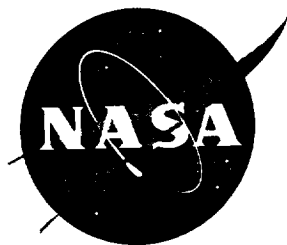


N 11  
97105

**NASA Contractor Report 195078**



# **Blade-Mounted Flap Control for BVI Noise Reduction Proof-of-Concept Test**

**Seth Dawson, Ahmed Hassan, Friedrich Straub and Hormoz Tadghighi**

***McDonnell Douglas Aerospace  
McDonnell Douglas Helicopter Systems  
Mesa, Arizona 85215***

**Contract NAS1-19060**

**July 1995**

**National Aeronautics and  
Space Administration  
Langley Research Center  
Hampton, Virginia 23681-0001**



## Table Of Contents

Section	Page Number
Summary . . . . .	1
1.0 Introduction . . . . .	2
2.0 Test Description . . . . .	4
3.0 Mechanical System Description . . . . .	5
3.1 Test Stand . . . . .	5
3.2 Rotor . . . . .	6
3.3 Blades . . . . .	6
3.5 Flap Actuation Mechanism . . . . .	6
3.6 Design Process, Mechanical Design of Hardware . . . . .	7
3.6.1 Aeroacoustic Analyses Summary . . . . .	7
3.6.2 Dynamic Analyses Summary . . . . .	8
3.6.3 Mechanical Design Summary . . . . .	9
3.7 Cam Profiles . . . . .	10
4.0 Data Acquisition . . . . .	11
4.1 Hardware Description For Data Acquisition . . . . .	11
4.2 Software Description . . . . .	12
4.3 Typical Test Day Description . . . . .	13
4.4 Acoustic Data Acquisition/Reduction . . . . .	16
4.4.1 Real-Time Data Acquisition . . . . .	16
4.4.1.1 Microphone and Kulite Pressure Transducer Data . . . . .	16
4.4.1.1.1 Transducer Calibrations . . . . .	17
4.4.1.1.2 Background and Reflected Noise Checks . . . . .	18
4.4.1.1.3 Test Point Data . . . . .	18
4.4.1.2 Microphone Traverse . . . . .	19
4.4.1.3 Wind Tunnel and Rotor Data . . . . .	19
4.4.2 Acoustic and Pressure Data Reduction . . . . .	19
4.4.2.1 Analytical Processing . . . . .	19
4.4.2.1.1 Engineering Units Conversion . . . . .	19
4.4.2.1.2 Ensemble Averages . . . . .	20
4.4.2.1.3 BVI Filtering . . . . .	20
4.4.2.1.4 Background and Reflected Signals . . . . .	20
4.4.2.2 Data Display . . . . .	21
4.4.2.3 Permanent Data Storage and Backup . . . . .	21
4.5 Dynamic Data Acquisition . . . . .	21
5.0 Test Procedures and Conduct . . . . .	21
5.1 Installation and Checkout . . . . .	22
5.2 Background Noise . . . . .	23
5.3 Weight Tares . . . . .	24
5.4 Aerodynamic Tares . . . . .	24
5.5 Track and Balance . . . . .	25

## Table Of Contents (cont'd)

Section	Page Number
5.6 Baseline Test Matrix . . . . .	25
5.7 -12.5 Degree Acoustic Cam . . . . .	27
5.8 -17.5 Degree Acoustic Cam . . . . .	28
5.9 -20.0 Degree Acoustic Cam . . . . .	30
5.10 2P3A Performance Cam . . . . .	32
5.11 2P6A Performance Cam . . . . .	33
5.12 Dynamics With Null Cam . . . . .	34
5.13 3P2A Dynamics Cam . . . . .	36
5.14 5P4A Dynamics Cam . . . . .	36
5.15 No Horn Baseline Case . . . . .	36
5.16 Removal of Model . . . . .	37
6.0 Test Results . . . . .	37
6.1 Stand Shake Test . . . . .	38
6.2 Dynamics data . . . . .	40
6.2.1 Rotor Dynamics . . . . .	40
6.2.1.1 Rotor Speed Sweeps . . . . .	40
6.2.1.2 Frequency Sweeps . . . . .	41
6.2.1.3 Transient Testing . . . . .	41
6.2.1.4 Standpipe Response . . . . .	42
6.2.2 Vibration Reduction . . . . .	42
6.2.3 Performance Improvement . . . . .	43
6.3 Sample Aerodynamic and Pressure Data . . . . .	44
6.3.1 Advancing Side BVI . . . . .	45
6.3.1.1 Effect of Trailing Edge Flap Deployment . . . . .	45
6.3.1.2 Effect of the Peak Flap Deflection Amplitude . . . . .	45
6.3.1.3 Effect of the Phase Shift in Azimuthal Flap Schedule . . . . .	47
6.3.2 Retreating Side BVI . . . . .	48
6.4 Sample Acoustic Data . . . . .	49
6.4.1 Advancing Side BVI . . . . .	49
6.4.1.1 Effect of Trailing Edge Flap Deployment . . . . .	49
6.4.1.2 Effect of Peak Deflection Amplitude . . . . .	51
6.4.1.3 Effect of the Phase Shift in Azimuthal Flap Schedule . . . . .	52
6.4.2 Retreating Side BVI . . . . .	53
6.5 Effect Of Acoustic Cams On Power Required . . . . .	54
7.0 Conclusions . . . . .	56
8.0 References . . . . .	57
Appendix A: Tunnel Test Tare Results and Correction Equation . . . . .	156
Appendix B: Test Log, Run Log, Instrumentation List, and Data Point Log . . . . .	159



## List Of Table Headings

Table	Page
1 Baseline Performance Test Matrix . . . . .	26
2 Baseline Acoustic Test Matrix . . . . .	27
3 Test Matrix For -12.5° Cam With 0° Azimuth . . . . .	27
4 Test Matrix For -12.5° Cam With -10° Azimuth . . . . .	27
5 Test Matrix For -12.5° Cam With +10° Azimuth . . . . .	28
6 Test Matrix For -12.5° Cam With +20° Azimuth . . . . .	28
7 Test Matrix For -17.5° Cam With -20° Azimuth . . . . .	28
8 Test Matrix For -17.5° Cam With 0° Azimuth . . . . .	28
9 Test Matrix For -17.5° Cam With -5° Azimuth . . . . .	29
10 Test Matrix For -17.5° Cam With -140° Azimuth . . . . .	30
11 Test Matrix For -20° Cam With -10° Azimuth . . . . .	30
12 Test Matrix For -20° Cam With 0° Azimuth . . . . .	31
13 Test Matrix For -20° Cam With -10° Azimuth . . . . .	31
14 Test Matrix For -20° Cam With -15° Azimuth . . . . .	31
15 Test Matrix For 2P3A Performance Cam With 11.7° Azimuth . . . . .	32
16 Test Matrix For 2P3A Performance Cam With 56.7° Azimuth . . . . .	32
17 Test Matrix For 2P3A Performance Cam With 101.7° Azimuth . . . . .	33
18 Test Matrix For 2P3A Performance Cam With 146.7° Azimuth . . . . .	33
19 Test Matrix For 2P6A Performance Cam With 11.7° Azimuth . . . . .	34
20 Test Matrix For Baseline Rotor Dynamic Excitation . . . . .	35
21 Test Conditions For Flow Visualization . . . . .	35
22 Conditions For Propulsive Force Comparison . . . . .	35
23 Test Conditions For 5P4A Dynamics Cam With -9° Azimuth . . . . .	36
24 Test Conditions For No Horn Baseline Rotor . . . . .	37
25 Shake Test Instrumentation (height relative to hub plane) . . . . .	39
26 Shake Test Frequency Sweeps . . . . .	39
27 Test Stand Modes And Response . . . . .	40
28 Ground Resonance Modal Data . . . . .	40
29 Frequencies Used In Transient Testing . . . . .	42
30 Shaft Angles Used . . . . .	42

## List Of Figure Captions

<b>Figure</b>		<b>Page</b>
Figure (1)	Active Flap Rotor and Test Stand At NASA Langley 14- by 22-Foot Subsonic Tunnel	59
Figure (2)	Schematic of Active Flap Model Rotor Hub and Rotor Mast.	60
Figure (3)	Cross Section of Active Flap Model Rotor Blade.	61
Figure (4)	Strain Gauges and Pressure Transducer Locations.	62
Figure (5)	Flap Actuation Mechanism.	63
Figure (6)	Typical BVI Noise Reduction Active Flap Deflection Profile Versus Azimuth Position.	64
Figure (7)	CAMRAD/JA Results. Bound Circulation versus Azimuth Position. $\mu = 0.15$ , $C_t = 0.007$ , $r/R = 0.93$ Solid Line is Baseline Rotor, Broken Line is Schedule 50 (20° Cam) Active Flap Deflection.	65
Figure (8)	Typical RFS2.BVI Results. Temporal Differential Pressure Gradients Near Blade Leading Edge versus Azimuth. $\mu = 0.15$ , $C_t = 0.007$ , $r/R = 0.93$ . Solid Line is Baseline Rotor, Broken Line is Schedule 50 (20° Cam) Active Flap Deflection.	66
Figure (9)	Typical WOPWOP Results. BVI Sound Pressure Level in dB Two Rotor Radius Under Rotor. $\mu = 0.15$ , $C_t = 0.007$ , $r/R = 0.93$ . Baseline Rotor Data; Schedule 50 (20° Cam) Active Flap Deflection Rotor Data; and Difference Between Baseline and Schedule 50 Is Shown.	67
Figure (10a)	Desired and Measured Flap Deflection Versus Azimuth Position For Acoustic Cam Profiles	68
Figure (10b)	Desired and Measured Flap Deflection Versus Azimuth Position For Harmonic Cam Profiles	69
Figure (11a)	Schedule 50 Cam Example of Trailing Edge Flap Deflection Over Four Revolutions	70

<b>Figure</b>		<b>Page</b>
Figure (11b)	Schedule 2P6A Cam Example of Trailing Edge Flap Deflection Over Four Revolutions	71
Figure (11c)	Schedule 5P4A Cam Example of Trailing Edge Flap Deflection Over Four Revolutions	72
Figure(12)	Acoustic Data Acquisition - Hardware Configuration.	73
Figure (13)	Acoustic Data Acquisition - Data Flow.	74
Figure (14)	Acoustic Data Acquisition - Overall Process Control.	75
Figure (15)	Position of Microphones Relative to Rotor in Wind Tunnel, Top View.	76
Figure (16)	Test Set Up For Shake Test.	77
Figure (17)	Frequency Response Function, R6 Hub Accelerometer, Lateral and R7, Balance Rolling Moment.	78
Figure (18)	Stand Frequency Response Function, R8 Mast Accelerometer, Lateral and R13 Mast Accelerometer Longitudinal.	79
Figure (19)	Stand Frequency Response, R14 Hub Accelerometer, Longitudinal and R12 Balance Pitch.	80
Figure (20a)	Blade Chord Bending at Station 23 Versus Rotor Speed.	81
Figure (20b)	Standpipe Torque Versus Rotor Speed.	81
Figure (21)	Power Spectra For Blade Flap, Chord and Torsion Response at Station 23, and For Main Rotor Shaft Torque at Nominal Rotor Speed (18.12 Hz).	82
Figure (22)	Longitudinal Cyclic Input and Chord Bending Response at Station 23.	83
Figure (23)	Rotor Balance Pitch Moment Frequency Response Baseline and 5P4A Cams.	84
Figure (24)	Rotor Balance Pitch Moment Time Histories, Baseline and 5P4A Cams.	85

<b>Figure</b>		<b>Page</b>
Figure (25)	Propulsive Force Versus Advance Ratio For Baseline and 2P3A Cams.	86
Figure (26)	L/D Versus Advance Ratio For Baseline And 2P3A Cams.	87
Figure (27)	Measured blade surface pressures ( $C_t/\sigma=0.0764$ , $\mu=0.149$ , $\alpha_{TPP}=5^\circ$ . aft, $x/C=0.03$ ) Baseline rotor configuration: Test # 0733, Point # 0891	88
Figure (28)	Measured blade surface pressures ( $C_t/\sigma=0.0764$ , $\mu=0.149$ , $\alpha_{TPP}=5^\circ$ . aft, $x/C=0.03$ ) Flapped rotor configuration: Test # 2916, Point # 2082	89
Figure (29)	Nominal flap schedule with a peak deflection of $-12.5^\circ$ and the schedule with a $-20^\circ$ of phase shift.	90
Figure (30)	Calculated differential pressures ( $C_t/\sigma=0.0764$ , $\mu=0.149$ , $\alpha_{TPP}=5^\circ$ . aft, $x/C=0.03$ ) Baseline rotor configuration: Test # 0733, Point # 0891	91
Figure (31)	Calculated differential pressures ( $C_t/\sigma=0.0764$ , $\mu=0.149$ , $\alpha_{TPP}=5^\circ$ . aft, $x/C=0.03$ ) Flapped rotor configuration: Test # 2916, Point # 2082	92
Figure (32)	Calculated differential pressures ( $C_t/\sigma=0.0760$ , $\mu=0.149$ , $\alpha_{TPP}=3^\circ$ . aft, $x/C=0.03$ ) Baseline rotor configuration: Test # 0731, Point # 0852	93
Figure (33)	Calculated differential pressures ( $C_t/\sigma=0.0764$ , $\mu=0.149$ , $\alpha_{TPP}=3^\circ$ . aft, peak deflection $-12.5^\circ$ , phase shift in azimuth $=-10^\circ$ , $x/C=0.03$ ) Flapped rotor configuration: Test # 2900, Point # 1774	94
Figure(34)	Calculated differential pressures ( $C_t/\sigma=0.0764$ , $\mu=0.149$ , $\alpha_{TPP}=3^\circ$ . aft, peak deflection $=-17.5^\circ$ , phase shift in azimuth $=-10^\circ$ , $x/C=0.03$ ) Flapped rotor configuration: Test # 3915, Point # 3105	95

<b>Figure</b>		<b>Page</b>
Figure (35)	Calculated differential pressures ( $C_t/\sigma=0.0764$ , $\mu=0.149$ , $\alpha_{TPP}=3^\circ$ . aft, peak deflection= $-17.5^\circ$ , phase shift in azimuth= $-20^\circ$ , $x/C=0.03$ ) Flapped rotor configuration: Test # 4034, Point # 4044	96
Figure (36)	Measured blade surface pressures ( $C_t/\sigma=0.076$ , $\mu=0.199$ , $\alpha_{TPP}=4^\circ$ . aft, $x/C=0.03$ ) Baseline rotor configuration: Test # 0738, Point # 1014	97
Figure (37)	Measured blade surface pressures ( $C_t/\sigma=0.076$ , $\mu=0.199$ , $\alpha_{TPP}=4^\circ$ . aft, peak deflection = $-12.5^\circ$ , phase shift in azimuth= $-10^\circ$ , $x/C=0.03$ ) Flapped rotor configuration: Test # 2904, Point # 1899	98
Figure (38)	Measured blade surface pressures ( $C_t/\sigma=0.076$ , $\mu=0.199$ , $\alpha_{TPP}=4^\circ$ . aft, peak deflection = $-17.5^\circ$ , phase shift in azimuth= $-10^\circ$ , $x/C=0.03$ ) Flapped rotor configuration: Test # 3922, Point # 3177	99
Figure (39)	Measured blade surface pressures ( $C_t/\sigma=0.076$ , $\mu=0.199$ , $\alpha_{TPP}=4^\circ$ . aft, peak deflection = $-20^\circ$ , phase shift in azimuth= $-10^\circ$ , $x/C=0.03$ ) Flapped rotor configuration: Test # 4047, Point # 3746	100
Figure (40)	Calculated differential pressures ( $C_t/\sigma=0.0865$ , $\mu=0.199$ , $\alpha_{TPP}=2.5^\circ$ . aft, $x/C=0.03$ ) Baseline rotor configuration: Test # 0741, Point # 1158	101
Figure (41)	Calculated differential pressures ( $C_t/\sigma=0.0865$ , $\mu=0.199$ , $\alpha_{TPP}=2.5^\circ$ . aft, peak deflection= $-17.5^\circ$ , phase shift in azimuth= $0^\circ$ , $x/C=0.03$ ) Flapped rotor configuration: Test # 3910, Point # 2845	102
Figure (42)	Calculated differential pressures ( $C_t/\sigma=0.0865$ , $\mu=0.199$ , $\alpha_{TPP}=2.5^\circ$ . aft, peak deflection= $-17.5^\circ$ , phase shift in azimuth= $-5^\circ$ , $x/C=0.03$ ) Flapped rotor configuration: Test # 3941, Point # 3084	103

<b>Figure</b>		<b>Page</b>
Figure (43)	Calculated differential pressures ( $C_t/\sigma=0.0865$ , $\mu=0.199$ , $\alpha_{TPP}=2.5^\circ$ . aft, peak deflection= $-17.5^\circ$ , phase shift in azimuth= $-10^\circ$ , $x/C=0.03$ ) Flapped rotor configuration: Test # 3925, Point # 3234	104
Figure (44)	Calculated differential pressures ( $C_t/\sigma=0.0865$ , $\mu=0.199$ , $\alpha_{TPP}=2.5^\circ$ . aft, peak deflection= $-17.5^\circ$ , phase shift in azimuth= $-20^\circ$ , $x/C=0.03$ ) Flapped rotor configuration: Test # 3741, Point # 2628	105
Figure (45)	Measured blade surface pressures ( $C_t/\sigma=0.0764$ , $\mu=0.149$ , $\alpha_{TPP}=3^\circ$ . aft, $x/C=0.03$ ) Baseline rotor configuration: Test # 0731, Point # 0852	106
Figure (46)	Measured blade surface pressures ( $C_t/\sigma=0.0764$ , $\mu=0.149$ , $\alpha_{TPP}=3^\circ$ . aft, peak deflection= $-17.5^\circ$ , phase shift= $+140^\circ$ , $x/C=0.03$ ) Flapped rotor configuration: Test # 5030, Point # 4373	107
Figure (47)	Measured blade surface pressures ( $C_t/\sigma=0.087$ , $\mu=0.199$ , $\alpha_{TPP}=2.5^\circ$ . aft, $x/C=0.03$ ) Baseline rotor configuration: Test # 0741, Point # 1158	108
Figure (48)	Measured blade surface pressures ( $C_t/\sigma=0.0764$ , $\mu=0.199$ , $\alpha_{TPP}=2.5^\circ$ aft, peak deflection= $-17.5^\circ$ , phase shift= $+140^\circ$ , $x/C=0.03$ ) Flapped rotor configuration: Test # 5050, Point # 4412	109
Figure (49a)	BVISPL Contour Plot Based on Spectra of Averaged Time Histories ( $C_t/\sigma = 0.0765$ , $\alpha_{TPP}=5$ degrees aft, $\mu=0.1488$ ) Baseline Rotor Configuration - Test # 0733	110
Figure (49b)	BVISPL Contour Plot Based on Spectra of Averaged Time Histories ( $C_t/\sigma = 0.0777$ , $\alpha_{TPP} = 5$ degrees aft, $\mu=0.1487$ , Peak Flap Deflection= $-12.5$ degrees, Azimuthal Phase Shift = $-20$ degrees ) Flapped Rotor Configuration - Test # 2916	111

<b>Figure</b>		<b>Page</b>
Figures (50a & 50b)	Average Acoustic Time Histories at Microphone Traverse Station 9 on the Advancing Side - Test #s 0733 & 2916	112
Figures (51a & 51b)	Ensemble-averaged Narrowband Spectra at Microphone Traverse Station 9 on the Advancing Side - Test #s 0733 & 2916	113
Figures (52a & 52b)	Average Acoustic Time Histories at Microphone Traverse Station 9 on the Retreating Side - Test #s 0733 & 2916	114
Figures (53a & 53b)	Ensemble-averaged Narrowband Spectra at Microphone Traverse Station 9 on the Retreating Side - Test #s 0733 & 2916	115
Figure (54a)	BVISPL Contour Plot Based on Ensemble-averaged Spectra ( $Ct/\sigma = 0.0868$ , $\alpha_{TPP} = 2.5$ degrees aft, $\mu=0.1987$ ) Baseline Rotor Configuration - Test #0741	116
Figure (54b)	BVISPL Contour Plot Based on Spectra of Averaged Time Histories ( $Ct/\sigma = 0.087$ , $\alpha_{TPP} = 2.5$ degrees aft, $\mu=0.1987$ ) Baseline Rotor Configuration - Test #0741	117
Figure (55a)	BVISPL Contour Plot Based on Ensemble-averaged Spectra ( $Ct/\sigma = 0.0875$ , $\alpha_{TPP} = 2.5$ degrees aft, $\mu=0.1986$ , Peak Flap Deflection = 12.5 degrees, Azimuthal Phase Shift = 0 degrees) Flapped Rotor Configuration - Test # 2741	118
Figure (55b)	BVISPL Contour Plot Based on Spectra of Averaged Time Histories ( $Ct/\sigma = 0.0875$ , $\alpha_{TPP} = 2.5$ degrees aft, $\mu=0.1986$ , Peak Flap Deflection = -12.5 degrees, Azimuthal Phase Shift = 0 degrees) Flapped Rotor Configuration - Test # 2741	119
Figure (56a)	BVISPL Contour Plot Based on Spectra of Averaged Time Histories ( $Ct/\sigma = 0.0773$ , $\alpha_{TPP} = 3$ degrees aft, $\mu=0.1492$ ) Baseline Rotor Configuration Test # 0731	120

<b>Figure</b>		<b>Page</b>
Figure (56b)	BVISPL Contour Plot Based on Spectra of Averaged Time Histories ( $Ct/\sigma = 0.0776$ , $\alpha_{Tpp} = 3$ degrees aft , $\mu = 0.1486$ , Peak Flap Deflection = -12.5 degrees, Azimuthal Phase Shift = -10 degrees ) Flapped Rotor Configuration - Test # 2900	121
Figure (56c)	BVISPL Contour Plot Based on Spectra of Averaged Time Histories ( $Ct/\sigma = 0.0778$ , $\alpha_{Tpp} = 3$ degrees aft, $\mu = 0.1488$ , Peak Flap Deflection = -17.5 degrees, Azimuthal Phase Shift = -5 degrees ) Flapped Rotor Configuration - Test # 3915	122
Figures (57a & 57b)	Average Acoustic Time Histories at Microphone Traverse Station 9 on the Advancing Side - Test #s 0731 & 2900	123
Figure (57c)	Average Acoustic Time Histories at Microphone Traverse Station 9 on the Advancing Side; Flapped Rotor - Test # 3915	124
Figures (58a & 58b)	Ensemble-averaged Narrowband Noise Spectra at Microphone Traverse Station 9 on the Advancing Side - Test #s 0731 & 2900	125
Figure (58c)	Ensemble-averaged Narrowband Noise Spectra at Microphone Traverse Station 9 on the Advancing Side ; Flapped Rotor - Test # 3915	126
Figure (59a)	BVISPL Contour Plot Based on Spectra of Averaged Time Histories ( $Ct/\sigma = 0.078$ , $\alpha_{Tpp} = 4$ degrees aft , $\mu = 0.1991$ ) Baseline Rotor Configuration Test # 0738	127
Figure (59b)	BVISPL Contour Plot Based on Spectra of Averaged Time Histories ( $Ct/\sigma = 0.0768$ , $\alpha_{Tpp} = 4$ degrees aft, $\mu = 0.1982$ , Peak Flap Deflection = -12.5 degrees, Azimuthal Phase Shift = -10 degrees ) Flapped Rotor Configuration - Test # 2904	128



<b>Figure</b>		<b>Page</b>
Figure (59c)	BVISPL Contour Plot Based on Spectra of Averaged Time Histories ( $Ct/\sigma = 0.0775$ , $\alpha_{TPP} = 4$ degrees aft , $\mu=0.1988$ , Peak Flap Deflection=-17.5 degrees, Azimuthal Phase Shift = -10 degrees ) Flapped Rotor Configuration Test # 3922	129
Figure (59d)	BVISPL Contour Plot Based on Spectra of Averaged Time Histories ( $Ct/\sigma = 0.0764$ , $\alpha_{TPP} = 4$ degrees aft, $\mu=0.198$ , Peak Flap Deflection=-20 degrees, Azimuthal Phase Shift = -10 degrees ) Flapped Rotor Configuration - Test # 4047	130
Figures (60a & 60b)	Average Acoustic Time Histories at Microphone Traverse Station 9 on the Advancing Side - Test #s 0734 & 2904	131
Figures (60c & 60d)	Average Acoustic Time Histories at Microphone Traverse Station 9 on the Advancing Side - Test #s 3922 & 4047	132
Figures (61a & 61b)	Ensemble-averaged Narrowband Noise Spectra at Microphone Traverse Station 9 on the Advancing Side - Test #s 0738 & 2904	133
Figures (61c & 61d)	Ensemble-averaged Narrowband Noise Spectra at Microphone Traverse Station 9 on the Advancing Side - Test #s 3922 & 4047	134
Figure (62a)	BVISPL Contour Plot Based on Spectra of Averaged Time Histories ( $Ct/\sigma = 0.0868$ , $\alpha_{TPP} = 2.5$ degrees aft , $\mu=0.1987$ ) Baseline Rotor Configuration Test # 0741	135
Figure (62b)	BVISPL Contour Plot Based on Spectra of Averaged Time Histories ( $Ct/\sigma = 0.0896$ , $\alpha_{TPP} = 2.5$ degrees aft, $\mu=0.1990$ , Peak Flap Deflection=-17.5 degrees, Azimuthal Phase Shift = 0 degrees) Flapped Rotor Configuration Test # 3910	136

<b>Figure</b>		<b>Page</b>
Figure (62c)	BVISPL Contour Plot Based on Spectra of Averaged Time Histories ( $Ct/\sigma = 0.0889$ , $\alpha_{TPP} = 2.5$ degrees aft , $\mu=0.1985$ , Peak Flap Deflection=-17.5 degrees, Azimuthal Phase Shift = -5 degrees) Flapped Rotor Configuration Test # 3941	137
Figure (62d)	BVISPL Contour Plot Based on Spectra of Averaged Time Histories ( $Ct/\sigma = 0.0887$ , $\alpha_{TPP} = 2.5$ degrees aft, $\mu=0.1983$ , Peak Flap Deflection=-17.5 degrees, Azimuthal Phase Shift = -10 degrees ) Flapped Rotor Configuration Test # 3925	138
Figure (62e)	BVISPL Contour Plot Based on Spectra of Averaged Time Histories ( $Ct/\sigma = 0.0879$ , $\alpha_{TPP} = 2.5$ degrees aft , $\mu=0.1990$ , Peak Flap Deflection=-17.5 degrees, Azimuthal Phase Shift = -20 degrees) Flapped Rotor Configuration Test # 3741	139
Figures (63a & 63b)	Average Acoustic Time Histories at Microphone Traverse Station 9 on the Advancing Side - Test #s 0741 & 3925	140
Figures (64a & 64b)	Ensemble-averaged Narrowband Noise Spectra at Microphone Traverse Station 9 on the Advancing Side - Test #s 0741 & 3910	141
Figure (64c)	Ensemble-averaged Narrowband Noise Spectra at Microphone Traverse Station 9 on the Advancing Side ; Flapped Rotor - Test # 3925	142
Figure (65a)	BVISPL Contour Plot Based on Spectra of Averaged Time Histories ( $Ct/\sigma = 0.0773$ , $\alpha_{TPP} = 3$ degrees aft , $\mu=0.1492$ ) Baseline Rotor Configuration Test # 0731	143
Figure (65b)	BVISPL Contour Plot Based on Spectra of Averaged Time Histories ( $Ct/\sigma = 0.0764$ , $\alpha_{TPP} = 3$ degrees aft, $\mu=0.1496$ , Peak Flap Deflection=-17.5 degrees, Azimuthal Phase Shift = +140 degrees ) Flapped Rotor Configuration - Test #5030	144

<b>Figure</b>		<b>Page</b>
Figures (66a & 66b)	Average Acoustic Time Histories at Microphone Traverse Station 9 on the Retreating Side - Test #s 0731 & 5030	145
Figures (67a & 67b)	Average Acoustic Time Histories at Microphone Traverse Station 9 on the Advancing Side - Test #s 0731 & 5030	146
Figures (68a & 68b)	Ensemble-averaged Narrowband Noise Spectra at Microphone Traverse Station 9 on the Retreating Side - Test #s 0731 & 5030	147
Figures (69a & 69b)	Ensemble-averaged Narrowband Noise Spectra at Microphone Traverse Station 9 on the Advancing Side - Test #s 0731 & 5030	148
Figure (70a)	BVISPL Contour Plot Based on Spectra of Averaged Time Histories ( $Ct/\sigma = 0.0868$ , $\alpha_{TPP} = 2.5$ degrees aft, $\mu=0.1987$ ) Baseline Rotor Configuration - Test # 0741	149
Figure (70b)	BVISPL Contour Plot Based on Spectra of Averaged Time Histories ( $Ct/\sigma = 0.0890$ , $\alpha_{TPP} = 2.5$ degrees aft, $\mu=0.1987$ , Peak Flap Deflection = -17.5 degrees, Azimuthal Phase Shift = +140 degrees ) Flapped Rotor Configuration - Test #5050	150
Figures (71a & 71b)	Average Acoustic Time Histories at Microphone Traverse Station 9 on the Retreating Side - Test #s 0741 & 5050	151
Figures (72a & 72b)	Average Acoustic Time Histories at Microphone Traverse Station 9 on the Advancing Side - Test #s 0741 & 5050	152
Figures (73a & 73b)	Ensemble-averaged Narrowband Noise Spectra at Microphone Traverse Station 9 on the Retreating Side - Test #s 0741 & 5050	153
Figures (74a & 74b)	Ensemble-averaged Narrowband Noise Spectra at Microphone Traverse Station 9 on the Advancing Side - Test #s 0741 & 5050	154

**Figure****Page**

Figure (75)

Power Required for Descent Flight Condition  
( $\mu = 0.20$  and  $C_t = 0.008$ ) for Baseline and Active  
Flap Rotor Configurations and Cruise Flight  
Condition for Baseline Rotor ( $\mu=0.3$ ,  $C_t=0.008$ )

155

## NOTATION

$C_t$	thrust coefficient
$M_h$	hover Mach number
NR	nominal rotor speed
$X, \bar{X}$	Propulsive force coefficient
$\alpha, \alpha_{TPP}$	tip path plane angle of attack
$\mu$	advance ratio
$\sigma$	rotor solidity
ASAP	database program
HP	Hewlett Packard
sps	samples per second
SPL	sound pressure level



## Summary

This report describes a wind tunnel test of the McDonnell Douglas Helicopter Systems (MDHS) Active Flap Model Rotor at the NASA Langley 14- by 22-Foot Subsonic Tunnel. The primary purpose of the test was to examine the reduction of BVI noise. This report is intended as a detailed record of the program, its conduct, and results. No analysis of the results is performed. This report briefly describes the aeroacoustic research leading to the initiation of this test program. The design of the model rotor and flap actuation profiles is described. The conduct of the test program is detailed. Examples of performance, aerodynamic and acoustic data are presented and discussed.

The test demonstrated that BVI noise reduction and vibration reduction were possible with the use of an active flap. Aerodynamic results supported the acoustic data trends, showing a reduction in the strength of the tip vortex with the deflection of the flap. Acoustic results showed that the flap deployment, depending on the peak deflection angle and azimuthal shift in its deployment schedule, can produce BVI noise reductions as much as 6 dB on the advancing and retreating sides. The noise reduction was accompanied by an increase in low frequency harmonic noise and high frequency broadband noise. A brief assessment of the effect of the flap on vibration showed that significant reductions were possible. The greatest vibration reductions were found in the four per rev pitching moment at the hub. Up to 76% reduction was measured at  $\mu = 0.30$ , and  $C_t = 0.006$ . Performance improvement cam results were inconclusive, as the improvements were predicted to be smaller than the resolution of the rotor balance.

## 1.0 Introduction

To investigate the use of a blade-mounted active flap for Blade Vortex Interaction Noise (BVI) reduction, rotor performance improvement, and vibration reduction, McDonnell Douglas Helicopter Systems (MDHS) and researchers from the NASA Langley Research Center performed a test of an active flap equipped model rotor in the Langley 14- by 22-Foot Subsonic Tunnel. The model and test stand were assembled and tested in hover in Mesa at MDHS's Remote Test Facility from September 1993 through January 1994. The six week tunnel entry at Langley's 14- by 22-Foot Subsonic Tunnel took place between 1 February 1994 and 15 March 1994.

The primary objective of this wind tunnel test was to perform an aeroacoustic investigation of the reduction of Blade Vortex Interaction (BVI) noise with the McDonnell Douglas Active Flap Rotor (MDAFR) system. The secondary objective was to study the performance characteristics of an active flap rotor with two per rev flap deflection. The tertiary goal was to investigate vibration reduction with N/rev flap deflection.

Low speed BVI occurring during descent in terminal area operations has been an objectionable noise source for many years. Unfortunately it continues to be a dominant source in present day helicopters and even plagues the promising new tiltrotor transport concept [1]. A great deal of effort has been expended in examining means to alleviate BVI noise [2-8]. Much of this work has been focused on methods of altering the characteristics of the rolled-up tip vortices which are the principal contributors to the high frequency impulsive noise. Investigators have examined both passive and active means of reducing the vortex strengths. Included among the passive techniques are tip shape variations that reduce tip loading to lower the tip vortex strength, and the use of subwings, extending beyond the rotor tip causing the formation of an additional tip vortex which interacts with and diffuses the primary vortex. Tip anhedral has also been used as a means of increasing the blade-vortex separation distance, although this was principally intended to improve hover performance. Active means of controlling tip vortex strength require additional weight, control system complexity and impacts reliability. Nevertheless, the severity of the problem dictates that these approaches be considered.

Recognizing the need to explore new technologies for BVI noise reduction, a National program was launched by NASA. The first phase, referred to as the *"National Rotorcraft Noise Reduction Program"* emphasized research in fundamental BVI noise prediction methodologies as they applied to conventional rotorcraft. At the end of the first phase of the program, NASA issued a Research Announcement for Innovative Noise Reduction Concept studies. Participants from academia, industry, and research establishments were asked to demonstrate, through numerical studies or wind tunnel testing, the potential benefits from using their respective active and/or passive BVI noise control concepts. Among the various concepts examined were doubly swept forward blade tips, passive trailing edge spoilers or drag generators, and the MDHS blade-mounted trailing edge flap concept. The MDHS study concluded that average noise reductions on the order



of 5 dB can be achieved with the unsteady deployment of the trailing edge flap. The active control concept rested on the validated premise that the rapid variations in blade airloads, which are to a large extent responsible for the generation of impulsive noise during BVI, can be reduced by the unsteady motion of the trailing edge flap. This is accomplished by direct changes in the vortex-wake trajectories and strengths.

It has been shown [9,10] that blade-mounted flaps are feasible for use in the helicopter operating environment as a primary rotor control device. Blade mounted flaps are used effectively to control the Kaman SH-2F Sea Sprite. Analytical studies [11] demonstrated that the flap appeared to offer a viable mechanism for reducing the impulsive aerodynamic response due to blade-vortex interaction. In both analytical and experimental studies, it has been shown [12] that strong leading edge pressure fluctuations occur during BVI conditions. Experience also shows that trailing edge flaps create aft pressure loading which might be utilized to alleviate the impulsive nature of BVI. Thus, in the concept tested in this experiment, the flap is applied in the regions where BVI occurs to alter the local blade response. As an active device, the flap motions can be tailored to achieve maximum benefit throughout a range of descent flight conditions. The flap can also be used to reduce the strength of portions of certain tip vortices which are most responsible for strong BVI. This is achieved by altering the spanwise lift distributions near the tip in those areas of the disk where the critical vortex elements are being generated.

With these goals in mind, a NASA Langley sponsored study was performed by MDHS to develop the active flap concept. The aerodynamic and acoustic tools previously used in the prediction of BVI [13] were modified to simulate a rotor having trailing edge flaps. The method was applied to analytically evaluate the performance, aerodynamics and acoustics of the one-seventh scale BELL AH-1G model rotor system (see reference [14]) employing a 25-percent chord, 18-percent span trailing edge flap. More specifically, flap deployment amplitudes, rates, duration and azimuthal location of the peak deflection were investigated in various flap schedules seeking maximum BVI noise reduction with minimum performance loss. For this study, a partial power descent flight condition at 65 knots, with 300 fpm descent rate was chosen as it represents a case where significant blade-vortex interactions were found in both blade surface pressures (aerodynamic) and microphone (acoustic) measurements obtained in the DNW wind tunnel tests [14] of the (unflapped) model rotor. Results of the analytical study [15] showed average reductions in the BVI noise levels on the order of 5 dB with moderate power penalties, on the order of 18% to 58% for a number of flap schedules.

Based on the results of this study, MDHS proposed to NASA Langley in 1991 a demonstration of this technique on a model rotor in the 14- by 22-foot Subsonic Tunnel. NASA Langley and MDHS agreed to a joint Proof-of-Concept wind tunnel test. NASA Langley funded portions of the aeroacoustic analysis to design the active flap deflection profiles, the preliminary design of the model rotor, bench testing of the flap actuation hardware, the wind tunnel test, and the final report. MDHS funded portions of the aeroacoustic analysis to design the active flap deflection profiles, the detailed design of the active flap model rotor, the fabrication

of the rotor, modifications to MDHS' Large Scale Test Rig, and an integration test of the hardware in Mesa, AZ. The wind tunnel test was a team effort with participants from NASA Langley's Aeroacoustics Branch and the Applied Acoustics Branch of the Acoustics Division, 14- by 22-Foot Subsonic Tunnel operations crew from the Tunnel Operations Branch, Technical Support Section D, US Army Aeroflightdynamics Directorate, and MDHS engineers and technicians. MDHS directed daily test operations, operated the rotor test stand and acquired performance data from the model, and evaluated the quality of aerodynamic and acoustic data. NASA Langley 14- by 22-Foot Subsonic Tunnel personnel operated the wind tunnel, motor generator set and supported model maintenance. NASA Subsonic Aerodynamics Branch, Applied Aerodynamics Division personnel supported the test program with mechanical and test engineering support. NASA Langley Acoustics Division personnel acquired pressure and acoustic data, processed, and evaluated that data.

## **2.0 Test Description**

The major milestones that were accomplished during installation and testing of the rotor system included:

1. Installation of test stand on sting support in tunnel.
2. Completion of shake test to identify stand modes.
3. Installation and checkout of rotor, control console and data acquisition system.
4. Hub balance and rotor track and balance.
5. Aerodynamic tare runs and acoustic background noise runs with hub turning, no blades.
6. Exploration of test envelope with rotor using flow visualization to ensure no ingestion of open jet shear layer for three acoustic test conditions and for performance test conditions.
7. Completion of baseline test matrix, with null cam, three acoustic test conditions and performance baseline points.
8. Completion of acoustic test matrix (3 test conditions) for  $-12.5^\circ$  active flap deflection cam (Schedule 63).
9. Completion of acoustic test matrix (3 test conditions) for  $-17.5^\circ$  active flap deflection cam (Schedule 65).
10. Completion of acoustic test matrix (3 test conditions) for  $-20.0^\circ$  active flap deflection cam, (Schedule 50).
11. Completion of performance test matrix for  $3.0^\circ$ , two per rev sinusoidal flap deflection.
12. Completion of performance test matrix for  $6.0^\circ$ , two per rev, sinusoidal flap deflection.
13. Completion of dynamics test matrix for  $2.0^\circ$ , three per rev sinusoidal flap deflection.
14. Completion of vibration test matrix for  $4.0^\circ$ , four per rev, sinusoidal flap deflection.
15. Completion of no horn baseline case.
16. Removal of model from wind tunnel test section.

### 3.0 Mechanical System Description

The MDHS Active Flap Rotor and Large Scale Test Rig were mounted on the NASA Langley 14- by 22-Foot Subsonic Tunnel Cart Number One in the front bay of the open jet test section. The test stand is shown mounted to the cart in Figure 1. The model rotor characteristics were as follows:

- Rotor radius, R	: 72.75 inches
- Blade chord length, C	: 5.25 inches
- Rotor solidity	: 0.0919
- Rotor airfoil section	: NACA 0015
- Flap span	: 17.9 % R
- Flap inboard radial station	: 79.4 % R
- Flap outboard radial station	: 97.3 % R
- Flap chord	: 25.0 % C
- Average blade twist	: -1.5°/linear foot

Each blade had a single trailing edge flap. The flap control system had provisions for adjusting the phase of the deflection profile. Three cams were used to provide different flap amplitudes and schedules for BVI noise reduction. Two additional cams were used to investigate rotor performance. Two cams were used to investigate vibration reduction. The cams included; one null cam with no flap deflection, three cams with flap deflection schedules designed to produce maximum BVI noise reduction (Schedule 63 with -12.5° deflection, Schedule 50 with -20°, and Schedule 65 with 17.5° deflection), one cam with 3.0° sinusoidal two per rev flap deflection, one cam with 6.0° sinusoidal two per rev flap deflection, one cam with 2.0° sinusoidal three per rev flap deflection, and one cam with 4.0° sinusoidal five per rev flap deflection.

### 3.1 Test Stand

The test stand was driven by a 200 HP, 400 Hz, three phase electric motor (supplied by deHavilland through NASA). The motor drove a 5:1 gear ratio transmission. The swashplate control system consisted of three hydraulic actuators located at the 60°, 180°, and 300° azimuth positions. The high rate actuators were capable of up to 40 Hz response with one half peak-to-peak amplitude of 0.100 inches. The actuators had six inches of stroke with full authority over 80% of the travel, and a 10% travel snubber to prevent hard-over conditions. Dual Linear Variable Displacement Transducers (LVDTs) measured actuator position and provided redundancy in the event of an LVDT malfunction. Progressing and regressing lag mode excitation was possible by nutating the swashplate at the fixed system frequencies.

The design load capabilities of the test stand components were far larger than the expected loads from the Active Flap Rotor at nominal operating conditions. This capability provided safety in the event of component failures in the flap actuation system. The five axis rotor balance could measure up to ±40,000 in-lbs of rolling

and pitching moments and up to  $\pm 1950$  lbs of side force and axial force. The test stand and rotor mounted in the 14- by 22-Foot Subsonic Tunnel are shown in Figure 1.

### **3.2 Rotor**

The four-bladed model rotor was 145.5 inches in diameter with a solidity of 0.0919 and a blade chord of 5.25 inches. The composite rotor blades used a NACA 0015 airfoil. Each blade had a single, integral trailing edge flap. The flap extended from the 79% radial position to the 97% radial position and spanned 25% of the blade chord. The arrangement of the hub, active flap control system and hub shaft in relationship to the root cuffs are shown in Figures 2.

### **3.3 Blades**

The composite model blades were designed and manufactured by Advanced Technologies Incorporated. A constant 5.25 inch chord NACA 0015 airfoil was used. A cross section of the active flap model rotor blade is shown in Figure 3. The hover tip Mach Number of this rotor was 0.619. Experimental aerodynamic data, describing the performance of flapped airfoils at high Mach Numbers, are limited. Some high Mach Number data was available, however, for the NACA 0015 airfoil with a flap, these data were used to check the accuracy of the numerically-generated airfoil coefficients.

Active flap angles were measured with a Hall effect transducer at the inboard end of the flap. Strain gauges were mounted at the 23.69 ( $r/R = .32$ ), and 50.4 ( $r/R = .70$ ) radial stations on the active flap rotor blades to measure the flap bending, chord bending and torsion moments. Four pairs of pressure transducers were located on the top and bottom surfaces near the leading edge of the blade ( $x/c = 0.03$ ), at radial stations  $r/R = 0.752, 0.821, 0.911, \text{ and } 0.970$ . The locations and types of these gauges and pressure transducers are shown in Figure 4.

### **3.5 Flap Actuation Mechanism**

The flap was driven by a cable running from a control horn on the flap, over a bellcrank, down the interior of the blade to a cam follower at the hub. The actuation cable was located along the blade's elastic axis to avoid any coupling between blade motion and active flap deflection. The cam follower rode on a non-rotating cam at the center of the hub. The flap was preloaded in the downward direction by a tension-torsion rod located in the flap's leading edge. As the cam follower rode up over the deflection profile on the interior surface of the cam, it retracted the actuation cable, deflecting the flap upwards. The flap actuation mechanism is shown in Figure 5. Different cams were used to provide flap schedules for performance improvements and for BVI noise reduction. The flap control system had provisions for adjusting the phase and amplitude of the deflection. A typical noise reduction flap deflection profile is shown in Figure 6.

### **3.6 Design Process, Mechanical Design of Hardware**

During the preliminary design phase, many different flap actuation concepts were evaluated including pneumatic, hydraulic, electromechanical, and mechanical types. Due to the high rates of flap deflection motion, and the high inertial forces, the best concept (for this demonstration-of-concept model) proved to be a mechanically operated active flap. The rotor hub preliminary design was performed by MDHS, while the detailed design and fabrication were completed by Advanced Technologies Incorporated (ATI). The flap actuation hardware proved to be the most challenging part of the design. The design process for the optimum cam profile involved a trade-off between minimizing allowable loads, and maximizing BVI noise reduction and fatigue life on the mechanical components.

#### **3.6.1 Aeroacoustic Analyses Summary**

A modified version of the CAMRAD/JA code [16] was used for the aerodynamic performance analyses of the Active Flap Model Rotor. CAMRAD/JA requires the physical geometry of the rotor, inertia and stiffness properties, flight conditions, and lookup tables of airfoil data. The code was modified at MDHS to allow for the aerodynamic and dynamic modeling of a blade mounted trailing edge flap. Input for the code included the flap deflection schedule, rotor advance ratio, tip Mach number and trim conditions. For given trim conditions the modified CAMRAD/JA code produced relevant blade motion parameters, the aerodynamic loads on the blade and flap, and the modal frequency placement. Potential blade-vortex encounters were also identified and tracked in time using the CAMRAD/JA code.

Typical CAMRAD/JA results are shown in Figure 7. Bound circulation versus rotor azimuth is shown for the baseline rotor and for the rotor with a  $-20^\circ$  active flap deflection for BVI noise reduction. Two  $-20^\circ$  active flap deflection cams were built. The first, Schedule 33, created unacceptably high loads in the flap actuation system. A second,  $-20^\circ$  active flap deflection cam was built with more gradual changes in flap deflection. The data presented here is for the second, Schedule 50 cam. For this case the advance ratio,  $\mu$ , was 0.15, with a thrust coefficient of  $C_t = 0.007$ . Data is shown for the blade station  $r/R = 0.93$ . The baseline rotor bound circulation is shown by the solid line. The bound circulation from the active flap deflection configuration is shown by the broken line. On the advancing side of the rotor, from  $90^\circ$  to  $160^\circ$  azimuth, bound circulation is sharply reduced as the flap is deflected upwards. The strength of the tip vortex, and thus the strength of the Blade Vortex Interaction encounter as the following blade reaches the vortex, is reduced.

The CAMRAD/JA code predicts far wake inflow angles of attack and BVI vortex element trajectories and strengths. These were then used as inputs for the RFS2.BVI aerodynamic code. RFS2.BVI [17] is an unsteady three-dimensional full potential rotor flow solver that computes the pressure field for the rotor during complex blade vortex interactions. Using the CAMRAD/JA results, RFS2.BVI utilizes an interpolation routine to compute the instantaneous position of the interaction vortex elements relative to the blade for the time-accurate calculation. The resulting predicted blade surface pressures were extracted and converted into

a readily usable format for the acoustic prediction code WOPWOP [18] to determine the impact of the flap deflection schedule on BVI noise.

Typical RFS2.BVI results are shown in Figure 8. The rate of change of the differential pressure versus azimuth is shown. The same test conditions are shown as for the previous CAMRAD/JA results. The blade station shown is  $r/R = 0.93$  with  $x/C = 0.03$ . The rate of change of the differential pressures is shown by the solid line for the baseline configuration. The data for the active flap deflection configuration is shown by the broken line. The baseline configuration shows the impulsive peaks at  $70^\circ$  azimuth typical of BVI encounters. RFS2.BVI results show a significant reduction in these impulsive peaks for the Schedule 50,  $-20^\circ$  active flap deflection configuration.

WOPWOP is a rotor acoustic prediction code based on the Ffowcs-Williams-Hawkings formulation [19]. WOPWOP uses Farassat's solution [20] to this equation. The program was originally developed at NASA Langley Research Center. WOPWOP has been coupled with the RFS2.BVI rotor flow solver via the computed blade surface pressures that are used as input to the acoustic analyses [13]. The code was modified to allow for the blade camber variations that result as a consequence of the trailing edge flap deflections. Average BVI noise reductions on the order of 5 dB from those of the baseline rotor were predicted.

Typical WOPWOP results are shown in Figure 9. For this case, average predicted reduction in BVI noise from the baseline rotor is 3.1 dB. The figure shows a carpet plot of overall sound pressure level ( $OASPL_{BVI}$ ) noise. The  $OASPL_{BVI}$  metric used here is a weighted average technique developed by NASA Langley. The amplitudes of the first two harmonics of the blade passage frequency have been removed from the OASPL average. BVI noise in this model scale rotor should dominate the spectrum in the range from 500 Hz to 3,000 Hz. The weighted average technique removes the first two rotor harmonics so that amplitudes in the time domain will not be biased by the rotor's lowest frequencies, which typically have the highest levels. The plot represents the noise levels predicted for Schedule 50, for microphone locations extending from two rotor radii downstream to three radii upstream. The integration of the  $OASPL_{BVI}$  noise level over this area results in an average noise level that is used as a metric to determine the effectiveness of the flap deflection schedule [15]. For the test conditions shown, it can be seen that the size and amplitude of the high intensity region below the rotor on the advancing side are reduced with the Schedule 50 cam. The average noise reduction over the area of the carpet plot is 3.1 dB.

### **3.6.2 Dynamic Analyses Summary**

Blade motion parameters and structural loads, aerodynamic loads on the blade and flap, and modal frequency placements for given trim conditions were also predicted with the modified CAMRAD/JA code [16]. Dynamic modeling of the flap actuation hardware and bench test hardware was performed using the ADAMS code [21]. ADAMS is a multi-body dynamic analysis model. The analysis uses prescribed rigid blade motions and aerodynamic loads on the flap, as well as the

mass, damping, elasticity and geometric properties of the flap actuation mechanism. Given prescribed cam follower motions, the analysis produces time histories of the dynamic loads on components, displacements of the linkage mechanism driving the flap, and flap motions.

### **3.6.3 Mechanical Design Summary**

The design process for the optimum cam profile involved a trade-off between minimizing allowable loads, maximizing BVI noise reduction, and maximizing fatigue life of the mechanical components. A number of flap schedule parameters had a direct impact on the level of the predicted BVI noise, and on the noise reductions. These included the duration, or dwell, of the maximum flap deflection, the azimuth location for initiating the dwell, the maximum amplitude of the flap deflection, and the initiation and completion points of the deflection on the rotor azimuth. Flap schedule parameters that directly affected the mechanical loads on the actuation hardware include the magnitude of the flap deflection, and the curvature of the ramp-up and ramp-down deflection profile, which directly impacted the cam follower acceleration. The design process consisted of an iterative procedure where all these factors were varied parametrically. The resulting aerodynamics, acoustics, dynamics and loads were then analyzed, and a new iteration was initiated based on these results.

During this iterative process it became clear that the ideal flap deflection profile, for an aerodynamics or acoustics engineer, moved instantaneously to its deflected position of  $-20^\circ$ , and back to the neutral position just as quickly. The dynamics engineer's ideal flap deflection profile was one with a smooth sinusoidal  $2/\text{rev}$  deflection of  $-20^\circ$ . The design engineer's ideal flap deflection profile had no deflection at all to reduce loads. Although sophisticated analysis tools were used to examine the effects of the flap deflection profile, the iterative design procedure was performed manually using a concurrent engineering approach. The final flap deflection profiles produced the required BVI noise reduction with loads resulting in an adequate fatigue life for key components.

As described in Section 3.0, three acoustic cams, two performance cams, and two vibration cams were tested. An iterative procedure was used to create the cam profile from the desired flap deflection profile.

### **3.7 Cam Profiles**

Time histories of trailing edge flap deflection with the objectives of reducing BVI noise, improving rotor performance, and reducing vibratory hub loads were defined by analysts in the respective disciplines. The azimuthal variations were then translated into a cam profile using the ADAMS computer code model of the flap actuation mechanism.

The schedule 50 cam (nominal  $-20^\circ$ ) used on the whirl tower was machined based on predictions from an early ADAMS model, which had 0.026 in/deg follower motion per flap deflection. Examination of whirl tower test data showed that the

actual flap deflection was higher. Four test points (90 - 93) at nominal rotor speed and collective of 2, 0, 2, and 4° were used to define an average flap amplitude. Using the ASAP database tools to average flap angles in the constant sections of the profile, the following values for flap amplitude were obtained for blades one through four: 22.24, 20.90, 22.57, 20.23. The average flap amplitude for this cam was thus determined to be 21.49°, resulting in 0.0242 in/deg follower motion per flap deflection.

The 2/rev performance cams were based on a later ADAMS model, updated from bench test data. This model had 0.01866 in/deg follower motion per flap deflection. Two cams were built as follows:

$$2P3A \text{ cam: } \delta_f = 3.25^\circ \cos 2(\psi + 15^\circ)$$

$$2P6A \text{ cam: } \delta_f = 6.5^\circ \cos 2(\psi + 15^\circ)$$

Both cams had a 15° azimuth lead, included to account for dynamics and to still place the maximum flap amplitude at zero azimuth. The amplitudes were increased from the nominal 3° and 6°, to obtain the desired amplitude around the azimuth in an average sense. Examining whirl tower test data, it was seen that the 2P6A cam produced a flap amplitude of 5.3° at an azimuth lead of 11.7°. This indicates 0.0228 in/deg follower motion per flap deflection.

Subsequent cams were built using 0.0242 in/deg follower motion per flap deflection. These included schedule 63 (12.5 cam), schedule 65 (17.5 cam) and schedule 50 (-20° cam) for noise reduction. Note that the previous schedule 50 cam was used during initial checkout in the wind tunnel, labeled as 22 cam. Two harmonic cams were built for vibration reduction as follows:

$$3P2A \text{ cam: } \delta_f = -2^\circ \cos 3\psi$$

$$5P4A \text{ cam: } \delta_f = -4^\circ \cos 5\psi$$

However, data could only be obtained with the 5/rev cam, because of a standpipe resonance near 3/rev. The azimuthal variation of flap deflection for all tested cam profiles is shown in Figures 10(a) and 10(b). Recall that the flap deflection is defined as positive with the trailing edge deflected down. Also, it should be noted that several conventions of cam phasing are used. Of these, the test data phase corresponds directly to the value read from the azimuth plate on top of the stand pipe.

Typical examples of trailing edge flap deflections over four rotor revolutions are shown in Figures 11a, b, c. For the -20° cam, data from all four flaps are shown to illustrate the variation in amplitudes from blade to blade. For the 2P6A and 5P4A cams, the data clearly shows that the azimuthally varying aerodynamic loading (at



an advance ratio of 0.3) causes a 1/rev modulation of the periodic flap angle motion amplitude.

#### **4.0 Data Acquisition**

The McDonnell Douglas Active Flap Rotor Test data acquisition and reduction system was used to perform the loads monitoring functions, to monitor test stand health, to acquire data from the test stand, to acquire data from the wind tunnel, to communicate with NASA acoustic data computer, and to store data. NASA Langley digitized and processed pressure and acoustic data. The McDonnell Douglas portion of the data acquisition system consisted of three HP-BASIC workstations. For each test condition, the rotor balance forces, blade parameters and rotor control positions were recorded for 40 revolutions at a rate of 64 points per revolution. During the 18 point acoustic traverses, the test stand data was acquired at all 18 points based on a predetermined option sent by the acoustic data computer. For each test condition, the tunnel speed, temperatures and pressures were read from the tunnel data computer.

#### **4.1 Hardware Description For Data Acquisition**

The McDonnell Douglas portion of the data acquisition system consisted of three HP workstations namely, the "Slave Computer", the "Master Computer", and the "Health Monitoring Computer". The operating system for each was HP-BASIC version 6.2.

The slave computer was a Motorola 68040 based HP 9000/382. This computer was used to perform all the data storage. It was configured with a 165 MByte LIF format internal SCSI hard disk, three external 110 MByte LIF format disk drives and one HP 9144 1/4 inch tape drive. The slave computer was equipped with an RS-232 port and two HP-IB cards. The RS-232 port was used at 19200 baud to send the derived  $C_l/\sigma$  and X parameters to the health monitor computer. The primary HP-IB port was used in non-active controller mode to communicate with the master computer to get the raw data parameters for loads monitoring and test point processing. The secondary HP-IB port was used to control the disk drives and the printer and to communicate with the NASA acoustic data acquisition computer. Since, HP BASIC does not support printer buffering, an Eventide buffer box was used to streamline the printing process. This buffer box allowed any printouts or graphics to quickly be dumped to the printer without holding up the computer. The slave computer information was displayed on a 17 inch color monitor.

The health monitoring computer was a Motorola 68030 based HP 9000/350 equipped with RS-232 and HP-IB interfaces. The health monitor was connected to an HP 3497A 20-channel scanner through the HP-IB card to acquire the test stand temperatures as well as the hydraulic pressure and oil pressure. The health monitor information was displayed on a 9 inch color touch screen monitor. The  $C_l/\sigma$  and X derived parameters were acquired from the slave computer through the RS-232 port. These parameters were displayed on the monitor, and used by the pilot

to fly the rotor. The disk drive and printer were also controlled through the HP-IB card.

The master computer was a Motorola 68040 based HP 9000/382. This computer was used primarily as a loads monitor. The loads monitored included the rotor balance parameters, blade parameters, and control actuator positions. The master computer was equipped with 3 GPIO cards, an RS-232 card, and an HP-IB card. The 3 GPIO cards were used to communicate with the HP 3852A Data Acquisition unit with 2 extends. The RS-232 port was used to communicate at 19200 baud with the wind tunnel data computer. The HP-IB card was used to send commands to the data acquisition unit and communicate with the slave computer. The master computer information was displayed on a 17 inch color monitor.

## 4.2 Software Description

The health monitor program was designed to provide the pilot and test team with a quick look of the test stand (not rotor) parameters. These parameters included 13 temperature sensing devices located on the hub, stand pipe, motor, and cooling water system. The health monitoring screen also displayed the hydraulic system low and high side pressures, the lubricating system pressure and the flow sensor. The health monitor was equipped with a touch screen which allowed for a quick, one touch screen dump of the display at any given time. The printout and continuous display included the test time and date. The health monitor screen was also used to display additional information for the pilot. While an additional monitor and faster bus (not RS-232) would have been preferable for this purpose, this solution was the best for the given resources. For this test the  $C_T/\sigma$  and X parameters were displayed on the health monitor screen.

The master computer program (BVIWHIRL14) primarily performed all of the data acquisition for the test stand, rotor and wind tunnel data computer. It was configured with icon menus and *softkey* menus. The icons which appeared on program status represent the assignments, rates, amplifier control, calibration, and loads monitor screens, respectively. The assignments screen was used to define the channels (72 in this case) with an instrument ID number, name and units. The load limits for each channel and warning limit were also included here. This screen was also used to change the active state of a channel as instrumentation was added or deleted from the configuration or if a channel were to malfunction. The rates screen was used to examine or change the rate (or E-U/volts) for each channel. The amplifier control screen was used to digitally control the programmable amplifier, but this feature was not used for this test. The calibration screen could be used to perform an RCAL for any of the channels or to simply examine the volts on each channel as opposed to its engineering units value. The screen could be used effectively as a voltmeter for every channel. The loads monitor screen was used to examine the steady and oscillatory values for each channel. In addition to the 72 raw channels, several derived quantities were displayed on this screen. For this test the quantities included,  $C_T/\sigma$ ,  $V/(\Omega \cdot R)$  (advance ratio), Mh, Vkts. The rotor speed was read by the optical encoder and displayed in both RPM and percent Nr. This screen had softkeys for recording

(setting) the non-rotating zero voltages. These zeros were used as the intercept when calculating the engineering unit values. Another softkey allowed a time history plot of the last revolution to be displayed for a selected channel. This plot was updated about every second. There were also softkeys for performance and stability. The performance softkey was used to acquire 40 revolutions of data and store it in memory. This feature was not used during actual testing. Instead, the slave computer sent a command to the master computer to send the results immediately to the slave computer. For stability data, a switch was used to change the data trigger from the one per revolution piper (used for performance data) to a voltage trigger keyed on the stop button in the dynamic control portion of the rotor control console. In this case, the stability data was stored in memory until the slave computer sent a request for it.

The slave computer program (BVISLAVE14) was used to control the communication between all of the computers as well as to archive, process, and print data. During testing, the slave computer was used primarily in the data monitor mode to review loads and to command data acquisition. The loads monitor mode was the only mode in which the  $C_f/\sigma$  and X values were transferred to the health monitor computer. There, values were only transferred when the slave computer wasn't busy performing other functions. When the rotor was not spinning, the slave computer was used to copy data to tape and to review the stored files with the time history plotting functions, the spectrum plotting functions and the moving block analysis function.

### **4.3 Typical Test Day Description**

The operation of the data acquisition and monitoring computer is described here for a typical test day. The beginning for each test day would start with a checkout of the health monitor to see if it was running properly. Usually the health monitor was running continuously. The next step was to ensure that both the master and slave computers were in the loads monitoring mode. The internal hard disk on the slave would be checked to see that it was clear of data files. The slave's internal hard disk could hold approximately 450 files or points. At this point, the data system was ready for testing and the test director was brought up to date on the status of the data system.

While the test director was going through the pre-test checklist, he would ask for the non-rotating zero to be taken. This was performed on the master computer where the zeros were set to the current voltage levels with blade #1 over the boom with zero shaft tilt. At the same time the "print volts" option on the slave would be used to print the current voltage levels. This was used to track any shifts in any of the parameters, particularly the balance channels. The test director would then call for rotor speed to be brought up. The data acquisition on the master computer would then be switched from static to dynamic mode. In static mode, screen updates occurred about every three seconds. This was due to a two second time-out while the program looked for the one per rev signal which was not present without rotor rotation. Once in dynamic mode, screen updates occurred about every second.

Once the rotor reached 100% RPM (1087 rpm), a dynamic zero (flat pitch 100% RPM) data point was taken. The test condition number for this point varied with the installed cam. The data point was acquired by selecting the GET&SEND PERFORM option on the slave computer. The data operator would then enter the test condition number. He would then confirm the point number. (The point number was unique for every data point. It began at 1 and ended at 4886 for this test.) He would then type in the test point description which would always include the cam configuration name and often included the RPM,  $Ct/\sigma$ , advance ratio and shaft angle. Once the data operator entered these five pieces of information, the slave would instantly command the master to acquire the wind tunnel condition, take 40 revolutions of rotor data, and to return control to the slave. When the results returned, the operator would have the choice of whether or not to save the data. After saving the raw data, the derived parameters would be calculated and printed on the line printer. At this point the slave computer would return to monitoring the loads.

For acoustic data points the procedure was similar. Once the rotor and wind tunnel were at the specified test condition, the test director would instruct the MDHS data engineer to begin the traverse process. The data engineer would first select the SETUP AUTOMATE option, then enter the test condition number, first point number and test point description. At this point the softkeys would turn from white to blue, indicating that IEEE-488 communication with address 825 (the acoustic VAX) would be allowed. The data engineer would then use the headset to tell the NASA data engineer that the data system was ready to take data and provide him with the data storage option. There were two data storage options for acoustic data. With option 1, the NASA computer commanded the MDHS computer to store the raw data disk and to print out a summary for each of the 18 points along the traverse path. With option 2, the NASA computer would instruct the MDHS computer to take all 18 points but only to save the data and printout the results for the first and 18th points. After receiving permission from the MDHS data engineer, the NASA data engineer would then begin the traverse process. The acoustic data computer would first ask the slave computer for the position for the hub in the tunnel. This was used to calculate the initial traverse position. Next, the acoustic data computer would command a data point to be taken. While the MDHS computer was getting the performance data, the acoustic data computer was acquiring data from the microphones and pressure transducers. Once the MDHS master computer received the data from the voltmeters, it would send a "1" back to the slave indicating that it had finished acquiring the data. The slave would then send the point number to the acoustic data computer. This action informed the acoustic data computer that it could now move the traverse and allowed it to open a file with the point number in the file name. The master would then send the data to the slave and the slave would calculate the derived parameters and return to the load monitoring mode. Once the acoustic data computer had finished storing its data to disk, it would send a command to the slave to send the results. The slave would then send a specified list of derived parameters to the acoustic data computer and return to the loads monitoring mode. This process would be repeated until the traverse was completed, at which time the acoustic data computer would tell the slave that the traverse was done. The slave would then disable communications with the acoustic data computer and the softkeys would return from blue to white.

The data acquisition process during the traverse was automated. Once the traverse was initiated, no further actions were required by the data engineer. Each traverse required seven to eight minutes. If at any time during the traverse, a loads or mechanical problem developed, the MDHS data engineer could select the QUIT AUTOMATE softkey which would return the softkeys to white, block out communications with the acoustic data computer, and allow both the master and slave computers to function in the loads monitoring mode without interruption. This allowed the test director and pilot to monitor parameters such as thrust,  $Ct/\sigma$  real time, while reacting to any emergency that might arise.

At the end of each test run, another data point would be taken at 100% RPM and flat pitch. The rotor speed would then be brought to zero. At this time a non-rotating data point would be taken, stored and printed. The current voltages would also be printed. The rotating data point and zeros were compared with previous point to check for zero drift or any other possible problems.

After the data acquisition run was completed, the slave computer would be put into archive mode. The first screen in the archive mode lists the number of files stored on the internal hard disk. The data engineer would place a 1/4-inch tape into the slave's tape drive. If it was a new tape, he would initialize it. With this drive, 175 data points would fit on each of the 65 Mb tapes. Once the tape was ready, he would select DISK TO TAPE action which would copy every data file on the hard disk to the 1/4-inch tape. If there were more than 175 files, he would be prompted to eject the tape, install a new one, and the copy would continue. This tape drive was one of the weakest links in the data system due to its slow data storage speed. It required four minutes to copy one file to tape, so to fill a tape required 11.5 hours. This extended duration was due to the tape winding and rewinding in order to write to the header at the beginning of the tape then append the data to the end of the tape. With 12 hours of scheduled testing each day, little time was available for data archiving. In practice, this was not a problem. When the copy to tape was complete, the tape was ejected and write locked. Then all of the files on the internal hard disk were copied to one of the three external hard disks. This operation required 10 seconds per file. This was particularly important if time constraints precluded a full archiving of all files on disk. The files which were not archived could be retrieved from the external hard disks and saved during the next archive operation. The external hard driver allowed the files to be recalled once the data was purged from the internal disk. After this operation, the files were then copied to the transfer disk (a 330 Mb HFS disk which is easily removable from the computer). This copy required 20 seconds per file. The transfer disk was then disconnected from the slave computer, mounted on an HP UNIX workstation (HP 9000/360 running HP-UX 9.0). The raw data files were then transferred over the ethernet network to an HP workstation in Mesa (HPR07, an HP 9000/735) via ftp (file transfer protocol). The network speed varied with type of data, but typically it required from 30-60 seconds per file to transfer them to Mesa. Once the raw data was on disk in Mesa, it was copied to 4mm tape in tar format. Then the data was loaded into the ASAP database denoted at BVINASA. The BVINASA database included the recorded channels as well as the derived parameters (recalculated on the HP in Mesa with the latest code corrections).

Once it was confirmed that the files transferred to Mesa were copied without error, the data on the slave's internal hard disk was purged, leaving only the data copied to the external disks. The data system was now ready for testing again.

During the many hours required to complete the two backups of the test data, the master computer and the health monitor computer were available to debug instrumentation problems, calibrate channels, and/or make changes to the software.

#### **4.4 Acoustic Data Acquisition/Reduction**

The acoustic data acquisition and reduction hardware was provided by NASA Langley, and coupled to the McDonnell Douglas Active Flap Rotor Test data acquisition and reduction system. Three figures are included to facilitate understanding of the involved processes and equipment. Figure 12 illustrates the major processes controlled by the host and remote computers. Figure 13 shows the major instrumentation and bus connections to facilitate the defined processes. Figure 14 is an overall data and process flow schematic.

As depicted in Figure 12, the control processes can be partitioned into two major categories, one to control the data acquisition processes and one to control digital signal processing. The major acquisition processes include real-time data acquisition and temporary data storage. The major signal processing areas include analytical processing, permanent data storage and backup, and data display. Separate computers controlled the acquisition and signal processing operations. The computers and hard disks were clustered for quick data file access, computations, and display. This also facilitated sharing of peripherals, such as digital tape drives and printers.

##### **4.4.1 Real-Time Data Acquisition**

Again referring to Figure 12, the real-time data acquisition control software was comprised of five modules that controlled the microphone and rotor blade pressure transducer (from the eight Kulite channels) data digitization, the microphone traverse, and the tunnel environment and rotor performance data transfer from the MDHS computer. These modules were all coupled together in an outer loop that allowed menu selection of various data acquisition types. The software then coupled the appropriate modules together to perform the desired function.

##### **4.4.1.1 Microphone and Kulite Pressure Transducer Data**

Sixteen analog microphones (B&K 4134 1/2 inch condenser type corrected for pressure response, with nose cone) were mounted on a traverse and systematically translated to pre-determined data acquisition stations. The microphones moved from upstream of the rotor to downstream of the rotor acquiring data at 17 positions as can be seen in Figure 15. Each microphone channel, consisting of a microphone cartridge, preamplifier, and power supply, was

directly wired to an amplifier/filter unit for signal conditioning, which was then connected to a 16-bit digitizer system. During rotor data acquisition, data were digitized using an external clock provided by a 1024/rev signal originating from the rotor head. Data acquired when the rotor hub was not rotating, such as microphone calibrations, were digitized using an internal clock. Continuous analog data were simultaneously digitized from all channels into discrete data which were entered into 8-Mbyte memory resident on each channel. Each channel could thus contain up to 4 million data samples. Memory contents were directly transferred to control computer memory via a high-speed parallel interface. In addition to the microphone data, the rotor 1/rev signal was also digitized by the acoustic data acquisition system. All of the digitized data were then written to magnetic disk as a single file of 17 channels (16 microphones plus the 1/rev) of dynamic data, along with rotor and tunnel information for each traverse location.

As described previously, one of the rotor blades was outfitted with eight Kulite pressure transducers. At the beginning of each microphone traverse sweep, data from these eight transducers were substituted for the eight retreating side microphone channels by an eight-channel software controllable data switch. Blade pressure data was sampled at the same frequency as acoustic data and processed in the same manner. Filter settings for the transducers were the same as acoustic channels. Binary count data were written into the same file with the advancing side acoustic data. A flag in the file header record indicates that channels 9-16 are Kulite channels.

The different data categories include microphone and Kulite blade surface pressure calibrations, tunnel background and reflected noise checks, and test point data taken with the traverse in operation. These categories were selectable from a main menu inside the data acquisition software. For each menu item, the data acquisition software would couple the appropriate control modules together to perform the selected operation.

#### **4.4.1.1.1 Transducer Calibrations**

Microphone calibrations were performed each day both before and after testing using a standard B&K 4220 pistonphone producing a pure tone at a frequency of 250 Hz and an amplitude of 124 dB. Calibration signals were digitized for 5 seconds at a rate of 20000 Hz to measure system amplitude response. The internal 6 MHz clock of the data acquisition computer was stepped down to generate the data acquisition clock signal. The signal conditioning filters were configured as for test point data acquisition, with settings of AC-coupled low-pass filters set at 10 kHz during the microphone calibrations. Spectral plots of channel amplitude were displayed on the data processing computer after each calibration to insure proper operation of all microphone data channels. In addition, calibration data files containing filter setting information and channel mean and standard deviation statistics were written to a file for use by the data acquisition system to convert raw digital counts into engineering units. This eliminated the intermediate step of converting raw digital counts to voltages, and then converting the voltages to engineering units.

Kulite channel calibration was performed by applying a series of known static pressures to each port, and acquiring data in the same way as for the microphone calibrations, with the exception that the filters were DC-coupled. A slope-intercept linear relation between pressure and digital counts was used to convert the Kulite signals into engineering units.

#### **4.4.1.1.2 Background and Reflected Noise Checks**

Tunnel background noise was measured at each of the speeds of interest with the rotor operating without blades. Since the hub was rotating, all filter settings and sample rates were the same as for normal rotor data acquisition. For reflection testing, blasting caps were mounted to a bar extending from the rotor hub in the nominal position of expected BVI. Data were acquired at 100 kHz sample rate for 5 seconds to insure that the blast and all of its reflections were captured.

#### **4.4.1.1.3 Test Point Data**

Sixteen channels of microphone data and one channel of 1/rev data were acquired for the various rotor operating conditions and flap configurations. For each condition, a complete microphone traverse sweep defined the noise field in a plane below the rotor system. Seventeen acoustic data sampling stations (shown in figure 15) defined where the traverse system was stopped, enabling data recording for approximately 32 rotor revolutions (about 1.8 seconds). The procedural order of events was as follows:

1. Advance traverse to full forward position, if not already there.
2. Acquire data at full forward position from all eight of the Kulite transducers and the eight microphones on the advancing side of the rotor and write data to file. Begin processing of that data on data processing computer.
3. Take data at full forward position using all 16 microphones. As soon as data are successfully acquired, move traverse to next position. Write data to file. Begin processing of that data.
4. Receive traverse position feedback from indexer. Verify correct position by comparison with station position table.
5. Repeat acquisition, move, data write, data processing, and verify process to last station.
6. Move traverse full forward to repeat the acquisition process for the next test point, while the rotor was trimmed for the next test condition.

Filter gain settings were adjusted to prevent signal clipping. A 4096/rev counter from the rotor, divided down to 1024/rev, served as an external clock for the digitizer. At a nominal rotor speed of 1087 RPM, this provided a sample rate of 18551 Hz.



#### **4.4.1.2 Microphone Traverse**

The microphone traverse system shown in Figure 13, which is comprised of traverse rails, 4 Compumotor single-axis indexer/drives (2 floor rails and 2 side rails), microphone wings, and interfaces, were software controlled by the data acquisition control computer. The standard RS-232C serial interface was used between the control computer and Compumotor indexer. Three basic commands will define two speeds (rack return and acquisition rates), desired position, and actual position. The step drives were commanded to stop at each acquisition point to allow the control computer to write digitized acoustic data to disk. A programmed sequence of instructions automated the positioning of the microphone wings at the known locations along the sweep shown in Figure 15.

#### **4.4.1.3 Wind Tunnel and Rotor Data**

Rotor and wind tunnel state data were all acquired via IEEE-488 interface from MDHS for each test point. Tunnel data were first acquired by MDHS from the MODCOMP, and then packaged with the rotor performance data for that test point for transfer to the acoustic data acquisition computer. These data were then written with that transducer data into one combined file for the test point.

### **4.4.2 Acoustic and Pressure Data Reduction**

#### **4.4.2.1 Analytical Processing**

As indicated in Figures 13 and 14, all analytical processing was accomplished on the acoustic data processing computer, which was clustered with the acoustic data acquisition computer. The data acquisition computer notified the data processing computer when data files were available for analytical processing.

##### **4.4.2.1.1 Engineering Units Conversion**

The 18-channel unformatted data files were read to input test point information (from the header record) and binary acoustic and/or rotor blade surface pressure data. The conversion process used digital counts data from the acoustic data files and channel calibration means and standard deviations from the calibration files. Converted pressure outputs were in units of Pascals for both microphone and Kulite data. The 1/rev signal channel did not require conversion, since it did not actually have any engineering value other than volts, and was only used to examine the stability of the rotor speed in any case.

#### **4.4.2.1.2 Ensemble Averages**

Time history averaging occurred over 30 rotor revolutions on an azimuthally dependent basis. This produced an average time history of 1024 points representing one complete rotor cycle. Spectral averaging also used the same 30 rotor revolutions that were Fast Fourier transformed and averaged across like frequency bins to produce a single spectral estimate of assumed Chi-square distribution with  $N=30$ , 60 degrees of freedom, and  $\pm 1.2$  dB confidence interval at 80% confidence level. The Chi-square distribution applies to non-tonal (broadband) data; data associated with tones are non-Chi-square distributed and thus do not ascribe to these confidence levels.

#### **4.4.2.1.3 BVI Filtering**

Integration of the narrowband spectra of all frequency bins from the 5th to 40th harmonics of the blade passage frequency were used to obtain a metric referred to hereafter as BVISPL. The BVISPL were used to compare the effectiveness of different flap motions in reducing BVI noise. The BVISPL were used to generate contour plots that displayed trends of both BVI amplitude and directivity for each rotor operating condition.

In order to focus on changes to the harmonic noise only, a second version of the BVISPL metric was also computed. Here, a narrowband spectrum was computed from each average time history, and that spectrum was then integrated over the same range as before. This permitted an examination of changes to the BVI noise, without including broadband noise increases due to the flap deflection. These are the values that are primarily used in this report.

#### **4.4.2.1.4 Background and Reflected Signals**

Data input and engineering units conversion were the same as for test point data. Individual microphone narrow band spectral analyses for each free stream velocity were computed and reviewed. Data from reflection testing were converted to engineering units and displayed as instantaneous time histories, to allow examination of the acoustic character of the test chamber. Relative time delays between direct and reflected signals were used to estimate the location of reflective surfaces. These data caused application of additional acoustic foam on the model when a model surface was indicated to be a substantial source of reflections. Examination of the background noise data, when compared with measured rotor data, showed that there was a significant signal-noise ratio except at the lowest rotor frequencies, when the rotor background noise began to approach the level of the rotor signal.

#### **4.4.2.2 Data Display**

Calibration data for microphones were displayed on the data processing computer terminal as soon as acquired. During test point data acquisition, min-max, average time history, and narrowband spectra data plots were generated on the data processing computer for display at the terminal. These plot files were also stored on hard disk for later display or printing. At the end of each traverse, a single color contour plot of BVISPL as a function of spatial position was generated and printed to a color printer. The combination of stored time history and spectrum line plots, in conjunction with the printed color contours, allowed quick on-line examination of all channels.

#### **4.4.2.3 Permanent Data Storage and Backup**

Data file storage on optical disks and 8-mm cassette tapes was completed daily during either lulls in the testing, or during first shift by a delayed batch process. Each 8-mm tape could hold approximately 2.1 Gbytes and each optical disk 594 Mbytes. All raw and processed data were stored in this manner, so all data are redundantly preserved.

### **4.5 Dynamic Data Acquisition**

In order to examine rotor dynamic stability, the hydraulically driven swashplate was used to excite rotor modes. Collective excitation was accomplished by a vertical sinusoidal excitation of the swashplate. Inplane mode excitation was accomplished by nutating the swashplate at the progressing or regressing mode frequencies. The basic performance data acquisition program was used with the exception of the trigger. Once the excitation level had been set to excite the blade mode with sufficient amplitude, the computer trigger was armed. When the excitation was cut off, the computer triggered the data acquisition program and recorded the transients over 40 rotor revolutions. The shake test and dynamic data are described in detail in Section 6.1 and 6.2.

## **5.0 Test Procedures and Conduct**

The wind tunnel test was conducted at the NASA Langley 14- by 22-Foot Subsonic Tunnel. The test stand was attached to Cart Number One in the front bay of the wind tunnel test section. The wind tunnel was operated in the open jet configuration with no side walls or top to the test section. The floor of the test section was lowered by two feet and acoustic treatment installed. Acoustic treatment was applied to the tunnel area around the test section. A traversing rake with microphones was installed to map the acoustic field below, and both upstream and downstream, of the rotor. The array of acoustic microphone data acquisition locations is shown in Figure 15. The smoke generator and traverse system located in the tunnel settling chamber were used for flow visualization to ensure that the rotor did not ingest the shear layer at lower tunnel speeds. Following shake tests of the rotor test stand (Section 6.1) and checkout of the motor control, rotor control

panel, dynamic control panel and test health monitoring system, the blades with active flaps were installed for the wind tunnel test. A complete instrumentation and data system verification and checkout were conducted. Oscillographs, oscilloscopes and digital monitors were used to monitor rotor parameters and to assure safe operation of the test.

The wind tunnel test lasted six weeks. The first two weeks were used to perform a brief shake test, and reinstall the acoustic treatment and acoustic traverse in the wind tunnel. Set up of test stand and instrumentation proceeded on a double shift operation during installation of the acoustic treatment. Four weeks of double shift operation were used for rotor checkout and testing. Before conducting the wind tunnel test, a checkout of the motor, controls, test stand, instrumentation, rotor system, and data acquisition system, was needed. The checkout proceeded in steps to verify the operation of the system.

### **5.1 Installation and Checkout**

The test stand was installed in wind tunnel. Power, lubrication, instrumentation and cooling lines were routed and secured. A crane was used to lift the model, in sections, into the tunnel. The model was assembled on the bayonet mount in the tunnel section. The hub was reassembled by MDHS personnel following the nondestructive testing inspection of the spiders by NASA Langley personnel.

A shake test of the test stand and hub was performed. A detailed description of the shake test can be found in section 6.1. Stand natural frequencies and damping were measured so that known stand resonances could be avoided. Dynamics engineers studied stand natural frequencies and rotor modes, identified resonances and ensured aeromechanical stability. Ground resonance stability characteristics were determined based on CAMRAD/JA results from isolated blade properties, and shake test results.

The shake test attachment fittings were removed. The blades and cable control turnbuckles were not installed. The null cam was installed and cam followers were left in place. The rotating system instrumentation was installed and its operation verified. The control system rigging was checked. Control system clearances were checked as well. The rotor control console operation, instrumentation and dynamic control console operation were verified.

Checks of the calibrations on the control system, motion indicators, drive system and rotor balance measurements were performed. The check calibration of the balance revealed that the balance normal force was not responding according to previous calibrations. Check loads were reapplied for three balance forces and two balance moments. The data was reduced, and a new balance calibration matrix derived. The corrected balance calibration matrix and a description of the balance calibration procedures can be found in Appendix A.

The shaft angle was swept from  $-15^{\circ}$  to  $15^{\circ}$  and clearances for model hardware and instrumentation checked. The precise position of the center of the hub was measured during the shaft angle sweep with surveying instruments. A table of

height (Z) corrections for shaft angle was developed to maintain the hub on position at the centerline of the tunnel. NASA Langley sting operators applied these corrections to the shaft for every shaft angle required during the test. The measurements of hub position were performed again with the shaft height (Z) corrections applied. The fore and aft position (x) versus shaft angle were recorded. This data was used to correct the acoustic traverse positions to maintain the same relationship between the microphone array and the rotor hub for every shaft angle.

The motor and test stand were operated to 110% nominal RPM to ensure correct operation. The hub imbalance was determined, and the rotor balanced to 15 in-grams. The HP3562 spectrum analyzer was used to develop a balance chart for the rotor. With the RPM stabilized, the balance phase and magnitude data were taken from the HP3562 analyzer. The magnitude was derived from the balance pitch moment reading at 1/rev rotational frequency. A known weight of approximately 40 grams was added to the damper bracket for blade number 1. The measurement was repeated. From the baseline delta weight balance and phase data, a correction delta weight and azimuth angle were calculated. This, in general, required that weight be added to two adjacent blades. If the imbalance was greater than 2000 in-grams, additional delta weights were generated to bring the blades into balance.

Occasionally, an alternative approach was used to simplify this procedure. It was assumed that the magnitude change was the same for all blades and that the phase shift was 90° difference between the adjacent blades for a given delta weight. This approach only required the addition of a delta weight once to any one of blades instead of to all blades.

On 14 February with a bare hub, the motor drive control was exercised up to 110 % RPM (1195 RPM) and the control system operated through 100% of its collective and cyclic pitch range. Collective pitch was exercised through the range 0° to 8.0° and lateral and longitudinal cyclic from 0° to 2.0°.

The data acquisition system operation was verified. Performance data on test stand and rotor were acquired with check loads. The digital data bus between the Langley wind tunnel computers and the MDHS data acquisition system was exercised and correct operation verified. Data with the acoustic microphone array was acquired. The digital data bus from the acoustic and pressure data acquisition system was exercised and correct operation verified.

Acoustically treated test stand fairings were then installed. NASA Langley Acoustics Division personnel performed a bang test to quantify the acoustic properties of the test section and model. Any "hard spots" identified which produced distinct echoes were treated with acoustic foam. A final bang test was performed to document and quantify all acoustic reflections.

## **5.2 Background Noise**

Background noise runs were performed on 16 February 1994. Background noise data was taken at tunnel speeds of  $m = 0, 0.10, 0.15, \text{ and } 0.20$ . For each tunnel

speed, an acoustic traverse was performed at shaft angles of  $\alpha_s = 0, 5.0, 10.0, -5.0, -10.0$  degrees.

### **5.3 Weight Tares**

The blades were installed and weight tares were acquired on 18 February 1994. The shaft angle was run throughout the range  $+13.0^\circ$  to  $-13.0^\circ$  in  $2.0^\circ$  increments. The rotor was not turning for these tare runs. Balance data was acquired at each point and at  $0^\circ$  shaft tilt. The blades were removed and weight tare data acquired for the bare hub only with the same shaft angles.

### **5.4 Aerodynamic Tares**

Rotor balance data were corrected for aero tares. These are subtracted from the rotor balance measurements to calculate the force due exclusively to the rotor blades. Aero tare runs were performed with the rotor at 100% RPM on 18 February without the blades. Performance data for the rotor test stand were acquired for a range of tunnel speed ( $\mu$ ) and shaft angles ( $\alpha_s$ ). The collective pitch was set to  $0.0^\circ$  ( $\theta_c=0.0^\circ$ ). Lateral and longitudinal cyclic were set to zero ( $A_1=0, B_1=0$ ). A sweep of shaft angles was also performed with the tunnel off and the rotor at 100% RPM. Shaft angle was swept from  $-13$  to  $+13^\circ$  in  $2^\circ$  increments ( $\alpha_s = 13, -11, -9, -7, -5, -3, -1, 0, 1, 3, 5, 7, 9, 11, 13$  degrees). It should be noted that the shaft angles used here are corrected values. The shaft angles were corrected for open jet effects using the method of Heyson [22]. Typical corrections were on the order of 0.5 degrees for the cases tested. The same shaft angle sweep was performed for tunnel speeds ranging from 69 ft/sec to 241 ft/sec, in 35 ft/sec increments ( $\mu = .10, .15, .20, .25, .30, .35$ ). The performance data were curve fit and used as tare values for measured rotor performance.

The cable control turnbuckles and blades were installed. The active flaps were set to the neutral position. The blade strain and pressure instrumentation were connected and operation of this instrumentation verified. The control system calibration with blade pitch measurements at 75% radius was rechecked. Static check loads were placed on the blades and the strain gauge calibrations verified.

Rotating aerodynamic tares were repeated on 22 February for the highest two tunnel velocities,  $\mu = .30$ , and  $.35$ . At zero tunnel speed, the rotor was run up to 100% RPM incrementally. Performance data was acquired at 544, 652, 870, 978, 1033, and 1087 RPM (50%, 60%, 80%, 90%, 95%, and 100%). At  $\mu = .05, .10, .15, .20$ , and  $.25$ , tare data was acquired at a shaft angle of zero. At  $\mu = .30$  and  $.35$ , the shaft angle was swept from  $-13$  to  $+13^\circ$  in  $2^\circ$  increments ( $\alpha_s = -13, -11, -9, -7, -5, -3, -1, 0, 1, 3, 5, 7, 9, 11, 13$  degrees). As mentioned earlier, the shaft angles used here are the corrected values. The performance data were curve fit and used as tare values for measured rotor performance.

## **5.5 Track and Balance**

On 22 February the rotor was run up to 100% RPM incrementally with blades on. The null cam, with no flap deflection, was installed. The rotor imbalance was measured and a rotor balance performed as described in Section 5.0. Performance data was acquired at 544, 652, 870, 978, 1033, 1087, and 1120 RPM (50%, 60%, 80%, 90%, 95%, 100%, and 103%). Stability data was not taken as the dynamics engineer had determined that stability was high based on the results of the shake test. Rotor track and balance runs were integrated with the performance testing.

The rotor was tracked during the run up. The blade tips were monitored on the video camera using a four per rev strobe. Both the track and balance needed to be within acceptable limits before increasing operational rotor speed. The final track and balance were done at 100% RPM (1087) with the track procedure completed first followed by the balance procedure. Below 100% RPM corrections to track and balance were made only if a blade was out of track by more than .7 inches or the blade imbalance was greater than 2000 in-grams. These units were used as the balance mass scale was calibrated in grams, and the mechanic's ruler was calibrated in inches.

At 100% rotor speed with the collective at flat pitch and with neutral cyclic, the rotor was tracked to within 0.1 inches and balanced to within 15 in-grams. Track and balance were checked at other collective pitch positions and tunnel speeds as the test envelope was expanded.

Once the rotor was tracked and balanced at 100% RPM, and a collective and cyclic sweep was performed, blade motion indicators were check calibrated. Flap motion indicators were calibrated over a range of  $-8^{\circ}$  to  $+8^{\circ}$ . Lag motion indicators were calibrated over a range of  $-5^{\circ}$  to  $5^{\circ}$ . The lag dampers were disconnected for this calibration. Check loads were applied to the rotor to verify the strain gauge calibrations.

Rotor speed sweeps, collective sweeps and cyclic sweeps were repeated on 24 February.

## **5.6 Baseline Test Matrix**

The rotor was tested in forward flight for the first time on 25 February. Data was acquired for the baseline test matrix with the null cam. For each test point, the rotor was established on the test condition defined by the parameters  $C_l/\sigma$ ,  $M_h$ ,  $\mu$ , and in some cases, shaft angle. Baseline data was taken for the performance test conditions, dynamics test conditions, and acoustic test conditions. These baseline data were acquired on 25 and 26 February. A sweep of rotor speed, collective pitch and cyclic pitch was performed for repeatability checks with prior runs.

The 12.125 foot diameter Active Flap Rotor was a large rotor for the 14- by 22-Foot Subsonic Tunnel open jet test section. At low tunnel speeds and advance ratios ( $m$ ) there was a significant possibility that the tunnel shear layer could be ingested by the rotor. Researchers at the US Army AFDD performed calculations that

suggested that this would not occur at the lowest advance ratio test point ( $C_t/\sigma = 0.0762$ ,  $\mu = 0.15$ ). In order to verify that shear layer was not significantly influenced by the rotor inflow, a flow visualization study was performed. The smoke generation system, located in the settling chamber upstream of the test section, was used to study this phenomena. Smoke streamlines were generated along the edge of the test section near the shear layer. Video cameras were used to monitor the smoke streamlines in the test section. Their behavior throughout the test envelope was used to judge whether the rotor was ingesting the shear layer. The flow visualization studies showed no shear layer ingestion throughout the test envelope.

Performance data was taken in forward flight at fixed shaft angles predicted by analysis. Since the normal forces required to produce the target propulsive force,  $X$ , were smaller than could be read by the balance, the shaft angle required for each test point was determined from theory. When the rotor was flown at velocities of over  $\mu = .20$ , the normal force measurements were large enough to produce reliable  $X$  measurements. The performance baseline data test matrix is shown in Table 1.

Table 1. Baseline Performance Test Matrix

$\mu$	$X$	$\alpha$	$C_t/\sigma$	$C_t$
0.15	0.12	-1.89	0.0653	0.0060
		-1.71	0.0762	0.0070
		-1.61	0.0871	0.0080
0.20	0.12	-3.24	0.0653	0.0060
		-2.72	0.0871	0.0080
0.25	0.12	-5.03	0.0653	0.0060
		-4.19	0.0871	0.0080
0.30	0.12	-7.38	0.0653	0.0060
		-6.12	0.0871	0.0080

The performance runs raised concerns over the calibration of the balance. A check calibration of the balance axial force was performed up to 200 lbs in 50 lbs increments. The data fit with previous calibrations.

For acoustic data, the microphone rake traverse was located in its most forward, upstream position. The shaft was then swept slowly back from  $\alpha = 0.0^\circ$  to  $\alpha = 10.0^\circ$  incrementally to aid in locating the shaft angle corresponding to maximum BVI noise. Sweeps of the acoustic traverse were performed for each discrete shaft angle. The shaft angles for maximum BVI noise could then be identified for each of the three acoustic test conditions. During the acoustic traverse, the model pilot maintained constant  $C_t/\sigma$ , while minimizing blade flapping. No adjustments in rotor speed to maintain  $M_h$  were required while the sweeps were completed.

Once the shaft angle for maximum BVI noise was determined, four data points bracketing this shaft angle were acquired. Data points were taken at shaft angles of the maximum BVI angle  $\pm 1$  degree and  $\pm 2$  degrees. At each test condition, the rotor was flown in trimmed condition by the pilot with first harmonic flapping,  $b_1$  and



$a_1$  minimized. The acoustic rake moved through the entire traverse range, acquiring data to create a "carpet plot" of acoustic pressures. Each traverse took up to eight minutes. During this time the pilot and test director carefully noted the control system position and first harmonic flapping. If the rotor drifted off trim or test condition due to a change in the tunnel conditions, the data point was repeated. In general, the rotor conditions and tunnel conditions remained stable for all of the acoustic sweeps.

The exploratory test matrix for acoustic data was performed with the baseline rotor with the null, or zero flap deflection cam. All points were flown with  $M_h = 0.618$ . The test points for the baseline configuration are shown in Table 2.

Table 2. Baseline Acoustic Test Matrix

$\mu$	$\alpha$	$C_t/\sigma$	$C_t$
0.15	3.0, 4.0, 5.0, 6.0, 7.0	0.0762	0.007
0.20	2.0, 3.0, 4.0, 5.0, 6.0	0.0762	0.007
0.20	2.5, 3.5, 4.5, 5.5, 6.5	0.0871	0.008

### 5.7. -12.5 Degree Acoustic Cam

The first BVI noise reduction cam tested was the -12.5° deflection cam, Schedule 63). Data was acquired for this configuration on 28 February, 1 March, and 2 March. In order to check out the rotor operation, and to provide a set of comparison data to this and other configurations, a collective sweep and cyclic sweep were performed in hover. The rotor was tested at each of the three acoustic test conditions with a set of shaft angles bracketing the maximum BVI points. For the first set of points the azimuth position of the cam was set to zero. Table 3 depicts the test matrix acquired.

Table 3. Test Matrix For -12.5° Cam With 0° Azimuth

$\mu$	$\alpha$	$C_t/\sigma$	$C_t$
0.15	3.0, 4.0, 5.0, 6.0, 7.0	0.0762	0.007
0.20	2.0, 3.0, 4.0, 5.0, 6.0	0.0762	0.007
0.20	2.5, 3.5, 4.5, 5.5, 6.5, 7.5, 8.5	0.0871	0.008

Two additional shaft angles 7.5°, and 8.5° were added to the shaft sweep at  $\mu = 0.20$ ,  $C_t/\sigma = 0.0871$  by the acoustics engineers to examine the effect of extreme aft shaft angles on BVI noise. The azimuth of the cam was moved to -10.0° and acoustic sweeps performed at the three test conditions. Intermediate shaft angles in the sweep were eliminated by the acoustics engineers. Table 4 depicts the test matrix for the -12.5° Cam With -10° Azimuth.

Table 4. Test Matrix For -12.5° Cam With -10° Azimuth

$\mu$	$\alpha$	$C_t/\sigma$	$C_t$
0.15	3.0, 5.0, 7.0	0.0762	0.007
0.20	2.0, 4.0, 6.0	0.0762	0.007
0.20	2.5, 4.5, 6.5	0.0871	0.008

The next azimuth tested for the Schedule 63 cam was +10.0°. A full matrix of shaft angle sweeps was performed for this configuration. The data points acquired are shown in Table 5.

Table 5. Test Matrix For -12.5° Cam With +10° Azimuth

$\mu$	$\alpha$	$C_t/\sigma$	$C_t$
0.15	3.0, 4.0, 5.0, 6.0, 7.0	0.0762	0.007
0.20	2.0, 3.0, 4.0, 5.0, 6.0	0.0762	0.007
0.20	2.5, 3.5, 4.5, 5.5, 6.5	0.0871	0.008

The final Schedule 63 azimuth position tested was -20.0°. Intermediate shaft angles in the sweep were eliminated by the acoustics engineers. The test matrix acquired is shown in Table 6 below.

Table 6. Test Matrix For -12.5° Cam With +20° Azimuth

$\mu$	$\alpha$	$C_t/\sigma$	$C_t$
0.15	3.0, 5.0, 7.0	0.0762	0.007
0.20	2.0, 4.0, 6.0	0.0762	0.007
0.20	2.5, 4.5, 6.5	0.0871	0.008

### 5.8 -17.5 Degree Acoustics Cam

The -17.5° acoustics cam, Schedule 65, was mounted on the model. The first azimuth tested was -20.0°. On 3 March, a collective and cyclic sweep was performed in hover to check flap operation, track, and to compare with hover data from other configurations. Acoustic sweeps were performed at this azimuth to compare with the baseline configuration. Table 7 depicts the data points acquired.

Table 7. Test Matrix For -17.5° Cam With -20° Azimuth

$\mu$	$\alpha$	$C_t/\sigma$	$C_t$
0.15	3.0, 4.0, 5.0, 6.0, 7.0	0.0762	0.007
0.20	2.0, 3.0, 4.0, 5.0, 6.0	0.0762	0.007
0.20	2.5, 3.5, 4.5, 5.5, 6.5	0.0871	0.008

The azimuth position of the cam was then moved back to 0.0° and the test matrix repeated, see Table 8.

Table 8. Test Matrix For -17.5° Cam With 0° Azimuth

$\mu$	$\alpha$	$C_t/\sigma$	$C_t$
0.15	3.0, 4.0, 5.0, 6.0, 7.0	0.0762	0.007
0.20	2.0, 3.0, 4.0, 5.0, 6.0	0.0762	0.007
0.20	2.5, 3.5, 4.5, 5.5, 6.5	0.0871	0.008

Flow visualization with smoke was performed during the first three test points to examine the wake structure. These runs were saved on video tape. Test

conditions 3905, 3906, and 3907, at  $\mu = 0.20$ ,  $C_T/\sigma = .0762$ ,  $C_T = 0070$  and  $\alpha = 2.0$ , 3.0, and 4.0 were examined with flow visualization as well as the stand acoustic sweeps.

Considering the trends observed in noise reduction with the two previous cam positions, an azimuth position of  $-5.0^\circ$  was chosen for the next data points. In order to minimize test time at this azimuth, intermediate shaft angles were eliminated from the data points. Table 9 illustrates the matrix of test points was acquired .

Table 9. Test Matrix For  $-17.5^\circ$  Cam With  $-5^\circ$  Azimuth

$\mu$	$\alpha$	$C_T/\sigma$	$C_T$
0.15	3.0, 5.0, 7.0	0.0762	0.007
0.20	2.0, 4.0, 6.0	0.0762	0.007
0.20	2.5, 4.5, 6.5	0.0871	0.008

The search for the best cam azimuth for noise reduction was continued and the cam moved to an azimuth position of  $-10.0^\circ$ . A limited test matrix, similar to that shown in Table 9 was acquired.

On 4 March, during the acquisition of test condition, 3920, at  $\mu = 0.20$ ,  $C_T/\sigma = 0.0762$ ,  $C_T = 0070$  and  $\alpha = 2.0$ , the flap actuation cable on blade station two failed. A performance point, test condition 3245 was taken after the tunnel velocity was brought down to zero, while the rotor was turning, to quantify rotor loads with a failed flap actuation cable. At this point the cables had run without a failure for 36 hours of data acquisition. Oscillatory loads on pitch link 4 continued to grow during these runs. The rod ends on pitch link 4 showed higher wear than the other rod ends, and were replaced.

Pitch link four showed increasingly high oscillatory loads during the course of the test. Loads on 5 March reached 220 lbs oscillatory. Relubrication of the pitch bearing alleviated the problem for 20 minutes, but the loads continued to increase with operating time on the rotor. The cam was moved to an azimuth position of  $-15.0^\circ$  and the same limited test matrix acquired.

On 5 March, during test condition 3956, at  $\mu = 0.20$ ,  $C_T/\sigma = 0.0762$ ,  $C_T = 0070$  and  $\alpha = 6.0$ , the flap actuation cable on blade station four failed. The cable was replaced, and shortly after the cable on blade station 1 failed. All cables were replaced at this point.

Continuing the data runs on 11 March, the  $-17.5^\circ$  Schedule 63 cam was installed at an azimuth position of  $\psi = -20.0^\circ$ . Two final acoustic sweeps with the cam on the advancing side of the rotor were completed at shaft angles of  $7.5^\circ$  and  $8.5^\circ$  with  $C_T/\sigma = 0.0871$  and  $C_T = 0.008$ .

As all of the priority one and two acoustic data points had been acquired, the acoustics engineers suggested that it would be interesting to examine the effect of

the cam on retreating side BVI. The cam was rotated to an azimuth position of  $\psi = 140.0^\circ$ . The matrix of acoustic sweeps was prioritized to ensure that the most important points were acquired first. All but two of the acoustic sweeps were acquired. Table 10 shows the test conditions acquired on the evening of 11 March and 12 March.

Table 10. Test Matrix For  $-17.5^\circ$  Acoustic Cam With  $140^\circ$  Azimuth

$\mu$	$\alpha$	$C_t/\sigma$	$C_t$
0.15	3.0, 4.0, 5.0, 6.0, 7.0	0.0762	0.007
0.20	2.0, 3.0, 4.0	0.0762	0.007
0.20	2.5, 3.5, 4.5, 5.5, 6.5	0.0871	0.008

Data channel MN 1018, blade two active flap angle failed on these runs. The console flapping resolver scope started to fade intermittently so that no trace was visible. A backup resolver scope was installed. Also, oscillatory loads on pitch link 4 continued to rise throughout these data runs. Several shutdowns were required to lubricate the bearings. This fix only served to relieve loads temporarily. Flow visualization was performed to study the wake vortex structure. These runs were recorded on videotape.

### 5.9 -20 Degree Acoustics Cam

The final  $-20^\circ$  acoustic cam, Schedule 50, was mounted on the model on 10 March. Experience in hover with this configuration had shown that the flap actuation cable life was limited to about 50 minutes of operation due to the extremely high loads on the actuation components. The cam was mounted at an azimuth position of  $\psi = -10.0^\circ$ . Hover data had been acquired for this configuration on 15 February. To maximize the acoustic test time, the forward flight data points were acquired immediately. The test points were prioritized so that flap activation cable breaks would not limit the acquisition of the most important data points. Acoustic sweeps were acquired for the conditions shown in Table 11.

Table 11. Test Matrix For  $-20^\circ$  Acoustic Cam With  $-10^\circ$  Azimuth

$\mu$	$\alpha$	$C_t/\sigma$	$C_t$
0.15	5.0	0.0762	0.007
0.20	4.0	0.0762	0.007
0.20	2.5, 3.5, 4.5, 5.5, 6.5	0.0871	0.008

The lower priority points in the matrix were omitted so that data with an azimuth angle of  $\psi = 0.0^\circ$  could be acquired. The lower priority points were acquired the next day, on 11 March, after the  $\psi = 0.0^\circ$  configuration data.

Four sweeps were completed in 51 minutes with the  $-20.0^\circ$  cam at an azimuth position of  $-20.0^\circ$  before the first cable break. The cable was replaced, and three more sweeps were completed in 40 minutes of run time before another cable failed. During these runs the control system actuators showed increasing levels of

error signals. These were attributable to the poor quality of the hydraulic fluid in the hydraulic cart. Several "patch tests" were completed, and filtering of the fluid performed. The fluid was brought up to a Class 6 or Class 7 level. The hydraulic fluid quality was a recurring problem throughout the test.

The Schedule 50 cam was installed at an azimuth position of  $\psi = 0.0^\circ$  on 10 March and acoustic data was acquired. Again, the order of acquisition of test points was prioritized to make the best use of available time on the rotor. Table 12 illustrates the conditions for the acquired test points.

Table 12. Test Matrix For  $-20^\circ$  Acoustic Cam With  $0^\circ$  Azimuth

$\mu$	$\alpha$	$C_t/\sigma$	$C_t$
0.15	5.0, 7.0, 3.0, 5.0	0.0762	0.007
0.20	2.0, 4.0, 6.0	0.0762	0.007
0.20	2.5, 4.5, 5.5, 6.5	0.0871	0.008

The cam azimuth position was then returned to  $\psi = -10.0^\circ$  and several more of the remaining acoustic sweeps for this matrix completed, see Table 13.

Table 13. Test Matrix For  $-20^\circ$  Acoustic Cam With  $-10^\circ$  Azimuth

$\mu$	$\alpha$	$C_t/\sigma$	$C_t$
0.15	7.0	0.0762	0.007
0.20	2.0, 6.0	0.0762	0.007
0.20	7.5, 8.5	0.0871	0.008

In the written test log, 4031 was also identified in a written comment as 4032 with test conditions for the Schedule 50 cam at an azimuth of  $\psi = -10.0^\circ$  and  $\mu = 0.15$ ,  $C_t/\sigma = .0762$ ,  $C_t = .0070$  and  $\alpha = 5$ . The computer performance data log retains the 4031 nomenclature and identifies the point with the test conditions with an azimuth of  $\psi = 0.0^\circ$  and  $\mu = 0.15$ ,  $C_t/\sigma = 0.0762$ ,  $C_t = 0.0070$  and  $\alpha = 5^\circ$ .

On 10 and 11 March the cable on hub position three failed after four acoustic sweeps. All four cables were replaced. The remaining five sweeps for the  $0.0^\circ$  cam azimuth position were completed. One sweep was completed at a cam azimuth position of  $-10.0^\circ$  before the hub position three cable failed again. The cable was replaced and five additional sweeps were performed.

The cam was repositioned at an azimuth position of  $\psi = -15.0$ , and a limited set of acoustic sweeps acquired, see Table 14.

Table 14. Test Matrix For  $-20^\circ$  Acoustic Cam With  $-15^\circ$  Azimuth

$\mu$	$\alpha$	$C_t/\sigma$	$C_t$
0.15	5.0	0.0762	0.007
0.20	5.0	0.0762	0.007
0.20	4.5	0.0871	0.008

A number of data channels failed during the data runs on 11 March. These included MN1025 pitch link 1, MN1030 blade two flap bending, MN 1031 blade two chord bending, and MN 1034 blade two torsion bending at the 23.7 radial station.

### 5.10 2P3A Performance

The 2P3A performance cam was tested next, on 2 and 3 March. The first azimuth position tested was 11.7°. In order to check out the rotor operation, and to provide a set of comparison data to this and other configurations, a rotor speed sweep, collective sweep and cyclic sweep were performed in hover.

Performance data points were acquired at the same shaft angle as for the baseline rotor, see Table 15.

Table 15. Test Matrix For 2P3A Performance Cam With 11.7° Azimuth

$\mu$	$\chi$	$\alpha$	$C_t/\sigma$	$C_t$
0.10	0.12	-0.92	0.0653	0.0060
		-0.81	0.0871	0.0080
0.15	0.12	-1.89	0.0653	0.0060
		-1.61	0.0871	0.0080
0.20	0.12	-3.24	0.0653	0.0060
		-2.72	0.0871	0.0080
0.25	0.12	-5.31	0.0653	0.0060
		-4.19	0.0871	0.0080
0.30	0.12	-7.38	0.0653	0.0060
		-6.12	0.0871	0.0080

High blade chord bending loads were encountered at  $\mu = 0.10$  and 0.15 for  $C_t/\sigma = 0.0871$ . The performance engineer requested an additional test point at  $\mu = 0.25$  for  $C_t/\sigma = 0.0979$ . High cyclic blade chord loads at station 23.67 precluded the acquisition of this data point.

The azimuth position of the cam was changed to 56.7°, and the test matrix acquired, see Table 16. No data was acquired at  $\mu = 0.10$ .

Table 16. Test Matrix For 2P3A Performance Cam With 56.7° Azimuth

$\mu$	$\chi$	$\alpha$	$C_t/\sigma$	$C_t$
0.15	0.12	-1.89	0.0653	0.0060
		-1.61	0.0871	0.0080
0.20	0.12	-3.24	0.0653	0.0060
		-2.72	0.0871	0.0080
0.25	0.12	-5.31	0.0653	0.0060
		-4.19	0.0871	0.0080
0.30	0.12	-7.38	0.0653	0.0060
		-6.12	0.0871	0.0080

One acoustic sweep to evaluate the effect of this cam on noise was performed. Data was taken for the acoustic test condition, 8036, at  $\mu = 0.20$ ,  $X = 0.12$ ,  $\alpha = 2.72^\circ$ ,  $C_t/\sigma = 0.0871$ , and  $C_t = 0.008$ .

The cam was moved to an azimuth position of  $101.7^\circ$  and the test matrix was repeated. Table 17 depicts the acquired test conditions.

Table 17. Test Matrix For 2P3A Performance Cam With  $101.7^\circ$  Azimuth

$\mu$	$X$	$\alpha$	$C_t/\sigma$	$C_t$
0.15	0.12	-1.89	0.0653	0.0060
		-1.61	0.0871	0.0080
0.20	0.12	-3.24	0.0653	0.0060
		-2.72	0.0871	0.0080
0.25	0.12	-5.31	0.0653	0.0060
		-4.19	0.0871	0.0080
0.30	0.12	-7.38	0.0653	0.0060
		-6.12	0.0871	0.0080

Again, one acoustic sweep was performed to evaluate the effect of this cam on noise. Data was taken for the acoustic test condition, 8044, at  $\mu = 0.20$ ,  $X = 0.12$ ,  $\alpha = -2.72^\circ$ ,  $C_t/\sigma = 0.0871$ , and  $C_t = 0.008$ .

The final azimuth tested was  $146.7^\circ$ . Table 18 illustrates the acquired test conditions.

Table 18. Test Matrix For 2P3A Performance Cam With  $146.7^\circ$  Azimuth

$\mu$	$X$	$\alpha$	$C_t/\sigma$	$C_t$
0.15	0.12	-1.89	0.0653	0.0060
		-1.61	0.0871	0.0080
0.20	0.12	-3.24	0.0653	0.0060
		-2.72	0.0871	0.0080
0.25	0.12	-5.31	0.0653	0.0060
		-4.19	0.0871	0.0080
0.30	0.12	-7.38	0.0653	0.0060
		-6.12	0.0871	0.0080

One last acoustic sweep was performed to evaluate the effect of this cam on noise. Data was taken for the acoustic test condition, 8052, at  $\mu = 0.20$ ,  $X = 0.12$ ,  $\alpha = -2.72^\circ$ ,  $C_t/\sigma = 0.0871$ , and  $C_t = 0.008$ .

### 5.11 2P6A Performance Cam

The next configuration tested was the sinusoidal 2P flap deflection cam with  $6.0^\circ$  peak flap deflection. The cam was mounted with an azimuth position of  $11.7^\circ$  on 7 March. A collective and cyclic sweep in hover was performed to verify flap and test stand operation and for comparison with hover data from other configurations.

During the first four forward flight data points the temperature on the standpipe bearing rose dramatically. The rotor was brought to a stop as quickly as possible. Because the temperatures on the bearing had exceeded 220° F, with no sign of stabilizing, the rotor was disassembled, and the standpipe and mast removed to examine the bearing. The standpipe was discolored from heating, and the bearing partially damaged with the inner bearing surface melted and partially removed. The remainder of the inner bearing surface was removed, leaving an oversized bearing that would act as a flail damper. The standpipe torsion gage that was previously damaged, was repaired, and the model reassembled. There was some suspicion that the 2P six degree cam was exciting a lateral bending mode in the standpipe. This mode was not observed in the standpipe torsion gage. No bending gage was available. To verify the test stand operation after the rebuild, the null cam was installed on the model. Several runs were completed in hover with no problems from the standpipe bearing.

Testing resumed with the completion of the test matrix for the 2P 6.0° cam. The cam was mounted at an azimuth position of  $\psi = 11.7^\circ$  and the test matrix for this position completed, see Table 19.

Table 19. Test Matrix For 2P6A Performance Cam With 11.7° Azimuth

$\mu$	$\alpha$	X	$C_t/\sigma$	$C_t$
0.20	-3.24	dependent	0.0653	0.006
0.20	dependent	0.12	0.0653	0.006
0.20	-2.72	dependent	0.0653	0.006
0.20	dependent	0.12	0.0653	0.006

An acoustic data sweep was acquired for test condition 8526, at  $\mu = 0.20$ ,  $C_t/\sigma = 0.0653$ ,  $C_t = .006$  and  $\alpha = -2.72^\circ$ . The same test matrix, with the acoustic data sweep was repeated for cam azimuth positions of  $\psi = 56.7^\circ$ ,  $101.7^\circ$ ,  $146.7^\circ$  and  $146.7^\circ$  on 9 March. The test matrix points at  $\mu = .25$ , and  $.30$  were deleted to minimize test time in this configuration.

## 5.12 Dynamics with Null Cam

With the null cam in place, the opportunity arose to complete the dynamics test matrix. Two rotor speed sweeps were performed, on 8 March, at collective angles of  $\theta = 0.0^\circ$  and  $\theta = 4.0^\circ$ . Performance and loads data were acquired at each rotor speed.

The flap, lag, and drive system modes were excited and the transients recorded for a number of rotor speeds on 8 and 9 March. The dynamic data acquisition procedure is described in Section 4.6. Table 20 shows the test conditions for the dynamics data.



Table 20. Test Matrix For Baseline Rotor Dynamic Excitation

RPM	Collective	Lateral Cyclic	Longitudinal Cyclic	Excitation Type
435	0.0°, 4.0°	0.0	0.0	Flap Lag
652	0.0°, 4.0°	0.0	0.0	Drive system Flap Lag
870	0.0°, 4.0°	0.0	0.0	Drive System Flap Lag
1087	0.0°, 4.0°	0.0	0.0	Flap Lag

Flow visualization runs (see Table 21) were performed in forward flight to reexamine the rotor wake structure. These were performed at a shaft angle of  $\alpha = 4.0^\circ$  and a hover tip Mach number of  $M_h = 0.618$ .

Table 21. Test Conditions For Flow Visualization

$\mu$	$\alpha$	$C_t/\sigma$	$C_t$
0.10	4.0	0.0762	0.007
0.15	4.0	0.0762	0.007
0.20	4.0	0.0762	0.007

For previous performance data, predicted shaft angles had been used, instead of flying to X. This procedure had been used, as the balance measurement of normal force at low advance ratios was imprecise. At higher advance ratios however, the measured propulsive force appeared to be more accurate. The shaft angles predicted by simple theory were not producing the correct propulsive force, X. In order to compare the predicted shaft angle data points to points with a fixed propulsive force, data was taken with each technique at a series of flight conditions, see Table 22.

Table 22. Conditions For Propulsive Force Comparison

$\mu$	$\alpha$	X.	$C_t/\sigma$	$C_t$
0.20	-3.24	dependent	0.0653	0.006
0.20	dependent	0.12	0.0653	0.006
0.20	-2.72	dependent	0.0653	0.006
0.20	dependent	0.12	0.0653	0.006
0.25	-5.3	dependent	0.0653	0.006
0.25	dependent	0.12	0.0653	0.006
0.25	-4.19	dependent	0.0653	0.006
0.25	dependent	0.12	0.0653	0.006
0.30	-7.38	dependent	0.0653	0.006
0.30	dependent	0.12	0.0653	0.006
0.30	-6.12	dependent	0.0653	0.006
0.30	dependent	0.12	0.0653	0.006

In order to fill out the baseline configuration acoustic test matrix, two acoustic sweeps were performed for test conditions 550 and 551. These were completed at test conditions of  $\mu = 0.20$ ,  $C_t/\sigma = 0.0871$ ,  $C_t = 0.0080$  and  $\alpha = 7.5^\circ$ , and  $8.5^\circ$ . No

increase in temperature was noted in the upper standpipe bearings during these runs. The removal of the inner bearing surface appeared to have addressed the heating problem.

### 5.13 3P2A Dynamics Cam

The first vibration reduction cam, 3P2A was installed on 12 March. A rotor speed and collective sweep were performed in hover to check the operation of the cam and test stand. The cam was installed at an azimuth position of  $\psi = 15.0^\circ$ . For this configuration, vibratory torsion loads on the standpipe increased significantly. The upper bearing temperature on the standpipe rose dramatically during these runs and showed no sign of stabilizing. The data runs were cut off when the standpipe bearing temperature reached 220 °F. It appeared that the 3P excitation of the standpipe was exciting the 2nd beam bending mode of the standpipe. As a result, the standpipe was rubbing on the upper bearing, which had been bored out to act as a flail damper. It was not possible to continue data runs with this cam because of this mechanical problem.

### 5.14 5P4A Dynamics Cam

The 5P4A dynamics cam was installed on 12 March with an azimuth position of  $\psi = -9.0^\circ$ . A hover checkout was performed to verify test stand operation, and to provide comparison data to other configurations. A rotor speed sweep, a collective sweep, and cyclic sweep were performed. Performance data points were acquired in forward flight as shown in Table 23.

Table 23. Test Conditions For 5P4A Dynamics Cam With  $-9^\circ$  Azimuth

$\mu$	$\alpha$	X	$C_t/\sigma$	$C_t$
0.10	-0.92	dependent	0.0653	0.006
0.15	-1.89	dependent	0.0653	0.006
0.20	-0.70	dependent	0.0653	0.006
0.20	-0.73	dependent	0.0871	0.008
0.20	3.5	dependent	0.0871	0.008
0.25	-3.0	dependent	0.0653	0.006
0.25	-2.5	dependent	0.0871	0.008
0.30	-5.0	dependent	0.0653	0.006
0.30	-4.0	dependent	0.0653	0.006

### 5.15 No Horn Baseline Case

The control horns were removed in order to study their effect on the tip vortex. Two hypotheses describing the effect of the external control horns on the tip vortex merited investigation. The first was that the control horns, protruding in the flow at the tip, produce a baseline rotor with higher broadband noise levels than expected. The second hypothesis was that the protruding external control horns had the effect of distributing the intensity of the bound circulation at the blade tip, hence weakening the BVI noise even before the flap was deployed.

In order to examine these hypotheses, the control horns and flap actuation cables were removed. The tips were modified with set screws to adjust the active flaps to an angle of 0.0°. The holes in the blade tips for the control cables were sealed with tape. The rotor in this configuration was tested on 14 March. A collective sweep in hover was performed and a limited acoustic matrix was acquired as shown in Table 24.

Table 24. Test Conditions For No Horn Baseline Rotor

$\mu$	$\alpha$	$C_t/\sigma$	$C_t$
0.15	3.0, 5.0, 7.0	0.0762	0.007
0.20	2.0, 4.0, 6.0	0.0762	0.007
0.20	2.5, 4.5, 6.5	0.0871	0.008

The results showed that the rotor was, on an average, approximately 2 dB louder than the baseline rotor with the control horns, in the BVI cases acquired here. This result tends to support the second theory, that the vortex structure was more diffused with the control horn. Flow visualization was performed during these runs and recorded on video tape. The results were inconclusive in supporting either theory. Further studies however, of blade pressures and acoustic time histories will be required to draw any definitive conclusions.

### 5.16 Removal of Model

The no control horn rotor configuration was the last configuration tested. The blades were removed from the hub, and a final check calibration performed on balance normal force. The results matched those taken previously during the test program. The model was removed from the test section in several major components. The instrumentation was removed from the control room by a combined crew of NASA and MDHS personnel.

## 6.0 Test Results

Data was acquired over a period of five weeks from 5 February to 15 March. A summary of all data points, i.e. with data acquired by the HP data system and stored in the ASAP database, and runs, i.e. rotor turning, is shown in Appendix B. This includes the respective test dates, test configuration and objective or cam phase (in degrees) as applicable. Initial checkout, tares, etc. were conducted up to run 70. The number of data points per segment of runs for each cam, and the total number of data points and run time per cam are also shown. In total 4886 data points and 81:02 hours of run time were accumulated in the tunnel. Note that 50 runs with a total run time of 17:07 hours were conducted during integration testing at the whirl tower in Mesa.

A summary of all runs conducted in the tunnel is shown in the run log, Appendix B. This includes the date, run number, start and end time of the run, the time per run (rotor turning), and the total cumulative run time in the tunnel. Additional information is listed for the data runs (71 through 156, total of 66:34 hours). Maintenance actions and comments, and the cumulative run time for the cam

follower bearings (CFB) are listed. This is followed by the cable log which shows when and on which hub arm a flap actuation cable failed. Last, the cam log shows the cumulative time per cam and phase value for each run.

Complete listings of measured and derived data, and of all data points, in chronological order, including condition number, test point number, description of test condition, as well as recorded values for the rotor speed (rpm), advance ratio ( $\nu$ ), corrected shaft angle of attack ( $\alpha_{fsc}$  - deg), thrust coefficient/solidity ( $c_T/\sigma$ ), and tip mach number ( $tipm$ ) are also included in Appendix B.

## **6.1 Stand Shake Test Data**

A ground vibration survey (GVS) of the MDHS Large Scale Test Rig mounted in the NASA Langley 14x22 Foot Subsonic Wind Tunnel was conducted to determine the dynamic characteristics of the rotor support. Specifically the objectives were:

1. Determine test stand modal frequencies, damping, and mass as well as mode shapes for use in an aeromechanical stability (ground and air resonance) analysis of the coupled rotor/support system.
2. Determine test stand modes within the range of 1 to 100 Hz to identify possible loads and vibration problems at rotor speed multiples.

The test article consisted of the MDHS Large Scale Test Rig which was bolted to the NASA Langley 14- by 22-Foot Subsonic Tunnel Cart 1, mounted in the forward bay. The complete active flap rotor hub, control system, mast and standpipe were installed, except for the blades, pitch links, and slip ring assembly. In place of the blades, four weights of approximately 3.44 pounds each were bolted to the hub arms. The test stand consisted of the rotor balance system, gearbox, motor, and test stand sled. No fairings were installed on the model. The drive system was installed with all flexures and couplings but without a motor lockout device. The test stand was mounted on the clamshell support normally used for the wind tunnel sting.

The shake test was conducted using a single input and recording multiple outputs. Lateral or longitudinal force inputs were provided by a hydraulic actuator over a frequency range of 1 to 100 Hz (including 5/rev) at a force level of 100 pounds peak-to peak. Using a 4 foot long rod and load cell, the shaker was connected to the test stand at the upper end of the auxiliary hub (4.5 inch below the hub plane). On the other end, the shaker was attached to a large mass of 2500 pounds, which was suspended by a 10 to 12 feet long chain. This large mass assured that the actuator output was effectively transmitted to the test stand. The length of the cable, together with the value of mass, provided enough frequency separation between the pendulum mode and the lowest test stand frequency of interest. Figure 16 shows the test setup.

An HP signal generator was used to provide a stepped sine sweep input to the actuator. Frequency steps were chosen at 0.01 Hz in the 1 to 30 Hz range, and at 0.1Hz in the 30 to 100 Hz range. Instrumentation used during the shake test (see Table 25) consisted of the load cell, an accelerometer located on the hub (3 inch above hub plane) and oriented in the direction of the applied load, the balance roll

and pitch moments, and the mast longitudinal and lateral accelerations. The latter four measurements were part of the instrumentation used during the wind tunnel test.

Table 25. Shake Test Instrumentation (height relative to hub plane)

No.	Item	Rate	Positive Polarity	Height, in
	load	10mV/lb	right/forward (compression)	-4.5
	hub accel	400mV/g	right/forward	3.0
1043	bal roll	.103mV/in-lb	right down	-46.55
1044	bal pitch	.088mV/in-lb	nose up	-46.55
1048	lon accel	387mV/g	aft	-38.0
1049	lat accel	397mV/g	right	-38.0

An HP dynamic analyzer (model 3562) was used to acquire the force input and one response measurement and to compute the frequency response (magnitude and phase) and coherence. Eight lateral and seven longitudinal sweeps were conducted. The first five lateral and three longitudinal sweeps (see Table 26) were used to establish an appropriate force level and analyzer sensitivity, and to examine the test stand mode shapes. Permanent records were obtained for all frequency response and some coherence functions. As noted above, the force level was 100 pounds peak-to-peak, except for sweep 1 where 50 pounds were used.

Table 26. Shake Test Frequency Sweeps

Lateral input

Run	Measurement	Freq. [Hz]	Comments
1	hub accel	1-30-100	modes at 7.6, 9.4, 21.3 Hz
2	hub accel	1-30-100	modes at 7.5, 9.3, 20.1 Hz
3	hub accel	1-34	examine vibrations on test stand
4	hub accel	15-24	mode at 20.1 Hz
5	hub accel	15-30	phase off, adjust analyzer sensitivity
6	hub accel	1-30-100	modes at 7.37, 9.0, 20 Hz
7	bal roll	1-33	out of range at peaks
8	lat accel	1-30	

Longitudinal Input

Run	Measurement	Freq. [Hz]	Comments
9	hub accel	1-30-100	modes at 7.1, 18.4, 25.6, 38.1 Hz
10	hub accel	12-50	explore large peak at 38 Hz
11	hub accel	25-50	out of range at 38 Hz
12	bal pitch	1-41-100	out of range at peaks
13	lat accel	1-41-100	
14	hub accel	1-42-100	move accel from standpipe to hub
15	hub accel	1-30	greater sensitivity

Typical frequency response functions, recorded for runs 6 through 8 and runs 12 through 14, are shown in Figures 17, 18 and 19. Based on this shake test data, stand modes and response levels at nominal rotor speed were identified, see table 27. Also shown in the table is a standpipe mode, which was later identified from standpipe torque strip chart data during runup and shutdown. None of these modes, with the exception of the standpipe, presented a problem.

Table 27. Test Stand Modes and Response

Mode	Rpm	%NR	Hub accel		Balance moment		Mast accel	
			Hz, mg/lb		Hz, in-lb/lb		Hz, mg/lb	
Lon 1	415	38.1	6.91	7.28	6.75	138.3	6.87	4.20
Lat 1	442	40.7	7.37	3.40	7.25	96.7	7.37	1.82
Lat 2	540	49.7	9.00	3.25	9.12	99.2	9.25	2.47
Lon 2	1097	100.9	18.28	3.29	18.00	65.1	18.50	0.85
Lat 3	1200	110.4	20.00	12.41	20.12	149.5	20.12	1.93
Lat	1087	100	18.12	2.98	18.12	59.8	18.12	0.13
Lon	1087	100	18.12	2.96	18.12	64.1	18.12	0.64
Lat 4		129	23.37	13.89	23.87	201.2	23.6	1.55
Lon 3		141	25.47	3.57	25.25	71.1	25.50	0.62
Lat 5		144	26.00	10.22	26.25	142.2	26.00	1.17
Lon 4		209	37.87	36.41	37.87	316.5	37.62	0.89
Lat 6		228	41.37	13.75	41.50	84.7	41.00	1.56
Standpipe		253	45.8					

Modes below 1/rev, i.e. the three lowest modes above, are of interest for ground resonance analysis. Modal damping for these modes was computed, using the HP analyzer, from a 3 pole, 3 zero curve fit at the response peak. The simple Deutsch criteria was then applied to show that no ground resonance problems were expected, see table 28.

Table 28. Ground Resonance Modal Data

Run	Mode	f-meas	A/F	f-fit	d-fit	$\zeta$	M-eff	c
		Hz	mg/lb	Hz	mHz	%c-cr	slug	lb-s/ft
6	Lat 1	7.37	3.40	7.39	-339.9	4.6	99	425
6	Lat 2	9.00	3.25	9.28	-442.0	4.8	100	558
15	Lon 1	6.91	7.28	6.93	-365.6	5.3	40	18

## 6.2 Dynamics Data

### 6.2.1 Rotor Dynamics

Dynamics data was acquired to better define and understand the dynamics of the active flap rotor. Of interest were the fundamental blade and drive system frequencies and damping, in particular for the lead-lag degree of freedom. The data of interest was obtained during run 120 on 8 March. Three different types of dynamic data were acquired.

#### 6.2.1.1 Rotor Speed Sweeps

Performance data was taken to identify rotor speeds where blade modal frequencies cross over rotor speed multiples. During rotor runup from 25 to 100 percent rotor speed, steady state (performance) data was taken at 16 rotor speeds (with increments of 5 percent NR). This data was acquired and stored using the HP data system. Test points 3534 - 3541 were for flat pitch and test points 3542 - 3549 were at 4° collective pitch.

Figures 20a, 20b show, respectively, the first five harmonics of blade chord bending at station 23 and standpipe torque versus rotor speed (normalized by the nominal rotor speed of 1087 rpm). From the peaks it is seen that a chordwise mode crosses 5/rev at .53NR, 2/rev at 0.6NR, and approaches 3/rev at NR. Similarly, it is seen that the standpipe's most prominent response peak occurs for the 4th harmonic near .65NR or 707 rpm.

### **6.2.1.2 Frequency Sweeps**

The dynamic control console was used to provide small amplitude sinusoidal inputs to the model rotor control system. The excitation frequency was swept manually from 1 to 30 Hz. Both cyclic (test points 3534 - 3541) and collective (test points 3542 - 3549) inputs were made at 40, 60, 80, and 100 percent rotor speed. Only flat pitch conditions were investigated. During cyclic excitation, blade flap and chord bending at station 23in were recorded on the HP analyzer and stored to disk. For collective excitation, blade torsion at station 23in and drive shaft torque number 2 were recorded and stored. Initially, the excitation frequency was adjusted, until a good response level was seen in the measurements of interest. The recorded power spectrum data was then used to identify modal frequencies for subsequent transient testing.

Figure 21 shows power spectra for the blade flap, chord and torsion responses at station 23in and for the main rotor shaft torque (gauge 2) at nominal rotor speed (18.12 Hz). Peaks at the rotor speed multiples clearly stand out in all four plots. The flap and torsion responses are rather flat in between. Small peaks, seen at 22Hz (flap only) and 76Hz, are a result of coupling with the chord motion. The chord and drive shaft responses are closely coupled, showing many peaks at common frequencies. The chord bending itself has a major peak at 23.25Hz or 1.28/rev. This is thought to be the fundamental chord mode.

### **6.2.1.3 Transient Testing**

Transient testing was performed to obtain damping estimates for specific modes of interest. The dynamic control console was used to provide sinusoidal inputs to the rotor control system at a given frequency. The amplitude of excitation was increased, until a good response level was seen in the measurement of interest. After reaching steady state, the excitation was terminated. Dynamic data was recorded on the HP data system over 40 rotor revolutions (64 points per revolution), starting at excitation cutoff. Modal damping and frequency can then be estimated using the moving block technique.

The blade flap and chord modes (bending station 23in) were excited using cyclic inputs. The drive system dynamics (torque 2) were excited using collective inputs. The blade torsion mode could not be sufficiently excited. The fixed system excitation frequencies used in transient testing are shown in the table 29. Figure 22 shows the longitudinal cyclic input (at 5Hz) and chord bending response at station 23in (at approximately 5+18 Hz) over 40 rotor revolutions.

Table 29. Frequencies used in transient testing

%NR	Flap	Chord	D/S
40	4.25	14.5	
60	3.70	5.4, 10.9	16.4
80	3.75	3.1, 8.1	17.9
100	3.80	6.7, 5.0	

#### 6.2.1.4 Standpipe Response

During rotor runup and shutdown, several peaks in the standpipe torque were observed on the strip chart. A Fourier analysis of this measurement at nominal rotor speed indicated a mode at 47.5 Hz or 2.6/rev. Consistent with this, the highest response peak always occurred around 680 rpm rotor speed. This corresponds to the crossover of the standpipe torsion mode with 4/rev. From the strip charts, a modal frequency of 45.8 Hz or 2.5/rev was determined. Smaller responses were observed around 340 rpm (crossover with 8/rev) and near 910 rpm (crossover with 3/rev). This mode did not present a problem, as long as the 680 rpm range was crossed rapidly, except for testing with the 3/rev vibration reduction cam.

#### 6.2.2 Vibration Reduction

Simulations have shown that a trailing edge flap can also be effective in reducing vibratory loads. Vibration reduction was therefore added to the test program as a third objective. Two vibration reduction cams were built, drawing on previous simulation results. Both cams had a cosine profile, one with 2° amplitude and 3/rev frequency, the other with 4° amplitude and 5/rev frequency.

In order to facilitate the data reduction for this objective, additional derived parameters were defined and added to the database. The 4/rev and 8/rev vibratory components of three hub forces and pitch and roll moments are added vectorially to form the vibration indices J4PRT and J8PRT, respectively. The 4/rev and 8/rev indices are then combined, using a relative weighting from ADS-27, to form the overall vibratory hub load index JRT. The mast longitudinal and lateral accelerations are similarly combined to form J4MST, J8MST, and JMST.

$$J4PRT = \left( DRAGRT_{4P}^2 + SIDERT_{4P}^2 + LIFTRT_{4P}^2 + (ROLLRT_{4P}^2 + PITCHRT_{4P}^2)/144 \right)^{1/2}$$

$$J8PRT = \left( DRAGRT_{8P}^2 + SIDERT_{8P}^2 + LIFTRT_{8P}^2 + (ROLLRT_{8P}^2 + PITCHRT_{8P}^2)/144 \right)^{1/2}$$

$$JRT = \left( J4PRT^2 + 0.486 J8PRT^2 \right)^{1/2}$$

$$J4MST = \left( MST\ ACCL\ LNG_{4P}^2 + MST\ ACCL\ LAT_{4P}^2 \right)^{1/2}$$

$$J8MST = \left( MST\ ACCL\ LNG_{8P}^2 + MST\ ACCL\ LAT_{8P}^2 \right)^{1/2}$$

$$JMST = \left( J4MST^2 + 0.486 J8MST^2 \right)^{1/2}$$



As noted above, the standpipe had a torsion mode near 2.5/rev, well separated from 3/rev. However, the 3/rev vibration reduction cam caused sufficient torsion and coupled bending motions of the standpipe, such that the standpipe would make contact with its centering bearing. As a result, bearing temperature rose very rapidly and exceeded limits when running at nominal rotor speed. Running with the null cam confirmed that the bearing temperature rise was caused by the 3/rev cam. Any further running with this cam had to be abandoned and only limited hover checkout test data was obtained.

Figure 23 shows the rotor balance pitch moment frequency response for the baseline case and with the flap moving at 4° and 5/rev (5P4A cam). Significant reductions in the response at 4, 5, and 8/rev are evident. Similarly, Figure 24 shows the balance pitch moment time histories for the baseline and active control case over four rotor revolutions. Again, substantial reductions in amplitudes are seen.

### 6.2.3 Performance Improvement

The application of active control to improve rotor performance is an attractive concept. In particular, 2/rev inputs have been investigated, to improve aerodynamic performance and alleviate stall. However, this type of input cannot be generated through a swashplate on rotors with four or more blades. In contrast, the active flap rotor provides control inputs to the trailing edge flap in the rotating system and can thus be used to apply inputs at any arbitrary harmonic.

Simulations with the CAMRAD/JA code showed that 2/rev inputs to the flap could improve rotor performance. This would occur at high thrust ( $C_T=.009$ ,  $\mu=.25$ ) and at high speed ( $C_T=.008$ ,  $\mu=.40$ ). Two cams were built to investigate possible performance improvements in the tunnel. Both cams have a 2/rev profile with amplitudes of 3 and 6°; they are denoted 2P3A and 2P6A cams.

In setting rotor trim conditions and measuring rotor performance accurately, two derived parameters are of importance. The nondimensional propulsive force X is

$$X = -\frac{C_x}{\sigma} \frac{\pi}{2\mu} = \frac{\pi f}{4 A_b}$$

$$\frac{C_x}{\sigma} = \frac{\text{DRAGNH}}{\rho A (\omega R)^2 \sigma}$$

where

with f is the equivalent flat plate drag area and  $A_b$  is the blade area. The equivalent lift to drag ratio is

$$\frac{L}{D} = \frac{1.688 * VKTS * LIFTNH}{HPNH * 550 + 1.688 * VKTS * DRAGNH}$$

where LIFTNH and DRAGNH are the rotor lift and drag forces in wind axis, including all corrections and tares (i.e. rotor minus hub forces).

Rotor performance testing in forward flight was performed simulating a fixed equivalent flat plate drag area and zero flapping. The value of the nondimensional propulsive force, X, was chosen as 0.12. Initial runs were made using precomputed shaft angles, based on simple equations. All runs using the 2P3A cam were made using the initial set of shaft angles. Later, runs with the null cam and 2P6A cam were made using the initial set of angles as well as trimming to X for advance ratios of 0.2 and higher. The 5P4A cam was run (when  $\mu \geq 0.2$ ) using shaft angles determined experimentally from trimming the null cam to X. Both sets of values are listed in table 30.

Table 30. Shaft Angles Used

$\mu$	Initial		Base, 5P4A	
	Ct=.006	Ct=.008	Ct=.006	Ct=.008
.10	-0.92	-0.81		
.15	-1.89	-1.61		
.20	-3.24	-2.72	-0.70	-0.73
.25	-5.30	-4.19	-3.00	-2.50
.30	-7.38	-6.12	-5.00	-4.00

The null cam and 2P6A cam were run using both precomputed shaft angles and trimming to X. Thus it is possible to assess the effect of propulsive force trim on rotor power. However, it is pointed out that the rotor balance was oversized for this rotor. The total balance load range for drag was 2000 pounds, resulting in less than desirable resolution in the range of actually measured drag.

Figure 25 shows the variation of the propulsive force X, versus advance ratio  $\mu$ , for the baseline and 2P3A cam. Large variations from the target value of 0.12 are seen, in particular at low speed. Figures 26 show L/D for the baseline and 2P3A cam (at phase angles of 0, 45, 90, and 135°) versus speed at two values of  $C_t$  (0.006, 0.008). Large variations in L/D are seen at a given flight condition, depending on the cam phase. However, closer examination of the data reveals that the changes in L/D are merely corresponding to changes in X, and thus do not represent actual performance improvements.

As a result, the trim procedure was changed to trim to X for testing with the 2/rev 6° cam. Results from the 2P6A cam have not been evaluated at this time.

### 6.3 Sample Aerodynamic and Pressure Data

For many years scientists have recognized the direct relation between the strength of blade-vortex interactions, BVI, (and hence BVI noise levels) and the temporal pressure gradients near the leading edge of the blade. In general, large gradients are indicative of the strong interaction(s) which typically result from the close proximity of the vortex-wake to the blade and/or from the presence of a relatively strong vortex wake near the surface of the blade. Quite often however, it is the

differential pressures or the temporal gradients of the differential pressures, rather than the pressures themselves, near the leading edge of the blade that are used to assess the intensity of BVI. These quantities also represent the blade lift or the time variation of the blade lift during the blade-vortex encounters. In this section, discussion of the acquired surface pressure data near the leading edge of the blade ( $x/C=0.03$ ) at four radial stations for the flapped model rotor as a function of the trailing edge flap schedule (peak deflection angle, phase shift in azimuth), tip path plane angle, advance ratio and blade thrust will be presented. Recall that the four radial stations with pressure instrumentation are located at  $R_{bar}=R/R_{tip}=0.7522, 0.8214, 0.9105, 0.9836$ . The first radial station is located just inboard of the inner unflapped/flapped blade juncture (i.e., on a blade section with no flap). The second, third and fourth radial stations are located on the flapped section of the rotor at the following positions; just outboard of the inner flap juncture, mid span and just inboard of the outer flap juncture. For contrast, where applicable, results for the baseline model rotor (i.e., with the flap in the neutral undeflected position) will also be presented.

### **6.3.1 Advancing Side BVI**

#### **6.2.1.1 Effects Of Trailing Edge Flap Deployment**

Figure 27 depicts the azimuthal variations of the measured upper (kulite # 1, 3, 5, 7) and lower (kulite # 2, 4, 6, 8) surface pressures (in Pascal) near the leading edge of the blade ( $x/C=0.03$ ) at the four blade radial stations  $R_{bar}= 0.7522, 0.8214, 0.9105, 0.9836$  respectively. For this case, the wind tunnel test conditions are: advance ratio  $\mu=0.149$ , tip path plane angle  $\alpha=5^\circ$  aft and  $C_{T/\sigma} = 0.0764$ . As seen, the presence of the advancing blade BVI characterized by the rapid, and sometimes impulsive, fluctuation in the surface pressures is evident in the  $40^\circ$ - $80^\circ$  azimuth range. On the retreating side, similar interactions can be seen in the  $260$ - $300$  azimuth range with the strongest interaction occurring in the vicinity of the  $280^\circ$  azimuth. In Figure 28, we illustrate the measured blade surface pressures for the flapped rotor utilizing the trailing edge flap schedule with a peak amplitude of  $-12.5$  (the minus sign indicates a flap up position) degrees and a  $-20^\circ$  azimuthal shift from the nominal position, see Figure 29. Clearly, with the exception of some weak interactions remaining between the  $60$  and the  $80^\circ$  azimuthal positions, all the previously observed advancing blade interactions seen in Figure 27 have been reduced in strength or completely eliminated. On the retreating side, a single interaction, rather than the multiple interactions seen in Figure 27, is seen near the  $300^\circ$  azimuth position. An alternative representation of the measured surface pressures shown in Figures 27 and 28 is given in Figures 30 and 31 which depict, respectively, the differential pressures (in KPa) at  $x/C=0.03$  for the baseline and the flapped model rotors as a function of blade azimuth.

#### **6.3.1.2 Effects Of The Peak Flap Deflection Amplitude**

Figures 32-35 depict the calculated differential pressures,  $(p_U - p_L)$ , using the measured individual upper and lower surface pressures) for the baseline rotor and for the flapped rotor with peak flap deflections of  $-12.5^\circ$ ,  $-17.5^\circ$  and  $-20.0^\circ$

respectively. For the flapped model rotors, a  $-10^\circ$  phase shift in azimuth from the nominal flap schedules was used. For these cases, the advance ratio is 0.148, the tip path plane angle  $\alpha$  is  $3^\circ$  aft and  $C_T/\sigma=0.076$ . As seen, with the increase in the peak deflection amplitude, the character of the advancing BVI is also changed. For example, for the baseline configuration, the impulsiveness which is observed in the interaction which occurs between the  $60^\circ$  and  $80^\circ$  azimuthal positions at all four radial stations is reduced with the  $-12.5^\circ$  peak flap deflection to a more gradual variation at  $R_{bar}= 0.8214, 0.9105, 0.9836$ . At  $R_{bar} = 0.7522$  and  $0.8214$ , one can also see some indication of BVI which may have resulted from a shift in the position of the vortex wake and/or a change in the strength of the wake due to the deployment of the flap. Unfortunately, with the absence of any detailed flowfield measurements of the strength of the vortex wake and its position relative to the blade, one can only infer that a combination of both must have resulted in these interactions. With the  $-17.5^\circ, -20.0^\circ$  peak flap deflections, very little evidence remains of the original BVI observed for the baseline rotor. However, in Figure 34 at  $R_{bar}=0.8214$ , significant changes in the blade surface pressure levels are observed. These changes are attributed to a possible erroneous reading of the lower surface pressures by kulite # 4 (see the pressure signal for kulite # 4 in Figure 35 at  $R_{bar}=0.8214$ ). On the retreating side, increasing the amplitude of the deflection seem to have no direct effect on the strength of the most dominant BVI which occurs near the  $280^\circ$  azimuthal position. (Note the change in scale between the figures)

For an advance ratio of  $\mu=0.2$ ,  $C_T/\sigma = 0.087$  and tip path plane angles of  $2.5^\circ, 4.5^\circ$  aft, similar blade pressure trends were observed for the unflapped and flapped model rotor with  $-12.5^\circ, -17.5^\circ$  and  $-20.0^\circ$  peak deflections.

Figures 36-39 depict respectively the measured surface pressures for the baseline rotor and for the flapped rotor with peak flap deflections of  $-12.5^\circ, -17.5^\circ$  and  $-20.0^\circ$  respectively for a higher forward speed flight condition. For the flapped rotor configurations, a  $-10^\circ$  phase shift from the nominal flap schedules were applied. For these cases, the advance ratio  $\mu$  is 0.199, the tip path plane angle is  $4^\circ$  aft and  $C_T/\sigma = 0.076$ . For the baseline rotor, the advancing blade BVI are evident between the  $20^\circ$  and the  $80^\circ$  azimuthal positions at all four radial stations. For the flapped rotor with  $-12.5^\circ$  peak deflection, it is clear that re-enforcement (due to the increase in the slopes of the pressure time histories) of the advancing BVI have taken place at  $R_{bar} = 0.7522, 0.8214$  with the most dominant interaction taking place between the  $60^\circ$  and the  $80^\circ$  azimuthal positions. At  $R_{bar} = 0.9105, 0.9836$ , a single interaction is seen in the vicinity of the  $50^\circ$  azimuth position. Similarly, for the flapped model rotor with a  $-17.5^\circ$  peak deflection, the number of advancing BVIs has been reduced with an obvious increase in their intensity (note the change of scale). This behavior is also seen for the flapped rotor with a  $-20.0^\circ$  peak deflection. Overall, the peak-to-peak amplitude of the measured pressure signals seem to increase with the increase in the amplitude of the peak deflection. Therefore, for this flight condition, one would therefore expect the BVI noise levels

to increase relative to those of the baseline rotor (i.e., the BVI noise levels using the  $-20.0^\circ$  peak deflection are higher than those using the  $-17.5$ ,  $-12.5^\circ$  peak deflections and, of course, are even higher than those for the baseline rotor). On the retreating side, no evidence in the change of the number and/or intensity of the BVI can be seen as a function of the peak flap deflection angle.

### **6.3.1.3 Effects Of the Phase Shift In Azimuthal Flap Schedule**

Figures 40-44 depict the calculated differential pressures (using the measured individual upper and lower surface pressures) for the baseline rotor and for the flapped rotor with a peak flap deflection of  $-17.5^\circ$  and  $0$ ,  $-5$ ,  $-10$ ,  $-20.0^\circ$  azimuthal phase shift respectively relative to the predicted nominal flap schedule. For these cases, the advance ratio is  $\mu = 0.199$ , the tip path plane angle  $\alpha$  is  $2.5^\circ$  aft and  $C_t/\sigma=0.0865$ . For the baseline rotor, four BVI can be identified between the  $0$  and  $80^\circ$  azimuthal positions at  $R_{bar}=0.7522$ ,  $0.8214$ . For  $R_{bar}=0.9105$ ,  $0.9836$ , a more dominant (due to its impulsiveness) BVI can be seen near the  $60^\circ$  azimuth position. The retreating blade BVI can also be identified in the vicinity of the  $300^\circ$  azimuth position. With the  $-17.5^\circ$  flap deflection and zero phase shift, it is clear that the number of dominant BVIs on the advancing side at  $R_{bar}=0.7522$ ,  $0.8214$  have been reduced to two. At  $R_{bar}=0.9105$ ,  $0.9836$ , the original impulsive BVI near the  $60^\circ$  azimuth can no longer be seen. For the  $-5^\circ$  phase shift, with the exception of the BVI seen at  $R_{bar}=0.7522$  between the  $60$  and  $80^\circ$  azimuthal positions, no evidence of BVI can be seen at the other three radial blade stations. At  $R_{bar}=0.8214$ , the pressure levels are also significantly different from those of the baseline rotor because of a possible malfunction of kulite # 4. For the  $-10^\circ$  phase shift, the character of the differential pressures at  $R_{bar}=0.7522$ ,  $0.8214$  is quite similar with some indication of BVI presence. The peak-to-peak amplitudes near the  $60^\circ$  azimuth at  $R_{bar}=0.9105$ ,  $0.9836$  are also slightly larger than those for the  $-5^\circ$  phase shift. Figures 41-44 also indicate that the strength of the retreating blade BVI is insensitive to the phase shift in azimuth. This, of course, is expected since the implemented flap deployment schedules were meant to only influence the advancing blade BVI by altering the strength of the vortex wake at its point of generation and its trajectory as it convects by the blade.

For an advance ratio of  $0.15$ ,  $C_t/\sigma = 0.076$ , reductions in the number of advancing side BVIs were also seen for tip path plane angles of  $3^\circ$ ,  $5^\circ$  aft and peak flap deflections of  $-12.5^\circ$ ,  $-17.5^\circ$  and  $-20.0^\circ$ . Similar reductions were also seen at an advance ratio of  $0.2$  and a tip path plane angle of  $3^\circ$  aft. However, for a tip path plane angle of  $4^\circ$  aft, though the number of advancing BVIs has also been reduced, their intensity was increased. This increase in intensity will undoubtedly be associated with higher BVI noise levels.

### 6.3.2 Retreating Side BVI

Thus far, we have shown how to reduce the strength, or completely eliminate, the advancing blade BVI. We have succeeded in achieving this goal by implementing flap schedules which affect the strength of the vortex wake at its generation azimuth and/or its trajectory and hence the blade-vortex separation distances at the interaction azimuth. In this section, we present results where our goal was to influence, by reducing the strength or by completely eliminating, the retreating blade BVI. To achieve this goal, one must also attempt to influence the strength of the vortex wake at its generation azimuth. Figures 45, 46 depict respectively the measured upper and lower blade surface pressures for the baseline rotor and for the flapped rotor (peak flap deflection= $-17.5^\circ$ , azimuthal phase shift= $+140^\circ$ ). In these tests, the advance ratio is 0.149, the tip path plane angle  $\alpha$  is equal to  $3^\circ$  aft and  $C_T/\sigma=0.0764$ . In Figure 45 one can clearly identify the retreating side BVI which take place between the  $260^\circ$  and the  $300^\circ$  azimuthal positions with the strongest interaction occurring near the  $280^\circ$  azimuth position, see the pressure signals for kulites 5-8 at  $R_{bar}=0.9105$  and  $0.9836$ . With the deployment of the trailing edge flap, Figure 46 indicates that there has been a considerable reduction in the strength of the retreating blade BVI by virtue of the significantly lower temporal gradients as compared with those for the baseline rotor. The constant reading provided by kulite # 4 on the lower surface of the blade at  $R_{bar}=0.8214$  is an indication of a malfunction in the circuitry of the pressure transducer. On the advancing side, note that there has been a slight increase in the intensity of the BVI with the deployment of the flap (note the different pressure scales in Figures 45, 46).

Figures 47, 48 illustrate respectively the measured upper and lower surface pressures for the baseline rotor and for the flapped rotor (peak flap deflection= $-17.5^\circ$ , azimuthal phase shift= $+140^\circ$ ). For these tests, the advance ratio is  $\mu = 0.199$ , the tip path plane angle  $\alpha$  is equal to  $2.5^\circ$  aft and  $C_T/\sigma=0.0764$ . As seen, with the deployment of this flap schedule, the retreating side BVI at  $R_{bar}=0.7522$ ,  $0.8214$  and  $0.9105$  has been completely eliminated. However, a much weaker retreating side BVI can be seen at  $R_{bar}=0.9836$  near the  $320^\circ$  azimuth. This is in contrast to the four much stronger interactions seen in the vicinity of the  $300^\circ$  azimuth for the baseline rotor. On the advancing side, milder variations in the surface pressures can be seen with the deployment of the trailing edge flap. Again, in Figure 48, the constant reading provided by kulite # 4 on the lower surface of the blade at  $R_{bar}=0.8214$  is an indication of a malfunction in the circuitry of the pressure transducer.

For an advance ratio of  $\mu = 0.2$ ,  $C_T/\sigma = 0.077$ , and tip path plane angles of  $3^\circ$  and  $4^\circ$  aft, significant reductions in the number, as well as intensity, of the retreating side BVIs were observed for the flapped model rotor with  $+140^\circ$  phase shift. In general, the observed reductions in the number of retreating side BVIs were accompanied by minimal changes to the advancing side BVI.

## **6.4 Sample Acoustic Data**

As discussed earlier, acoustic data were obtained using a traversing microphone array (see section 4.4.1.1). The reduced acoustic data presented in this report is based on the on-line data reduction techniques employed by NASA during the wind tunnel test. The microphone signals were digitized at a rate of 1024 16-bit samples per rotor revolution, which corresponds to an approximate sample rate of 18,200 samples per second. The acoustic time histories were acquired for a total of 30 rotor revolutions for each of the 16 microphones of the traversing array. On-line data processing included ensemble-averaged time histories ensemble averaged over 30 revolutions. Narrowband spectra for ensemble-averaged time history as well as single rotor revolution time history were generated. In addition, single rotor revolution spectra were averaged over 30 revolutions to obtain ensemble-averaged spectra. It should be noted that while the ensemble-averaged spectra contain the rotor broadband noise component, it is filtered out in the spectra based on averaged time history.

In order to assess the overall BVI noise reduction achieved using the trailing edge flap, the acoustic results are presented here in three formats. These are;

- noise contour plots (over the microphone traverse plane) using the BVI noise metric BVISPL, which is based on the sum of the energy contained in the narrowband spectra between the 5th and the 40th harmonics (frequency range dominated usually by BVI noise),
- ensemble-averaged time histories and,
- ensemble-averaged narrowband noise spectral data.

The BVISPL contour plots are based on the spectra of averaged time histories and therefore do not include the rotor broadband noise component. These contour plots, however, show the effect of flaps on the harmonic BVI noise and its directivity. The averaged time histories and the ensemble-averaged narrowband spectra are presented only for some of the microphones which are located at microphone traverse station 9, as shown schematically in Figure 15. Since the locations of these microphones generally correspond to the max BVI lobe position, the acoustic information furnished through these microphones is considered to be fairly accurate in assessing the effectiveness of the trailing edge flap in reducing the rotor BVI noise. Because the reduced acoustic data presented here are from the on-line data, it was not possible to correct the variations in the Y-axis scale limits between the different time history plots presented here.

### **6.4.1 Advancing Side BVI**

#### **6.4.1.1 Effect of Trailing Edge Flap Deployment**

Figures 49a and 49b, show the contour plots respectively for the rotor baseline and the flapped rotor with  $-12.5^\circ$  peak flap deflection and  $-20^\circ$  phase azimuthal shift from the predicted nominal schedule. The rotor operating conditions for this

case are; advance ratio,  $\mu=0.1488$ , tip path plane angle,  $\alpha=5^\circ$  aft, and  $Ct/\sigma=0.0765$ . As shown, the flap deployment on the rotor advancing side reduced the max BVI noise lobe by more than 5 dB. The corresponding BVISPL values for the rotor retreating side were reduced by a very small amount.

Figures 50a and 50b, illustrate the acoustic time histories for mics 9 to 12 (see Figure 15) which are located on the rotor advancing side for the baseline and the flapped rotor respectively. Clearly, the time histories for the baseline rotor show a stronger 4-per-rev impulsive BVI signal compared with the flapped rotor results. Also, despite of lack of significant reduction in amplitude of the signal between the baseline and the flapped rotor, the BVI characteristics of the time histories for the baseline are much more acoustically impulsive in nature.

Figures 51a and 51b, show the ensemble-averaged narrowband noise spectra at the same microphone locations selected for the time history plots for the baseline and for the flapped rotor respectively. It is shown that the harmonic content of the noise spectra for the baseline rotor is higher compared with the corresponding spectral data for the flapped rotor. For the baseline spectra data, the mid-range frequencies, where the BVI noise is normally dominated, is higher by as much as 10 dB (maximum). Also, as shown in the spectra for the flapped rotor (Figure 51b), the sound pressure levels associated with the first few harmonics have been increased significantly (by 8-10 dB) for the flapped rotor relative to the baseline. The narrowband spectra also reveal that the flap deployment has increased the high frequency (>3 kHz) broadband noise levels by about 2 to 4 dB. The increase in the noise levels in the first few harmonics for the flapped rotor could be due to an increase in low frequency unsteady airloads given the rotor trim conditions remained unchanged relative to the baseline rotor. The broadband noise increase could be due to the vortices shed from the separated flow behind the deflected flap.

Figures 52a, 52b and 53a, 53b show pressure time histories and spectral data respectively for the baseline and flapped rotors at the retreating side microphone locations (mics 1 - 4, see Figure 15). Clearly, the flap deployment on the advancing side had very little influence on acoustic data at these microphone locations.

Sample contour plots are also presented where the BVISPL was computed from the ensemble-averaged narrowband spectra and therefore contain the additional rotor broadband noise component in the frequency range between the 5th and 40th harmonics. Figures 54a and 54b show the contour plots based on BVISPL computed from ensemble-averaged narrowband spectra and spectra based on averaged time history for the baseline rotor. Figures 55a and 55b show similar contour plots for the flapped rotor with  $-12.5^\circ$  peak flap deflection and nominal phase setting. The test conditions for these plots are; advance ratio,  $\mu=0.1987$ , tip path plane angle,  $\alpha=2.5^\circ$  aft, and  $Ct/\sigma=0.0868$ . As seen, on the advancing side, the inclusion of the broadband noise component has increased the max BVISPL lobe



by approximately 2 dB for the baseline and flapped rotors. However, no noticeable change in the max BVI lobe on the retreating side is observed. Since, both the baseline and the flapped rotor results increased by similar amounts, the assessment of the BVI noise reductions provided in this report is thus accurate in establishing the effectiveness of the trailing edge flap in reducing the rotor BVI noise. In fact, a comparison of Figures 54a and 55a show noise reduction on the order of 3 to 4 dB in the maximum BVI lobe even when the broadband noise component is included in the BVISPL estimation. It should also be noted that there are some test conditions where the flap deployment has increased BVI and the high frequency broadband noise levels, as will be discussed later.

#### **6.4.1.2 Effect of Peak Deflection Amplitude**

Figures 56a-c, show the BVISPL contour plots for the baseline and the flapped rotor configurations (with peak flap deflections of  $-12.5^\circ$  and  $-17.5^\circ$ ) respectively. For the flapped rotor with a peak deflection angle of  $-12.5^\circ$ , a  $-10^\circ$  azimuthal phase shift from the nominal flap schedule was used while for the  $-17.5^\circ$  peak deflection, an azimuthal phase shift of  $-5^\circ$  from the nominal schedule was used. For these cases, the advance ratio is  $\mu=0.1492$ , tip path plane angle is  $\alpha=3^\circ$ , and  $C_t/\sigma=0.0773$ . As shown, there is a reduction of 3-4 dB in the maximum BVISPL for the  $-12.5^\circ$  schedule and about 1-2 dB for the  $-17.5^\circ$ . As for the retreating side, there is virtually no significant changes in the BVISPL values from those of the baseline rotor for all the schedules presented here.

Figures 57a-c, illustrate the acoustic time histories for the microphone locations in the vicinity of the maximum BVISPL lobe (i.e., mics# 9 - 12; see Figure 15) for the baseline and flapped (with  $-12.5^\circ$ ,  $-17.5^\circ$  peak flap deflections) rotors respectively. Clearly, the depicted time histories for the baseline are more impulsive in nature in terms of pulse width and amplitude as compared to the flapped rotor data. Also, as shown in Figures 57b and 57c, there are some changes in pulse shape from semi-impulsive for the baseline rotor to a broader signal due to the flap deployment. As a result, a reduction in the BVI noise in the mid-range frequency is observed in the noise spectra as depicted in the Figures 58a-c. From these noise spectra, it is also observed that the rotor broadband noise levels were increased by as much as 4-5 dB for the flapped rotor as compared to the baseline rotor. It should be mentioned here that it is not possible to provide any tangible technical discussion pertaining to the details of the broadband noise source(s) without performing further analyses.

For the test condition considered, the increase in the peak flap deflection angle did not significantly affect the noise data, although from the contour plots, one can deduce that the  $-12.5^\circ$  flap deflection produced slightly larger BVI noise reductions than the  $-17.5^\circ$  flap deflection. This observation, however, is not totally supported by the limited spectral data shown.

For completeness, in order to truly assess the effectiveness of all flap schedules employed in the wind tunnel test to reduce the rotor BVI noise, we now present a set of acoustic data for a test condition where flap deployment, in combination with some azimuthal shift (e.g.,  $-10^\circ$ ) increased the BVI noise. Figures 59a-d illustrate the contour plots for the baseline rotor and for the flapped rotor for peak flap deflections equal to  $-12.5^\circ$ ,  $-17.5^\circ$ , and  $-20^\circ$  respectively. For these cases, the advance ratio is  $\mu=0.199$ , the rotor shaft angle  $\alpha=4^\circ$  aft and  $Ct/\sigma=0.0764$ . As seen, the maximum BVI lobe on the rotor advancing side has increased by 3 to 10 dB due to the deployment of the flap for all the flap. On the retreating side, with the exception of the  $-17.5^\circ$  schedule where the BVISPL actually increased by 4 dB, there was no significant changes in the BVI noise intensity for the flapped rotor.

Figures 60a-d depict the measured time histories for the baseline and the flapped rotor (mics 9 - 12) with peak flap deflection of  $-12.5^\circ$ ,  $-17.5^\circ$ , and  $-20^\circ$  (azimuthal phase shift of  $-10^\circ$ ) respectively. Noting that the plot scales are different, all the depicted time histories are impulsive in nature illustrating clearly 4-per-rev BVI type pulses. The peak-to-peak pressure values for all the flap schedules considered here are significantly higher. This confirms the adverse effects of the trailing edge flap on the BVI noise attenuation (an average increase of 100%) for this particular rotor flight condition. Figures 61a-d illustrate the sound pressure level spectra for the baseline and flapped rotors. As observed in these spectra, consistent with the time histories and the contour plots, the harmonic content in the baseline data is detectable up to 1200 Hz as compared to the 2000 Hz for the flapped rotor. Also the harmonic noise and broadband noise are significantly higher for the flapped rotor test cases. Overall, it is obvious that the flap deployment for this rotor flight condition has adversely affected the BVI noise. Additional detailed analysis is needed to determine the reasons behind the increase in BVI with flap deployment for this test condition.

#### **6.4.1.3 Effect of the Phase Shift in Azimuthal Flap Schedule**

Figures 62a-e, illustrate the contour plots respectively for the baseline and flapped rotors with peak flap deflection of  $-17.5^\circ$  and azimuthal phasing of 0 (nominal),  $-5^\circ$ ,  $-10^\circ$  and  $-20^\circ$ . The test conditions for this data are; advance ratio,  $\mu=0.199$ , tip path plane,  $\alpha=2.5^\circ$  aft, and  $Ct/\sigma=0.0896$ . It is shown that the flap deployment on the advancing side reduced the max BVI noise lobe by 2 dB without any significant effects on the retreating side BVI noise intensity. Shifting the cam from  $0^\circ$  to  $-20^\circ$  from the nominal, further reduced the max BVISPL noise lobes by 4 dB as well as reducing the max BVI lobe domain, see Figures 62b-e. Note that similar phase variations in the use of higher harmonic control [7] have resulted in optimizing the maximum BVI noise reduction.

Figures 63a and 63b, depict the measured acoustic time histories for the baseline and flapped rotor with  $-10^\circ$  phase shift. The time histories are shown only for mics.

9 - 12 which are located on the rotor advancing side. In comparing the baseline data with that for the flapped rotor, it is clear that despite the mismatch in the y-scale of the plots, the baseline acoustic time histories are more impulsive in nature and a clear 4-per-rev BVI signal can be detected. Also, a reduction in peak-to-peak sound pressures is achieved with the flapped rotor by as much as 30% in comparison with the baseline data. The time histories support the results presented in the contour plots.

In order to assess the benefits associated with the flap azimuthal phasing, the measured noise spectra for the baseline and flapped rotor ( $-17.5^\circ$ ) with 0 (nominal) and  $-10^\circ$  azimuthal shift are compared in Figures 64a-c respectively. As shown, in a progressive fashion, the harmonic content of the noise spectra has been reduced from 2600 Hz for the baseline rotor to 800 Hz for the flapped rotor with a  $-10^\circ$  phase shift. However, whereas there is a clear reduction in the sound pressure levels at the blade passage frequency for the flapped rotor, the rotor broadband noise level was noticeably increased by 3 to 4 dB at frequencies above 2000 Hz. In addition, the first few noise harmonics (i.e. up to the 3rd) increased by as much as 6 dB for the flapped rotor as compared to the baseline rotor, see Figures 64a-c.

#### 6.4.2 Retreating Side BVI

Figures 65a and 65b depict contour plots for the baseline and for the flapped rotor (peak flap deflection  $=-17.5^\circ$ , azimuth phase of  $+140^\circ$ ) respectively for an advance ratio,  $\mu=0.1492$ , tip path plane angle,  $\alpha=3^\circ$  aft and  $Ct/\sigma=0.0764$ . Pre-test predictions have shown that the azimuthal phase shift of  $+140^\circ$  relative to the nominal schedule selected for advancing side BVI noise reduction may affect the tip vortex generated in the rotor third quadrant and hence the retreating side BVI noise. As shown in these figures, the maximum BVISPL lobe on the rotor retreating side has been reduced by as much as 4 dB, whereas on the advancing side the noise levels in maximum BVI lobe have increased by as much as 4 to 5 dB.

In order to accurately assess the impact of the trailing edge flap, the acoustic time history results are presented in Figures 66a and 66b for mics 5 - 8. These microphones are located in the vicinity of the maximum BVI lobe, see Figure (15). As shown, it is clear that there is a moderate reduction in the peak-to-peak sound pressures for the flapped rotor configuration (by up to 30 to 40%). There is a general 4-per-rev nature to the signature for the baseline rotor, but there is a lack of clear impulsive BVI signal for the flapped rotor. In contrast, the noise signatures for mics 9 - 11 (Figures 67a and 67b) which are located on the rotor advancing side are clearly more impulsive for the flapped rotor as compared to the baseline rotor. In addition, there is a significant increase in the peak-to-peak sound pressures for the flapped rotor by as much as 400%. A consistent trend is also observed from the measured narrowband noise spectra for these microphones, see Figures 68a, 68b and Figures 69a, 69b. In the noise spectra for mics 5 - 8, the sound harmonics levels are higher and more distinguishable for the noise spectra corresponding to

the baseline rotor versus the flapped rotor. It appears that the noise spectra located on the rotor advancing side are also contaminated with somewhat stronger high frequency broadband noise. As a result, a typical broadband noise hump is clearly visible in the spectra for mics 9 - 12, Figures 69a and 69b.

Figures 70a and 70b, depict the contour plots for baseline and flapped rotors with  $-17.5^\circ$  flap schedule and  $+140^\circ$  azimuth phase shift at an advance ratio  $\mu=0.1987$ , tip path plane  $\alpha=2.5^\circ$  aft, and  $Ct/\sigma=0.086$ . The overall trend observed for this rotor test condition is very similar to the one observed for the lower  $Ct/\sigma$  and the 0.1492 advance ratio discussed above, where the max BVI noise level has been reduced on the rotor retreating side by about 6 dB and increased on the advancing side by about 2 dB, see Figures. 70a and 70b. Figures 71a and 71b show the reductions in the peak-to-peak sound pressures from those of the baseline rotor at microphones 5 - 8. Figures. 72a and 72b depict a clear 4-per-rev BVI noise signature with an increase (by as much as 100%) in the peak-to-peak sound pressures for the flapped rotor on the advancing side. The corresponding narrowband noise spectra (mics 5 - 12) for the baseline versus the flapped rotor is somewhat mixed with no noticeable reduction for mics 9 - 12 on the advancing side, but a more clear reduction for the mics 5 - 8 on the retreating side, see Figures. 73a, 73b and Figures 74a, 74b.

In summary, the preceding discussion showed, through sample plots of measured acoustic data, that the flap deployment, and in particular the peak deflection angle and azimuthal shift can produce BVI noise reductions of the order of 6 dB on the advancing and retreating sides. However, it is often accompanied by increases in low frequency harmonic noise and high frequency broadband noise. We have also shown that for certain test conditions, most notably for  $\mu=0.2$  and  $Ct/\sigma=0.076$ , that the BVI noise levels increased with the deployment of the flap. It should be noted that most of the conclusions reached here are based on limited acoustic data. A more comprehensive analysis of the data should be conducted to establish more clearly the effects of the trailing edge flap on BVI noise.

## **6.5. Effects Of Acoustic Cams On Power Required**

The deflection of the flap for acoustic noise reduction, vibration reduction or performance improvements added additional power requirements to the rotor. These requirements came from two sources, the mechanical power required to operate the flap actuation mechanism, and the power required to overcome the aerodynamic drag of the deflected flap.

The torque required by the rotor and active flap actuation system was measured with strain gauges on the drive shaft. The cam for the flap actuation system was held stationary by a nonrotating standpipe, which ran up the center of the drive shaft. The standpipe torque was measured with strain gauges and represented the torque required to actuate the active flaps. The difference between the drive shaft torque and the standpipe torque was the torque delivered to the rotor itself.

Hover results showed that at  $C_t/\sigma = 0.04$ , a  $23.5^\circ$  nonharmonic active flap deflection configuration rotor in hover required 79% more power to operate, while the flap actuation mechanism added an additional 7% to the power required. The power increment due to the active flap deflection for the  $20.0^\circ$  nonharmonic deflection ranged from 10% to 30% in hover, while for the  $17.5^\circ$  nonharmonic deflection profile it ranged from 7% to 12% in hover.

In forward flight, for descent conditions of  $C_t/\sigma = 0.0762$  and  $(\mu = 0.15)$ , the power increment due to the  $17.5^\circ$  nonharmonic deflection profile was 21%. The baseline rotor with no flap deflection at this condition required 36.3 HP while the rotor with  $17.5^\circ$  nonharmonic flap deflection required 42.8 HP. An examination of all descent data showed power increases of from 11% to 24% for the  $12.5^\circ$  flap, from 21% to 57% for the  $17.5^\circ$  flap, and from 33% to 76% for the  $20^\circ$  flap.

Figure 75 shows the measured power required for the model rotor at a descent flight condition ( $\mu=0.20$ ,  $C_t=0.008$ ) and a cruise flight condition ( $\mu=0.30$ ,  $C_t=0.008$ ). The data for the descent flight condition is shown for the baseline rotor (i.e., with the flap in the neutral position) and for the active flap rotor with peak flap deflections equal to  $-20^\circ$ ,  $-17.5^\circ$  and  $-12.5^\circ$ . and phase angles equal to  $0^\circ$ ,  $-20^\circ$  and  $+140^\circ$ . Although there is a penalty in power to pay for noise reduction, in a descent or heliport approach flight profile, the power required for cruise is higher, see Figure 75. Thus, excess power is available for this noise reduction technique in the flight regimes where noise reduction is needed.

## 7.0 Conclusions

This model rotor wind tunnel test demonstrated that BVI noise reduction and vibration reduction were possible with an active flap. Results from the performance deflection profiles were inconclusive. The test program demonstrated the mechanical operation of a model rotor with an active flap operating at up to 105 Hz. Over 100 hours of operation on this rotor system were achieved during the test program. Aerodynamic results supported the acoustic data trends, showing a reduction in the strength of the tip vortex with the deflection of the flap. Acoustic results showed, that the flap deployment, depending upon the peak deflection angle and azimuthal shift in its deployment schedule, can produce BVI noise reductions as much as 6 dB on the advancing and retreating sides. The noise reduction is often accompanied by an increase in low frequency harmonic noise and high frequency broadband noise. For certain test conditions, most notably  $\mu=0.2$  and  $C_t/\sigma=0.076$ , the BVI noise levels increased with flap deployment. A brief assessment of the effect of the flap on vibration showed that significant reductions were possible. The greatest vibration reductions were found in the four per rev pitching moment at the hub. Up to 76% reduction was measured at  $\mu = 0.30$ , and  $C_t = 0.006$ . Performance improvement cam results were inconclusive, as the improvements were predicted to be smaller than the resolution of the rotor balance. The test program accomplished all of the goals established at the onset of the program.

## 8.0 References

1. Thompson, P., Neir, R., Reber, R. Scholes, R., Alexander, H., Sweet, D., Berry, D. "Civil Tiltrotor Missions and Applications Phase II: The Commercial Passenger Market," NASA CR 177576, February 1991.
2. Hoad, Danny R., "Helicopter Model Scale Results of Blade-Vortex Interaction Impulsive Noise as Affected by Tip Vortex Modification," 36th Annual Forum Proceedings, American Helicopter Society Inc., May 1980, pp. 80-62-1-80-62- 13.
3. Martin, R.M., and Connor, Andrew B., "Wind-Tunnel Acoustic Results of Two Rotor Models With Several Tip Designs," NASA TM-87698, 1986.
4. Carlin, G., and Farrance, K., "Results of Wake Surveys on Advanced Rotor Planforms," 46th Annual Forum Proceedings, American Helicopter Society Inc., Vol 2, May 21-23, 1980.
5. Hardin, J.C. and Lamkin, S.L., "Concepts for Reduction of Blade-Vortex Interaction Noise," AIAA Journal of Aircraft, Vol. 24, No. 2, February 1987.
6. Pegg, Robert, J., Hosier, Robert N., Balcerak, John C., and Johnson, Kevin H., "Design and Preliminary Tests of a Blade Tip Air Mass Injection System for Vortex Modification and Possible Noise Reduction on a Full-Scale Helicopter Rotor," NASA TMX-3314, December 1975.
7. Brooks, F. Thomas, Booth, Earl R., Jolly, Ralph J., Yeager, William, T., and Wilbur, Matthew L., "Reduction of Blade-Vortex Interaction Noise Using Higher Harmonic Pitch Control," NASA TM 101624, July 1989.
8. Childress, O. S., "Helicopter Noise Reduction Program - 1989" NASA CP10047, July 1990.
9. Lemnios, A.Z., and Howes, H.E., "Wind Tunnel Investigation of the Controllable Twist Rotor Performance and Dynamic Behavior," USAAMRDL TR 77-10, June 1977.
10. Wei, Fu-Shang, and Jones, Robert, "Correlation and Analysis for SH-2F 101 Rotor," AIAA Journal of Aircraft, Vol. 25, No. 7, July 1988.
11. Charles, B.D., Tadghighi, H., and Hassan, A.A., "Effects of a Trailing Edge Flap on the Aerodynamics of Rotor Blade-vortex Interactions", DGLR/AIAA 14th Aeroacoustics Conference, May 11-14, 1992, Aachen, Germany.
12. Lorber, P. F., "Blade-Vortex Interaction Data Obtained From A Pressure-Instrumented Model Rotor At The DNW," AHS/RAS International Technical Specialist Meeting on Rotorcraft Acoustics and Rotor Fluid Dynamics, Philadelphia, PA, October 1991.

## 8.0 References (cont'd)

13. Hassan, A.A., Tadghighi, H., and Charles, B.D., "Aerodynamics and Acoustics of Three-Dimensional Blade-Vortex Interactions," NASA CR 182026, July 1990.
14. Boxwell, D.A., Schmitz, F.H., Splettstoesser, W.R., and Schultz, K.J., "Helicopter Model Rotor-Blade Vortex Interaction Impulsive Noise: Scalability and Parametric Variations," Journal of the American Helicopter Society, Vol. 32, No. 1, January 1987.
15. Hassan, A.A., Charles, B.D., Tadghighi, H., and Sankar, L.N., "Blade Mounted Trailing Edge Flap Control for BVI Noise Reduction," NASA CR 4426, February 1992.
16. Straub, F.K., and Robinson, L.H., "Dynamics of a Rotor with Nonharmonic Control," Proceedings of the American Helicopter Society 49th Annual Forum, St. Louis, MO, 19-21 May, 1993.
17. Hassan, A.A., and Charles, B.D., "Simulation of Realistic Rotor Blade Vortex Interactions Using a Finite-Difference Technique," Journal of the American Helicopter Society, Vol. 31, No. 3, pp 71-81, July 1991.
18. Brentner, K.S., "Prediction of Helicopter Rotor Discrete Frequency Noise, - A Computer Program Incorporating Realistic Blade Motions and Advanced Acoustic Formulation," NASA TM-87721, October 1986.
19. Ffowcs Williams, J. E., and Hawkings, D.L., "Sound Generated by Turbulence and Surfaces in Arbitrary Motion," Philos. Trans. Roy. London, Ser. A, Vol. 264, no. 1151, May 8, 1969, 321-342.
20. Farassat, F., and Succi, G. P., "The Prediction of Helicopter Rotor Discrete Frequency Noise," Vertica, Volume ,7 No. 4, 1983, pgs 309-320.
21. "ADAMS Reference Manual, Version 6.0," Mechanical Dynamics, Ann Arbor, MI, Nov. 1991.
22. Heyson, H. H., "Use of Superposition in Digital Computers to Obtain Wind Tunnel Interference Factors for Arbitrary Configurations," NASA TR R-302, Feb. 1964.





Figure 1. Active Flap Rotor and Test Stand at NASA Langley 14 x 22 Foot Subsonic Wind Tunnel

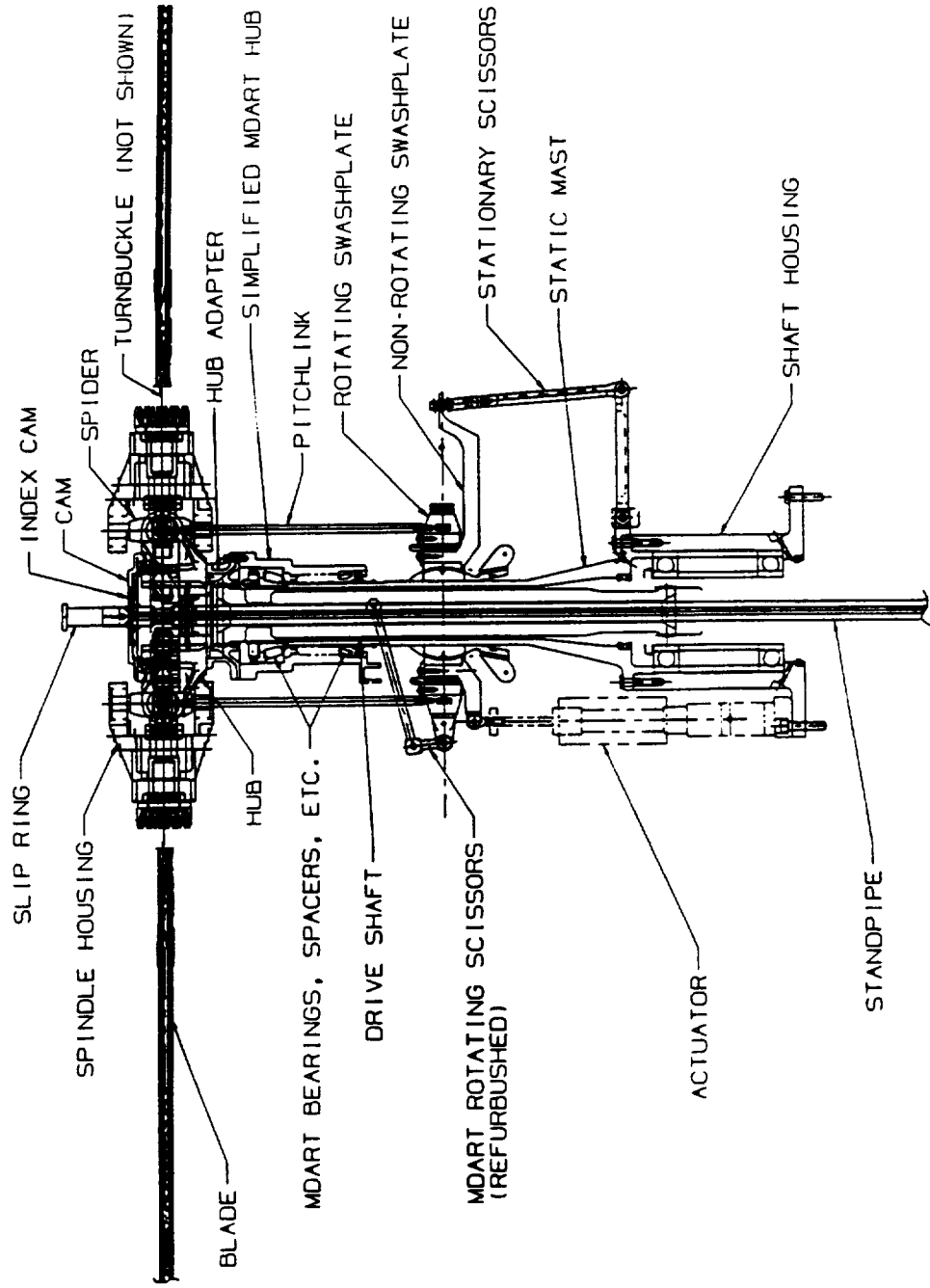
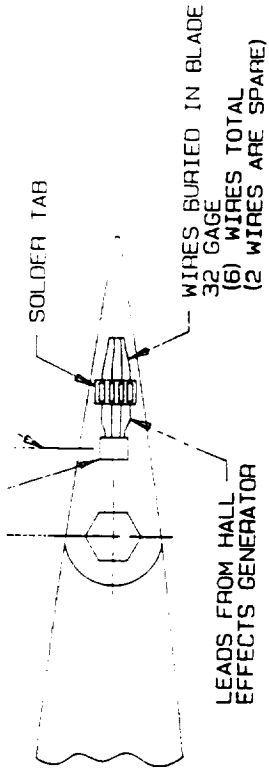


Figure 2. Schematic of Active Flap Model Rotor Hub and Rotor Mast.



**SECTION @ STA. 58.50 LOOKING INBOARD**

SCALE: 2/1  
(SECTION ROTATED 90°)

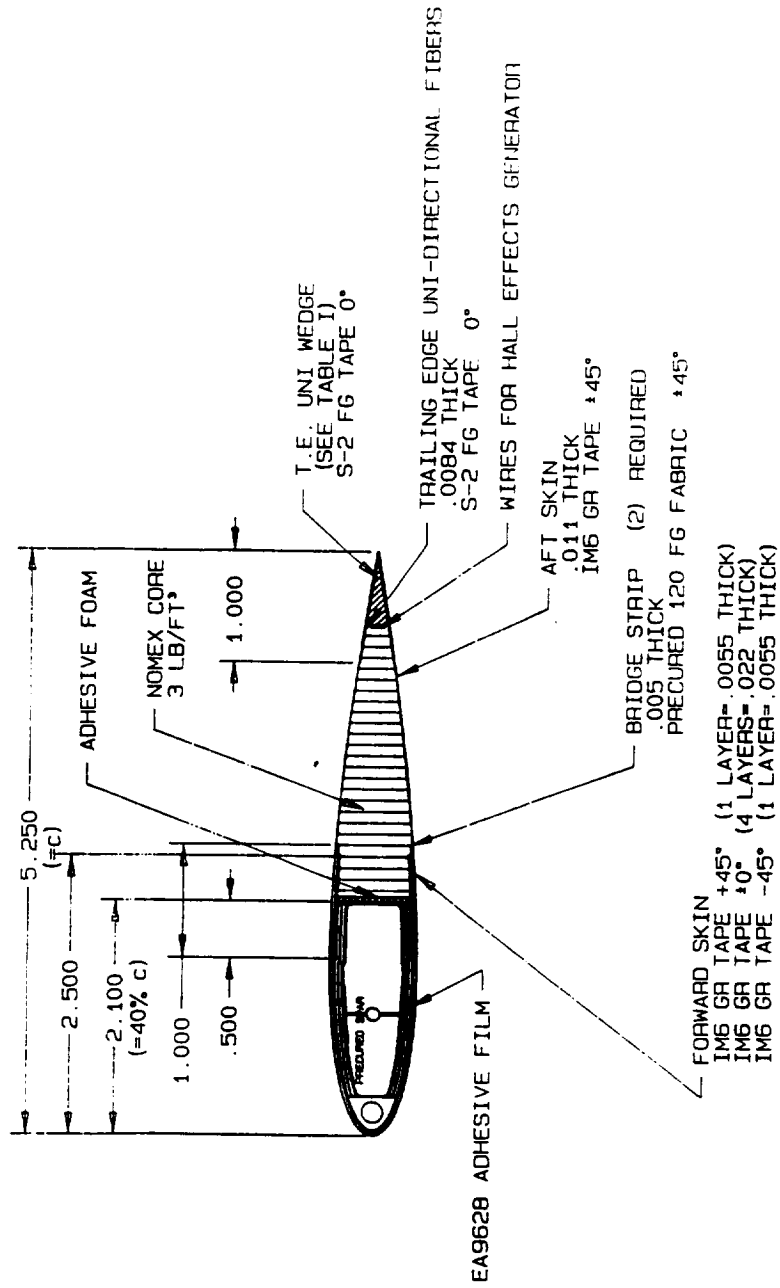


Figure 3. Cross Section of Active Flap Model Rotor Blade.

Blade Instrumentation	
Item	Radial Station [in]
flap, lag, torsion strain gauges	23.69
flap, lag strain gauges	50.40
pressure transducers	54.72
pressure transducers	59.76
pressure transducers	66.24
pressure transducers	70.56

Rotor Data and Geometry		
no. of blades	$N$	4
rotor radius	[in] $R$	72.75
rotor speed	[rpm] $\Omega$	1087
chord	[in] $c$	5.25
Lock number	$\gamma$	2.2
solidity	$\sigma$	0.092
linear twist	[deg] $\theta_{tw}$	-9
flap chord	$c_f/c$	0.25
flap.lag hinge	$r_\beta/R, r_\gamma/R$	.0825
feather bearing	$r_\theta/R$	.1409
blade pins	$r_{bp}/R$	.2016
root cutout	$r_a/R$	.2500
flap inboard	$r_1/R$	.7937
flap outboard	$r_2/R$	.9729
pitch horn arm	[in] $x_{ph}$	4.6648
damper arm	[in] $x_d$	4.4665

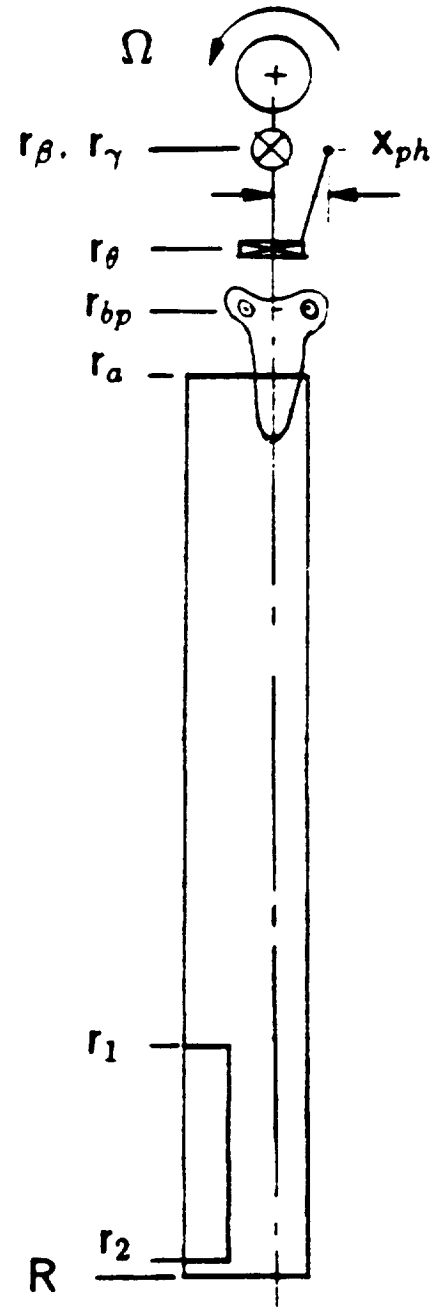


Figure 4. Strain Gauges and Pressure Transducer Locations.

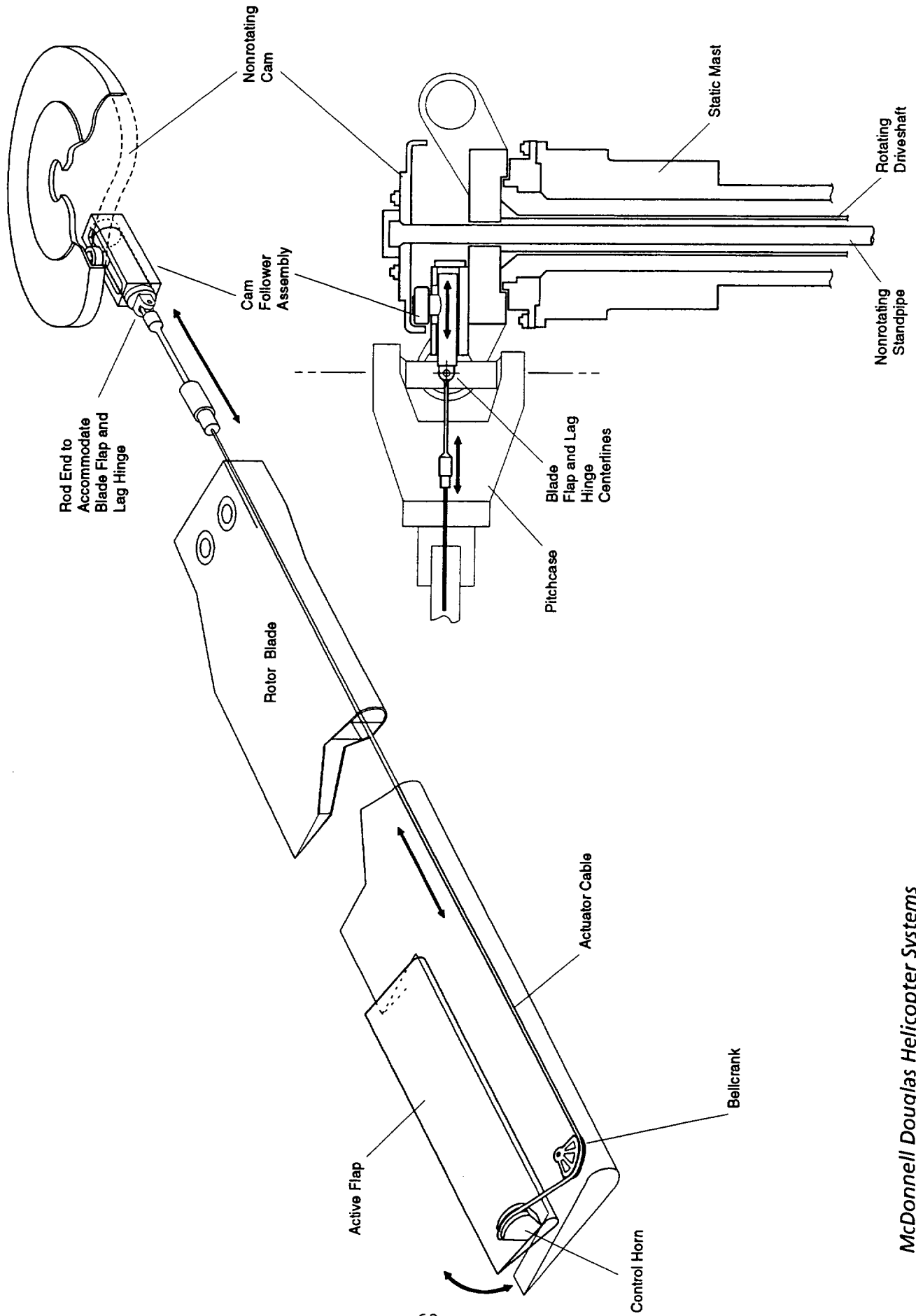


Figure 5. Flap Actuation Mechanism.

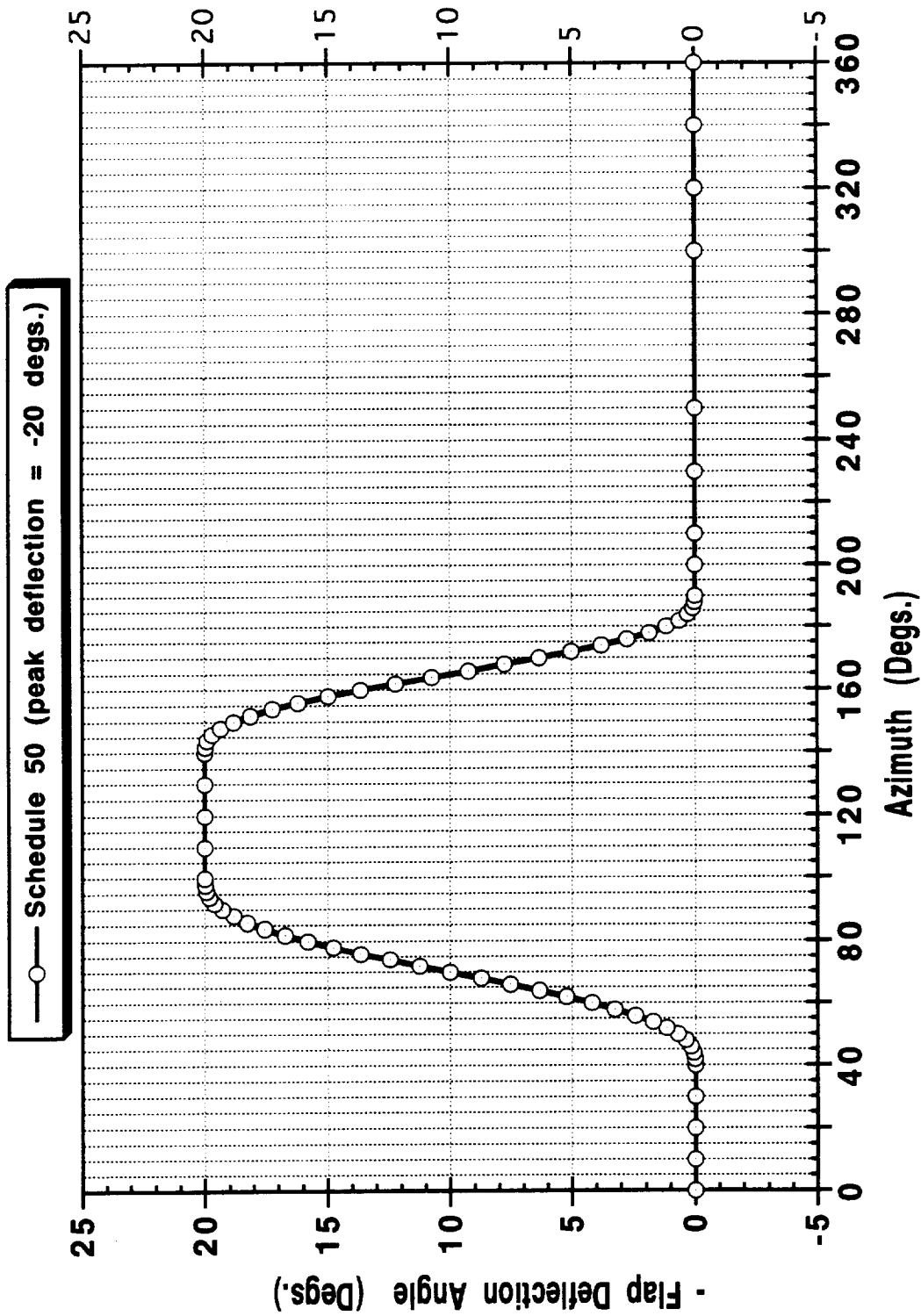


Figure 6. Typical BVI Noise Reduction Active Flap Deflection Profile Versus Azimuth Position.

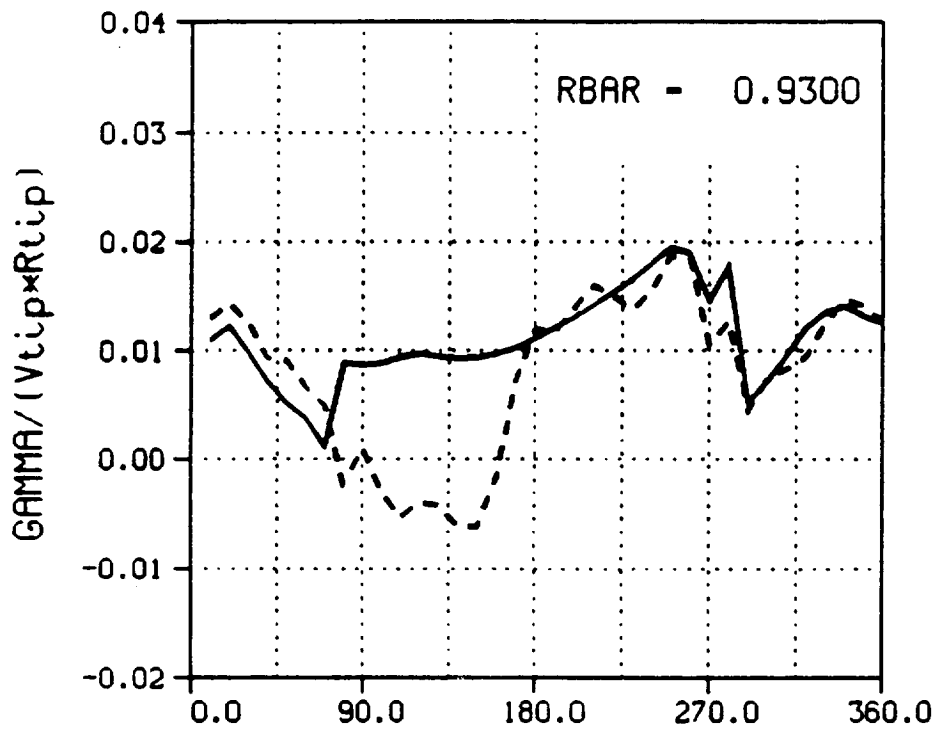


Figure (7) CAMRAD/JA Results. Bound Circulation versus Azimuth Position.  $\mu = 0.15$ ,  $C_t = 0.007$ ,  $r/R = 0.93$ . Solid Line is Baseline Rotor, Broken Line is Schedule 50 (20° Cam) Active Flap Deflection.

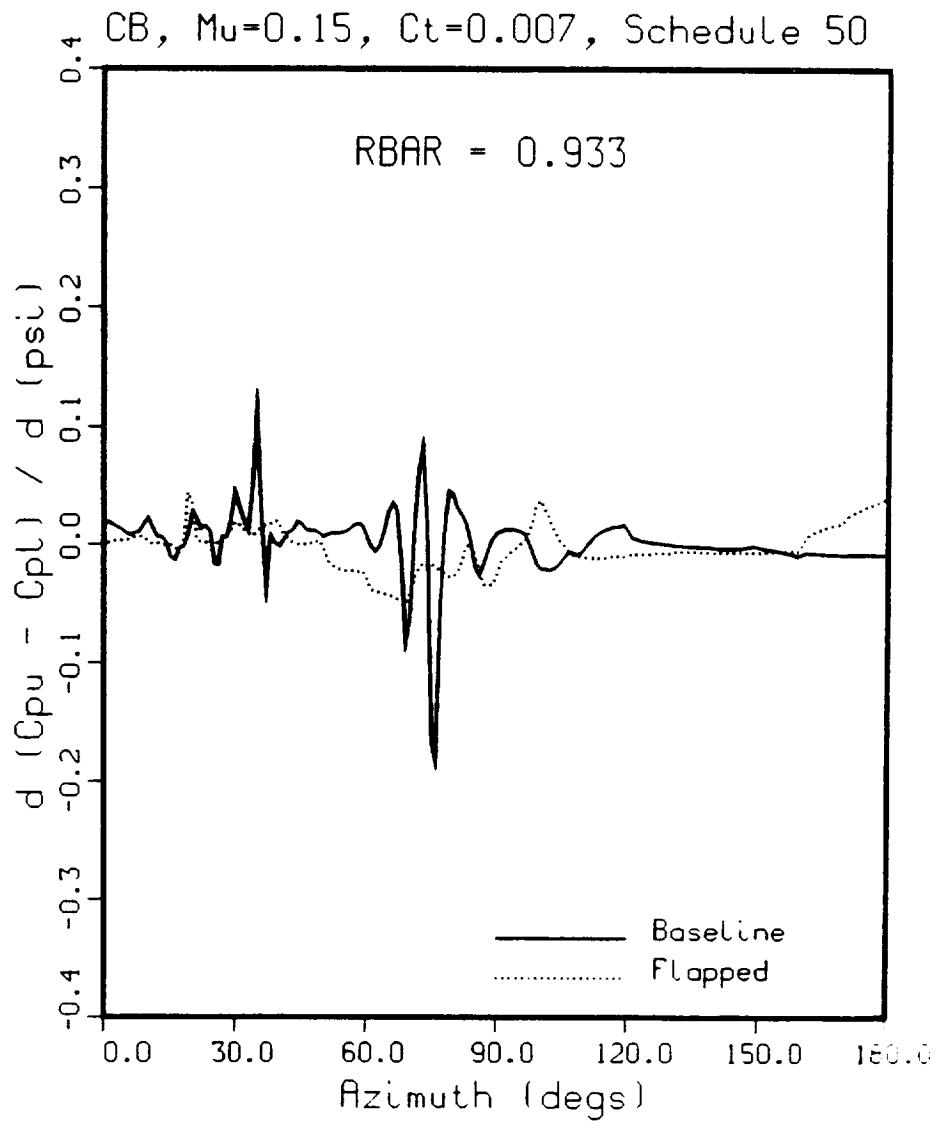


Figure (8) Typical RFS2.BVI Results. Temporal Differential Pressure Gradients Near Blade Leading Edge versus Azimuth.  $\mu = 0.15$ ,  $C_t = 0.007$ .  $r/R = 0.93$ . Solid Line is Baseline Rotor, Broken Line is Schedule 50 (20° Cam) Active Flap Deflection.



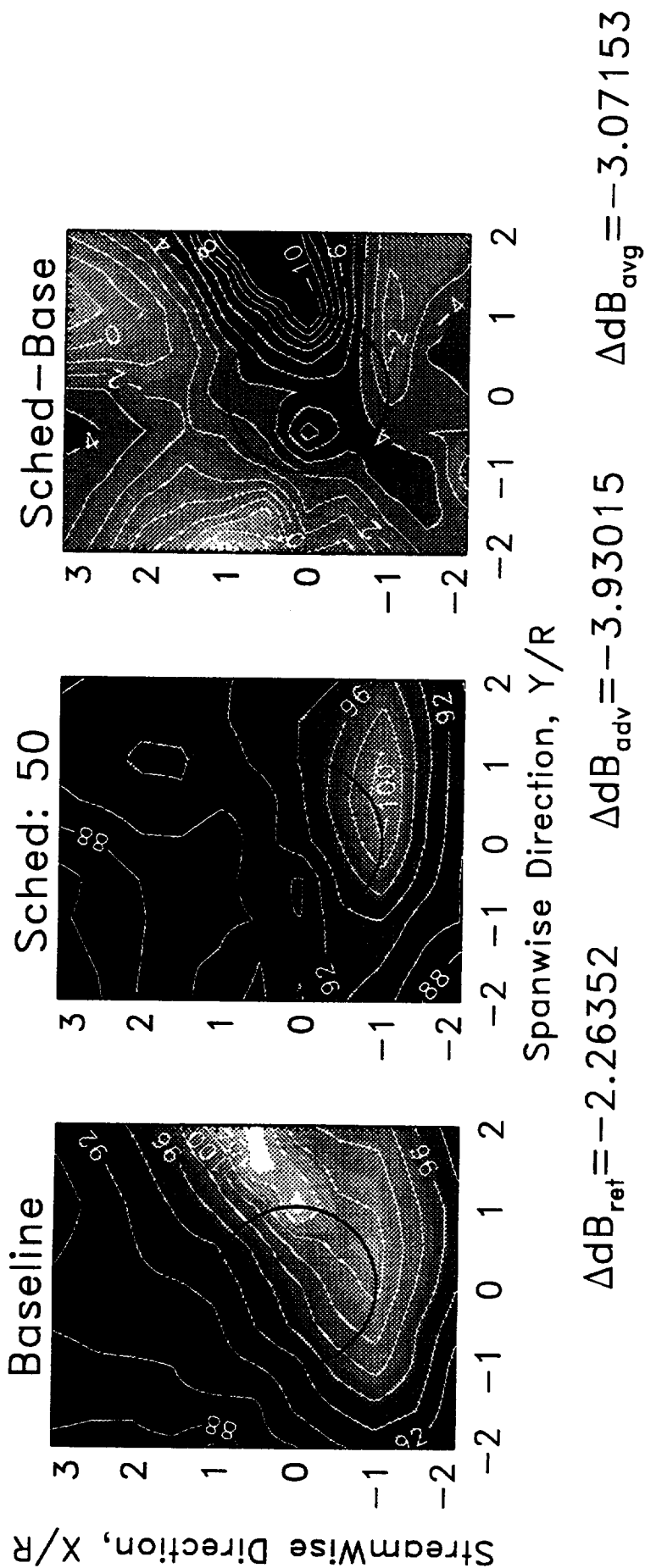


Figure (9) Typical WOPWOP Results. BVI Sound Pressure Level in dB Two Rotor Radius Under Rotor.  $\mu = 0.15$ ,  $C_t = 0.007$ ,  $r/R = 0.93$ . Baseline Rotor Data; Schedule 50 (20° Cam) Active Flap Deflection Rotor Data; and Difference Between Baseline and Schedule 50 Is Shown.

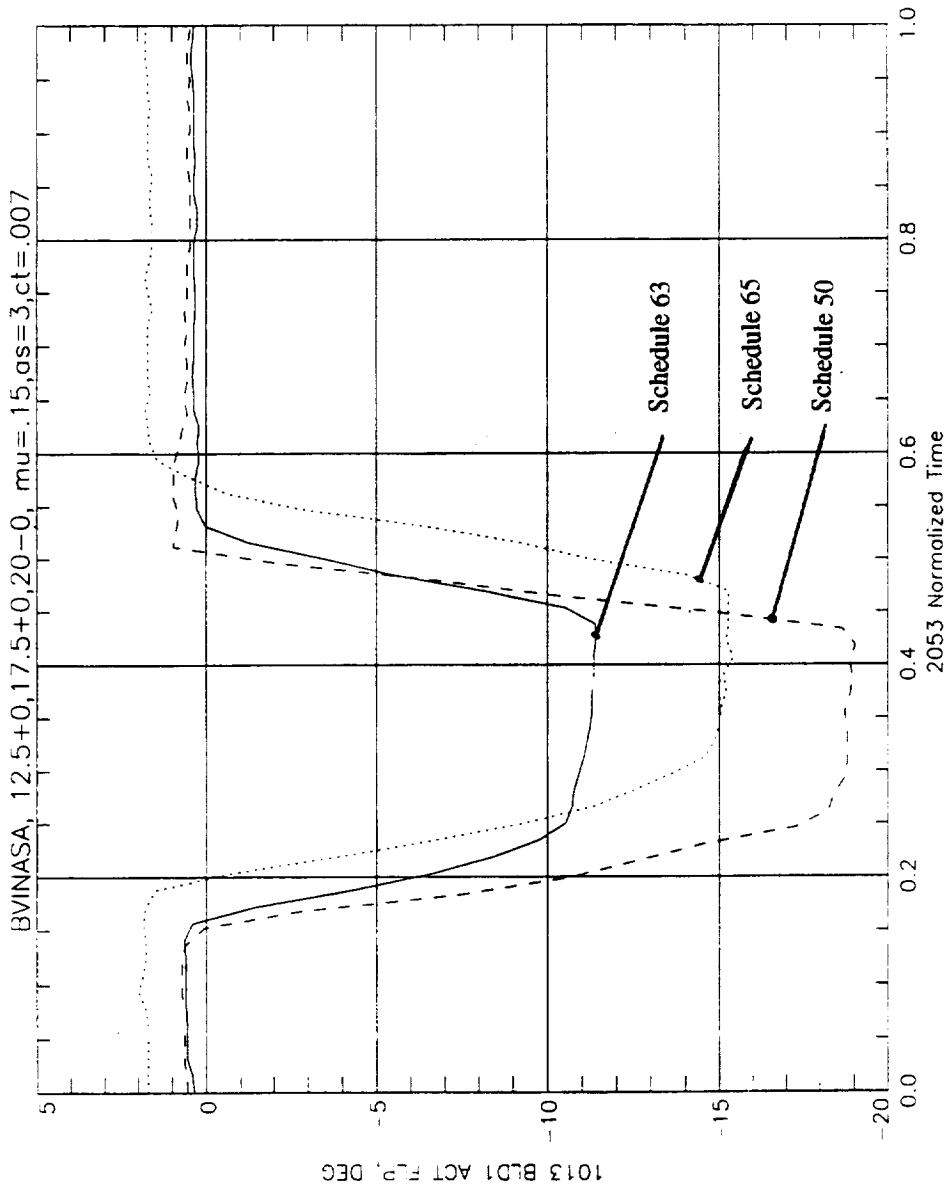
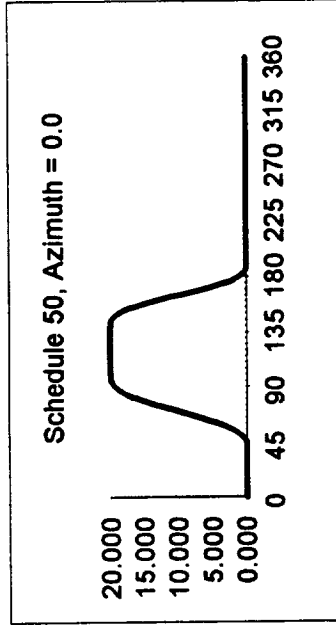
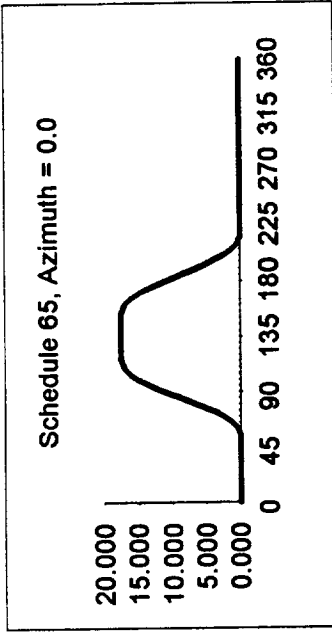
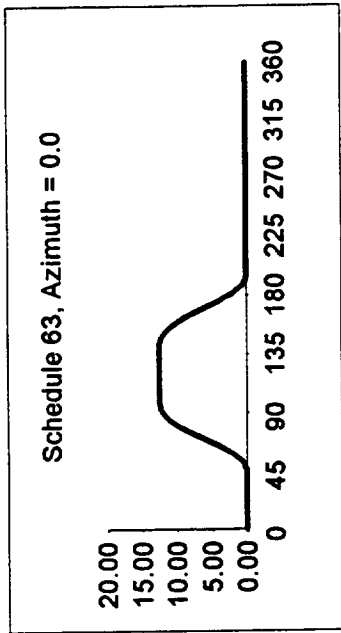


Figure (10a) Desired and Measured Flap Deflection Versus Azimuth Position For Acoustic Cam Profiles

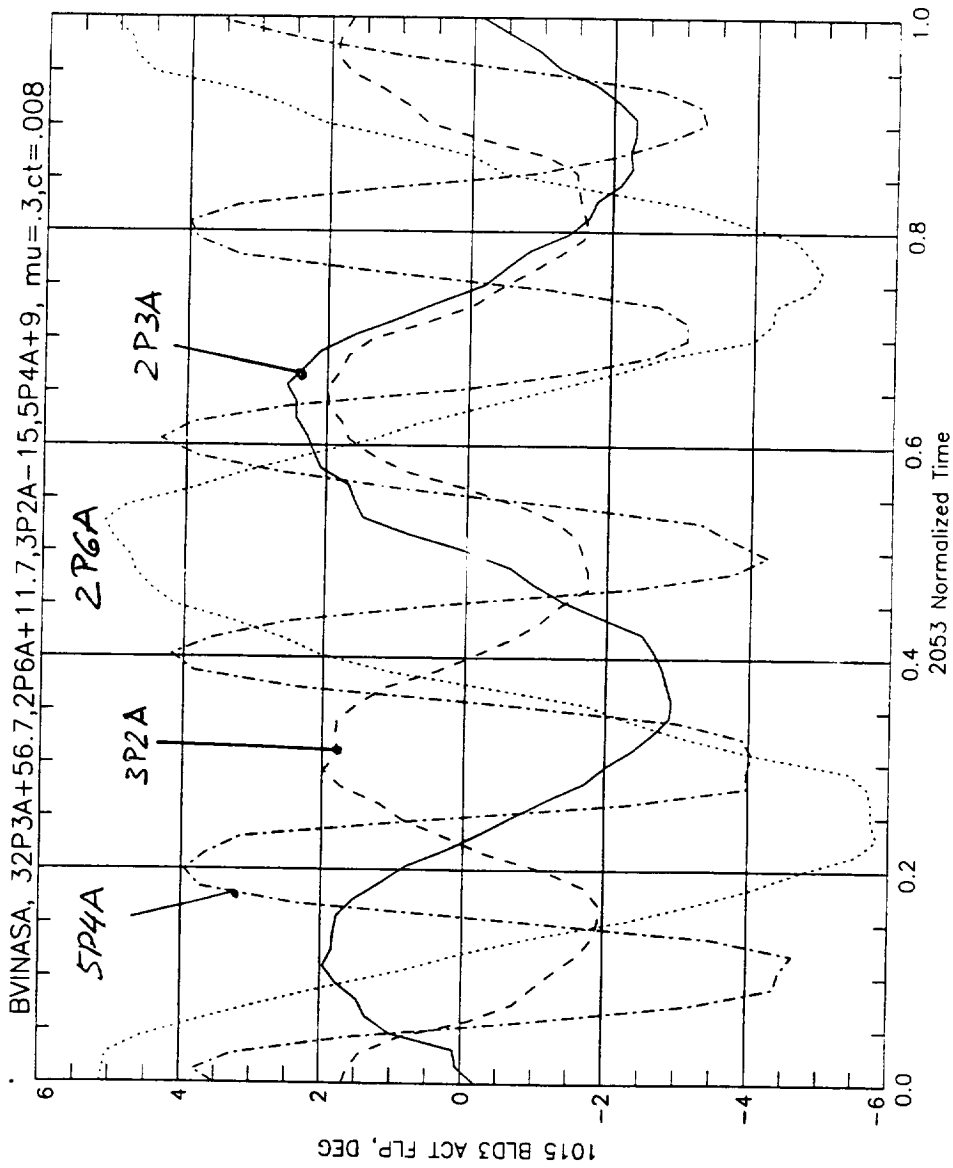
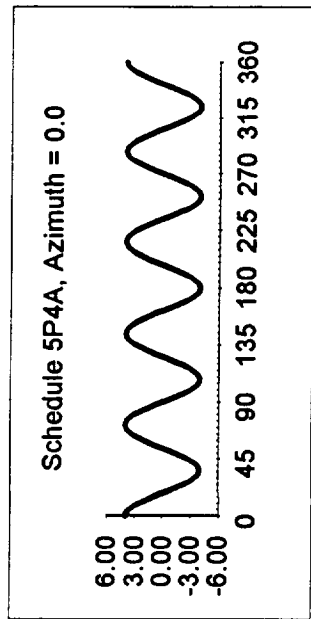
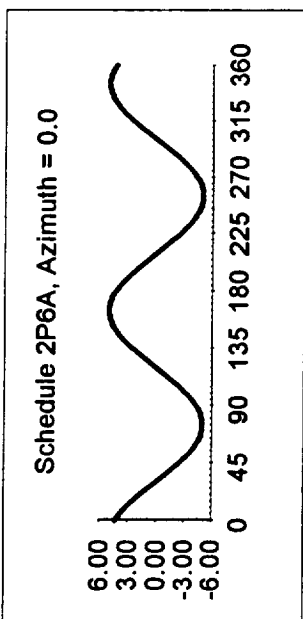
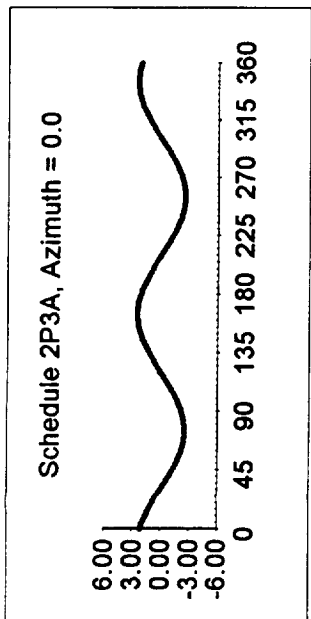


Figure (10b) Desired and Measured Flap Deflection Versus Azimuth Position For Harmonic Cam Profiles

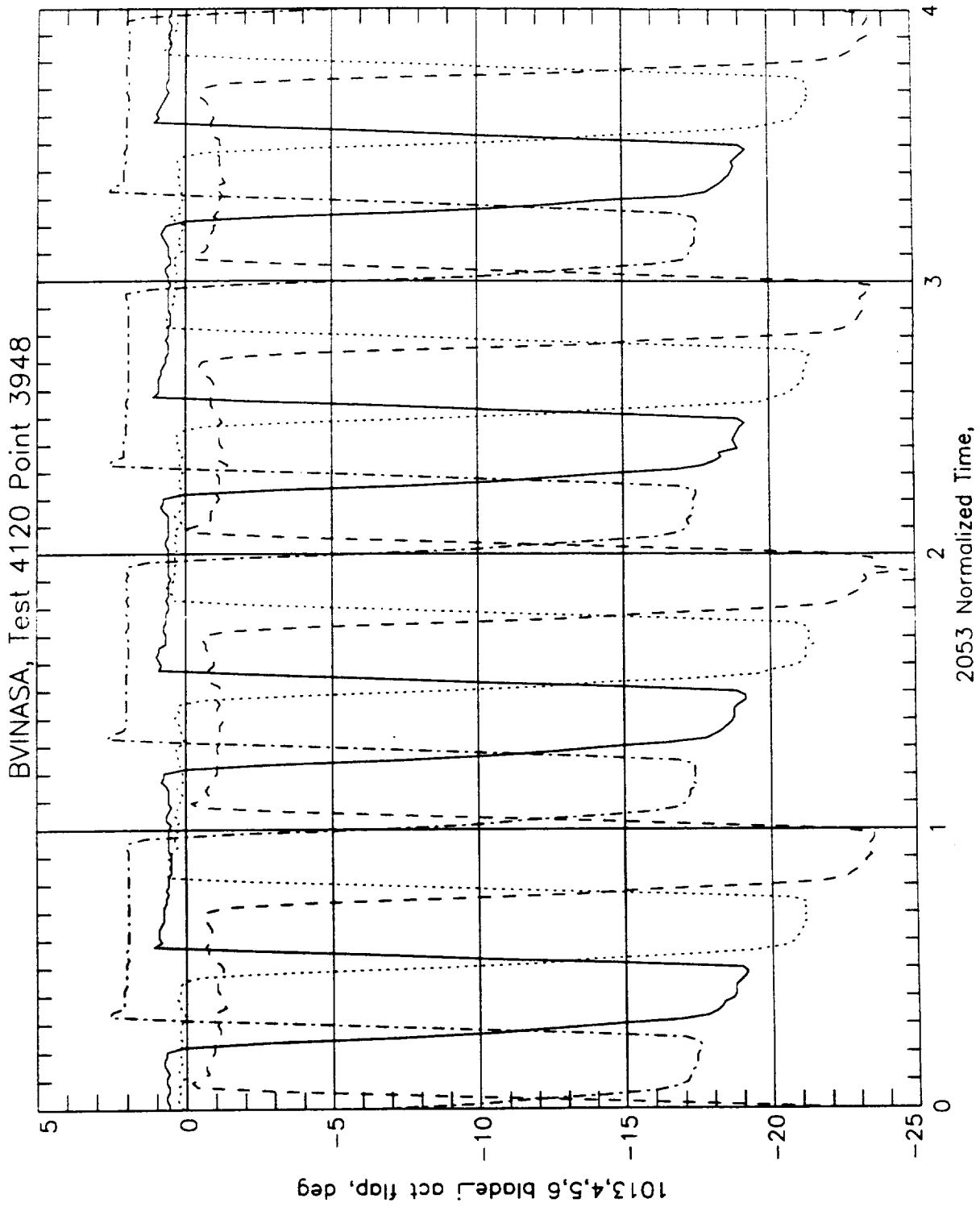
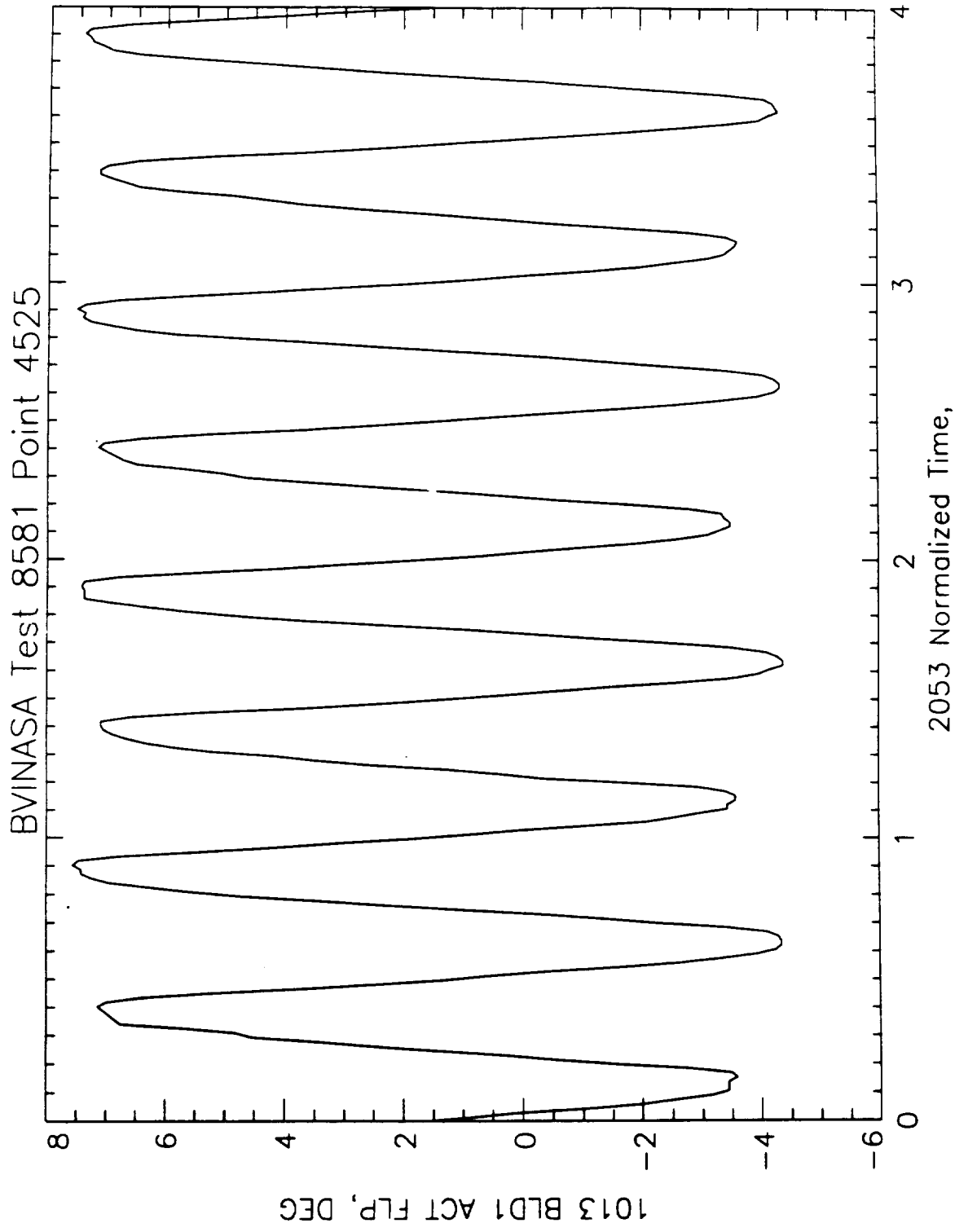
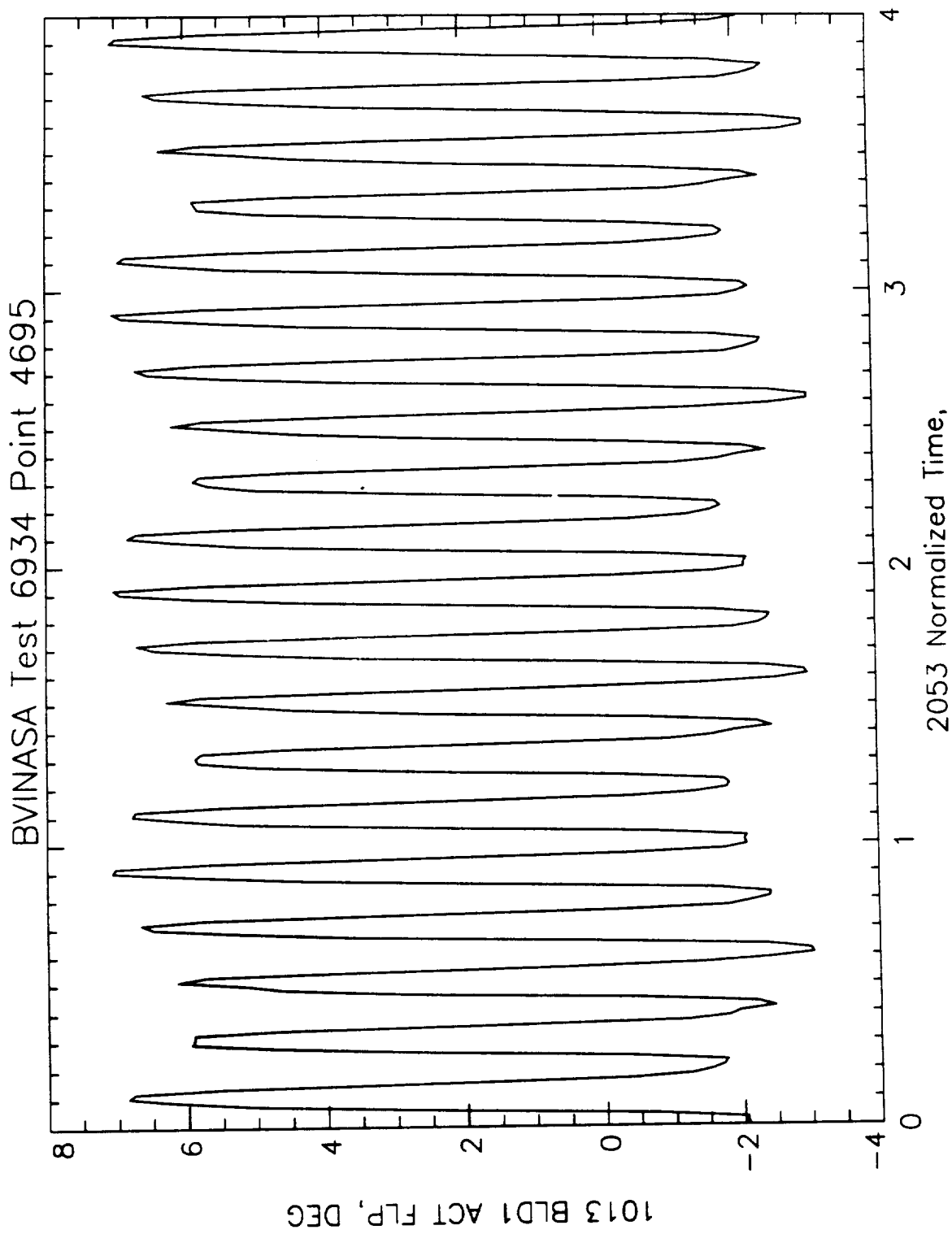


Figure (11a) Schedule 50 Cam Example of Trailing Edge Flap Deflection Over Four Revolutions



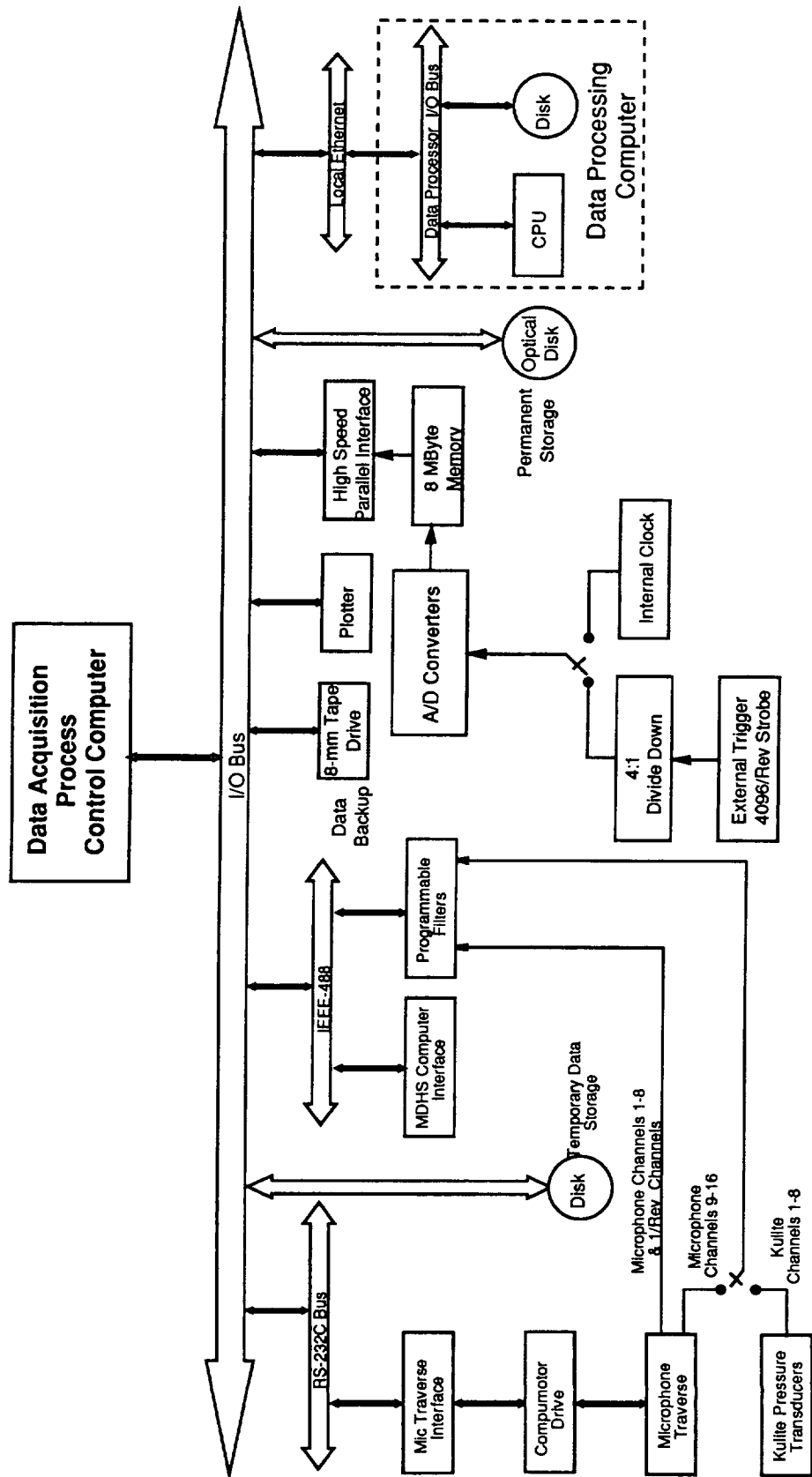
2P6+146.7 CAM, RPM= 1094 VOR = 0.30 ALFS

Figure (11b) Schedule 2P6A Cam Example of Trailing Edge Flap Deflection Over Four Revolutions



5P4A+0 CAM, RPM= 1100 VOR=0.30 ALFSU=-5.

Figure (11c) Schedule 5P4A Cam Example of Trailing Edge Flap Deflection Over Four Revolutions



Figure(12) Acoustic Data Acquisition - Hardware Configuration

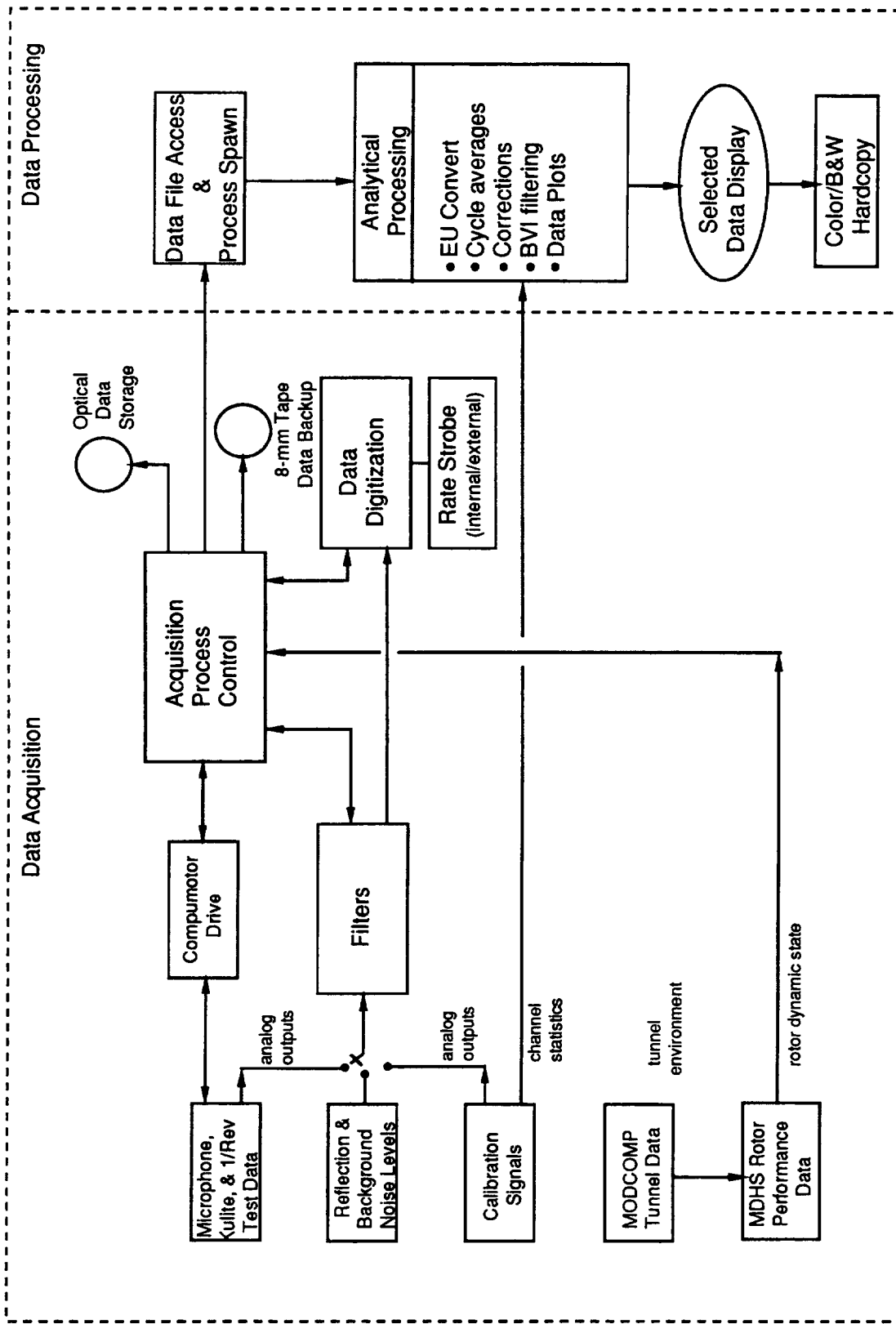


Figure (13) Acoustic Data Acquisition - Data Flow



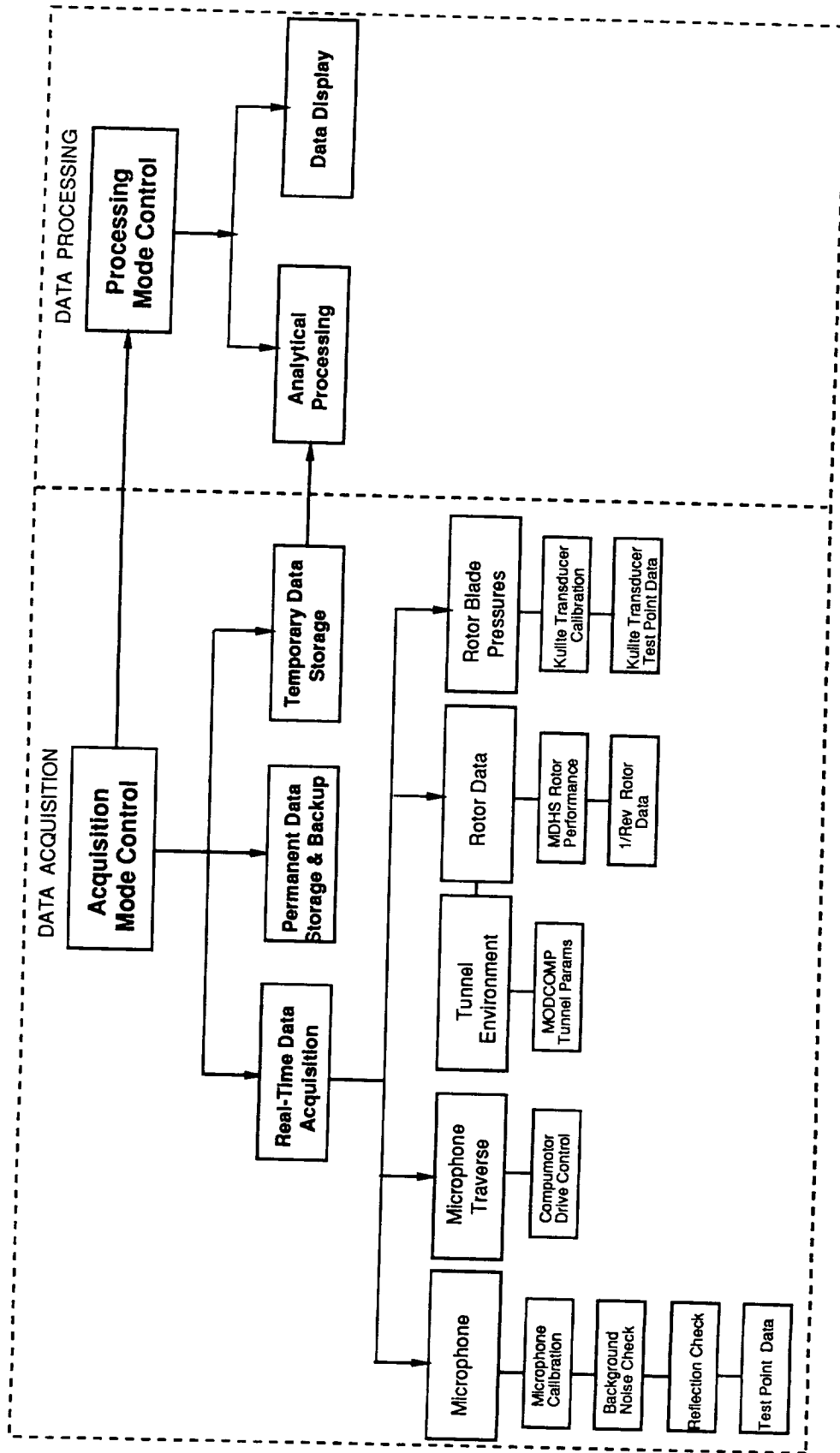


Figure (14) Acoustic Data Acquisition - Overall Process Control

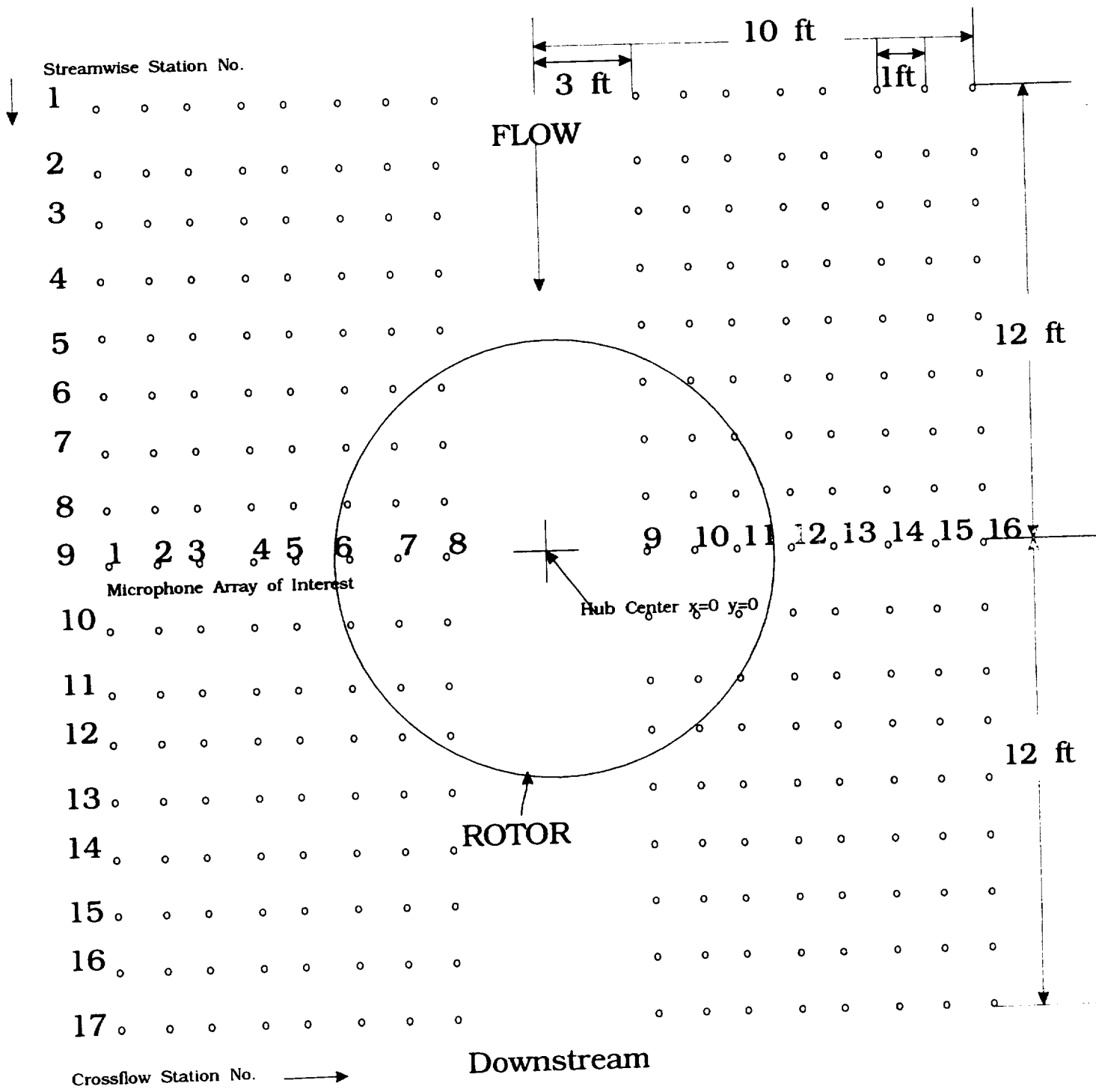


Figure (15) Position of Microphones Relative to Rotor in Wind Tunnel, Top View.



Figure (16) Test Set Up For Shake Test.

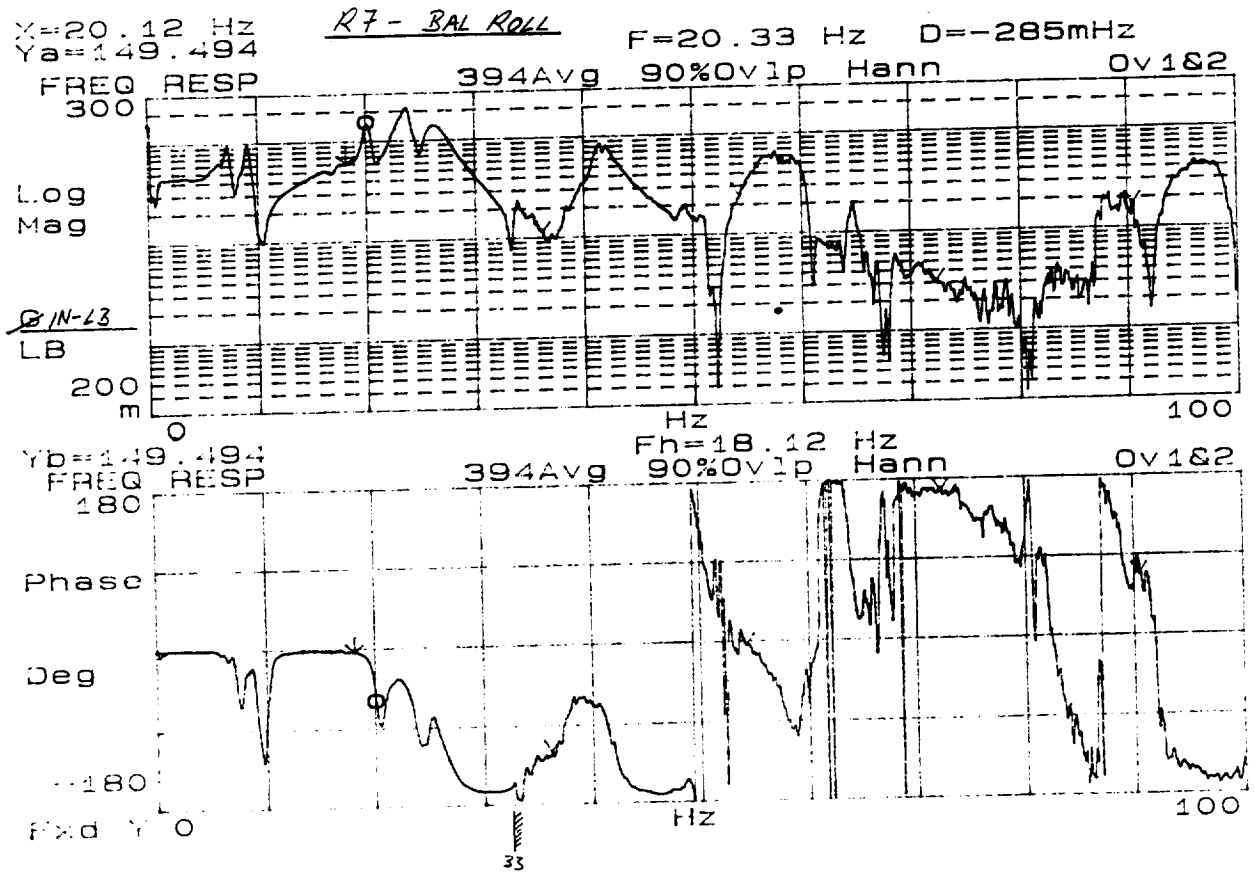
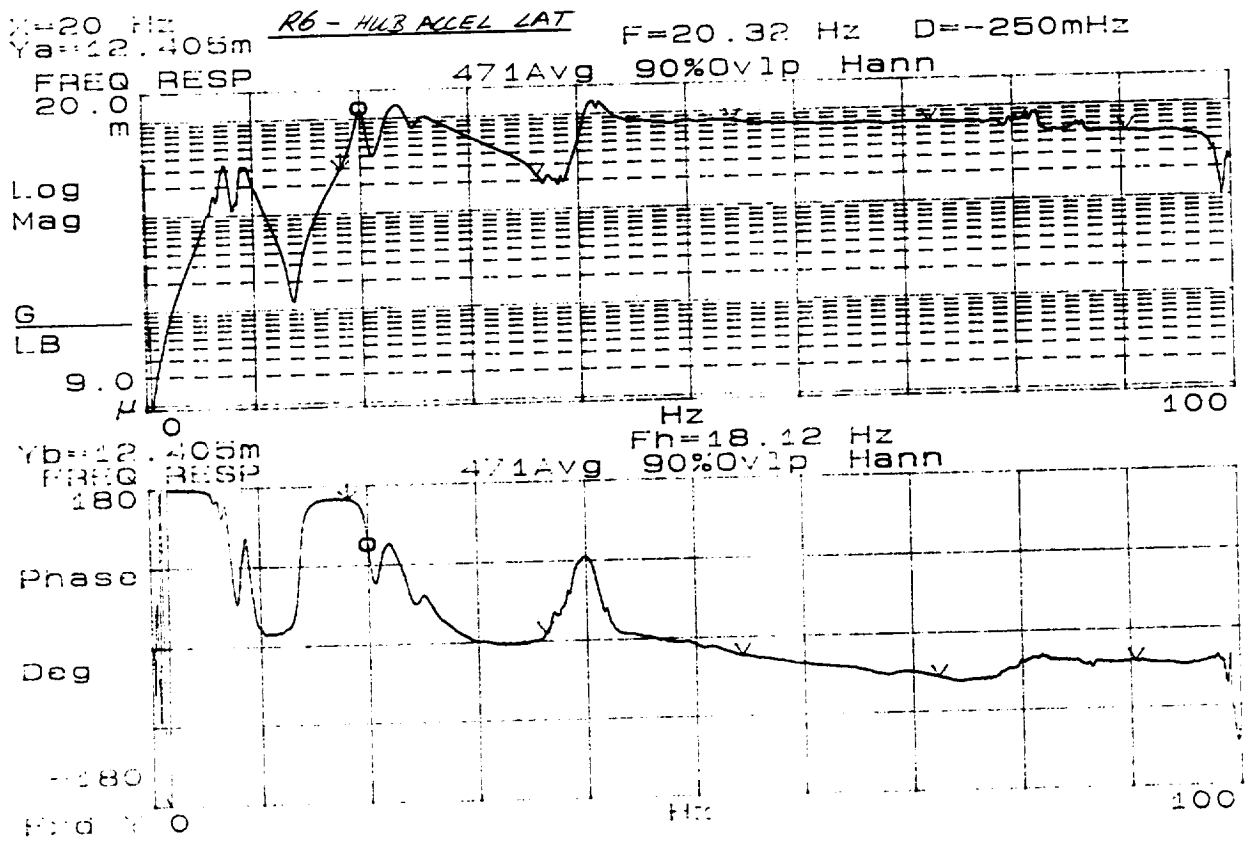


Figure (17) Frequency Response Function, R6 Hub Accelerometer, Lateral and R7, Balance Rolling Moment.

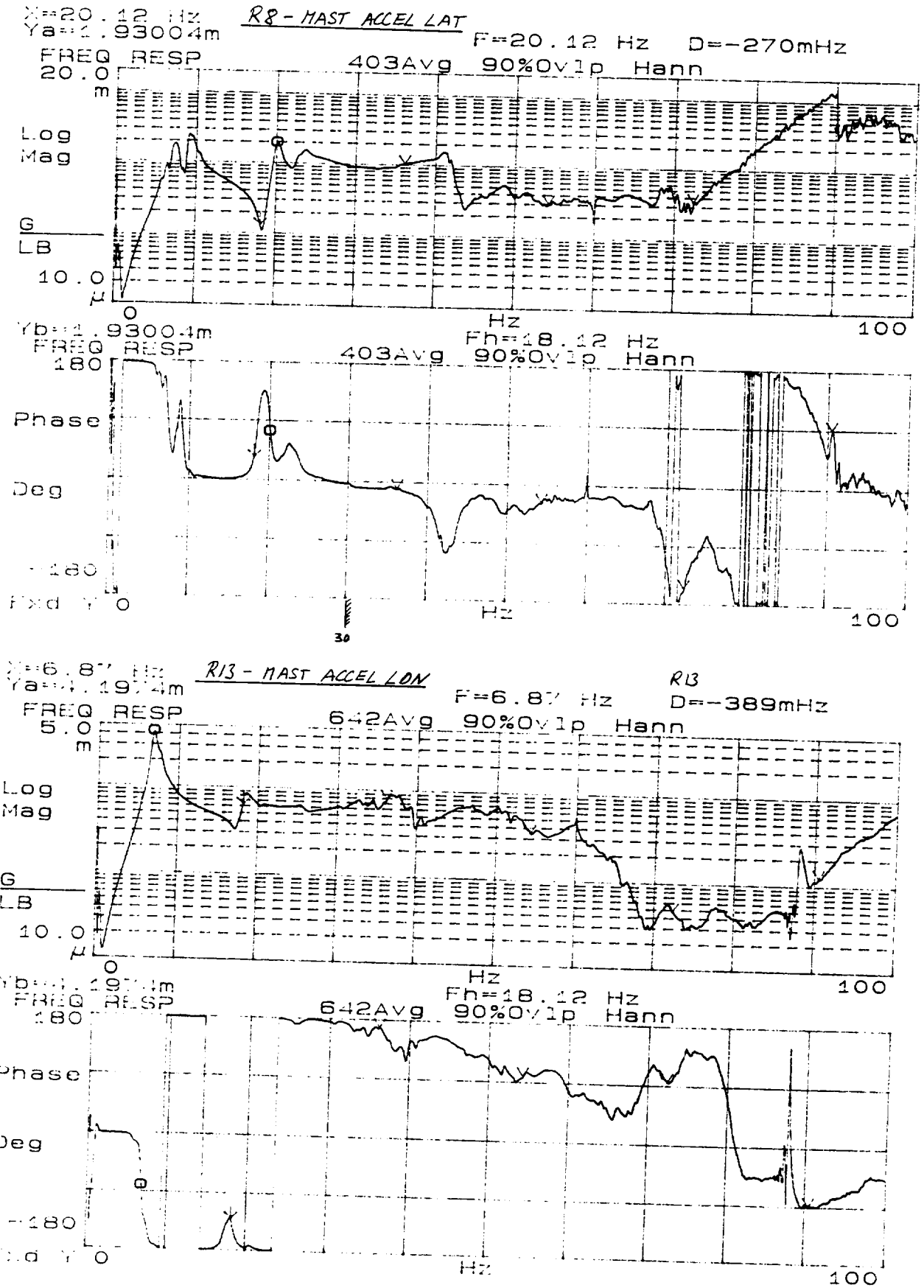


Figure (18) Stand Frequency Response Function, R8 Mast Accelerometer, Lateral and R13 Mast Accelerometer Longitudinal.

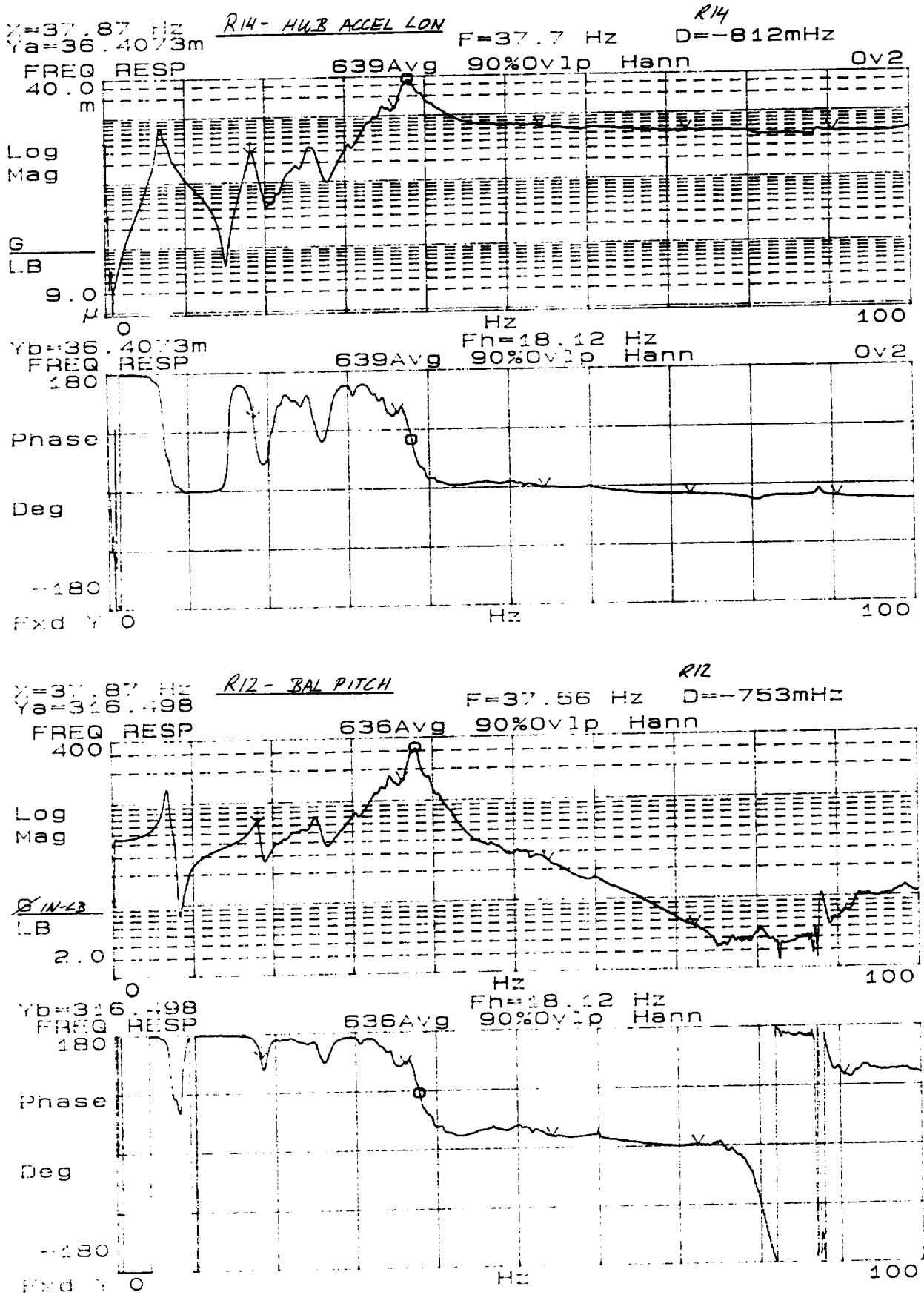
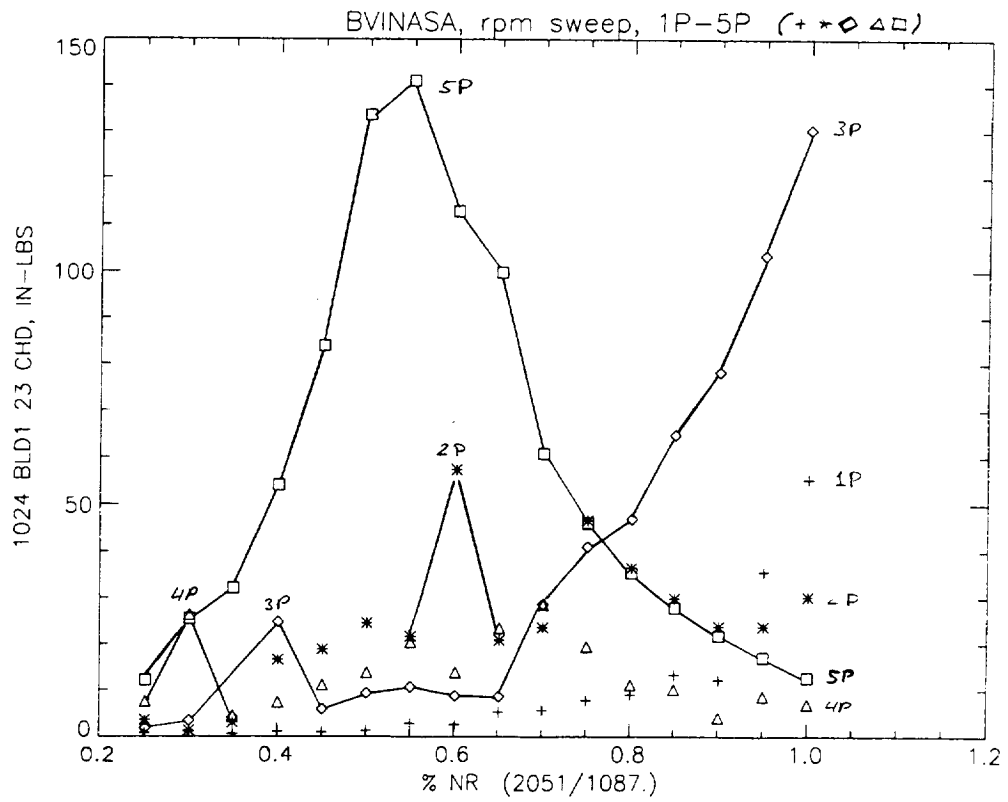
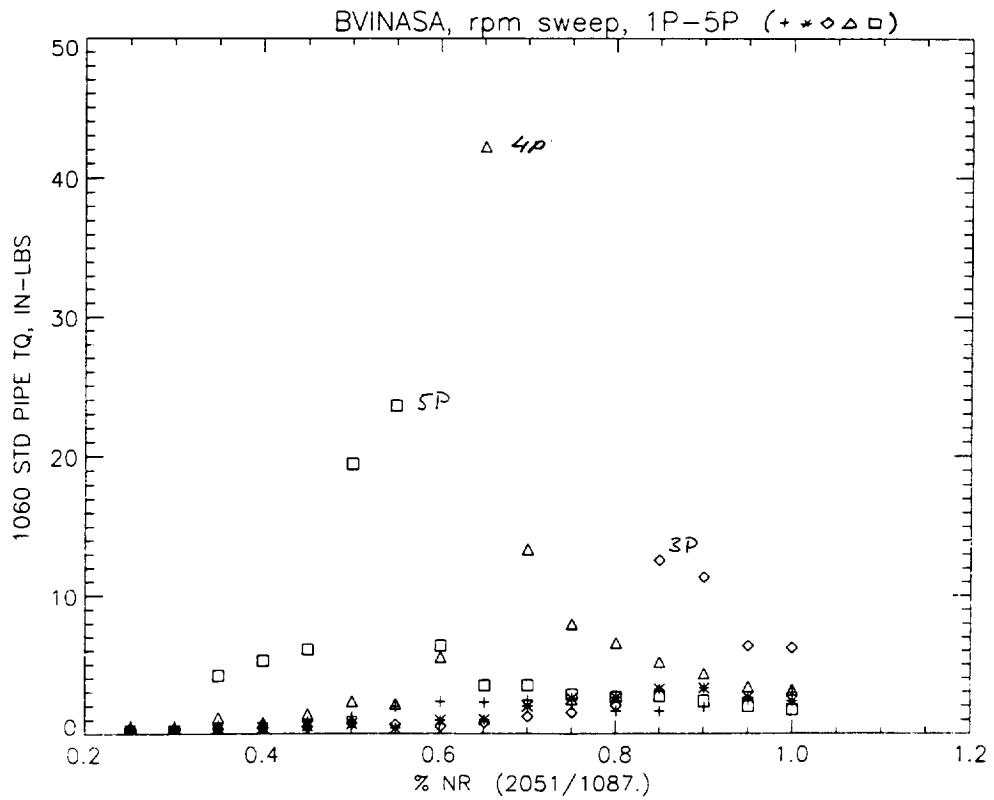


Figure (19) Stand Frequency Response, R14 Hub Accelerometer, Longitudinal and R12 Balance Pitch.



Figure(20a) Blade Chord Bending at Station 23 Versus Rotor Speed.



Figure(20b) Standpipe Torque Versus Rotor Speed.

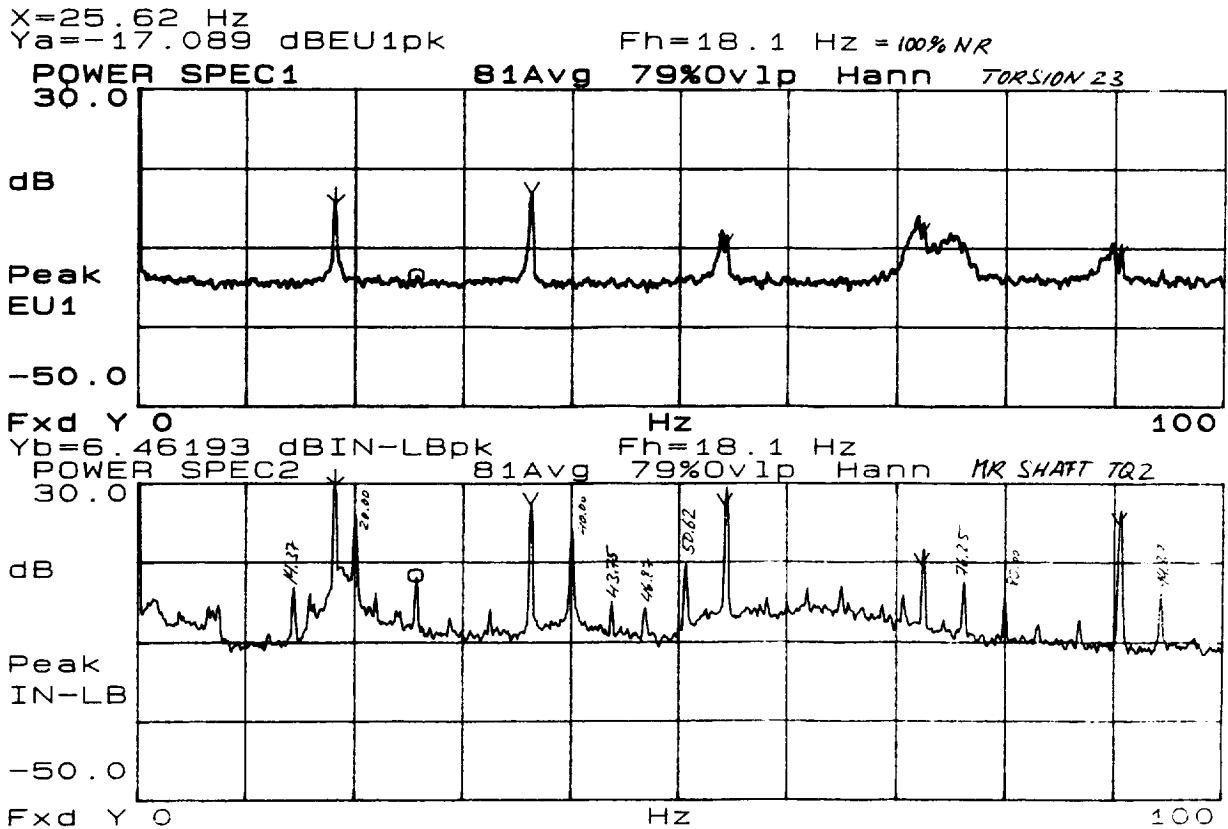
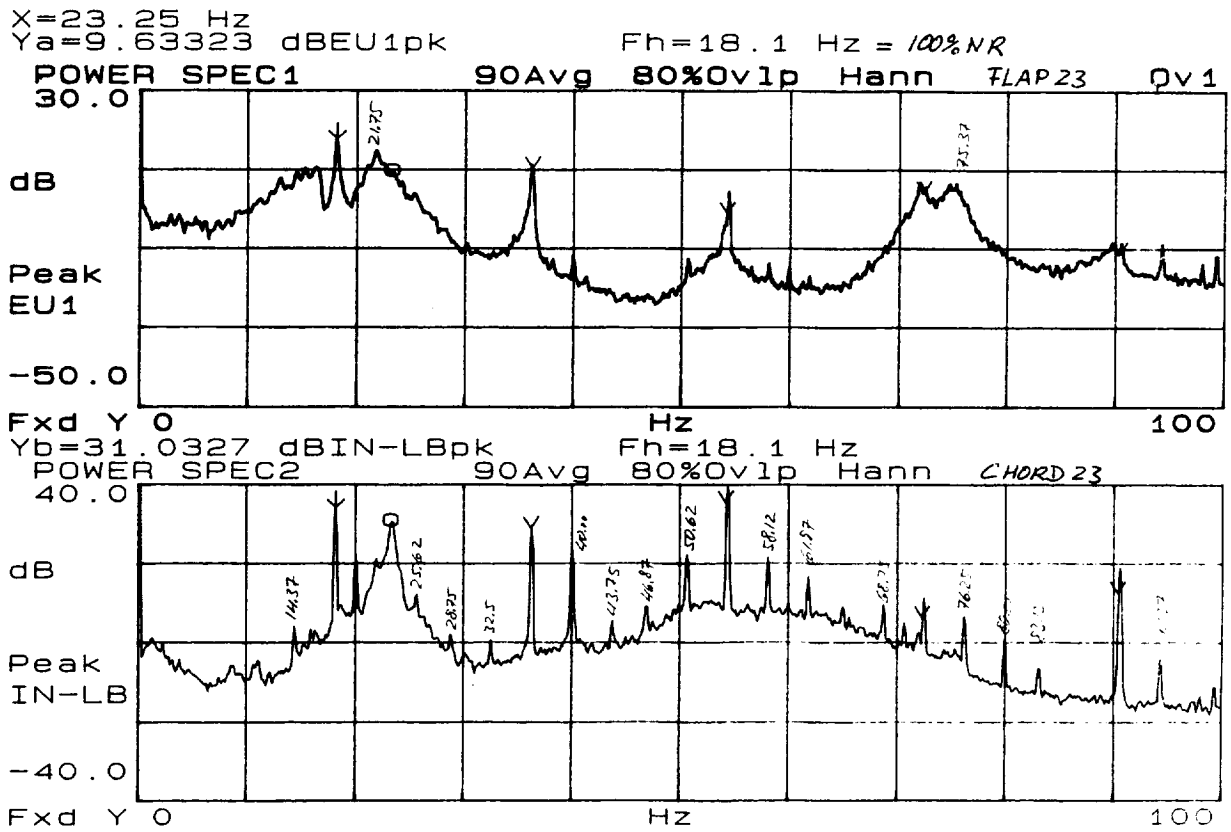


Figure (21) Power Spectra For Blade Flap, Chord and Torsion Response at Station 23, and For Main Rotor Shaft Torque at Nominal Rotor Speed (18.12 Hz).



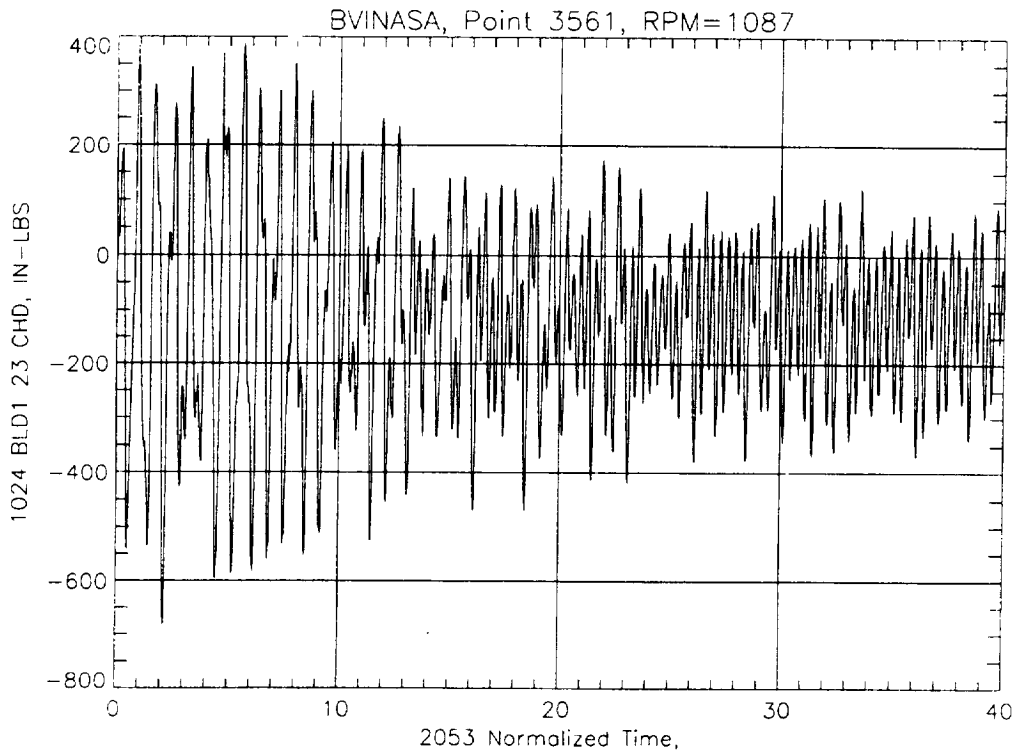
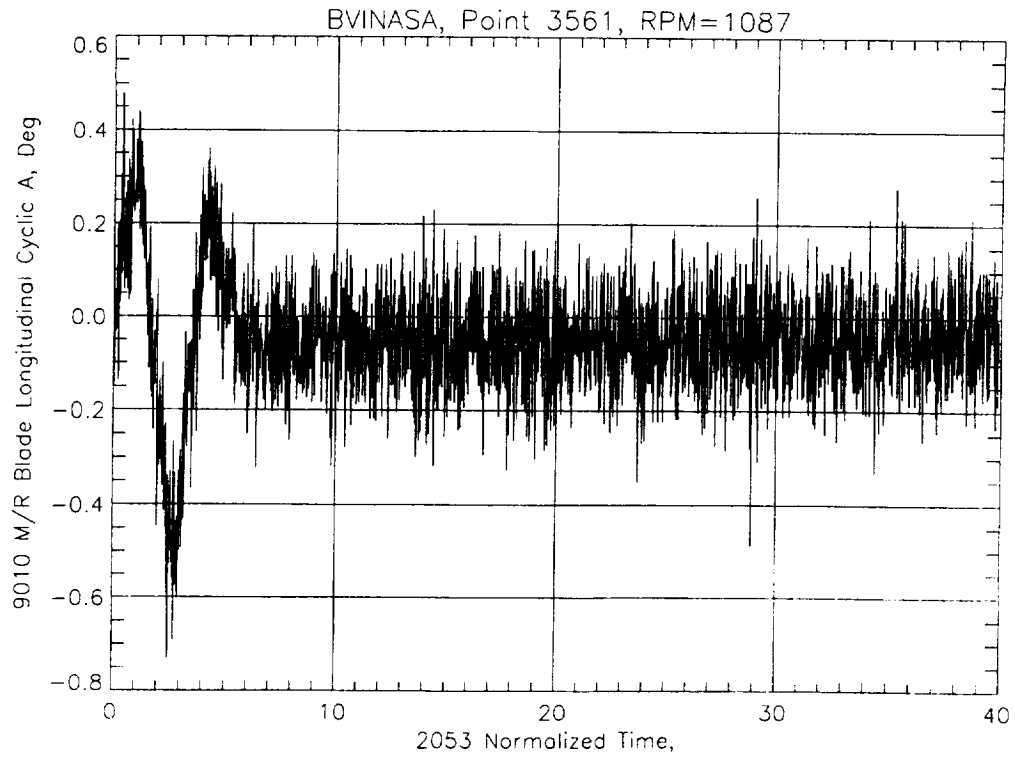


Figure (22) Longitudinal Cyclic Input and Chord Bending Response at Station 23.

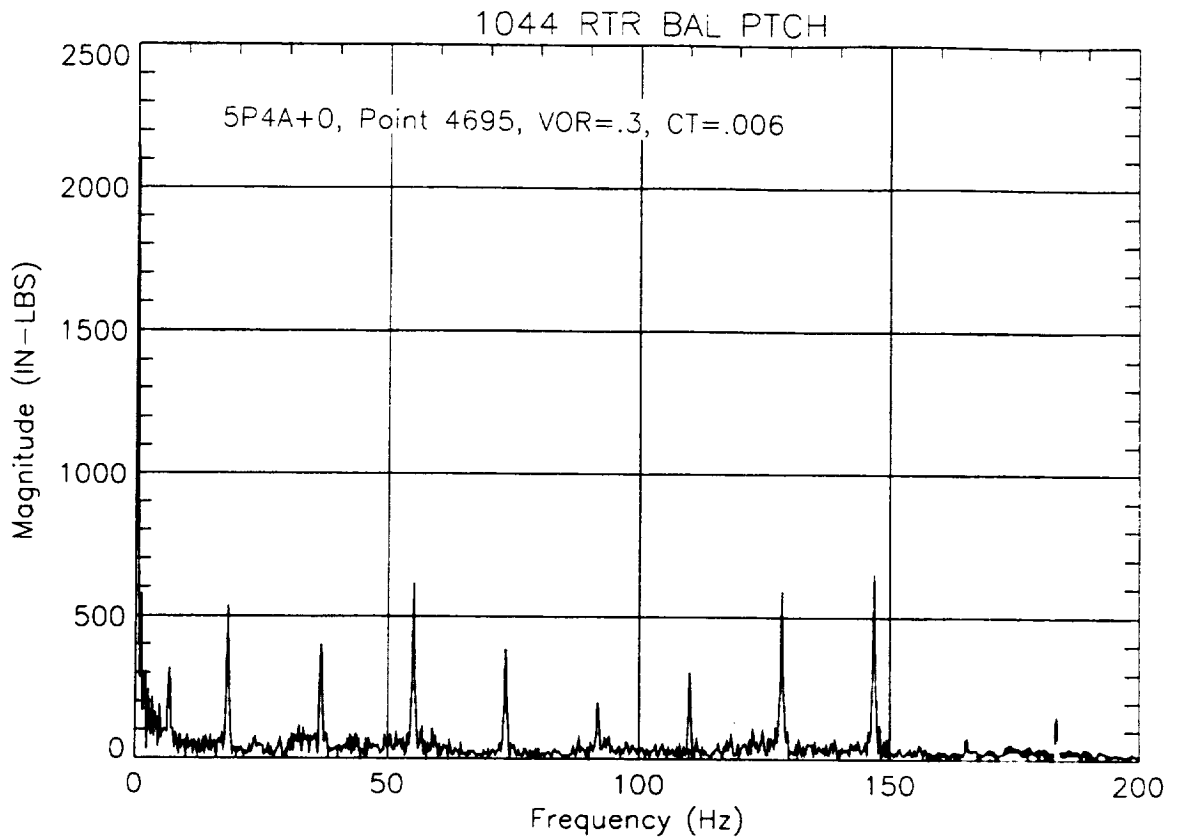
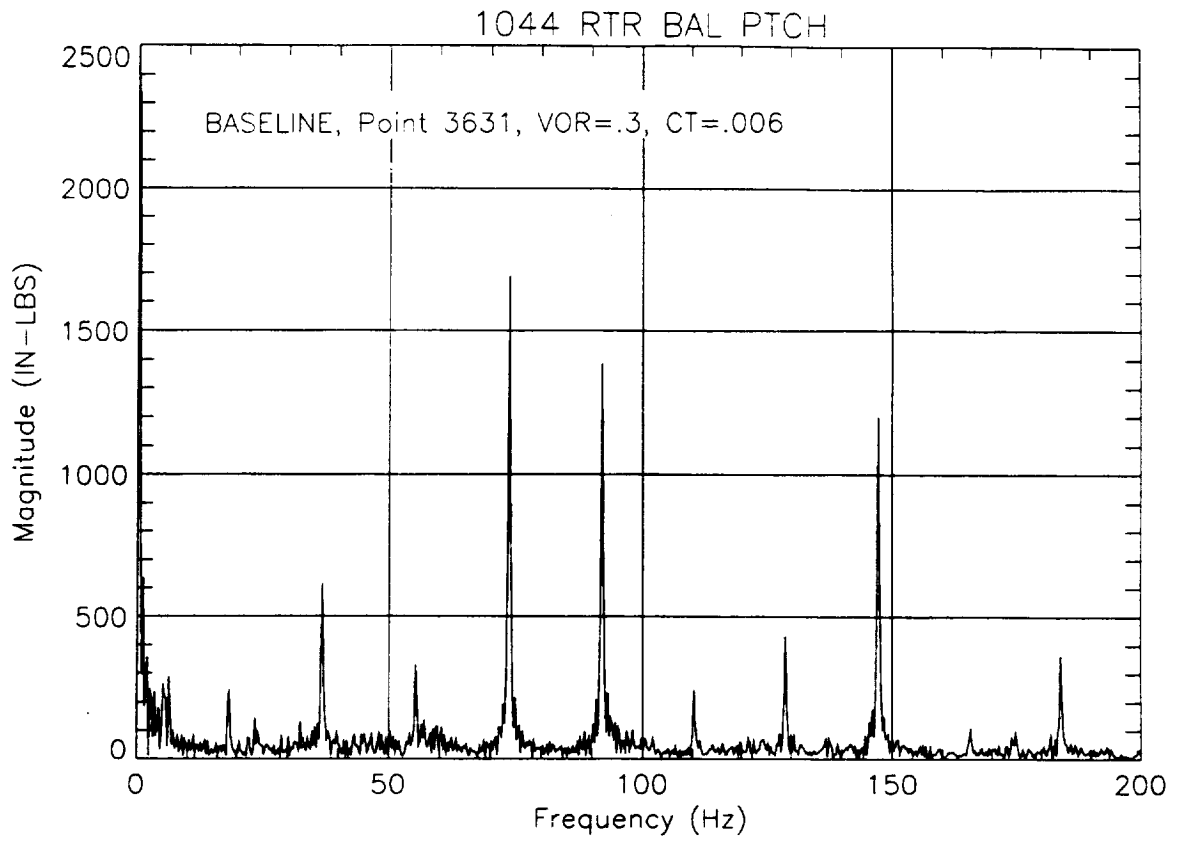


Figure (23) Rotor Balance Pitch Moment Frequency Response, Baseline and 5P4A Cams.

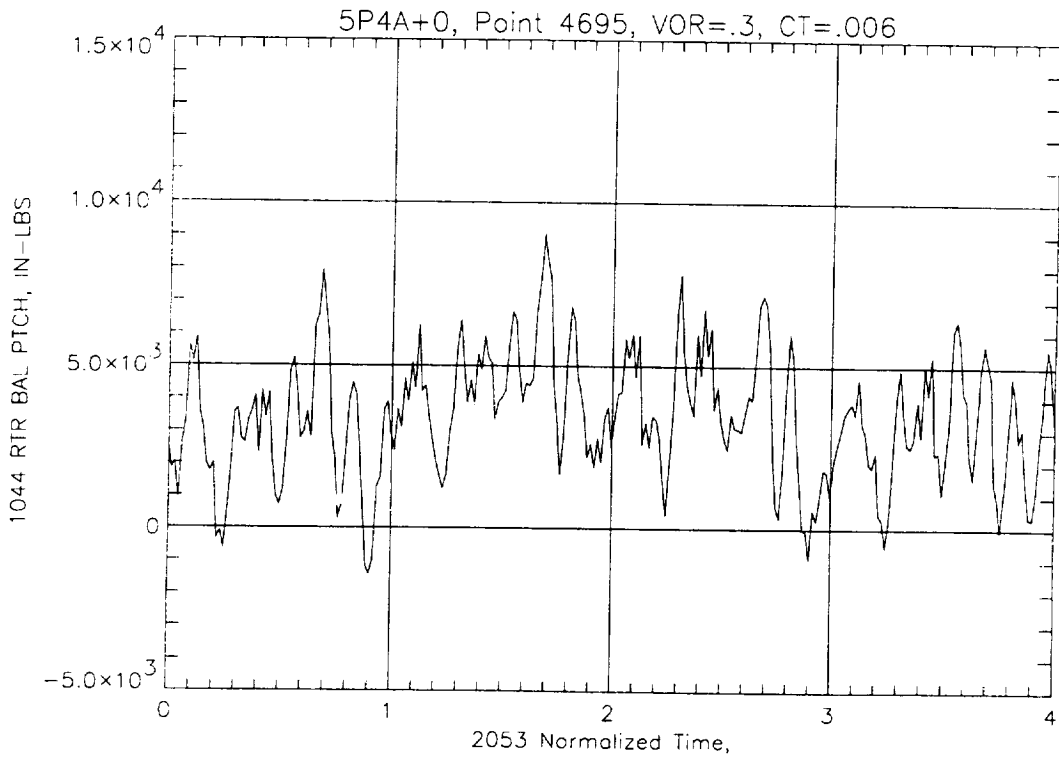
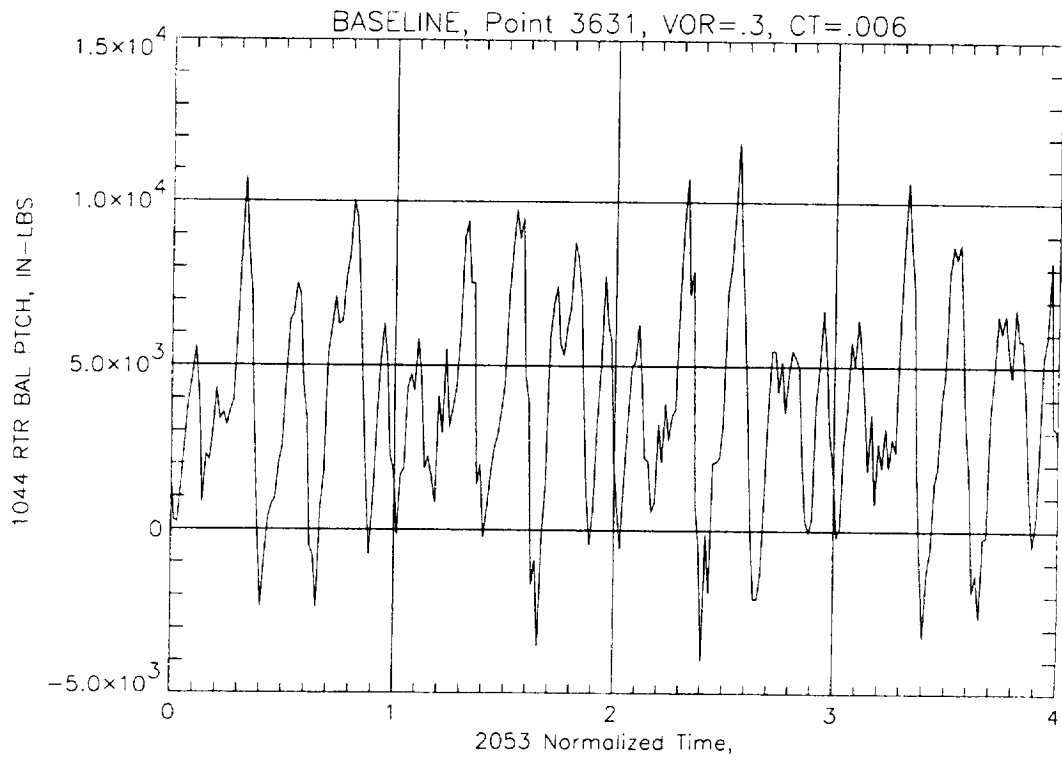


Figure (24) Rotor Balance Pitch Moment Time Histories, Baseline and 5P4A Cams.

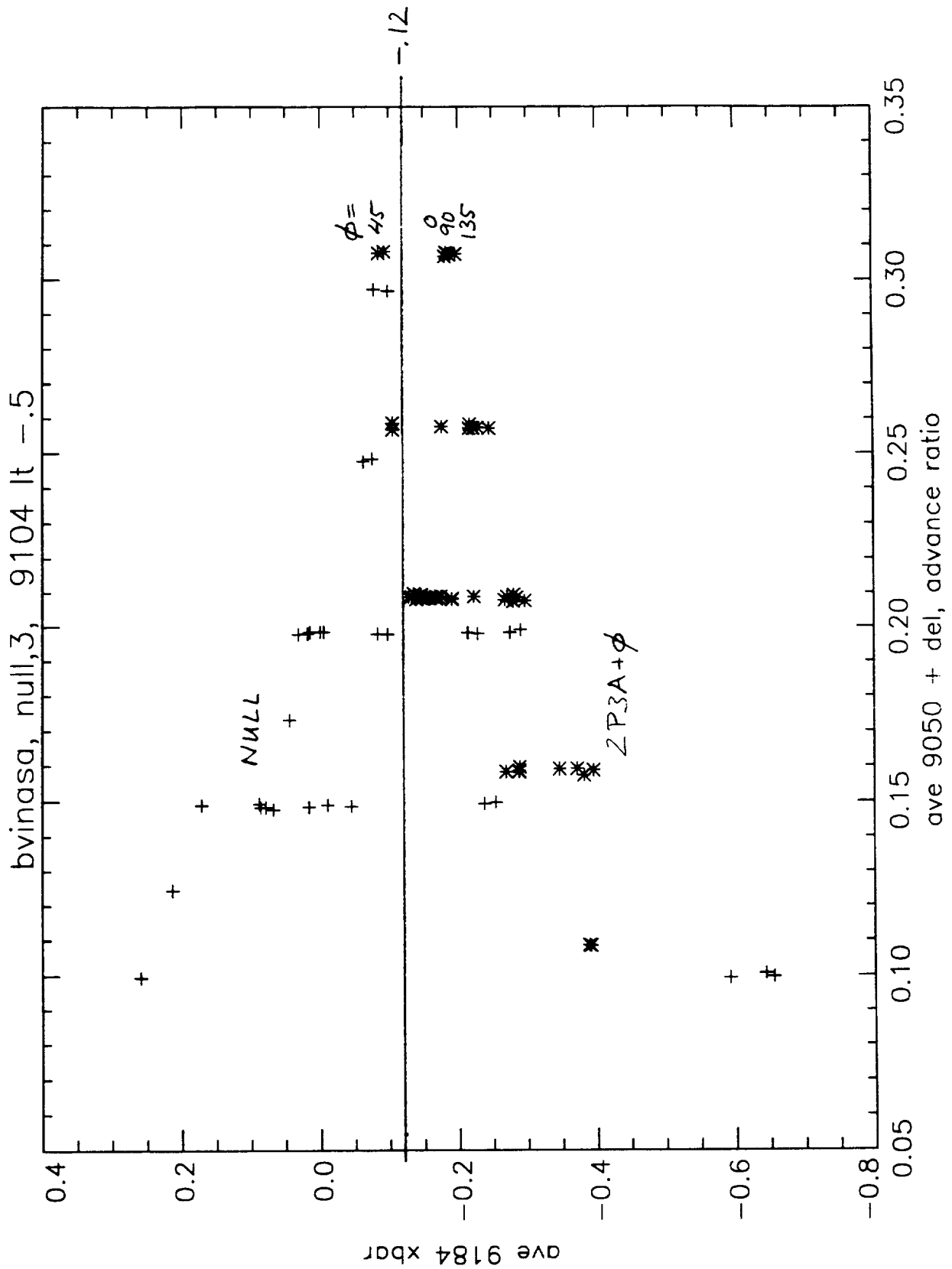


Figure (25) Propulsive Force Versus Advance Ratio For Baseline and 2P3A Cams.

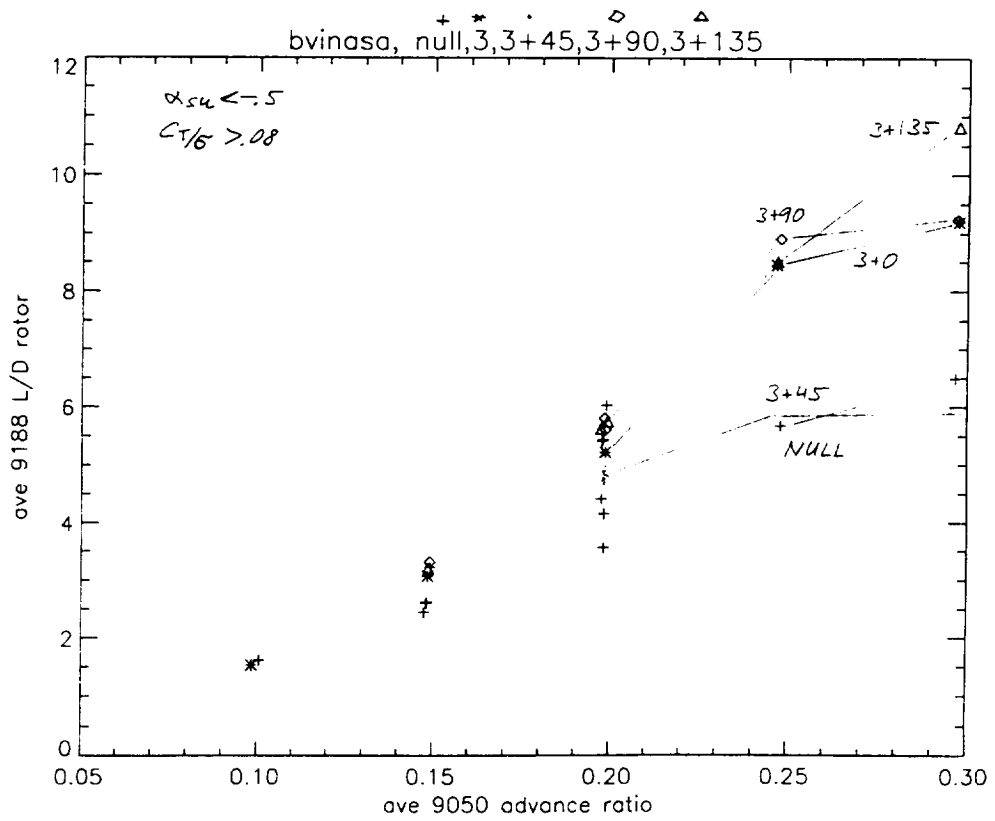
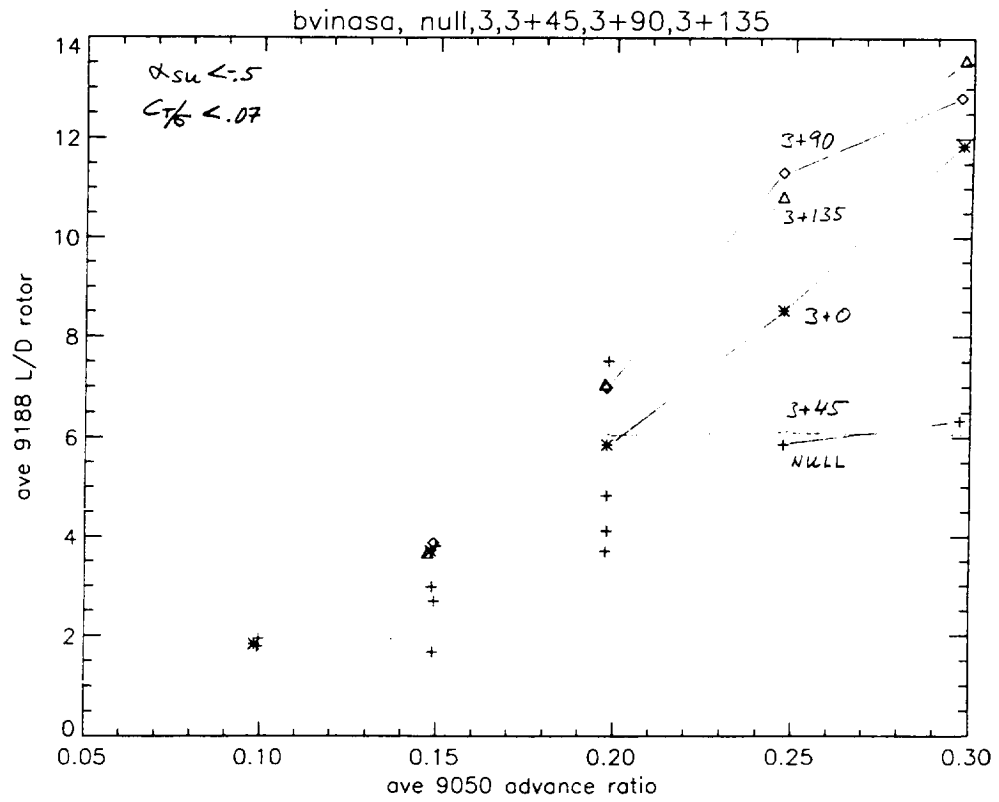


Figure (26) L/D Versus Advance Ratio For Baseline And 2P3A Cams.

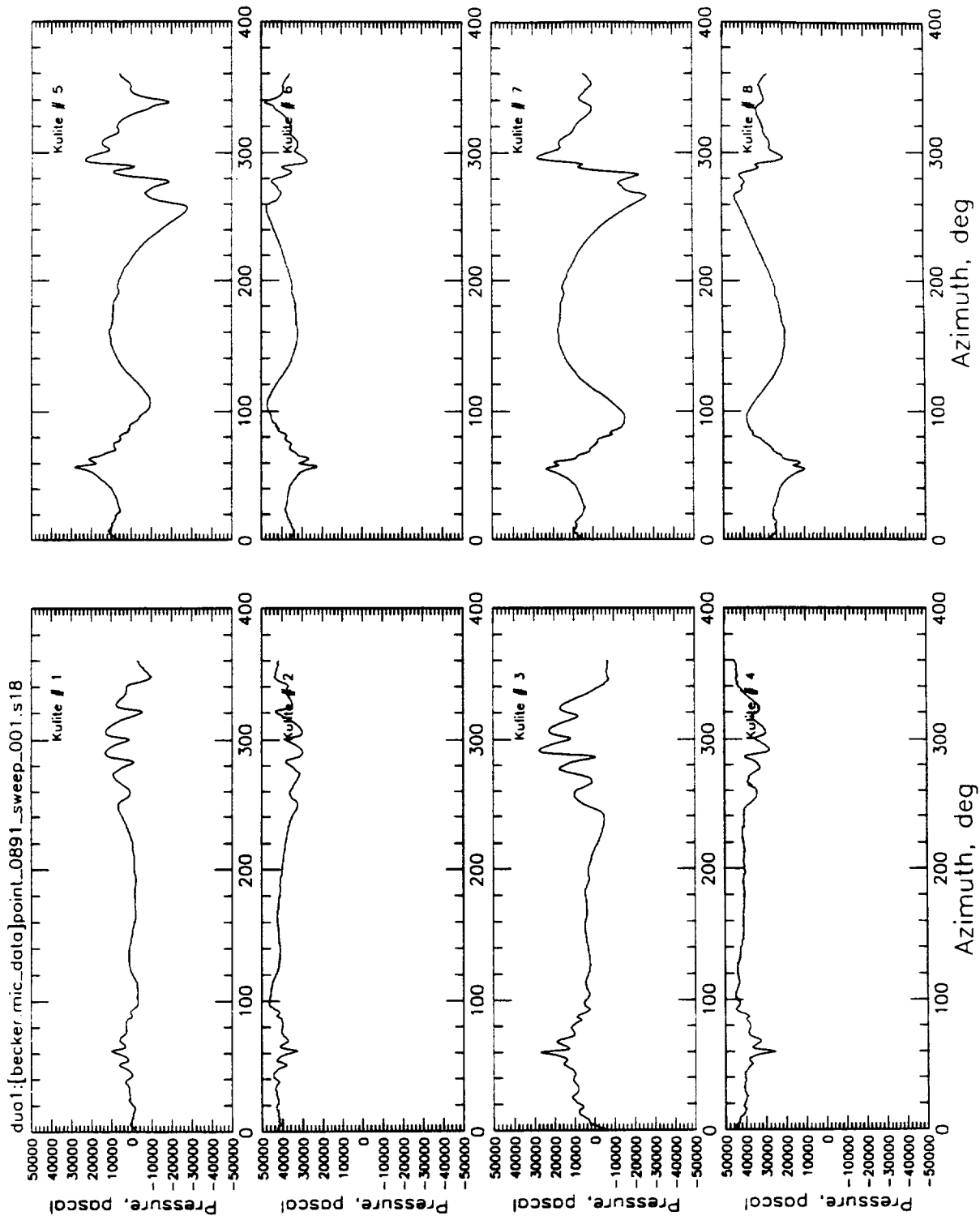


Figure (27) Measured blade surface pressures ( $C_l/\sigma=0.0764$ ,  $\mu=0.149$ ,  $\alpha_{TPP}=5^\circ$ . aft,  $x/C=0.03$ ) Baseline rotor configuration: Test # 0733, Point # 0891

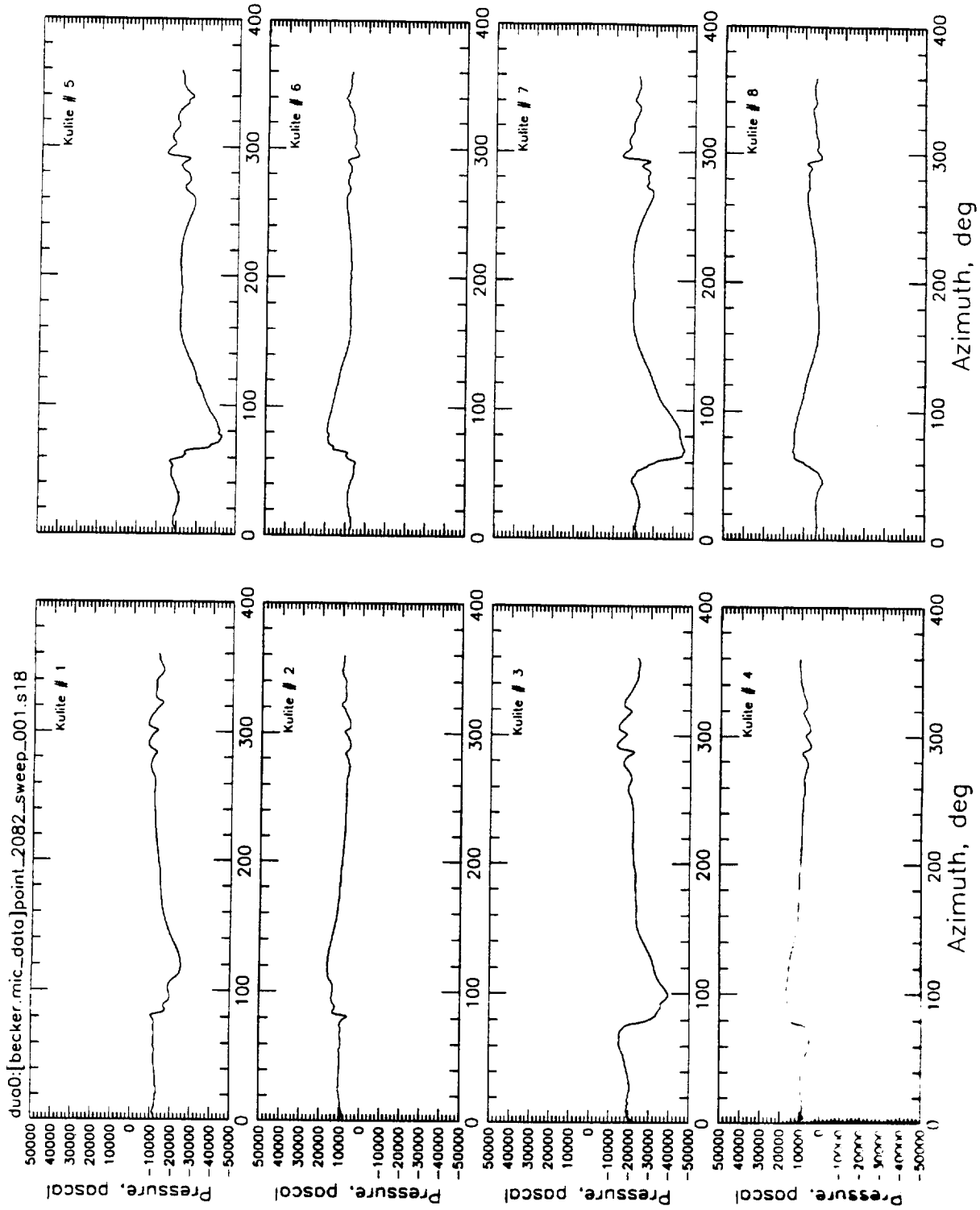


Figure (28) Measured blade surface pressures ( $C_l/\sigma=0.0764$ ,  $\mu=0.149$ ,  $\alpha_{TPP}=5^\circ$ . aft,  $x/C=0.03$ ) Flapped rotor configuration: Test # 2916, Point # 2082

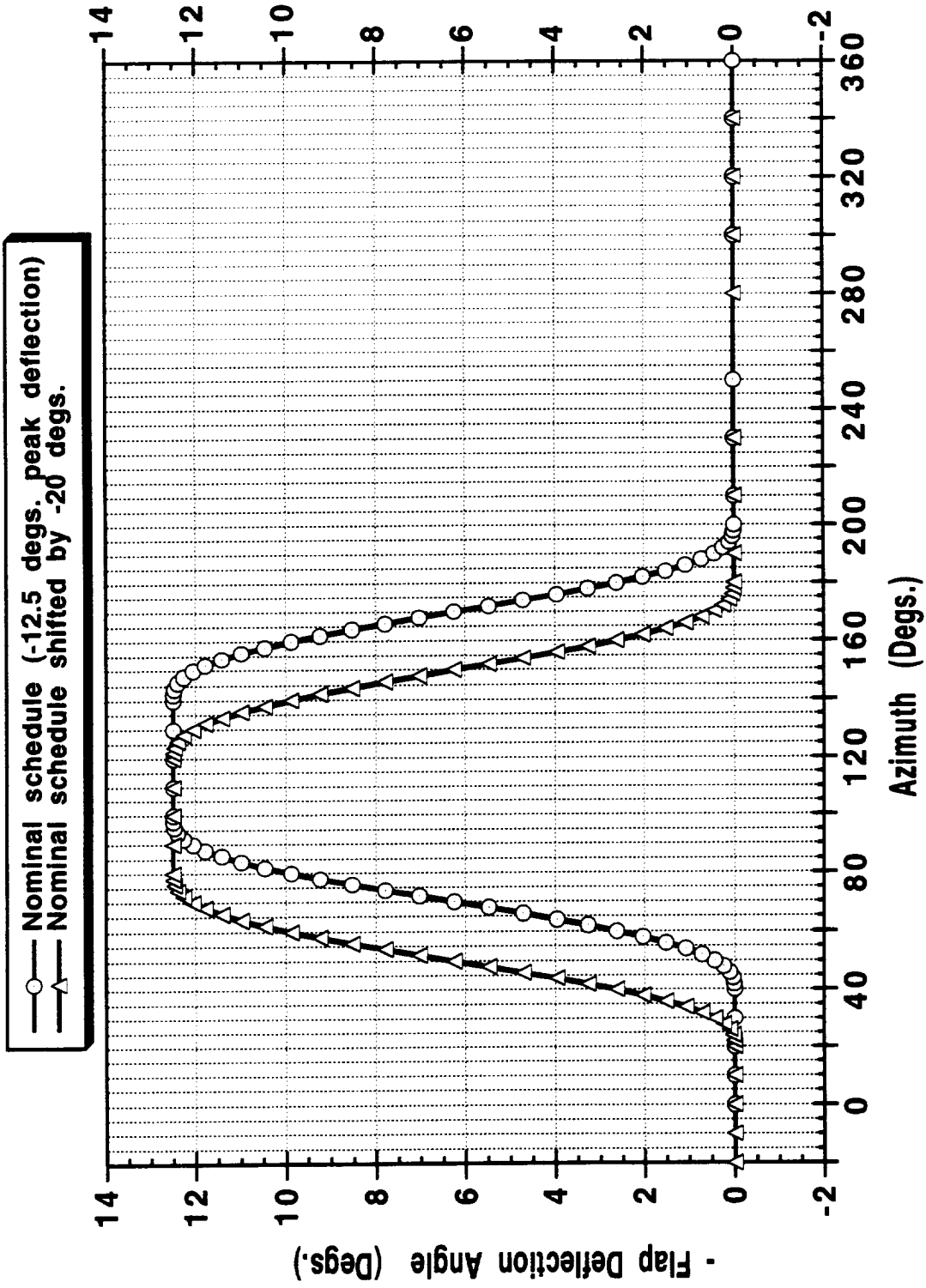


Figure (29) Nominal flap schedule with a peak deflection of  $-12.5^\circ$  and the schedule with a  $-20^\circ$  of phase shift.



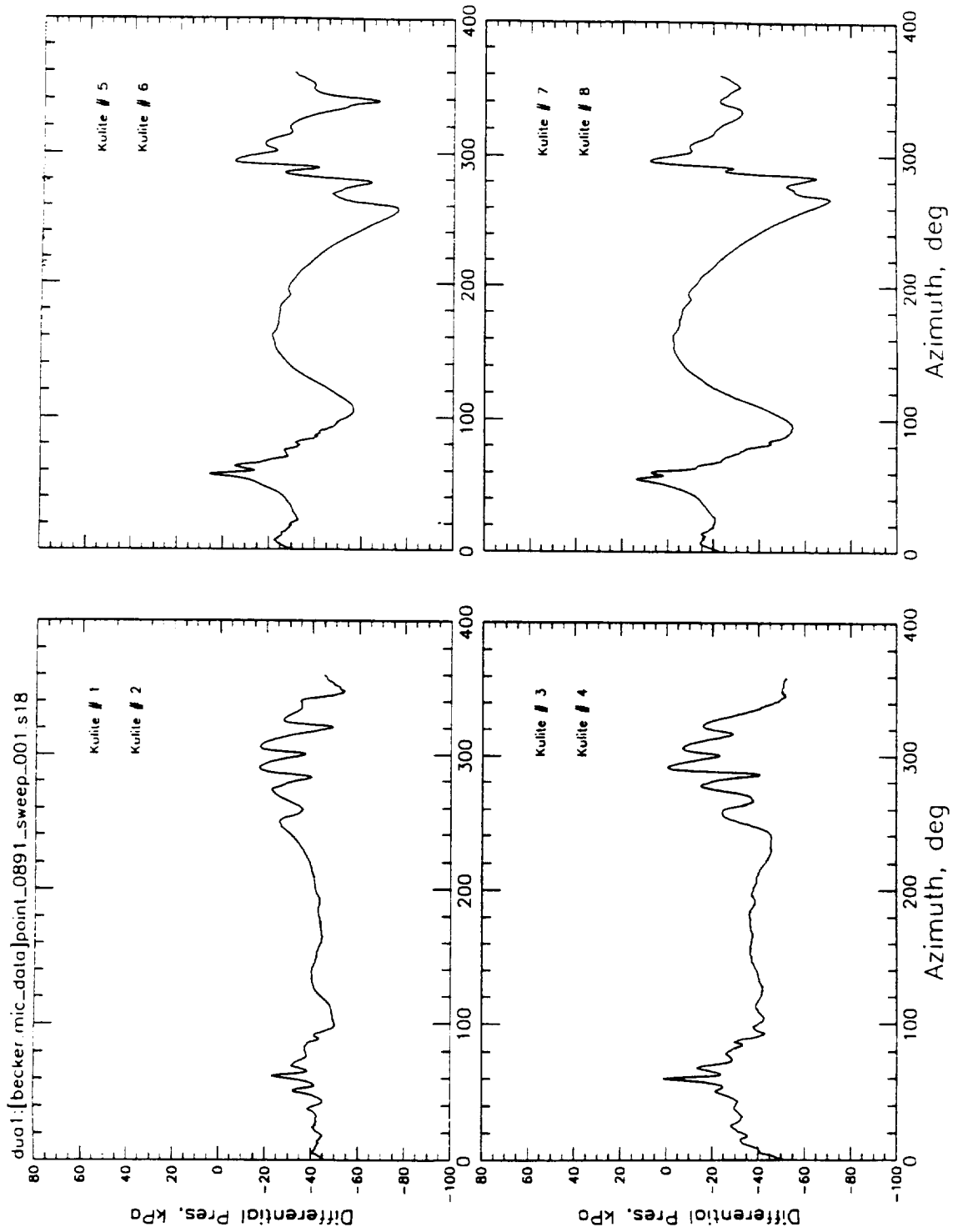


Figure (30) Calculated differential pressures ( $C_L/\sigma=0.0764$ ,  $\mu=0.149$ ,  $\alpha_{TPP}=5^\circ$ . aft,  $x/C=0.03$ ) Baseline rotor configuration: Test # 0733, Point # 0891

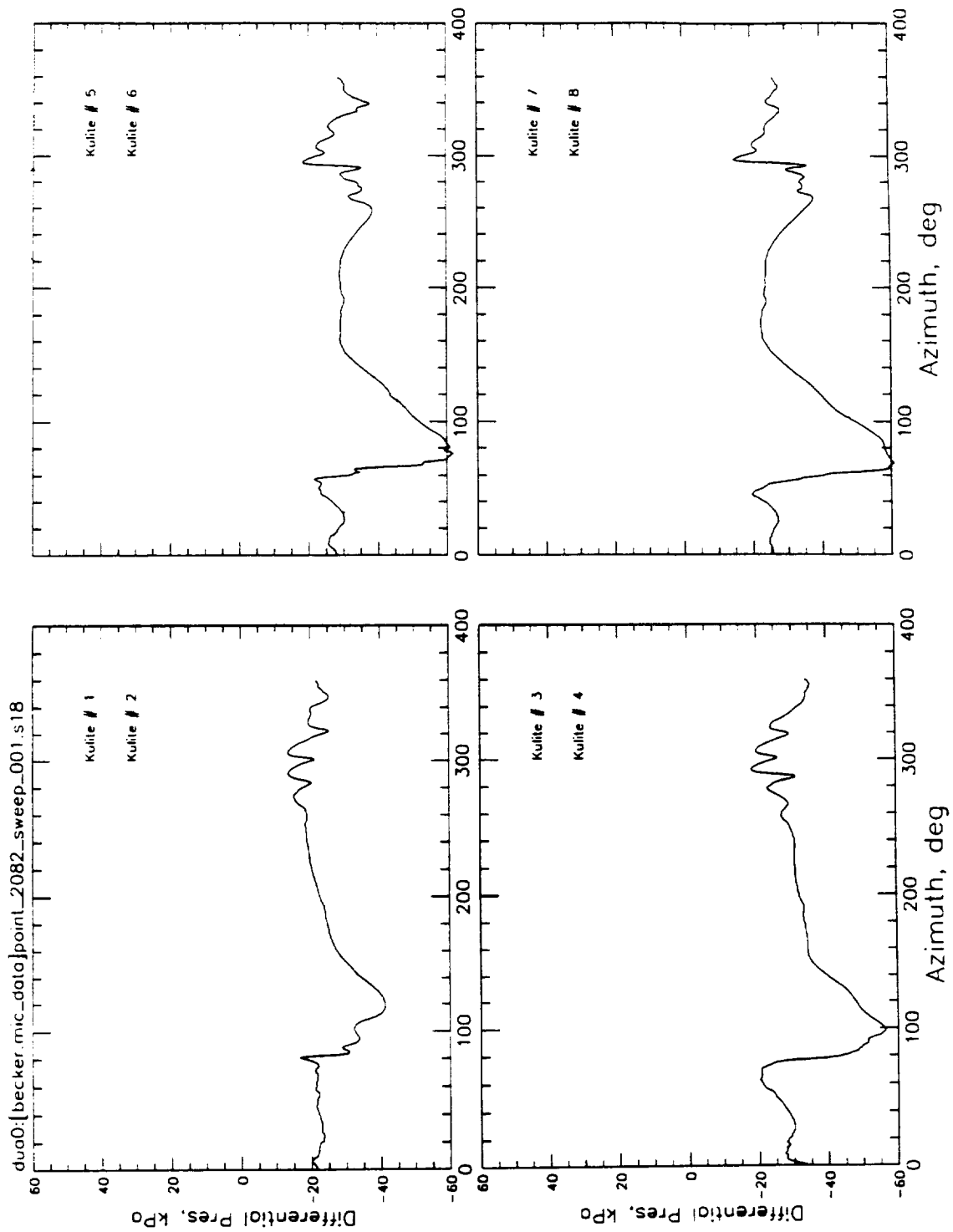


Figure (31) Calculated differential pressures ( $C_l/\sigma=0.0764$ ,  $\mu=0.149$ ,  $\alpha_{TPP}=5^\circ$  . aft,  $x/C=0.03$ ) Flapped rotor configuration: Test # 2916, Point # 2082

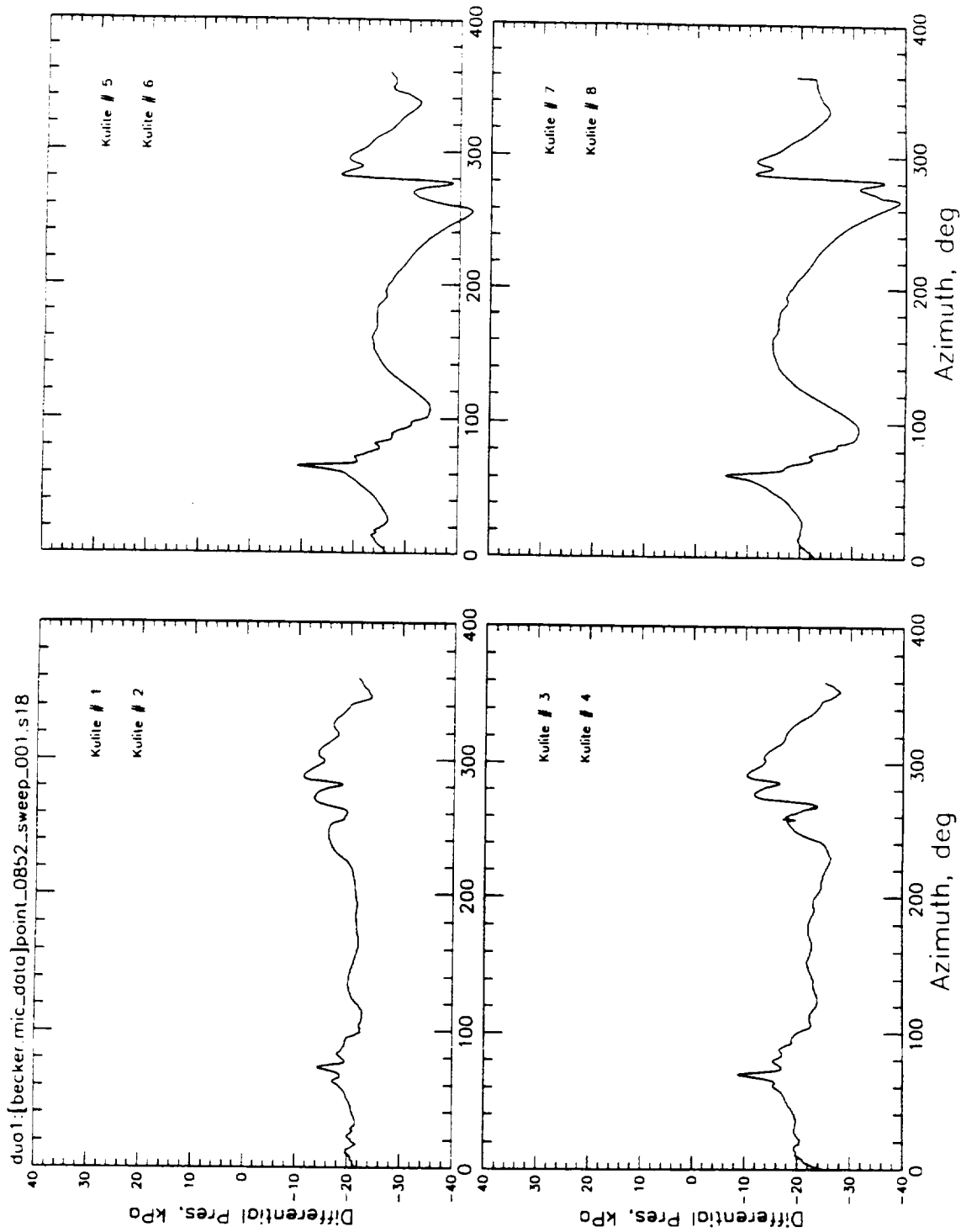


Figure (32) Calculated differential pressures ( $C_T/\sigma=0.0760$ ,  $\mu=0.149$ ,  $\alpha_{TPP}=3^\circ$ . aft,  $x/C=0.03$ ) Baseline rotor configuration: Test # 0731, Point # 0852

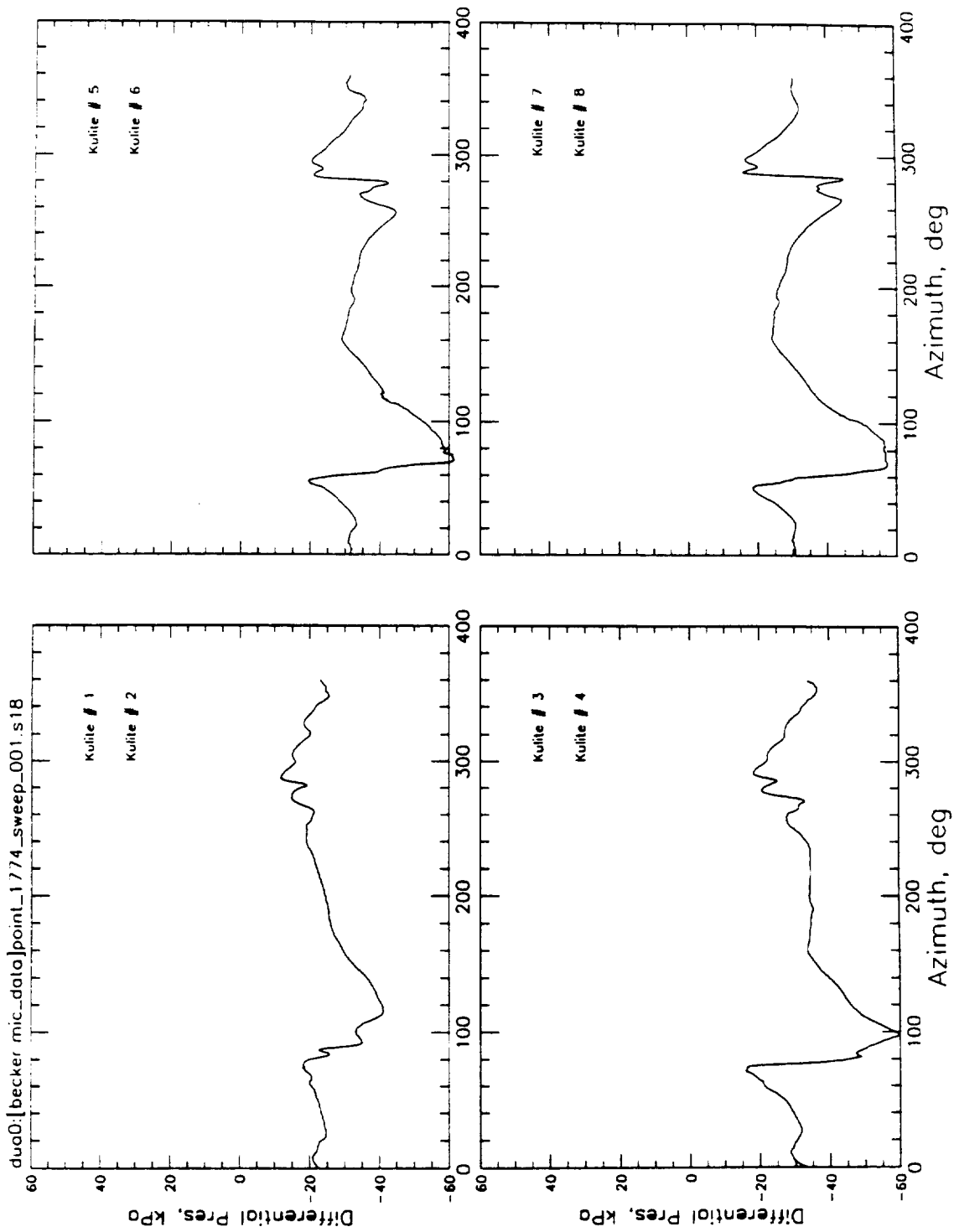
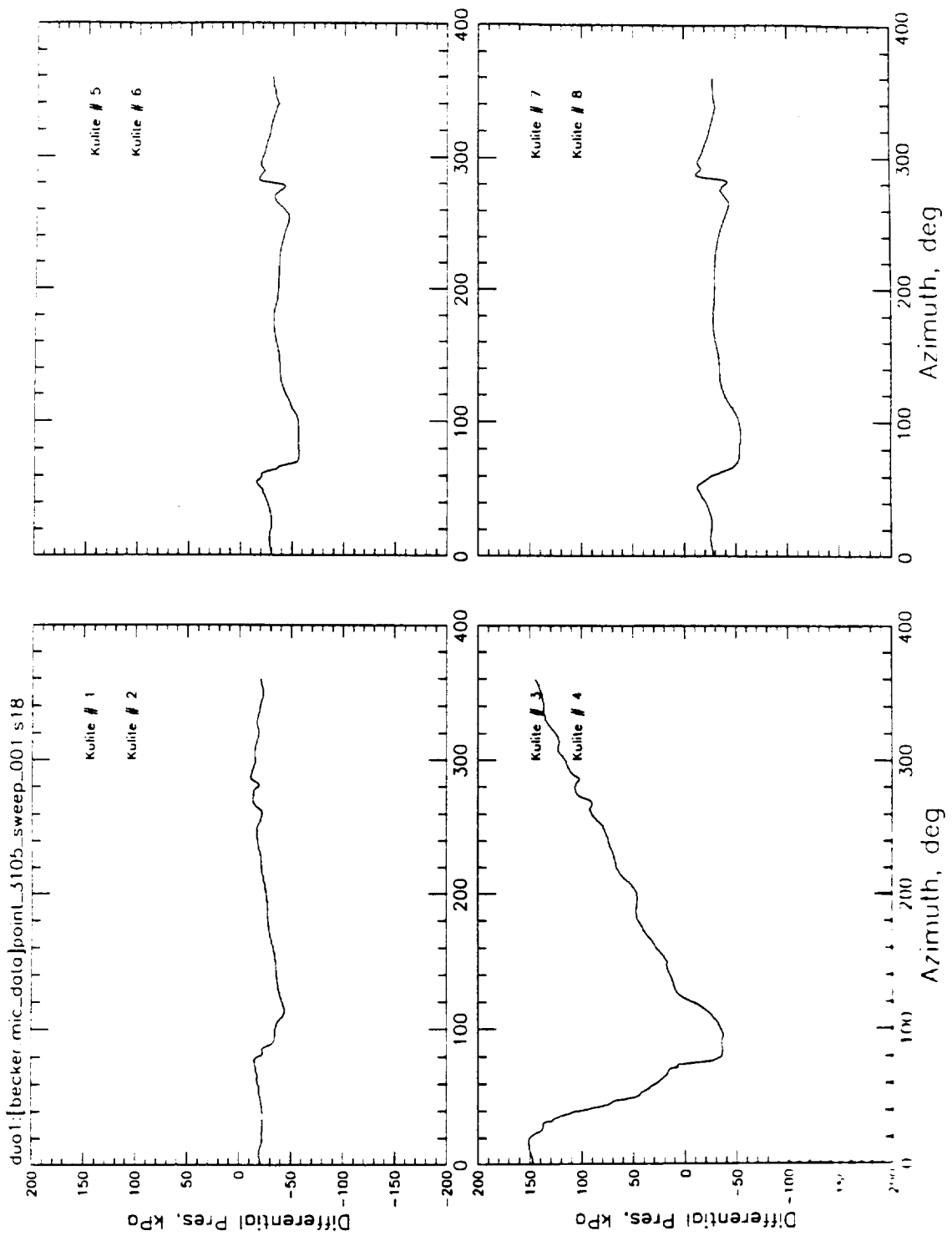


Figure (33) Calculated differential pressures ( $C_T/\sigma=0.0764$ ,  $\mu=0.149$ ,  $\alpha_{TPP}=3^\circ$  aft, peak deflection-12.5°, phase shift in azimuth=-10°,  $x/C=0.03$ )  
 Flapped rotor configuration: Test # 2900, Point # 1774



Figure(34) Calculated differential pressures ( $C_l/\sigma=0.0764$ ,  $\mu=0.149$ ,  $\alpha_{TPP}=3^\circ$ . aft, peak deflection=-17.5°, phase shift in azimuth=-10°,  $x/C=0.03$ )  
 Flapped rotor configuration: Test # 3915, Point # 3105

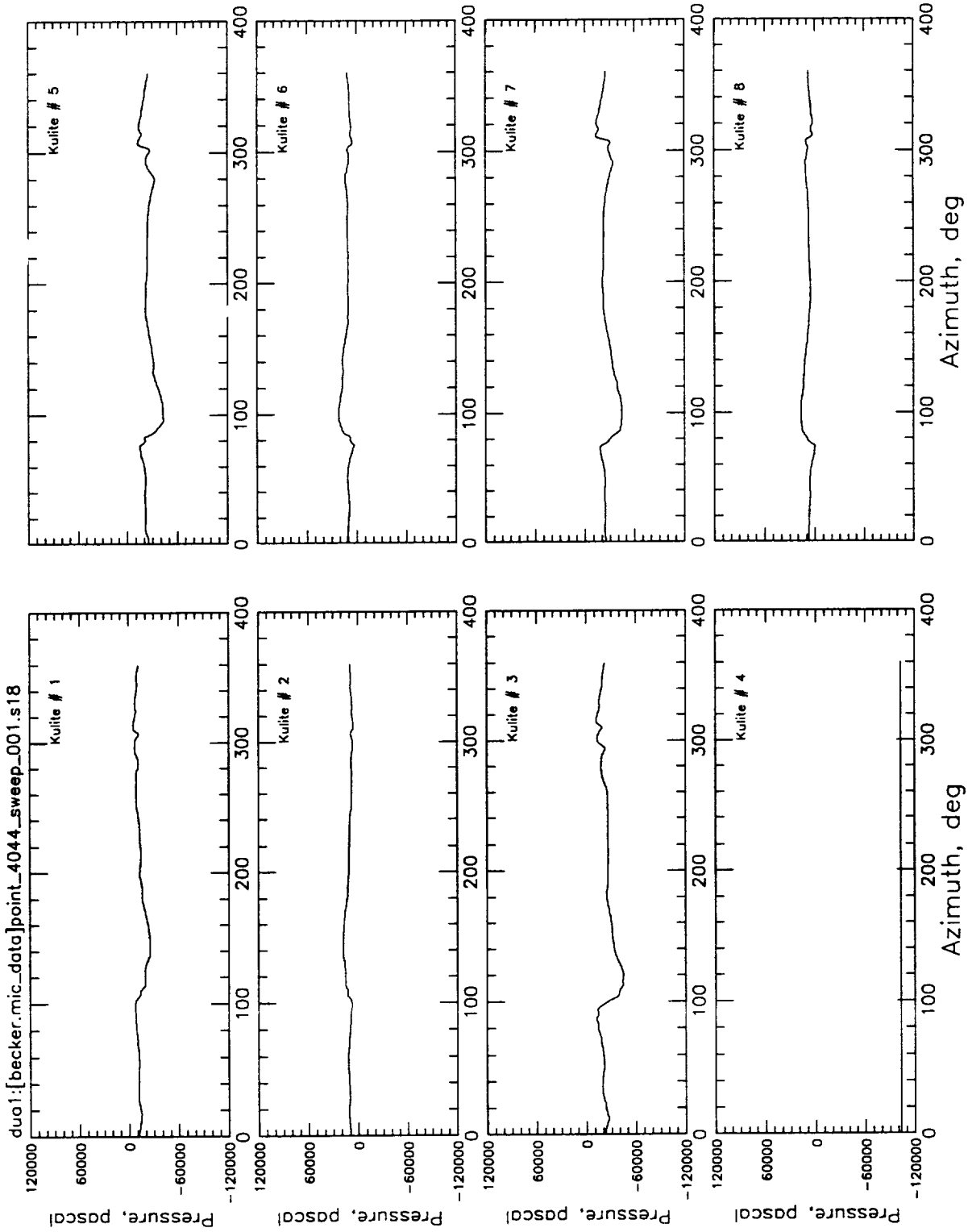


Figure (35) Calculated differential pressures ( $C_l/\alpha=0.0764$ ,  $\mu=0.149$ ,  $\alpha_{TPP}=3^\circ$ . aft, peak deflection=-17.5°, phase shift in azimuth=-20°,  $x/C=0.03$ )  
 Flapped rotor configuration: Test # 4034, Point # 4044

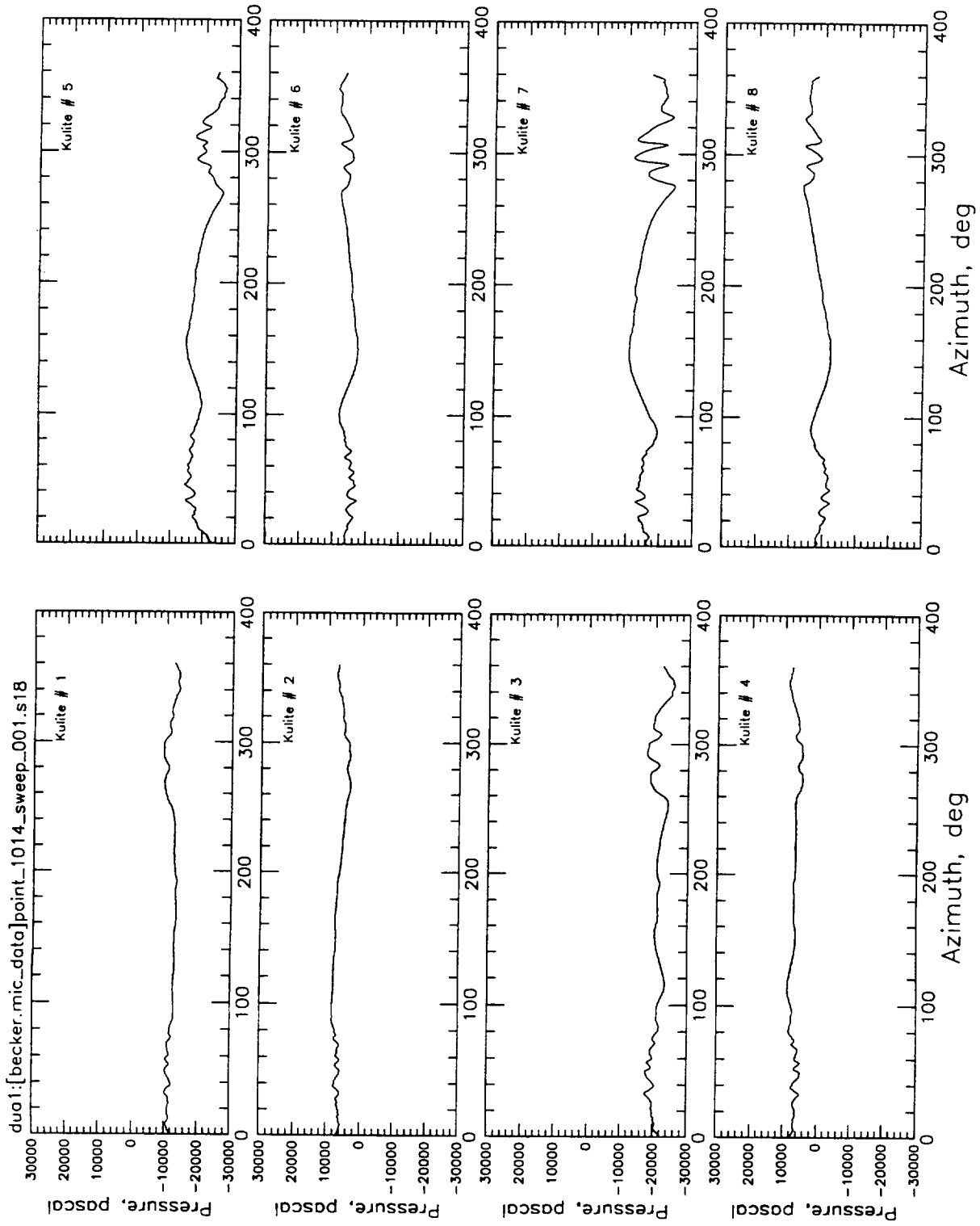


Figure (36) Measured blade surface pressures ( $C_l/\sigma=0.076$ ,  $\mu=0.199$ ,  $\alpha_{TPP}=4^\circ$ , aft,  $x/C=0.03$ ) Baseline rotor configuration: Test # 0738, Point # 1014

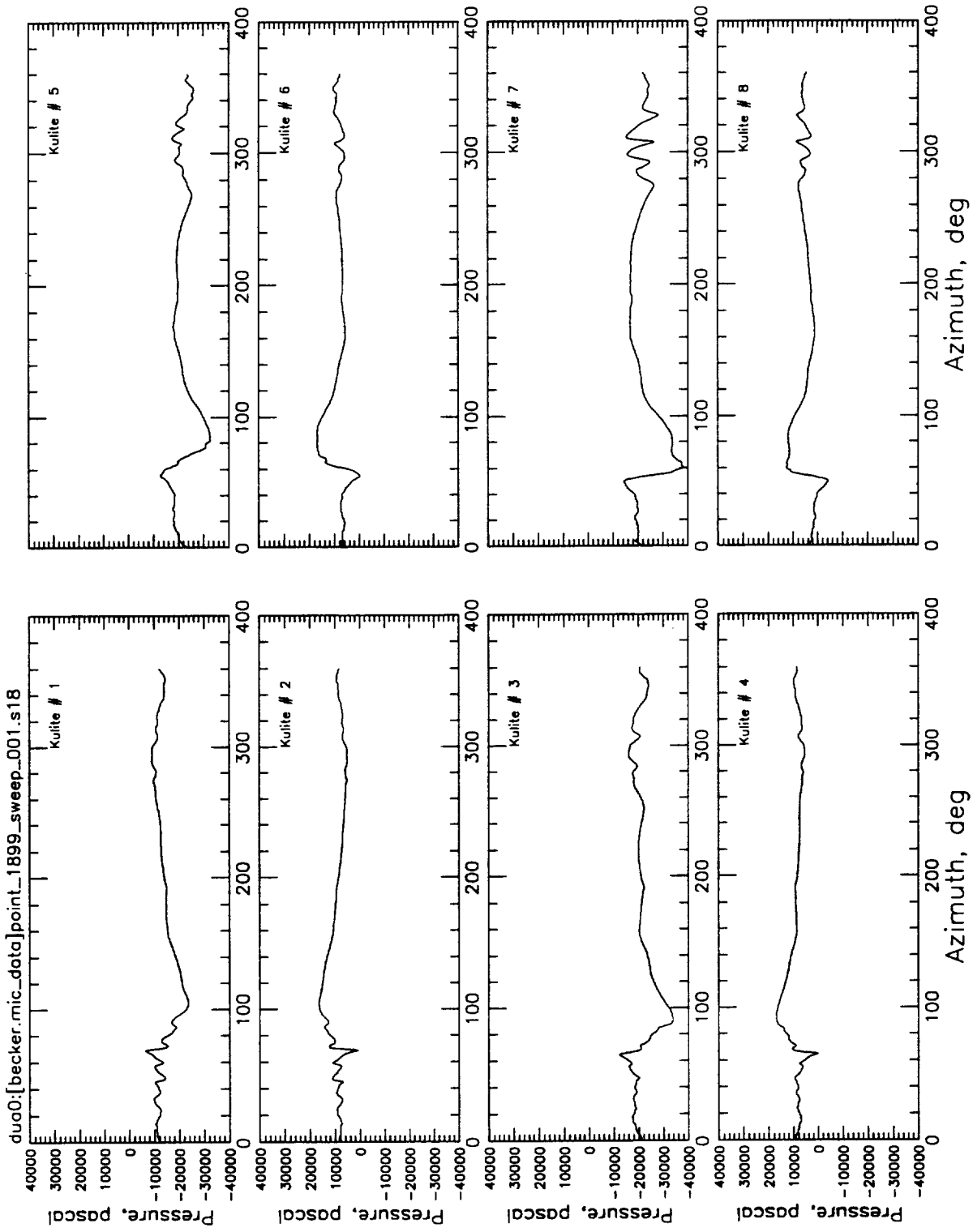


Figure (37) Measured blade surface pressures ( $C_l/\sigma=0.076$ ,  $\mu=0.199$ ,  $\alpha_{TPP}=4^\circ$ . aft, peak deflection =  $-12.5^\circ$ , phase shift in azimuth =  $-10^\circ$ ,  $x/C=0.03$ )  
 Flapped rotor configuration: Test # 2904, Point # 1899



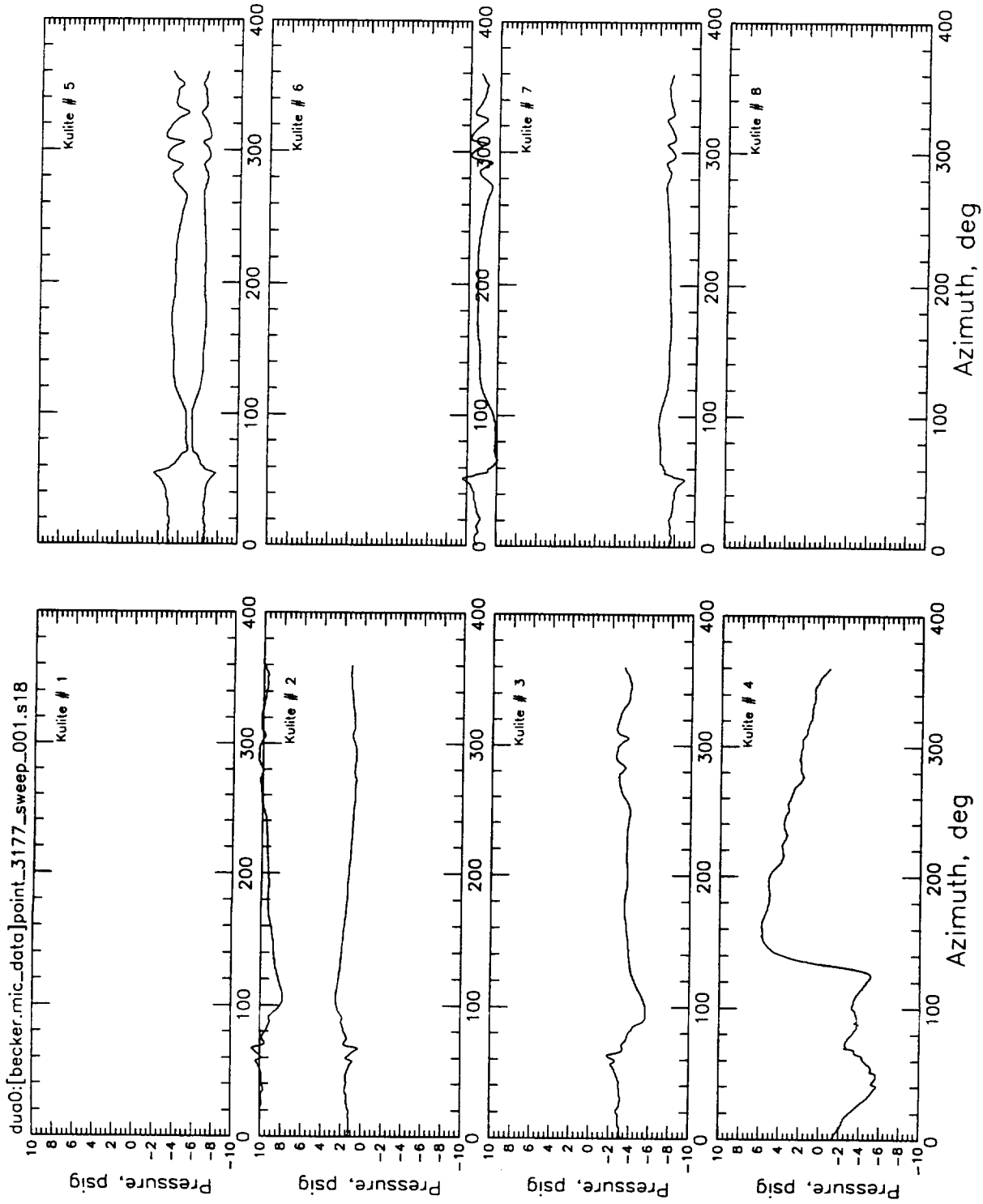
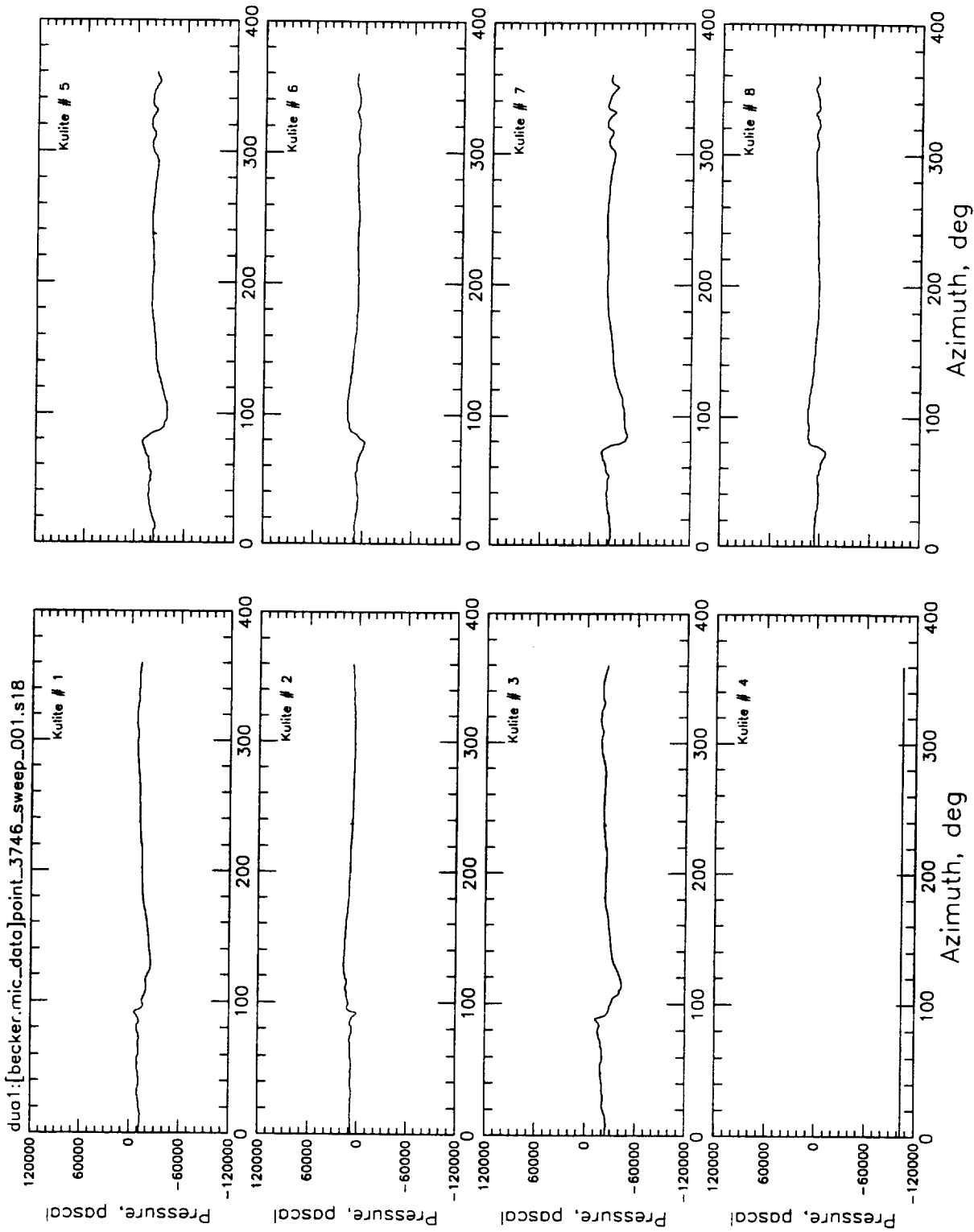


Figure (38) Measured blade surface pressures ( $C_l/\sigma=0.076$ ,  $\mu=0.199$ ,  $\alpha_{TPP}=4^\circ$ . aft, peak deflection =  $-17.5^\circ$ , phase shift in azimuth =  $-10^\circ$ ,  $x/C=0.03$ )  
 Flapped rotor configuration: Test # 3922, Point # 3177



**Figure (39)** Measured blade surface pressures ( $C_l/\sigma=0.076$ ,  $\mu=0.199$ ,  $\alpha_{TTPP}=4^\circ$ .  
aft, peak deflection =  $-20^\circ$ , phase shift in azimuth =  $-10^\circ$ ,  $\chi/C=0.03$ )  
Flapped rotor configuration: Test # 4047, Point # 3746

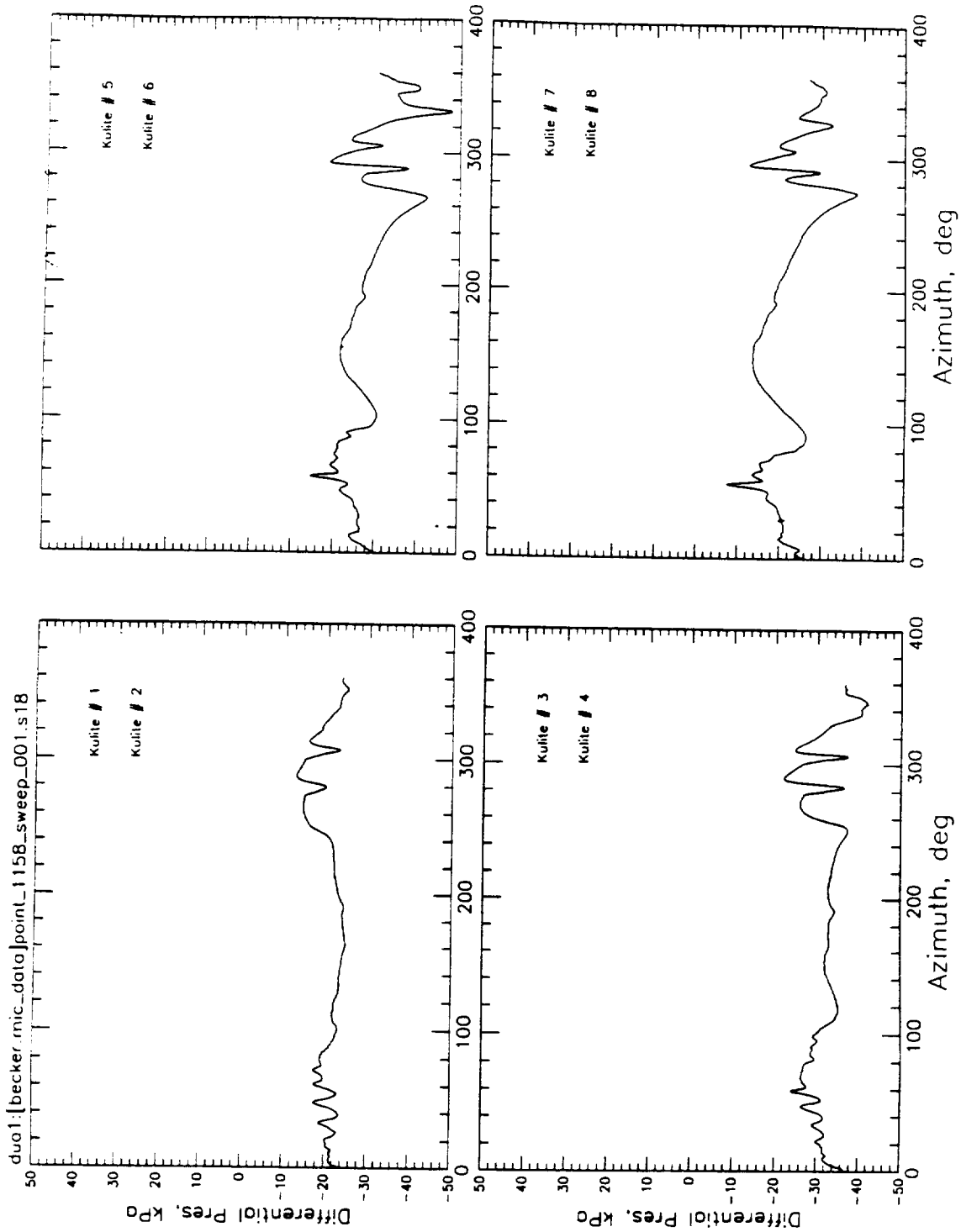


Figure (40) Calculated differential pressures ( $C_l/\sigma=0.0865$ ,  $\mu=0.199$ ,  $\alpha_{TPP}=2.5^\circ$  aft,  $x/C=0.03$ ) Baseline rotor configuration: Test # 0741, Point # 1158

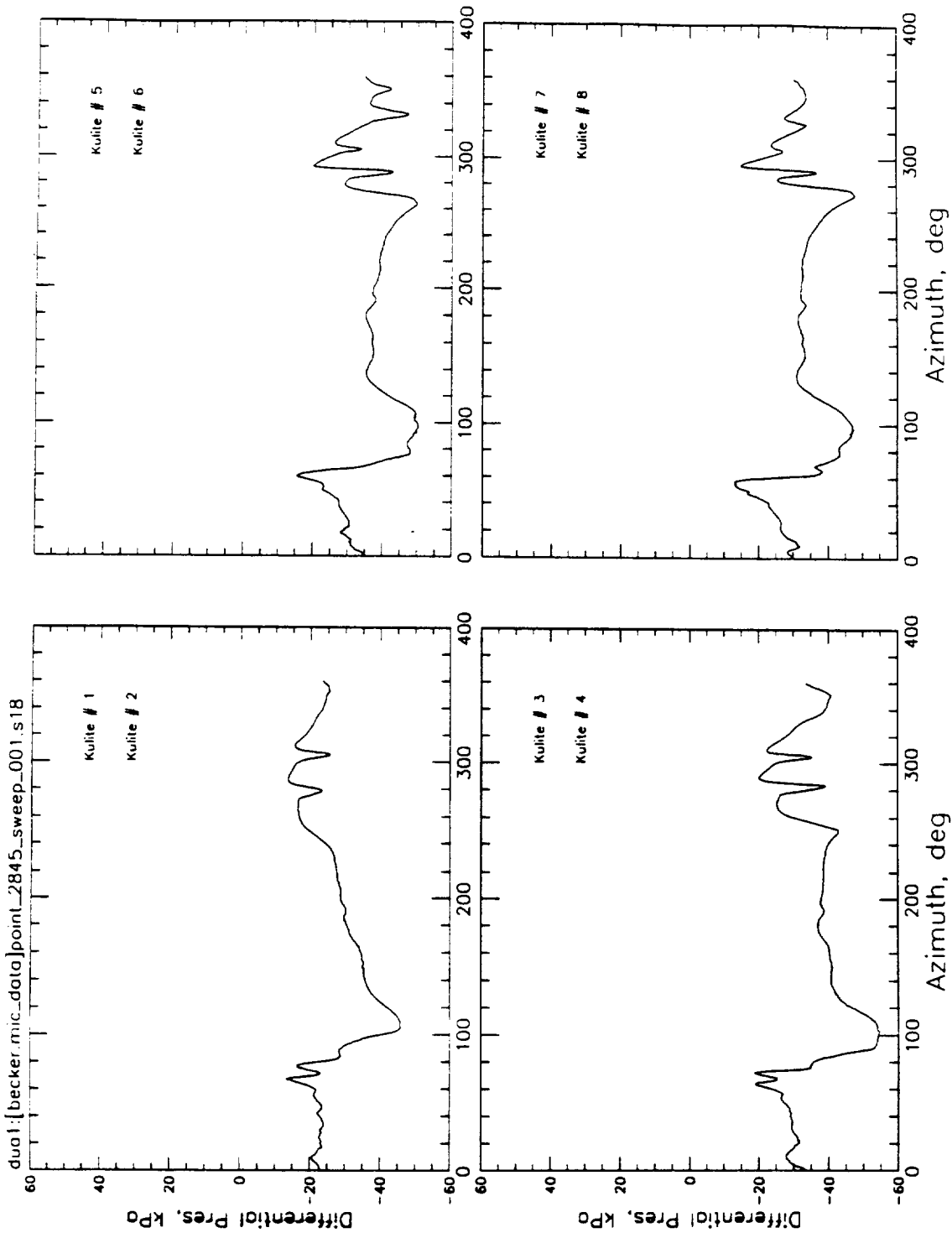


Figure (41) Calculated differential pressures ( $C_l/\sigma=0.0865$ ,  $\mu=0.199$ ,  $\alpha_{TPP}=2.5^\circ$ , aft, peak deflection=-17.5°, phase shift in azimuth=0°,  $x/C=0.03$ )  
 Flapped rotor configuration: Test # 3910, Point # 2845

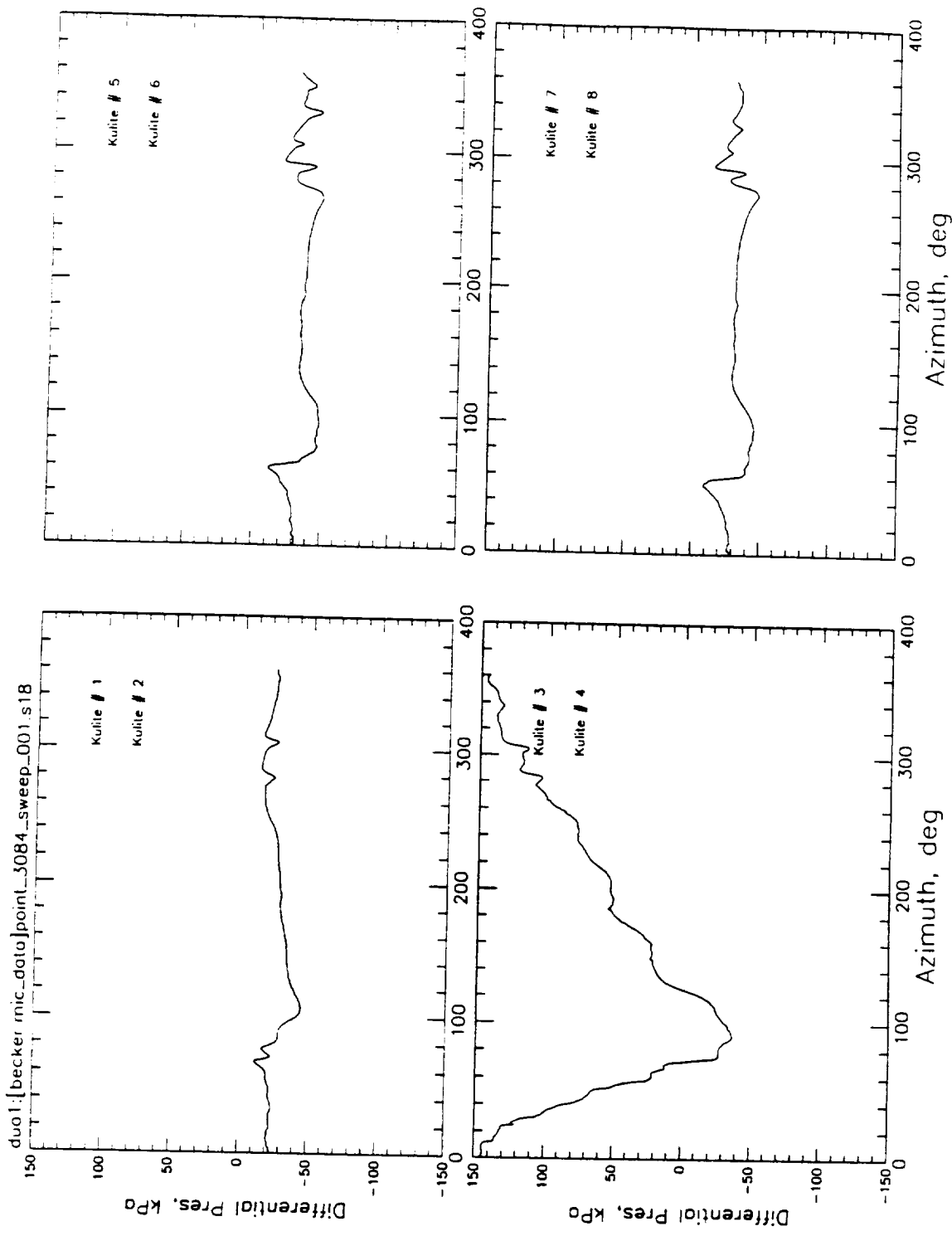


Figure (42) Calculated differential pressures ( $C_l/\sigma=0.0865$ ,  $\mu=0.199$ ,  $\alpha_{TPP}=2.5^\circ$ . aft, peak deflection=-17.5°, phase shift in azimuth=-5°,  $x/C=0.03$ )  
 Flapped rotor configuration: Test # 3941, Point # 3084

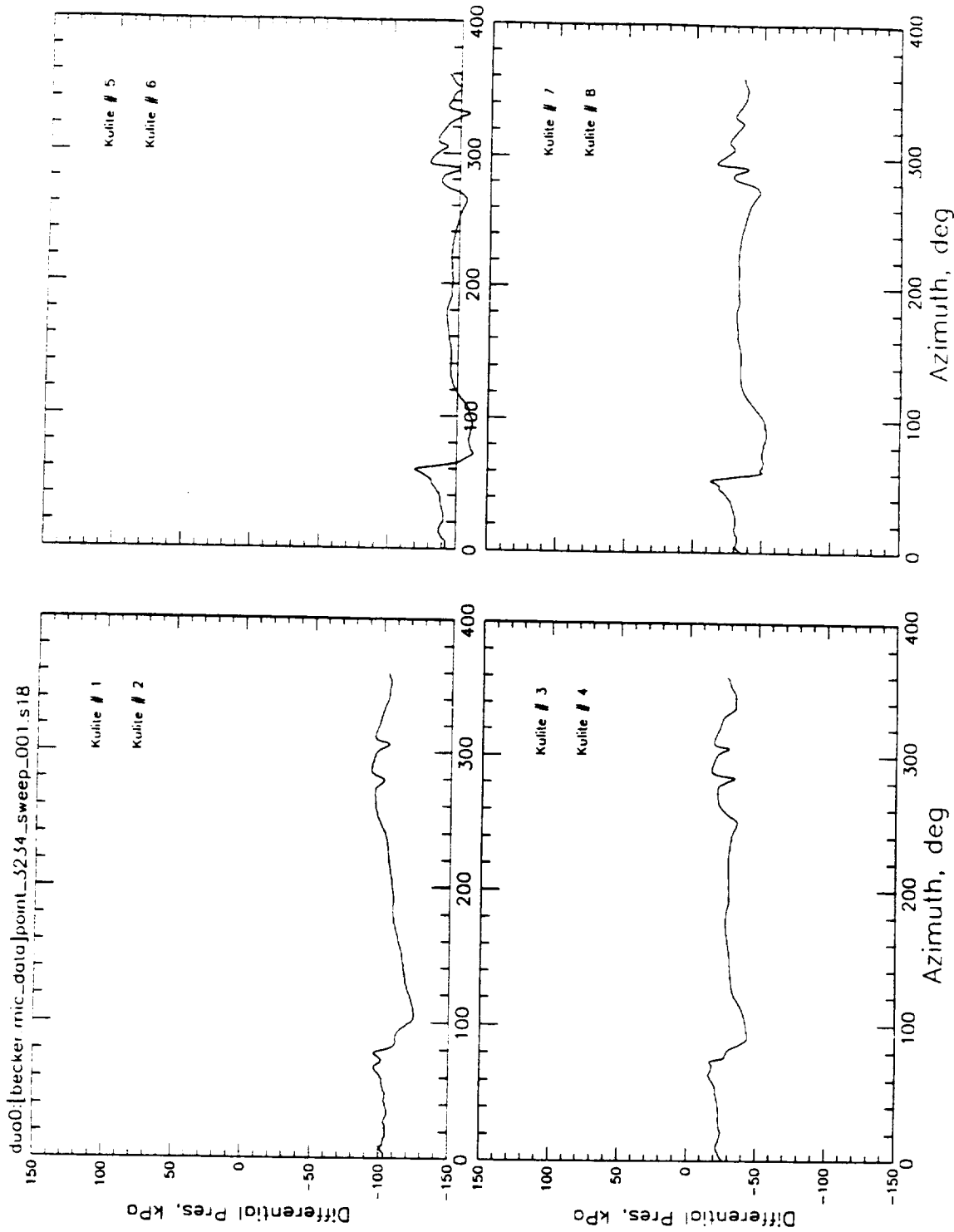


Figure (43) Calculated differential pressures ( $C_l/\sigma=0.0865$ ,  $\mu=0.199$ ,  $\alpha_{TPP}=2.5^\circ$ , aft, peak deflection= $-17.5^\circ$ , phase shift in azimuth= $-10^\circ$ ,  $x/C=0.03$ )  
 Flapped rotor configuration: Test # 3925, Point # 3234

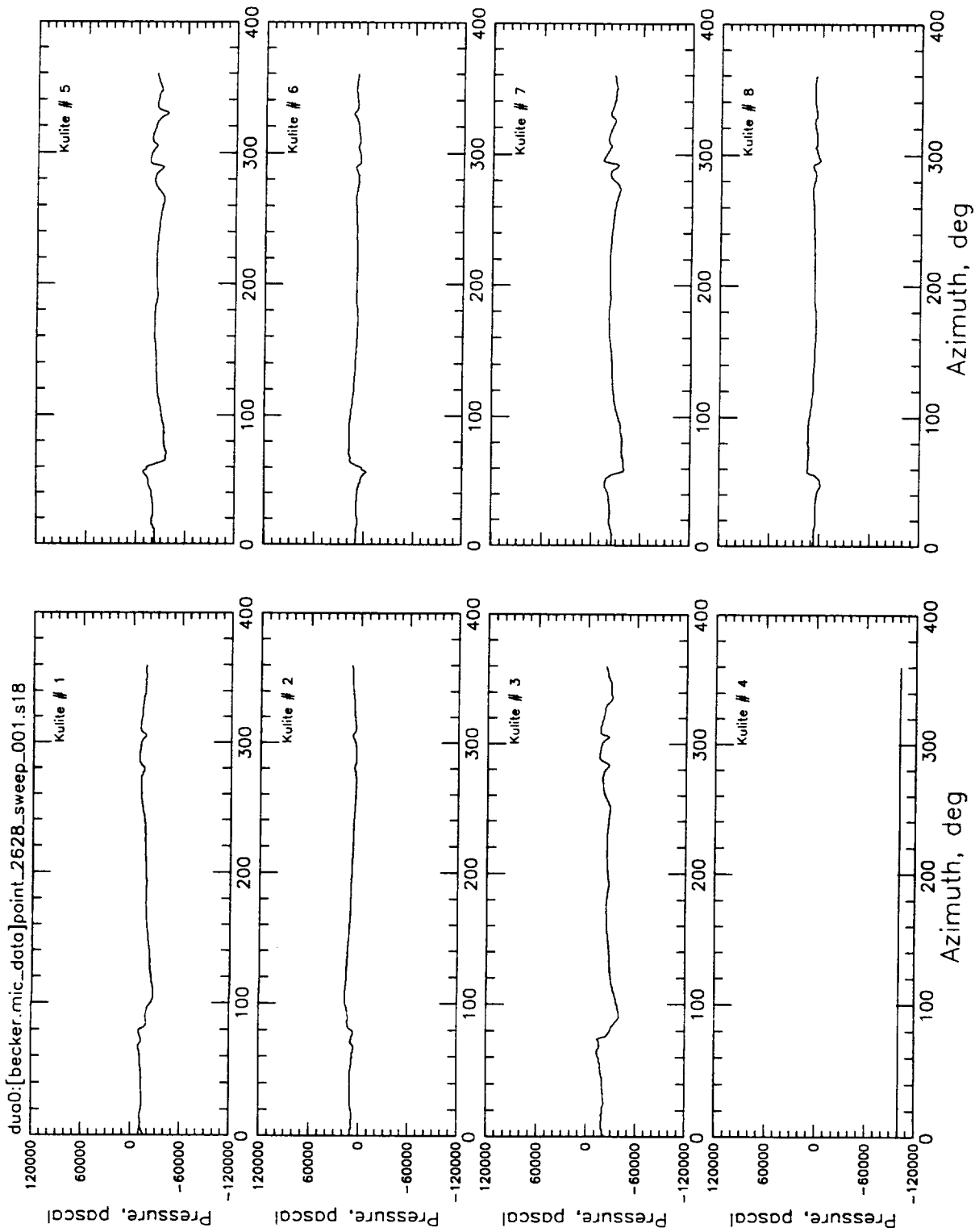


Figure (44) Calculated differential pressures ( $C_l/\sigma=0.0865$ ,  $\mu=0.199$ ,  $\alpha_{TPP}=2.5^\circ$ . aft, peak deflection=-17.5°, phase shift in azimuth=-20°,  $x/C=0.03$ )  
 Flapped rotor configuration: Test # 3741, Point # 2628

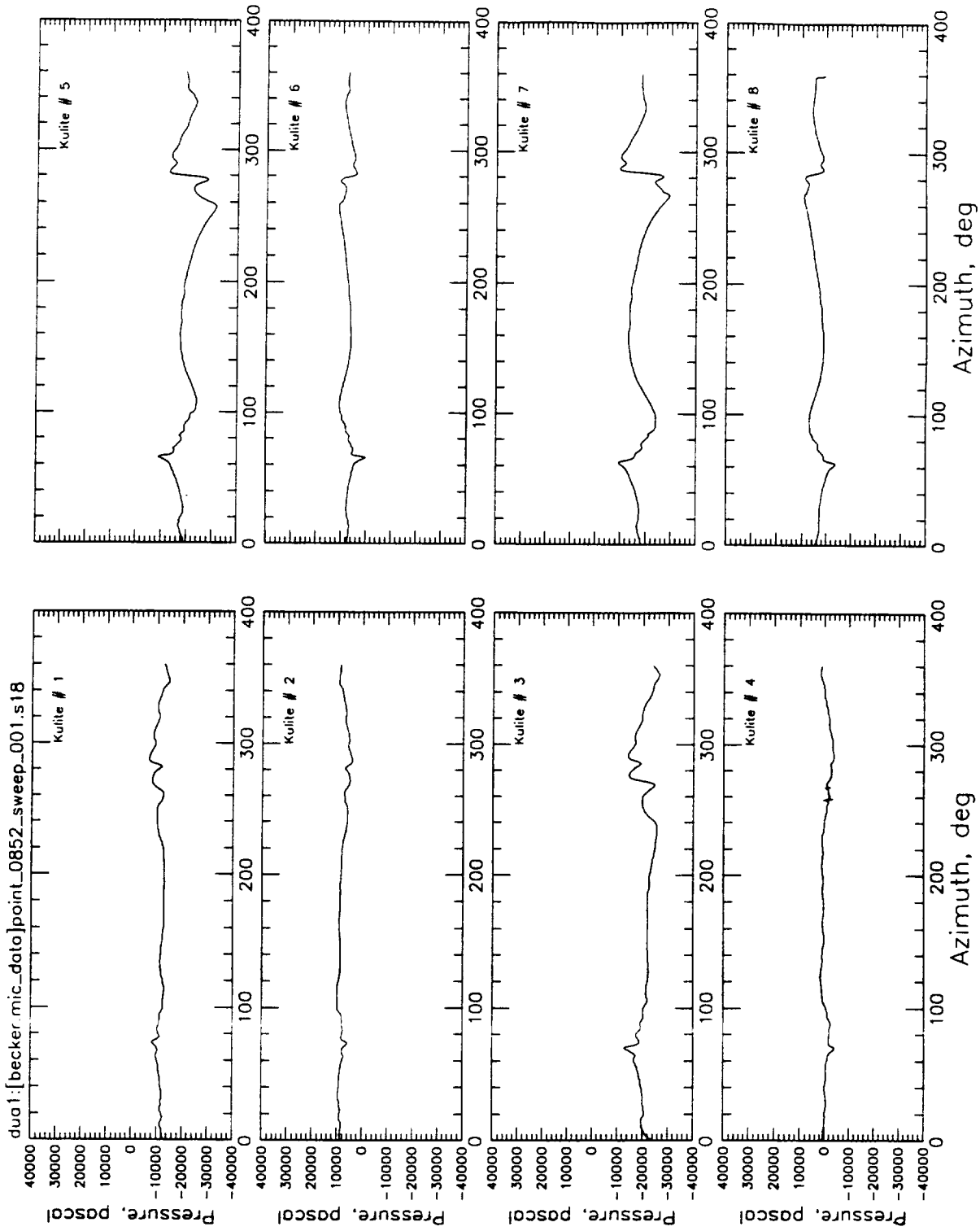


Figure (45) Measured blade surface pressures ( $C_l/\sigma=0.0764$ ,  $\mu=0.149$ ,  $\alpha_{TPP}=3^\circ$ , aft,  $x/C=0.03$ ) Baseline rotor configuration: Test # 0731, Point # 0852



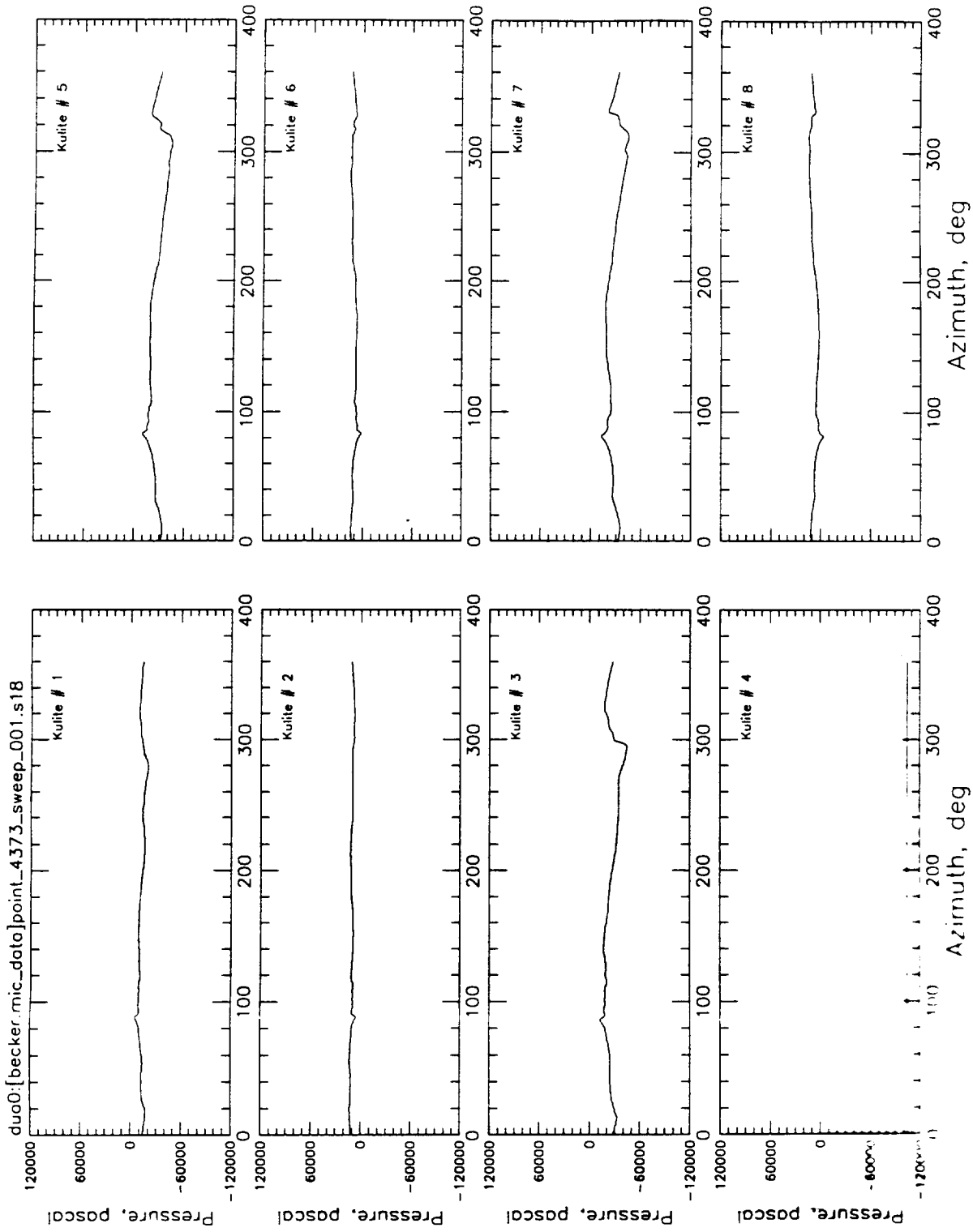


Figure (46) Measured blade surface pressures ( $C_l/\sigma=0.0764$ ,  $\mu=0.149$ ,  $\alpha_{TPP}=3^\circ$ . aft, peak deflection=-17.5°, phase shift=+140°,  $x/C=0.03$ ) Flapped rotor configuration: Test # 5030, Point # 4373

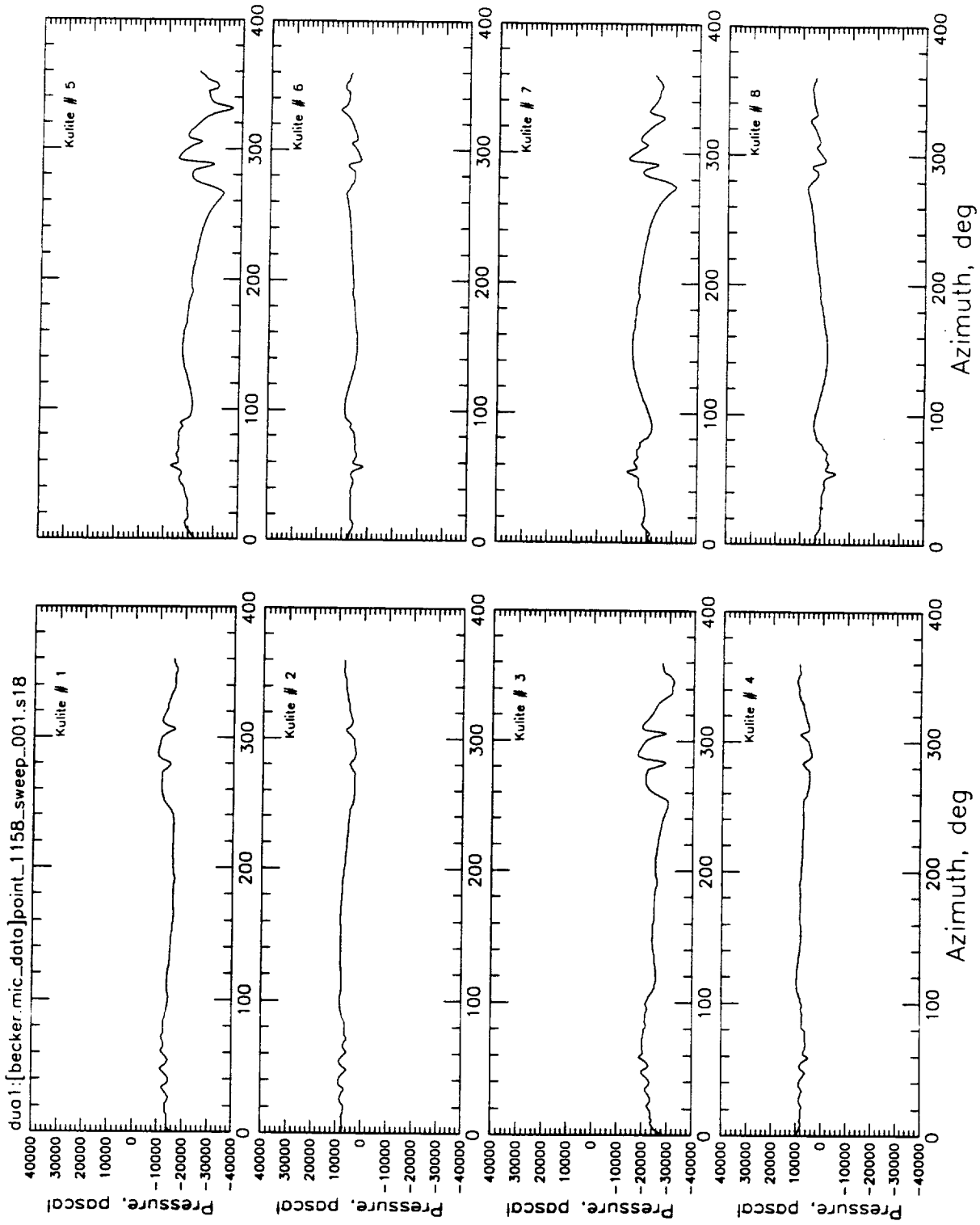


Figure (47) Measured blade surface pressures ( $C_l/\sigma=0.087$ ,  $\mu=0.199$ ,  $\alpha_{TPP}=2.5^\circ$ . aft,  $x/C=0.03$ ) Baseline rotor configuration: Test # 0741, Point # 1158

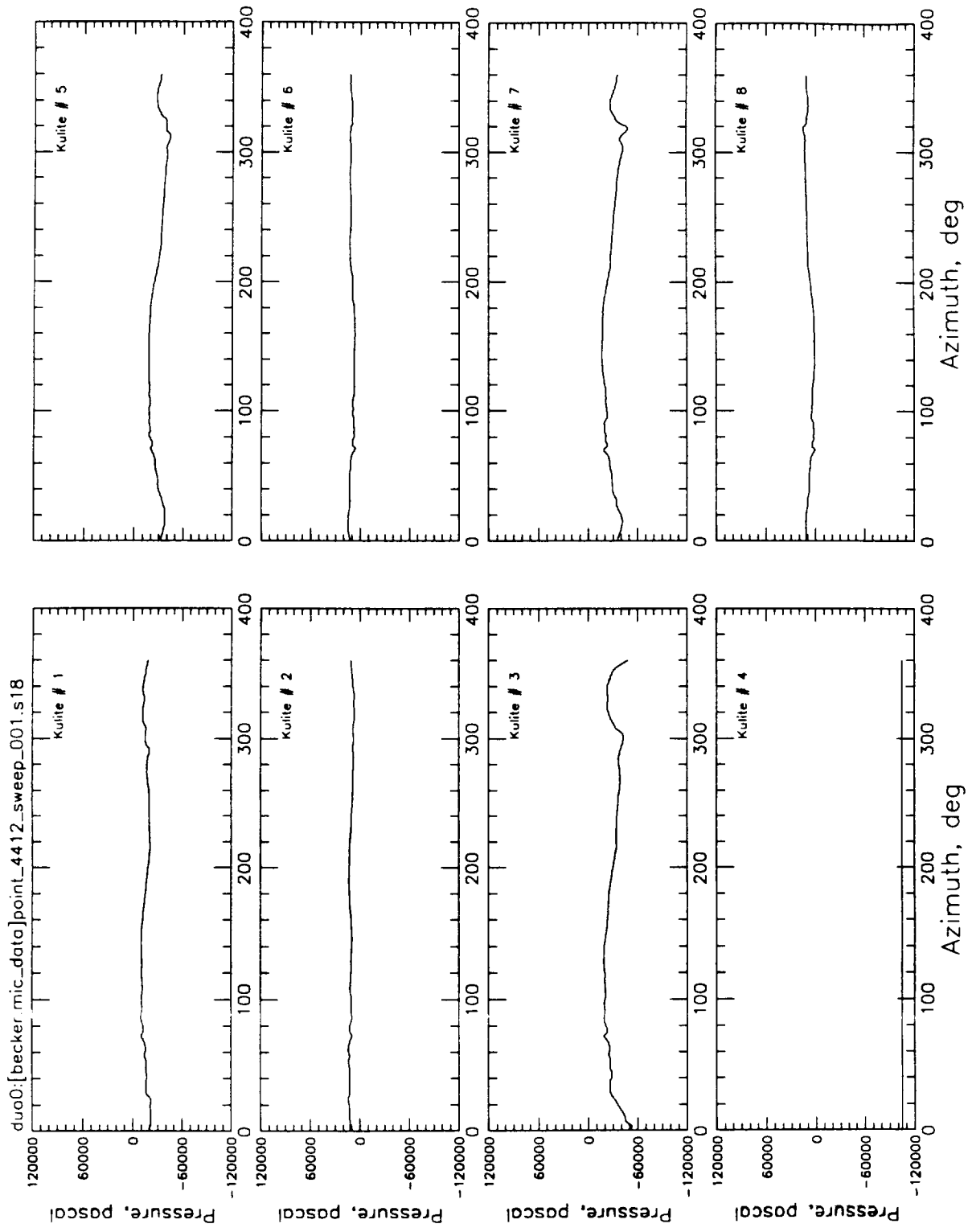
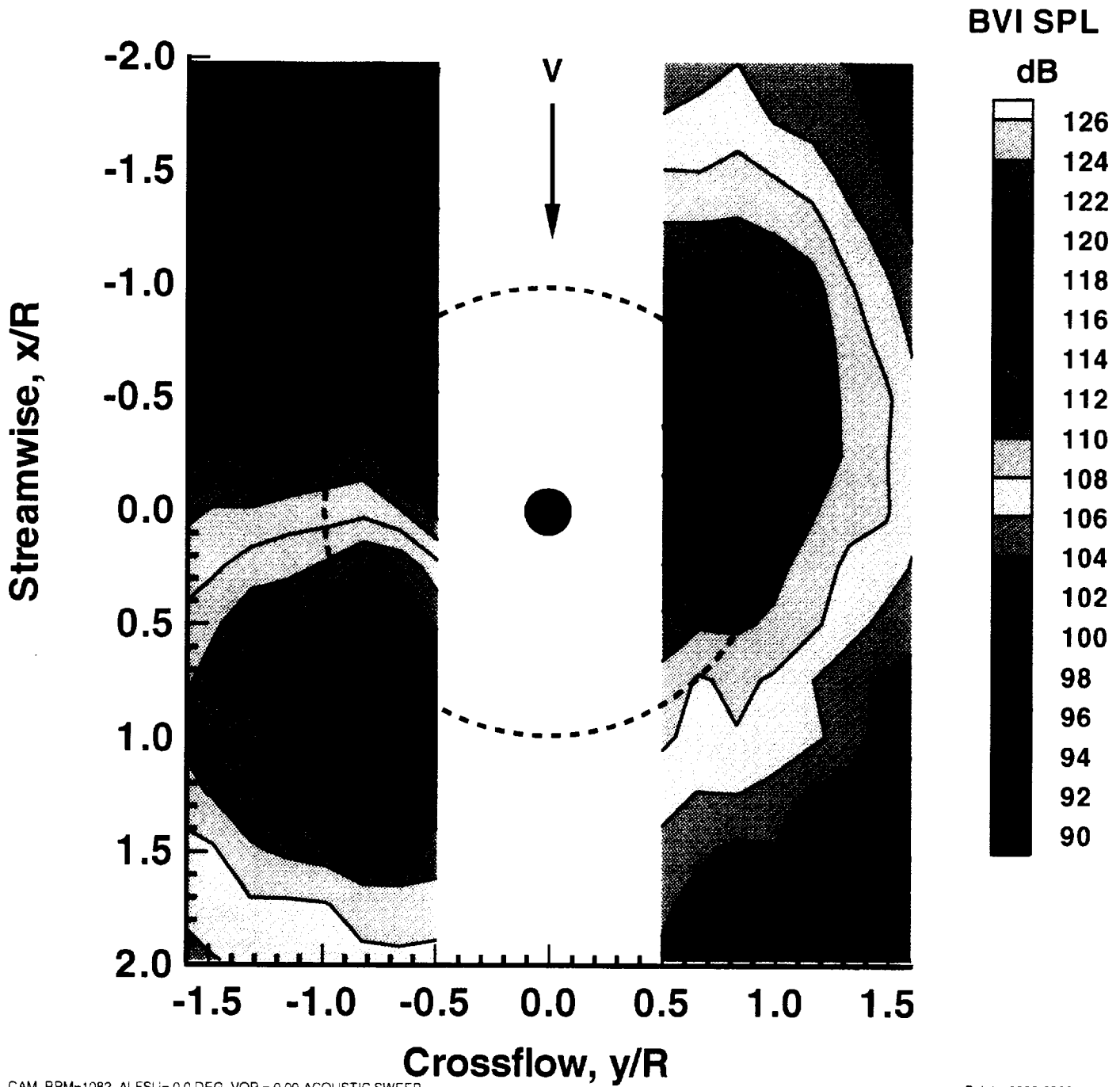


Figure (48) Measured blade surface pressures ( $C_l/\sigma=0.0764$ ,  $\mu=0.199$ ,  $\alpha_{TPP}=2.5^\circ$  aft, peak deflection=-17.5°, phase shift=+140°,  $x/C=0.03$ ) Flapped rotor configuration: Test # 5050, Point # 4412

Condition: 0733 Date: 25 Feb 1994

$\alpha_{\text{shaft}}$ : 5.013  $\mu$ : 0.1488  $C_t/\sigma$ : 0.0765



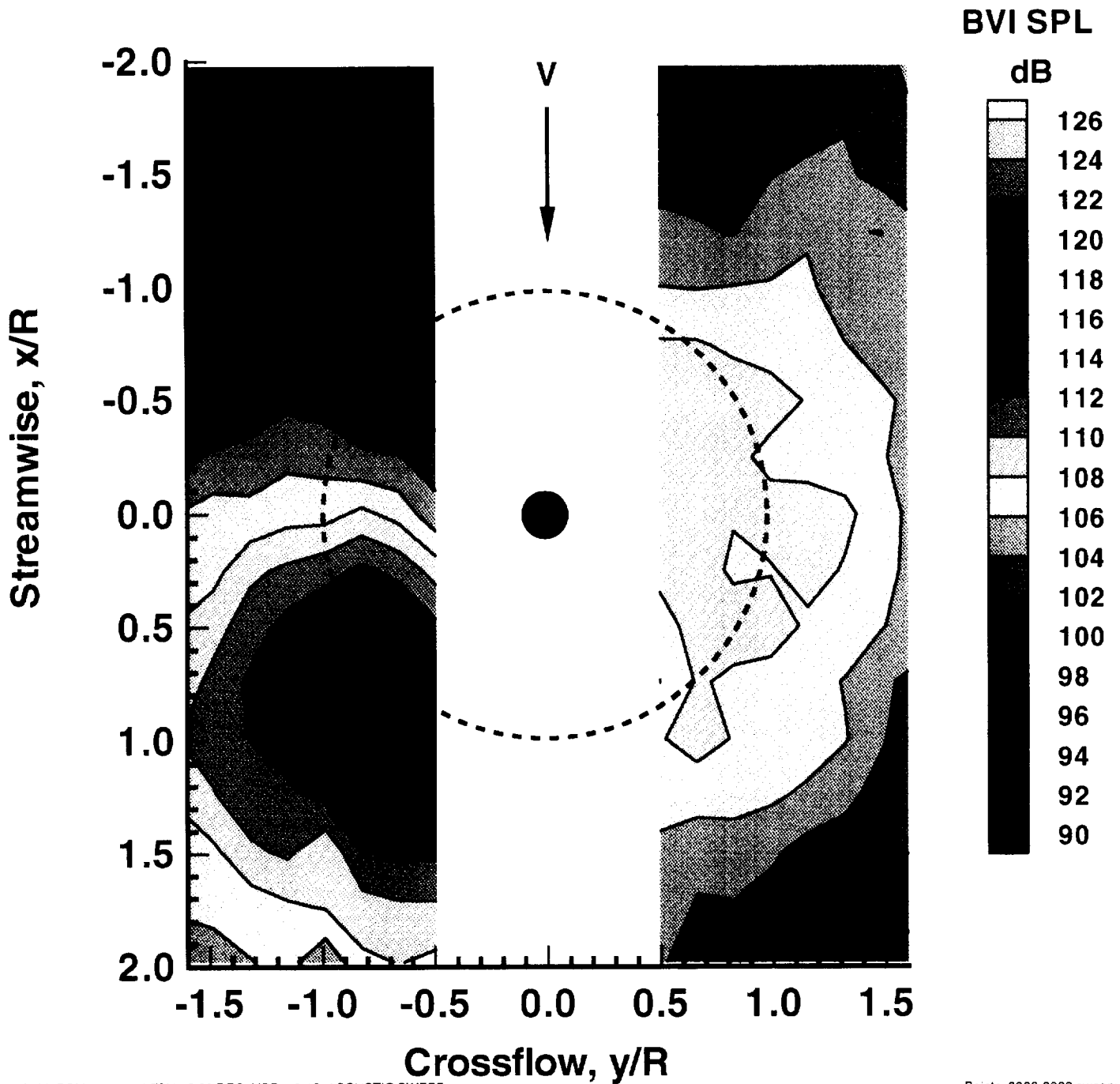
NULL CAM, RPM=1082, ALFSU=0.0 DEG, VOR = 0.00, ACOUSTIC SWEEP

Points: 0892-0908 sweep: 001

Figure (49a) BVISPL Contour Plot Based on Spectra of Averaged Timehistories ( $C_t/s = 0.0765$ ,  $\alpha_{\text{TPP}} = 5$  degrees aft,  $\mu=0.1488$ ) Baseline Rotor Configuration - Test # 0733

Condition: 2916 Date: 2 Mar 1994

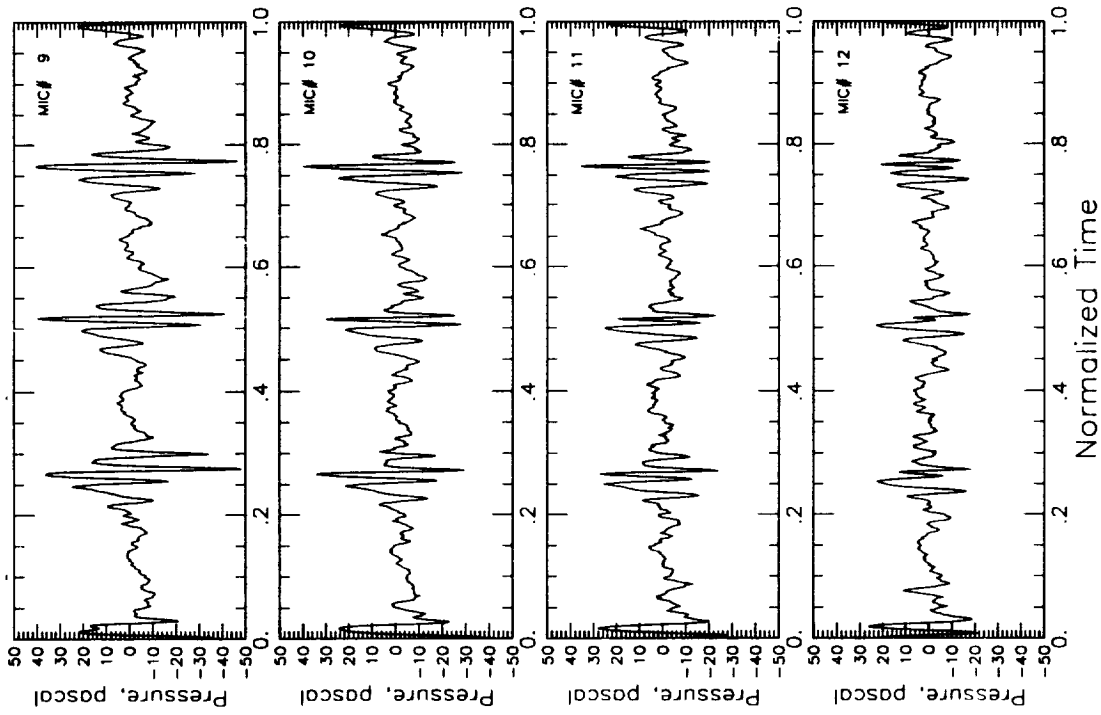
$\alpha_{\text{shaft}}$ : 5.007  $\mu$ : 0.1487  $C_t/\sigma$ : 0.0777



12.5-20CAM, RPM= 1075, ALFSU= 5.00 DEG, VOR = 0 15, ACOUSTIC SWEEP

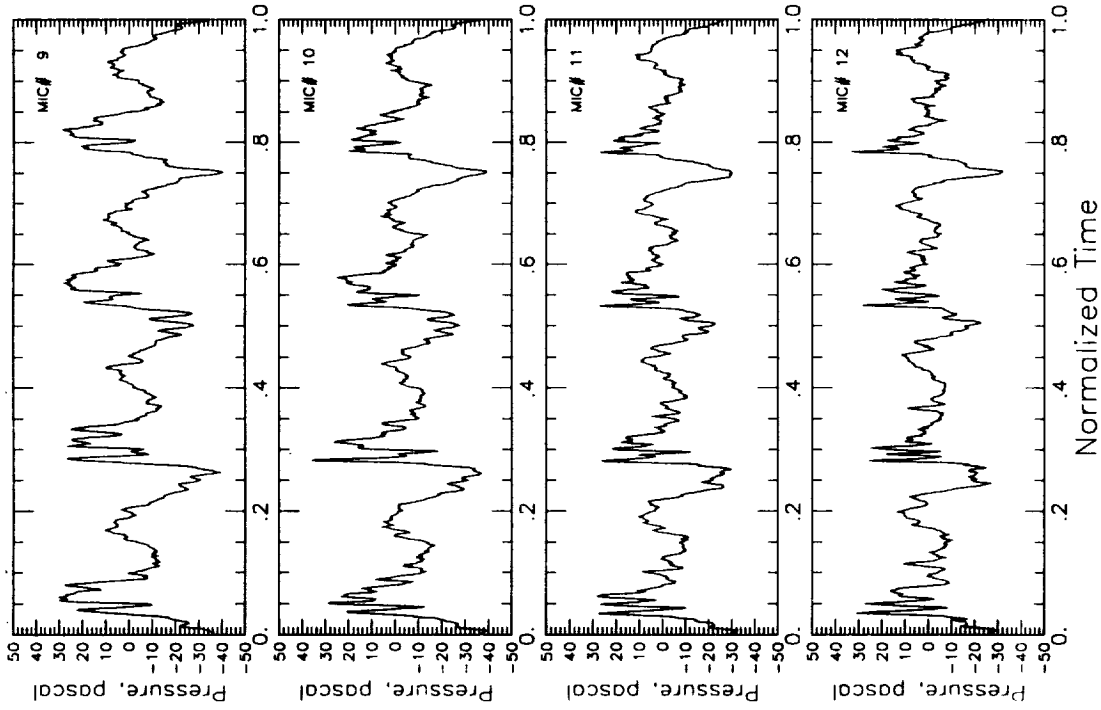
Points: 2083-2099 sweep:

Figure (49b) BVISPL Contour Plot Based on Spectra of Averaged Time Histories ( $C_t/\sigma = 0.0777$ ,  $\alpha_{\text{TPP}} = 5$  degrees aft,  $\mu = 0.1487$ , Peak Flap Deflection = -12.5 degrees, Azimuthal Phase Shift = -20 degrees) Flapped Rotor Configuration - Test # 2916

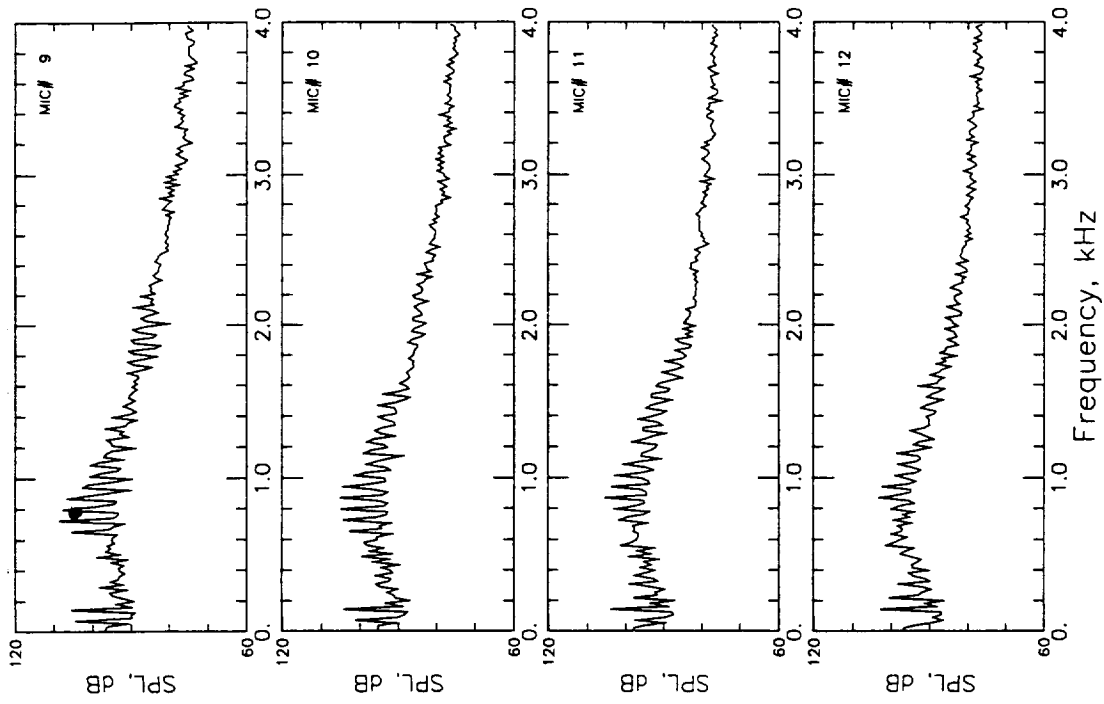


**a - Baseline Rotor [No Flap] - Test # 0733**

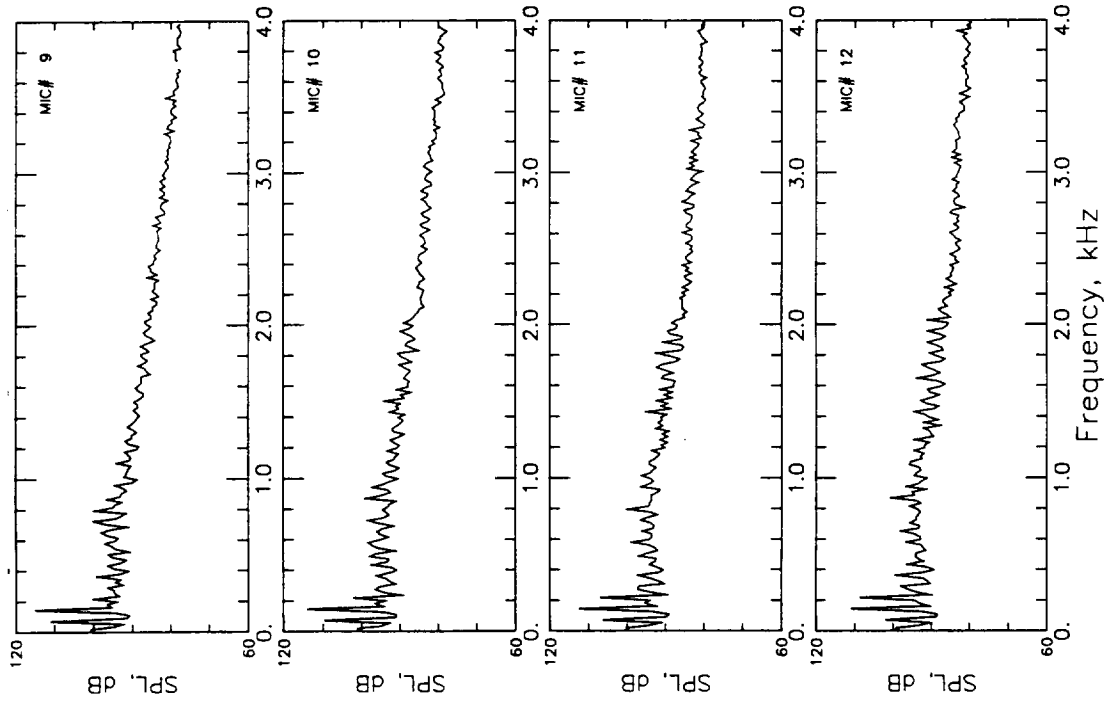
**Figures (50a & 50b) Average Acoustic Time Histories at Microphone  
 Traverse Station 9 on the Advancing Side - Test #s  
 0733 & 2916**



**b - Flapped Rotor  
 [Peak Flap Deflection=-12.5 degrees, Azimuthal  
 Phase Shift = -20 degrees ] - Test # 2916**

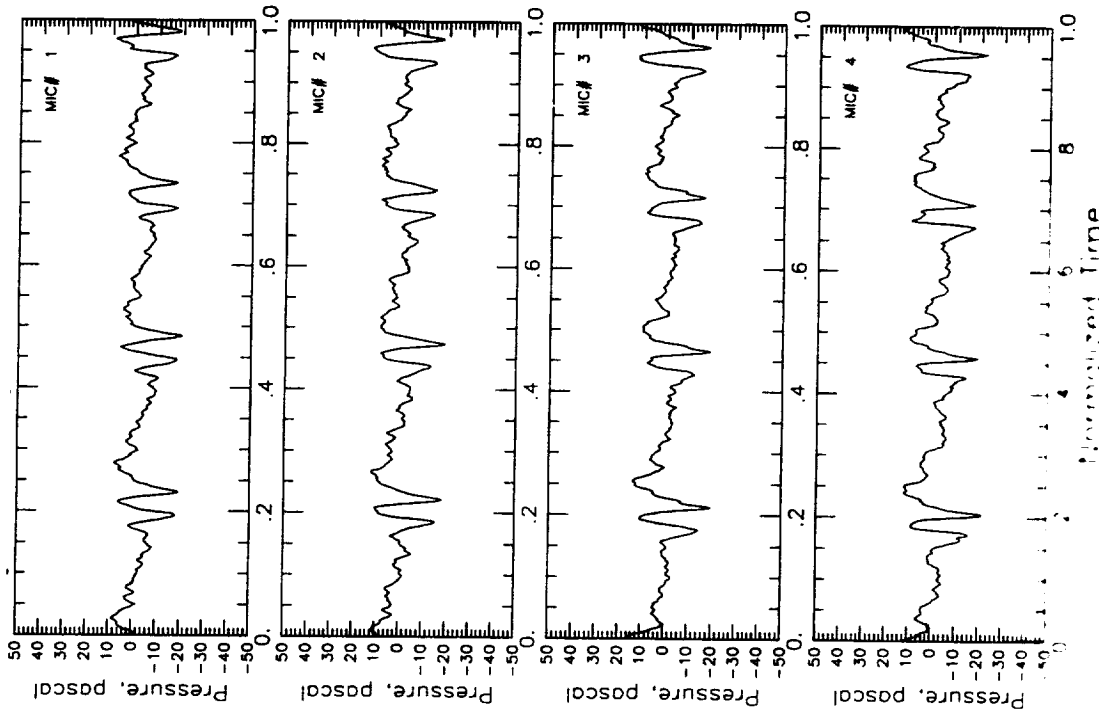


**a - Baseline Rotor [No Flap]- Test # 0733**

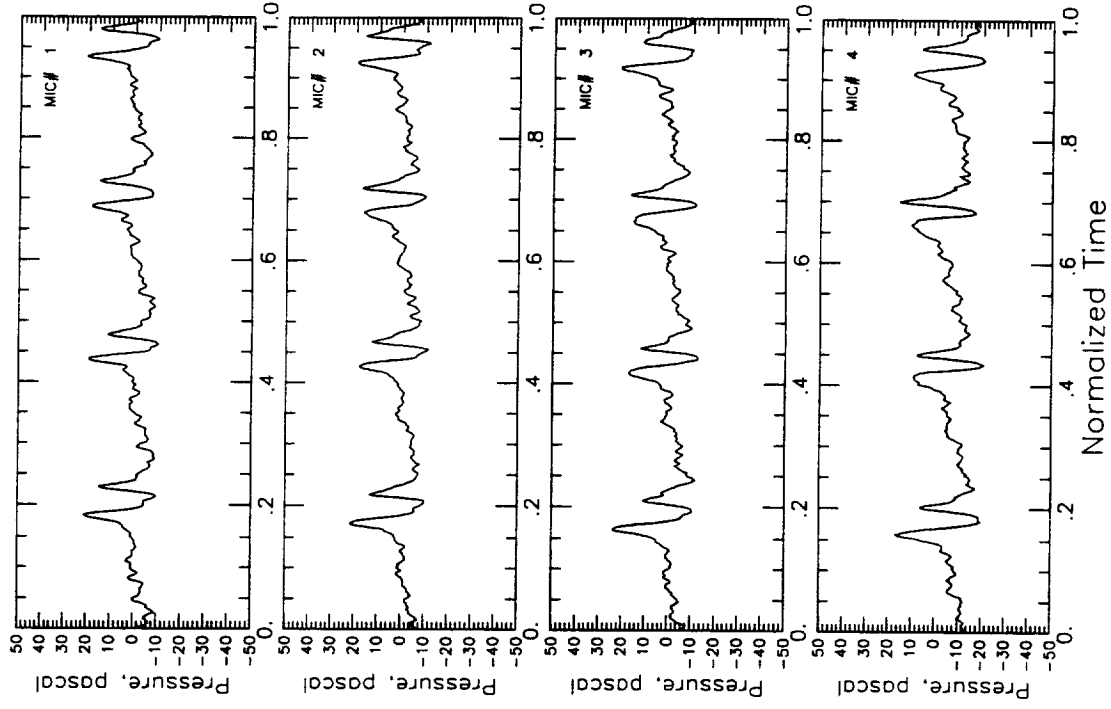


**b - Flapped Rotor**  
**[Peak Flap Deflection=-12.5 degrees, Azimuthal**  
**Phase Shift = -20 degrees ] - Test # 2916**

**Figures (51a & 51b) Ensemble-averaged Narrowband Spectra at**  
**Microphone Traverse Station 9 on the Advancing Side**  
**- Test #s 0733 & 2916**



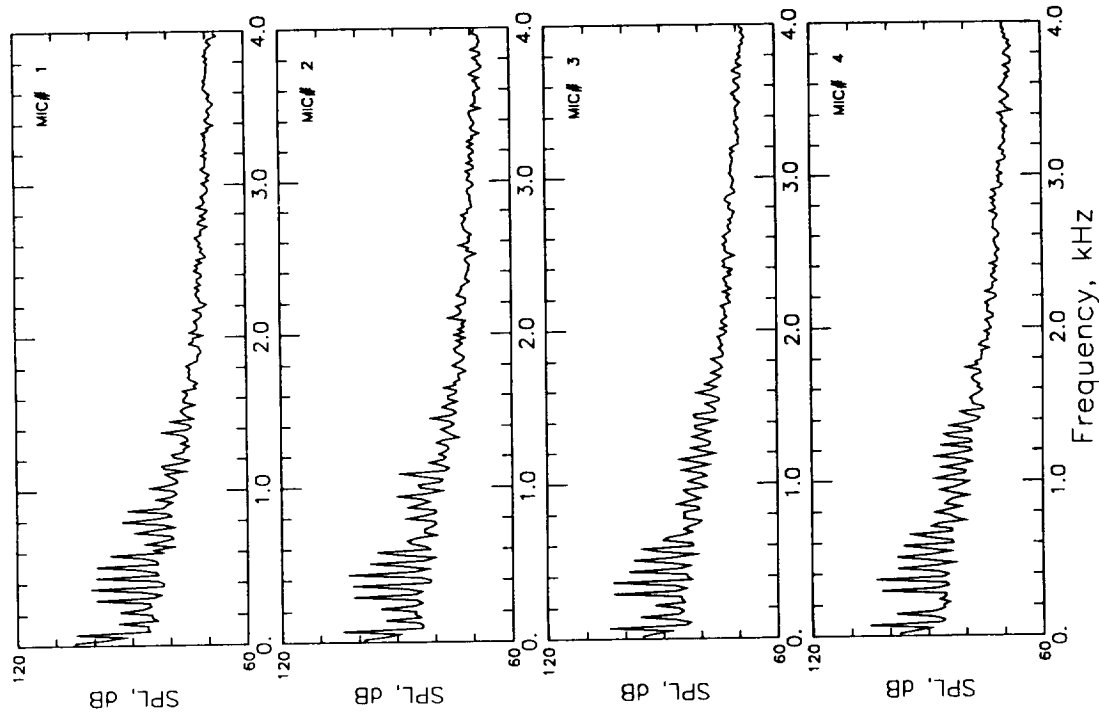
**a - Baseline Rotor [No Flap] - Test # 0733**



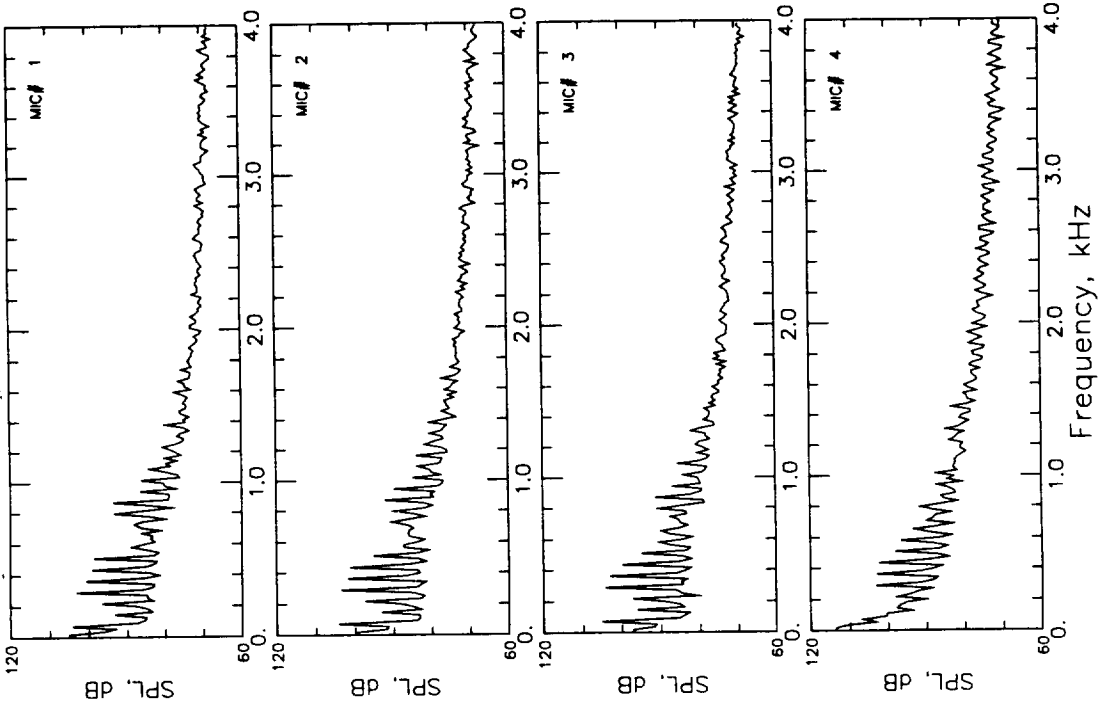
**b - Flapped Rotor**  
**[Peak Flap Deflection=-12.5 degrees, Azimuthal**  
**Phase Shift = -20 degrees ] - Test # 2916**

**Figures (52a & 52b) Average Acoustic Time Histories at Microphone**  
**Traverse Station 9 on the Retreating Side - Test #s**  
**0733 & 2916**





**a - Baseline Rotor [No Flap]- Test # 0733**



**b - Flapped Rotor**  
**[Peak Flap Deflection=-12.5 degrees, Azimuthal**  
**Phase Shift = -20 degrees ]- Test # 2916**

**Figures (53a & 53b) Ensemble-averaged Narrowband Spectra at**  
**Microphone Traverse Station 9 on the Retreating Side**  
**- Test #s 0733 & 2916**

Condition: 0741 Date: 26 Feb 1994

$\alpha_{\text{shaft}}$ : 2.502  $\mu$ : 0.1987  $C_t/\sigma$ : 0.0868

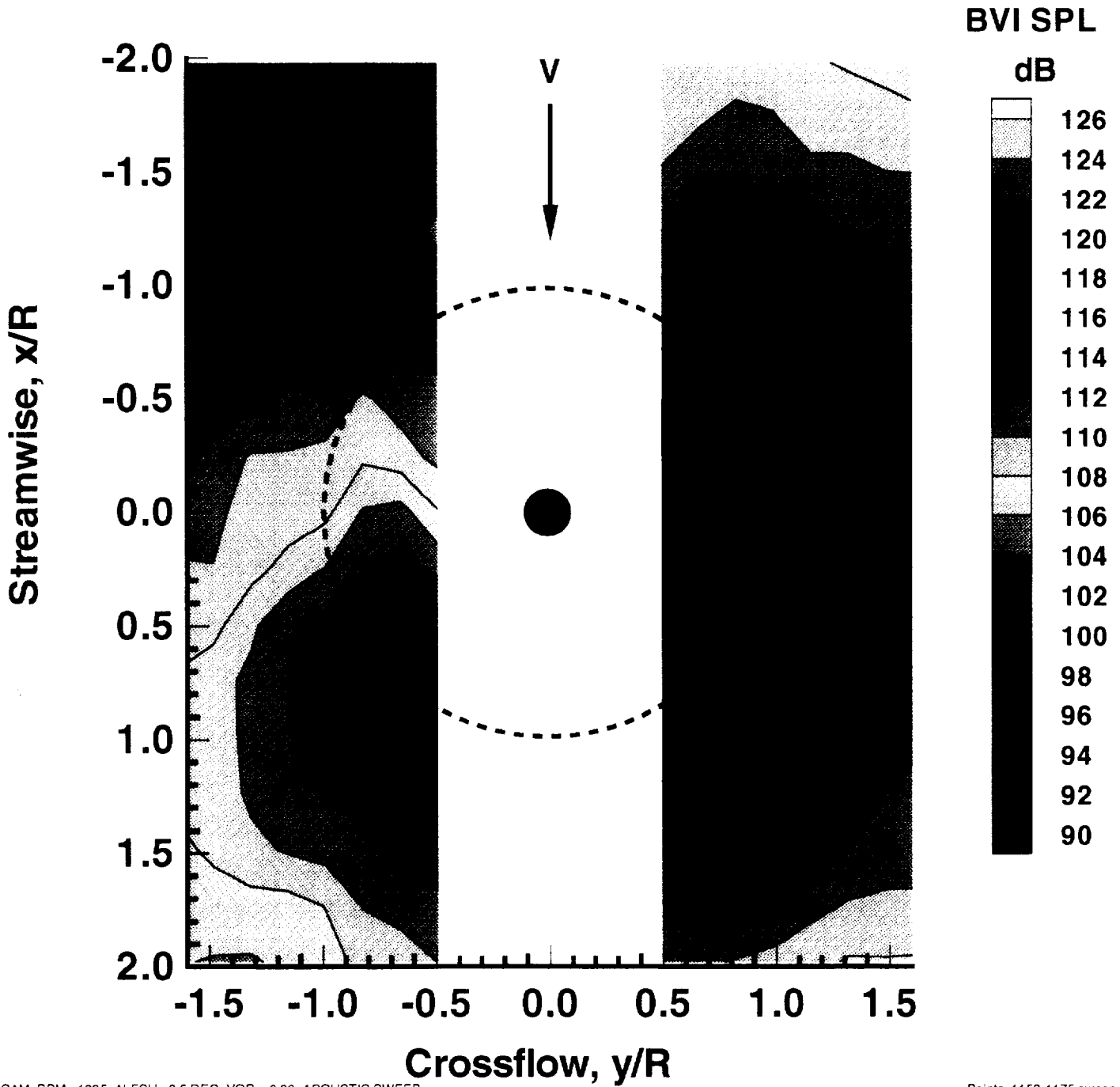


Figure (54a) BVISPL Contour Plot Based on Ensemble-averaged Spectra ( $C_t/\sigma = 0.0868$ ,  $\alpha_{\text{TRP}} = 2.5$  degrees aft,  $\mu=0.1987$ ) Baseline Rotor Configuration - Test #0741

Condition: 0741 Date: 26 Feb 1994

$\alpha_{\text{shaft}}$ : 2.502  $\mu$ : 0.1987  $C_t/\sigma$ : 0.0868

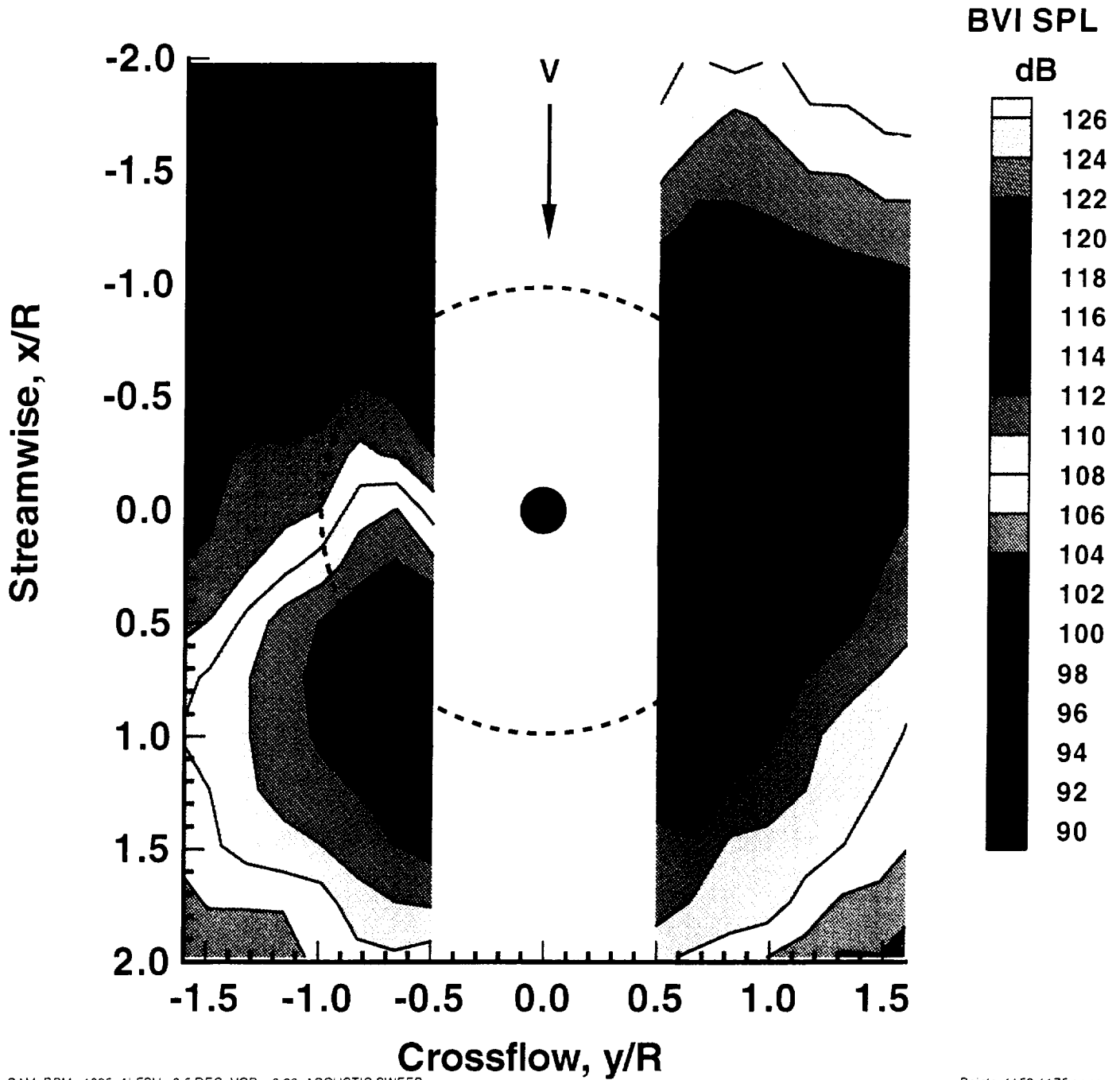
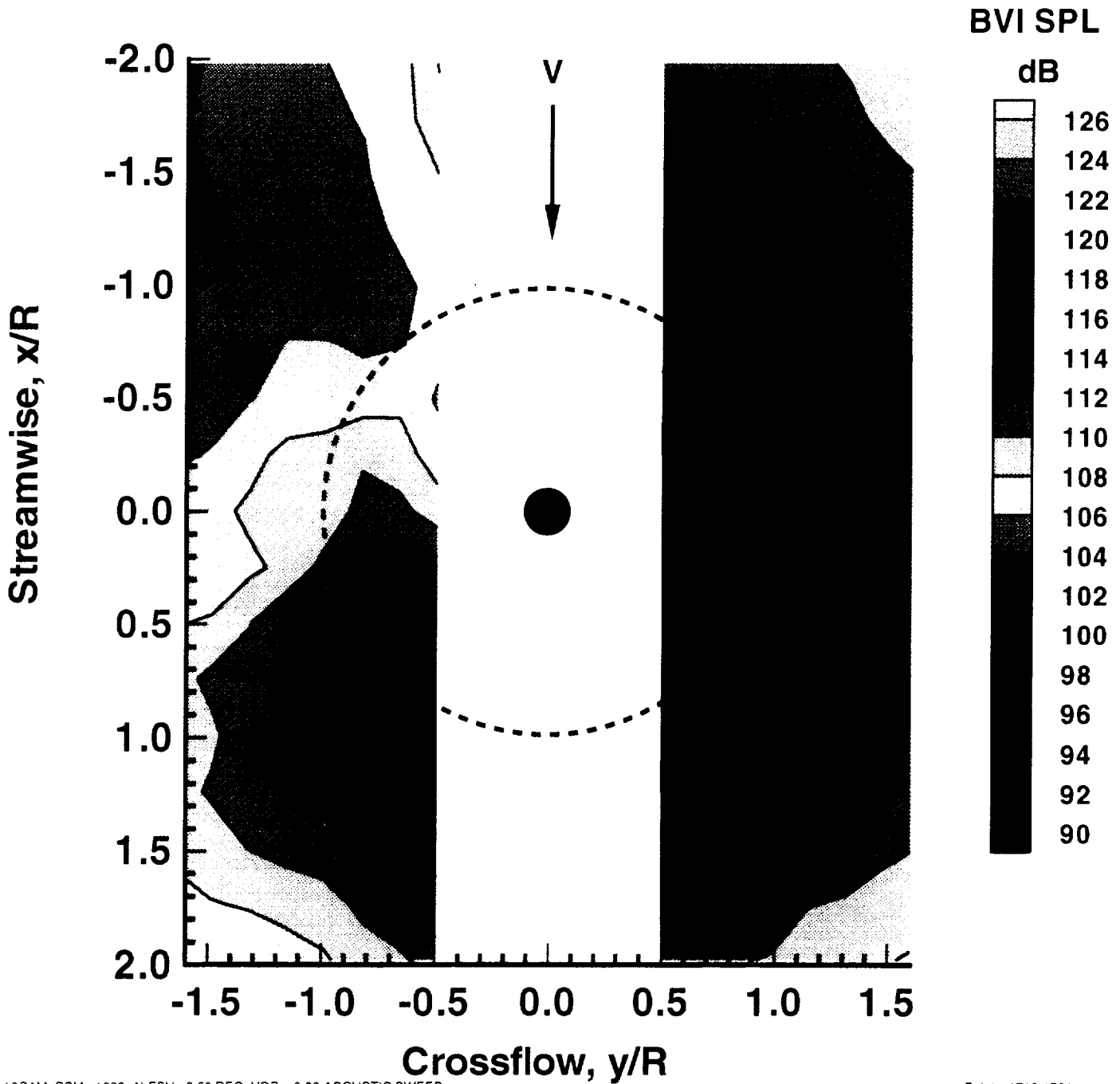


Figure (54b) BVISPL Contour Plot Based on Spectra of Averaged Time Histories ( $C_t/\sigma = 0.087$ ,  $\alpha_{\text{TRP}} = 2.5$  degrees aft,  $\mu=0.1987$ ) Baseline Rotor Configuration - Test #0741

Condition: 2741 Date: 1 Mar 1994

$\alpha_{\text{shaft}}$ : 2.502  $\mu$ : 0.1986  $C_t/\sigma$ : 0.0875



12.5+10CAM, RPM= 1082, ALFSU= 2.50 DEG, VOR = 0.20, ACOUSTIC SWEEP

Points: 1718-1734 sweep: 001

Figure (55a) BVISPL Contour Plot Based on Ensemble-averaged Spectra  
( $C_t/\sigma=0.0875$ ,  $\alpha_{\text{TPP}}= 2.5$  degrees aft,  $\mu=0.1986$ , Peak Flap  
Deflection = 12.5 degrees, Azimuthal Phase Shift = 0 degrees )  
Flapped Rotor Configuration - Test # 2741

Condition: 2741 Date: 1 Mar 1994

$\alpha_{\text{shaft}}$ : 2.502  $\mu$ : 0.1986  $C_t/\sigma$ : 0.0875

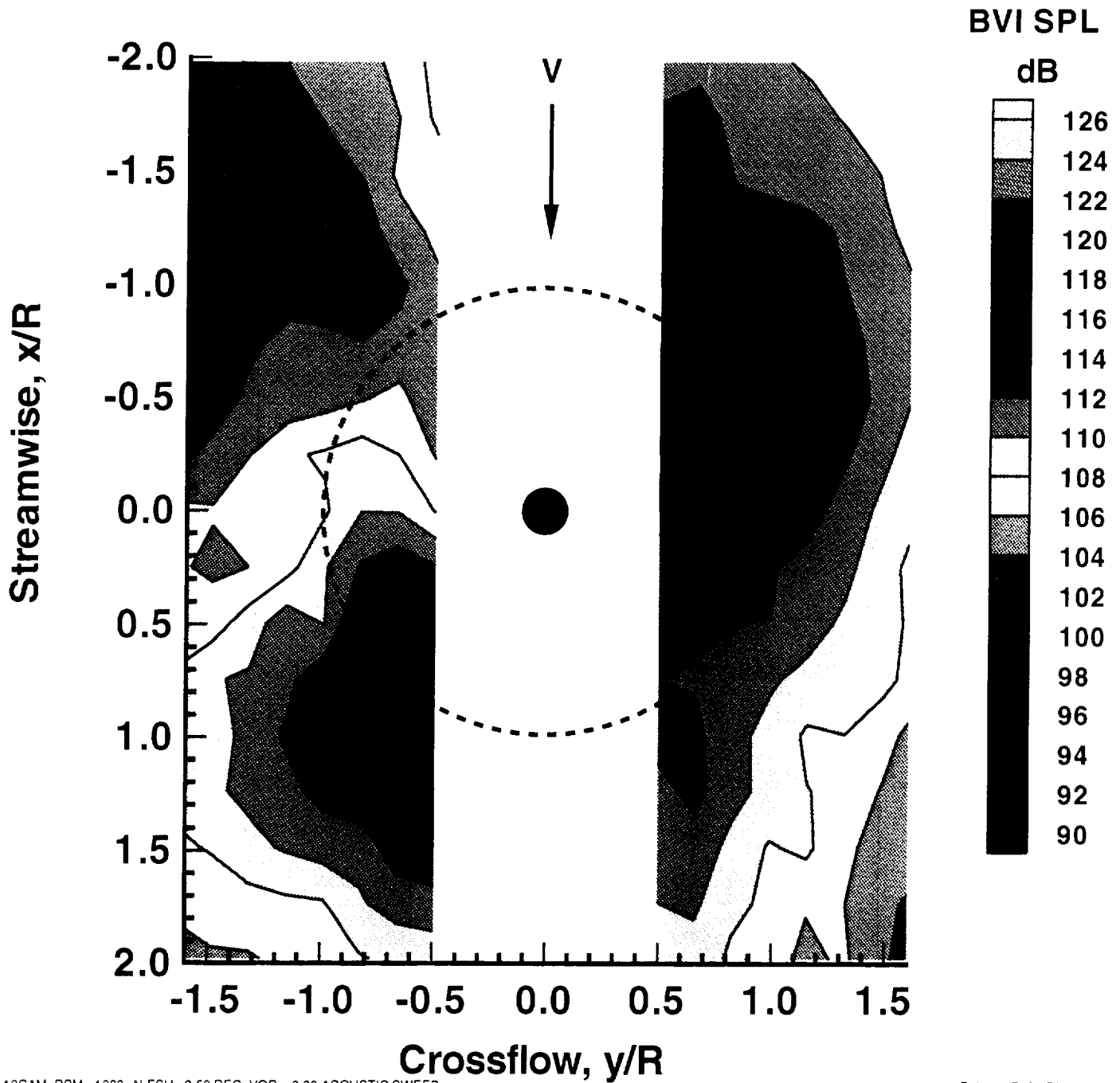


Figure (55b) BVISPL Contour Plot Based on Spectra of Averaged Time Histories ( $C_t/\sigma = 0.0875$ ,  $\alpha_{\text{TPP}} = 2.5$  degrees aft,  $\mu = 0.1986$ , Peak Flap Deflection = -12.5 degrees, Azimuthal Phase Shift = 0 degrees) Flapped Rotor Configuration - Test # 2741

Condition: 0731 Date: 25 Feb 1994

$\alpha_{\text{shaft}}$ : 3.016  $\mu$ : 0.1492  $C_t/\sigma$ : 0.0773

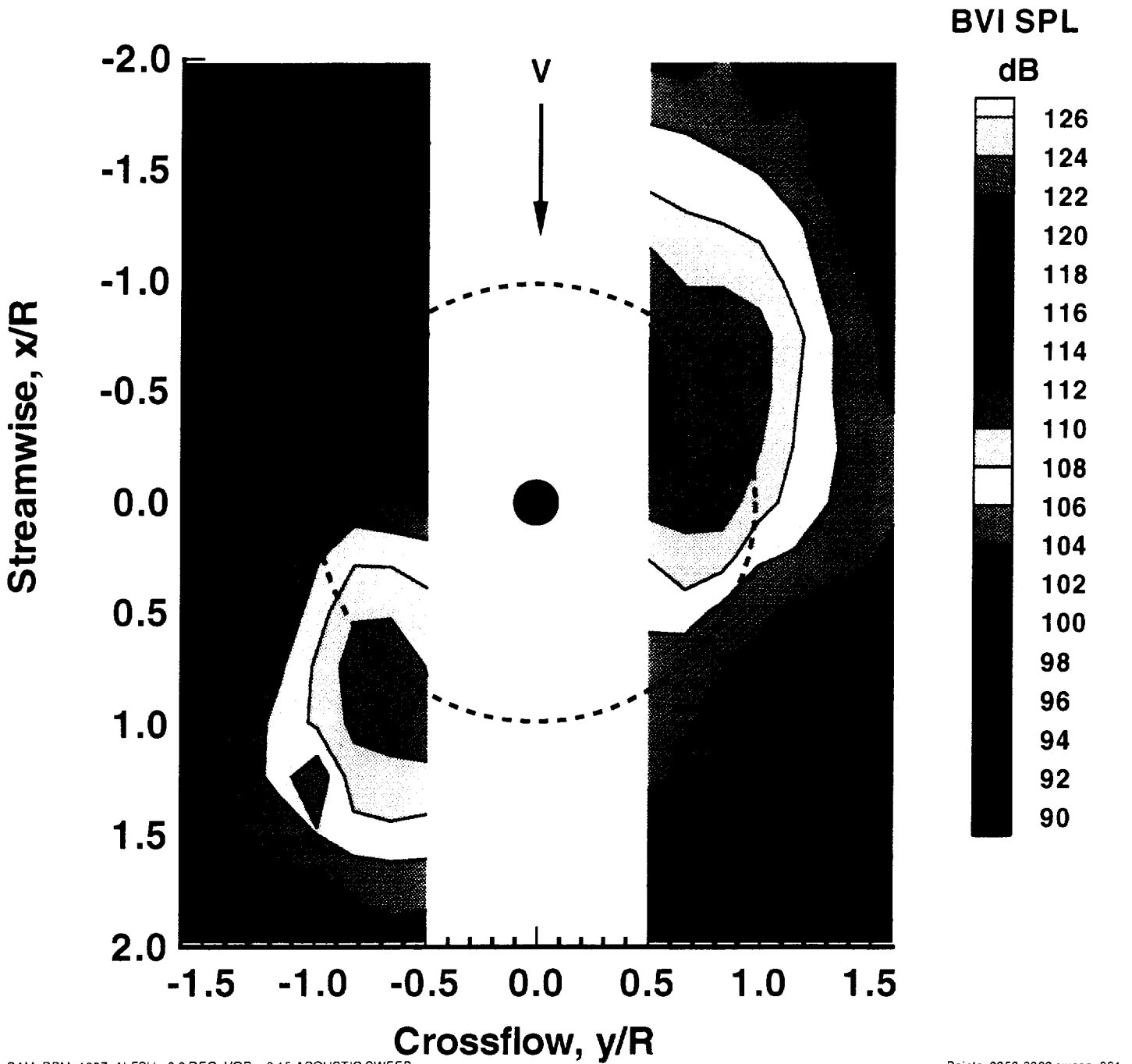
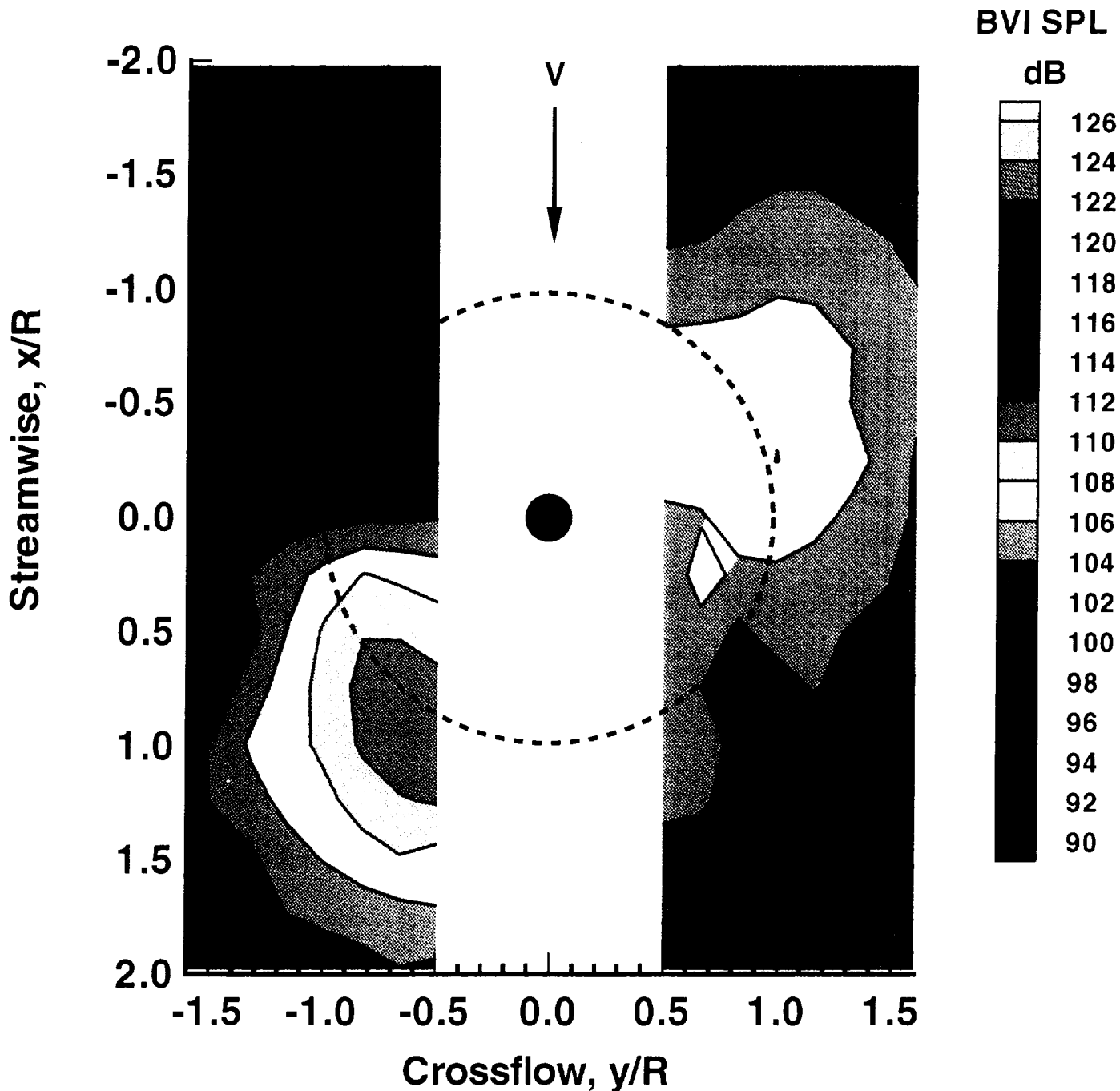


Figure (56a) BVISPL Contour Plot Based on Spectra of Averaged Time Histories ( $C_t/\sigma = 0.0773$ ,  $\alpha_{\text{TRP}} = 3$  degrees aft,  $\mu=0.1492$ ) Baseline Rotor Configuration Test # 0731

Condition: 2900 Date: 1 Mar 1994

$\alpha_{\text{shaft}}$ : 3.023  $\mu$ : 0.1486  $C_t/\sigma$ : 0.0776



12.5-10CAM, RPM= 1074, ALFSU= 3.00 DEG, VOR = 0.15, ACOUSTIC SWEEP

Points: 1775-1791 sweep:

Figure (56b) BVISPL Contour Plot Based on Spectra of Averaged Time Histories ( $C_t/\sigma = 0.0776$ ,  $\alpha_{\text{TRP}} = 3$  degrees aft,  $\mu = 0.1486$ , Peak Flap Deflection = -12.5 degrees, Azimuthal Phase Shift = -10 degrees) Flapped Rotor Configuration - Test # 2900

Condition: 3915 Date: 4 Mar 1994

$\alpha_{\text{shaft}}$ : 3.018  $\mu$ : 0.1488  $C_t/\sigma$ : 0.0778

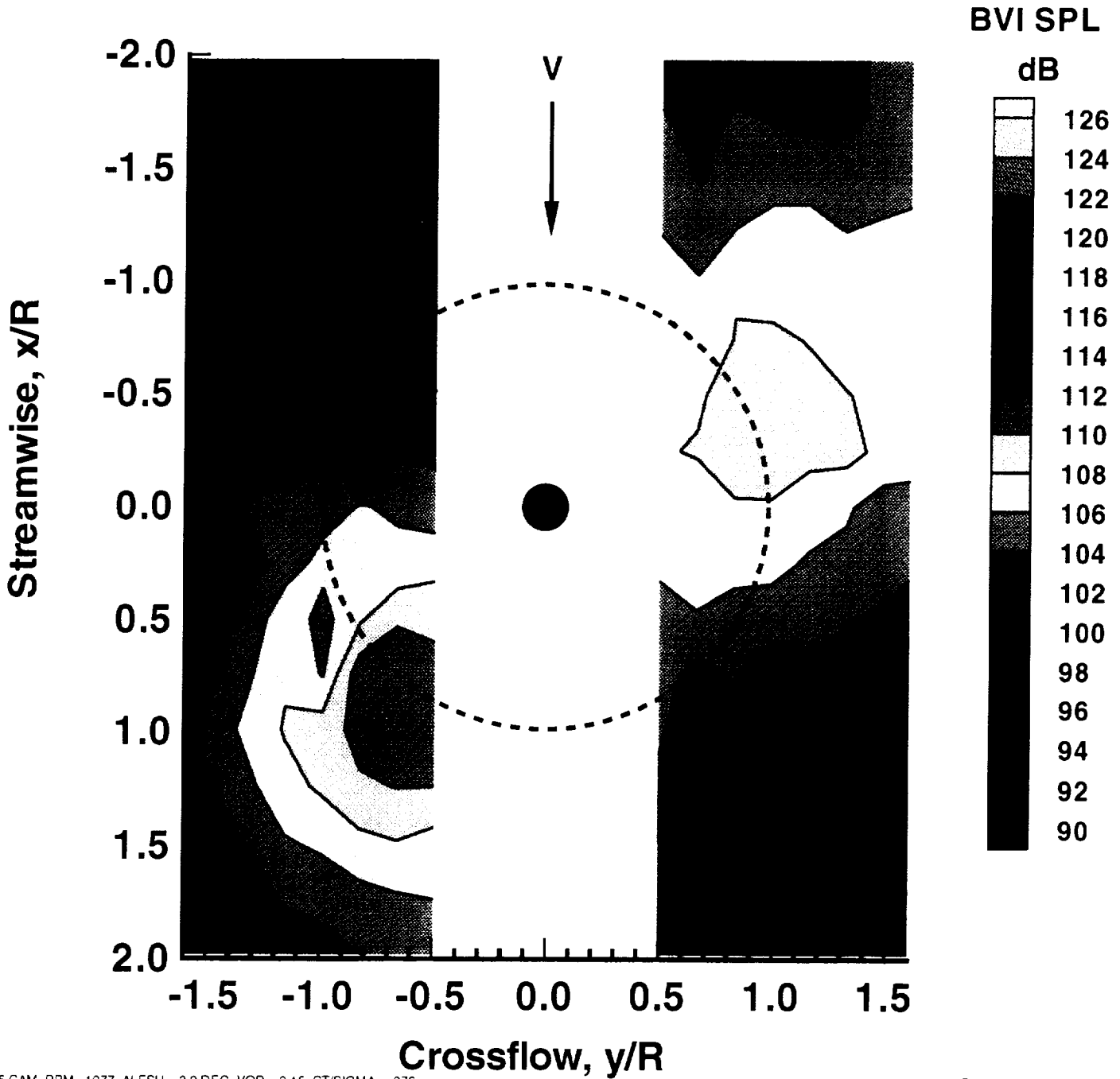
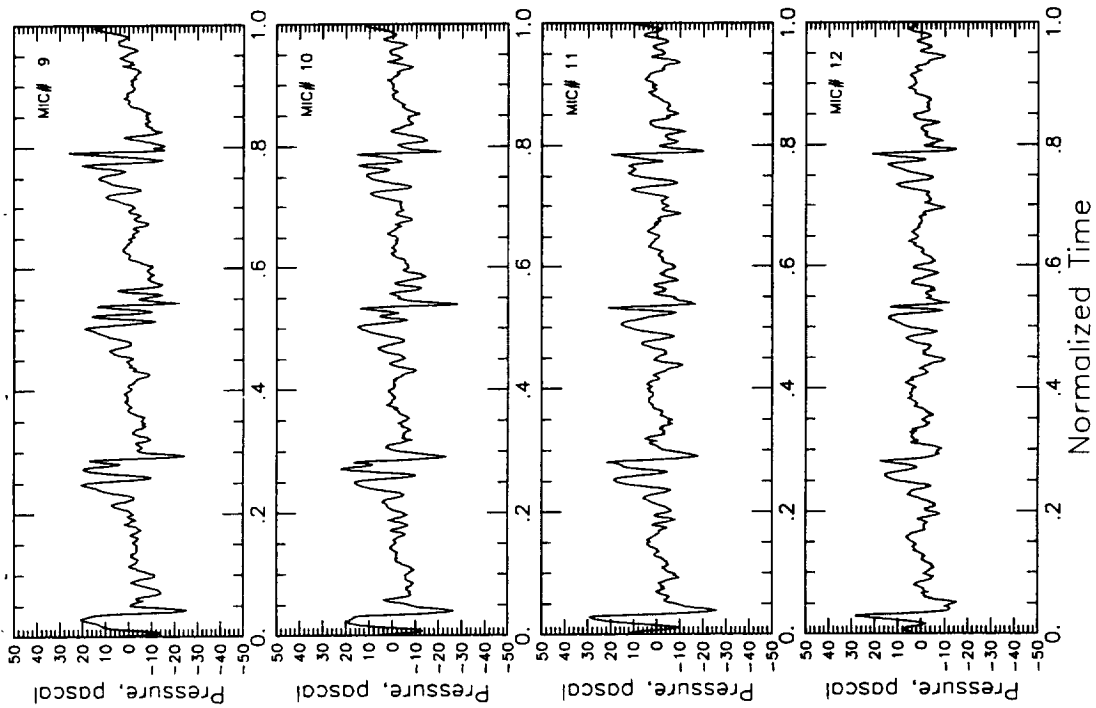
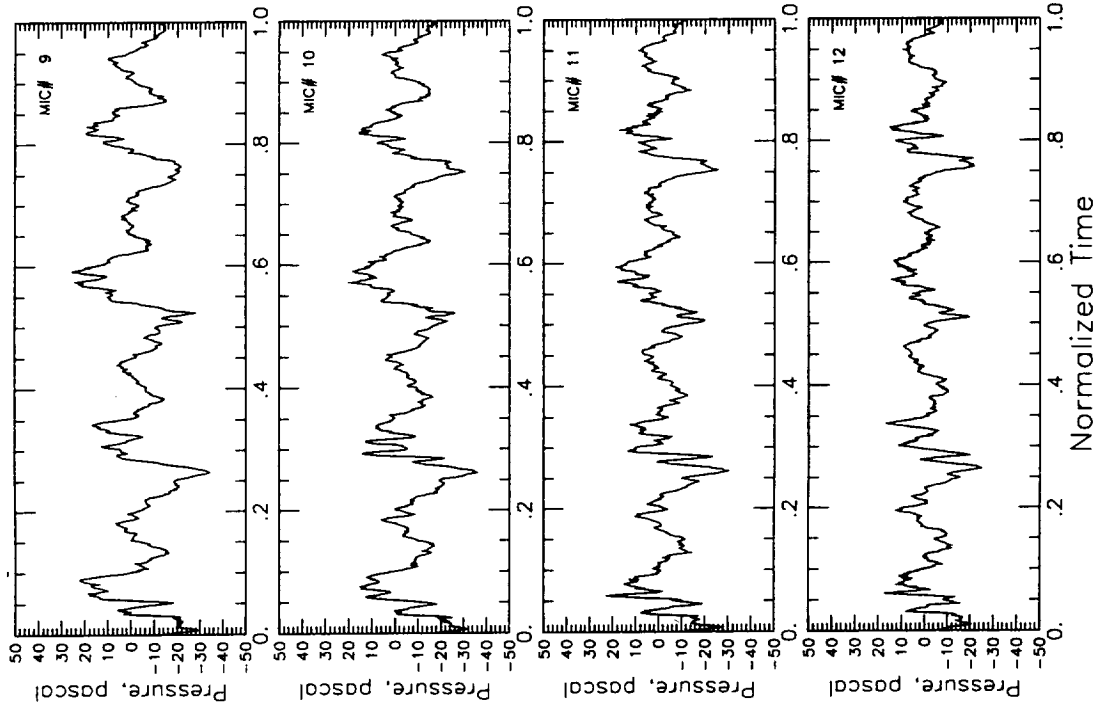


Figure (56c) BVISPL Contour Plot Based on Spectra of Averaged Time Histories ( $C_t/\sigma = 0.0778$ ,  $\alpha_{\text{TRP}} = 3$  degrees aft,  $\mu = 0.1488$ , Peak Flap Deflection = -17.5 degrees, Azimuthal Phase Shift = -5 degrees) Flapped Rotor Configuration - Test # 3915



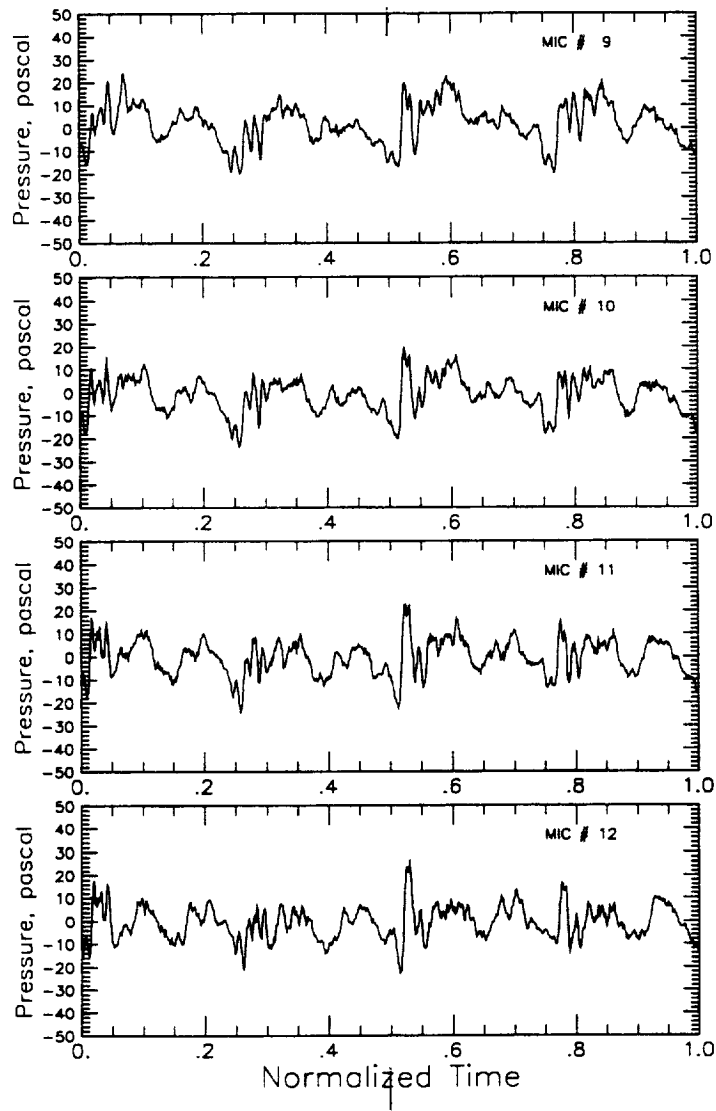


**a - Baseline Rotor [No Flap]- Test # 0731**



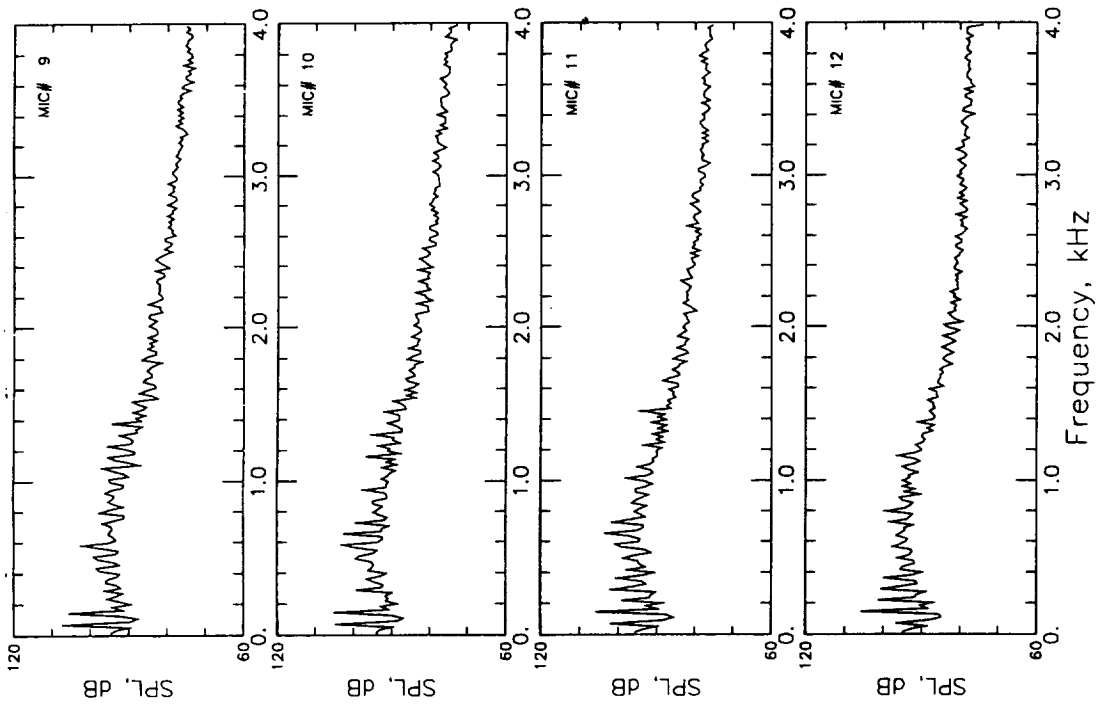
**b - Flapped Rotor**  
**[Peak Flap Deflection= -12.5 degrees, Azimuthal**  
**Phase Shift = -10 degrees ]- Test # 2900**

Figures (57a & 57b) Average Acoustic Time Histories at Microphone  
 Traverse Station 9 on the Advancing Side - Test #s 0731  
 & 2900

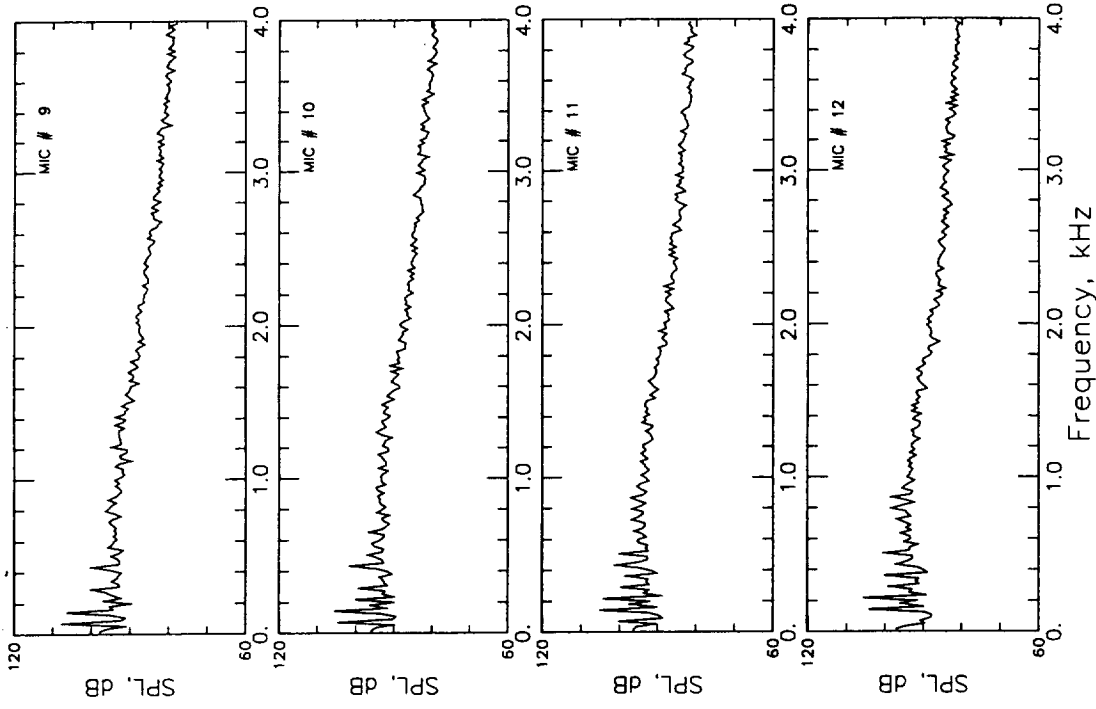


**[Peak Flap Deflection = -17.5 degrees, Azimuthal Phase Shift = -10 degrees]**

Figure (57c) Average Acoustic Time Histories at Microphone Traverse Station 9 on the Advancing Side; Flapped Rotor - Test # 3915

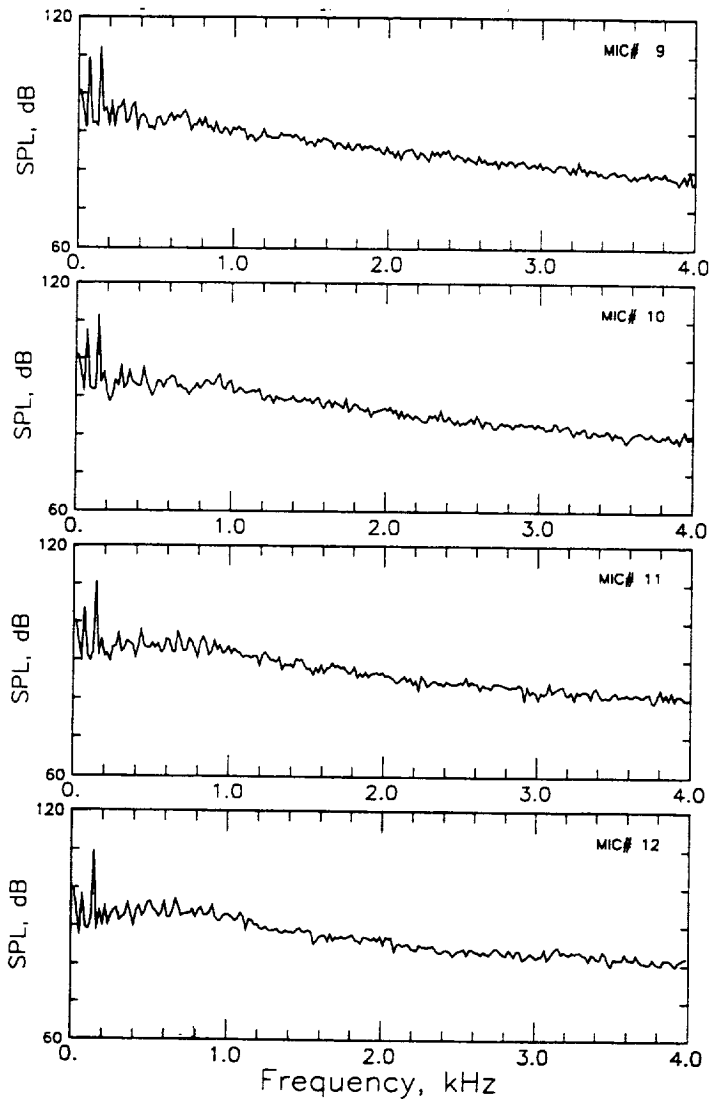


**a - Baseline Rotor [No Flap]- Test # 0731**



**b - Flapped Rotor**  
**[Peak Flap Deflection= -12.5 degrees, Azimuthal**  
**Phase Shift = -10 degrees ]- Test # 2900**

Figures (58a & 58b) Ensemble-averaged Narrowband Noise Spectra at  
 Microphone Traverse Station 9 on the Advancing Side -  
 Test #s 0731 & 2900



**[Peak Flap Deflection = -17.5 degrees, Azimuthal Phase Shift = -10 degrees]**

Figure (58c) Ensemble-averaged Narrowband Noise Spectra at Microphone Traverse Station 9 on the Advancing Side ; Flapped Rotor - Test # 3915

Condition: 0738 Date: 26 Feb 1994

$\alpha_{\text{shaft}}$ : 3.996  $\mu$ : 0.1991  $C_t/\sigma$ : 0.0780

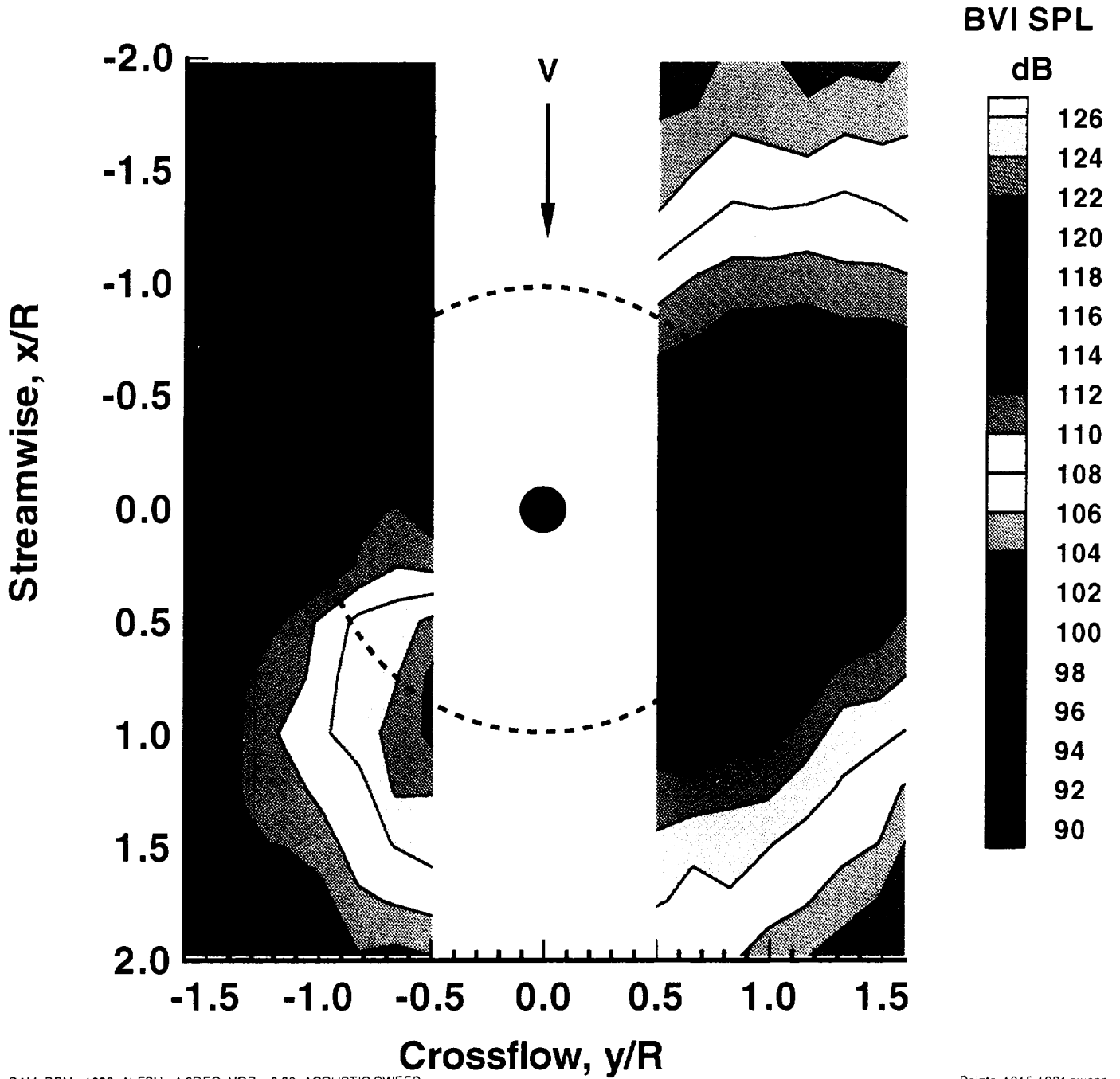


Figure (59a) BVISPL Contour Plot Based on Spectra of Averaged Time Histories ( $C_t/\sigma = 0.078$ ,  $\alpha_{\text{TRP}} = 4$  degrees aft,  $\mu=0.1991$ ) Baseline Rotor Configuration Test # 0738

Condition: 2904 Date: 1 Mar 1994

$\alpha_{\text{shaft}}$ : 4.001  $\mu$ : 0.1982  $C_t/\sigma$ : 0.0768

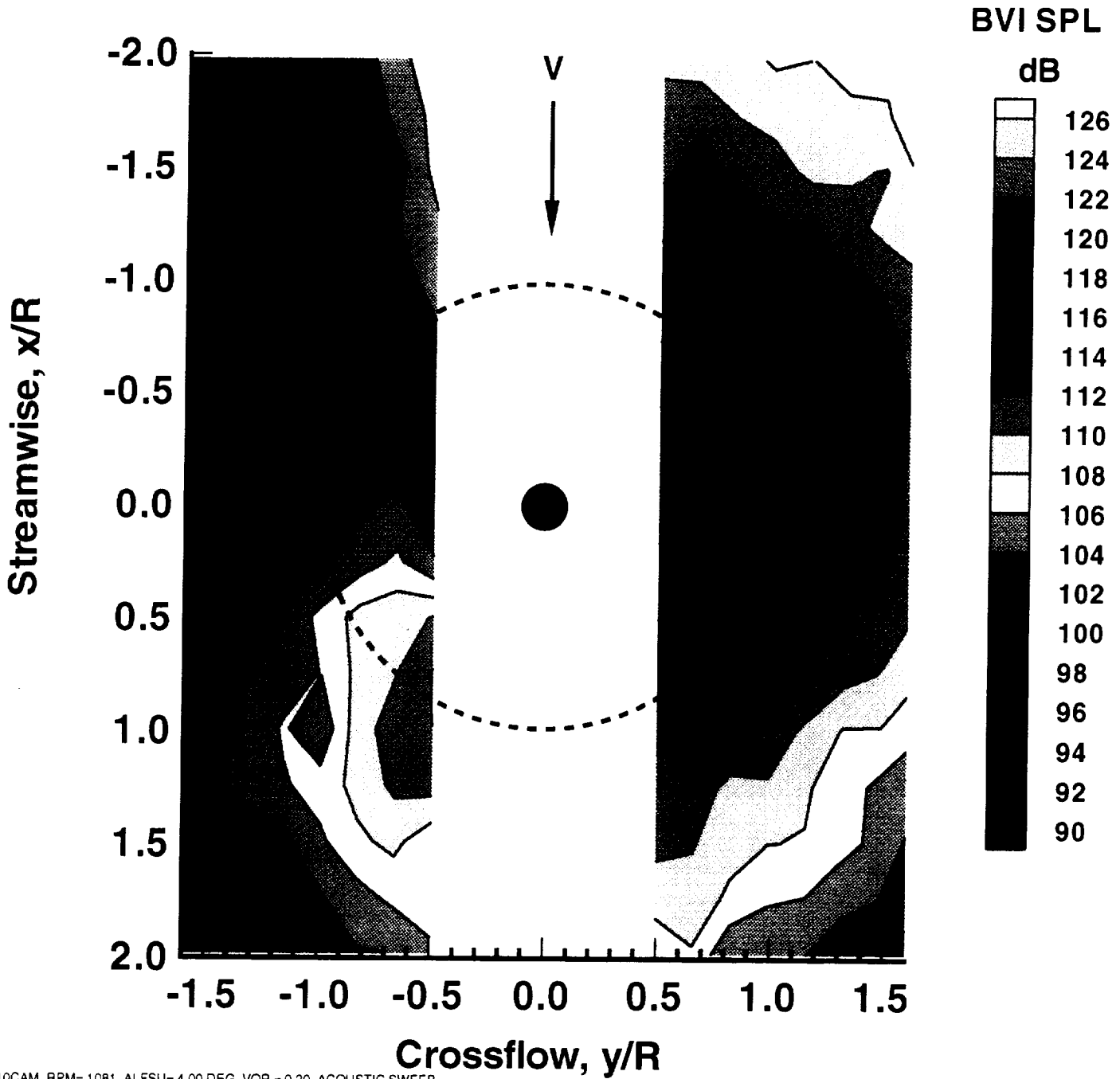
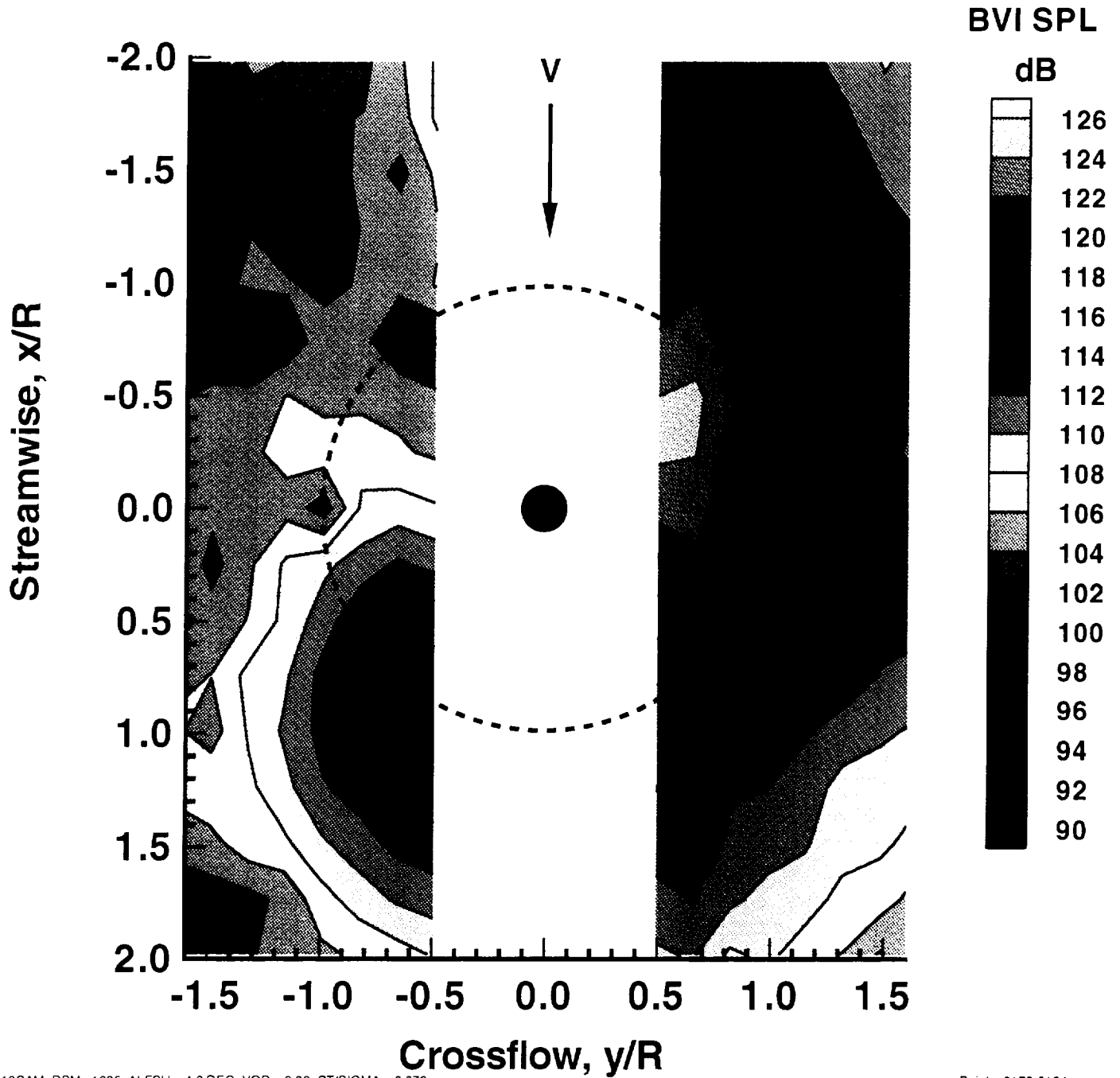


Figure (59b) BVISPL Contour Plot Based on Spectra of Averaged Time Histories ( $C_t/\sigma = 0.0768$ ,  $\alpha_{\text{TPP}} = 4$  degrees aft,  $\mu = 0.1982$ , Peak Flap Deflection = -12.5 degrees, Azimuthal Phase Shift = -10 degrees) Flapped Rotor Configuration - Test # 2904

Condition: 3922 Date: 4 Mar 1994

$\alpha_{\text{shaft}}$ : 4.031  $\mu$ : 0.1988  $C_t/\sigma$ : 0.0775



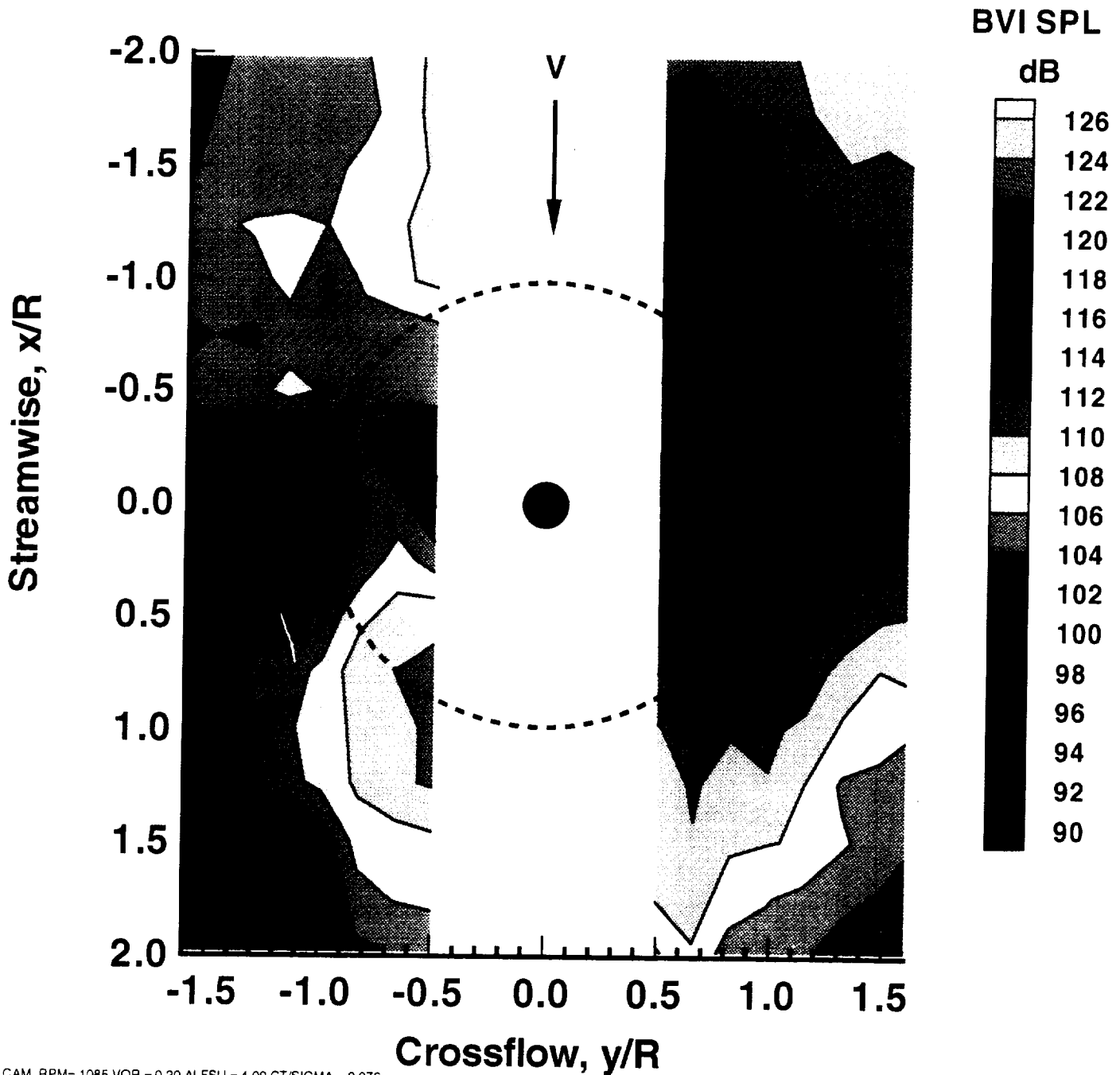
17.5-10CAM, RPM= 1095, ALFSU = 4.0 DEG, VOR = 0.20, CT/SIGMA = 0.076

Points: 3178-3194 sweep:

Figure (59c) BVISPL Contour Plot Based on Spectra of Averaged Time Histories ( $C_t/\sigma = 0.0775$ ,  $\alpha_{\text{TPP}} = 4$  degrees aft,  $\mu=0.1988$ , Peak Flap Deflection=-17.5 degrees, Azimuthal Phase Shift = -10 degrees) Flapped Rotor Configuration Test # 3922

Condition: 4047 Date: 10 Mar 1994

$\alpha_{\text{shaft}}$ : 4.042  $\mu$ : 0.1980  $C_t/\sigma$ : 0.0764

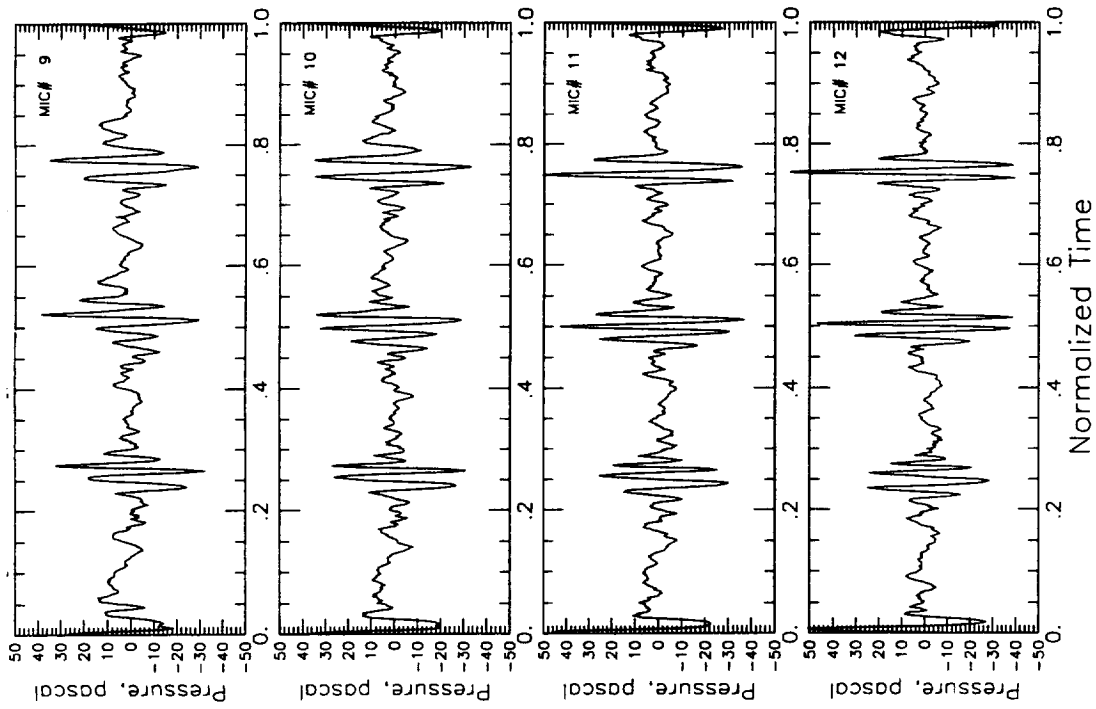


20-10 CAM. RPM= 1085 VOR = 0.20 ALFSU = 4.00 CT/SIGMA = 0.076

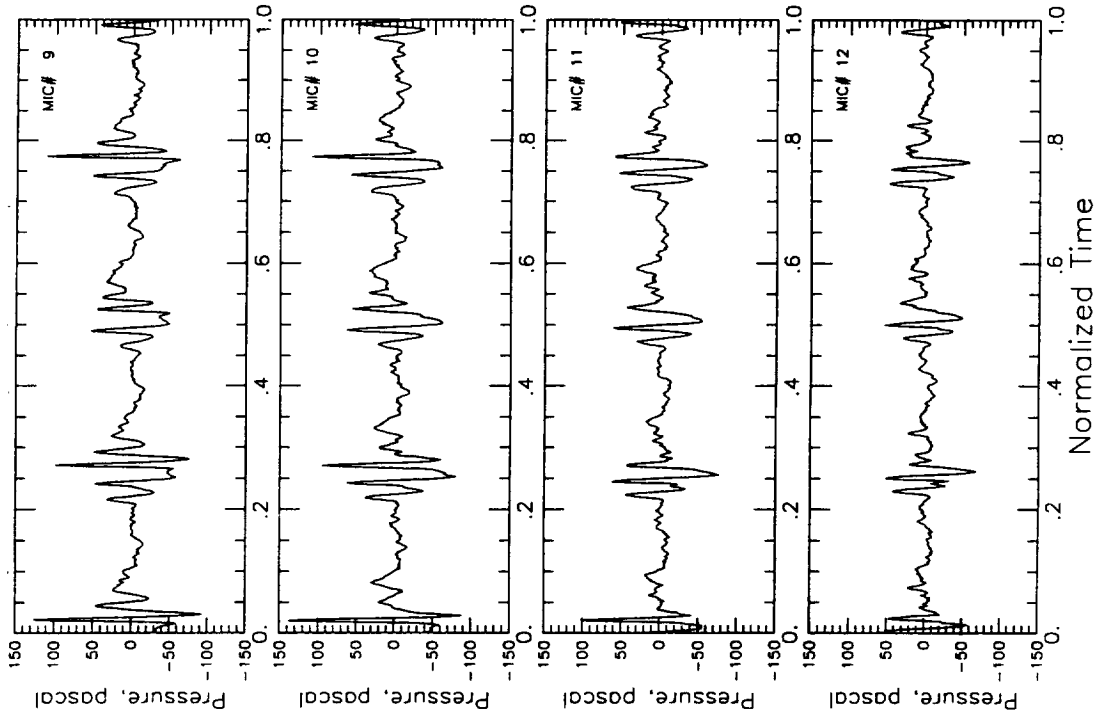
Points: 3747-3763 sweep: 001

Figure (59d) BVISPL Contour Plot Based on Spectra of Averaged Time Histories ( $C_t/\sigma = 0.0764$ ,  $\alpha_{\text{TPP}} = 4$  degrees aft,  $\mu=0.198$ , Peak Flap Deflection=-20 degrees, Azimuthal Phase Shift = -10 degrees ) Flapped Rotor Configuration - Test # 4047



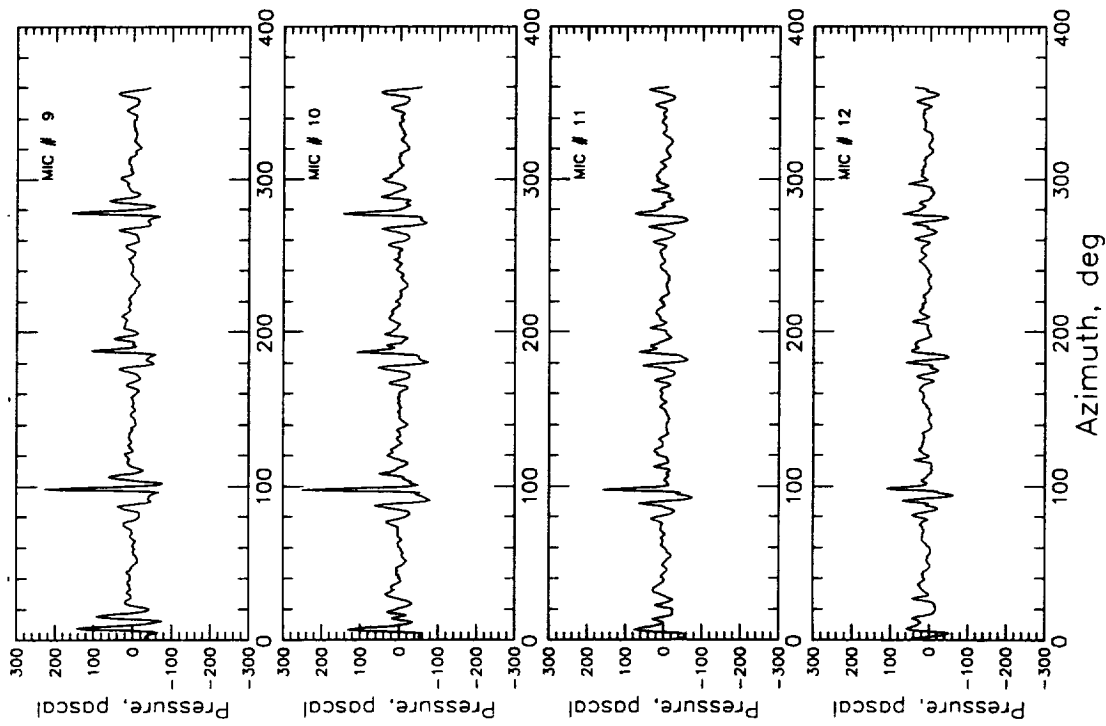


**a - Baseline Rotor [No Flap]- Test # 0738**



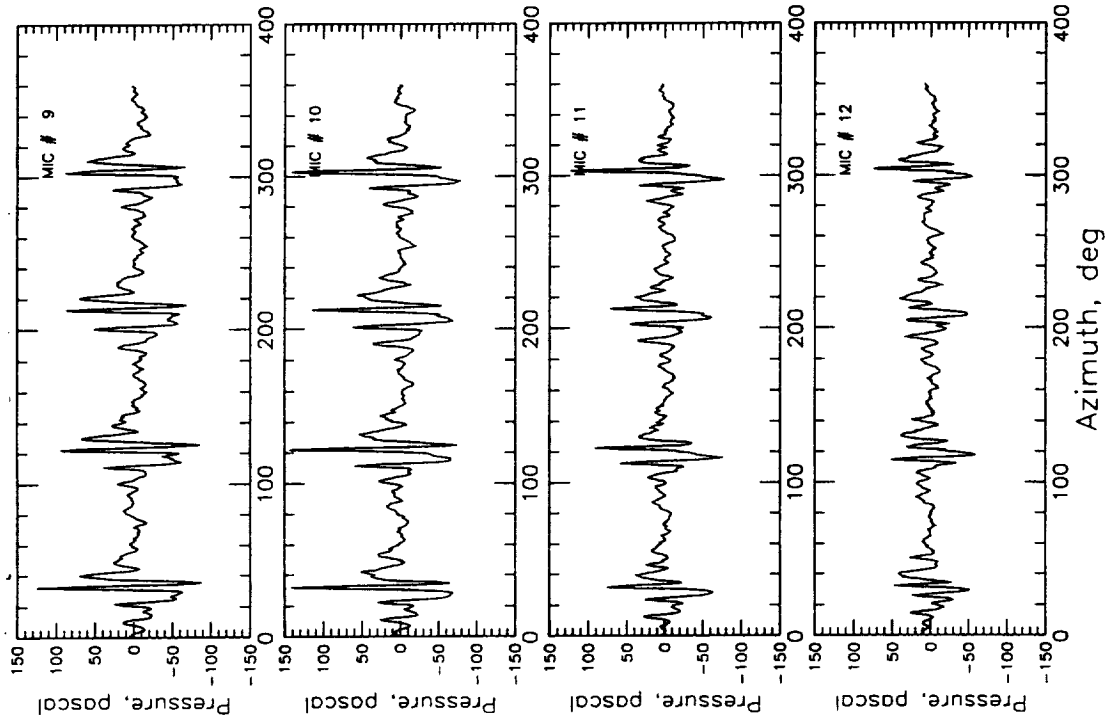
**b - Flapped Rotor**  
**[Peak Flap Deflection= -12.5 degrees, Azimuthal**  
**Phase Shift = -10 degrees ] - Test # 2904**

Figures (60a & 60b) Average Acoustic Time Histories at Microphone  
 Traverse Station 9 on the Advancing Side - Test #s  
 0734 & 2904



**c - Flapped Rotor**

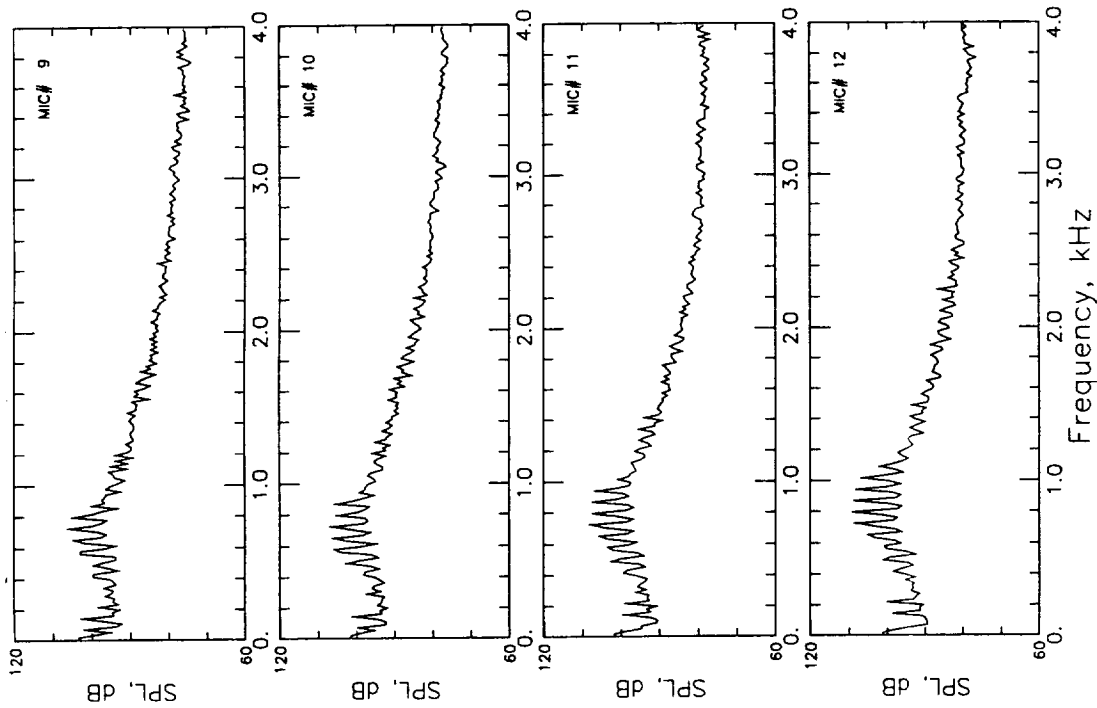
**[Peak Flap Deflection= -17.5 degrees, Azimuthal Phase Shift = -10 degrees ] - Test # 3922**



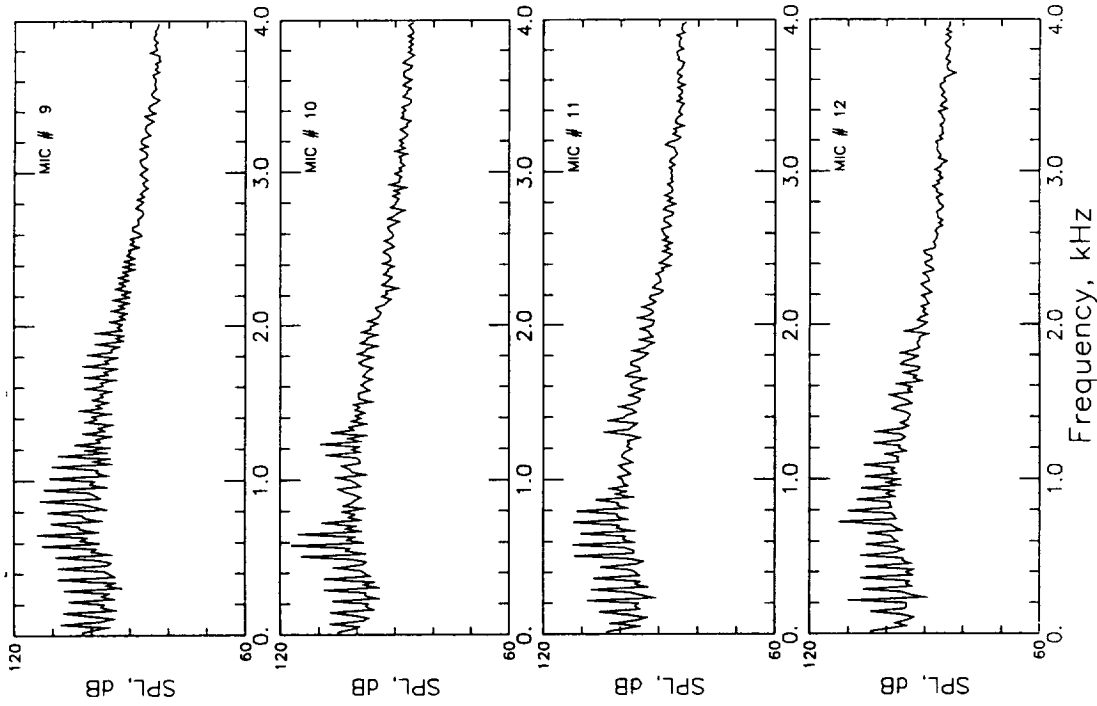
**d - Flapped Rotor**

**[Peak Flap Deflection= -20.0 degrees, Azimuthal Phase Shift = -10 degrees ] - Test # 4047**

Figures (60c & 60d) Average Acoustic Time Histories at Microphone Traverse Station 9 on the Advancing Side - Test #s 3922 & 4047

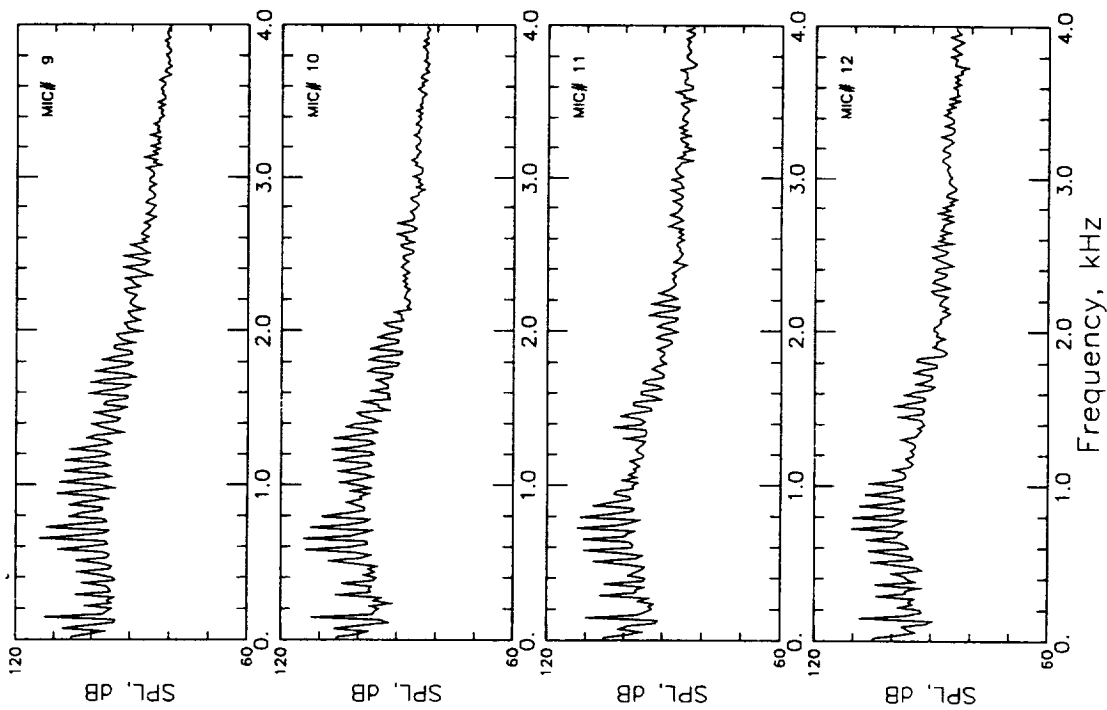


**a - Baseline Rotor [No Flap]- Test # 0738**



**b - Flapped Rotor  
[Peak Flap Deflection= -12.5 degrees, Azimuthal  
Phase Shift = -10 degrees ] - Test # 2904**

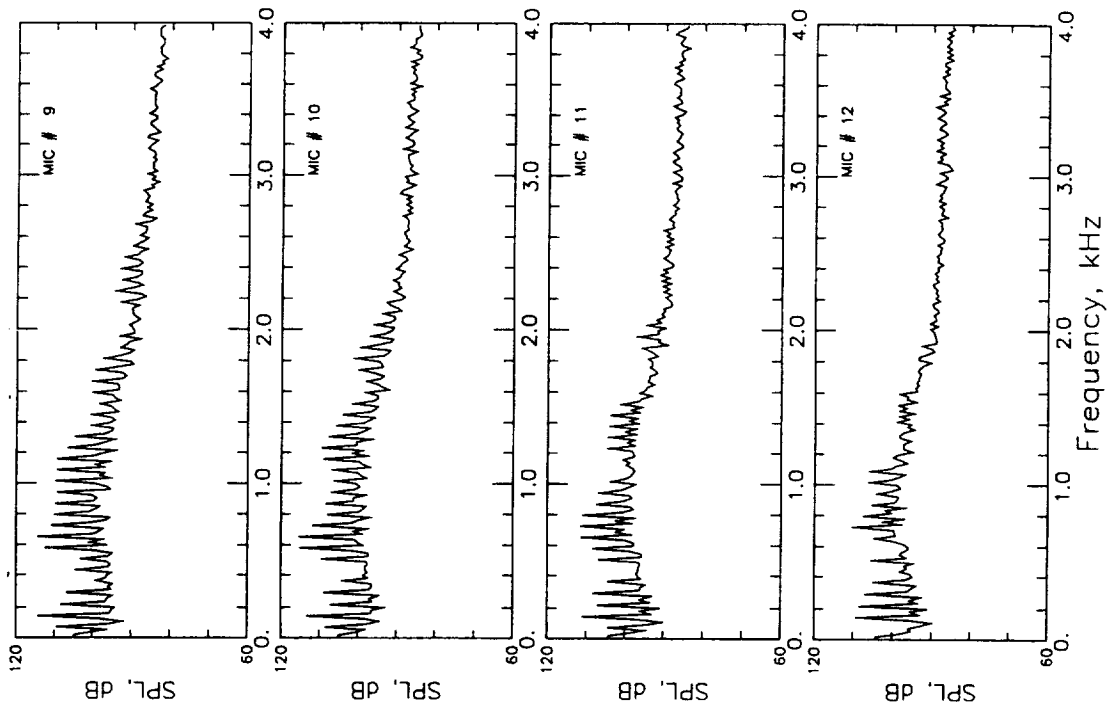
Figures (61a & 61b) Ensemble-averaged Narrowband Noise Spectra at  
Microphone Traverse Station 9 on the Advancing Side -  
Test #s 0738 & 2904



**c - Flapped Rotor**

**[Peak Flap Deflection= -17.5 degrees, Azimuthal  
Phase Shift = -10 degrees ] - Test # 3922**

Figures (61c & 61d) Ensemble-averaged Narrowband Noise Spectra at  
Microphone Traverse Station 9 on the Advancing Side -  
Test #s 3922 & 4047

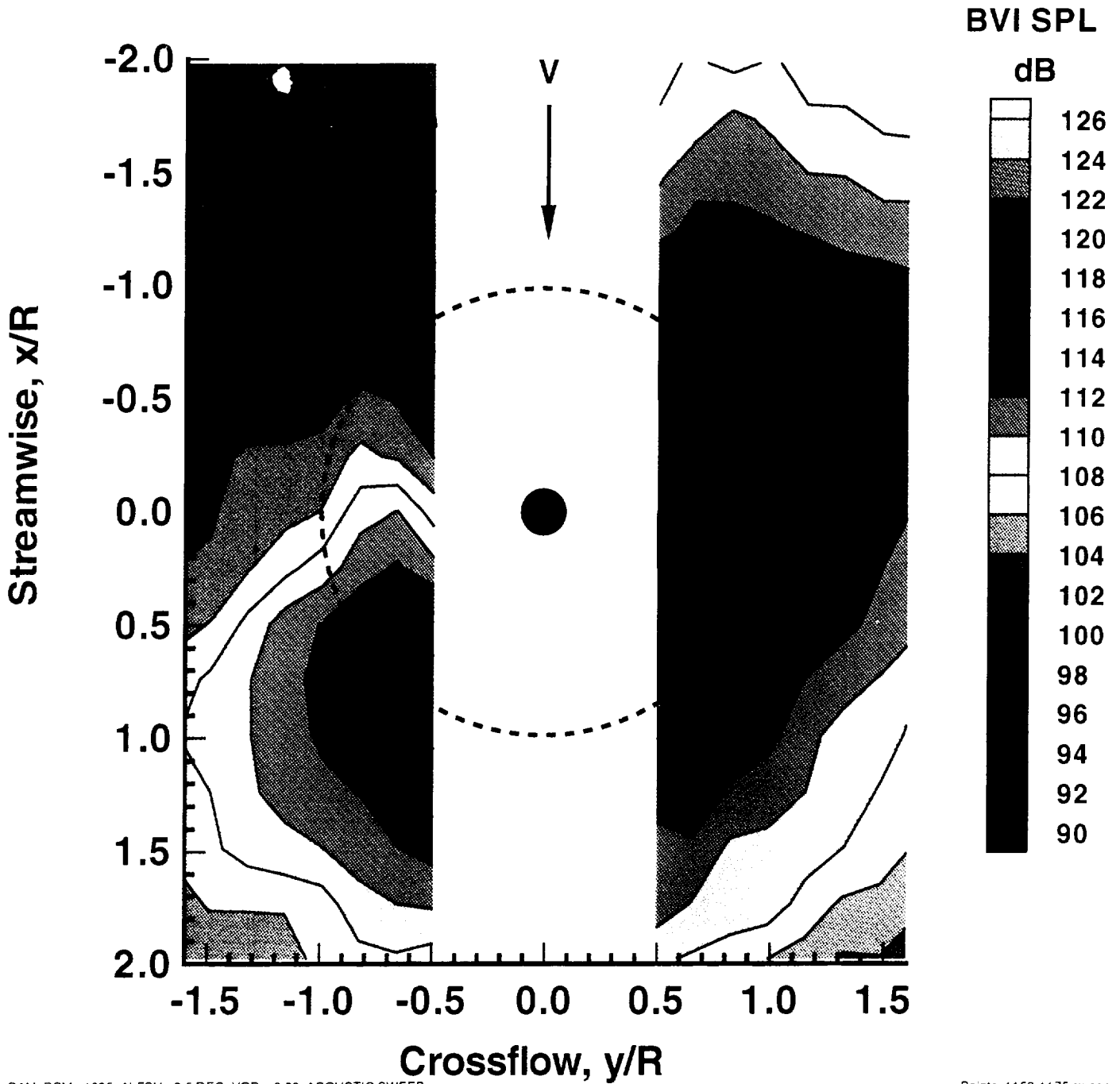


**d - Flapped Rotor**

**[Peak Flap Deflection= -20.0 degrees, Azimuthal  
Phase Shift = -10 degrees ] - Test # 4047**

Condition: 0741 Date: 26 Feb 1994

$\alpha_{\text{shaft}}$ : 2.502  $\mu$ : 0.1987  $C_t/\sigma$ : 0.0868



NULL CAM, RPM= 1095, ALFSU= 2.5 DEG, VOR = 0.20, ACOUSTIC SWEEP

Points: 1159-1175 sweep

Figure (62a) BVISPL Contour Plot Based on Spectra of Averaged Time Histories ( $C_t/\sigma = 0.0868$ ,  $\alpha_{\text{TPP}} = 2.5$  degrees aft,  $\mu=0.1987$ ) Baseline Rotor Configuration Test # 0741

Condition: 3910 Date: 3 Mar 1994

$\alpha_{\text{shaft}}$ : 2.515  $\mu$ : 0.1990  $C_t/\sigma$ : 0.0896

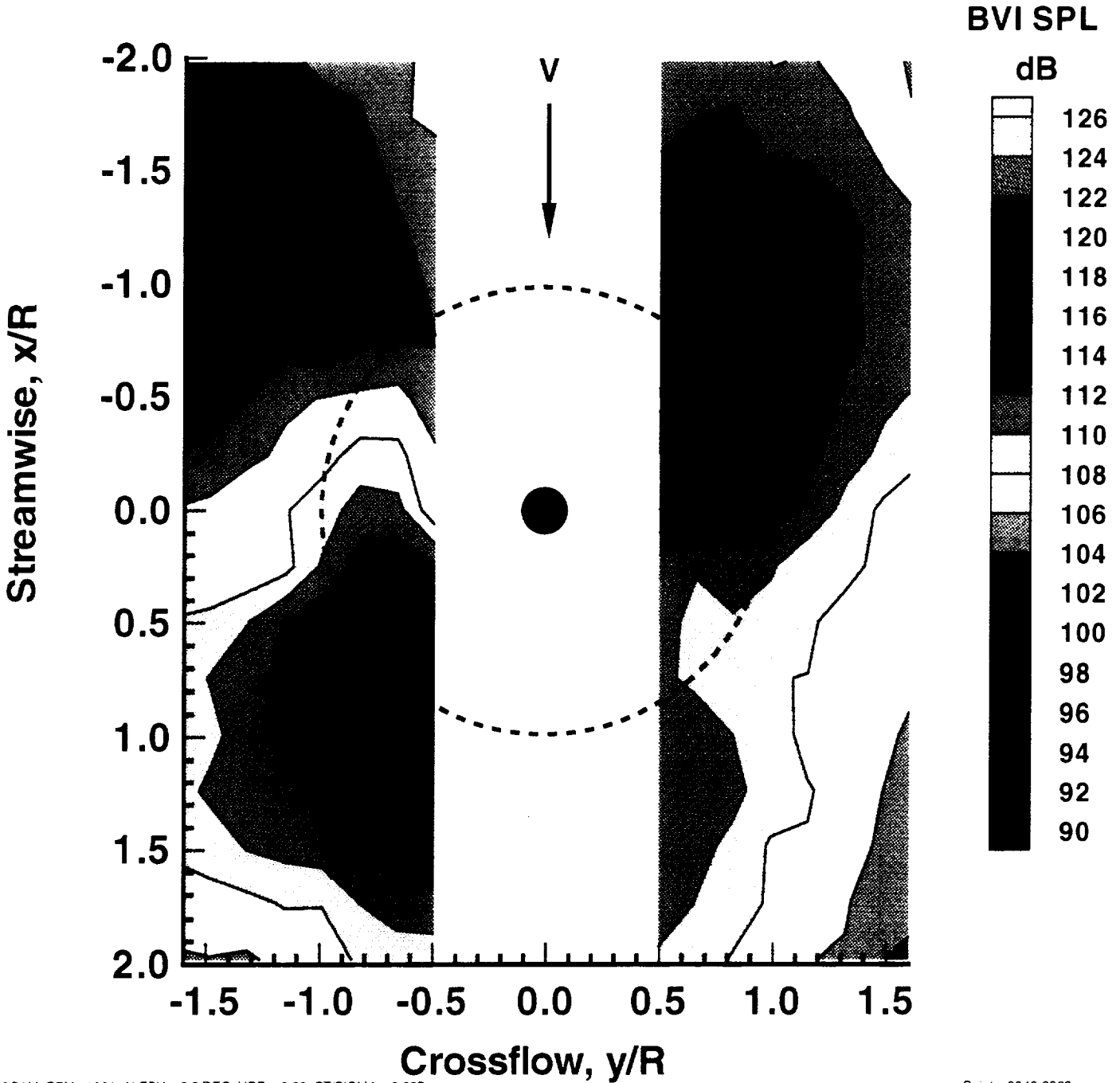


Figure (62b) BVISPL Contour Plot Based on Spectra of Averaged Time Histories ( $C_t/\sigma = 0.0896$ ,  $\alpha_{\text{TPP}} = 2.5$  degrees aft,  $\mu=0.1990$ , Peak Flap Deflection=-17.5 degrees, Azimuthal Phase Shift = 0 degrees ) Flapped Rotor Configuration Test # 3910

Condition: 3941 Date: 4 Mar 1994

$\alpha_{\text{shaft}}$ : 2.496  $\mu$ : 0.1985  $C_t/\sigma$ : 0.0889

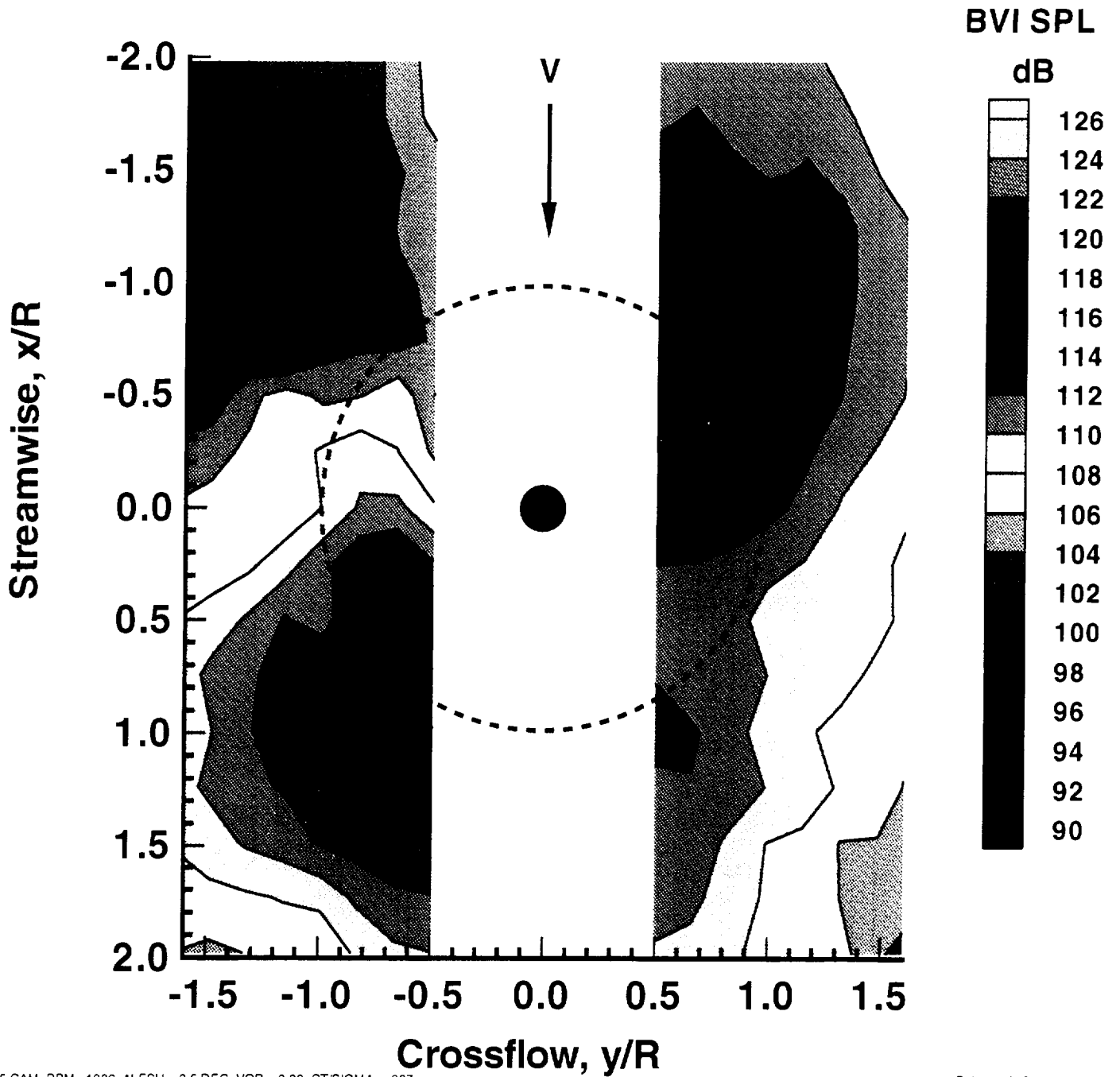


Figure (62c) BVISPL Contour Plot Based on Spectra of Averaged Time Histories ( $C_t/\sigma = 0.0889$ ,  $\alpha_{\text{TRP}} = 2.5$  degrees aft,  $\mu=0.1985$ , Peak Flap Deflection= -17.5 degrees, Azimuthal Phase Shift = -5 degrees ) Flapped Rotor Configuration Test # 3941

Condition: 3925 Date: 4 Mar 1994

$\alpha_{\text{shaft}}$ : 2.511  $\mu$ : 0.1983  $C_t/\sigma$ : 0.0887

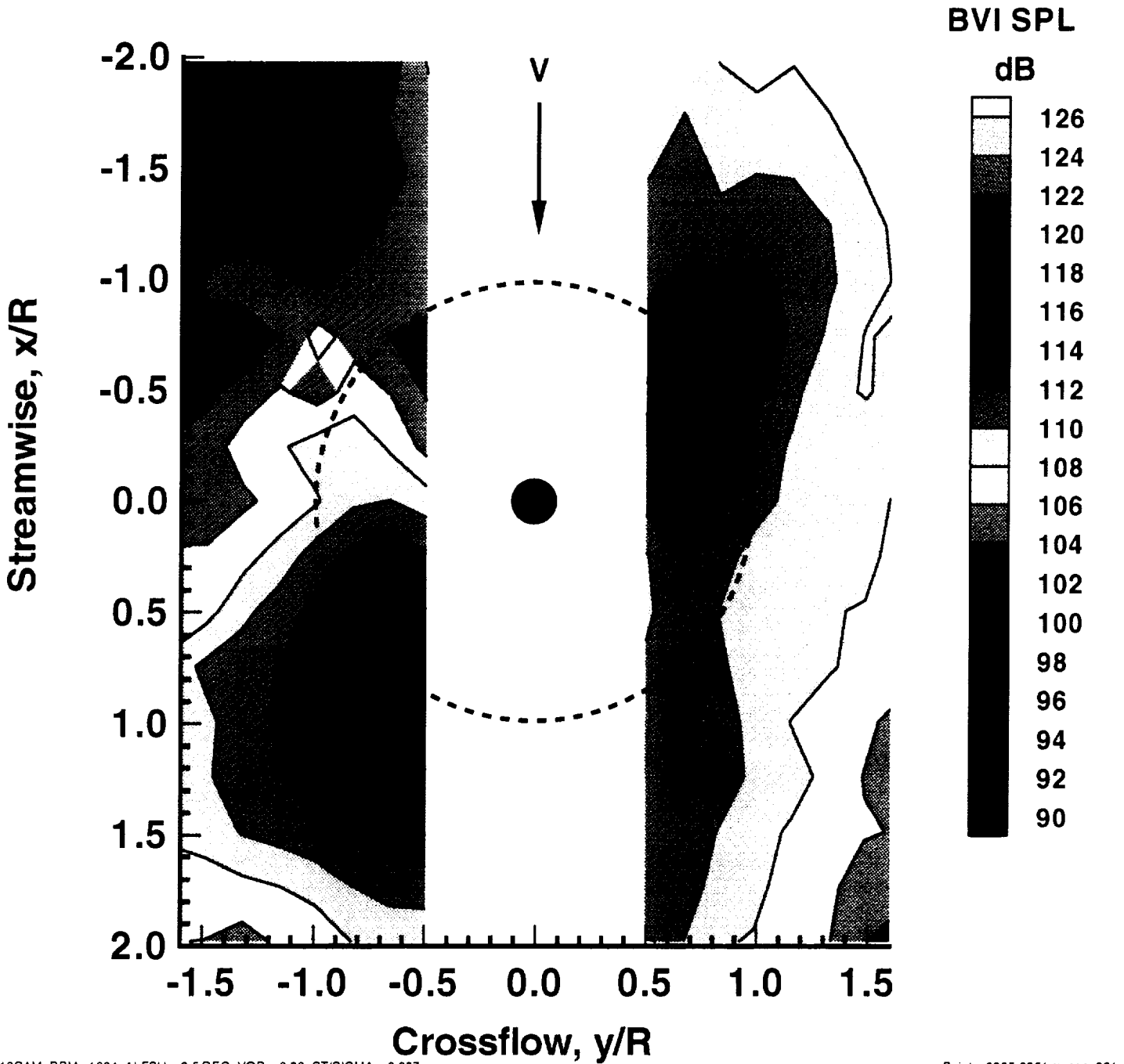
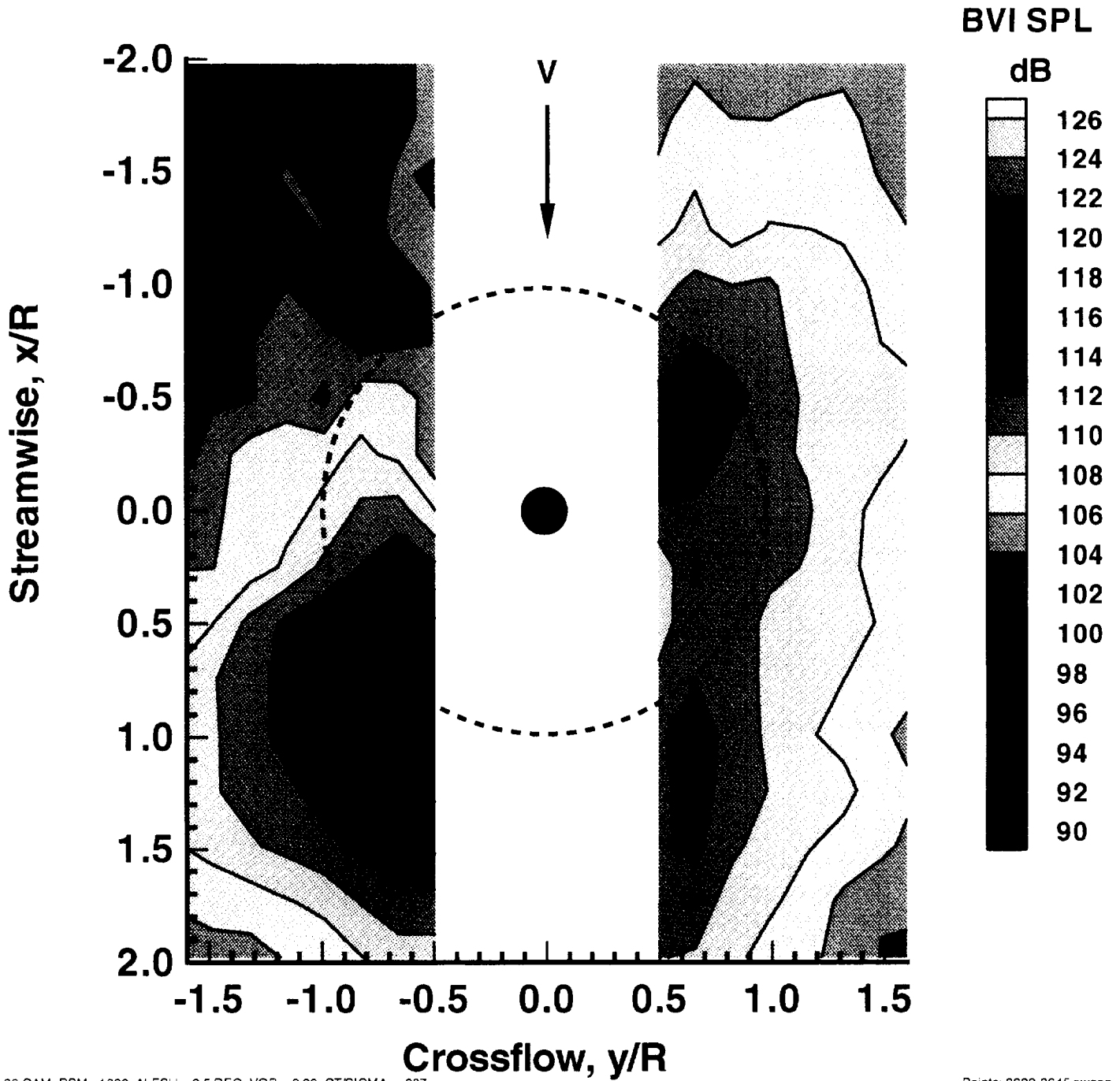


Figure (62d) BVISPL Contour Plot Based on Spectra of Averaged Time Histories ( $C_t/\sigma = 0.0887$ ,  $\alpha_{\text{TPP}} = 2.5$  degrees aft,  $\mu=0.1983$ , Peak Flap Deflection=-17.5 degrees, Azimuthal Phase Shift = -10 degrees) Flapped Rotor Configuration Test # 3925



Condition: 3741 Date: 3 Mar 1994

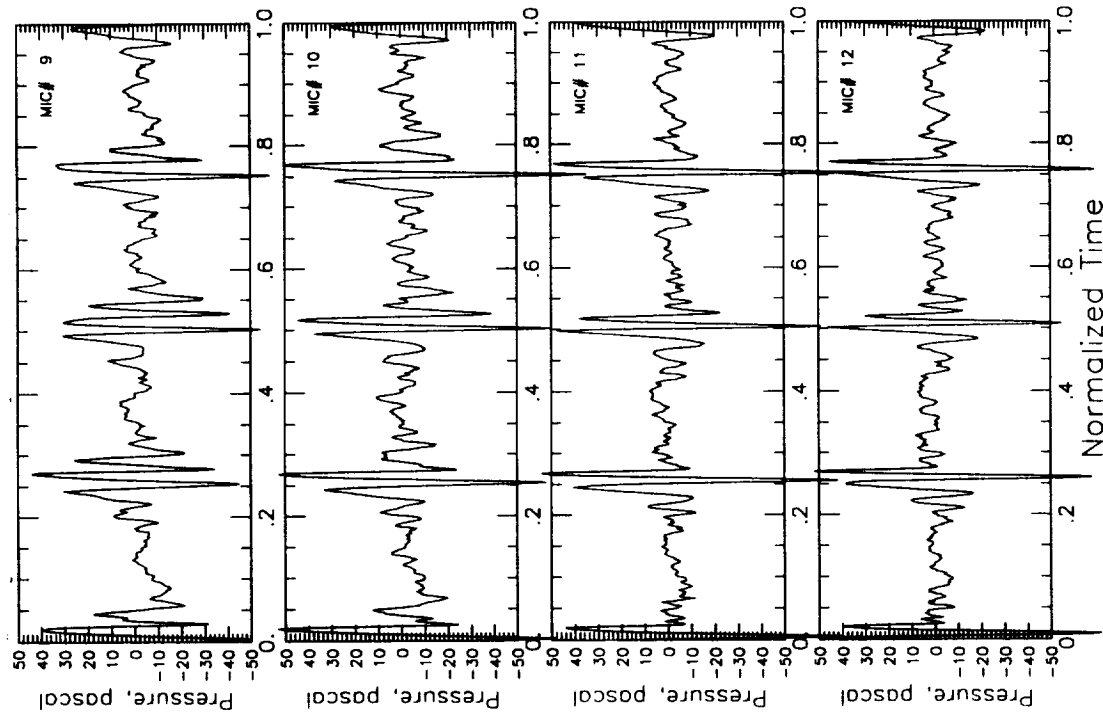
$\alpha_{\text{shaft}}$ : 2.508  $\mu$ : 0.1990  $C_t/\sigma$ : 0.0879



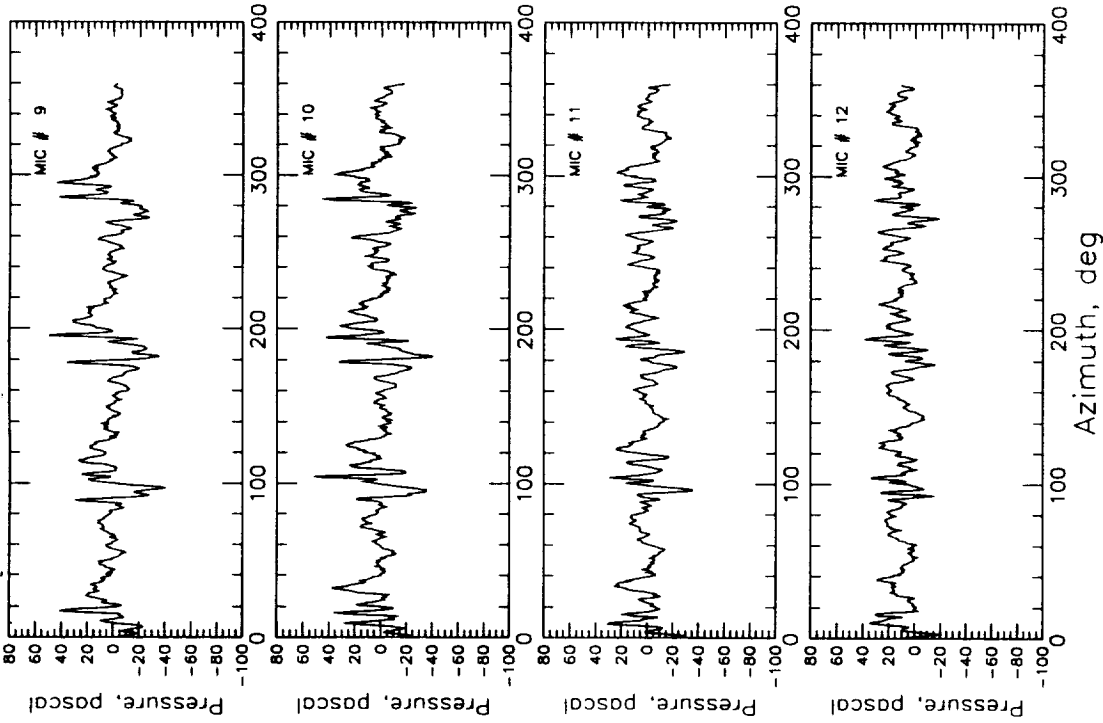
17.5-20 CAM. RPM=1086. ALFSU = 2.5 DEG. VOR = 0.20. CT/SIGMA = .087

Points: 2629-2645 sweep

Figure (62e) BVISPL Contour Plot Based on Spectra of Averaged Time Histories ( $C_t/\sigma = 0.0879$ ,  $\alpha_{\text{TPP}} = 2.5$  degrees aft,  $\mu = 0.1990$ , Peak Flap Deflection = -17.5 degrees, Azimuthal Phase Shift = -20 degrees) Flapped Rotor Configuration Test # 3741



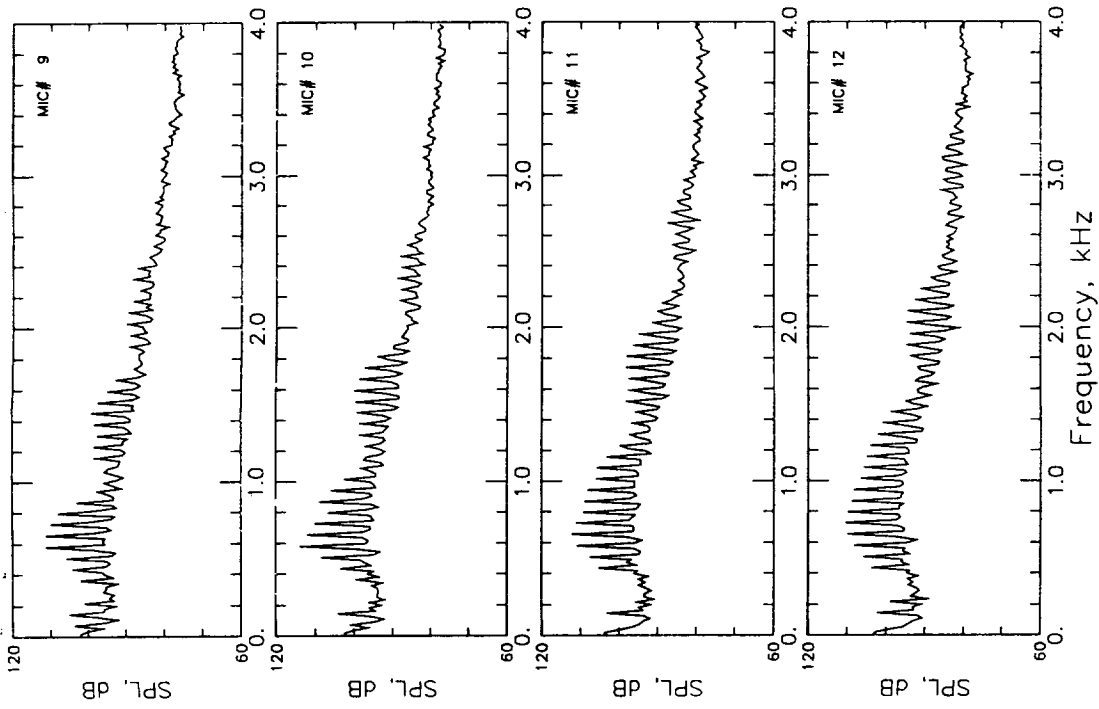
**a - Baseline Rotor [No Flap]- Test # 0741**



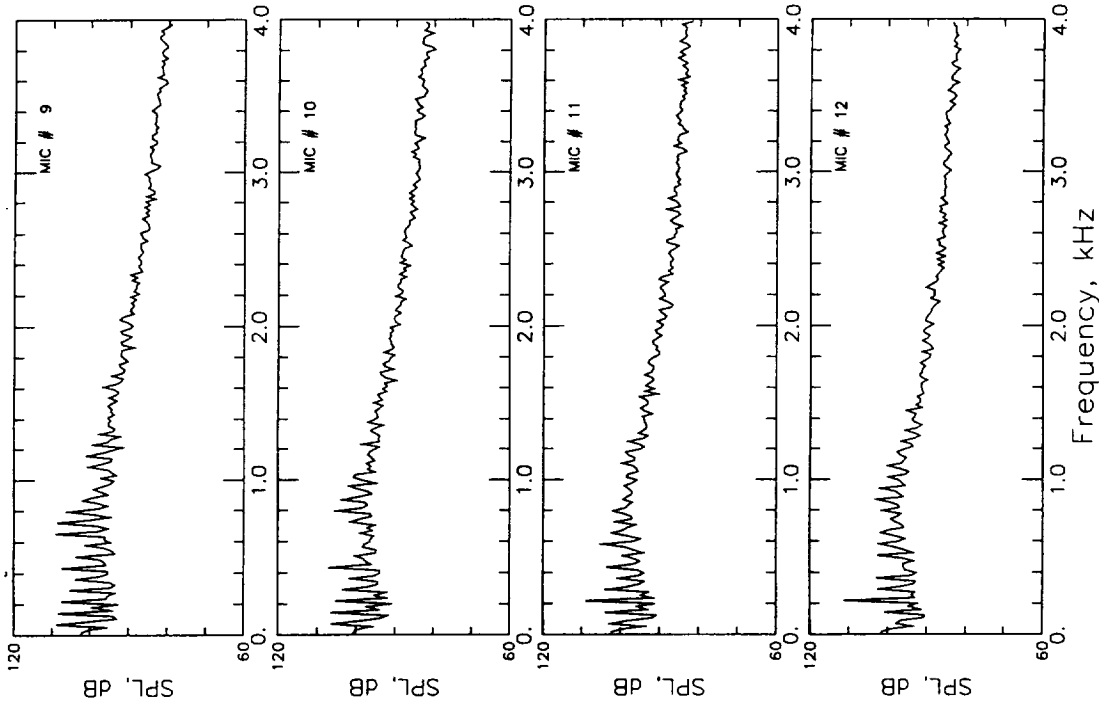
**b - Flapped Rotor**

**[Peak Flap Deflection= -17.5 degrees, Azimuthal Phase Shift = -10 degrees ] - Test # 3925**

**Figures (63a & 63b) Average Acoustic Time Histories at Microphone Traverse Station 9 on the Advancing Side - Test #s 0741 & 3925**

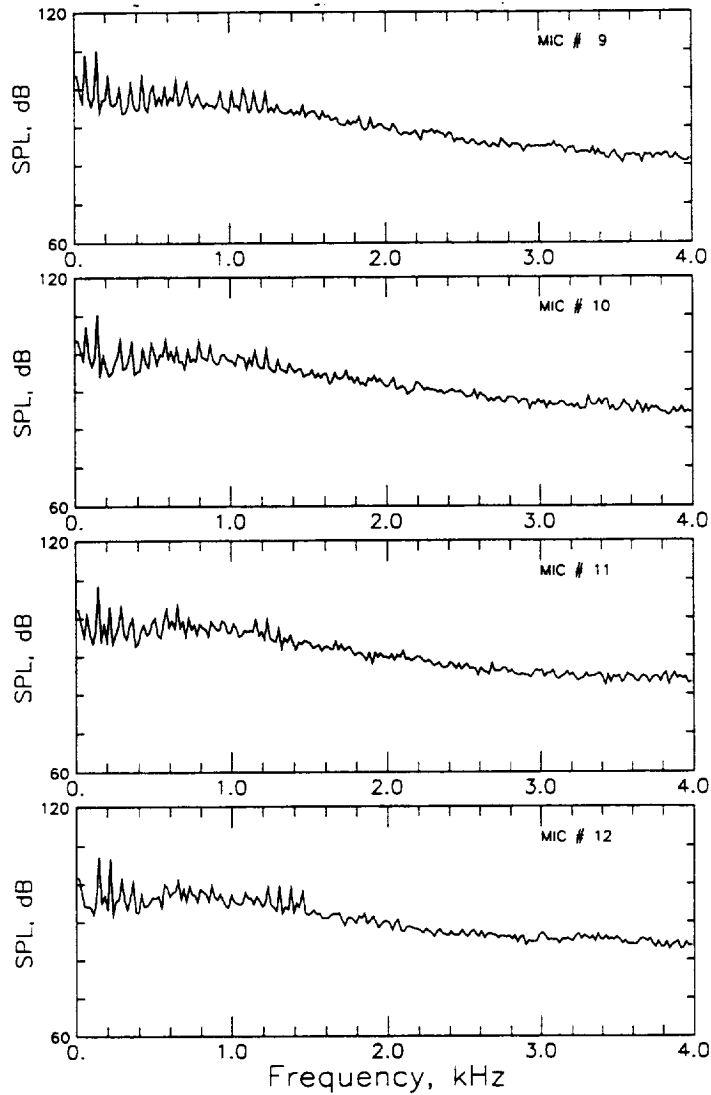


**a - Baseline Rotor [No Flap]- Test # 0741**



**b - Flapped Rotor**  
**[Peak Flap Deflection= -17.5 degrees, Azimuthal**  
**Phase Shift = -10 degrees ] - Test # 3910**

**Figures (64a & 64b) Ensemble-averaged Narrowband Noise Spectra at**  
**Microphone Traverse Station 9 on the Advancing Side**  
**- Test #s 0741 & 3910**



**[Peak Flap Deflection = -17.5 degrees, Azimuthal Phase Shift = -10 degrees]**

Figure (64c) Ensemble-averaged Narrowband Noise Spectra at Microphone Traverse Station 9 on the Advancing Side ; Flapped Rotor - Test # 3925

Condition: 0731 Date: 25 Feb 1994

$\alpha_{\text{shaft}}$ : 3.016  $\mu$ : 0.1492  $C_t/\sigma$ : 0.0773

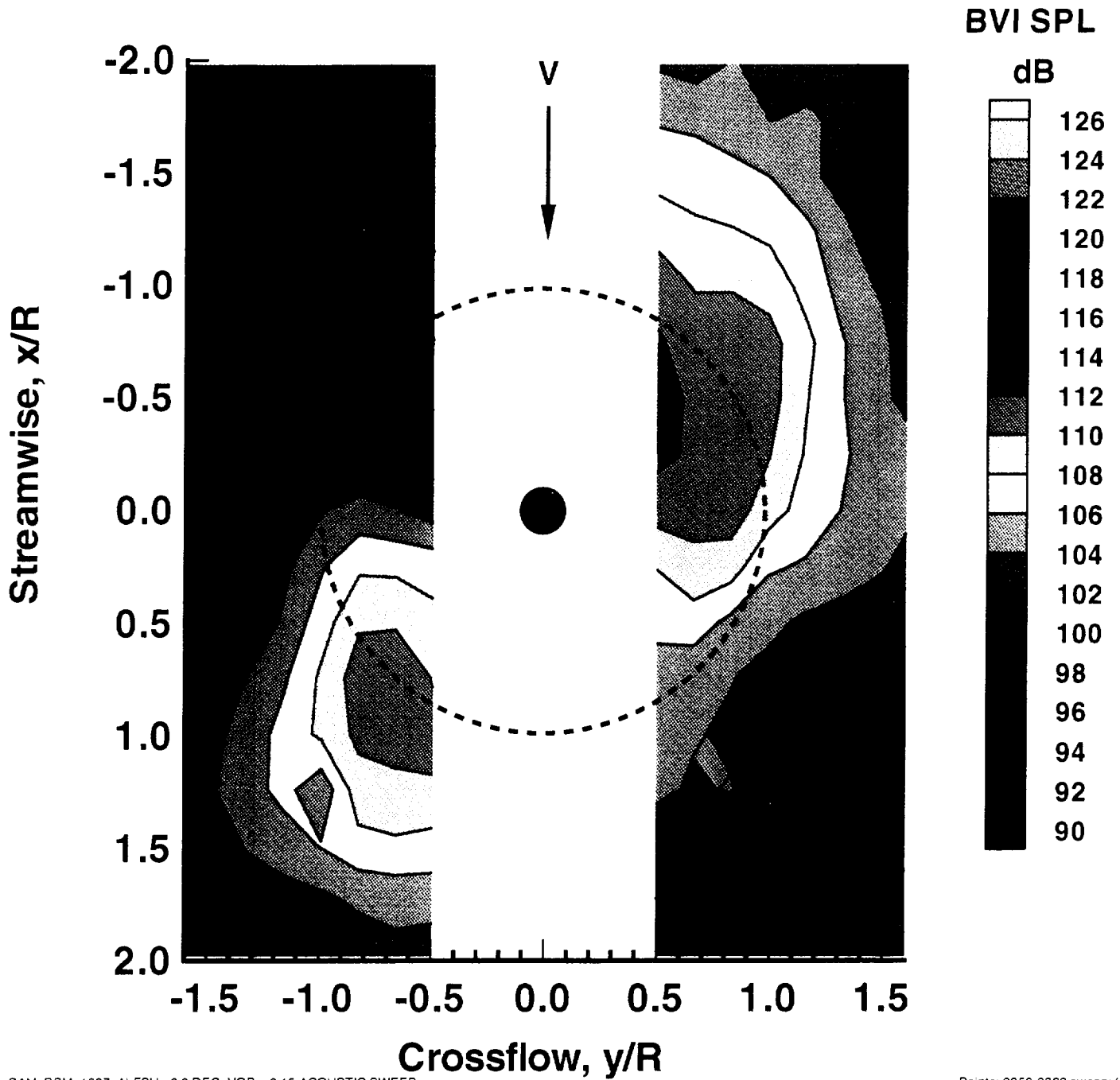
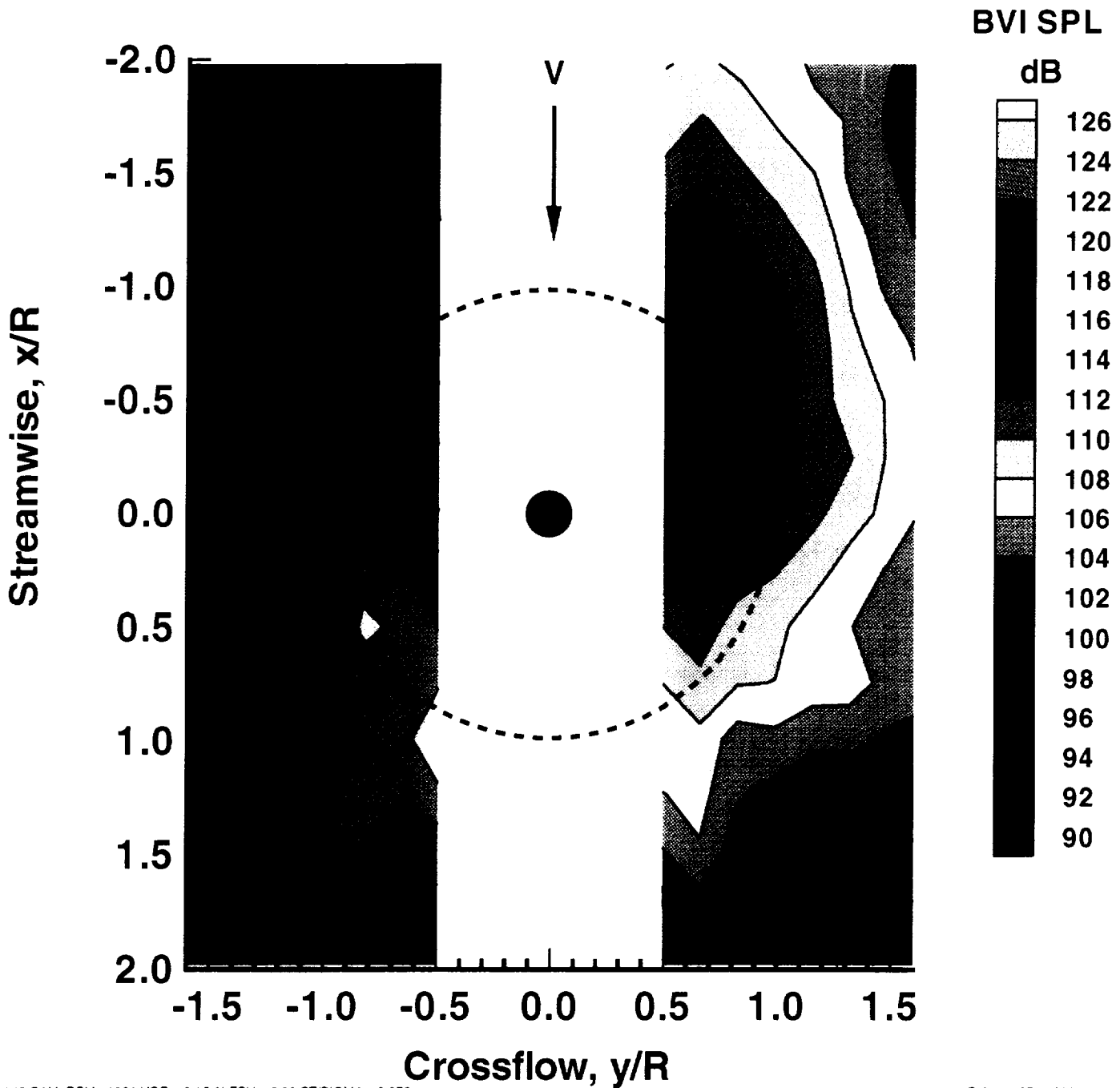


Figure (65a) BVISPL Contour Plot Based on Spectra of Averaged Time Histories ( $C_t/\sigma = 0.0773$ ,  $\alpha_{\text{TPP}} = 3$  degrees aft,  $\mu=0.1492$ ) Baseline Rotor Configuration Test # 0731

Condition: 5030 Date: 11 Mar 1994

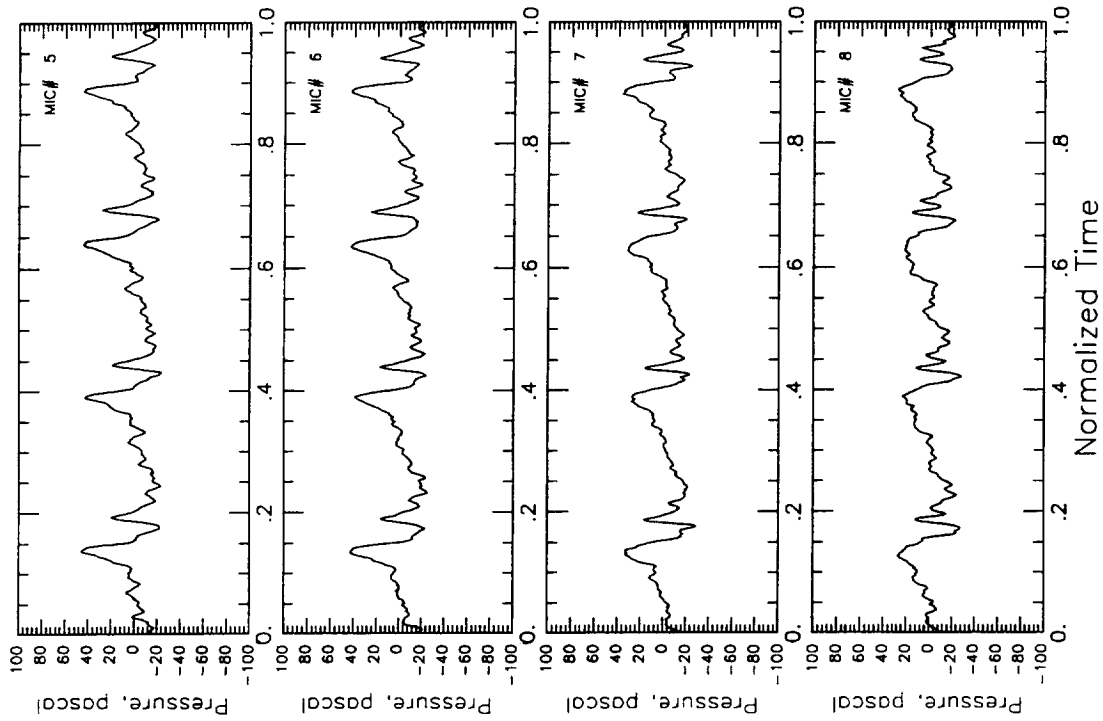
$\alpha_{\text{shaft}}$ : 3.072  $\mu$ : 0.1496  $C_t/\sigma$ : 0.0764



17.5+140 CAM, RPM= 1081 VOR = 0.15 ALFSU = 3.00 CT/SIGMA = 0.076

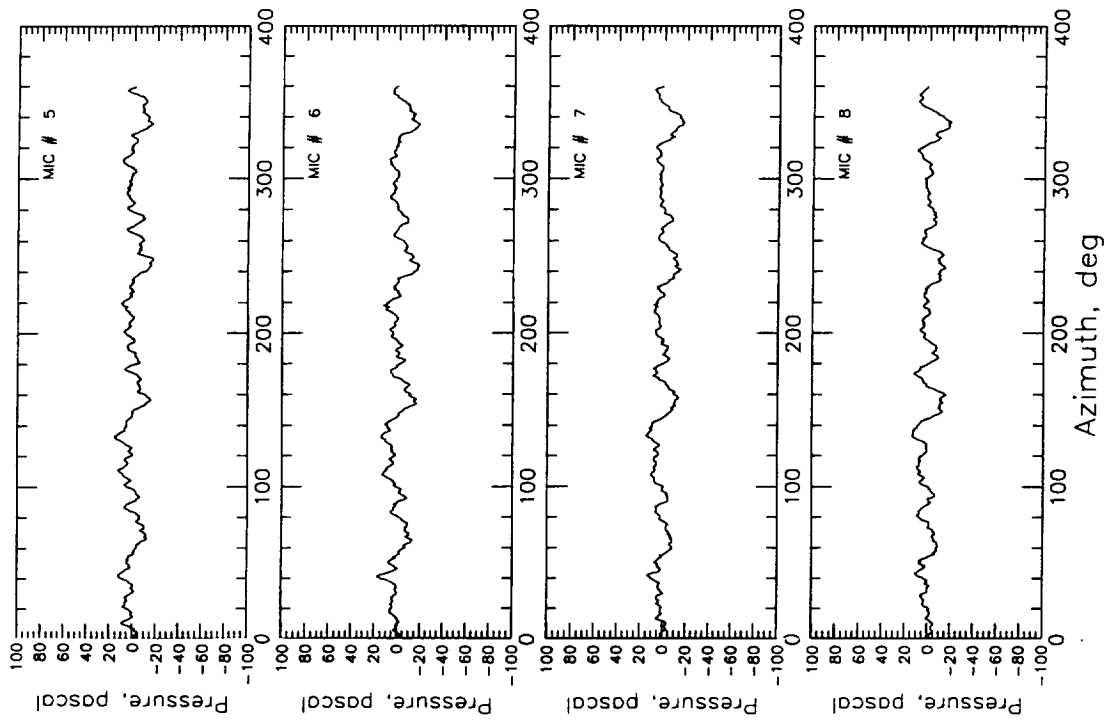
Points: 4374-4390 sweep: 001

Figure (65b) BVISPL Contour Plot Based on Spectra of Averaged Time Histories ( $C_t/\sigma = 0.0764$ ,  $\alpha_{\text{TPP}} = 3$  degrees aft,  $\mu=0.1496$ , Peak Flap Deflection=-17.5 degrees, Azimuthal Phase Shift = +140 degrees ) Flapped Rotor Configuration - Test #5030



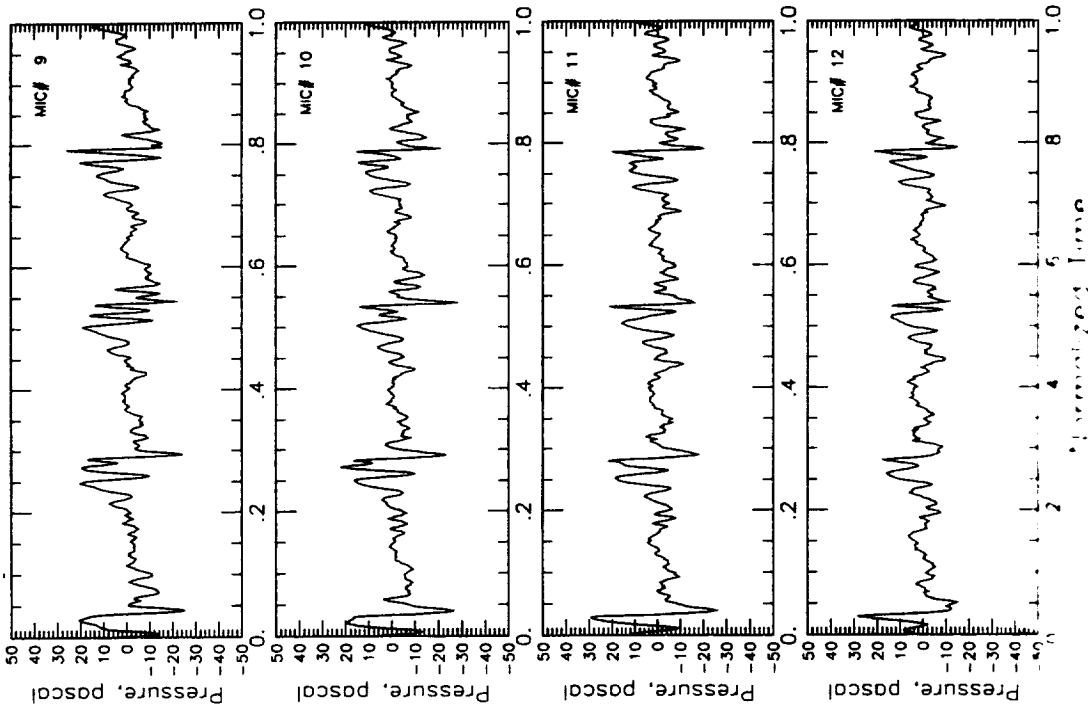
**a - Baseline Rotor [No Flap]- Test # 0731**

Figures (66a & 66b) Average Acoustic Time Histories at Microphone Traverse Station 9 on the Retreating Side - Test #s 0731 & 5030

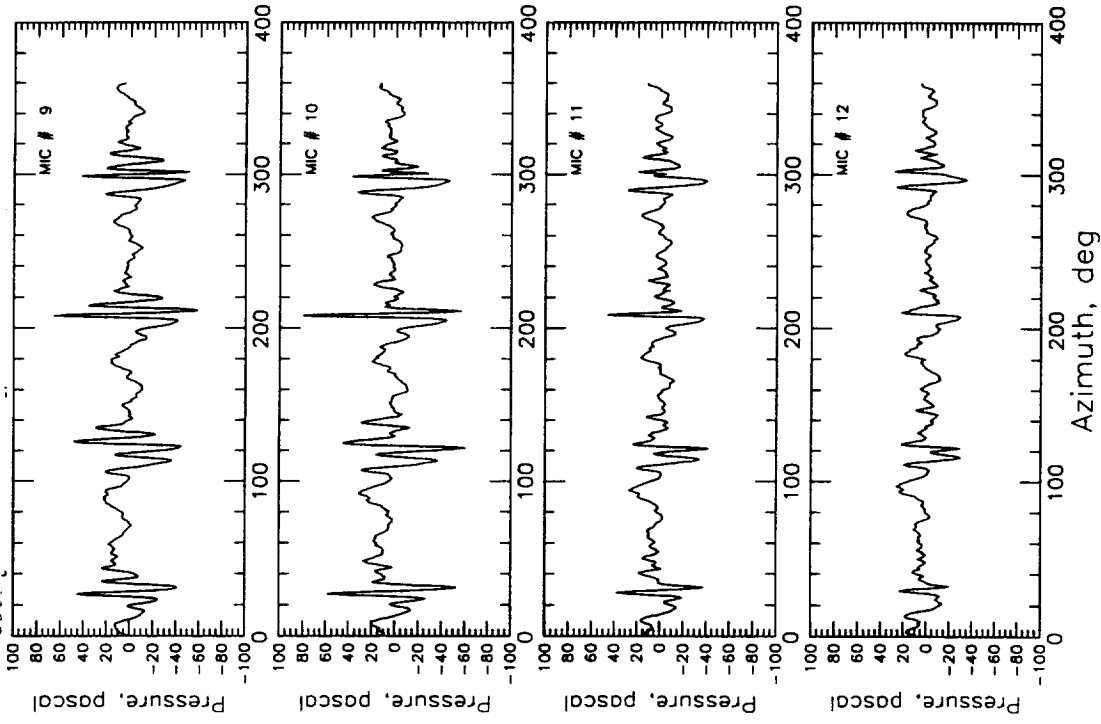


**b - Flapped Rotor**

[Peak Flap Deflection= -17.5 degrees, Azimuthal Phase Shift = +140 degrees ] - Test # 5030



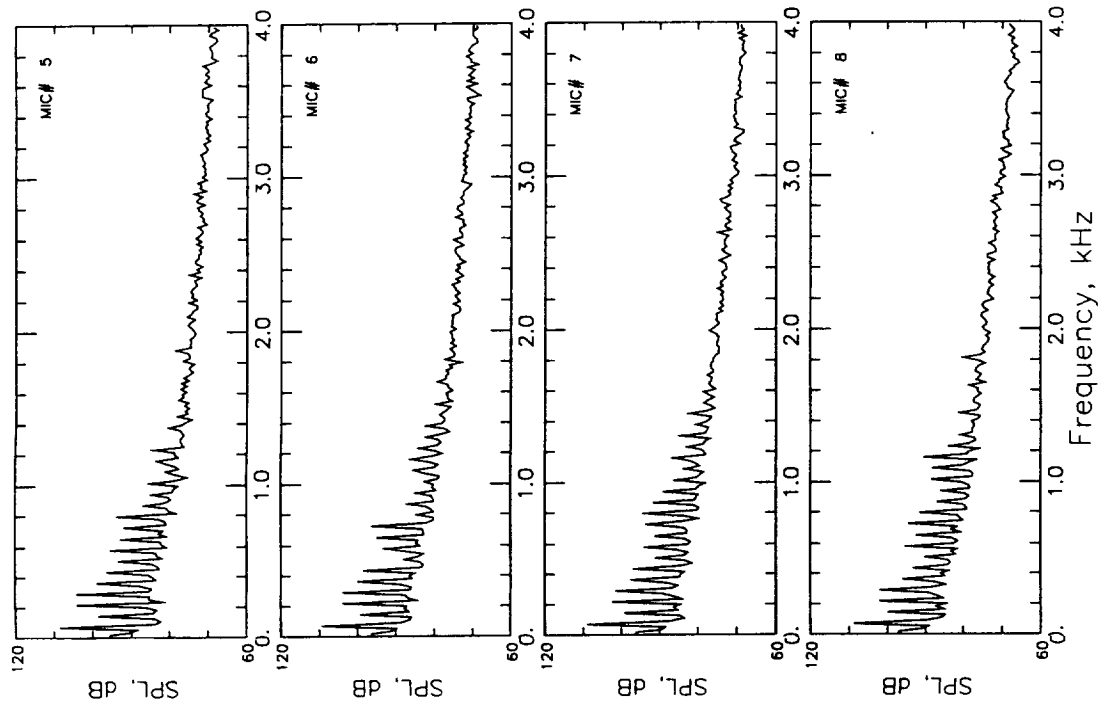
**a - Baseline Rotor [No Flap]- Test # 0731**



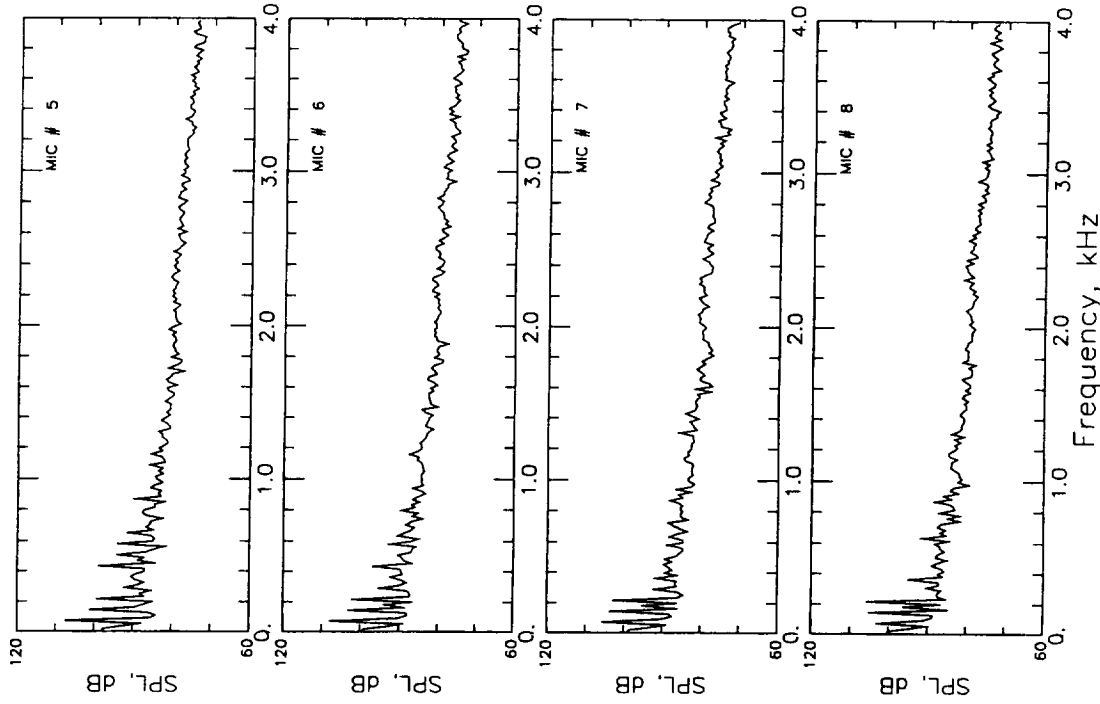
**b - Flapped Rotor  
[Peak Flap Deflection= -17.5 degrees, Azimuthal  
Phase Shift = +140 degrees ] - Test # 5030**

**Figures (67a & 67b) Average Acoustic Time Histories at Microphone  
Traverse Station 9 on the Advancing Side - Test #s  
0731 & 5030**





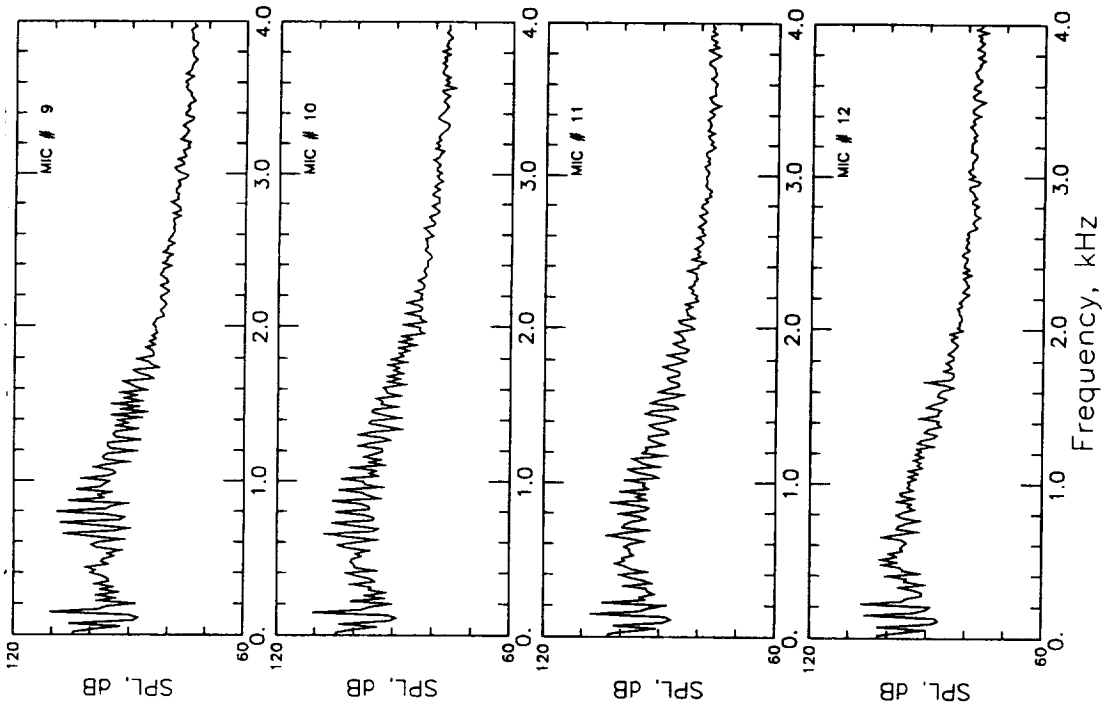
**a - Baseline Rotor [No Flap]- Test # 0731**



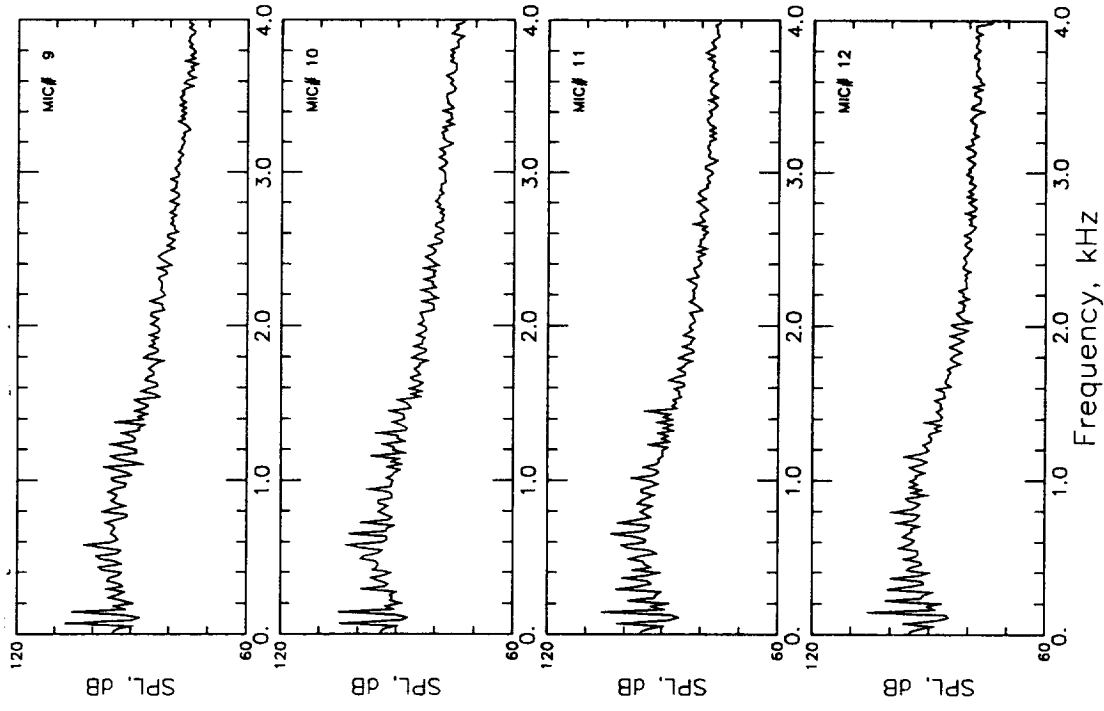
**b - Flapped Rotor**

**[Peak Flap Deflection= -17.5 degrees, Azimuthal  
Phase Shift = +140 degrees ] - Test # 5030**

Figures (68a & 68b) Ensemble-averaged Narrowband Noise Spectra at  
Microphone Traverse Station 9 on the Retreating Side -  
Test #s 0731 & 5030



**a - Baseline Rotor [No Flap]- Test # 0731**



**b - Flapped Rotor**  
**[Peak Flap Deflection= -17.5 degrees, Azimuthal**  
**Phase Shift = +140 degrees ] - Test # 5030**

**Figures (69a & 69b) Ensemble-averaged Narrowband Noise Spectra at**  
**Microphone Traverse Station 9 on the Advancing Side**  
**- Test #s 0731 & 5030**

Condition: 0741 Date: 26 Feb 1994

$\alpha_{\text{shaft}}$ : 2.502  $\mu$ : 0.1987  $C_t/\sigma$ : 0.0868

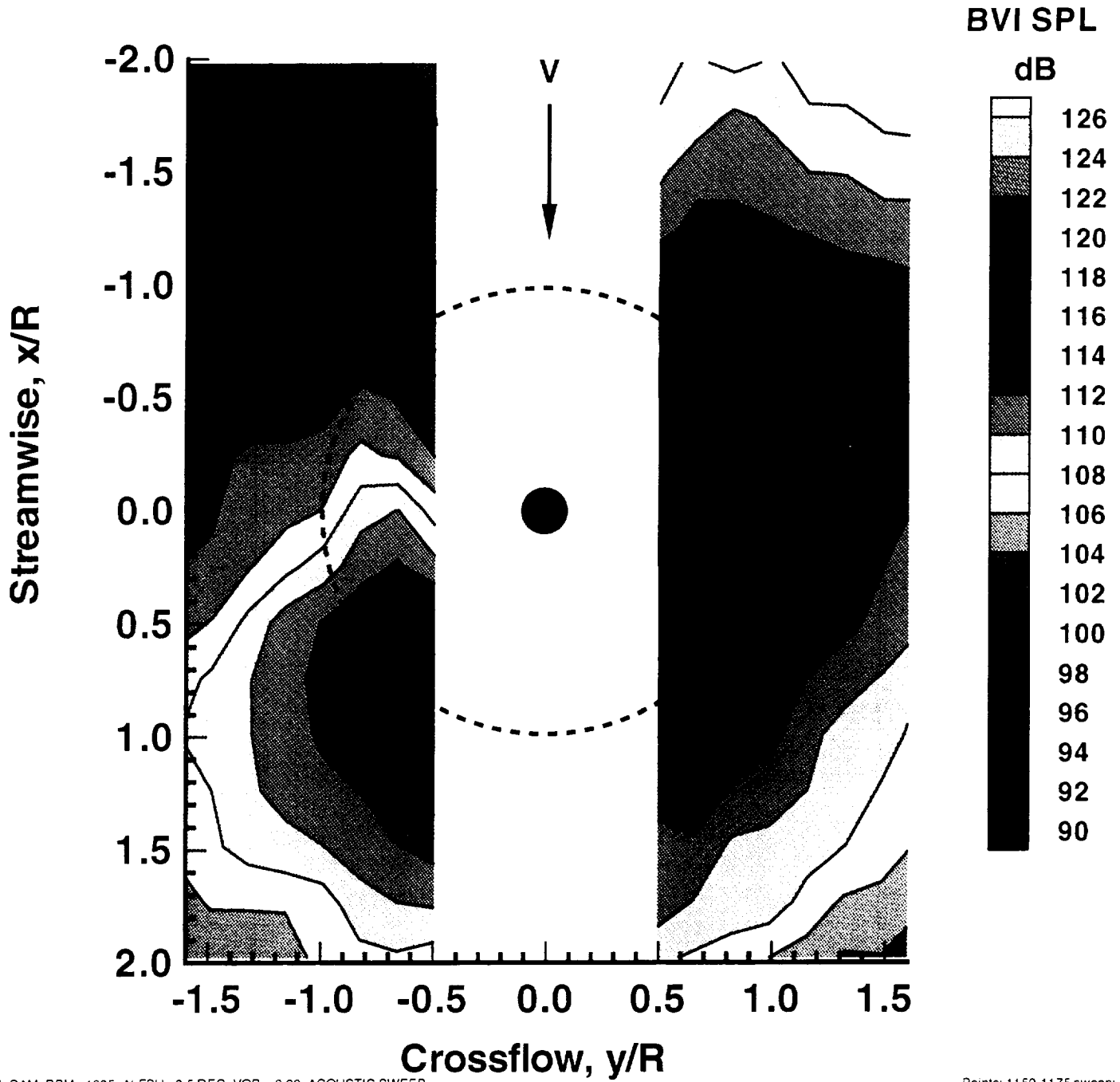


Figure (70a) BVISPL Contour Plot Based on Spectra of Averaged Time Histories ( $C_t/\sigma = 0.0868$ ,  $\alpha_{\text{TRP}} = 2.5$  degrees aft,  $\mu=0.1987$ ) Baseline Rotor Configuration - Test # 0741

Condition: 5050 Date: 12 Mar 1994

$\alpha_{\text{shaft}}$ : 2.514  $\mu$ : 0.1987  $C_t/\sigma$ : 0.0890

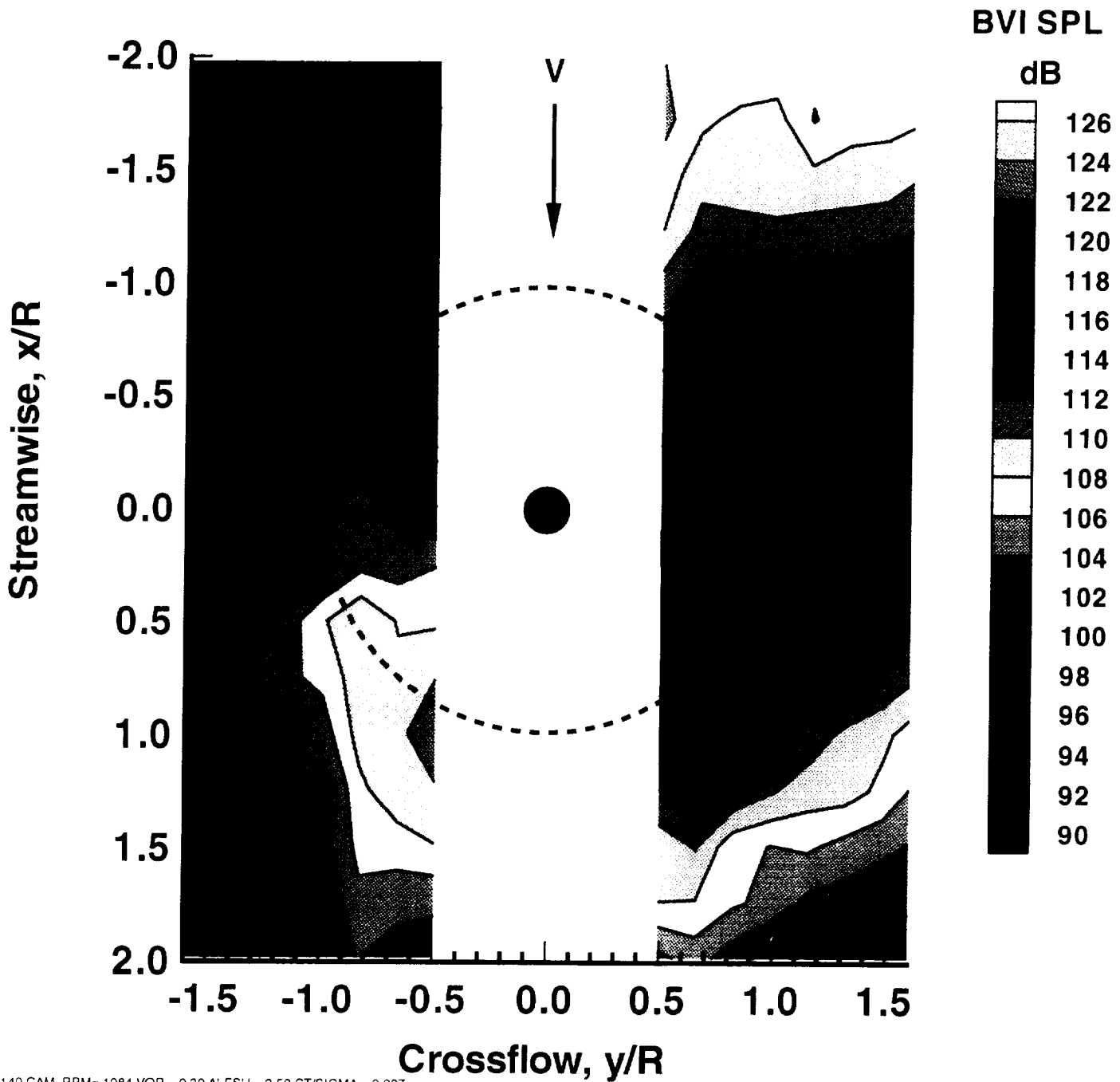
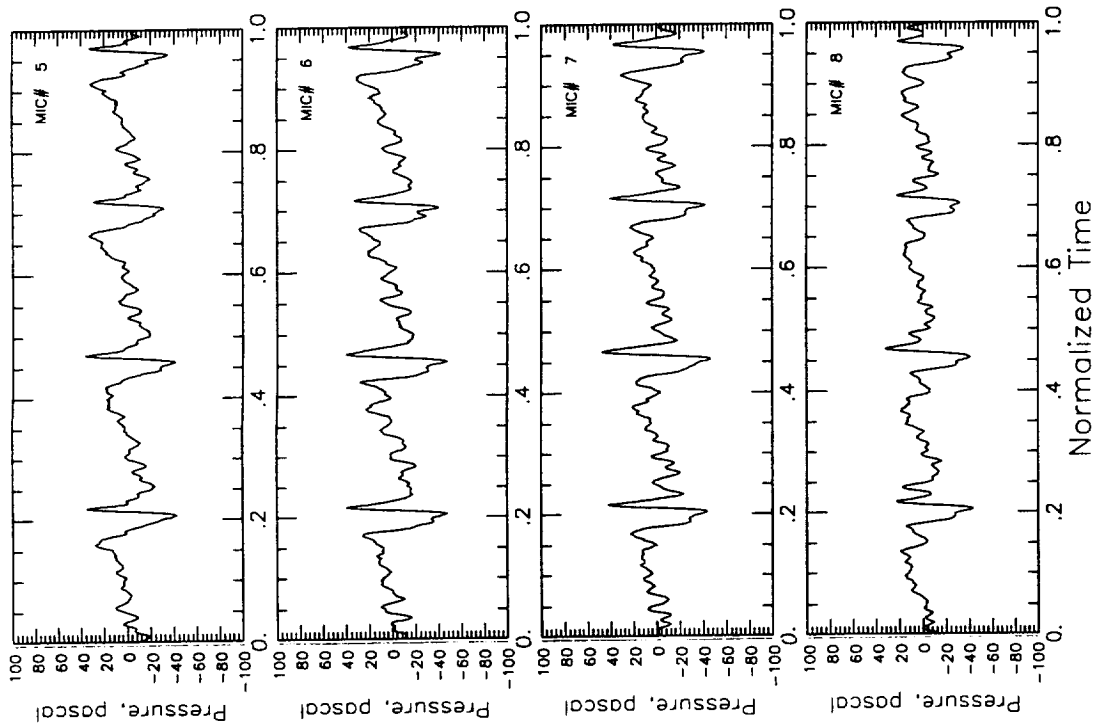
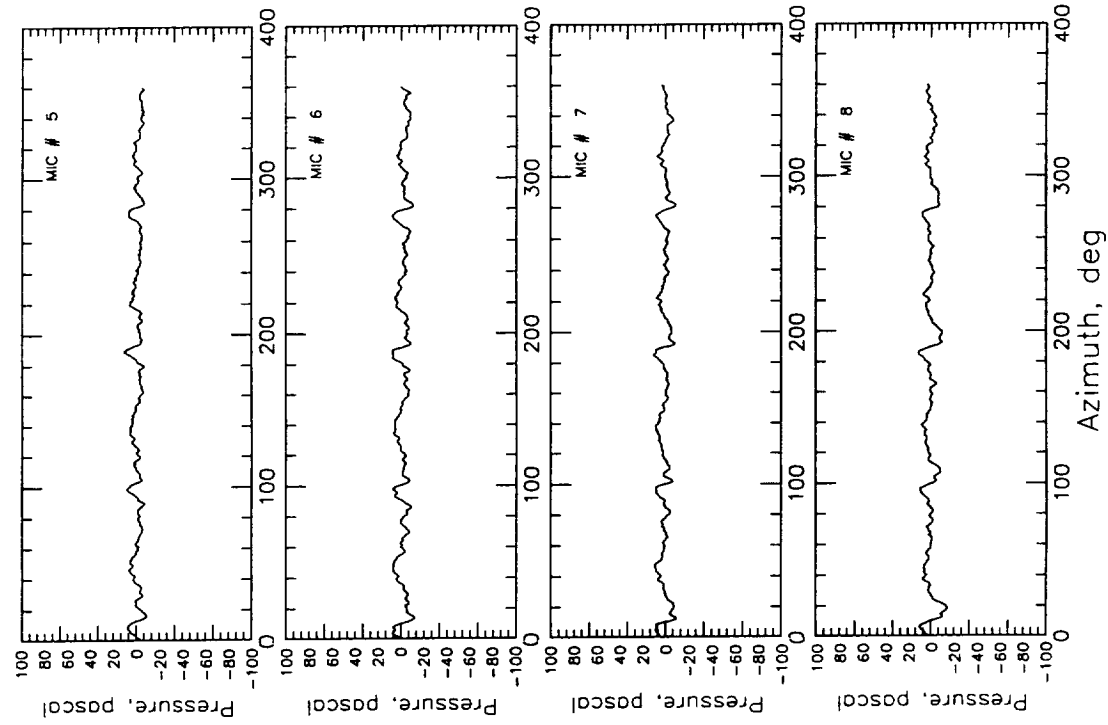


Figure (70b) BVISPL Contour Plot Based on Spectra of Averaged Time Histories ( $C_t/\sigma = 0.0890$ ,  $\alpha_{TPP} = 2.5$  degrees aft,  $\mu=0.1987$ , Peak Flap Deflection=-17.5 degrees, Azimuthal Phase Shift = +140 degrees ) Flapped Rotor Configuration - Test #5050

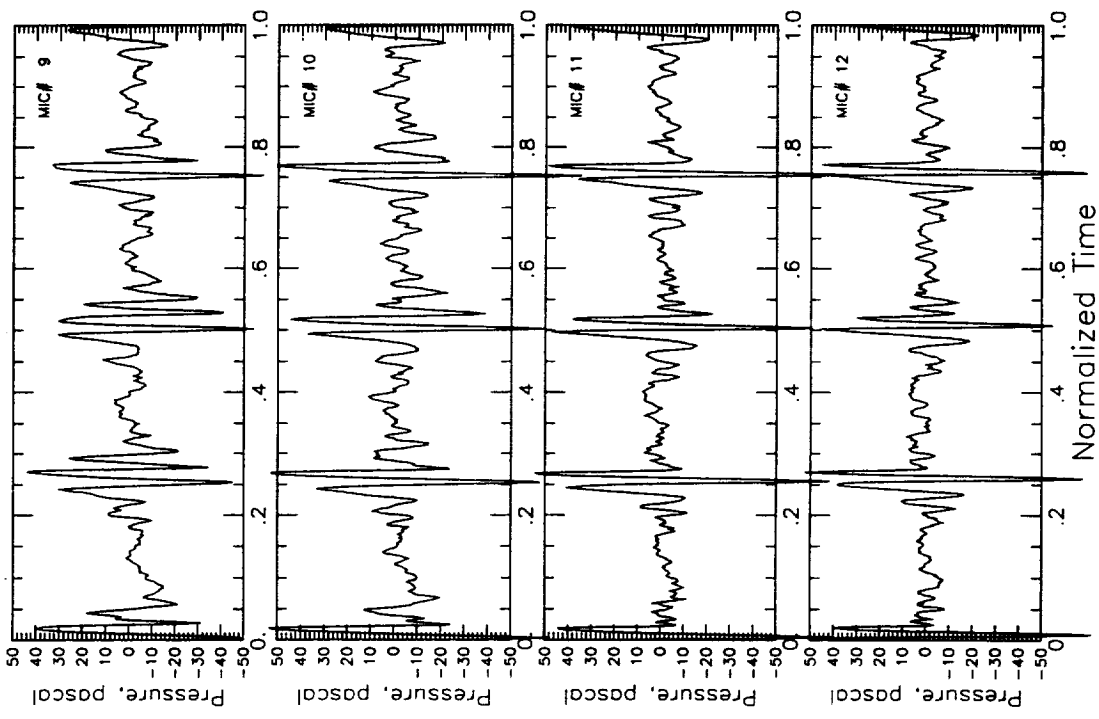


**a - Baseline Rotor [No Flap]- Test # 0741**



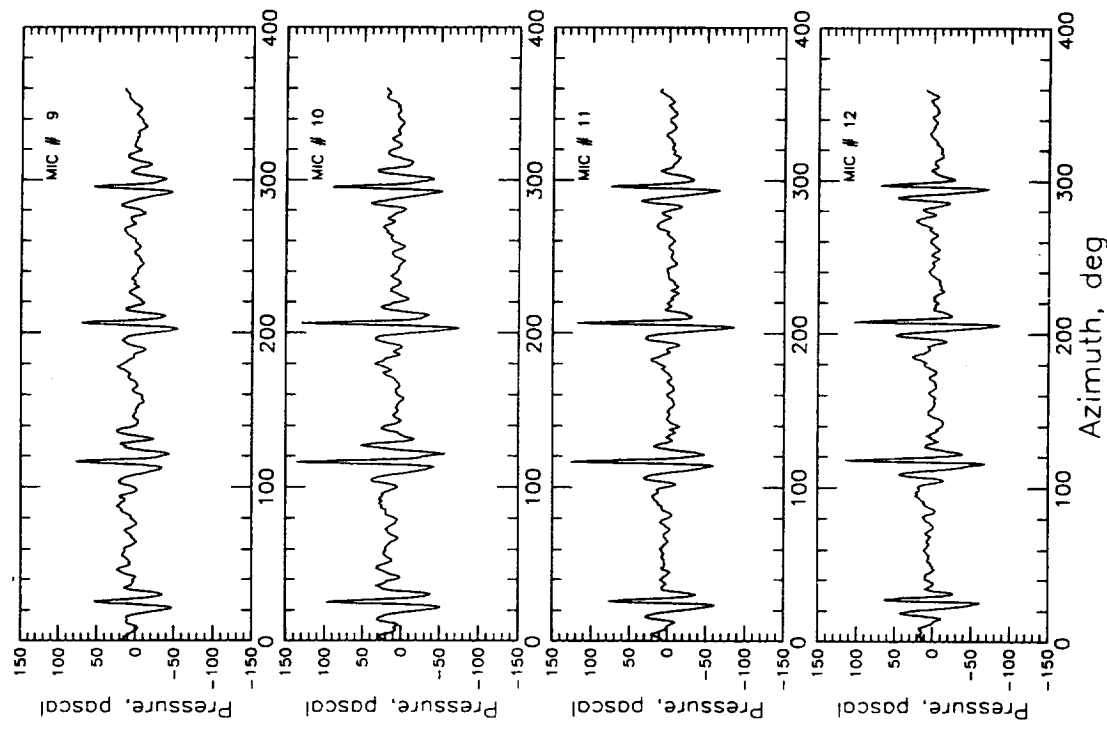
**b - Flapped Rotor  
[Peak Flap Deflection= -17.5 degrees, Azimuthal  
Phase Shift = +140 degrees ] - Test # 5050**

**Figures (71a & 71b) Average Acoustic Time Histories at Microphone  
Traverse Station 9 on the Retreating Side - Test #s  
0741 & 5050**

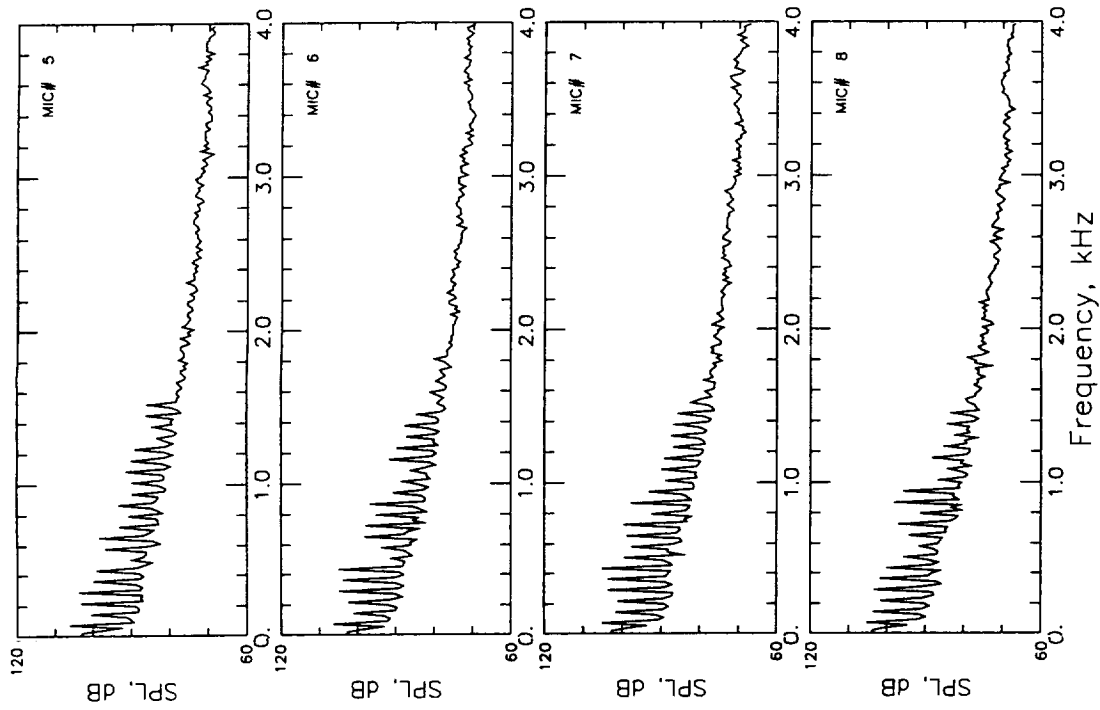


**a - Baseline Rotor [No Flap]- Test # 0741**

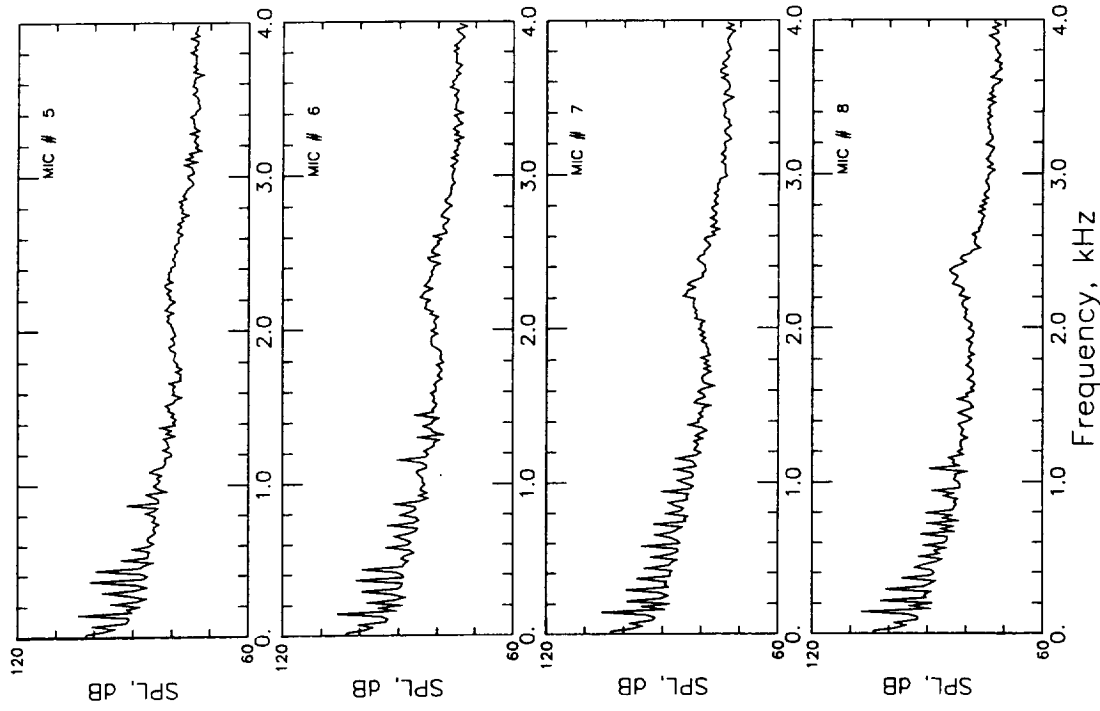
Figures (72a & 72b) Average Acoustic Time Histories at Microphone Traverse Station 9 on the Advancing Side - Test #s 0741 & 5050



**b - Flapped Rotor [Peak Flap Deflection= -17.5 degrees, Azimuthal Phase Shift = +140 degrees ] - Test # 5050**



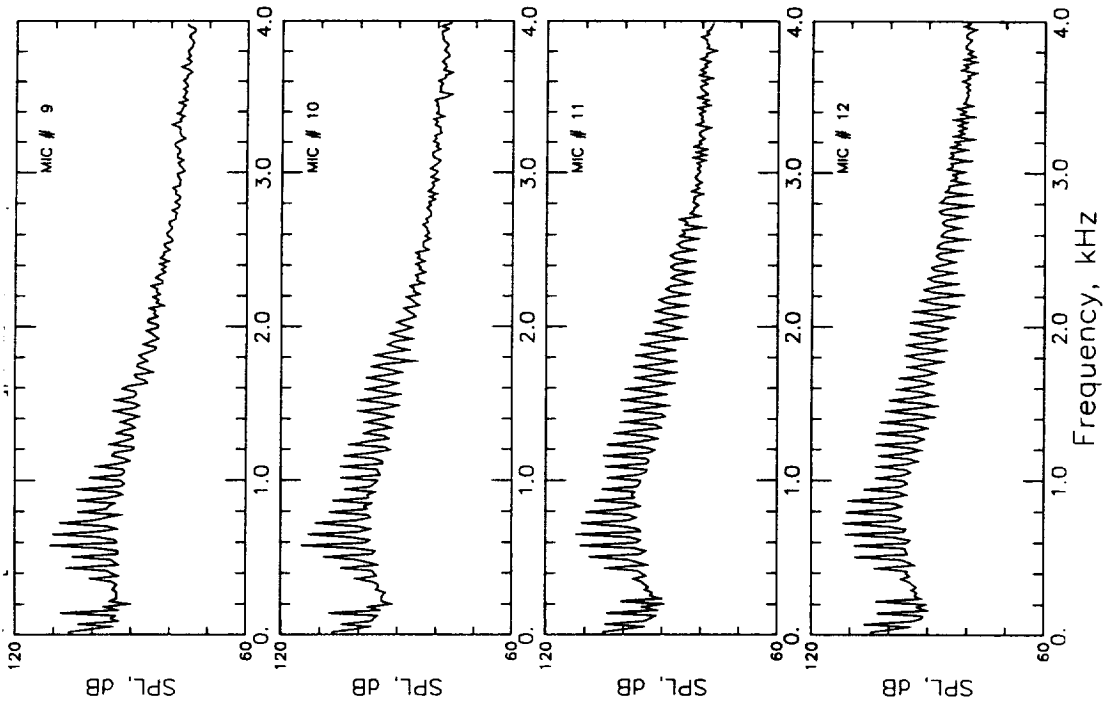
**a - Baseline Rotor [No Flap]- Test # 0741**



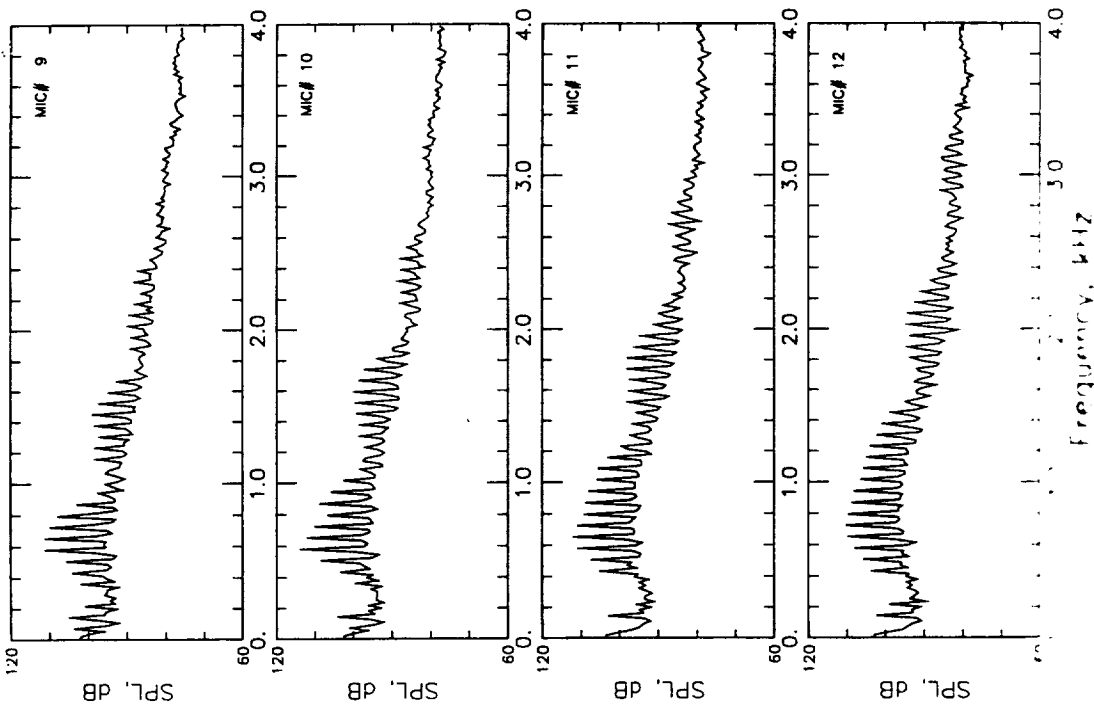
**b - Flapped Rotor**

**[Peak Flap Deflection = -17.5 degrees, Azimuthal Phase Shift = +140 degrees ] - Test # 5050**

**Figures (73a & 73b) Ensemble-averaged Narrowband Noise Spectra at Microphone Traverse Station 9 on the Retreating Side - Test #s 0741 & 5050**



**b - Flapped Rotor**  
 [Peak Flap Deflection= -17.5 degrees, Azimuthal  
 Phase Shift = +140 degrees ] - Test # 5050



**a - Baseline Rotor [No Flap]- Test # 0741**

Figures (74a & 74b) Ensemble-averaged Narrowband Noise Spectra at  
 Microphone Traverse Station 9 on the Advancing Side  
 - Test #s 0741 & 5050



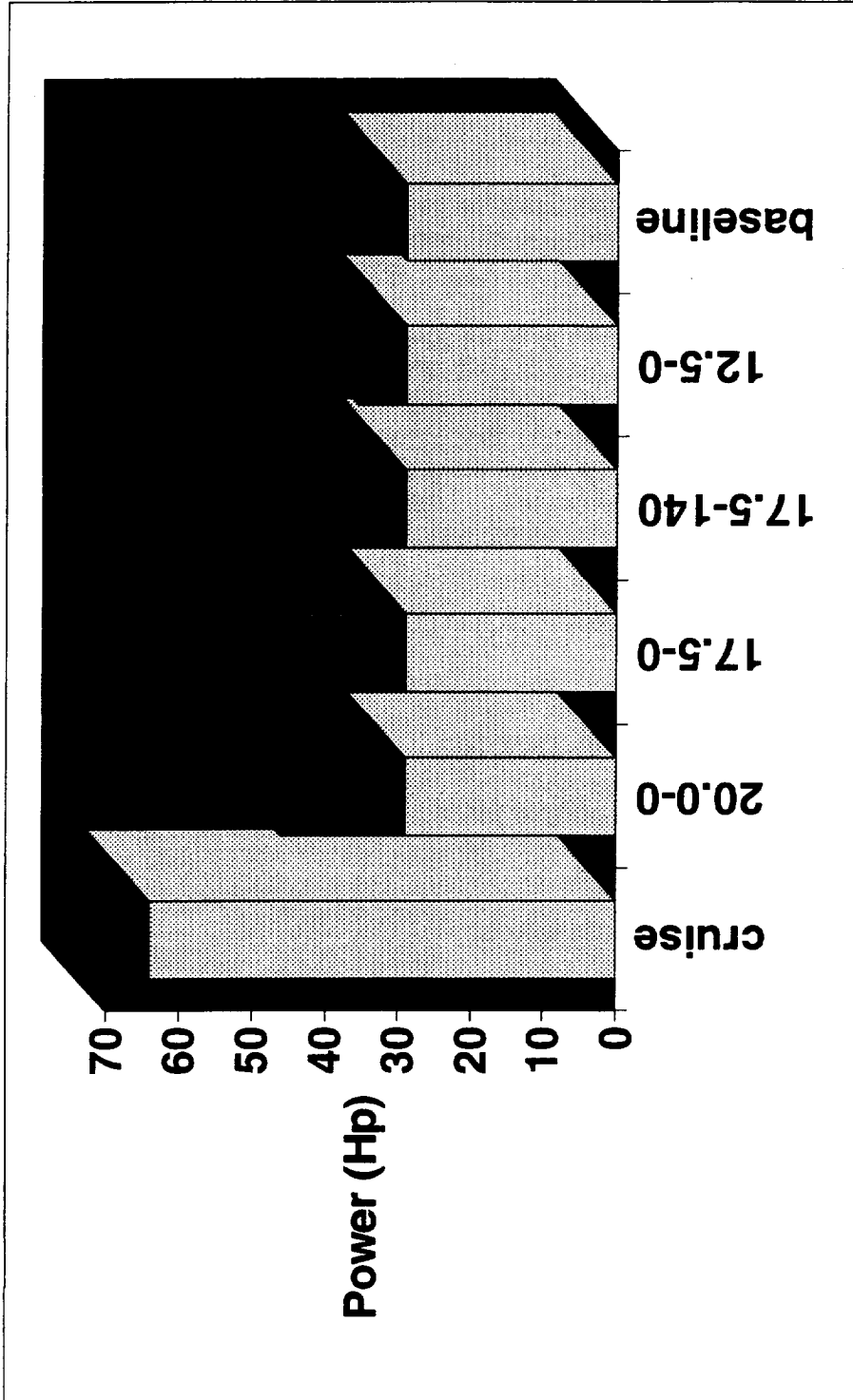


Figure (75) Power Required for Descent Flight Condition ( $\mu = 0.20$  and  $Ct = 0.008$ ) for Baseline and Active Flap Rotor Configurations and Cruise Flight Condition for Baseline Rotor ( $\mu=0.3, Ct=0.008$ )

## Appendix A

### BVI Tunnel test Tare Results and Correction Equations

The tare runs were completed in the Langley 14- by 22-foot Subsonic Tunnel on Friday, February 18, Saturday February 19, and Tuesday, February 22 1994. The values from the runs on the 18th and 19th are stored in the file BVI\_TARE.XLS for all five balance forces and torque. The weight Tares were calculated from data in this file. Three additional files were created to calculate tares for lift, drag, pitch and torque. The lift file was not used, but it is called LIFTTARE.XLS. The file AXLTARE.XLS contains the data and correction equations for both DRAG and PITCH. The file TORQTARE.XLS contains the data and correction equation for the torque gauges. The corrections below use the variable naming convention used in the test plan and are the correction used in all post processing programs and the online system beginning on Monday the 28 of February 1994.

**Lift:** The balance appeared to drift in all five axes and the data from the aero and rotation tare runs indicate mostly drift and it is my conclusion the change in lift during the rotation and wind on runs are due only to drift and not aerodynamics or dynamics at least to the extent to which the instrumentation is accurate. Thus, the only lift tare is for weight. The weight tares were acquired with both blades on and blades off. The blades off points were used to generate the aero tares. The blades on weight tares are shown below. The Lift tares are:

$$\begin{aligned} \text{TWNFRB} &= 27.32075 * \text{SIN}(\text{ALFSU}) + 1008.355 * (1. - \text{COS}(\text{ALFSU})) \\ \text{TRNFRB} &= 0. \\ \text{TMNFRB} &= 0. \end{aligned}$$

$$\text{LIFT,RT} = \text{NFRHC} - \text{TWNFRB} - \text{TRNFRB}$$

where NFRHC is the corrected normal force at the hub

$$\text{LIFT,HT} = \text{LIFT,RT} - \text{TMNFRB}$$

for reference the blades off weight tare is:

$$\text{twnfrb (no blades)} = 26.19128 * \text{SIN}(\text{ALFSU}) + 1016.023 * (1. - \text{COS}(\text{ALFSU}))$$

**Drag:** The balance appeared to drift a considerable amount during the runs on February 18th and 19th, but the run on the 22nd was performed with a quick q sweep the results seem consistent, so this run was used to generate the aero tares for both DRAG and PITCH. The results suggest some effect of RPM changes on drag, but these were attributed to drift and not the physics of the rotor system. Thus, only the effects of weight and q are shown in the tares. The drag tares are:

$$\begin{aligned} \text{TWAFRB} &= 992.4972 * \text{SIN}(\text{ALFSU}) - 14.858 * (1. - \text{COS}(\text{ALFSU})) \\ \text{TRAFRB} &= 0. \end{aligned}$$

$$\text{TMAFRB}=0.012195*\text{qpsfA2}+1.580381 * \text{qpsf}$$

$$\text{DRAG,RT}=\text{AFRHC}-\text{TWAFRB}-\text{TRAFRB}$$

where AFRHC is the corrected axial force at the hub)

$$\text{DRAG,HT}=\text{DRAG,RT}-\text{TMAFRB}$$

for reference the blades off weight tare is:

$$\text{tw sfrb}(\text{no blades})=971.329*\text{SIN}(\text{ALFSU})+43.47764*(1.-\text{COS}(\text{ALFSU}))$$

**Side:** All of the change appears to be drift in the measurement and no physical meaning can be applied to the data. Also, no trend seems to exist, so no aerodynamic or rotation tares were applied to the side force. The side tares are:

$$\text{TWSFRB}=-13.7467*\text{SIN}(\text{ALFSU})+27.94548*(1.-\text{COS}(\text{ALFSU}))$$

$$\text{TRSFRB}=0.$$

$$\text{TMSFRB}=0.$$

$$\text{SIDE,RT}=\text{SFRHC}-\text{TWSFRB}-\text{TRSFRB}$$

where SFRHC is the corrected side force at the hub

$$\text{SIDE,HT}=\text{SIDE,RT}-\text{TMSFRB}$$

for reference the blades of weight tare is:

$$\text{tw sfrb}(\text{no blades})=-11.1573*\text{SIN}(\text{ALFSU})+-5.36711*(1.-\text{COS}(\text{ALFSU}))$$

**Roll:** None of the roll tare values seem to be significant except for the weight tare. Thus only the weight tare was applied to the roll force. The roll tares are:

$$\text{TWRMRB}=979.6701 * \text{SIN}(\text{ALFSU})-1568.76*(1.-\text{COS}(\text{ALFSU}))$$

$$\text{TRRMRB}=0.$$

$$\text{TMRMRB}=0.$$

$$\text{ROLL,RT}=\text{RMRHC}-\text{TWRMRB}-\text{TRRMRB}$$

RMRHC is the corrected roll moment at the hub

$$\text{ROLL,HT}=\text{ROLL,RT}-\text{TMRMRB}$$

for reference the blades of weight tare is:

$$\text{tw rmr}(\text{no blades})=898.9695*\text{SIN}(\text{ALFSU})-189.23*(1.-\text{COS}(\text{ALFSU}))$$

**Pitch:** The pitch aero tares at the hub seem to match the 46.55 inch offset from the balance times the axial force. However, a better correlation was found using a polynomial based on qpsf since using the axial force directly created a system with two linearly dependent variables. Also, it was determined the pitch did not vary significantly with RPM. The pitch tares are:

$$\text{TWPMRB}=-25301.9*\text{SIN}(\text{ALFSU})+1493.207(1.-\text{COS}(\text{ALFSU}))$$

$$\text{TRPMRB}=0.$$

$$\text{TMPMRB}=-0.00641 * \text{qpsfA3}-0.09434 * \text{qpsf}^2+5.121993 * \text{qpsf}$$

$$\text{PITCH,RT}=\text{PMRHC}-\text{TWPMRB}-\text{TRPMRB}$$

PMRHC is the corrected pitch moment at the hub

$$\text{PITCH,HT}=\text{PITCH,RT}-\text{TMPMRB}$$

for reference the blades of weight tare is:

$$\text{twnfrb}(\text{no blades})=26.19128 * \text{SIN}(\text{ALFSU})+1016.023 * (1.-\text{COS}(\text{ALFSU}))$$

**Torque:** The primary torque bridge was out during the tare runs, but the backup gauge was very repeatable during the runs. Of course there is no weight tare for torque and shaft angle seemed to have no effect on torque. It is a very strong function of RPM and a mild function of q. A linear estimating process was used to determine a function of both RPM and q. The average of the torque values acquired at a specific q and 100% RPM over a range of shaft angles was used to determine the dependency on q and the results of a couple of RPM sweeps was used for the dependency on RPM. The torque tares are given by:

$$\text{TTORQ1}=0.0000726 * \text{qpsf}^3-$$

$$0.03063 * \text{qpsfA2}+5.101959 * \text{qpsf}+0.257654 * \text{RPM}$$

$$\text{TTORQ2}=0.0000726 * \text{qpsf}^3-$$

$$0.03063 * \text{qpsf}^2+5.101959 * \text{qpsf}+0.257654 * \text{RPM}$$

$$\text{TORQ, HT} =\text{TORQ}-\text{TTORQ1}$$

$$\text{TORQ2, HT}=\text{TORQ2}-\text{TTORQ2}$$

## **Appendix B**

### **Test Log, Run Log, Instrumentation List, and Data Point Log**

								Active Flap Rotor, Run Log			
TEST	POINT	DATE				CT	Mu	Lft (lbs)	HP		
9500	1	Feb-94	9:49:09	RCAL AXL 980		####	0.00	-12.47	0.0		
9500	2	5-Feb-94	9:52:43	RCAL AXL 980		####	0.00	-12.68	0.0		
9500	3	5-Feb-94	9:53:18	RCAL AXL-980		####	0.00	6.02	0.0		
9501	4	5-Feb-94	9:55:28	RCAL SIDE 956.4		####	0.00	5.67	0.0		
9501	5	5-Feb-94	9:55:59	RCAL SIDE-956.4		####	0.00	-11.38	0.0		
9502	6	5-Feb-94	9:57:39	RCAL NORM 2180.		####	0.00	2159.30	0.0		
9502	7	5-Feb-94	9:58:32	RCAL NORM-2180.		####	0.00	-2174.40	0.0		
9503	8	5-Feb-94	10:00:08	RCAL ROLL 44651		####	0.00	-0.76	0.0		
9503	9	5-Feb-94	10:00:47	RCAL ROLL-44651		####	0.00	-4.81	0.0		
9504	10	5-Feb-94	10:01:58	RCAL PITCH 44357		####	0.00	-40.40	0.0		
9504	11	5-Feb-94	10:02:34	RCAL PITCH-44357		####	0.00	35.30	0.0		
9505	12	5-Feb-94	10:13:03	APPLIED LOAD PITCH 2300		####	0.00	-0.58	0.0		
9506	13	5-Feb-94	10:14:01	APPLIED LOAD PITCH 4600		####	0.00	0.05	0.0		
9507	14	5-Feb-94	10:14:41	APPLIED LOAD PITCH 6900		####	0.00	-0.19	0.0		
9508	15	5-Feb-94	10:15:23	APPLIED LOAD PITCH 9200		####	0.00	-0.28	0.0		
9509	16	5-Feb-94	10:16:01	APPLIED LOAD PITCH 11500		####	0.00	-0.02	0.0		
9510	17	5-Feb-94	10:16:58	APPLIED LOAD PITCH 13800		####	0.00	0.12	0.0		
9511	18	5-Feb-94	10:18:07	APPLIED LOAD PITCH 175*92		####	0.00	2.21	0.0		
9512	19	5-Feb-94	10:18:50	APPLIED LOAD PITCH 200*92		####	0.00	1.99	0.0		
9513	20	5-Feb-94	10:19:30	APPLIED LOAD PITCH 225*92		####	0.00	0.62	0.0		
9514	21	5-Feb-94	10:20:16	APPLIED LOAD PITCH 250*92		####	0.00	0.49	0.0		
9515	22	5-Feb-94	10:21:02	APPLIED LOAD PITCH 275*92		####	0.00	0.82	0.0		
9516	23	5-Feb-94	10:21:51	APPLIED LOAD PITCH 300*92		####	0.00	0.07	0.0		
9517	24	5-Feb-94	10:22:48	APPLIED LOAD PITCH 275*92		####	0.00	-0.70	0.0		
9518	25	5-Feb-94	10:23:37	APPLIED LOAD PITCH 250*92		####	0.00	0.20	0.0		
9519	26	5-Feb-94	10:24:30	APPLIED LOAD PITCH 225*92		####	0.00	4.06	0.0		
9520	27	5-Feb-94	10:25:19	APPLIED LOAD PITCH 200*92		####	0.00	-0.60	0.0		
9521	28	5-Feb-94	10:26:04	APPLIED LOAD PITCH 175*92		####	0.00	-0.10	0.0		
9522	29	5-Feb-94	10:26:44	APPLIED LOAD PITCH 150*92		####	0.00	-0.45	0.0		
9523	30	5-Feb-94	10:27:30	APPLIED LOAD PITCH 125*92		####	0.00	-0.35	0.0		
9524	31	5-Feb-94	10:28:17	APPLIED LOAD PITCH 100*92		####	0.00	-0.02	0.0		
9525	32	5-Feb-94	10:29:07	APPLIED LOAD PITCH 75*92		####	0.00	0.01	0.0		
9526	33	5-Feb-94	10:30:03	APPLIED LOAD PITCH 50*92		####	0.00	-0.35	0.0		
9527	34	5-Feb-94	10:30:46	APPLIED LOAD PITCH 25*92		####	0.00	-0.54	0.0		
9528	35	5-Feb-94	10:31:26	APPLIED LOAD PITCH 0*92		####	0.00	-1.53	0.0		
9530	36	5-Feb-94	11:22:17	APPLIED LOAD AXIAL 0		####	0.00	-0.25	0.0		
9530	37	5-Feb-94	11:22:58	APPLIED LOAD AXIAL 25		####	0.00	-0.26	0.0		
9530	38	5-Feb-94	11:23:53	APPLIED LOAD AXIAL 50 LBS		####	0.00	0.01	0.0		
9530	39	5-Feb-94	11:24:24	APPLIED LOAD AXIAL 75 LBS		####	0.00	0.00	0.0		
9530	40	5-Feb-94	11:25:03	APPLIED LOAD AXIAL 100 LBS		####	0.00	0.08	0.0		
9530	41	5-Feb-94	11:26:15	APPLIED LOAD AXIAL 125 LBS		####	0.00	-0.18	0.0		
9530	42	5-Feb-94	11:26:50	APPLIED LOAD AXIAL 150 LBS		####	0.00	0.02	0.0		
9530	43	5-Feb-94	11:27:46	APPLIED LOAD AXIAL 175 LBS		####	0.00	-0.36	0.0		
9530	44	5-Feb-94	11:28:24	APPLIED LOAD AXIAL 200 LBS		####	0.00	-0.84	0.0		
9530	45	5-Feb-94	11:28:55	APPLIED LOAD AXIAL 225 LBS		####	0.00	-1.78	0.0		
9530	46	5-Feb-94	11:30:06	APPLIED LOAD AXIAL 225 LBS		####	0.00	0.88	0.0		
9530	47	5-Feb-94	11:30:53	APPLIED LOAD AXIAL 250 LBS		####	0.00	-0.05	0.0		
9530	48	5-Feb-94	11:31:24	APPLIED LOAD AXIAL 275 LBS		####	0.00	-0.59	0.0		
9530	49	5-Feb-94	11:32:02	APPLIED LOAD AXIAL 300 LBS		####	0.00	-1.65	0.0		
9530	50	5-Feb-94	11:32:44	APPLIED LOAD AXIAL 275 LBS		####	0.00	-1.47	0.0		
9530	51	5-Feb-94	11:33:30	APPLIED LOAD AXIAL 250 LBS		####	0.00	-1.38	0.0		
9530	52	5-Feb-94	11:34:17	APPLIED LOAD AXIAL 225 LBS		####	0.00	-1.68	0.0		
9530	53	5-Feb-94	11:34:56	APPLIED LOAD AXIAL 200 LBS		####	0.00	-1.32	0.0		
9530	54	5-Feb-94	11:35:34	APPLIED LOAD AXIAL 175 LBS		####	0.00	-1.22	0.0		
9530	55	5-Feb-94	11:36:13	APPLIED LOAD AXIAL 150 LBS		####	0.00	-0.71	0.0		
9530	56	5-Feb-94	11:37:37	APPLIED LOAD AXIAL 150 LBS		####	0.00	1.90	0.0		
9530	57	5-Feb-94	11:38:14	APPLIED LOAD AXIAL 125 LBS		####	0.00	1.37	0.0		
9530	58	5-Feb-94	11:38:45	APPLIED LOAD AXIAL 100 LBS		####	0.00	1.23	0.0		
9530	59	5-Feb-94	11:39:43	APPLIED LOAD AXIAL 75 LBS		####	0.00	0.75	0.0		
9530	60	5-Feb-94	11:40:22	APPLIED LOAD AXIAL 50 LBS		####	0.00	0.91	0.0		
9530	61	5-Feb-94	11:41:04	APPLIED LOAD AXIAL 25 LBS		####	0.00	0.80	0.0		
9530	62	5-Feb-94	11:41:39	APPLIED LOAD AXIAL 0 LBS		####	0.00	0.42	0.0		
9531	63	5-Feb-94	11:50:00	APPLIED LOAD SIDE =300LBS WITH CHANNEL SWITCH (LOAD WAS REALL		####	0.00	5.62	0.0		
21	64	15-Feb-94	2:37:10	NULL CAM ZERO PITCH 978RPM		0.001	0.00	-39.33	19.5		
45	65	15-Feb-94	2:43:40	NULL CAM ZERO PITCH 1087RPM		0.001	0.00	-28.50	25.9		
45	66	15-Feb-94	3:17:22	NULL CAM ZERO PITCH 1087RPM		0.001	0.00	-27.89	26.4		
47	67	15-Feb-94	3:29:58	NULL CAM ZERO PITCH 1087RPM 2DEG COL.		0.001	0.00	114.91	30.1		
49	68	15-Feb-94	3:32:51	NULL CAM ZERO PITCH 1087RPM 4DEG COL.		0.002	0.01	315.67	42.1		
51	69	15-Feb-94	3:34:46	NULL CAM ZERO PITCH 1087RPM 6DEG COL.		0.004	0.02	530.03	61.1		
52	70	15-Feb-94	3:39:41	NULL CAM ZERO PITCH 1087RPM 7DEG COL.		0.005	0.02	645.16	73.2		
53	71	15-Feb-94	3:42:50	NULL CAM ZERO PITCH 1087RPM 8DEG COL.		0.006	0.03	757.51	87.2		
47	72	15-Feb-94	3:47:14	NULL CAM ZERO PITCH 1087RPM 2DEG COL 1DEG RIGHT ROLL		0.001	0.01	121.16	30.7		
47	73	15-Feb-94	3:48:49	NULL CAM ZERO PITCH 1087RPM 2DEG COL 1.5DEG RIGHT ROLL		0.001	0.01	123.47	31.6		
47	74	15-Feb-94	3:50:56	NULL CAM ZERO PITCH 1087RPM 2DEG COL 1.0DEG LEFT ROLL		0.001	0.01	112.31	30.9		
47	75	15-Feb-94	3:52:02	NULL CAM ZERO PITCH 1087RPM 2DEG COL 1.5DEG LEFT ROLL		0.001	0.00	114.27	31.1		
47	76	15-Feb-94	3:54:22	NULL CAM ZERO PITCH 1087RPM 2DEG COL 1.0DEG NOSE UP		0.001	0.01	109.61	30.5		
47	77	15-Feb-94	3:55:06	NULL CAM ZERO PITCH 1087RPM 2DEG COL 1.5DEG NOSE UP		0.001	0.00	110.56	31.1		
47	78	15-Feb-94	3:56:37	NULL CAM ZERO PITCH 1087RPM 2DEG COL 1.0DEG NOSE DOWN		0.001	0.01	103.19	31.0		
47	79	15-Feb-94	3:57:34	NULL CAM ZERO PITCH 1087RPM 2DEG COL 1.5DEG NOSE DOWN		0.001	0.01	102.05	30.8		
45	80	15-Feb-94	3:59:31	NULL CAM ZERO PITCH 1087RPM 0DEG COL 0.0DEG NOSE DOWN		0.001	0.00	-31.06	26.1		
32	81	15-Feb-94	4:02:06	NULL CAM ZERO PITCH 1033RPM 0DEG COL 0.0DEG NOSE DOWN		0.001	0.00	-42.27	22.8		
34	82	15-Feb-94	4:03:18	NULL CAM ZERO PITCH 1033RPM 2 DEG COL 0.0DEG NOSE DOWN		0.001	0.01	74.54	25.8		
35	83	15-Feb-94	4:04:25	NULL CAM ZERO PITCH 1033RPM 4 DEG COL 0.0DEG NOSE DOWN		0.002	0.02	242.82	36.1		
36	84	15-Feb-94	4:05:27	NULL CAM ZERO PITCH 1033RPM 6 DEG COL 0.0DEG NOSE DOWN		0.004	0.01	437.52	51.5		

TEST	POINT	DATE			CT	Mu	Lift (lbs)	HP
37	85	15-Feb-94	4:06:45	NULL CAM ZERO PITCH 1033RPM 8 DEG COL 0.0DEG NOSE DOWN	0.005	0.02	662.55	74.6
21	86	15-Feb-94	4:09:51	NULL CAM ZERO PITCH 978RPM 0 DEG COL 0.0DEG NOSE DOWN	0.001	0.00	-50.49	19.7
22	87	15-Feb-94	4:11:15	NULL CAM ZERO PITCH 978RPM 2 DEG COLL	0.001	0.00	46.96	21.8
23	88	15-Feb-94	4:12:15	NULL CAM ZERO PITCH 978RPM 4 DEG COLL	0.002	0.02	193.21	30.4
24	89	15-Feb-94	4:13:57	NULL CAM ZERO PITCH 978RPM 6 DEG COLL	0.003	0.02	363.08	42.8
25	90	15-Feb-94	4:15:08	NULL CAM ZERO PITCH 978RPM 8 DEG COLL	0.005	0.03	566.26	62.7
18	91	15-Feb-94	4:17:44	NULL CAM ZERO PITCH 870RPM 2 DEG COLL	0.001	0.00	19.69	15.8
12	92	15-Feb-94	4:19:41	NULL CAM ZERO PITCH 652RPM 2 DEG COLL	0.001	0.00	-11.90	7.2
877	93	15-Feb-94	20:39:05	20+0 CAM 652 RPM PERF.PT	0.001	0.00	-8.11	10.0
878	94	15-Feb-94	20:40:50	20+0 CAM 652 RPM 2 DEG COLL. PERF	0.002	0.00	42.76	9.7
875	95	15-Feb-94	20:43:52	20+0 CAM 870 RPM 0 DEG COLL. PERF	0.001	0.00	-22.13	22.1
876	96	15-Feb-94	20:44:42	20+0 CAM 870 RPM 2 DEG COLL. PERF	0.001	0.00	66.26	21.3
911	97	15-Feb-94	20:47:23	20+0 CAM 978 RPM 0 DEG COLL. PERF	0.001	0.00	-16.28	30.4
813	98	15-Feb-94	20:55:07	20+0 CAM 1087 RPM 0 DEG COLL. PERF	0.001	0.00	-8.72	40.9
853	99	15-Feb-94	20:56:17	20+0 CAM 1087 RPM 1 DEG COLL. PERF	0.001	0.00	57.41	40.2
812	100	15-Feb-94	20:57:19	20+0 CAM 1087 RPM 2 DEG COLL. PERF	0.002	0.01	125.94	40.4
854	101	15-Feb-94	20:58:31	20+0 CAM 1087 RPM 3 DEG COLL. PERF	0.002	0.01	236.38	45.4
814	102	15-Feb-94	20:59:23	20+0 CAM 1087 RPM 4 DEG COLL. PERF	0.003	0.01	329.52	51.5
821	103	15-Feb-94	21:00:19	20+0 CAM 1087 RPM 5 DEG COLL. PERF	0.003	0.02	423.35	58.7
902	104	15-Feb-94	21:01:09	20+0 CAM 1087 RPM 6 DEG COLL. PERF	0.004	0.02	524.77	67.4
863	105	15-Feb-94	21:02:47	20+0 CAM 1087 RPM 7 DEG COLL. PERF	0.005	0.02	630.52	77.9
864	106	15-Feb-94	21:03:52	20+0 CAM 1087 RPM 8 DEG COLL. PERF	0.006	0.03	753.21	94.0
812	107	15-Feb-94	21:09:22	20+0 CAM 1087 RPM 2 DEG COLL. ACOUSTIC	0.002	0.01	120.41	41.0
813	108	16-Feb-94	0:48:22	20+0 CAM 1087 RPM	0.001	0.00	-80.55	40.6
812	109	16-Feb-94	0:52:23	20+0 CAM 1087 RPM 2 DEG COLL	0.001	0.01	72.91	41.2
856	110	16-Feb-94	0:54:18	20+0 CAM 1087 RPM 2 DEG COLL 1 DEG RIGHT	0.002	0.01	78.26	42.5
858	111	16-Feb-94	0:56:29	20+0 CAM 1087 RPM 2 DEG COLL 2 DEG RIGHT	0.001	0.01	96.01	45.6
999	112	16-Feb-94	1:00:59	20+0 CAM 00 RPM 0 DEG COLL 0 DEG RIGHT	####	0.00	-15.44	0.0
813	115	16-Feb-94	5:18:45	20+0 1087 RPM	0.001	0.00	-31.92	40.2
860	119	16-Feb-94	5:27:32	20+0 1087 RPM 2 DEG COLL 1 DEG NOSE UP	0.002	0.00	152.70	41.0
862	120	16-Feb-94	5:28:35	20+0 1087 RPM 2 DEG COLL 2 DEG NOSE UP	0.001	0.01	152.12	40.9
812	121	16-Feb-94	5:29:44	20+0 1087 RPM 2 DEG COLL	0.002	0.01	140.89	40.8
8880	122	16-Feb-94	5:30:56	20+0 1087 RPM 2 DEG COLL 1 DEG NOSE DOWN	0.002	0.00	147.76	43.1
881	123	16-Feb-94	5:32:08	20+0 1087 RPM 2 DEG COLL 2 DEG NOSE DOWN	0.002	0.01	150.63	45.1
865	125	16-Feb-94	5:37:11	20+0 1033 RPM	0.001	0.00	3.71	35.0
866	126	16-Feb-94	5:38:12	20+0 1033 RPM 1 DEG COLL	0.001	0.00	59.82	34.4
811	127	16-Feb-94	5:39:00	20+0 1033 RPM 2 DEG COLL	0.002	0.01	135.61	35.4
867	128	16-Feb-94	5:39:51	20+0 1033 RPM 3 DEG COLL	0.002	0.01	230.56	39.4
868	129	16-Feb-94	5:40:46	20+0 1033 RPM 4 DEG COLL	0.003	0.02	311.75	44.6
869	130	16-Feb-94	5:41:34	20+0 1033 RPM 5 DEG COLL	0.003	0.02	398.81	50.9
870	131	16-Feb-94	5:42:43	20+0 1033 RPM 6 DEG COLL	0.004	0.01	492.57	58.9
871	132	16-Feb-94	5:43:37	20+0 1033 RPM 7 DEG COLL	0.005	0.03	595.13	69.3
872	133	16-Feb-94	5:44:22	20+0 1033 RPM 8 DEG COLL	0.006	0.02	702.41	81.8
865	134	16-Feb-94	5:46:24	20+0 1033 RPM 0 DEG COLL	0.001	0.00	10.12	35.3
911	135	16-Feb-94	5:47:51	20+0 978 RPM 0 DEG COLL	0.001	0.00	4.02	30.4
912	136	16-Feb-94	5:48:37	20+0 978 RPM 1 DEG COLL	0.001	0.00	48.62	29.6
910	137	16-Feb-94	5:49:17	20+0 978 RPM 2 DEG COLL	0.001	0.00	117.47	31.0
913	138	16-Feb-94	5:49:56	20+0 978 RPM 3 DEG COLL	0.002	0.01	197.19	33.4
914	139	16-Feb-94	5:50:43	20+0 978 RPM 4 DEG COLL	0.003	0.02	268.72	37.3
915	140	16-Feb-94	5:51:22	20+0 978 RPM 5 DEG COLL	0.003	0.02	368.51	43.9
916	141	16-Feb-94	5:51:58	20+0 978 RPM 6 DEG COLL	0.004	0.02	455.77	51.1
873	142	16-Feb-94	5:52:48	20+0 978 RPM 7 DEG COLL	0.005	0.02	538.73	59.2
999	143	16-Feb-94	5:54:57	POST TEST POINT	####	0.00	22.52	0.0
1900	144	16-Feb-94	21:18:03	HUB,ALFSU=0.,RPM=1087,VOR=0.	0.001	0.00	9.23	4.4
1901	162	16-Feb-94	21:27:21	HUB,ALFSU=5.,RPM=1087,VOR=0.	0.001	0.00	41.26	15.6
1902	180	16-Feb-94	21:36:45	HUB,ALFSU=10.,RPM=1087,VOR=0.	0.001	0.00	52.84	25.4
1903	198	16-Feb-94	21:46:48	HUB,ALFSU=5.,RPM=1087,VOR=0.	0.001	0.00	35.16	24.6
1904	218	16-Feb-94	21:56:33	HUB,ALFSU=10.,RPM=1087,VOR=0.	0.001	0.00	24.37	25.5
1909	234	16-Feb-94	22:17:30	HUB,ALFSU=10.,RPM=1087,VOR=0.15	0.001	0.14	5.25	6.8
1908	252	16-Feb-94	22:26:45	HUB,ALFSU=5.,RPM=1087,VOR=0.15	0.001	0.15	1.06	6.6
1905	270	16-Feb-94	22:35:54	HUB,ALFSU=0.,RPM=1087,VOR=0.15	0.001	0.15	-3.63	5.9
1906	288	16-Feb-94	22:45:02	HUB,ALFSU=5.,RPM=1087,VOR=0.15	0.001	0.15	-6.96	5.9
1907	306	16-Feb-94	22:56:19	HUB,ALFSU=10.,RPM=1087,VOR=0.15	0.001	0.15	-11.04	6.0
1912	327	16-Feb-94	23:17:15	HUB,ALFSU=10.,RPM=1087,VOR=0.20	0.001	0.20	-4.72	6.7
1911	345	16-Feb-94	23:28:52	HUB,ALFSU=5.,RPM=1087,VOR=0.20	0.001	0.20	10.51	6.6
1910	363	16-Feb-94	23:39:15	HUB,ALFSU=0.,RPM=1087,VOR=0.20	0.001	0.20	21.43	6.5
1913	381	16-Feb-94	23:49:15	HUB,ALFSU=5.,RPM=1087,VOR=0.20	0.001	0.20	28.24	7.7
1914	401	17-Feb-94	0:14:16	HUB,ALFSU=10.,RPM=1087,VOR=0.20	0.001	0.20	29.45	8.0
1701	419	18-Feb-94	23:55:50	BLADES ON TARE,ALFSU=13.0DEG	####	9.00	-1.33	0.0
1702	420	19-Feb-94	0:07:13	BLADES ON TARE,ALFSU=11.0DEG	####	0.00	-1.06	0.0
1703	421	19-Feb-94	0:08:26	BLADES ON TARE,ALFSU=09.0DEG	####	0.00	-1.09	0.0
1704	422	19-Feb-94	0:10:03	BLADES ON TARE,ALFSU=07.0DEG	####	0.00	-1.03	0.0
1705	423	19-Feb-94	0:11:09	BLADES ON TARE,ALFSU=05.0DEG	####	0.00	-1.27	0.0
1706	424	19-Feb-94	0:12:04	BLADES ON TARE,ALFSU=03.0DEG	####	0.00	-0.95	0.0
1707	425	19-Feb-94	0:13:21	BLADES ON TARE,ALFSU=01.0DEG	####	0.00	-0.85	0.0
1708	426	19-Feb-94	0:14:21	BLADES ON TARE,ALFSU=00.0 DEG	####	0.00	-1.04	0.0
1709	427	19-Feb-94	0:15:22	BLADES ON TARE,ALFSU=-01.0 DEG	####	0.00	-0.99	0.0
1710	428	19-Feb-94	0:16:30	BLADES ON TARE,ALFSU=-03.0 DEG	####	0.00	-1.22	0.0
1711	429	19-Feb-94	0:17:39	BLADES ON TARE,ALFSU=-05.0 DEG	####	0.00	-0.86	0.0
1712	430	19-Feb-94	0:18:57	BLADES ON TARE,ALFSU=-07.0 DEG	####	0.00	-1.01	0.0
1713	431	19-Feb-94	0:19:45	BLADES ON TARE,ALFSU=-09.0 DEG	####	0.00	-0.74	0.0
1714	432	19-Feb-94	0:20:47	BLADES ON TARE,ALFSU=-11.0 DEG	####	0.00	-0.68	0.0
1715	433	19-Feb-94	0:21:42	BLADES ON TARE,ALFSU=-13.0 DEG	####	0.00	-0.72	0.0
1716	434	19-Feb-94	0:39:18	BLADES OFF TARE,ALFSU=-13.0 DEG	####	0.00	26.63	0.0
1717	435	19-Feb-94	0:40:28	BLADES OFF TARE,ALFSU=-11.0 DEG	####	0.00	26.24	0.0

TEST	POINT	DATE			CT	Mu	LIFT (lbs)	HP
1718	436	19-Feb-94	0:41:27	BLADES OFF TARE,ALFSU=-09.0 DEG	####	0.00	26.06	0.0
1719	437	19-Feb-94	0:42:30	BLADES OFF TARE,ALFSU=-07.0 DEG	####	0.00	25.35	0.0
1720	438	19-Feb-94	0:43:35	BLADES OFF TARE,ALFSU=-05.0 DEG	####	0.00	25.47	0.0
1721	439	19-Feb-94	0:44:38	BLADES OFF TARE,ALFSU=-03.0 DEG	####	0.00	25.57	0.0
1722	440	19-Feb-94	0:45:34	BLADES OFF TARE,ALFSU=-01.0 DEG	####	0.00	25.22	0.0
1723	441	19-Feb-94	0:46:30	BLADES OFF TARE,ALFSU= 00.0 DEG	####	0.00	25.31	0.0
1724	442	19-Feb-94	0:47:16	BLADES OFF TARE,ALFSU= 01.0 DEG	####	0.00	25.05	0.0
1725	443	19-Feb-94	0:48:11	BLADES OFF TARE,ALFSU= 03.0 DEG	####	0.00	24.82	0.0
1726	444	19-Feb-94	0:48:56	BLADES OFF TARE,ALFSU= 05.0 DEG	####	0.00	24.75	0.0
1727	445	19-Feb-94	0:49:52	BLADES OFF TARE,ALFSU= 07.0 DEG	####	0.00	24.68	0.0
1728	446	19-Feb-94	0:51:23	BLADES OFF TARE,ALFSU= 09.0 DEG	####	0.00	24.69	0.0
1729	447	19-Feb-94	0:52:38	BLADES OFF TARE,ALFSU= 11.0 DEG	####	0.00	24.53	0.0
1730	448	19-Feb-94	0:53:36	BLADES OFF TARE,ALFSU= 13.0 DEG	####	0.00	25.16	0.0
1733	449	19-Feb-94	1:18:49	BLADES OFF TARE, RPM= 1087, ALFSU= 13.0 DEG	0.001	0.00	35.28	0.9
1734	450	19-Feb-94	1:20:23	BLADES OFF TARE, RPM= 1087, ALFSU= 11.0 DEG	0.001	0.00	43.29	0.8
1735	451	19-Feb-94	1:22:02	BLADES OFF TARE, RPM= 1087, ALFSU= 09.0 DEG	0.001	0.00	51.03	0.8
1736	452	19-Feb-94	1:23:19	BLADES OFF TARE, RPM= 1087, ALFSU= 07.0 DEG	0.001	0.00	54.67	0.8
1737	453	19-Feb-94	1:24:42	BLADES OFF TARE, RPM= 1087, ALFSU= 05.0 DEG	0.001	0.00	58.57	0.9
1738	454	19-Feb-94	1:26:04	BLADES OFF TARE, RPM= 1087, ALFSU= 03.0 DEG	0.001	0.00	59.64	0.9
1739	455	19-Feb-94	1:27:15	BLADES OFF TARE, RPM= 1087, ALFSU= 01.0 DEG	0.001	0.00	60.46	0.9
1740	456	19-Feb-94	1:28:23	BLADES OFF TARE, RPM= 1087, ALFSU= 00.0 DEG	0.001	0.00	61.73	0.9
1741	457	19-Feb-94	1:29:30	BLADES OFF TARE, RPM= 978, ALFSU= 00.0 DEG	0.001	0.00	62.65	0.7
1742	458	19-Feb-94	1:30:28	BLADES OFF TARE, RPM= 1033, ALFSU= 00.0 DEG	0.001	0.00	64.92	0.8
1743	459	19-Feb-94	1:31:51	BLADES OFF TARE, RPM= 1141, ALFSU= 00.0 DEG	0.001	0.00	63.64	0.9
1744	460	19-Feb-94	1:32:35	BLADES OFF TARE, RPM= 1196, ALFSU= 00.0 DEG	0.001	0.00	65.27	0.9
1745	462	19-Feb-94	1:34:35	BLADES OFF TARE, RPM= 1087, ALFSU= -1.0 DEG	0.001	0.00	63.06	0.9
1746	463	19-Feb-94	1:35:55	BLADES OFF TARE, RPM= 1087, ALFSU= -3.0 DEG	0.001	0.00	62.83	0.9
1747	464	19-Feb-94	1:37:19	BLADES OFF TARE, RPM= 1087, ALFSU= -5.0 DEG	0.001	0.00	60.63	0.9
1748	465	19-Feb-94	1:38:50	BLADES OFF TARE, RPM= 1087, ALFSU= -7.0 DEG	0.001	0.00	59.64	0.9
1749	466	19-Feb-94	1:40:08	BLADES OFF TARE, RPM= 1087, ALFSU= -9.0 DEG	0.001	0.00	56.61	0.8
1750	467	19-Feb-94	1:41:35	BLADES OFF TARE, RPM= 1087, ALFSU= -11.0 DEG	0.001	0.00	55.40	0.8
1751	468	19-Feb-94	1:42:55	BLADES OFF TARE, RPM= 1087, ALFSU= -13.0 DEG	0.001	0.00	54.51	0.9
1767	469	19-Feb-94	1:46:58	BLADES OFF TARE, RPM= 1087, ALFSU= -13.0 DEG, VOR = 0.10	0.001	0.10	54.63	0.9
1768	470	19-Feb-94	1:48:54	BLADES OFF TARE, RPM= 1087, ALFSU= -11.0 DEG, VOR = 0.10	0.001	0.10	52.37	0.9
1765	471	19-Feb-94	1:49:52	BLADES OFF TARE, RPM= 1087, ALFSU= -9.0 DEG, VOR = 0.10	0.001	0.10	52.45	0.9
1764	472	19-Feb-94	1:50:57	BLADES OFF TARE, RPM= 1087, ALFSU= -7.0 DEG, VOR = 0.10	0.001	0.10	50.63	0.9
1763	473	19-Feb-94	1:51:54	BLADES OFF TARE, RPM= 1087, ALFSU= -5.0 DEG, VOR = 0.10	0.001	0.10	50.17	0.9
1762	474	19-Feb-94	1:52:49	BLADES OFF TARE, RPM= 1087, ALFSU= -3.0 DEG, VOR = 0.10	0.001	0.10	50.29	0.9
1761	475	19-Feb-94	1:53:40	BLADES OFF TARE, RPM= 1087, ALFSU= -1.0 DEG, VOR = 0.10	0.001	0.10	49.59	0.8
1760	476	19-Feb-94	1:54:33	BLADES OFF TARE, RPM= 1087, ALFSU= 0.0 DEG, VOR = 0.10	0.001	0.10	48.27	0.9
1759	477	19-Feb-94	1:55:31	BLADES OFF TARE, RPM= 1087, ALFSU= 1.0 DEG, VOR = 0.10	0.001	0.10	45.07	0.9
1758	478	19-Feb-94	1:56:22	BLADES OFF TARE, RPM= 1087, ALFSU= 3.0 DEG, VOR = 0.10	0.001	0.10	44.69	0.8
1757	479	19-Feb-94	1:57:38	BLADES OFF TARE, RPM= 1087, ALFSU= 5.0 DEG, VOR = 0.10	0.001	0.10	43.02	0.8
1756	480	19-Feb-94	1:58:31	BLADES OFF TARE, RPM= 1087, ALFSU= 7.0 DEG, VOR = 0.10	0.001	0.10	41.00	0.9
1755	481	19-Feb-94	1:59:27	BLADES OFF TARE, RPM= 1087, ALFSU= 9.0 DEG, VOR = 0.10	0.001	0.10	38.95	0.9
1754	482	19-Feb-94	2:00:24	BLADES OFF TARE, RPM= 1087, ALFSU= 11.0 DEG, VOR = 0.10	0.001	0.10	36.31	0.9
1753	483	19-Feb-94	2:01:34	BLADES OFF TARE, RPM= 1087, ALFSU= 13.0 DEG, VOR = 0.10	0.001	0.10	34.82	0.9
1786	484	19-Feb-94	2:03:58	BLADES OFF TARE, RPM= 1087, ALFSU= 13.0 DEG, VOR = 0.15	0.001	0.15	27.88	0.9
1785	485	19-Feb-94	2:04:57	BLADES OFF TARE, RPM= 1087, ALFSU= 11.0 DEG, VOR = 0.15	0.001	0.15	27.62	0.9
1784	486	19-Feb-94	2:06:16	BLADES OFF TARE, RPM= 1087, ALFSU= 9.0 DEG, VOR = 0.15	0.001	0.15	26.04	0.8
1783	487	19-Feb-94	2:07:08	BLADES OFF TARE, RPM= 1087, ALFSU= 7.0 DEG, VOR = 0.15	0.001	0.15	24.44	0.9
1782	488	19-Feb-94	2:08:04	BLADES OFF TARE, RPM= 1087, ALFSU= 5.0 DEG, VOR = 0.15	0.001	0.15	24.29	0.8
1781	489	19-Feb-94	2:09:01	BLADES OFF TARE, RPM= 1087, ALFSU= 3.0 DEG, VOR = 0.15	0.001	0.15	23.65	0.9
1780	490	19-Feb-94	2:10:02	BLADES OFF TARE, RPM= 1087, ALFSU= 1.0 DEG, VOR = 0.15	0.001	0.15	22.95	0.9
1775	491	19-Feb-94	2:11:17	BLADES OFF TARE, RPM= 1087, ALFSU= 0.0 DEG, VOR = 0.15	0.001	0.15	22.29	0.9
1776	492	19-Feb-94	2:13:37	BLADES OFF TARE, RPM= 978, ALFSU= 0.0 DEG, VOR = 0.15	0.001	0.15	17.38	0.8
1777	493	19-Feb-94	2:15:27	BLADES OFF TARE, RPM= 1033, ALFSU= 0.0 DEG, VOR = 0.15	0.001	0.15	15.83	0.8
1778	494	19-Feb-94	2:16:33	BLADES OFF TARE, RPM= 1141, ALFSU= 0.0 DEG, VOR = 0.15	0.000	0.15	17.27	0.9
1779	495	19-Feb-94	2:17:46	BLADES OFF TARE, RPM= 1196, ALFSU= 0.0 DEG, VOR = 0.15	0.000	0.15	14.13	1.0
1774	496	19-Feb-94	2:20:36	BLADES OFF TARE, RPM= 1087, ALFSU= -1.0 DEG, VOR = 0.15	0.001	0.15	12.84	0.8
1773	497	19-Feb-94	2:21:38	BLADES OFF TARE, RPM= 1087, ALFSU= -3.0 DEG, VOR = 0.15	0.001	0.15	14.05	0.9
1772	498	19-Feb-94	2:22:56	BLADES OFF TARE, RPM= 1087, ALFSU= -5.0 DEG, VOR = 0.15	0.001	0.15	14.67	0.9
1771	499	19-Feb-94	2:24:06	BLADES OFF TARE, RPM= 1087, ALFSU= -7.0 DEG, VOR = 0.15	0.001	0.15	15.56	0.9
1770	500	19-Feb-94	2:25:13	BLADES OFF TARE, RPM= 1087, ALFSU= -9.0 DEG, VOR = 0.15	0.001	0.15	17.37	0.8
1769	501	19-Feb-94	2:26:18	BLADES OFF TARE, RPM= 1087, ALFSU= -11.0 DEG, VOR = 0.15	0.001	0.15	17.51	0.8
1768	502	19-Feb-94	2:27:46	BLADES OFF TARE, RPM= 1087, ALFSU= -13.0 DEG, VOR = 0.15	0.001	0.15	18.85	0.8
1789	503	19-Feb-94	2:55:29	BLADES OFF TARE, RPM= 1087, ALFSU= 13.0 DEG, VOR = 0.20	0.001	0.20	-53.64	0.9
1790	504	19-Feb-94	2:56:37	BLADES OFF TARE, RPM= 1087, ALFSU= 11.0 DEG, VOR = 0.20	0.001	0.20	-46.70	0.9
1791	505	19-Feb-94	2:57:36	BLADES OFF TARE, RPM= 1087, ALFSU= 9.0 DEG, VOR = 0.20	0.001	0.20	-40.56	0.9
1792	506	19-Feb-94	2:58:41	BLADES OFF TARE, RPM= 1087, ALFSU= 7.0 DEG, VOR = 0.20	0.001	0.20	-36.20	0.8
1793	507	19-Feb-94	2:59:34	BLADES OFF TARE, RPM= 1087, ALFSU= 5.0 DEG, VOR = 0.20	0.001	0.20	-31.97	0.9
1794	508	19-Feb-94	3:00:31	BLADES OFF TARE, RPM= 1087, ALFSU= 3.0 DEG, VOR = 0.20	0.001	0.20	-28.32	0.8
1795	509	19-Feb-94	3:01:33	BLADES OFF TARE, RPM= 1087, ALFSU= 1.0 DEG, VOR = 0.20	0.001	0.20	-26.00	0.8
1796	510	19-Feb-94	3:02:46	BLADES OFF TARE, RPM= 1087, ALFSU= 0.0 DEG, VOR = 0.20	0.001	0.20	-23.23	0.9
1797	511	19-Feb-94	3:04:44	BLADES OFF TARE, RPM= 978, ALFSU= 0.0 DEG, VOR = 0.20	0.001	0.20	-20.80	0.8
1798	512	19-Feb-94	3:05:43	BLADES OFF TARE, RPM= 1033, ALFSU= 0.0 DEG, VOR = 0.20	0.001	0.20	-18.44	0.8
1799	513	19-Feb-94	3:07:14	BLADES OFF TARE, RPM= 1141, ALFSU= 0.0 DEG, VOR = 0.20	0.001	0.20	-14.16	0.8
1800	514	19-Feb-94	3:08:21	BLADES OFF TARE, RPM= 1196, ALFSU= 0.0 DEG, VOR = 0.20	0.001	0.20	-12.19	0.9
1801	515	19-Feb-94	3:10:21	BLADES OFF TARE, RPM= 1087, ALFSU= -1.0 DEG, VOR = 0.20	0.001	0.20	-11.70	0.8
1802	516	19-Feb-94	3:11:43	BLADES OFF TARE, RPM= 1087, ALFSU= -3.0 DEG, VOR = 0.20	0.001	0.20	-7.92	1.0
1803	517	19-Feb-94	3:12:56	BLADES OFF TARE, RPM= 1087, ALFSU= -5.0 DEG, VOR = 0.20	0.001	0.20	-5.28	0.9
1804	518	19-Feb-94	3:13:50	BLADES OFF TARE, RPM= 1087, ALFSU= -7.0 DEG, VOR = 0.20	0.001	0.20	-2.23	1.0
1805	519	19-Feb-94	3:14:56	BLADES OFF TARE, RPM= 1087, ALFSU= -9.0 DEG, VOR = 0.20	0.001	0.20	0.69	1.0
1806	520	19-Feb-94	3:17:56	BLADES OFF TARE, RPM= 1087, ALFSU= -11.0 DEG, VOR = 0.20	0.001	0.20	3.11	0.8
1807	521	19-Feb-94	3:19:06	BLADES OFF TARE, RPM= 1087, ALFSU= -13.0 DEG, VOR = 0.20	0.001	0.20	6.66	0.9



TEST	POINT	DATE			CT	Mu	Lift (lbs)	HP
1808	522	19-Feb-94	3:21:41	BLADES OFF TARE, RPM= 1087, ALFSU= -13.0 DEG, VOR = 0.25	0.001	0.25	10.70	1.1
1809	523	19-Feb-94	3:22:52	BLADES OFF TARE, RPM= 1087, ALFSU= -11.0 DEG, VOR = 0.25	0.001	0.25	10.35	0.8
1810	524	19-Feb-94	3:24:13	BLADES OFF TARE, RPM= 1087, ALFSU= -9.0 DEG, VOR = 0.25	0.001	0.25	9.40	1.1
1811	525	19-Feb-94	3:25:20	BLADES OFF TARE, RPM= 1087, ALFSU= -7.0 DEG, VOR = 0.25	0.001	0.25	6.32	1.0
1812	526	19-Feb-94	3:26:20	BLADES OFF TARE, RPM= 1087, ALFSU= -5.0 DEG, VOR = 0.25	0.001	0.25	6.85	0.9
1813	527	19-Feb-94	3:27:30	BLADES OFF TARE, RPM= 1087, ALFSU= -3.0 DEG, VOR = 0.25	0.001	0.25	5.32	0.8
1814	528	19-Feb-94	3:28:45	BLADES OFF TARE, RPM= 1087, ALFSU= -1.0 DEG, VOR = 0.25	0.001	0.25	3.32	0.9
1815	529	19-Feb-94	3:30:03	BLADES OFF TARE, RPM= 1087, ALFSU= 0.0 DEG, VOR = 0.25	0.001	0.25	2.72	1.0
1816	530	19-Feb-94	3:30:58	BLADES OFF TARE, RPM= 1087, ALFSU= 1.0 DEG, VOR = 0.25	0.001	0.25	1.54	1.3
1817	531	19-Feb-94	3:32:44	BLADES OFF TARE, RPM= 1087, ALFSU= 3.0 DEG, VOR = 0.25	0.001	0.25	-0.32	0.9
1818	532	19-Feb-94	3:34:10	BLADES OFF TARE, RPM= 1087, ALFSU= 5.0 DEG, VOR = 0.25	0.001	0.25	-2.80	1.1
1819	533	19-Feb-94	3:35:15	BLADES OFF TARE, RPM= 1087, ALFSU= 7.0 DEG, VOR = 0.25	0.001	0.25	-6.75	1.0
1820	534	19-Feb-94	3:36:32	BLADES OFF TARE, RPM= 1087, ALFSU= 9.0 DEG, VOR = 0.25	0.001	0.25	-9.77	1.2
1821	535	19-Feb-94	3:37:54	BLADES OFF TARE, RPM= 1087, ALFSU= 11.0 DEG, VOR = 0.25	0.001	0.25	-13.30	1.0
1822	536	19-Feb-94	3:40:13	BLADES OFF TARE, RPM= 1087, ALFSU= 13.0 DEG, VOR = 0.25	0.001	0.25	-17.31	0.8
1854	537	19-Feb-94	3:44:06	BLADES OFF TARE, RPM= 1087, ALFSU= 13.0 DEG, VOR = 0.30	0.001	0.30	-14.84	0.8
1853	538	19-Feb-94	3:45:30	BLADES OFF TARE, RPM= 1087, ALFSU= 11.0 DEG, VOR = 0.30	0.001	0.30	-8.74	0.8
1852	539	19-Feb-94	3:46:44	BLADES OFF TARE, RPM= 1087, ALFSU= 9.0 DEG, VOR = 0.30	0.001	0.30	-3.97	0.8
1851	540	19-Feb-94	3:47:45	BLADES OFF TARE, RPM= 1087, ALFSU= 7.0 DEG, VOR = 0.30	0.001	0.30	2.06	0.8
1850	541	19-Feb-94	3:49:20	BLADES OFF TARE, RPM= 1087, ALFSU= 5.0 DEG, VOR = 0.30	0.001	0.30	6.25	0.8
1849	542	19-Feb-94	3:50:56	BLADES OFF TARE, RPM= 1087, ALFSU= 3.0 DEG, VOR = 0.30	0.001	0.30	24.89	0.9
1848	543	19-Feb-94	3:51:57	BLADES OFF TARE, RPM= 1087, ALFSU= 1.0 DEG, VOR = 0.30	0.001	0.30	27.06	1.0
1847	544	19-Feb-94	3:53:00	BLADES OFF TARE, RPM= 1087, ALFSU= 0.0 DEG, VOR = 0.30	0.001	0.30	27.61	0.9
1846	545	19-Feb-94	3:54:06	BLADES OFF TARE, RPM= 1087, ALFSU= -1.0 DEG, VOR = 0.30	0.001	0.30	28.68	1.0
1845	546	19-Feb-94	3:55:23	BLADES OFF TARE, RPM= 1087, ALFSU= -3.0 DEG, VOR = 0.30	0.001	0.30	33.15	0.9
1844	547	19-Feb-94	4:18:58	BLADES OFF TARE, RPM= 1087, ALFSU= -5.0 DEG, VOR = 0.30	0.001	0.30	123.95	1.1
1843	548	19-Feb-94	4:20:14	BLADES OFF TARE, RPM= 1087, ALFSU= -7.0 DEG, VOR = 0.30	0.001	0.30	129.32	1.1
1842	549	19-Feb-94	4:22:03	BLADES OFF TARE, RPM= 1087, ALFSU= -9.0 DEG, VOR = 0.30	0.001	0.30	136.09	0.9
1841	550	19-Feb-94	4:23:12	BLADES OFF TARE, RPM= 1087, ALFSU= -11.0 DEG, VOR = 0.30	0.001	0.30	132.97	1.0
1840	551	19-Feb-94	4:24:31	BLADES OFF TARE, RPM= 1087, ALFSU= -13.0 DEG, VOR = 0.30	0.001	0.30	134.20	0.8
1871	552	19-Feb-94	4:26:49	BLADES OFF TARE, RPM= 1087, ALFSU= -13.0 DEG, VOR = 0.35	0.001	0.35	149.01	1.1
1870	553	19-Feb-94	4:28:00	BLADES OFF TARE, RPM= 1087, ALFSU= -11.0 DEG, VOR = 0.35	0.001	0.35	159.43	1.0
1869	554	19-Feb-94	4:44:31	BLADES OFF TARE, RPM= 1087, ALFSU= -9.0 DEG, VOR = 0.35	0.001	0.35	146.99	1.1
1868	555	19-Feb-94	5:00:33	BLADES OFF TARE, RPM= 1087, ALFSU= -7.0 DEG, VOR = 0.35	0.001	0.35	191.65	0.8
1873	556	22-Feb-94	15:38:44	BLADES OFF TARE, RPM= 544, ALFSU= 0.0 DEG, VOR = 0.00	0.001	0.01	39.30	1.2
1874	557	22-Feb-94	15:39:27	BLADES OFF TARE, RPM= 652, ALFSU= 0.0 DEG, VOR = 0.00	0.001	0.01	55.21	1.8
1875	558	22-Feb-94	15:40:41	BLADES OFF TARE, RPM= 761, ALFSU= 0.0 DEG, VOR = 0.00	0.001	0.01	79.21	2.3
1876	559	22-Feb-94	15:41:41	BLADES OFF TARE, RPM= 870, ALFSU= 0.0 DEG, VOR = 0.00	0.001	0.01	108.98	3.1
1741	560	22-Feb-94	15:42:47	BLADES OFF TARE, RPM= 978, ALFSU= 0.0 DEG, VOR = 0.00	0.001	0.01	138.06	3.9
1742	561	22-Feb-94	15:43:33	BLADES OFF TARE, RPM= 1033, ALFSU= 0.0 DEG, VOR = 0.00	0.001	0.01	144.67	4.5
1740	562	22-Feb-94	15:44:10	BLADES OFF TARE, RPM= 1087, ALFSU= 0.0 DEG, VOR = 0.00	0.001	0.01	136.66	4.9
1872	563	22-Feb-94	15:51:40	BLADES OFF TARE, RPM= 1087, ALFSU= 0.0 DEG, VOR = 0.05	0.001	0.05	169.41	5.2
1760	564	22-Feb-94	15:54:06	BLADES OFF TARE, RPM= 1087, ALFSU= 0.0 DEG, VOR = 0.10	0.001	0.10	137.78	5.5
1775	565	22-Feb-94	15:56:03	BLADES OFF TARE, RPM= 1087, ALFSU= 0.0 DEG, VOR = 0.15	0.001	0.15	126.11	5.9
1796	566	22-Feb-94	15:57:30	BLADES OFF TARE, RPM= 1087, ALFSU= 0.0 DEG, VOR = 0.20	0.001	0.20	113.16	6.6
1832	567	22-Feb-94	15:58:55	BLADES OFF TARE, RPM= 1087, ALFSU= 0.0 DEG, VOR = 0.25	0.001	0.25	130.90	7.1
1847	568	22-Feb-94	16:00:18	BLADES OFF TARE, RPM= 1087, ALFSU= 0.0 DEG, VOR = 0.30	0.001	0.30	128.02	7.9
1864	569	22-Feb-94	16:03:59	BLADES OFF TARE, RPM= 1087, ALFSU= 0.0 DEG, VOR = 0.35	0.001	0.34	132.93	8.7
1840	570	22-Feb-94	16:07:25	BLADES OFF TARE, RPM= 1087, ALFSU= 13.0 DEG, VOR = 0.30	0.001	0.30	178.70	7.8
1841	571	22-Feb-94	16:08:31	BLADES OFF TARE, RPM= 1087, ALFSU= 11.0 DEG, VOR = 0.30	0.001	0.30	163.48	7.8
1842	572	22-Feb-94	16:09:23	BLADES OFF TARE, RPM= 1087, ALFSU= 9.0 DEG, VOR = 0.30	0.001	0.30	176.68	7.8
1843	573	22-Feb-94	16:10:14	BLADES OFF TARE, RPM= 1087, ALFSU= 7.0 DEG, VOR = 0.30	0.001	0.30	167.83	7.9
1844	574	22-Feb-94	16:11:03	BLADES OFF TARE, RPM= 1087, ALFSU= 5.0 DEG, VOR = 0.30	0.001	0.30	155.66	7.9
1845	575	22-Feb-94	16:12:00	BLADES OFF TARE, RPM= 1087, ALFSU= 3.0 DEG, VOR = 0.30	0.001	0.30	161.47	7.9
1846	576	22-Feb-94	16:12:50	BLADES OFF TARE, RPM= 1087, ALFSU= 1.0 DEG, VOR = 0.30	0.001	0.30	151.32	8.1
1847	577	22-Feb-94	16:13:35	BLADES OFF TARE, RPM= 1087, ALFSU= 0.0 DEG, VOR = 0.30	0.001	0.30	142.11	8.1
1848	578	22-Feb-94	16:14:20	BLADES OFF TARE, RPM= 1087, ALFSU= 1.0 DEG, VOR = 0.30	0.001	0.30	146.07	8.0
1849	579	22-Feb-94	16:15:20	BLADES OFF TARE, RPM= 1087, ALFSU= 3.0 DEG, VOR = 0.30	0.001	0.30	134.45	8.0
1850	580	22-Feb-94	16:16:11	BLADES OFF TARE, RPM= 1087, ALFSU= 5.0 DEG, VOR = 0.30	0.001	0.30	119.79	8.0
1851	581	22-Feb-94	16:17:04	BLADES OFF TARE, RPM= 1087, ALFSU= 7.0 DEG, VOR = 0.30	0.001	0.30	131.73	8.1
1852	582	22-Feb-94	16:17:54	BLADES OFF TARE, RPM= 1087, ALFSU= 9.0 DEG, VOR = 0.30	0.001	0.30	118.49	8.2
1853	583	22-Feb-94	16:19:01	BLADES OFF TARE, RPM= 1087, ALFSU= 11.0 DEG, VOR = 0.30	0.001	0.30	115.37	8.2
1854	584	22-Feb-94	16:19:51	BLADES OFF TARE, RPM= 1087, ALFSU= 13.0 DEG, VOR = 0.30	0.001	0.30	101.99	8.2
1857	585	22-Feb-94	16:22:17	BLADES OFF TARE, RPM= 1087, ALFSU= 13.0 DEG, VOR = 0.35	0.001	0.35	102.14	8.5
1858	586	22-Feb-94	16:23:11	BLADES OFF TARE, RPM= 1087, ALFSU= 11.0 DEG, VOR = 0.35	0.001	0.35	109.87	8.5
1859	587	22-Feb-94	16:24:24	BLADES OFF TARE, RPM= 1087, ALFSU= 9.0 DEG, VOR = 0.35	0.001	0.35	114.20	8.3
1860	588	22-Feb-94	16:24:59	BLADES OFF TARE, RPM= 1087, ALFSU= 7.0 DEG, VOR = 0.35	0.001	0.32	105.04	7.3
1740	589	22-Feb-94	16:27:17	BLADES OFF TARE, RPM= 1087, ALFSU= 0.0 DEG, VOR = 0.00	0.001	0.02	84.15	4.9
999	590	22-Feb-94	16:28:36	POST TEST ZERO, RPM= 0, ALFSU= 0.0 DEG, VOR = 0.00	####	9.00	-26.12	0.0
999	591	22-Feb-94	17:05:09	POST TEST ZERO, RPM= 0, ALFSU= 0.0 DEG, VOR = 0.00	####	0.00	-90.82	0.0
1740	592	22-Feb-94	17:18:19	HUB ONLY TARE, RPM= 1087, ALFSU= 0.0 DEG, VOR = 0.00	0.001	0.00	110.55	4.9
1864	593	22-Feb-94	17:23:58	HUB ONLY TARE, RPM= 1087, ALFSU= 0.0 DEG, VOR = 0.35	0.001	0.35	168.67	8.5
1859	594	22-Feb-94	17:25:19	HUB ONLY TARE, RPM= 1087, ALFSU= 9.0 DEG, VOR = 0.35	0.002	0.35	175.91	8.3
1860	595	22-Feb-94	17:26:10	HUB ONLY TARE, RPM= 1087, ALFSU= 7.0 DEG, VOR = 0.35	0.001	0.35	170.85	8.4
1861	596	22-Feb-94	17:26:45	HUB ONLY TARE, RPM= 1087, ALFSU= 5.0 DEG, VOR = 0.35	0.001	0.35	173.43	8.4
1862	597	22-Feb-94	17:27:21	HUB ONLY TARE, RPM= 1087, ALFSU= 3.0 DEG, VOR = 0.35	0.001	0.35	176.29	8.2
1740	598	22-Feb-94	17:29:29	HUB ONLY TARE, RPM= 1087, ALFSU= 0.0 DEG, VOR = 0.00	0.001	0.02	151.52	4.8
1862	599	22-Feb-94	17:36:43	HUB ONLY TARE, RPM= 1087, ALFSU= 3.0 DEG, VOR = 0.35	0.001	0.35	181.51	8.2
1863	600	22-Feb-94	17:37:15	HUB ONLY TARE, RPM= 1087, ALFSU= 1.0 DEG, VOR = 0.35	0.002	0.35	186.50	8.4
1864	601	22-Feb-94	17:37:52	HUB ONLY TARE, RPM= 1087, ALFSU= 0.0 DEG, VOR = 0.35	0.001	0.35	175.48	8.4
1865	602	22-Feb-94	17:38:31	HUB ONLY TARE, RPM= 1087, ALFSU= -1.0 DEG, VOR = 0.35	0.001	0.35	182.32	8.5
1866	603	22-Feb-94	17:39:17	HUB ONLY TARE, RPM= 1087, ALFSU= -3.0 DEG, VOR = 0.35	0.001	0.35	183.40	8.2
1867	604	22-Feb-94	17:40:12	HUB ONLY TARE, RPM= 1087, ALFSU= -5.0 DEG, VOR = 0.35	0.001	0.35	180.07	8.2
1868	605	22-Feb-94	17:40:45	HUB ONLY TARE, RPM= 1087, ALFSU= -5.0 DEG, VOR = 0.35	0.001	0.28	173.85	6.9
1740	606	22-Feb-94	17:42:25	HUB ONLY TARE, RPM= 1087, ALFSU= 0.0 DEG, VOR = 0.03	0.001	0.03	163.20	4.7

TEST	POINT	DATE			CT	Mu	Lift (lbs)	HP
999	607	22-Feb-94	17:43:28	POST TEST ZERO, RPM= 1087, ALFSU= 0.0 DEG, VOR = 0.00	####	9.00	45.15	0.0
999	608	22-Feb-94	17:57:14	POST TEST ZERO, RPM= 0000, ALFSU= 0.0 DEG, VOR = 0.00	####	0.00	5.00	0.0
1740	609	22-Feb-94	18:02:19	HUB ONLY TARE, RPM= 1087, ALFSU= 0.0 DEG, VOR = 0.00	0.001	0.00	108.61	5.8
1867	610	22-Feb-94	18:06:58	HUB ONLY TARE, RPM= 1087, ALFSU= -5.0 DEG, VOR = 0.35	0.001	0.35	138.01	8.4
1868	611	22-Feb-94	18:07:29	HUB ONLY TARE, RPM= 1087, ALFSU= -7.0 DEG, VOR = 0.35	0.001	0.34	139.09	8.4
1869	612	22-Feb-94	18:08:08	HUB ONLY TARE, RPM= 1087, ALFSU= -9.0 DEG, VOR = 0.35	0.001	0.35	140.23	8.3
1870	613	22-Feb-94	18:08:44	HUB ONLY TARE, RPM= 1087, ALFSU= -11.0 DEG, VOR = 0.35	0.001	0.35	139.38	8.4
1871	614	22-Feb-94	18:09:25	HUB ONLY TARE, RPM= 1087, ALFSU= -13.0 DEG, VOR = 0.35	0.001	0.35	135.09	8.3
999	615	22-Feb-94	18:17:06	POST TEST ZERO, RPM= 1087, ALFSU= -13.0 DEG, VOR = 0.35	####	0.00	23.87	0.0
700	616	22-Feb-94	23:39:53	NULL CAM, RPM= 544, ALFSU= 0.0 DEG, VOR = 0.00	0.003	0.04	112.97	4.1
701	617	22-Feb-94	23:40:55	NULL CAM, RPM= 652, ALFSU= 0.0 DEG, VOR = 0.00	0.003	0.03	142.53	6.5
702	618	22-Feb-94	23:41:36	NULL CAM, RPM= 761, ALFSU= 0.0 DEG, VOR = 0.00	0.003	0.03	180.40	9.8
703	619	22-Feb-94	23:42:13	NULL CAM, RPM= 870, ALFSU= 0.0 DEG, VOR = 0.00	0.003	0.02	225.30	14.1
21	620	22-Feb-94	23:42:57	NULL CAM, RPM= 978, ALFSU= 0.0 DEG, VOR = 0.00	0.002	0.02	263.20	19.3
704	621	22-Feb-94	23:43:35	NULL CAM, RPM= 1033, ALFSU= 0.0 DEG, VOR = 0.00	0.002	0.02	287.39	22.6
45	622	22-Feb-94	23:44:02	NULL CAM, RPM= 1087, ALFSU= 0.0 DEG, VOR = 0.00	0.002	0.02	290.00	26.6
705	623	22-Feb-94	23:44:36	NULL CAM, RPM= 1120, ALFSU= 0.0 DEG, VOR = 0.00	0.002	0.02	338.47	30.4
45	624	22-Feb-94	23:45:15	NULL CAM, RPM= 1087, ALFSU= 0.0 DEG, VOR = 0.00	0.002	0.02	307.11	26.0
706	625	22-Feb-94	23:45:47	NULL CAM, RPM= 1087, ALFSU= 0.0 DEG, VOR = 0.00	0.003	0.02	381.23	29.4
47	626	22-Feb-94	23:46:17	NULL CAM, RPM= 1087, ALFSU= 0.0 DEG, VOR = 0.00	0.003	0.02	427.97	30.0
707	627	22-Feb-94	23:46:43	NULL CAM, RPM= 1087, ALFSU= 0.0 DEG, VOR = 0.00	0.004	0.02	518.15	35.3
49	628	22-Feb-94	23:47:19	NULL CAM, RPM= 1087, ALFSU= 0.0 DEG, VOR = 0.00	0.004	0.03	590.33	45.1
708	629	22-Feb-94	23:48:55	NULL CAM, RPM= 1087, ALFSU= 0.0 DEG, VOR = 0.00	0.006	0.03	729.40	51.7
51	630	22-Feb-94	23:49:50	NULL CAM, RPM= 1087, ALFSU= 0.0 DEG, VOR = 0.00	0.006	0.03	821.48	60.3
52	631	22-Feb-94	23:51:42	NULL CAM, RPM= 1087, ALFSU= 0.0 DEG, VOR = 0.00	0.007	0.02	953.98	75.3
709	632	22-Feb-94	23:53:56	NULL CAM, RPM= 1087, ALFSU= 0.0 DEG, VOR = 0.00	0.008	0.04	1049.40	89.5
999	633	22-Feb-94	23:57:32	POST TEST ZERO, RPM= 1087, ALFSU= 0.0 DEG, VOR = 0.00	####	9.00	-11.79	0.0
999	634	23-Feb-94	0:30:01	POST TEST ZERO, RPM= 1087, ALFSU= 0.0 DEG, VOR = 0.00	####	9.00	-8.30	0.0
45	635	23-Feb-94	0:49:00	NULL CAM, RPM= 1087, ALFSU= 0.0 DEG, VOR = 0.00	0.002	0.02	192.47	27.2
47	636	23-Feb-94	0:49:34	NULL CAM, RPM= 1087, ALFSU= 0.0 DEG, VOR = 0.00	0.003	0.02	400.44	30.6
700	637	24-Feb-94	3:09:03	NULL CAM, RPM= 544, ALFSU= 0.0 DEG, VOR = 0.00	0.001	0.01	1.06	4.2
701	638	24-Feb-94	3:11:37	NULL CAM, RPM= 652, ALFSU= 0.0 DEG, VOR = 0.00	0.001	0.01	6.70	6.4
702	639	24-Feb-94	3:13:03	NULL CAM, RPM= 761, ALFSU= 0.0 DEG, VOR = 0.00	0.001	0.01	15.00	9.4
703	640	24-Feb-94	3:14:12	NULL CAM, RPM= 870, ALFSU= 0.0 DEG, VOR = 0.00	0.001	0.01	23.57	13.5
21	641	24-Feb-94	3:15:00	NULL CAM, RPM= 978, ALFSU= 0.0 DEG, VOR = 0.00	0.001	0.01	40.75	18.6
704	642	24-Feb-94	3:16:13	NULL CAM, RPM= 1033, ALFSU= 0.0 DEG, VOR = 0.00	0.001	0.01	49.79	21.3
45	643	24-Feb-94	3:17:15	NULL CAM, RPM= 1087, ALFSU= 0.0 DEG, VOR = 0.00	0.001	0.01	59.43	26.7
705	644	24-Feb-94	3:19:52	NULL CAM, RPM= 1120, ALFSU= 0.0 DEG, VOR = 0.00	0.001	0.00	68.27	31.8
45	645	24-Feb-94	3:22:51	NULL CAM, RPM= 1087, ALFSU= 0.0 DEG, VOR = 0.00	0.001	0.01	66.18	30.6
47	646	24-Feb-94	3:24:12	NULL CAM, RPM= 1087, ALFSU= 0.0 DEG, COLL = 2.0 DEG	0.002	0.02	195.41	33.4
47	647	24-Feb-94	3:25:26	NULL CAM, RPM= 1087, ALFSU= 0.0 DEG, COLL = 2.0 DEG, LAT = .5 DEG	0.002	0.01	199.18	33.3
47	648	24-Feb-94	3:27:29	NULL CAM, RPM= 1087, ALFSU= 0.0 DEG, COLL = 2.0 DEG, LAT = 1.0 DEG	0.002	0.01	203.82	32.8
47	649	24-Feb-94	3:29:09	NULL CAM, RPM= 1087, ALFSU= 0.0 DEG, COLL = 2.0 DEG, LAT = 1.5 DEG	0.002	0.02	211.51	34.0
47	650	24-Feb-94	3:29:49	NULL CAM, RPM= 1087, ALFSU= 0.0 DEG, COLL = 2.0 DEG, LAT = 2.0 DEG	0.002	0.01	214.65	37.7
47	651	24-Feb-94	3:30:41	NULL CAM, RPM= 1087, ALFSU= 0.0 DEG, COLL = 2.0 DEG, LAT = 0.0 DEG	0.002	0.01	194.13	32.1
47	652	24-Feb-94	3:31:42	NULL CAM, RPM= 1087, ALFSU= 0.0 DEG, COLL = 2.0 DEG, LONGA = 0.5 DE	0.002	0.01	194.35	33.2
47	653	24-Feb-94	3:32:31	NULL CAM, RPM= 1087, ALFSU= 0.0 DEG, COLL = 2.0 DEG, LONGA = 1.0 DE	0.002	0.01	202.14	32.3
47	654	24-Feb-94	3:33:08	NULL CAM, RPM= 1087, ALFSU= 0.0 DEG, COLL = 2.0 DEG, LONGA = 1.5 DE	0.002	0.01	206.03	30.2
47	655	24-Feb-94	3:34:08	NULL CAM, RPM= 1087, ALFSU= 0.0 DEG, COLL = 2.0 DEG, LONGA = 2.0 DE	0.002	0.01	206.34	31.2
45	656	24-Feb-94	3:35:39	NULL CAM, RPM= 1087, ALFSU= 0.0 DEG,	0.001	0.00	62.89	25.4
999	657	24-Feb-94	4:05:25	NULL CAM, RPM= 0, ALFSU= 0.0 DEG, 0,0	####	9.00	-40.21	0.0
45	658	24-Feb-94	4:23:08	NULL CAM, RPM= 1087, ALFSU= 0.0 DEG, 0,0,0	0.001	0.01	14.03	27.4
45	659	24-Feb-94	4:26:21	NULL CAM, RPM= 1087, ALFSU= 0.0 DEG, 0,0,0	0.001	0.01	23.14	26.3
45	660	24-Feb-94	4:27:19	NULL CAM, RPM= 1087, ALFSU= 0.0 DEG, 0,0,0	0.001	0.01	23.65	26.0
45	661	24-Feb-94	4:27:40	NULL CAM, RPM= 1087, ALFSU= 0.0 DEG, 0,0,0	0.001	0.01	25.83	26.5
45	662	24-Feb-94	4:28:00	NULL CAM, RPM= 1087, ALFSU= 0.0 DEG, 0,0,0	0.001	0.01	26.69	26.5
45	663	24-Feb-94	4:28:20	NULL CAM, RPM= 1087, ALFSU= 0.0 DEG, 0,0,0	0.001	0.01	23.82	26.0
45	664	24-Feb-94	4:28:41	NULL CAM, RPM= 1087, ALFSU= 0.0 DEG, 0,0,0	0.001	0.01	26.57	26.5
45	665	24-Feb-94	4:29:02	NULL CAM, RPM= 1087, ALFSU= 0.0 DEG, 0,0,0	0.001	0.01	27.08	25.7
45	666	24-Feb-94	4:29:22	NULL CAM, RPM= 1087, ALFSU= 0.0 DEG, 0,0,0	0.001	0.01	30.06	26.8
45	667	24-Feb-94	4:29:42	NULL CAM, RPM= 1087, ALFSU= 0.0 DEG, 0,0,0	0.001	0.01	27.81	26.3
45	668	24-Feb-94	4:30:03	NULL CAM, RPM= 1087, ALFSU= 0.0 DEG, 0,0,0	0.001	0.01	28.33	26.0
45	669	24-Feb-94	4:30:23	NULL CAM, RPM= 1087, ALFSU= 0.0 DEG, 0,0,0	0.001	0.01	27.43	25.5
45	670	24-Feb-94	4:30:44	NULL CAM, RPM= 1087, ALFSU= 0.0 DEG, 0,0,0	0.001	0.01	25.90	26.3
45	671	24-Feb-94	4:31:04	NULL CAM, RPM= 1087, ALFSU= 0.0 DEG, 0,0,0	0.001	0.01	29.58	26.5
45	672	24-Feb-94	4:31:25	NULL CAM, RPM= 1087, ALFSU= 0.0 DEG, 0,0,0	0.001	0.01	26.30	25.7
45	673	24-Feb-94	4:31:46	NULL CAM, RPM= 1087, ALFSU= 0.0 DEG, 0,0,0	0.001	0.01	29.57	25.9
45	674	24-Feb-94	4:32:06	NULL CAM, RPM= 1087, ALFSU= 0.0 DEG, 0,0,0	0.001	0.01	32.49	26.7
45	675	24-Feb-94	4:32:27	NULL CAM, RPM= 1087, ALFSU= 0.0 DEG, 0,0,0	0.001	0.01	29.40	26.6
45	676	24-Feb-94	4:32:48	NULL CAM, RPM= 1087, ALFSU= 0.0 DEG, 0,0,0	0.001	0.01	27.93	26.3
47	677	24-Feb-94	4:35:40	NULL CAM, RPM= 1087, ALFSU= 0.0 DEG, COLL = 2.0 DEG	0.001	0.01	152.25	29.8
47	678	24-Feb-94	4:37:22	NULL CAM, RPM= 1087, ALFSU= 0.0 DEG, COLL = 2.0 DEG	0.001	0.01	154.11	29.6
47	679	24-Feb-94	4:37:56	NULL CAM, RPM= 1087, ALFSU= 0.0 DEG, COLL = 2.0 DEG	0.001	0.01	152.16	29.1
47	680	24-Feb-94	4:38:17	NULL CAM, RPM= 1087, ALFSU= 0.0 DEG, COLL = 2.0 DEG	0.001	0.01	152.75	29.1
47	681	24-Feb-94	4:38:37	NULL CAM, RPM= 1087, ALFSU= 0.0 DEG, COLL = 2.0 DEG	0.001	0.02	155.98	29.5
47	682	24-Feb-94	4:38:58	NULL CAM, RPM= 1087, ALFSU= 0.0 DEG, COLL = 2.0 DEG	0.001	0.02	154.03	29.7
47	683	24-Feb-94	4:39:18	NULL CAM, RPM= 1087, ALFSU= 0.0 DEG, COLL = 2.0 DEG	0.001	0.01	155.28	29.5
47	684	24-Feb-94	4:39:39	NULL CAM, RPM= 1087, ALFSU= 0.0 DEG, COLL = 2.0 DEG	0.001	0.02	152.25	29.4
47	685	24-Feb-94	4:40:00	NULL CAM, RPM= 1087, ALFSU= 0.0 DEG, COLL = 2.0 DEG	0.001	0.02	152.75	28.9
47	686	24-Feb-94	4:40:21	NULL CAM, RPM= 1087, ALFSU= 0.0 DEG, COLL = 2.0 DEG	0.001	0.01	152.57	28.9
47	687	24-Feb-94	4:40:42	NULL CAM, RPM= 1087, ALFSU= 0.0 DEG, COLL = 2.0 DEG	0.001	0.02	153.52	29.4
47	688	24-Feb-94	4:41:02	NULL CAM, RPM= 1087, ALFSU= 0.0 DEG, COLL = 2.0 DEG	0.001	0.02	150.24	29.1
47	689	24-Feb-94	4:41:23	NULL CAM, RPM= 1087, ALFSU= 0.0 DEG, COLL = 2.0 DEG	0.001	0.02	150.95	29.6
47	690	24-Feb-94	4:41:43	NULL CAM, RPM= 1087, ALFSU= 0.0 DEG, COLL = 2.0 DEG	0.001	0.02	152.54	29.1
47	691	24-Feb-94	4:42:05	NULL CAM, RPM= 1087, ALFSU= 0.0 DEG, COLL = 2.0 DEG	0.001	0.01	155.39	29.7

TEST	POINT	DATE			CT	Mu	Lift (lbs)	HP
47	692	24-Feb-94	4:42:26	NULL CAM, RPM= 1087, ALFSU= 0.0 DEG, COLL = 2.0 DEG	0.001	0.02	152.54	29.4
47	693	24-Feb-94	4:42:46	NULL CAM, RPM= 1087, ALFSU= 0.0 DEG, COLL = 2.0 DEG	0.001	0.02	153.67	29.4
47	694	24-Feb-94	4:43:07	NULL CAM, RPM= 1087, ALFSU= 0.0 DEG, COLL = 2.0 DEG	0.001	0.01	154.81	29.6
47	695	24-Feb-94	4:43:28	NULL CAM, RPM= 1087, ALFSU= 0.0 DEG, COLL = 2.0 DEG	0.001	0.01	151.86	28.8
45	696	24-Feb-94	4:46:49	NULL CAM, RPM= 1087, ALFSU= 0.0 DEG,	0.001	0.01	31.39	25.3
999	697	24-Feb-94	4:48:17	NULL CAM, RPM= 0, ALFSU= 0.0 DEG,	####	9.00	-28.47	0.0
700	698	24-Feb-94	21:42:37	NULL CAM, RPM= 544, ALFSU= 0.0 DEG,	0.001	0.03	-18.25	4.3
701	699	24-Feb-94	21:43:29	NULL CAM, RPM= 652, ALFSU= 0.0 DEG,	0.001	0.02	-12.54	6.5
702	700	24-Feb-94	21:44:26	NULL CAM, RPM= 761, ALFSU= 0.0 DEG	0.001	0.02	-4.42	9.5
703	701	24-Feb-94	21:45:33	NULL CAM, RPM= 870, ALFSU= 0.0 DEG	0.001	0.02	7.72	13.4
21	702	24-Feb-94	21:46:43	NULL CAM, RPM= 978, ALFSU= 0.0 DEG	0.001	0.01	19.83	18.1
704	703	24-Feb-94	21:49:07	NULL CAM, RPM= 1033, ALFSU= 0.0 DEG	0.001	0.01	38.41	21.0
45	704	24-Feb-94	21:50:32	NULL CAM, RPM= 1087, ALFSU= 0.0 DEG	0.001	0.01	53.13	25.9
999	705	24-Feb-94	21:52:03	POST ZERO, RPM= 0000, ALFSU= 0.0 DEG	####	9.00	-7.45	0.0
700	706	24-Feb-94	22:46:18	NULL CAM, RPM= 544, ALFSU= 0.0 DEG	0.001	0.02	-16.75	4.2
21	707	24-Feb-94	22:47:39	NULL CAM, RPM= 978, ALFSU= 0.0 DEG	0.001	0.01	9.77	18.5
700	708	24-Feb-94	23:21:24	NULL CAM, RPM= 544, ALFSU= 0.0 DEG	0.001	0.02	9.03	4.0
21	709	24-Feb-94	23:22:37	NULL CAM, RPM= 978, ALFSU= 0.0 DEG	0.001	0.01	44.40	18.5
45	710	24-Feb-94	23:24:15	NULL CAM, RPM= 1087, ALFSU= 0.0 DEG	0.001	0.01	68.28	26.2
700	711	24-Feb-94	23:53:08	NULL CAM, RPM= 544, ALFSU= 0.0 DEG	0.001	0.02	-11.48	4.0
21	712	24-Feb-94	23:54:28	NULL CAM, RPM= 978, ALFSU= 0.0 DEG	0.001	0.01	19.97	18.5
45	713	24-Feb-94	23:55:29	NULL CAM, RPM= 1087, ALFSU= 0.0 DEG	0.001	0.01	38.62	25.0
21	714	25-Feb-94	0:31:43	NULL CAM, RPM= 978, ALFSU= 0.0 DEG	0.001	0.01	20.44	18.4
45	715	25-Feb-94	0:32:41	NULL CAM, RPM= 1087, ALFSU= 0.0 DEG	0.001	0.01	41.45	25.9
705	716	25-Feb-94	0:33:55	NULL CAM, RPM= 1120, ALFSU= 0.0 DEG	0.001	0.01	51.46	27.8
45	717	25-Feb-94	0:34:35	NULL CAM, RPM= 1087, ALFSU= 0.0 DEG	0.001	0.01	50.94	25.5
706	718	25-Feb-94	0:35:31	NULL CAM, RPM= 1087, ALFSU= 0.0 DEG, COLL = 1.0 DEG	0.001	0.02	104.83	26.9
47	719	25-Feb-94	0:37:07	NULL CAM, RPM= 1087, ALFSU= 0.0 DEG, COLL = 2.0 DEG	0.002	0.02	192.88	30.9
707	720	25-Feb-94	0:37:38	NULL CAM, RPM= 1087, ALFSU= 0.0 DEG, COLL = 3.0 DEG	0.002	0.02	286.43	35.2
49	721	25-Feb-94	0:38:15	NULL CAM, RPM= 1087, ALFSU= 0.0 DEG, COLL = 4.0 DEG	0.003	0.02	384.12	42.6
708	722	25-Feb-94	0:38:46	NULL CAM, RPM= 1087, ALFSU= 0.0 DEG, COLL = 5.0 DEG	0.004	0.02	488.21	50.9
51	723	25-Feb-94	0:39:14	NULL CAM, RPM= 1087, ALFSU= 0.0 DEG, COLL = 6.0 DEG	0.005	0.03	602.86	62.3
52	724	25-Feb-94	0:39:52	NULL CAM, RPM= 1087, ALFSU= 0.0 DEG, COLL = 7.0 DEG	0.006	0.03	722.17	75.6
709	725	25-Feb-94	0:40:39	NULL CAM, RPM= 1087, ALFSU= 0.0 DEG, COLL = 8.0 DEG	0.007	0.04	847.51	93.0
710	726	25-Feb-94	0:43:28	NULL CAM, RPM= 1087, ALFSU= 0.0 DEG, COLL = 9.0 DEG	0.007	0.04	970.18	109.0
711	727	25-Feb-94	0:45:33	NULL CAM, RPM= 1087, ALFSU= 0.0 DEG, COLL = 10.0 DEG	0.008	0.04	1101.80	129.8
45	728	25-Feb-94	0:47:14	NULL CAM, RPM= 1087, ALFSU= 0.0 DEG, COLL = 0.0 DEG	0.001	0.01	75.17	25.0
47	729	25-Feb-94	0:48:13	NULL CAM, RPM= 1087, ALFSU= 0.0 DEG, COLL = 2.0 DEG	0.002	0.02	205.62	29.9
47	730	25-Feb-94	0:51:44	NULL CAM, RPM= 1087, ALFSU= 0.0 DEG, COLL = 2.0 DEG, LAT = 0.5 DEG	0.002	0.02	205.24	30.6
47	731	25-Feb-94	0:53:06	NULL CAM, RPM= 1087, ALFSU= 0.0 DEG, COLL = 2.0 DEG, LONGA = 1.0 DE	0.002	0.02	204.47	30.8
47	732	25-Feb-94	0:53:46	NULL CAM, RPM= 1087, ALFSU= 0.0 DEG, COLL = 2.0 DEG, LONGA = 1.5 DE	0.002	0.02	208.61	31.2
47	733	25-Feb-94	0:54:30	NULL CAM, RPM= 1087, ALFSU= 0.0 DEG, COLL = 2.0 DEG, LONGA = 2.0 DE	0.002	0.01	213.88	32.2
47	734	25-Feb-94	0:56:03	NULL CAM, RPM= 1087, ALFSU= 0.0 DEG, COLL = 2.0 DEG, LAT = 0.5 DEG	0.002	0.02	201.05	30.6
47	735	25-Feb-94	0:56:35	NULL CAM, RPM= 1087, ALFSU= 0.0 DEG, COLL = 2.0 DEG, LAT = 1.0 DEG	0.002	0.02	204.93	31.0
47	736	25-Feb-94	0:57:06	NULL CAM, RPM= 1087, ALFSU= 0.0 DEG, COLL = 2.0 DEG, LAT = 1.5 DEG	0.002	0.01	207.63	31.8
47	737	25-Feb-94	0:57:35	NULL CAM, RPM= 1087, ALFSU= 0.0 DEG, COLL = 2.0 DEG, LAT = 2.0 DEG	0.002	0.02	217.71	32.9
47	738	25-Feb-94	1:00:04	NULL CAM, RPM= 1087, ALFSU= 0.0 DEG, COLL = 2.0 DEG, LAT = -2.0 DEG	0.002	0.02	205.03	32.4
45	739	25-Feb-94	1:01:23	NULL CAM, RPM= 1087, ALFSU= 0.0 DEG, COLL = 0.0 DEG, LAT = 0.0 DEG	0.001	0.01	60.41	25.3
714	740	25-Feb-94	1:03:54	NULL CAM, RPM= 1087, ALFSU= 0.0 DEG, COLL = 0.0 DEG, LAT = 0.0 DEG C	0.007	0.04	913.40	102.5
716	741	25-Feb-94	1:13:52	NULL CAM, RPM= 1087, ALFSU= 0.0 DEG, COLL = 0.0 DEG, VOR = 0.05	0.003	0.05	366.45	38.3
716	742	25-Feb-94	1:21:14	NULL CAM, RPM= 1087, ALFSU= 0.0 DEG, COLL = 0.0 DEG, VOR = 0.05	0.007	0.05	942.09	99.3
717	743	25-Feb-94	1:28:15	NULL CAM, RPM= 1087, ALFSU= 0.0 DEG, VOR = 0.075	0.007	0.07	929.98	90.7
718	744	25-Feb-94	1:33:08	NULL CAM, RPM= 1087, ALFSU= 0.0 DEG, VOR = 0.100	0.003	0.10	405.19	35.4
718	745	25-Feb-94	1:38:00	NULL CAM, RPM= 1087, ALFSU= -0.85 DEG, VOR = 0.100	0.007	0.10	931.18	81.9
719	746	25-Feb-94	1:43:40	NULL CAM, RPM= 1087, ALFSU= -0.85 DEG, VOR = 0.125	0.007	0.12	928.20	72.3
723	747	25-Feb-94	1:47:05	NULL CAM, RPM= 1087, ALFSU= -0.85 DEG, VOR = 0.15	0.002	0.15	271.37	30.6
723	748	25-Feb-94	1:51:18	NULL CAM, RPM= 1087, ALFSU= -1.71 DEG, VOR = 0.15	0.006	0.15	801.65	58.8
720	749	25-Feb-94	1:52:29	NULL CAM, RPM= 1087, ALFSU= -1.71 DEG, VOR = 0.15	0.007	0.15	930.09	71.1
724	750	25-Feb-94	1:53:46	NULL CAM, RPM= 1087, ALFSU= -1.71 DEG, VOR = 0.15	0.008	0.15	1051.90	83.4
721	751	25-Feb-94	2:02:43	NULL CAM, RPM= 1081, ALFSU= -2.20 DEG, VOR = 0.175	0.007	0.17	913.31	66.4
725	752	25-Feb-94	2:09:25	NULL CAM, RPM= 1082, ALFSU= -2.90 DEG, VOR = 0.200	0.006	0.20	785.16	56.6
722	753	25-Feb-94	2:10:51	NULL CAM, RPM= 1082, ALFSU= -2.90 DEG, VOR = 0.200	0.007	0.20	911.01	66.4
726	754	25-Feb-94	2:12:49	NULL CAM, RPM= 1084, ALFSU= -2.90 DEG, VOR = 0.200	0.008	0.20	1042.50	79.5
45	755	25-Feb-94	2:20:39	NULL CAM, RPM= 1087, ALFSU= 0.0 DEG, VOR = 0.000	0.001	0.01	-8.73	26.6
999	756	25-Feb-94	2:22:15	NULL CAM, RPM= 0, ALFSU= 0.0 DEG, VOR = 0.000	####	9.00	-52.40	0.0
727	757	25-Feb-94	3:57:02	NULL CAM, RPM= 1077, ALFSU= 0.0 DEG, VOR = 0.150	0.007	0.15	916.93	56.3
727	758	25-Feb-94	3:58:29	NULL CAM, RPM= 1077, ALFSU= 0.0 DEG, VOR = 0.150 KULITE POINT	0.007	0.15	914.79	56.2
45	759	25-Feb-94	4:12:53	NULL CAM, RPM= 1087, ALFSU= 0	0.001	0.01	99.91	26.2
999	760	25-Feb-94	4:14:20	NULL CAM, RPM= 0, ALFSU= 0	####	9.00	28.67	0.0
45	761	25-Feb-94	4:40:00	NULL CAM, RPM= 1087, ALFSU= 0	0.001	0.01	22.07	24.7
727	762	25-Feb-94	4:47:06	NULL CAM, RPM= 1087, ALFSU= 0, VOR = .150	0.007	0.15	914.20	58.0
727	763	25-Feb-94	4:49:11	NULL CAM, RPM= 1077, ALFSU= SWEEP FOR ACOUSTIC, VOR = .150	0.007	0.15	924.69	58.5
727	764	25-Feb-94	4:52:14	NULL CAM, RPM= 1077, ALFSU= SWEEP FOR ACOUSTIC, VOR = .150	0.007	0.15	916.31	54.5
727	765	25-Feb-94	4:54:20	NULL CAM, RPM= 1077, ALFSU= SWEEP FOR ACOUSTIC, VOR = .150	0.007	0.15	918.09	51.0
727	766	25-Feb-94	4:55:58	NULL CAM, RPM= 1077, ALFSU= SWEEP FOR ACOUSTIC, VOR = .150	0.007	0.15	912.04	47.6
727	767	25-Feb-94	4:57:25	NULL CAM, RPM= 1077, ALFSU= SWEEP FOR ACOUSTIC, VOR = .150	0.007	0.15	920.32	44.7
727	768	25-Feb-94	4:59:00	NULL CAM, RPM= 1077, ALFSU= SWEEP FOR ACOUSTIC, VOR = .150	0.007	0.15	915.44	41.8
727	769	25-Feb-94	5:00:34	NULL CAM, RPM= 1077, ALFSU= SWEEP FOR ACOUSTIC, VOR = .150	0.007	0.15	908.83	38.0
727	770	25-Feb-94	5:02:55	NULL CAM, RPM= 1077, ALFSU= SWEEP FOR ACOUSTIC, VOR = .150	0.007	0.15	908.80	35.1
727	771	25-Feb-94	5:04:50	NULL CAM, RPM= 1077, ALFSU= SWEEP FOR ACOUSTIC, VOR = .150	0.007	0.15	913.37	32.7
727	772	25-Feb-94	5:07:04	NULL CAM, RPM= 1077, ALFSU= SWEEP FOR ACOUSTIC, VOR = .150	0.007	0.15	905.45	28.9
727	773	25-Feb-94	5:08:57	NULL CAM, RPM= 1077, ALFSU= SWEEP FOR ACOUSTIC, VOR = .150	0.007	0.15	906.33	27.1
728	774	25-Feb-94	5:17:00	NULL CAM, RPM= 1078, ALFSU= SWEEP FOR ACOUSTIC, VOR = 200	0.007	0.20	905.71	47.1
728	775	25-Feb-94	5:18:53	NULL CAM, RPM= 1078, ALFSU= SWEEP FOR ACOUSTIC, VOR = 200	0.007	0.20	916.02	43.6
728	776	25-Feb-94	5:20:11	NULL CAM, RPM= 1078, ALFSU= SWEEP FOR ACOUSTIC, VOR = 200	0.007	0.20	919.95	39.6

TEST	POINT	DATE			CT	Mu	Lift (lbs)	HP
728	777	25-Feb-94	5:21:34	NULL CAM, RPM= 1078, ALFSU= SWEEP FOR ACOUSTIC, VOR = 200	0.007	0.20	912.70	35.8
728	778	25-Feb-94	5:23:13	NULL CAM, RPM= 1078, ALFSU= SWEEP FOR ACOUSTIC, VOR = 200	0.007	0.20	908.97	31.8
728	779	25-Feb-94	5:24:39	NULL CAM, RPM= 1078, ALFSU= SWEEP FOR ACOUSTIC, VOR = 200	0.007	0.20	909.72	28.7
728	780	25-Feb-94	5:26:05	NULL CAM, RPM= 1078, ALFSU= SWEEP FOR ACOUSTIC, VOR = 200	0.007	0.20	902.32	25.3
728	781	25-Feb-94	5:27:51	NULL CAM, RPM= 1078, ALFSU= SWEEP FOR ACOUSTIC, VOR = 200	0.007	0.20	907.65	21.9
728	782	25-Feb-94	5:29:26	NULL CAM, RPM= 1078, ALFSU= SWEEP FOR ACOUSTIC, VOR = 200	0.007	0.20	907.92	18.5
728	783	25-Feb-94	5:30:55	NULL CAM, RPM= 1078, ALFSU= SWEEP FOR ACOUSTIC, VOR = 200	0.007	0.20	903.43	15.0
728	784	25-Feb-94	5:32:51	NULL CAM, RPM= 1078, ALFSU= SWEEP FOR ACOUSTIC, VOR = 200	0.007	0.20	902.45	12.6
729	785	25-Feb-94	5:36:10	NULL CAM, RPM= 1081, ALFSU= SWEEP FOR ACOUSTIC, VOR = 200	0.008	0.20	1037.80	14.8
729	786	25-Feb-94	5:37:52	NULL CAM, RPM= 1081, ALFSU= SWEEP FOR ACOUSTIC, VOR = 200	0.008	0.20	1031.70	18.2
729	787	25-Feb-94	5:39:28	NULL CAM, RPM= 1081, ALFSU= SWEEP FOR ACOUSTIC, VOR = 200	0.008	0.20	1037.20	21.3
729	788	25-Feb-94	5:40:53	NULL CAM, RPM= 1081, ALFSU= SWEEP FOR ACOUSTIC, VOR = 200	0.008	0.20	1041.10	25.3
729	789	25-Feb-94	5:42:22	NULL CAM, RPM= 1081, ALFSU= SWEEP FOR ACOUSTIC, VOR = 200	0.008	0.20	1038.80	28.8
729	790	25-Feb-94	5:43:34	NULL CAM, RPM= 1081, ALFSU= SWEEP FOR ACOUSTIC, VOR = 200	0.008	0.20	1046.30	33.3
729	791	25-Feb-94	5:44:58	NULL CAM, RPM= 1081, ALFSU= SWEEP FOR ACOUSTIC, VOR = 200	0.008	0.20	1050.40	37.7
729	792	25-Feb-94	5:46:18	NULL CAM, RPM= 1081, ALFSU= SWEEP FOR ACOUSTIC, VOR = 200	0.008	0.20	1038.70	41.7
729	793	25-Feb-94	5:47:51	NULL CAM, RPM= 1081, ALFSU= SWEEP FOR ACOUSTIC, VOR = 200	0.008	0.20	1040.30	46.4
729	794	25-Feb-94	5:49:28	NULL CAM, RPM= 1081, ALFSU= SWEEP FOR ACOUSTIC, VOR = 200	0.008	0.20	1046.30	51.5
729	795	25-Feb-94	5:51:00	NULL CAM, RPM= 1081, ALFSU= SWEEP FOR ACOUSTIC, VOR = 200	0.008	0.20	1051.90	56.3
730	796	25-Feb-94	5:53:51	NULL CAM, RPM= 1082, ALFSU= 0.0 DEG, VOR = 200	0.004	0.20	461.33	31.0
45	797	25-Feb-94	5:56:18	NULL CAM, RPM= 1081, ALFSU= 0.0 DEG, VOR = 0.00	0.001	0.01	102.51	27.1
999	798	25-Feb-94	5:57:33	NULL CAM, RPM= 0, ALFSU= 0.0 DEG, VOR = 0.00	#####	9.00	32.63	0.0
9530	799	25-Feb-94	16:26:08	AXIAL CAL AXIAL=0LBS	#####	9.00	-1.04	0.0
9530	800	25-Feb-94	16:26:43	AXIAL CAL AXIAL=50LBS	#####	9.00	-1.13	0.0
9530	801	25-Feb-94	16:28:37	AXIAL CAL AXIAL=100LBS	#####	9.00	-1.19	0.0
9530	802	25-Feb-94	16:36:16	AXIAL CAL AXIAL=0LBS	#####	9.00	0.32	0.0
9530	803	25-Feb-94	16:37:00	AXIAL CAL AXIAL= 50LBS	#####	9.00	0.24	0.0
9530	804	25-Feb-94	16:37:35	AXIAL CAL AXIAL=100LBS	#####	9.00	-0.25	0.0
9530	805	25-Feb-94	16:38:20	AXIAL CAL AXIAL=150LBS	#####	9.00	-0.35	0.0
9530	806	25-Feb-94	16:38:55	AXIAL CAL AXIAL=200LBS	#####	9.00	0.03	0.0
9530	807	25-Feb-94	16:39:35	AXIAL CAL AXIAL=150LBS	#####	9.00	-0.34	0.0
9530	808	25-Feb-94	16:40:23	AXIAL CAL AXIAL=100LBS	#####	9.00	-0.75	0.0
9530	809	25-Feb-94	16:41:05	AXIAL CAL AXIAL= 50LBS	#####	9.00	-0.75	0.0
9530	810	25-Feb-94	16:41:48	AXIAL CAL AXIAL= 0LBS	#####	9.00	-1.09	0.0
45	812	25-Feb-94	18:36:17	NULL CAM, RPM=1087, ALFSU= 0.0 DEG, VOR = 0.00	0.001	0.02	32.47	26.5
706	813	25-Feb-94	18:41:36	NULL CAM, RPM=1087, ALFSU= 0.0 DEG, VOR = 0.00, COLL=2DEG	0.001	0.02	114.26	27.1
47	814	25-Feb-94	18:42:13	NULL CAM, RPM=1087, ALFSU= 0.0 DEG, VOR = 0.00, COLL=2DEG	0.002	0.02	197.58	30.3
707	815	25-Feb-94	18:42:47	NULL CAM, RPM=1087, ALFSU= 0.0 DEG, VOR = 0.00, COLL=3DEG	0.002	0.02	297.10	36.3
49	816	25-Feb-94	18:43:25	NULL CAM, RPM=1087, ALFSU= 0.0 DEG, VOR = 0.00, COLL=4DEG	0.003	0.02	393.04	43.0
708	817	25-Feb-94	18:43:53	NULL CAM, RPM=1087, ALFSU= 0.0 DEG, VOR = 0.00, COLL=5DEG	0.004	0.03	501.68	52.3
51	818	25-Feb-94	18:44:40	NULL CAM, RPM=1087, ALFSU= 0.0 DEG, VOR = 0.00, COLL=6DEG	0.005	0.03	610.89	63.7
52	819	25-Feb-94	18:45:15	NULL CAM, RPM=1087, ALFSU= 0.0 DEG, VOR = 0.00, COLL=7DEG	0.006	0.04	720.56	76.6
709	820	25-Feb-94	18:46:17	NULL CAM, RPM=1087, ALFSU= 0.0 DEG, VOR = 0.00, COLL=8DEG	0.007	0.04	842.89	91.4
710	821	25-Feb-94	18:47:33	NULL CAM, RPM=1087, ALFSU= 0.0 DEG, VOR = 0.00, COLL=9DEG	0.008	0.04	978.28	110.2
711	822	25-Feb-94	18:48:42	NULL CAM, RPM=1087, ALFSU= 0.0 DEG, VOR = 0.00, COLL=10DEG	0.009	0.03	1109.70	129.7
45	823	25-Feb-94	18:50:46	NULL CAM, RPM=1087, ALFSU= 0.0 DEG, VOR = 0.00, COLL=0DEG	0.001	0.02	80.14	25.2
47	824	25-Feb-94	18:51:46	NULL CAM, RPM=1087, ALFSU= 0.0 DEG, VOR = 0.00, COLL=2DEG	0.002	0.02	207.46	30.6
47	825	25-Feb-94	18:52:36	NULL CAM, RPM=1087, ALFSU= 0.0 DEG, VOR = 0.00, COLL=2DEG, LONG=2	0.002	0.02	222.27	33.1
47	826	25-Feb-94	18:53:47	NULL CAM, RPM=1087, ALFSU= 0.0 DEG, VOR = 0.00, COLL=2DEG, LAT=2DE	0.002	0.02	225.18	33.3
45	827	25-Feb-94	18:55:03	NULL CAM, RPM=1087, ALFSU= 0.0 DEG, VOR = 0.00, COLL=0DEG	0.001	0.02	76.00	26.2
723	828	25-Feb-94	19:12:02	NULL CAM, RPM=1087, ALFSU=-1.9 DEG, VOR = 0.15	0.006	0.15	792.10	56.6
720	829	25-Feb-94	19:14:25	NULL CAM, RPM=1087, ALFSU=-1.7 DEG, VOR = 0.15	0.007	0.15	919.99	66.8
724	830	25-Feb-94	19:16:39	NULL CAM, RPM=1087, ALFSU=-1.6 DEG, VOR = 0.15 ACOUSTICS	0.008	0.15	1043.30	79.2
724	847	25-Feb-94	19:22:43	NULL CAM, RPM=1087, ALFSU=-1.6 DEG, VOR = 0.15 ACOUSTICS	0.008	0.15	1032.80	76.8
45	848	25-Feb-94	19:29:19	NULL CAM, RPM=1087, ALFSU= 0.0 DEG, VOR = 0.00	0.001	0.01	13.36	25.8
999	849	25-Feb-94	19:31:17	NULL CAM, RPM=0000, ALFSU= 0.0 DEG, VOR = 0.00	#####	9.00	-31.58	0.0
21	850	25-Feb-94	21:08:46	NULL CAM, RPM= 978, ALFSU= 0.0 DEG, VOR = 0.00	0.001	0.02	8.80	17.4
45	851	25-Feb-94	21:11:38	NULL CAM, RPM=1087, ALFSU= 0.0 DEG, VOR = 0.00	0.001	0.02	27.58	24.5
731	852	25-Feb-94	21:21:23	NULL CAM, RPM=1087, ALFSU= 3.0 DEG, VOR = 0.15 ACOUSTIC SWEEP	0.007	0.15	911.12	47.6
731	869	25-Feb-94	21:27:30	NULL CAM, RPM=1087, ALFSU= 3.0 DEG, VOR = 0.15 ACOUSTIC SWEEP	0.007	0.15	923.61	47.2
732	870	25-Feb-94	21:31:52	NULL CAM, RPM=1087, ALFSU= 4.0 DEG, VOR = 0.15 ACOUSTIC SWEEP	0.007	0.15	904.69	44.0
732	887	25-Feb-94	21:35:00	NULL CAM, RPM=1087, ALFSU= 4.0 DEG, VOR = 0.15 ACOUSTIC SWEEP	0.007	0.15	915.15	43.9
45	888	25-Feb-94	21:44:10	NULL CAM, RPM=1087, ALFSU= 0.0 DEG, VOR = 0.00	0.001	0.01	92.46	25.1
45	889	25-Feb-94	22:04:13	NULL CAM, RPM=1082, ALFSU= 0.0 DEG, VOR = 0.00	0.001	0.01	26.03	24.1
45	890	25-Feb-94	22:18:00	NULL CAM, RPM=1082, ALFSU= 0.0 DEG, VOR = 0.00	0.001	0.01	47.48	24.0
733	891	25-Feb-94	22:27:18	NULL CAM, RPM=1082, ALFSU= 0.0 DEG, VOR = 0.00 ACOUSTIC SWEEP	0.007	0.15	908.62	42.3
733	908	25-Feb-94	22:33:23	NULL CAM, RPM=1082, ALFSU= 0.0 DEG, VOR = 0.00 ACOUSTIC SWEEP	0.007	0.15	907.95	42.1
734	912	25-Feb-94	22:44:34	NULL CAM, RPM=1082, ALFSU= 0.6 DEG, VOR = 0.15 ACOUSTIC SWEEP	0.007	0.15	903.14	39.1
734	929	25-Feb-94	22:50:44	NULL CAM, RPM=1082, ALFSU= 0.6 DEG, VOR = 0.15 ACOUSTIC SWEEP	0.007	0.15	917.84	38.4
734	930	25-Feb-94	22:53:02	NULL CAM, RPM=1082, ALFSU= 0.6 DEG, VOR = 0.15 ACOUSTIC SWEEP	0.007	0.15	896.44	38.7
734	948	25-Feb-94	22:58:44	NULL CAM, RPM=1082, ALFSU= 0.6 DEG, VOR = 0.15 ACOUSTIC SWEEP	0.007	0.15	905.95	37.8
735	947	25-Feb-94	23:01:39	NULL CAM, RPM=1084, ALFSU= 7.0 DEG, VOR = 0.15 ACOUSTIC SWEEP	0.007	0.15	904.36	36.0
735	964	25-Feb-94	23:06:18	NULL CAM, RPM=1084, ALFSU= 7.0 DEG, VOR = 0.15 ACOUSTIC SWEEP	0.007	0.15	918.55	35.9
725	965	25-Feb-94	23:15:50	NULL CAM, RPM=1087, ALFSU=-3.24DEG, VOR = 0.20	0.006	0.20	773.86	52.3
726	966	25-Feb-94	23:21:21	NULL CAM, RPM=1088, ALFSU=-2.72DEG, VOR = 0.20	0.008	0.20	1045.50	72.4
736	967	25-Feb-94	23:25:04	NULL CAM, RPM=1088, ALFSU=-2.0DEG, VOR = 0.20 ACOUSTIC SWEEP	0.007	0.20	904.14	40.6
736	984	25-Feb-94	23:32:01	NULL CAM, RPM=1088, ALFSU=3.0DEG, VOR = 0.20 ACOUSTIC SWEEP	0.007	0.20	912.28	40.3
737	985	25-Feb-94	23:34:32	NULL CAM, RPM=1088, ALFSU=3.0DEG, VOR = 0.20 ACOUSTIC SWEEP	0.007	0.20	912.86	37.7
737	1002	25-Feb-94	23:42:00	NULL CAM, RPM=1088, ALFSU=3.0DEG, VOR = 0.20 ACOUSTIC SWEEP	0.007	0.20	924.58	37.4
756	1003	25-Feb-94	23:53:11	NULL CAM, RPM=1095, ALFSU=5.0DEG, VOR = 0.25	0.006	0.25	784.37	57.9
757	1004	25-Feb-94	23:55:54	NULL CAM, RPM=1095, ALFSU=-4.19DEG, VOR = 0.25	0.008	0.25	1031.80	75.1
758	1005	26-Feb-94	0:02:57	NULL CAM, RPM=1102, ALFSU=-7.4DEG, VOR = 0.30	0.008	0.30	791.75	74.5
759	1006	26-Feb-94	0:05:26	NULL CAM, RPM=1102, ALFSU=-8.12DEG, VOR = 0.30	0.008	0.30	1054.80	83.9
725	1007	26-Feb-94	0:15:08	NULL CAM, RPM=1095, ALFSU=-3.2DEG, VOR = 0.20	0.006	0.20	771.33	52.0
726	1008	26-Feb-94	0:17:16	NULL CAM, RPM=1095, ALFSU=-2.7DEG, VOR = 0.20	0.008	0.20	1047.80	69.7

TEST	POINT	DATE			CT	Mu	Lift (lbs)	HP
45	1009	26-Feb-94	0:24:22	NULL CAM, RPM=1087, ALFSU= 0.0DEG, VOR = 0.00	0.001	0.01	64.86	26.1
999	1010	26-Feb-94	0:25:58	NULL CAM, RPM=0000, ALFSU= 0.0DEG, VOR = 0.00	####	9.00	11.42	0.0
45	1011	26-Feb-94	1:27:07	NULL CAM, RPM= 1087, ALFSU= 0.0DEG, VOR = 0.00	0.001	0.01	8.65	23.8
736	1012	26-Feb-94	1:37:31	NULL CAM, RPM= 1089, ALFSU= 2.0DEG, VOR = 0.20	0.007	0.20	913.30	41.7
738	1013	26-Feb-94	1:40:50	NULL CAM, RPM= 1090, ALFSU= 4.0DEG, VOR = 0.20	0.007	0.20	899.44	33.0
738	1014	26-Feb-94	1:43:15	NULL CAM, RPM= 1090, ALFSU= 4.0DEG, VOR = 0.20, ACOUSTIC SWEEP	0.007	0.20	906.82	33.1
738	1015	26-Feb-94	1:43:52	NULL CAM, RPM= 1090, ALFSU= 4.0DEG, VOR = 0.20, ACOUSTIC SWEEP	0.007	0.20	903.83	33.0
738	1031	26-Feb-94	1:49:35	NULL CAM, RPM= 1090, ALFSU= 4.0DEG, VOR = 0.20, ACOUSTIC SWEEP	0.007	0.20	920.67	33.1
736	1032	26-Feb-94	1:52:47	NULL CAM, RPM= 1092, ALFSU= 2.0DEG, VOR = 0.20, ACOUSTIC SWEEP	0.007	0.20	904.82	39.3
736	1049	26-Feb-94	1:59:15	NULL CAM, RPM= 1092, ALFSU= 2.0DEG, VOR = 0.20, ACOUSTIC SWEEP	0.007	0.20	917.34	38.9
739	1050	26-Feb-94	2:02:23	NULL CAM, RPM= 1091, ALFSU= 5.0DEG, VOR = 0.20, ACOUSTIC SWEEP	0.007	0.20	899.72	28.9
739	1067	26-Feb-94	2:08:50	NULL CAM, RPM= 1091, ALFSU= 5.0DEG, VOR = 0.20, ACOUSTIC SWEEP	0.007	0.20	914.25	28.3
740	1068	26-Feb-94	2:12:08	NULL CAM, RPM= 1093, ALFSU= 6.0DEG, VOR = 0.20, ACOUSTIC SWEEP	0.007	0.20	903.91	25.9
740	1085	26-Feb-94	2:18:34	NULL CAM, RPM= 1093, ALFSU= 6.0DEG, VOR = 0.20, ACOUSTIC SWEEP	0.007	0.20	907.02	25.1
745	1086	26-Feb-94	2:22:58	NULL CAM, RPM= 1093, ALFSU= 6.5 DEG, VOR = 0.20, ACOUSTIC SWEEP	0.008	0.20	1022.40	27.7
745	1103	26-Feb-94	2:29:19	NULL CAM, RPM= 1093, ALFSU= 6.5 DEG, VOR = 0.20, ACOUSTIC SWEEP	0.008	0.20	1034.50	27.2
744	1104	26-Feb-94	2:34:11	NULL CAM, RPM= 1095, ALFSU= 5.5 DEG, VOR = 0.20, ACOUSTIC SWEEP	0.008	0.20	1030.80	31.8
744	1121	26-Feb-94	2:49:21	NULL CAM, RPM= 1095, ALFSU= 5.5 DEG, VOR = 0.20, ACOUSTIC SWEEP	0.008	0.20	1036.70	31.6
743	1122	26-Feb-94	2:54:54	NULL CAM, RPM= 1095, ALFSU= 4.5 DEG, VOR = 0.20, ACOUSTIC SWEEP	0.008	0.20	1025.90	36.3
743	1139	26-Feb-94	3:01:25	NULL CAM, RPM= 1095, ALFSU= 4.5 DEG, VOR = 0.20, ACOUSTIC SWEEP	0.008	0.20	1037.70	35.8
742	1140	26-Feb-94	3:04:59	NULL CAM, RPM= 1095, ALFSU= 3.5 DEG, VOR = 0.20, ACOUSTIC SWEEP	0.008	0.20	1034.50	40.9
742	1157	26-Feb-94	3:13:28	NULL CAM, RPM= 1095, ALFSU= 3.5 DEG, VOR = 0.20, ACOUSTIC SWEEP	0.008	0.20	1045.10	40.1
741	1158	26-Feb-94	3:16:48	NULL CAM, RPM= 1095, ALFSU= 2.5 DEG, VOR = 0.20, ACOUSTIC SWEEP	0.008	0.20	1025.10	44.4
741	1175	26-Feb-94	3:23:24	NULL CAM, RPM= 1095, ALFSU= 2.5 DEG, VOR = 0.20, ACOUSTIC SWEEP	0.008	0.20	1029.80	44.2
45	1176	26-Feb-94	3:29:30	NULL CAM, RPM= 1087, ALFSU= 0.0 DEG, VOR = 0.00,	0.001	0.01	85.85	25.5
999	1177	26-Feb-94	3:31:01	NULL CAM, RPM= 0, ALFSU= 0.0 DEG, VOR = 0.00,	####	9.00	20.96	0.0
760	1178	26-Feb-94	4:19:09	NULL CAM, RPM= 1087, ALFSU= -0.914 DEG, VOR = 0.100,	0.006	0.10	778.83	65.2
761	1179	26-Feb-94	4:24:14	NULL CAM, RPM= 1087, ALFSU= -0.81 DEG, VOR = 0.100,	0.008	0.10	1040.10	93.0
760	1180	26-Feb-94	4:26:32	NULL CAM, RPM= 1087, ALFSU= -0.92 DEG, VOR = 0.100,	0.006	0.10	778.67	61.5
725	1181	26-Feb-94	4:32:35	NULL CAM, RPM= 1092, ALFSU= -3.24 DEG, VOR = 0.200,	0.006	0.20	780.29	53.0
726	1182	26-Feb-94	4:35:00	NULL CAM, RPM= 1092, ALFSU= -2.72 DEG, VOR = 0.200,	0.008	0.20	1040.70	71.7
736	1183	26-Feb-94	4:40:40	NULL CAM, RPM= 1092, ALFSU= 2.00 DEG, VOR = 0.200,	0.007	0.20	909.93	41.8
737	1184	26-Feb-94	4:43:07	NULL CAM, RPM= 1092, ALFSU= 3.00 DEG, VOR = 0.200,	0.007	0.20	903.47	37.5
739	1185	26-Feb-94	4:45:20	NULL CAM, RPM= 1092, ALFSU= 5.00 DEG, VOR = 0.200,	0.007	0.20	898.50	30.2
744	1186	26-Feb-94	4:48:12	NULL CAM, RPM= 1092, ALFSU= 5.50 DEG, VOR = 0.200,	0.008	0.20	1029.30	33.9
745	1187	26-Feb-94	4:51:17	NULL CAM, RPM= 1092, ALFSU= 6.50 DEG, VOR = 0.200,	0.008	0.20	1024.60	29.3
720	1188	26-Feb-94	4:59:40	NULL CAM, RPM= 1092, ALFSU= -1.61 DEG, VOR = 0.150,	0.008	0.15	1028.30	73.4
723	1189	26-Feb-94	5:02:55	NULL CAM, RPM= 1092, ALFSU= -1.89 DEG, VOR = 0.150,	0.006	0.15	778.15	52.5
762	1190	26-Feb-94	5:08:52	NULL CAM, RPM= 1092, ALFSU= 8.00 DEG, VOR = 0.150, ACOUSTIC SWEEP	0.007	0.15	892.61	32.6
762	1207	26-Feb-94	5:15:35	NULL CAM, RPM= 1092, ALFSU= 8.00 DEG, VOR = 0.150, ACOUSTIC SWEEP	0.007	0.15	910.41	32.5
726	1208	26-Feb-94	5:23:50	NULL CAM, RPM= 1093, ALFSU= -2.72 DEG, VOR = 0.200, ACOUSTIC SWEEP	0.008	0.20	1034.10	71.1
726	1226	26-Feb-94	5:35:13	NULL CAM, RPM= 1093, ALFSU= -2.72 DEG, VOR = 0.200, ACOUSTIC SWEEP	0.008	0.20	1051.30	70.6
45	1227	26-Feb-94	5:39:58	NULL CAM, RPM= 1087, ALFSU= 0.0 DEG, VOR = 0.000	0.001	0.00	75.73	25.1
999	1228	26-Feb-94	5:41:46	NULL CAM, RPM= 0, ALFSU= 0.0 DEG, VOR = 0.000	####	9.00	15.64	0.0
2045	1229	28-Feb-94	21:05:38	12.5+OCAM, RPM= 1087, ALFSU= 0.00 DEG, VOR = 0.000	0.001	0.00	-10.50	30.9
2045	1230	28-Feb-94	21:09:18	12.5+OCAM, RPM= 1087, ALFSU= 0.00 DEG, VOR = 0.000	0.001	0.00	-1.48	31.2
2706	1231	28-Feb-94	21:10:03	12.5+OCAM, RPM= 1087, ALFSU= 0.00 DEG, VOR = 0.000, COLL=1DEG	0.001	0.01	58.24	30.6
2047	1232	28-Feb-94	21:10:36	12.5+OCAM, RPM= 1087, ALFSU= 0.00 DEG, VOR = 0.000, COLL=2DEG	0.002	0.01	142.46	33.0
2707	1233	28-Feb-94	21:11:11	12.5+OCAM, RPM= 1087, ALFSU= 0.00 DEG, VOR = 0.000, COLL= 3 DEG	0.002	0.01	245.88	38.4
2049	1234	28-Feb-94	21:11:41	12.5+OCAM, RPM= 1087, ALFSU= 0.00 DEG, VOR = 0.000, COLL= 4 DEG	0.003	0.02	340.84	44.7
2708	1235	28-Feb-94	21:12:12	12.5+OCAM, RPM= 1087, ALFSU= 0.00 DEG, VOR = 0.000, COLL= 5 DEG	0.003	0.02	433.63	52.4
2051	1236	28-Feb-94	21:13:41	12.5+OCAM, RPM= 1087, ALFSU= 0.00 DEG, VOR = 0.000, COLL= 6 DEG	0.004	0.02	540.85	62.2
2052	1237	28-Feb-94	21:14:15	12.5+OCAM, RPM= 1087, ALFSU= 0.00 DEG, VOR = 0.000, COLL= 7 DEG	0.005	0.04	641.12	74.4
2709	1238	28-Feb-94	21:15:05	12.5+OCAM, RPM= 1087, ALFSU= 0.00 DEG, VOR = 0.000, COLL= 8 DEG	0.006	0.03	758.75	88.4
2710	1239	28-Feb-94	21:16:41	12.5+OCAM, RPM= 1087, ALFSU= 0.00 DEG, VOR = 0.000, COLL= 9 DEG	0.007	0.03	871.49	103.3
2711	1240	28-Feb-94	21:17:34	12.5+OCAM, RPM= 1087, ALFSU= 0.00 DEG, VOR = 0.000, COLL= 10DEG	0.008	0.02	1018.40	124.0
2045	1241	28-Feb-94	21:19:03	12.5+OCAM, RPM= 1087, ALFSU= 0.00 DEG, VOR = 0.000, COLL= 0DEG	0.001	0.00	3.64	31.7
2047	1242	28-Feb-94	21:19:48	12.5+OCAM, RPM= 1087, ALFSU= 0.00 DEG, VOR = 0.000, COLL= 2DEG	0.002	0.01	147.08	33.4
2047	1243	28-Feb-94	21:21:07	12.5+OCAM, RPM= 1087, ALFSU= 0.00 DEG, VOR = 0.000, COLL= 2DEG, LAT=2	0.001	0.01	148.97	34.5
2047	1244	28-Feb-94	21:21:45	12.5+OCAM, RPM= 1087, ALFSU= 0.00 DEG, VOR = 0.000, COLL= 2DEG, LAT=0	0.001	0.01	145.88	33.6
2047	1245	28-Feb-94	21:22:42	12.5+OCAM, RPM= 1087, ALFSU= 0.00 DEG, VOR = 0.000, COLL= 2DEG, LONG	0.001	0.01	157.11	33.9
2045	1246	28-Feb-94	21:23:41	12.5+OCAM, RPM= 1087, ALFSU= 0.00 DEG, VOR = 0.000, COLL= 0DEG, LONG	0.001	0.00	-3.88	31.9
2045	1247	28-Feb-94	21:51:08	12.5+OCAM, RPM= 1087, ALFSU= 0.00 DEG, VOR = 0.000, COLL= 0DEG, LONG	0.001	0.00	-34.02	31.5
2731	1248	28-Feb-94	22:08:08	12.5+OCAM, RPM= 1071, ALFSU= 3.00 DEG, VOR = 0.150, ACOUSTIC SWEEP	0.007	0.15	918.95	56.5
2731	1265	28-Feb-94	22:14:15	12.5+OCAM, RPM= 1071, ALFSU= 3.00 DEG, VOR = 0.150, ACOUSTIC SWEEP	0.007	0.15	918.37	56.2
2732	1266	28-Feb-94	22:25:02	12.5+OCAM, RPM= 1074, ALFSU= 4.00 DEG, VOR = 0.150, ACOUSTIC SWEEP	0.007	0.15	921.50	54.6
2732	1283	28-Feb-94	22:31:06	12.5+OCAM, RPM= 1074, ALFSU= 4.00 DEG, VOR = 0.150, ACOUSTIC SWEEP	0.007	0.15	923.08	54.1
2732	1284	28-Feb-94	22:33:49	12.5+OCAM, RPM= 1074, ALFSU= 4.00 DEG, VOR = 0.150, ACOUSTIC SWEEP	0.007	0.15	933.96	54.7
2732	1301	28-Feb-94	22:40:33	12.5+OCAM, RPM= 1074, ALFSU= 4.00 DEG, VOR = 0.150, ACOUSTIC SWEEP	0.007	0.15	931.06	54.7
2733	1302	28-Feb-94	22:43:01	12.5+OCAM, RPM= 1077, ALFSU= 5.00 DEG, VOR = 0.150, ACOUSTIC SWEEP	0.007	0.15	926.46	51.6
2733	1318	28-Feb-94	22:48:57	12.5+OCAM, RPM= 1077, ALFSU= 5.00 DEG, VOR = 0.150, ACOUSTIC SWEEP	0.007	0.15	927.27	51.3
2733	1319	28-Feb-94	22:49:19	12.5+OCAM, RPM= 1077, ALFSU= 5.00 DEG, VOR = 0.150, ACOUSTIC SWEEP	0.007	0.15	926.19	51.2
2734	1320	28-Feb-94	22:52:06	12.5+OCAM, RPM= 1077, ALFSU= 6.00 DEG, VOR = 0.150, ACOUSTIC SWEEP	0.007	0.15	920.29	48.6
2734	1337	28-Feb-94	22:58:14	12.5+OCAM, RPM= 1077, ALFSU= 6.00 DEG, VOR = 0.150, ACOUSTIC SWEEP	0.007	0.15	928.92	48.1
2735	1338	28-Feb-94	23:01:18	12.5+OCAM, RPM= 1077, ALFSU= 7.00 DEG, VOR = 0.150, ACOUSTIC SWEEP	0.007	0.15	915.73	45.2
2735	1355	28-Feb-94	23:07:19	12.5+OCAM, RPM= 1077, ALFSU= 7.00 DEG, VOR = 0.150, ACOUSTIC SWEEP	0.007	0.15	918.00	45.2
2045	1356	28-Feb-94	23:12:32	12.5+OCAM, RPM= 1087, ALFSU= 0.00 DEG, VOR = 0.000	0.001	0.01	-38.15	32.2
999	1357	28-Feb-94	23:13:58	12.5+OCAM, RPM= 0000, ALFSU= 0.00 DEG, VOR = 0.000	####	9.00	-42.55	0.0
2045	1358	1-Mar-94	0:01:30	12.5+OCAM, RPM= 1087, ALFSU= 0.00 DEG, VOR = 0.000	0.001	0.01	-31.40	32.2
2736	1359	1-Mar-94	0:11:38	12.5+OCAM, RPM= 1087, ALFSU= 2.00 DEG, VOR = 0.200	0.007	0.20	941.11	49.1
2736	1376	1-Mar-94	0:18:01	12.5+OCAM, RPM= 1087, ALFSU= 2.00 DEG, VOR = 0.200	0.007	0.20	964.69	48.6
2737	1377	1-Mar-94	0:21:07	12.5+OCAM, RPM= 1087, ALFSU= 3.00 DEG, VOR = 0.200	0.007	0.20	920.55	43.7
2737	1394	1-Mar-94	0:27:31	12.5+OCAM, RPM= 1087, ALFSU= 3.00 DEG, VOR = 0.200	0.007	0.20	936.60	42.7
2738	1395	1-Mar-94	0:30:18	12.5+OCAM, RPM= 1087, ALFSU= 4.00 DEG, VOR = 0.200, ACOUSTIC SWEEP	0.007	0.20	926.97	39.6
2738	1412	1-Mar-94	0:36:55	12.5+OCAM, RPM= 1087, ALFSU= 4.00 DEG, VOR = 0.200, ACOUSTIC SWEEP	0.007	0.20	938.73	39.3



TEST	POINT	DATE			CT	Mu	Lift (lbs)	HP
2739	1413	1-Mar-94	0:39:29	12.5+0CAM, RPM= 1087, ALFSU= 5.00 DEG, VOR = 0.20, ACOUSTIC SWEEP	0.007	0.20	919.13	35.3
2739	1430	1-Mar-94	0:45:41	12.5+0CAM, RPM= 1087, ALFSU= 5.00 DEG, VOR = 0.20, ACOUSTIC SWEEP	0.007	0.20	926.44	35.0
2740	1431	1-Mar-94	0:52:10	12.5+0CAM, RPM= 1087, ALFSU= 6.00 DEG, VOR = 0.20, ACOUSTIC SWEEP	0.007	0.20	922.16	32.7
2740	1448	1-Mar-94	0:58:41	12.5+0CAM, RPM= 1087, ALFSU= 6.00 DEG, VOR = 0.20, ACOUSTIC SWEEP	0.007	0.20	934.34	32.2
2045	1449	1-Mar-94	1:54:30	12.5+0CAM, RPM= 1087, ALFSU= 0.00 DEG, VOR = 0.00	0.001	0.00	-30.08	31.7
2741	1450	1-Mar-94	2:04:18	12.5+0CAM, RPM= 1087, ALFSU= 2.50 DEG, VOR = 0.20, ACOUSTIC SWEEP	0.008	0.20	1081.80	53.1
2741	1467	1-Mar-94	2:10:38	12.5+0CAM, RPM= 1087, ALFSU= 2.50 DEG, VOR = 0.20, ACOUSTIC SWEEP	0.008	0.20	1082.30	52.1
2742	1468	1-Mar-94	2:13:03	12.5+0CAM, RPM= 1087, ALFSU= 3.50 DEG, VOR = 0.20, ACOUSTIC SWEEP	0.008	0.20	1059.10	46.8
2742	1485	1-Mar-94	2:19:42	12.5+0CAM, RPM= 1087, ALFSU= 3.50 DEG, VOR = 0.20, ACOUSTIC SWEEP	0.008	0.20	1079.90	46.2
2743	1486	1-Mar-94	2:22:10	12.5+0CAM, RPM= 1087, ALFSU= 4.50 DEG, VOR = 0.20, ACOUSTIC SWEEP	0.008	0.20	1058.00	42.5
2743	1503	1-Mar-94	2:28:39	12.5+0CAM, RPM= 1087, ALFSU= 4.50 DEG, VOR = 0.20, ACOUSTIC SWEEP	0.008	0.20	1070.70	41.4
2744	1504	1-Mar-94	2:31:46	12.5+0CAM, RPM= 1087, ALFSU= 5.50 DEG, VOR = 0.20, ACOUSTIC SWEEP	0.008	0.20	1059.00	37.9
2744	1521	1-Mar-94	2:37:50	12.5+0CAM, RPM= 1087, ALFSU= 5.50 DEG, VOR = 0.20, ACOUSTIC SWEEP	0.008	0.20	1065.50	37.3
2745	1522	1-Mar-94	2:40:33	12.5+0CAM, RPM= 1087, ALFSU= 6.50 DEG, VOR = 0.20, ACOUSTIC SWEEP	0.008	0.20	1048.70	33.9
2745	1539	1-Mar-94	2:47:36	12.5+0CAM, RPM= 1087, ALFSU= 6.50 DEG, VOR = 0.20, ACOUSTIC SWEEP	0.008	0.20	1057.20	33.0
2746	1540	1-Mar-94	2:50:52	12.5+0CAM, RPM= 1087, ALFSU= 7.50 DEG, VOR = 0.20, ACOUSTIC SWEEP	0.008	0.20	1045.90	29.7
2746	1557	1-Mar-94	2:57:04	12.5+0CAM, RPM= 1087, ALFSU= 7.50 DEG, VOR = 0.20, ACOUSTIC SWEEP	0.008	0.20	1054.40	29.1
2747	1558	1-Mar-94	3:03:01	12.5+0CAM, RPM= 1087, ALFSU= 8.50 DEG, VOR = 0.20, ACOUSTIC SWEEP	0.008	0.20	1040.80	26.2
2747	1575	1-Mar-94	3:09:30	12.5+0CAM, RPM= 1087, ALFSU= 8.50 DEG, VOR = 0.20, ACOUSTIC SWEEP	0.008	0.20	1048.20	25.6
2045	1576	1-Mar-94	3:17:55	12.5+0CAM, RPM= 1087, ALFSU= 0.00 DEG, VOR = 0.00	0.001	0.00	51.34	31.4
999	1577	1-Mar-94	3:18:37	12.5+0CAM, RPM= 0000, ALFSU= 0.00 DEG, VOR = 0.00	####	0.00	42.08	0.0
2045	1578	1-Mar-94	4:09:49	12.5+0CAM, RPM= 1087, ALFSU= 0.00 DEG, VOR = 0.00	0.001	0.01	-32.79	31.5
2900	1579	1-Mar-94	4:17:51	12.5-10CAM, RPM= 1076, ALFSU= 3.00 DEG, VOR = 0.15, ACOUSTIC SWEEP	0.007	0.15	928.24	54.4
2900	1596	1-Mar-94	4:24:04	12.5-10CAM, RPM= 1076, ALFSU= 3.00 DEG, VOR = 0.15, ACOUSTIC SWEEP	0.007	0.15	950.53	54.3
2902	1597	1-Mar-94	4:28:13	12.5-10CAM, RPM= 1077, ALFSU= 5.00 DEG, VOR = 0.15, ACOUSTIC SWEEP	0.007	0.15	931.77	47.6
2902	1614	1-Mar-94	4:34:53	12.5-10CAM, RPM= 1077, ALFSU= 5.00 DEG, VOR = 0.15, ACOUSTIC SWEEP	0.007	0.15	941.44	47.4
2904	1615	1-Mar-94	4:37:35	12.5-10CAM, RPM= 1077, ALFSU= 7.00 DEG, VOR = 0.15, ACOUSTIC SWEEP	0.007	0.15	914.58	40.6
2904	1632	1-Mar-94	4:43:44	12.5-10CAM, RPM= 1077, ALFSU= 7.00 DEG, VOR = 0.15, ACOUSTIC SWEEP	0.007	0.15	917.15	40.0
2905	1633	1-Mar-94	4:49:34	12.5-10CAM, RPM= 1080, ALFSU= 2.00 DEG, VOR = 0.20, ACOUSTIC SWEEP	0.007	0.20	923.03	45.6
2905	1650	1-Mar-94	4:55:39	12.5-10CAM, RPM= 1080, ALFSU= 2.00 DEG, VOR = 0.20, ACOUSTIC SWEEP	0.007	0.20	933.42	45.0
2045	1651	1-Mar-94	18:17:25	12.5+10CAM, RPM= 1087, ALFSU= 0.00 DEG, VOR = 0.00	0.001	0.01	-22.28	30.2
2706	1652	1-Mar-94	18:18:05	12.5+10CAM, RPM= 1087, ALFSU= 0.00 DEG, VOR = 0.00, COLL=1DEG	0.001	0.01	37.20	29.9
2047	1653	1-Mar-94	18:18:45	12.5+10CAM, RPM= 1087, ALFSU= 0.00 DEG, VOR = 0.00, COLL=2DEG	0.001	0.02	132.62	31.9
2707	1654	1-Mar-94	18:19:16	12.5+10CAM, RPM= 1087, ALFSU= 0.00 DEG, VOR = 0.00, COLL=3DEG	0.002	0.02	234.39	37.4
2049	1655	1-Mar-94	18:19:44	12.5+10CAM, RPM= 1087, ALFSU= 0.00 DEG, VOR = 0.00, COLL=4DEG	0.003	0.02	324.48	43.7
2708	1656	1-Mar-94	18:20:19	12.5+10CAM, RPM= 1087, ALFSU= 0.00 DEG, VOR = 0.00, COLL=5DEG	0.003	0.02	420.44	51.4
2051	1657	1-Mar-94	18:20:48	12.5+10CAM, RPM= 1087, ALFSU= 0.00 DEG, VOR = 0.00, COLL=6DEG	0.004	0.02	523.38	61.5
2052	1658	1-Mar-94	18:21:23	12.5+10CAM, RPM= 1087, ALFSU= 0.00 DEG, VOR = 0.00, COLL=7DEG	0.006	0.02	636.63	73.8
2709	1659	1-Mar-94	18:21:58	12.5+10CAM, RPM= 1087, ALFSU= 0.00 DEG, VOR = 0.00, COLL=8DEG	0.006	0.03	746.04	86.8
2710	1660	1-Mar-94	18:22:38	12.5+10CAM, RPM= 1087, ALFSU= 0.00 DEG, VOR = 0.00, COLL=9DEG	0.007	0.03	876.82	103.6
2045	1661	1-Mar-94	18:24:12	12.5+10CAM, RPM= 1087, ALFSU= 0.00 DEG, VOR = 0.00, COLL=0DEG	0.001	0.01	15.02	30.2
2736	1662	1-Mar-94	18:32:50	12.5+10CAM, RPM= 1076, ALFSU= 2.00 DEG, VOR = 0.20, ACOUSTIC SWEEP	0.007	0.20	926.07	47.0
2736	1679	1-Mar-94	18:38:52	12.5+10CAM, RPM= 1076, ALFSU= 2.00 DEG, VOR = 0.20, ACOUSTIC SWEEP	0.007	0.20	929.12	45.8
2738	1680	1-Mar-94	18:41:29	12.5+10CAM, RPM= 1079, ALFSU= 4.00 DEG, VOR = 0.20, ACOUSTIC SWEEP	0.007	0.20	915.72	38.9
2738	1698	1-Mar-94	18:49:55	12.5+10CAM, RPM= 1079, ALFSU= 4.00 DEG, VOR = 0.20, ACOUSTIC SWEEP	0.007	0.20	919.49	37.7
2740	1699	1-Mar-94	18:52:35	12.5+10CAM, RPM= 1079, ALFSU= 6.00 DEG, VOR = 0.20, ACOUSTIC SWEEP	0.007	0.20	920.14	31.4
2740	1716	1-Mar-94	18:58:34	12.5+10CAM, RPM= 1079, ALFSU= 6.00 DEG, VOR = 0.20, ACOUSTIC SWEEP	0.007	0.20	917.37	30.7
2741	1717	1-Mar-94	19:02:35	12.5+10CAM, RPM= 1082, ALFSU= 2.50 DEG, VOR = 0.20, ACOUSTIC SWEEP	0.008	0.20	1047.30	51.9
2741	1734	1-Mar-94	19:08:34	12.5+10CAM, RPM= 1082, ALFSU= 2.50 DEG, VOR = 0.20, ACOUSTIC SWEEP	0.008	0.20	1056.30	51.6
2743	1735	1-Mar-94	19:11:35	12.5+10CAM, RPM= 1083, ALFSU= 4.50 DEG, VOR = 0.20, ACOUSTIC SWEEP	0.008	0.20	1049.10	43.7
2743	1752	1-Mar-94	19:17:56	12.5+10CAM, RPM= 1083, ALFSU= 4.50 DEG, VOR = 0.20, ACOUSTIC SWEEP	0.008	0.20	1046.60	42.7
2745	1753	1-Mar-94	19:20:37	12.5+10CAM, RPM= 1083, ALFSU= 6.50 DEG, VOR = 0.20, ACOUSTIC SWEEP	0.008	0.20	1036.50	35.2
2745	1770	1-Mar-94	19:26:37	12.5+10CAM, RPM= 1083, ALFSU= 6.50 DEG, VOR = 0.20, ACOUSTIC SWEEP	0.008	0.20	1043.50	35.2
2045	1771	1-Mar-94	19:32:02	12.5+10CAM, RPM= 1087, ALFSU= 0.00 DEG, VOR = 0.00	0.001	0.01	-26.49	30.7
999	1772	1-Mar-94	19:33:03	12.5+10CAM, RPM= 0000, ALFSU= 0.00 DEG, VOR = 0.00	####	9.00	-41.06	0.0
2045	1773	1-Mar-94	21:02:13	12.5-10CAM, RPM= 1087, ALFSU= 0.00 DEG, VOR = 0.00	0.001	0.01	-19.89	29.1
2900	1774	1-Mar-94	21:09:36	12.5-10CAM, RPM= 1074, ALFSU= 3.00 DEG, VOR = 0.15, ACOUSTIC SWEEP	0.007	0.15	923.06	53.8
2900	1791	1-Mar-94	21:16:42	12.5-10CAM, RPM= 1074, ALFSU= 3.00 DEG, VOR = 0.15, ACOUSTIC SWEEP	0.007	0.15	938.59	53.6
2901	1792	1-Mar-94	21:19:23	12.5-10CAM, RPM= 1077, ALFSU= 5.00 DEG, VOR = 0.15, ACOUSTIC SWEEP	0.007	0.15	922.47	47.5
2901	1809	1-Mar-94	21:25:41	12.5-10CAM, RPM= 1077, ALFSU= 5.00 DEG, VOR = 0.15, ACOUSTIC SWEEP	0.007	0.15	938.33	47.3
2902	1810	1-Mar-94	21:27:57	12.5-10CAM, RPM= 1077, ALFSU= 7.00 DEG, VOR = 0.15, ACOUSTIC SWEEP	0.007	0.15	920.38	40.7
2902	1827	1-Mar-94	21:33:57	12.5-10CAM, RPM= 1077, ALFSU= 7.00 DEG, VOR = 0.15, ACOUSTIC SWEEP	0.007	0.15	926.81	40.4
2909	1828	1-Mar-94	21:36:29	12.5-10CAM, RPM= 1078, ALFSU= 6.00 DEG, VOR = 0.15, ACOUSTIC SWEEP	0.007	0.15	917.66	43.2
2909	1845	1-Mar-94	21:42:32	12.5-10CAM, RPM= 1078, ALFSU= 6.00 DEG, VOR = 0.15, ACOUSTIC SWEEP	0.007	0.15	914.88	43.1
2910	1846	1-Mar-94	21:45:04	12.5-10CAM, RPM= 1078, ALFSU= 4.00 DEG, VOR = 0.15, ACOUSTIC SWEEP	0.007	0.15	924.33	50.7
2910	1863	1-Mar-94	21:51:34	12.5-10CAM, RPM= 1078, ALFSU= 4.00 DEG, VOR = 0.15, ACOUSTIC SWEEP	0.007	0.15	939.11	50.2
2903	1864	1-Mar-94	21:57:10	12.5-10CAM, RPM= 1080, ALFSU= 2.00 DEG, VOR = 0.20, ACOUSTIC SWEEP	0.007	0.20	926.28	46.7
2903	1881	1-Mar-94	22:03:10	12.5-10CAM, RPM= 1080, ALFSU= 2.00 DEG, VOR = 0.20, ACOUSTIC SWEEP	0.007	0.20	928.65	46.2
2911	1882	1-Mar-94	22:05:50	12.5-10CAM, RPM= 1080, ALFSU= 3.00 DEG, VOR = 0.20, ACOUSTIC SWEEP	0.007	0.20	916.50	42.9
2911	1896	1-Mar-94	22:12:59	12.5-10CAM, RPM= 1080, ALFSU= 3.00 DEG, VOR = 0.20, ACOUSTIC SWEEP	0.007	0.20	925.07	42.2
2904	1899	1-Mar-94	22:17:03	12.5-10CAM, RPM= 1081, ALFSU= 4.00 DEG, VOR = 0.20, ACOUSTIC SWEEP	0.007	0.20	915.97	39.0
2904	1916	1-Mar-94	22:23:41	12.5-10CAM, RPM= 1081, ALFSU= 4.00 DEG, VOR = 0.20, ACOUSTIC SWEEP	0.007	0.20	922.79	38.3
2912	1917	1-Mar-94	22:26:09	12.5-10CAM, RPM= 1081, ALFSU= 5.00 DEG, VOR = 0.20, ACOUSTIC SWEEP	0.007	0.20	923.21	36.0
2912	1934	1-Mar-94	22:32:09	12.5-10CAM, RPM= 1081, ALFSU= 5.00 DEG, VOR = 0.20, ACOUSTIC SWEEP	0.007	0.20	921.88	36.0
2905	1935	1-Mar-94	22:34:43	12.5-10CAM, RPM= 1081, ALFSU= 6.00 DEG, VOR = 0.20, ACOUSTIC SWEEP	0.007	0.20	912.03	33.2
2905	1952	1-Mar-94	22:40:48	12.5-10CAM, RPM= 1081, ALFSU= 6.00 DEG, VOR = 0.20, ACOUSTIC SWEEP	0.007	0.20	921.47	32.1
2905	1963	1-Mar-94	22:42:27	12.5-10CAM, RPM= 1081, ALFSU= 6.00 DEG, VOR = 0.20, ACOUSTIC SWEEP	0.007	0.20	914.62	33.8
2905	1970	1-Mar-94	22:50:32	12.5-10CAM, RPM= 1081, ALFSU= 6.00 DEG, VOR = 0.20, ACOUSTIC SWEEP	0.007	0.20	927.19	31.9
2908	1971	1-Mar-94	22:54:54	12.5-10CAM, RPM= 1082, ALFSU= 2.50 DEG, VOR = 0.20, ACOUSTIC SWEEP	0.008	0.20	1057.30	52.2
2908	1988	1-Mar-94	23:00:56	12.5-10CAM, RPM= 1082, ALFSU= 2.50 DEG, VOR = 0.20, ACOUSTIC SWEEP	0.008	0.20	1065.00	52.1
2913	1989	1-Mar-94	23:03:13	12.5-10CAM, RPM= 1082, ALFSU= 3.50 DEG, VOR = 0.20, ACOUSTIC SWEEP	0.008	0.20	1056.00	48.5
2913	2006	1-Mar-94	23:09:17	12.5-10CAM, RPM= 1082, ALFSU= 3.50 DEG, VOR = 0.20, ACOUSTIC SWEEP	0.008	0.20	1066.70	47.4
2907	2007	1-Mar-94	23:12:02	12.5-10CAM, RPM= 1082, ALFSU= 4.50 DEG, VOR = 0.20, ACOUSTIC SWEEP	0.008	0.20	1052.00	43.5
2907	2024	1-Mar-94	23:18:37	12.5-10CAM, RPM= 1082, ALFSU= 4.50 DEG, VOR = 0.20, ACOUSTIC SWEEP	0.008	0.20	1059.00	42.8
2914	2025	1-Mar-94	23:20:59	12.5-10CAM, RPM= 1082, ALFSU= 5.50 DEG, VOR = 0.20, ACOUSTIC SWEEP	0.008	0.20	1037.30	39.5



TEST	POINT	DATE		CT	Mu	Lift (lbs)	HP
8046	2321	2-Mar-94	21:14:21 3+101.7CAM, RPM= 1102, ALFSU=-4.19 DEG, VOR = 0.25	0.008	0.25	1013.50	74.5
8047	2322	2-Mar-94	21:19:20 3+101.7CAM, RPM= 1106, ALFSU=-7.38 DEG, VOR = 0.30	0.006	0.30	776.70	75.5
8048	2323	2-Mar-94	21:21:16 3+101.7CAM, RPM= 1108, ALFSU=-6.12 DEG, VOR = 0.30	0.008	0.30	1016.70	96.3
8006	2324	2-Mar-94	21:28:09 3+101.7CAM, RPM= 1087, ALFSU= 0.00 DEG, VOR = 0.00	0.001	0.01	35.32	23.7
999	2325	2-Mar-94	21:29:23 3+101.7CAM, RPM= 0000, ALFSU= 0.00 DEG, VOR = 0.00	####	9.00	13.28	0.0
8006	2326	2-Mar-94	22:10:46 3+146.7 CAM, RPM= 10870, ALFSU= 0.00 DEG, VOR = 0.00	0.001	0.01	-4.35	24.1
8049	2327	2-Mar-94	22:16:18 3+146.7 CAM, RPM= 1096, ALFSU=-1.89 DEG, VOR = 0.15	0.006	0.15	762.56	56.1
8050	2328	2-Mar-94	22:18:08 3+146.7 CAM, RPM= 1096, ALFSU=-1.61 DEG, VOR = 0.15	0.008	0.15	1017.20	77.9
8051	2329	2-Mar-94	22:21:59 3+146.7 CAM, RPM= 1099, ALFSU=-3.24 DEG, VOR = 0.20	0.006	0.20	764.97	53.9
8052	2330	2-Mar-94	22:25:42 3+146.7 CAM, RPM= 1099, ALFSU=-2.72 DEG, VOR = 0.20	0.008	0.20	1020.40	73.7
8052	2347	2-Mar-94	22:31:47 3+146.7 CAM, RPM= 1099, ALFSU=-2.72 DEG, VOR = 0.20	0.008	0.20	1038.80	73.1
8053	2348	2-Mar-94	22:36:22 3+146.7 CAM, RPM= 1103, ALFSU=-5.30 DEG, VOR = 0.25	0.006	0.25	782.22	61.1
8054	2349	2-Mar-94	22:38:49 3+146.7 CAM, RPM= 1103, ALFSU=-4.19 DEG, VOR = 0.25	0.008	0.25	1031.10	78.2
8055	2350	2-Mar-94	22:42:38 3+146.7 CAM, RPM= 1106, ALFSU=-7.38 DEG, VOR = 0.30	0.006	0.30	761.18	74.7
8056	2351	2-Mar-94	22:44:54 3+146.7 CAM, RPM= 1108, ALFSU=-6.12 DEG, VOR = 0.30	0.008	0.30	1019.20	92.7
8006	2352	2-Mar-94	22:49:56 3+146.7 CAM, RPM= 1087, ALFSU= 0.00 DEG, VOR = 0.00	0.001	0.00	37.36	24.1
999	2353	2-Mar-94	22:50:57 3+146.7 CAM, RPM= 0000, ALFSU= 0.00 DEG, VOR = 0.00	####	0.00	7.13	0.0
3045	2354	3-Mar-94	0:04:49 3+146.7 CAM, RPM= 1087, ALFSU= 0.00 DEG, VOR = 0.00	0.001	0.00	-11.27	34.0
3046	2355	3-Mar-94	0:05:47 3+146.7 CAM, RPM= 1087, COLL = 1.0 DEG, ALFSU= 0.00 DEG, VOR = 0.00	0.001	0.01	41.75	33.5
3047	2356	3-Mar-94	0:06:36 17.5-20 CAM, RPM= 1087, COLL = 2.0 DEG, ALFSU= 0.00 DEG, VOR = 0.00	0.002	0.02	123.75	34.9
3048	2357	3-Mar-94	0:07:18 17.5-20 CAM, RPM= 1087, COLL = 3.0 DEG, ALFSU= 0.00 DEG, VOR = 0.00	0.002	0.02	227.10	39.4
3049	2358	3-Mar-94	0:07:50 17.5-20 CAM, RPM= 1087, COLL = 4.0 DEG, ALFSU= 0.00 DEG, VOR = 0.00	0.003	0.02	316.26	44.9
3708	2359	3-Mar-94	0:08:29 17.5-20 CAM, RPM= 1087, COLL = 5.0 DEG, ALFSU= 0.00 DEG, VOR = 0.00	0.003	0.02	406.03	52.5
3051	2361	3-Mar-94	0:09:34 17.5-20 CAM, RPM= 1087, COLL = 6.0 DEG, ALFSU= 0.00 DEG, VOR = 0.00	0.004	0.03	504.83	62.0
3052	2362	3-Mar-94	0:10:16 17.5-20 CAM, RPM= 1087, COLL = 7.0 DEG, ALFSU= 0.00 DEG, VOR = 0.00	0.005	0.03	622.16	73.7
3709	2363	3-Mar-94	0:11:06 17.5-20 CAM, RPM= 1087, COLL = 8.0 DEG, ALFSU= 0.00 DEG, VOR = 0.00	0.006	0.03	724.57	85.2
3710	2364	3-Mar-94	0:11:48 17.5-20 CAM, RPM= 1087, COLL = 9.0 DEG, ALFSU= 0.00 DEG, VOR = 0.00	0.007	0.03	825.83	99.2
3711	2365	3-Mar-94	0:12:46 17.5-20 CAM, RPM= 1087, COLL = 10.0 DEG, ALFSU= 0.00 DEG, VOR = 0.00	0.007	0.03	943.26	116.8
3045	2366	3-Mar-94	0:14:14 17.5-20 CAM, RPM= 1087, COLL = 0.0 DEG, ALFSU= 0.00 DEG, VOR = 0.00	0.001	0.00	9.19	33.8
3047	2367	3-Mar-94	0:14:56 17.5-20 CAM, RPM= 1087, COLL = 2.0 DEG, ALFSU= 0.00 DEG, VOR = 0.00	0.002	0.01	139.18	34.8
3047	2368	3-Mar-94	0:16:47 17.5-20 CAM, RPM= 1087, COLL = 2.0 DEG, LAT = 2.0 DEG	0.002	0.01	142.10	36.0
3047	2369	3-Mar-94	0:18:36 17.5-20 CAM, RPM= 1087, COLL = 2.0 DEG, LONG = 2.0 DEG	0.002	0.01	162.41	36.5
3045	2370	3-Mar-94	0:19:49 17.5-20 CAM, RPM= 1087, COLL = 0.0 DEG, LONG = 0.0 DEG	0.001	0.00	13.09	35.2
3731	2371	3-Mar-94	0:27:23 17.5-20 CAM, RPM= 1087, ALFSU = 3.0 DEG, VOR = 0.150	0.007	0.15	884.42	57.6
3731	2388	3-Mar-94	0:33:28 17.5-20 CAM, RPM= 1087, ALFSU = 3.0 DEG, VOR = 0.150	0.007	0.15	892.35	56.7
3732	2389	3-Mar-94	0:35:58 17.5-20 CAM, RPM= 1087, ALFSU = 4.0 DEG, VOR = 0.150, CT/SIGMA = .076	0.007	0.15	888.17	54.4
3732	2408	3-Mar-94	0:42:12 17.5-20 CAM, RPM= 1087, ALFSU = 4.0 DEG, VOR = 0.150, CT/SIGMA = .076	0.007	0.15	893.67	54.1
3733	2407	3-Mar-94	0:44:31 17.5-20 CAM, RPM= 1087, ALFSU = 5.0 DEG, VOR = 0.150, CT/SIGMA = .076	0.007	0.15	889.06	52.1
3733	2424	3-Mar-94	0:50:52 17.5-20 CAM, RPM= 1087, ALFSU = 5.0 DEG, VOR = 0.150, CT/SIGMA = .076	0.007	0.15	897.56	51.4
3734	2425	3-Mar-94	0:53:59 17.5-20 CAM, RPM= 1087, ALFSU = 6.0 DEG, VOR = 0.150, CT/SIGMA = .076	0.007	0.15	880.93	47.6
3734	2442	3-Mar-94	1:00:04 17.5-20 CAM, RPM= 1087, ALFSU = 6.0 DEG, VOR = 0.150, CT/SIGMA = .076	0.007	0.15	883.40	47.5
3735	2443	3-Mar-94	1:02:28 17.5-20 CAM, RPM= 1087, ALFSU = 7.0 DEG, VOR = 0.150, CT/SIGMA = .076	0.007	0.15	873.96	45.1
3735	2461	3-Mar-94	1:08:29 17.5-20 CAM, RPM= 1087, ALFSU = 7.0 DEG, VOR = 0.150, CT/SIGMA = .076	0.007	0.15	880.16	44.9
3045	2461	3-Mar-94	1:15:59 17.5-20 CAM, RPM= 1087, ALFSU = 0.0 DEG, VOR = 0.00, CT/SIGMA = .000	0.001	0.00	8.36	34.9
999	2462	3-Mar-94	1:19:32 17.5-20 CAM, RPM= 0000, ALFSU = 0.0 DEG, VOR = 0.00, CT/SIGMA = .000	####	0.00	7.62	0.0
3045	2463	3-Mar-94	3:49:28 17.5-20 CAM, RPM= 1087, ALFSU = 0.0 DEG, VOR = 0.00, CT/SIGMA = .000	0.001	0.01	-29.01	33.8
3736	2464	3-Mar-94	3:57:38 17.5-20 CAM, RPM= 1080, ALFSU = 2.0 DEG, VOR = 0.20, CT/SIGMA = .076	0.007	0.20	901.88	50.4
3736	2481	3-Mar-94	4:04:17 17.5-20 CAM, RPM= 1080, ALFSU = 2.0 DEG, VOR = 0.20, CT/SIGMA = .076	0.007	0.20	928.14	50.2
3737	2482	3-Mar-94	4:06:47 17.5-20 CAM, RPM= 1080, ALFSU = 3.0 DEG, VOR = 0.20, CT/SIGMA = .076	0.007	0.20	885.49	45.9
3737	2489	3-Mar-94	4:13:01 17.5-20 CAM, RPM= 1080, ALFSU = 3.0 DEG, VOR = 0.20, CT/SIGMA = .076	0.007	0.20	907.31	45.8
3738	2500	3-Mar-94	4:15:31 17.5-20 CAM, RPM= 1080, ALFSU = 4.0 DEG, VOR = 0.20, CT/SIGMA = .076	0.007	0.20	881.08	42.5
3738	2517	3-Mar-94	4:22:13 17.5-20 CAM, RPM= 1080, ALFSU = 4.0 DEG, VOR = 0.20, CT/SIGMA = .076	0.007	0.20	890.72	40.7
3739	2518	3-Mar-94	4:24:36 17.5-20 CAM, RPM= 1085, ALFSU = 5.0 DEG, VOR = 0.20, CT/SIGMA = .076	0.007	0.20	879.20	37.8
3740	2536	3-Mar-94	5:00:35 17.5-20 CAM, RPM= 1085, ALFSU = 6.0 DEG, VOR = 0.20, CT/SIGMA = .076	0.007	0.20	876.10	35.4
3740	2553	3-Mar-94	5:07:45 17.5-20 CAM, RPM= 1085, ALFSU = 6.0 DEG, VOR = 0.20, CT/SIGMA = .076	0.007	0.20	883.97	34.2
3743	2554	3-Mar-94	5:10:21 17.5-20 CAM, RPM= 1085, ALFSU = 6.5 DEG, VOR = 0.20, CT/SIGMA = .087	0.008	0.20	998.81	37.7
3743	2571	3-Mar-94	5:16:31 17.5-20 CAM, RPM= 1085, ALFSU = 6.5 DEG, VOR = 0.20, CT/SIGMA = .087	0.008	0.20	1008.80	37.1
3745	2572	3-Mar-94	5:19:12 17.5-20 CAM, RPM= 1085, ALFSU = 5.5 DEG, VOR = 0.20, CT/SIGMA = .087	0.008	0.20	997.98	41.8
3745	2589	3-Mar-94	5:25:24 17.5-20 CAM, RPM= 1085, ALFSU = 5.5 DEG, VOR = 0.20, CT/SIGMA = .087	0.008	0.20	1008.00	41.1
3744	2590	3-Mar-94	5:27:47 17.5-20 CAM, RPM= 1085, ALFSU = 4.5 DEG, VOR = 0.20, CT/SIGMA = .087	0.008	0.20	1010.20	46.1
3744	2607	3-Mar-94	5:34:40 17.5-20 CAM, RPM= 1086, ALFSU = 4.5 DEG, VOR = 0.20, CT/SIGMA = .087	0.008	0.20	1021.50	45.8
3742	2608	3-Mar-94	5:37:07 17.5-20 CAM, RPM= 1086, ALFSU = 3.5 DEG, VOR = 0.20, CT/SIGMA = .087	0.008	0.20	1017.00	49.8
3742	2627	3-Mar-94	5:46:27 17.5-20 CAM, RPM= 1086, ALFSU = 3.5 DEG, VOR = 0.20, CT/SIGMA = .087	0.008	0.20	1025.50	49.8
3741	2628	3-Mar-94	5:48:59 17.5-20 CAM, RPM= 1086, ALFSU = 2.5 DEG, VOR = 0.20, CT/SIGMA = .087	0.008	0.20	1016.00	54.4
3741	2645	3-Mar-94	5:55:48 17.5-20 CAM, RPM= 1086, ALFSU = 2.5 DEG, VOR = 0.20, CT/SIGMA = .087	0.008	0.20	1026.30	54.0
3045	2646	3-Mar-94	5:59:31 17.5-20 CAM, RPM= 1087, ALFSU = 0.0 DEG, VOR = 0.00, CT/SIGMA = .000	0.001	0.00	18.07	34.6
999	2647	3-Mar-94	6:00:38 17.5-20 CAM, RPM= 0000, ALFSU = 0.0 DEG, VOR = 0.00, CT/SIGMA = .000	####	0.00	30.25	0.0
3145	2648	3-Mar-94	18:38:24 17.5+OCAM, RPM= 1087, ALFSU = 0.0 DEG, VOR = 0.00, CT/SIGMA = .000	0.001	0.01	-31.11	34.3
3900	2648	3-Mar-94	18:50:04 17.5+OCAM, RPM= 1076, ALFSU = 3.0 DEG, VOR = 0.15, CT/SIGMA = .076	0.007	0.15	898.04	55.4
3900	2666	3-Mar-94	18:56:16 17.5+OCAM, RPM= 1076, ALFSU = 3.0 DEG, VOR = 0.15, CT/SIGMA = .076	0.007	0.15	907.65	55.7
3901	2667	3-Mar-94	18:58:34 17.5+OCAM, RPM= 1079, ALFSU = 4.0 DEG, VOR = 0.15, CT/SIGMA = .076	0.007	0.15	898.17	53.0
3901	2684	3-Mar-94	19:04:32 17.5+OCAM, RPM= 1079, ALFSU = 4.0 DEG, VOR = 0.15, CT/SIGMA = .076	0.007	0.15	898.14	53.2
3902	2685	3-Mar-94	19:06:23 17.5+OCAM, RPM= 1080, ALFSU = 5.0 DEG, VOR = 0.15, CT/SIGMA = .076	0.007	0.15	893.13	51.1
3902	2702	3-Mar-94	19:12:40 17.5+OCAM, RPM= 1080, ALFSU = 5.0 DEG, VOR = 0.15, CT/SIGMA = .076	0.007	0.15	893.18	50.0
3903	2703	3-Mar-94	19:14:41 17.5+OCAM, RPM= 1080, ALFSU = 6.0 DEG, VOR = 0.15, CT/SIGMA = .076	0.007	0.15	887.53	48.2
3903	2720	3-Mar-94	19:20:48 17.5+OCAM, RPM= 1080, ALFSU = 6.0 DEG, VOR = 0.15, CT/SIGMA = .076	0.007	0.15	886.85	48.6
3904	2721	3-Mar-94	19:22:46 17.5+OCAM, RPM= 1080, ALFSU = 7.0 DEG, VOR = 0.15, CT/SIGMA = .076	0.007	0.15	886.63	48.8
3904	2738	3-Mar-94	19:28:51 17.5+OCAM, RPM= 1080, ALFSU = 7.0 DEG, VOR = 0.15, CT/SIGMA = .076	0.007	0.15	885.77	46.0
3145	2739	3-Mar-94	19:33:42 17.5+OCAM, RPM= 1085, ALFSU = 0.0 DEG, VOR = 0.00, CT/SIGMA = .000	0.001	0.01	-24.77	35.9
999	2740	3-Mar-94	19:34:51 17.5+OCAM, RPM= 0000, ALFSU = 0.0 DEG, VOR = 0.00, CT/SIGMA = .000	####	9.00	-22.89	0.0
3145	2741	3-Mar-94	21:19:52 17.5+OCAM, RPM= 1087, ALFSU = 0.0 DEG, VOR = 0.00, CT/SIGMA = .000	0.001	0.01	-42.07	35.3
3905	2742	3-Mar-94	21:28:55 17.5+OCAM, RPM= 1080, ALFSU = 2.0 DEG, VOR = 0.20, CT/SIGMA = .076	0.007	0.20	893.35	50.9
3905	2750	3-Mar-94	21:34:57 17.5+OCAM, RPM= 1080, ALFSU = 2.0 DEG, VOR = 0.20, CT/SIGMA = .076	0.007	0.20	911.21	50.2
3906	2770	3-Mar-94	21:50:38 17.5+OCAM, RPM= 1080, ALFSU = 3.0 DEG, VOR = 0.20, CT/SIGMA = .076	0.007	0.20	893.08	45.9
3906	2787	3-Mar-94	21:56:46 17.5+OCAM, RPM= 1080, ALFSU = 3.0 DEG, VOR = 0.20, CT/SIGMA = .076	0.007	0.20	907.60	45.3



TEST	POINT	DATE				CT	Mu	Lift (lbs)	HP
3907	2788	3-Mar-94	21:59:43	17.5+OCAM, RPM= 1085, ALFSU = 4.0 DEG, VOR = 0.20, CT/SIGMA = .076		0.007	0.20	895.70	42.3
3907	2805	3-Mar-94	22:05:58	17.5+OCAM, RPM= 1085, ALFSU = 4.0 DEG, VOR = 0.20, CT/SIGMA = .076		0.007	0.20	902.26	41.5
3908	2806	3-Mar-94	22:08:33	17.5+OCAM, RPM= 1086, ALFSU = 5.0 DEG, VOR = 0.20, CT/SIGMA = .076		0.007	0.20	895.38	39.2
3908	2823	3-Mar-94	22:14:38	17.5+OCAM, RPM= 1086, ALFSU = 5.0 DEG, VOR = 0.20, CT/SIGMA = .076		0.007	0.20	902.33	38.8
3909	2824	3-Mar-94	22:17:12	17.5+OCAM, RPM= 1087, ALFSU = 6.0 DEG, VOR = 0.20, CT/SIGMA = .076		0.007	0.20	899.03	35.8
3909	2841	3-Mar-94	22:23:13	17.5+OCAM, RPM= 1087, ALFSU = 6.0 DEG, VOR = 0.20, CT/SIGMA = .076		0.007	0.20	905.10	35.1
3145	2842	3-Mar-94	22:28:00	17.5+OCAM, RPM= 1087, ALFSU = 0.0 DEG, VOR = 0.00, CT/SIGMA =		0.001	0.01	13.61	35.6
999	2843	3-Mar-94	22:28:55	17.5+OCAM, RPM= 0000, ALFSU = 0.0 DEG, VOR = 0.00, CT/SIGMA =	#####	9.00		-1.36	0.0
3145	2844	3-Mar-94	22:54:27	17.5+OCAM, RPM= 1087, ALFSU = 0.0 DEG, VOR = 0.00, CT/SIGMA =		0.001	0.01	-14.32	33.9
3910	2845	3-Mar-94	23:04:06	17.5+OCAM, RPM= 1081, ALFSU = 2.5 DEG, VOR = 0.20, CT/SIGMA = 0.087		0.008	0.20	1027.40	54.8
3910	2862	3-Mar-94	23:10:14	17.5+OCAM, RPM= 1081, ALFSU = 2.5 DEG, VOR = 0.20, CT/SIGMA = 0.087		0.008	0.20	1054.70	54.6
3911	2864	3-Mar-94	23:16:32	17.5+OCAM, RPM= 1085, ALFSU = 3.5 DEG, VOR = 0.20, CT/SIGMA = 0.087		0.008	0.20	1033.90	49.7
3911	2881	3-Mar-94	23:22:41	17.5+OCAM, RPM= 1085, ALFSU = 3.5 DEG, VOR = 0.20, CT/SIGMA = 0.087		0.008	0.20	1048.40	49.2
3912	2882	3-Mar-94	23:25:07	17.5+OCAM, RPM= 1085, ALFSU = 4.5 DEG, VOR = 0.20, CT/SIGMA = 0.087		0.008	0.20	1026.70	44.4
3912	2899	3-Mar-94	23:31:51	17.5+OCAM, RPM= 1085, ALFSU = 4.5 DEG, VOR = 0.20, CT/SIGMA = 0.087		0.008	0.20	1037.70	43.6
3913	2900	3-Mar-94	23:34:12	17.5+OCAM, RPM= 1085, ALFSU = 5.5 DEG, VOR = 0.20, CT/SIGMA = 0.087		0.008	0.20	1023.80	40.3
3913	2917	3-Mar-94	23:40:40	17.5+OCAM, RPM= 1085, ALFSU = 5.5 DEG, VOR = 0.20, CT/SIGMA = 0.087		0.008	0.20	1035.40	39.4
3914	2918	3-Mar-94	23:44:21	17.5+OCAM, RPM= 1087, ALFSU = 6.5 DEG, VOR = 0.20, CT/SIGMA = 0.087		0.008	0.20	1011.60	36.5
3914	2935	3-Mar-94	23:50:34	17.5+OCAM, RPM= 1087, ALFSU = 6.5 DEG, VOR = 0.20, CT/SIGMA = 0.087		0.008	0.20	1025.30	35.9
3145	2936	3-Mar-94	23:56:59	17.5+OCAM, RPM= 1087, ALFSU = 0.0 DEG, VOR = 0.00, CT/SIGMA =		0.001	0.00	34.78	33.9
999	2937	3-Mar-94	23:58:30	17.5+OCAM, RPM= 0000, ALFSU = 0.0 DEG, VOR = 0.00, CT/SIGMA =	#####	0.00		36.29	0.0
3345	2938	4-Mar-94	1:10:45	17.5+OCAM, RPM= 1087, ALFSU = 0.0 DEG, VOR = 0.00, CT/SIGMA =		0.001	0.01	-24.73	34.2
3930	2939	4-Mar-94	1:17:43	17.5-5 CAM, RPM= 1076, ALFSU = 3.0 DEG, VOR = 0.15, CT/SIGMA = .075		0.007	0.15	891.48	55.8
3930	2956	4-Mar-94	1:23:47	17.5-5 CAM, RPM= 1076, ALFSU = 3.0 DEG, VOR = 0.15, CT/SIGMA = .075		0.007	0.15	910.46	55.5
3932	2957	4-Mar-94	1:26:31	17.5-5 CAM, RPM= 1078, ALFSU = 5.0 DEG, VOR = 0.15, CT/SIGMA = .076		0.007	0.15	887.43	48.5
3932	2974	4-Mar-94	1:32:47	17.5-5 CAM, RPM= 1078, ALFSU = 5.0 DEG, VOR = 0.15, CT/SIGMA = .076		0.007	0.15	901.33	48.5
3934	2975	4-Mar-94	1:35:41	17.5-5 CAM, RPM= 1079, ALFSU = 7.0 DEG, VOR = 0.15, CT/SIGMA = .076		0.007	0.15	894.19	43.2
3934	2992	4-Mar-94	1:41:41	17.5-5 CAM, RPM= 1079, ALFSU = 7.0 DEG, VOR = 0.15, CT/SIGMA = .076		0.007	0.15	906.04	43.0
3935	2993	4-Mar-94	1:48:11	17.5-5 CAM, RPM= 1081, ALFSU = 2.0 DEG, VOR = 0.20, CT/SIGMA = .076		0.007	0.20	906.10	48.7
3935	2994	4-Mar-94	1:50:49	17.5-5 CAM, RPM= 1081, ALFSU = 2.0 DEG, VOR = 0.20, CT/SIGMA = .076		0.007	0.20	905.96	48.9
3935	3011	4-Mar-94	1:57:01	17.5-5 CAM, RPM= 1081, ALFSU = 2.0 DEG, VOR = 0.20, CT/SIGMA = .076		0.007	0.20	916.89	47.9
3937	3012	4-Mar-94	1:59:57	17.5-5 CAM, RPM= 1082, ALFSU = 4.0 DEG, VOR = 0.20, CT/SIGMA = .076		0.007	0.20	893.97	40.3
3937	3029	4-Mar-94	2:05:55	17.5-5 CAM, RPM= 1082, ALFSU = 4.0 DEG, VOR = 0.20, CT/SIGMA = .076		0.007	0.20	908.34	39.9
3940	3030	4-Mar-94	2:08:29	17.5-5 CAM, RPM= 1084, ALFSU = 6.0 DEG, VOR = 0.20, CT/SIGMA = .076		0.007	0.20	898.87	33.6
3940	3047	4-Mar-94	2:14:32	17.5-5 CAM, RPM= 1084, ALFSU = 6.0 DEG, VOR = 0.20, CT/SIGMA = .076		0.007	0.20	900.68	33.5
3946	3048	4-Mar-94	2:17:40	17.5-5 CAM, RPM= 1085, ALFSU = 6.5 DEG, VOR = 0.20, CT/SIGMA = .087		0.008	0.20	1025.30	36.8
3946	3065	4-Mar-94	2:23:54	17.5-5 CAM, RPM= 1085, ALFSU = 6.5 DEG, VOR = 0.20, CT/SIGMA = .087		0.008	0.20	1035.80	36.0
3943	3066	4-Mar-94	2:26:25	17.5-5 CAM, RPM= 1085, ALFSU = 4.5 DEG, VOR = 0.20, CT/SIGMA = .087		0.008	0.20	1022.40	44.6
3943	3083	4-Mar-94	2:32:38	17.5-5 CAM, RPM= 1085, ALFSU = 4.5 DEG, VOR = 0.20, CT/SIGMA = .087		0.008	0.20	1033.10	43.8
3941	3084	4-Mar-94	2:34:58	17.5-5 CAM, RPM= 1086, ALFSU = 2.5 DEG, VOR = 0.20, CT/SIGMA = .087		0.008	0.20	1034.20	53.8
3941	3101	4-Mar-94	2:41:12	17.5-5 CAM, RPM= 1086, ALFSU = 2.5 DEG, VOR = 0.20, CT/SIGMA = .087		0.008	0.20	1047.90	53.0
3345	3102	4-Mar-94	2:45:11	17.5-5 CAM, RPM= 1087, ALFSU = 0.0 DEG, VOR = 0.00, CT/SIGMA = .000		0.002	0.00	41.04	34.4
999	3103	4-Mar-94	2:46:22	17.5-5 CAM, RPM= 0000, ALFSU = 0.0 DEG, VOR = 0.00, CT/SIGMA = .000	#####	0.00		35.73	0.0
3245	3104	4-Mar-94	3:20:06	17.5-5 CAM, RPM= 1087, ALFSU = 0.0 DEG, VOR = 0.00, CT/SIGMA = .000		0.001	0.00	-27.73	34.3
3915	3105	4-Mar-94	3:26:12	17.5-5 CAM, RPM= 1077, ALFSU = 3.0 DEG, VOR = 0.15, CT/SIGMA = .076		0.007	0.15	898.14	57.3
3915	3122	4-Mar-94	3:32:19	17.5-5 CAM, RPM= 1077, ALFSU = 3.0 DEG, VOR = 0.15, CT/SIGMA = .076		0.007	0.15	916.02	56.2
3917	3123	4-Mar-94	3:34:59	17.5-5 CAM, RPM= 1079, ALFSU = 5.0 DEG, VOR = 0.15, CT/SIGMA = .076		0.007	0.15	902.68	50.4
3917	3140	4-Mar-94	3:41:08	17.5-5 CAM, RPM= 1079, ALFSU = 5.0 DEG, VOR = 0.15, CT/SIGMA = .076		0.007	0.15	916.91	51.0
3919	3141	4-Mar-94	3:43:47	17.5-5 CAM, RPM= 1079, ALFSU = 7.0 DEG, VOR = 0.15, CT/SIGMA = .076		0.007	0.15	891.98	44.2
3919	3158	4-Mar-94	3:49:50	17.5-5 CAM, RPM= 1079, ALFSU = 7.0 DEG, VOR = 0.15, CT/SIGMA = .076		0.007	0.15	910.19	43.9
3920	3159	4-Mar-94	3:55:08	17.5-5 CAM, RPM= 1082, ALFSU = 2.0 DEG, VOR = 0.20, CT/SIGMA = .076		0.007	0.20	892.91	49.4
3245	3173	4-Mar-94	4:03:45	17.5-5 CAM, RPM= 1087, LOST FLAP CABLE #2		0.002	0.00	52.52	34.9
999	3174	4-Mar-94	4:04:43	17.5-5 CAM, RPM= 0000, LOST FLAP CABLE #2	#####	9.00		14.83	0.0
3245	3175	4-Mar-94	18:33:34	17.5-10CAM, RPM= 1087, ALFSU = 0.0 DEG, VOR = 0.00, CT/SIGMA =		0.002	0.01	-5.53	34.5
3245	3178	4-Mar-94	19:19:45	17.5-10CAM, RPM= 1087, ALFSU = 0.0 DEG, VOR = 0.00, CT/SIGMA =		0.002	0.01	-43.23	33.6
3922	3177	4-Mar-94	19:27:36	17.5-10CAM, RPM= 1095, ALFSU = 4.0 DEG, VOR = 0.20, CT/SIGMA = 0.076		0.007	0.20	898.42	45.9
3922	3194	4-Mar-94	19:33:40	17.5-10CAM, RPM= 1095, ALFSU = 4.0 DEG, VOR = 0.20, CT/SIGMA = 0.076		0.007	0.20	906.68	45.7
3924	3195	4-Mar-94	19:36:13	17.5-10CAM, RPM= 1099, ALFSU = 6.0 DEG, VOR = 0.20, CT/SIGMA = 0.076		0.007	0.20	897.82	38.9
3924	3212	4-Mar-94	19:42:16	17.5-10CAM, RPM= 1099, ALFSU = 6.0 DEG, VOR = 0.20, CT/SIGMA = 0.076		0.007	0.20	892.46	37.9
3245	3213	4-Mar-94	19:46:36	17.5-10CAM, RPM= 1087, ALFSU = 0.0 DEG, VOR = 0.00, CT/SIGMA =		0.002	0.01	-34.56	34.7
999	3214	4-Mar-94	19:47:33	17.5-10CAM, RPM= 0000, ALFSU = 0.0 DEG, VOR = 0.00, CT/SIGMA =	#####	9.00		-27.62	0.0
3245	3215	4-Mar-94	21:01:32	17.5-10CAM, RPM= 1087, ALFSU = 0.0 DEG, VOR = 0.00, CT/SIGMA =		0.002	0.01	-46.09	35.3
3920	3216	4-Mar-94	21:06:54	17.5-10CAM, RPM= 1087, ALFSU = 2.0 DEG, VOR = 0.20, CT/SIGMA = 0.076		0.007	0.20	911.84	54.7
3920	3233	4-Mar-94	21:12:55	17.5-10CAM, RPM= 1087, ALFSU = 2.0 DEG, VOR = 0.20, CT/SIGMA = 0.076		0.007	0.20	906.89	54.0
3925	3234	4-Mar-94	21:16:25	17.5-10CAM, RPM= 1094, ALFSU = 2.5 DEG, VOR = 0.20, CT/SIGMA = 0.087		0.008	0.20	1021.10	59.3
3925	3251	4-Mar-94	21:22:25	17.5-10CAM, RPM= 1094, ALFSU = 2.5 DEG, VOR = 0.20, CT/SIGMA = 0.087		0.008	0.20	1049.10	58.9
3927	3252	4-Mar-94	21:24:59	17.5-10CAM, RPM= 1093, ALFSU = 4.5 DEG, VOR = 0.20, CT/SIGMA = 0.087		0.008	0.20	1020.60	49.8
3927	3269	4-Mar-94	21:31:03	17.5-10CAM, RPM= 1093, ALFSU = 4.5 DEG, VOR = 0.20, CT/SIGMA = 0.087		0.008	0.20	1023.80	49.1
3929	3270	4-Mar-94	21:33:14	17.5-10CAM, RPM= 1093, ALFSU = 6.5 DEG, VOR = 0.20, CT/SIGMA = 0.087		0.008	0.20	1018.60	40.9
3929	3287	4-Mar-94	21:39:16	17.5-10CAM, RPM= 1093, ALFSU = 6.5 DEG, VOR = 0.20, CT/SIGMA = 0.087		0.008	0.20	1025.50	40.6
3245	3288	4-Mar-94	21:43:52	17.5-10CAM, RPM= 1087, ALFSU = 0.0 DEG, VOR = 0.00, CT/SIGMA =		0.002	0.00	-11.00	34.9
999	3289	4-Mar-94	21:44:49	17.5-10CAM, RPM= 0000, ALFSU = 0.0 DEG, VOR = 0.00, CT/SIGMA =	#####	9.00		2.46	0.0
3445	3290	4-Mar-94	23:04:45	17.5-15CAM, RPM= 1087, ALFSU = 0.0 DEG, VOR = 0.00, CT/SIGMA = 0.000		0.002	0.01	-61.10	35.4
999	3291	4-Mar-94	23:16:39	17.5-15CAM, RPM= 0000, ALFSU = 0.0 DEG, VOR = 0.00, CT/SIGMA = 0.000	#####	9.00		-10.15	0.0
3445	3292	5-Mar-94	2:59:10	17.5-15CAM, RPM= 1087, ALFSU = 0.0 DEG, VOR = 0.00, CT/SIGMA = 0.000		0.002	0.01	10.98	33.9
3962	3293	5-Mar-94	3:06:23	17.5-15CAM, RPM= 1078, ALFSU = 3.0 DEG, VOR = 0.15, CT/SIGMA = 0.076		0.007	0.15	900.14	56.4
3962	3310	5-Mar-94	3:12:32	17.5-15CAM, RPM= 1078, ALFSU = 3.0 DEG, VOR = 0.15, CT/SIGMA = 0.076		0.007	0.15	914.67	56.0
3948	3311	5-Mar-94	3:14:51	17.5-15CAM, RPM= 1080, ALFSU = 5.0 DEG, VOR = 0.15, CT/SIGMA = 0.076		0.007	0.15	892.33	49.6
3948	3328	5-Mar-94	3:21:28	17.5-15CAM, RPM= 1080, ALFSU = 5.0 DEG, VOR = 0.15, CT/SIGMA = 0.076		0.007	0.15	901.36	49.1
3951	3329	5-Mar-94	3:23:37	17.5-15CAM, RPM= 1080, ALFSU = 7.0 DEG, VOR = 0.15, CT/SIGMA = 0.076		0.007	0.15	895.13	44.5
3951	3346	5-Mar-94	3:29:47	17.5-15CAM, RPM= 1080, ALFSU = 7.0 DEG, VOR = 0.15, CT/SIGMA = 0.076		0.007	0.15	903.00	44.3
999	3347	5-Mar-94	3:38:57	17.5-15CAM, RPM= 0000, ALFSU = 0.0 DEG, VOR = 0.00, CT/SIGMA = 0.000	#####	9.00		16.41	0.0
3445	3348	5-Mar-94	4:02:22	17.5-15CAM, RPM= 1087, ALFSU = 0.0 DEG, VOR = 0.00, CT/SIGMA = 0.000		0.001	0.01	-38.11	35.0
3952	3349	5-Mar-94	4:11:03	17.5-15CAM, RPM= 1082, ALFSU = 2.0 DEG, VOR = 0.20, CT/SIGMA = 0.076		0.007	0.20	908.80	53.8
3952	3366	5-Mar-94	4:17:08	17.5-15CAM, RPM= 1082, ALFSU = 2.0 DEG, VOR = 0.20, CT/SIGMA = 0.076		0.007	0.20	933.92	52.8

TEST	POINT	DATE					CT	Mu	Lift (lbs)	HP
3954	3367	5-Mar-94	4:21:08	17.5-15CAM, RPM= 1084, ALFSU = 4.0 DEG, VOR = 0.20, CT/SIGMA = 0.076		0.007	0.20	906.06	44.7	
3954	3384	5-Mar-94	4:27:40	17.5-15CAM, RPM= 1084, ALFSU = 4.0 DEG, VOR = 0.20, CT/SIGMA = 0.076		0.007	0.20	917.87	44.1	
3956	3385	5-Mar-94	4:30:18	17.5-15CAM, RPM= 1084, ALFSU = 6.0 DEG, VOR = 0.20, CT/SIGMA = 0.076		0.007	0.20	890.96	36.8	
3445	3387	5-Mar-94	4:35:26	17.5-15CAM, RPM= 1087, ALFSU = 0.0 DEG, VOR = 0.00, CT/SIGMA = 0.000		0.001	0.01	30.26	33.2	
999	3388	5-Mar-94	4:36:30	17.5-15CAM, RPM= 0000, ALFSU = 0.0 DEG, VOR = 0.00, CT/SIGMA = 0.000	#####		0.00	-1.54	0.0	
3445	3389	7-Mar-94	22:10:50	17.5-15CAM, RPM= 1087, ALFSU = 0.0 DEG, VOR = 0.00, CT/SIGMA =		0.002	0.00	15.59	36.1	
3956	3390	7-Mar-94	22:18:39	17.5-15CAM, RPM= 1102, ALFSU = 6.0 DEG, VOR = 0.20, CT/SIGMA = 0.076		0.007	0.20	913.93	38.8	
3956	3407	7-Mar-94	22:24:43	17.5-15CAM, RPM= 1102, ALFSU = 6.0 DEG, VOR = 0.20, CT/SIGMA = 0.076		0.007	0.20	920.85	38.0	
3957	3408	7-Mar-94	22:29:01	17.5-15CAM, RPM= 1105, ALFSU = 2.5 DEG, VOR = 0.20, CT/SIGMA = 0.087		0.008	0.20	1058.40	60.3	
3957	3425	7-Mar-94	22:35:04	17.5-15CAM, RPM= 1105, ALFSU = 2.5 DEG, VOR = 0.20, CT/SIGMA = 0.087		0.008	0.20	1059.40	59.9	
3959	3426	7-Mar-94	22:37:45	17.5-15CAM, RPM= 1105, ALFSU = 4.5 DEG, VOR = 0.20, CT/SIGMA = 0.087		0.008	0.20	1040.40	50.5	
3959	3443	7-Mar-94	22:43:58	17.5-15CAM, RPM= 1105, ALFSU = 4.5 DEG, VOR = 0.20, CT/SIGMA = 0.087		0.008	0.20	1041.80	49.6	
3961	3444	7-Mar-94	22:50:57	17.5-15CAM, RPM= 1106, ALFSU = 6.5 DEG, VOR = 0.20, CT/SIGMA = 0.087		0.008	0.20	1023.80	41.9	
3961	3481	7-Mar-94	22:57:04	17.5-15CAM, RPM= 1106, ALFSU = 6.5 DEG, VOR = 0.20, CT/SIGMA = 0.087		0.008	0.20	1022.40	41.5	
3445	3462	7-Mar-94	23:02:21	17.5-15CAM, RPM= 1087, ALFSU = 0.0 DEG, VOR = 0.00, CT/SIGMA =		0.001	0.00	-22.70	35.8	
999	3463	7-Mar-94	23:03:46	17.5-15CAM, RPM= 0000, ALFSU = 0.0 DEG, VOR = 0.00, CT/SIGMA =	#####		0.00	-19.03	0.0	
3445	3464	7-Mar-94	23:48:33	17.5-15CAM, RPM= 1087, ALFSU = 0.0 DEG, VOR = 0.00, CT/SIGMA =		0.001	0.00	-56.57	36.1	
3963	3465	7-Mar-94	23:58:36	17.5-15CAM, RPM= 1087, ALFSU = 4.0 DEG, VOR = 0.10, CT/SIGMA = 0.076		0.007	0.08	910.65	88.2	
3445	3466	8-Mar-94	0:19:16	17.5-15CAM, RPM= 1087, ALFSU = 0.0 DEG, VOR = 0.00, CT/SIGMA =		0.001	0.00	-9.41	36.1	
999	3467	8-Mar-94	0:20:12	17.5-15CAM, RPM= 0000, ALFSU = 0.0 DEG, VOR = 0.00, CT/SIGMA =	#####		0.00	-19.77	0.0	
8500	3468	8-Mar-94	1:35:26	2P6+11.7, RPM= 0544, ALFSU = 0.0 DEG, VOR = 0.00, CT/SIGMA =		0.002	0.00	-23.54	4.1	
8501	3469	8-Mar-94	1:36:50	2P6+11.7, RPM= 0652, ALFSU = 0.0 DEG, VOR = 0.00, CT/SIGMA =		0.002	0.00	-26.52	6.4	
8502	3470	8-Mar-94	1:38:07	2P6+11.7, RPM= 0761, ALFSU = 0.0 DEG, VOR = 0.00, CT/SIGMA =		0.002	0.00	-28.22	9.6	
8503	3471	8-Mar-94	1:39:16	2P6+11.7, RPM= 0870, ALFSU = 0.0 DEG, VOR = 0.00, CT/SIGMA =		0.001	0.00	-31.48	13.6	
8504	3472	8-Mar-94	1:40:14	2P6+11.7, RPM= 0878, ALFSU = 0.0 DEG, VOR = 0.00, CT/SIGMA =		0.001	0.00	-27.87	19.0	
8505	3473	8-Mar-94	1:41:24	2P6+11.7, RPM= 1033, ALFSU = 0.0 DEG, VOR = 0.00, CT/SIGMA =		0.001	0.00	-26.63	22.2	
8506	3474	8-Mar-94	1:42:18	2P6+11.7, RPM= 1087, ALFSU = 0.0 DEG, VOR = 0.00, CT/SIGMA =		0.001	0.00	-25.53	25.9	
8507	3475	8-Mar-94	1:45:50	2P6+11.7, RPM= 1120, ALFSU = 0.0 DEG, VOR = 0.00, CT/SIGMA =		0.001	0.00	-20.32	28.3	
8508	3476	8-Mar-94	1:46:49	2P6+11.7, RPM= 1087, ALFSU = 0.0 DEG, VOR = 0.00, CT/SIGMA =		0.001	0.00	-18.31	26.3	
8509	3477	8-Mar-94	1:47:42	2P6+11.7, RPM= 1087, COLL = 1 DEG, ALFSU = 0.0 DEG, VOR = 0.00, CT/SIG		0.001	0.00	52.53	28.5	
8510	3478	8-Mar-94	1:48:20	2P6+11.7, RPM= 1087, COLL = 2 DEG, ALFSU = 0.0 DEG, VOR = 0.00, CT/SIG		0.001	0.01	123.61	31.7	
8511	3479	8-Mar-94	1:49:04	2P6+11.7, RPM= 1087, COLL = 3 DEG, ALFSU = 0.0 DEG, VOR = 0.00, CT/SIG		0.002	0.01	204.58	37.3	
8512	3480	8-Mar-94	1:49:34	2P6+11.7, RPM= 1087, COLL = 4 DEG, ALFSU = 0.0 DEG, VOR = 0.00, CT/SIG		0.002	0.02	297.08	45.0	
8513	3481	8-Mar-94	1:50:03	2P6+11.7, RPM= 1087, COLL = 5 DEG, ALFSU = 0.0 DEG, VOR = 0.00, CT/SIG		0.003	0.02	404.33	54.7	
8514	3482	8-Mar-94	1:50:32	2P6+11.7, RPM= 1087, COLL = 6 DEG, ALFSU = 0.0 DEG, VOR = 0.00, CT/SIG		0.004	0.03	498.63	64.5	
8515	3483	8-Mar-94	1:51:31	2P6+11.7, RPM= 1087, COLL = 7 DEG, ALFSU = 0.0 DEG, VOR = 0.00, CT/SIG		0.005	0.04	625.98	78.3	
8516	3484	8-Mar-94	1:52:07	2P6+11.7, RPM= 1087, COLL = 8 DEG, ALFSU = 0.0 DEG, VOR = 0.00, CT/SIG		0.006	0.03	753.83	93.2	
8517	3485	8-Mar-94	1:52:38	2P6+11.7, RPM= 1087, COLL = 9 DEG, ALFSU = 0.0 DEG, VOR = 0.00, CT/SIG		0.007	0.03	867.33	110.7	
8506	3486	8-Mar-94	1:54:53	2P6+11.7, RPM= 1087, COLL = 0 DEG, ALFSU = 0.0 DEG, VOR = 0.00, CT/SIG		0.001	0.00	-11.96	25.7	
8510	3487	8-Mar-94	1:55:45	2P6+11.7, RPM= 1087, COLL = 2 DEG, ALFSU = 0.0 DEG, VOR = 0.00, CT/SIG		0.001	0.01	141.64	31.8	
8519	3488	8-Mar-94	1:56:58	2P6+11.7, RPM= 1087, COLL = 2 DEG, LAT = 2.0 DEG, VOR = 0.00, CT/SIG		0.001	0.01	151.87	34.8	
8510	3489	8-Mar-94	1:57:51	2P6+11.7, RPM= 1087, COLL = 2 DEG, LAT = 0.0 DEG, VOR = 0.00, CT/SIG		0.001	0.00	141.42	32.0	
8520	3490	8-Mar-94	1:58:46	2P6+11.7, RPM= 1087, COLL = 2 DEG, LONG = 2.0 DEG, VOR = 0.00, CT/SIG		0.001	0.02	140.93	34.0	
8506	3491	8-Mar-94	1:59:50	2P6+11.7, RPM= 1087, COLL = 0 DEG, LONG = 0.0 DEG, VOR = 0.00, CT/SIG		0.001	0.00	2.36	26.3	
8521	3492	8-Mar-94	2:08:17	2P6+11.7, RPM= 1086, ALPHA = 0.92 DEG, VOR = 0.10, CT/SIGMA = .064		0.008	0.10	788.49	71.4	
8522	3493	8-Mar-94	2:08:27	2P6+11.7, RPM= 1086, ALPHA = -0.81 DEG, VOR = 0.10, CT/SIGMA = .087		0.008	0.10	1039.70	103.3	
8523	3494	8-Mar-94	2:13:08	2P6+11.7, RPM= 1086, ALPHA = -1.89 DEG, VOR = 0.15, CT/SIGMA = .085		0.006	0.15	791.06	63.0	
8524	3495	8-Mar-94	2:15:22	2P6+11.7, RPM= 1086, ALPHA = -1.81 DEG, VOR = 0.15, CT/SIGMA = .087		0.008	0.15	1055.30	87.8	
999	3496	8-Mar-94	2:22:51	2P6+11.7, RPM= 0000, ALPHA = -0.00 DEG, VOR = 0.00, CT/SIGMA = .000	#####		0.00	17.36	0.0	
45	3497	8-Mar-94	22:07:07	NULL CAM, RPM= 1087, ALPHA = 0.00 DEG, VOR = 0.00, CT/SIGMA =		0.001	0.00	-18.61	24.6	
500	3498	8-Mar-94	22:11:35	NULL CAM, RPM= 272, ALPHA = 0.00 DEG, VOR = 0.00, DYNAMICS		0.002	0.00	4.72	0.8	
501	3499	8-Mar-94	22:12:34	NULL CAM, RPM= 326, ALPHA = 0.00 DEG, VOR = 0.00, DYNAMICS		0.001	0.00	5.98	1.1	
502	3500	8-Mar-94	22:13:37	NULL CAM, RPM= 380, ALPHA = 0.00 DEG, VOR = 0.00, DYNAMICS		0.001	0.00	6.44	1.6	
503	3501	8-Mar-94	22:14:18	NULL CAM, RPM= 435, ALPHA = 0.00 DEG, VOR = 0.00, DYNAMICS		0.001	0.00	6.18	2.2	
504	3502	8-Mar-94	22:15:08	NULL CAM, RPM= 489, ALPHA = 0.00 DEG, VOR = 0.00, DYNAMICS		0.001	0.00	5.28	2.9	
505	3503	8-Mar-94	22:15:55	NULL CAM, RPM= 544, ALPHA = 0.00 DEG, VOR = 0.00, DYNAMICS		0.001	0.00	3.46	3.7	
506	3504	8-Mar-94	22:16:33	NULL CAM, RPM= 598, ALPHA = 0.00 DEG, VOR = 0.00, DYNAMICS		0.001	0.00	2.29	4.7	
507	3505	8-Mar-94	22:17:18	NULL CAM, RPM= 652, COLL = 0.00 DEG, DYNAMICS		0.001	0.00	1.91	5.9	
508	3506	8-Mar-94	22:17:52	NULL CAM, RPM= 707, COLL = 0.00 DEG, DYNAMICS		0.002	0.00	-1.14	7.3	
509	3507	8-Mar-94	22:18:33	NULL CAM, RPM= 761, COLL = 0.00 DEG, DYNAMICS		0.001	0.00	-1.16	8.8	
510	3508	8-Mar-94	22:19:12	NULL CAM, RPM= 815, COLL = 0.00 DEG, DYNAMICS		0.001	0.00	-2.08	10.6	
532	3509	8-Mar-94	22:19:56	NULL CAM, RPM= 870, COLL = 0.00 DEG, DYNAMICS		0.001	0.00	-1.97	12.7	
511	3510	8-Mar-94	22:20:32	NULL CAM, RPM= 824, COLL = 0.00 DEG, DYNAMICS		0.001	0.00	-1.36	15.2	
21	3511	8-Mar-94	22:21:05	NULL CAM, RPM= 978, COLL = 0.00 DEG, DYNAMICS		0.001	0.00	-2.57	17.9	
512	3512	8-Mar-94	22:21:46	NULL CAM, RPM= 1033, COLL = 0.00 DEG, DYNAMICS		0.001	0.00	-0.91	21.0	
45	3513	8-Mar-94	22:22:19	NULL CAM, RPM= 1087, COLL = 0.00 DEG, DYNAMICS		0.001	0.00	1.70	24.6	
514	3514	8-Mar-94	22:25:30	NULL CAM, RPM= 272, COLL = 4.00 DEG, DYNAMICS		0.004	0.00	28.11	1.0	
515	3515	8-Mar-94	22:26:09	NULL CAM, RPM= 328, COLL = 4.00 DEG, DYNAMICS		0.003	0.00	36.44	1.5	
516	3516	8-Mar-94	22:27:06	NULL CAM, RPM= 380, COLL = 4.00 DEG, DYNAMICS		0.003	0.00	43.93	2.2	
517	3517	8-Mar-94	22:27:44	NULL CAM, RPM= 435, COLL = 4.00 DEG, DYNAMICS		0.003	0.01	53.61	3.1	
518	3518	8-Mar-94	22:28:22	NULL CAM, RPM= 489, COLL = 4.00 DEG, DYNAMICS		0.003	0.02	63.87	4.2	
519	3519	8-Mar-94	22:29:01	NULL CAM, RPM= 544, COLL = 4.00 DEG, DYNAMICS		0.003	0.01	76.82	5.7	
520	3520	8-Mar-94	22:29:42	NULL CAM, RPM= 598, COLL = 4.00 DEG, DYNAMICS		0.003	0.02	90.15	7.3	
521	3521	8-Mar-94	22:30:23	NULL CAM, RPM= 652, COLL = 4.00 DEG, DYNAMICS		0.002	0.02	105.33	9.2	
522	3522	8-Mar-94	22:31:17	NULL CAM, RPM= 707, COLL = 4.00 DEG, DYNAMICS		0.002	0.00	120.57	11.5	
523	3523	8-Mar-94	22:32:04	NULL CAM, RPM= 761, COLL = 4.00 DEG, DYNAMICS		0.003	0.02	141.09	14.4	
524	3524	8-Mar-94	22:32:42	NULL CAM, RPM= 815, COLL = 4.00 DEG, DYNAMICS		0.002	0.02	162.08	17.5	
533	3525	8-Mar-94	22:33:23	NULL CAM, RPM= 870, COLL = 4.00 DEG, DYNAMICS		0.002	0.01	189.32	21.3	
525	3526	8-Mar-94	22:34:19	NULL CAM, RPM= 924, COLL = 4.00 DEG, DYNAMICS		0.002	0.02	214.74	25.6	
526	3527	8-Mar-94	22:34:58	NULL CAM, RPM= 978, COLL = 4.00 DEG, DYNAMICS		0.003	0.02	244.91	30.6	
527	3528	8-Mar-94	22:35:40	NULL CAM, RPM= 1033, COLL = 4.00 DEG, DYNAMICS		0.002	0.01	275.65	36.1	
49	3529	8-Mar-94	22:36:25	NULL CAM, RPM= 1087, COLL = 4.00 DEG, DYNAMICS		0.002	0.02	308.05	42.6	
45	3530	8-Mar-94	22:37:36	NULL CAM, RPM= 1087, COLL = 0.00 DEG, DYNAMICS		0.001	0.00	-9.95	24.6	
513	3531	8-Mar-94	22:41:03	NULL CAM, RPM= 568, COLL = 4.00 DEG, DYNAMICS		0.002	0.01	75.43	6.3	
999	3532	8-Mar-94	22:43:18	NULL CAM, RPM= 0000, COLL = 0.00 DEG, DYNAMICS	#####		0.00	7.36	0.0	

TEST	POINT	DATE			CT	MU	Lift (lbs)	HP
45	3533	8-Mar-94	22:44:50	NULL CAM, RPM= 1087, COLL = 0.00 DEG, DYNAMICS	0.001	0.00	-20.91	24.3
503	3534	8-Mar-94	22:46:29	NULL CAM, RPM= 435, COLL = 0.00 DEG, DYNAMICS	0.002	0.00	-11.12	2.1
503	3535	8-Mar-94	22:55:50	NULL CAM, RPM= 435, COLL = 0.00 DEG, DYNAMICS	0.002	0.00	-23.39	2.2
507	3536	8-Mar-94	22:58:00	NULL CAM, RPM= 652, COLL = 0.00 DEG, DYNAMICS	0.002	0.00	-31.71	5.9
507	3537	8-Mar-94	23:02:26	NULL CAM, RPM= 652, COLL = 0.00 DEG, DYNAMICS	0.002	0.00	-33.40	5.9
532	3538	8-Mar-94	23:04:03	NULL CAM, RPM= 870, COLL = 0.00 DEG, DYNAMICS	0.001	0.00	-38.40	12.9
532	3539	8-Mar-94	23:08:37	NULL CAM, RPM= 870, COLL = 0.00 DEG, DYNAMICS	0.001	0.00	-37.39	13.0
45	3540	8-Mar-94	23:09:30	NULL CAM, RPM= 1087, COLL = 0.00 DEG, DYNAMICS	0.001	0.00	-41.65	24.9
45	3541	8-Mar-94	23:13:56	NULL CAM, RPM= 1087, COLL = 0.00 DEG, DYNAMICS	0.001	0.00	-39.55	24.6
45	3542	8-Mar-94	23:21:00	NULL CAM, RPM= 1087, COLL = 0.00 DEG, DYNAMICS	0.001	0.00	-37.57	24.6
45	3543	8-Mar-94	23:25:20	NULL CAM, RPM= 1087, COLL = 0.00 DEG, DYNAMICS	0.001	0.00	-42.57	24.6
532	3544	8-Mar-94	23:26:26	NULL CAM, RPM= 870, COLL = 0.00 DEG, DYNAMICS	0.001	0.00	-36.60	12.8
532	3545	8-Mar-94	23:31:40	NULL CAM, RPM= 870, COLL = 0.00 DEG, DYNAMICS	0.001	0.00	-36.03	12.8
507	3546	8-Mar-94	23:33:02	NULL CAM, RPM= 652, COLL = 0.00 DEG, DYNAMICS	0.001	0.00	-35.14	5.8
507	3547	8-Mar-94	23:36:53	NULL CAM, RPM= 652, COLL = 0.00 DEG, DYNAMICS	0.001	0.00	-40.50	5.9
503	3548	8-Mar-94	23:38:14	NULL CAM, RPM= 435, COLL = 0.00 DEG, DYNAMICS	0.002	0.00	-40.46	2.2
503	3549	8-Mar-94	23:41:53	NULL CAM, RPM= 435, COLL = 0.00 DEG, DYNAMICS	0.002	0.00	-43.30	2.2
550	3550	8-Mar-94	23:52:27	NULL CAM, RPM= 652, DYN STAB, DRIVE	0.002	0.00	-59.06	5.9
548	3551	8-Mar-94	23:57:01	NULL CAM, RPM= 870, DYN STAB, DRIVE	0.001	0.00	-68.43	13.0
542	3552	9-Mar-94	0:02:41	NULL CAM, RPM= 870, DYN STAB, FLAP	0.001	0.00	-61.38	12.9
540	3553	9-Mar-94	0:08:19	NULL CAM, RPM= 652, DYN STAB, FLAP	0.002	0.00	-58.24	5.9
538	3554	9-Mar-94	0:12:09	NULL CAM, RPM= 435, DYN STAB, FLAP	0.003	0.00	-58.16	2.2
544	3555	9-Mar-94	0:15:38	NULL CAM, RPM= 1087, DYN STAB, FLAP	0.001	0.00	-85.69	24.9
539	3556	9-Mar-94	0:24:13	NULL CAM, RPM= 1087, DYN STAB, LAG	0.003	0.00	-63.12	2.2
541	3557	9-Mar-94	0:27:34	NULL CAM, RPM= 652, DYN STAB, LAG	0.002	0.00	-71.61	6.0
551	3558	9-Mar-94	0:30:04	NULL CAM, RPM= 652, DYN STAB, LAG	0.002	0.00	-69.39	5.9
543	3559	9-Mar-94	0:33:03	NULL CAM, RPM= 870, DYN STAB, LAG	0.001	0.00	-74.11	13.0
552	3560	9-Mar-94	0:35:04	NULL CAM, RPM= 870, DYN STAB, LAG	0.001	0.00	-69.51	13.0
545	3561	9-Mar-94	0:37:52	NULL CAM, RPM= 1087, DYN STAB, LAG	0.001	0.00	-81.29	24.8
553	3562	9-Mar-94	0:39:34	NULL CAM, RPM= 1087, DYN STAB, LAG	0.001	0.00	-86.08	24.9
45	3563	9-Mar-94	0:40:41	NULL CAM, RPM= 1087, VOR = 0.00 ALFSU = 0.0	0.001	0.00	-82.86	24.8
999	3564	9-Mar-94	0:41:44	NULL CAM, RPM= 0000, VOR = 0.00 ALFSU = 0.0	####	0.00	-60.09	0.0
45	3565	9-Mar-94	1:36:16	NULL CAM, RPM= 1087, VOR = 0.00 ALFSU = 0.0	0.001	0.01	-7.31	24.7
529	3566	9-Mar-94	1:42:37	NULL CAM, RPM= 1087, VOR = 0.10 ALFSU = 4.0, CT/SIGMA = .076	0.007	0.10	927.21	69.9
530	3567	9-Mar-94	1:46:39	NULL CAM, RPM= 1082, VOR = 0.15 ALFSU = 4.0, CT/SIGMA = .076	0.007	0.15	926.42	48.5
531	3568	9-Mar-94	1:51:13	NULL CAM, RPM= 1082, VOR = 0.20 ALFSU = 4.0, CT/SIGMA = .076	0.007	0.20	924.94	34.4
725	3569	9-Mar-94	2:14:04	NULL CAM, RPM= 1087, VOR = 0.20 ALFSU = -3.25 CT/SIGMA = .076	0.006	0.20	788.32	53.2
532	3570	9-Mar-94	2:26:02	NULL CAM, RPM= 1089, VOR = 0.20 ALFSU = -0.70 CT/SIGMA = .065	0.006	0.20	801.67	45.0
726	3571	9-Mar-94	2:33:32	NULL CAM, RPM= 1090, VOR = 0.20 ALFSU = -2.70 CT/SIGMA = .087	0.008	0.20	1034.50	70.7
726	3588	9-Mar-94	2:39:53	NULL CAM, RPM= 1090, VOR = 0.20 ALFSU = -2.70 CT/SIGMA = .087	0.008	0.20	1050.10	70.5
533	3589	9-Mar-94	2:42:37	NULL CAM, RPM= 1090, VOR = 0.20 ALFSU = -0.73 CT/SIGMA = .087	0.008	0.20	1051.20	62.9
551	3590	9-Mar-94	2:46:13	NULL CAM, RPM= 1090, VOR = 0.20 ALFSU = 7.5, CT/SIGMA = .087	0.008	0.20	1042.50	26.1
551	3607	9-Mar-94	2:53:49	NULL CAM, RPM= 1090, VOR = 0.20 ALFSU = 7.5, CT/SIGMA = .087	0.008	0.20	1053.30	25.2
538	3608	9-Mar-94	2:56:41	NULL CAM, RPM= 1092, VOR = 0.20 ALFSU = 8.5, CT/SIGMA = .087	0.008	0.20	1032.70	21.0
538	3625	9-Mar-94	3:02:51	NULL CAM, RPM= 1092, VOR = 0.20 ALFSU = 8.5, CT/SIGMA = .087	0.008	0.20	1040.80	20.4
756	3626	9-Mar-94	3:09:06	NULL CAM, RPM= 1095, VOR = 0.25 ALFSU = -5.3, CT/SIGMA = .065	0.006	0.25	775.47	59.7
534	3627	9-Mar-94	3:12:29	NULL CAM, RPM= 1095, VOR = 0.25 ALFSU = -3.0, CT/SIGMA = .065	0.006	0.25	800.07	51.7
757	3628	9-Mar-94	3:15:33	NULL CAM, RPM= 1098, VOR = 0.25 ALFSU = -4.19 CT/SIGMA = .087	0.008	0.25	1051.80	76.8
535	3629	9-Mar-94	3:17:57	NULL CAM, RPM= 1097, VOR = 0.25 ALFSU = -2.50 CT/SIGMA = .087	0.008	0.25	1057.50	67.2
758	3630	9-Mar-94	3:21:59	NULL CAM, RPM= 1101, VOR = 0.30 ALFSU = -7.37 CT/SIGMA = .065	0.006	0.30	792.19	74.6
536	3631	9-Mar-94	3:24:13	NULL CAM, RPM= 1104, VOR = 0.30 ALFSU = -5.00 CT/SIGMA = .065	0.006	0.30	788.17	62.5
759	3632	9-Mar-94	3:26:35	NULL CAM, RPM= 1105, VOR = 0.30 ALFSU = -6.12 CT/SIGMA = .087	0.008	0.30	1069.50	95.5
537	3633	9-Mar-94	3:28:40	NULL CAM, RPM= 1105, VOR = 0.30 ALFSU = -4.00 CT/SIGMA = .087	0.008	0.30	1069.90	79.8
45	3634	9-Mar-94	3:32:51	NULL CAM, RPM= 1087, VOR = 0.00 ALFSU = 0.00 CT/SIGMA = .000	0.001	0.00	77.94	25.3
999	3635	9-Mar-94	3:33:46	NULL CAM, RPM= 0000, VOR = 0.00 ALFSU = 0.00 CT/SIGMA = .000	####	0.00	42.28	0.0
8506	3636	9-Mar-94	4:38:20	NULL CAM, RPM= 1087, VOR = 0.00 ALFSU = 0.00 CT/SIGMA = .000	0.002	0.00	-113.36	26.9
8586	3637	9-Mar-94	4:45:30	NULL CAM, RPM= 1089, VOR = 0.20 ALFSU = -3.24 CT/SIGMA = .065	0.006	0.20	795.36	64.8
826	3638	9-Mar-94	4:48:22	NULL CAM, RPM= 1089, VOR = 0.20 ALFSU = 0.50 CT/SIGMA = .065	0.006	0.20	791.09	52.2
8527	3639	9-Mar-94	4:51:51	NULL CAM, RPM= 1089, VOR = 0.20 ALFSU = -2.75 CT/SIGMA = .087	0.008	0.20	1076.20	89.6
8527	3656	9-Mar-94	4:57:57	NULL CAM, RPM= 1089, VOR = 0.20 ALFSU = -2.75 CT/SIGMA = .087	0.008	0.20	1105.80	89.7
8528	3657	9-Mar-94	5:01:10	NULL CAM, RPM= 1089, VOR = 0.20 ALFSU = 0.06 CT/SIGMA = .087	0.008	0.20	1049.20	68.4
8506	3658	9-Mar-94	5:08:30	NULL CAM, RPM= 1087, VOR = 0.00 ALFSU = 0.00 CT/SIGMA = .000	0.001	0.00	-13.62	27.2
999	3659	9-Mar-94	5:09:41	NULL CAM, RPM= 0000, VOR = 0.00 ALFSU = 0.00 CT/SIGMA = .000	####	0.00	26.77	0.0
8537	3660	9-Mar-94	5:26:33	NULL CAM, RPM= 1087, VOR = 0.00 ALFSU = 0.00 CT/SIGMA = .000	0.001	0.00	-55.78	26.1
8538	3661	9-Mar-94	5:31:52	2P6 @ 56.7 CAM, RPM= 1087 VOR = 0.15 ALFSU = -1.89 CT/SIGMA = .065	0.006	0.15	794.46	62.4
8539	3662	9-Mar-94	5:34:12	2P6 @ 56.7 CAM, RPM= 1087 VOR = 0.15 ALFSU = -1.61 CT/SIGMA = .087	0.008	0.15	1049.30	86.4
8540	3663	9-Mar-94	5:38:27	2P6 @ 56.7 CAM, RPM= 1087 VOR = 0.20 ALFSU = -3.24 CT/SIGMA = .065	0.006	0.20	791.94	60.0
8541	3664	9-Mar-94	5:42:12	2P6 @ 56.7 CAM, RPM= 1088 VOR = 0.20 ALFSU = 0.70 CT/SIGMA = .065	0.006	0.20	785.21	43.4
8542	3665	9-Mar-94	5:45:09	2P6 @ 56.7 CAM, RPM= 1088 VOR = 0.20 ALFSU = -2.72 CT/SIGMA = .087	0.008	0.20	1057.00	80.2
8542	3682	9-Mar-94	5:51:20	2P6 @ 56.7 CAM, RPM= 1088 VOR = 0.20 ALFSU = -2.72 CT/SIGMA = .087	0.008	0.20	1070.90	79.9
8543	3683	9-Mar-94	5:53:31	2P6 @ 56.7 CAM, RPM= 1088 VOR = 0.20 ALFSU = 0.30 CT/SIGMA = .087	0.008	0.20	1047.60	62.8
8537	3684	9-Mar-94	5:56:23	2P6 @ 56.7 CAM, RPM= 1087 VOR = 0.00 ALFSU = 0.00 CT/SIGMA = .000	0.001	0.00	10.34	26.4
999	3685	9-Mar-94	5:57:24	2P6 @ 56.7 CAM, RPM= 0000 VOR = 0.00 ALFSU = 0.00 CT/SIGMA = .000	####	0.00	36.54	0.0
8553	3686	9-Mar-94	20:48:56	2P6+101.7CAM, RPM= 1087 VOR = 0.00 ALFSU = 0.00 CT/SIGMA =	0.002	0.01	-77.37	25.5
8554	3687	9-Mar-94	20:54:49	2P6+101.7CAM, RPM= 1078 VOR = 0.15 ALFSU = -1.89 CT/SIGMA = 0.065	0.006	0.15	788.54	63.1
8555	3688	9-Mar-94	20:56:49	2P6+101.7CAM, RPM= 1078 VOR = 0.15 ALFSU = -1.61 CT/SIGMA = 0.087	0.008	0.15	1045.70	89.1
8556	3689	9-Mar-94	21:00:58	2P6+101.7CAM, RPM= 1082 VOR = 0.20 ALFSU = -3.24 CT/SIGMA = 0.065	0.006	0.20	788.47	60.8
8557	3690	9-Mar-94	21:05:02	2P6+101.7CAM, RPM= 1082 VOR = 0.20 ALFSU = -1.83 CT/SIGMA = 0.065	0.006	0.20	787.95	54.5
8558	3691	9-Mar-94	21:08:13	2P6+101.7CAM, RPM= 1084 VOR = 0.20 ALFSU = -2.72 CT/SIGMA = 0.087	0.008	0.20	1040.20	79.6
8558	3708	9-Mar-94	21:14:16	2P6+101.7CAM, RPM= 1084 VOR = 0.20 ALFSU = -2.72 CT/SIGMA = 0.087	0.008	0.20	1040.30	78.6
8559	3709	9-Mar-94	21:17:33	2P6+101.7CAM, RPM= 1086 VOR = 0.20 ALFSU = -2.00 CT/SIGMA = 0.087	0.008	0.20	1053.50	79.6
8553	3710	9-Mar-94	21:21:20	2P6+101.7CAM, RPM= 1087 VOR = 0.00 ALFSU = 0.00 CT/SIGMA =	0.001	0.01	-46.63	25.9
999	3711	9-Mar-94	21:22:29	2P6+101.7CAM, RPM= 0000 VOR = 0.00 ALFSU = 0.00 CT/SIGMA =	####	9.00	10.84	0.0
8568	3712	9-Mar-94	22:24:29	2P6+146.7CAM, RPM= 1087 VOR = 0.00 ALFSU = 0.00 CT/SIGMA =	0.002	0.01	-71.07	24.8
8569	3713	9-Mar-94	22:30:54	2P6+146.7CAM, RPM= 1080 VOR = 0.15 ALFSU = -1.89 CT/SIGMA = 0.065	0.006	0.15	784.81	60.8

TEST	POINT	DATE			CT	Mu	LIR (lbs)	HP
8570	3714	9-Mar-94	22:32:54	2P6+146.7CAM, RPM= 1080 VOR = 0.15 ALFSU =-1.81 CT/SIGMA = 0.087	0.008	0.15	1043.70	84.9
8571	3715	9-Mar-94	22:38:05	2P6+146.7CAM, RPM= 1085 VOR = 0.20 ALFSU =-3.24 CT/SIGMA = 0.065	0.006	0.20	788.70	58.6
8572	3716	9-Mar-94	22:42:00	2P6+146.7CAM, RPM= 1085 VOR = 0.20 ALFSU =-0.90 CT/SIGMA = 0.065	0.006	0.20	793.33	49.9
8568	3717	9-Mar-94	22:45:49	2P6+146.7CAM, RPM= 1085 VOR = 0.00 ALFSU = 0.00 CT/SIGMA =	0.001	0.01	-19.20	25.6
999	3718	9-Mar-94	22:46:33	2P6+146.7CAM, RPM= 0000 VOR = 0.00 ALFSU = 0.00 CT/SIGMA =	####	9.00	29.51	0.0
8568	3719	9-Mar-94	23:50:26	2P6+146.7CAM, RPM= 1087 VOR = 0.00 ALFSU = 0.00 CT/SIGMA = 0.000	0.001	0.01	-73.58	24.6
8573	3720	9-Mar-94	23:59:07	2P6+146.7CAM, RPM= 1083 VOR = 0.20 ALFSU =-2.70 CT/SIGMA = 0.087	0.008	0.20	1044.50	79.9
8574	3721	10-Mar-94	0:00:54	2P6+146.7CAM, RPM= 1083 VOR = 0.20 ALFSU =-0.35 CT/SIGMA = 0.087	0.008	0.20	1041.80	67.1
8568	3722	10-Mar-94	0:04:48	2P6+146.7CAM, RPM= 1087 VOR = 0.00 ALFSU = 0.00 CT/SIGMA = 0.000	0.001	0.01	-30.67	25.3
999	3723	10-Mar-94	0:05:47	2P6+146.7CAM, RPM= 0000 VOR = 0.00 ALFSU = 0.00 CT/SIGMA = 0.000	####	9.00	14.41	0.0
4045	3724	10-Mar-94	1:20:49	20-10 CAM, RPM= 1087 VOR = 0.00 ALFSU = 0.00 CT/SIGMA = 0.000	0.002	0.01	0.33	38.1
4032	3725	10-Mar-94	1:24:57	20-10 CAM, RPM= 1080 VOR = 0.15 ALFSU = 5.00 CT/SIGMA = 0.076	0.007	0.15	900.08	54.9
4032	3726	10-Mar-94	1:25:54	20-10 CAM, RPM= 1080 VOR = 0.15 ALFSU = 5.00 CT/SIGMA = 0.076	0.007	0.15	903.32	55.2
4032	3728	10-Mar-94	1:33:56	20-10 CAM, RPM= 1080 VOR = 0.15 ALFSU = 5.00 CT/SIGMA = 0.076	0.007	0.15	916.83	54.9
4032	3745	10-Mar-94	1:40:22	20-10 CAM, RPM= 1080 VOR = 0.15 ALFSU = 5.00 CT/SIGMA = 0.076	0.007	0.15	925.49	54.5
4047	3746	10-Mar-94	1:44:18	20-10 CAM, RPM= 1085 VOR = 0.20 ALFSU = 4.00 CT/SIGMA = 0.076	0.007	0.20	897.94	46.9
4047	3763	10-Mar-94	1:50:35	20-10 CAM, RPM= 1085 VOR = 0.20 ALFSU = 4.00 CT/SIGMA = 0.076	0.007	0.20	907.53	46.2
4052	3764	10-Mar-94	1:53:02	20-10 CAM, RPM= 1088 VOR = 0.20 ALFSU = 4.50 CT/SIGMA = 0.087	0.008	0.20	1035.10	50.9
4052	3781	10-Mar-94	1:59:22	20-10 CAM, RPM= 1088 VOR = 0.20 ALFSU = 4.50 CT/SIGMA = 0.087	0.008	0.20	1039.40	50.0
4050	3782	10-Mar-94	2:01:42	20-10 CAM, RPM= 1089 VOR = 0.20 ALFSU = 2.50 CT/SIGMA = 0.087	0.008	0.20	1029.50	58.9
999	3799	10-Mar-94	2:11:07	20-10 CAM, RPM= 0000 VOR = 0.00 ALFSU = 0.00 CT/SIGMA = 0.000	####	9.00	22.86	0.0
4045	3800	10-Mar-94	4:23:50	20-10 CAM, RPM= 1087 VOR = 0.00 ALFSU = 0.00 CT/SIGMA = 0.000	0.002	0.02	-16.48	38.7
4051	3801	10-Mar-94	4:30:36	20-10 CAM, RPM= 1089 VOR = 0.20 ALFSU = 3.50 CT/SIGMA = 0.087	0.008	0.20	1027.40	56.4
4051	3818	10-Mar-94	4:36:41	20-10 CAM, RPM= 1089 VOR = 0.20 ALFSU = 3.50 CT/SIGMA = 0.087	0.008	0.20	1053.20	55.6
4053	3819	10-Mar-94	4:39:07	20-10 CAM, RPM= 1093 VOR = 0.20 ALFSU = 5.50 CT/SIGMA = 0.087	0.008	0.20	1024.70	47.4
4053	3836	10-Mar-94	4:45:12	20-10 CAM, RPM= 1093 VOR = 0.20 ALFSU = 5.50 CT/SIGMA = 0.087	0.008	0.20	1041.40	46.3
4054	3837	10-Mar-94	4:47:15	20-10 CAM, RPM= 1095 VOR = 0.20 ALFSU = 6.50 CT/SIGMA = 0.087	0.008	0.20	1015.30	42.6
999	3853	10-Mar-94	4:56:32	20-10 CAM, RPM= 0000 VOR = 0.00 ALFSU = 0.00 CT/SIGMA = 0.000	####	9.00	30.58	0.0
4145	3854	10-Mar-94	23:48:35	20-0 CAM, RPM= 1087 VOR = 0.00 ALFSU = 0.00 CT/SIGMA = 0.000	0.001	0.01	-24.68	38.6
4117	3855	10-Mar-94	23:53:40	20-0 CAM, RPM= 1076 VOR = 0.15 ALFSU = 5.00 CT/SIGMA = 0.076	0.007	0.15	887.20	56.1
4117	3872	10-Mar-94	23:59:53	20-0 CAM, RPM= 1076 VOR = 0.15 ALFSU = 5.00 CT/SIGMA = 0.076	0.007	0.15	900.57	55.6
4123	3873	11-Mar-94	0:02:51	20-0 CAM, RPM= 1076 VOR = 0.20 ALFSU = 4.00 CT/SIGMA = 0.076	0.007	0.20	895.70	48.1
4123	3890	11-Mar-94	0:09:02	20-0 CAM, RPM= 1076 VOR = 0.20 ALFSU = 4.00 CT/SIGMA = 0.076	0.007	0.20	901.18	47.6
4128	3891	11-Mar-94	0:11:10	20-0 CAM, RPM= 1082 VOR = 0.20 ALFSU = 4.50 CT/SIGMA = 0.087	0.008	0.20	1040.90	53.8
4128	3908	11-Mar-94	0:17:23	20-0 CAM, RPM= 1082 VOR = 0.20 ALFSU = 4.50 CT/SIGMA = 0.087	0.008	0.20	1041.40	53.6
4119	3909	11-Mar-94	0:20:41	20-0 CAM, RPM= 1082 VOR = 0.15 ALFSU = 7.00 CT/SIGMA = 0.076	0.007	0.15	903.03	51.6
4119	3926	11-Mar-94	0:26:50	20-0 CAM, RPM= 1082 VOR = 0.15 ALFSU = 7.00 CT/SIGMA = 0.076	0.007	0.15	908.03	51.4
4120	3927	11-Mar-94	0:30:09	20-0 CAM, RPM= 1082 VOR = 0.20 ALFSU = 2.00 CT/SIGMA = 0.076	0.007	0.20	896.60	58.1
999	3929	11-Mar-94	0:34:20	20-0 CAM, RPM= 0000 VOR = 0.00 ALFSU = 0.00 CT/SIGMA = 0.000	####	0.00	-37.70	0.0
4145	3930	11-Mar-94	2:22:24	20-0 CAM, RPM= 1087 VOR = 0.00 ALFSU = 0.00 CT/SIGMA = 0.000	0.001	0.01	-37.88	39.6
4120	3931	11-Mar-94	2:26:22	20-0 CAM, RPM= 1077 VOR = 0.20 ALFSU = 2.00 CT/SIGMA = 0.076	0.007	0.20	911.90	58.4
4120	3948	11-Mar-94	2:32:32	20-0 CAM, RPM= 1077 VOR = 0.20 ALFSU = 2.00 CT/SIGMA = 0.076	0.007	0.20	937.64	57.7
4126	3949	11-Mar-94	2:34:42	20-0 CAM, RPM= 1080 VOR = 0.20 ALFSU = 2.50 CT/SIGMA = 0.087	0.008	0.20	1040.20	62.0
4126	3968	11-Mar-94	2:40:50	20-0 CAM, RPM= 1080 VOR = 0.20 ALFSU = 2.50 CT/SIGMA = 0.087	0.008	0.20	1055.20	61.4
4125	3967	11-Mar-94	2:42:50	20-0 CAM, RPM= 1082 VOR = 0.20 ALFSU = 6.00 CT/SIGMA = 0.076	0.007	0.20	899.57	42.2
4125	3984	11-Mar-94	2:49:10	20-0 CAM, RPM= 1082 VOR = 0.20 ALFSU = 6.00 CT/SIGMA = 0.076	0.007	0.20	911.88	41.1
4157	3985	11-Mar-94	2:51:10	20-0 CAM, RPM= 1083 VOR = 0.20 ALFSU = 6.50 CT/SIGMA = 0.087	0.008	0.20	1020.90	43.8
4157	4002	11-Mar-94	2:57:18	20-0 CAM, RPM= 1083 VOR = 0.20 ALFSU = 6.50 CT/SIGMA = 0.087	0.008	0.20	1028.20	43.2
4030	4003	11-Mar-94	3:00:18	20-0 CAM, RPM= 1083 VOR = 0.15 ALFSU = 3.00 CT/SIGMA = 0.076	0.007	0.15	921.00	62.9
4030	4020	11-Mar-94	3:06:25	20-0 CAM, RPM= 1083 VOR = 0.15 ALFSU = 3.00 CT/SIGMA = 0.076	0.007	0.15	919.89	63.1
4145	4021	11-Mar-94	3:08:28	20-0 CAM, RPM= 1087 VOR = 0.00 ALFSU = 0.00 CT/SIGMA = 0.000	0.002	0.00	18.49	39.9
999	4022	11-Mar-94	3:09:35	20-0 CAM, RPM= 0000 VOR = 0.00 ALFSU = 0.00 CT/SIGMA = 0.000	####	0.00	5.30	0.0
4045	4023	11-Mar-94	3:27:12	20-0 CAM, RPM= 1087 VOR = 0.00 ALFSU = 0.00 CT/SIGMA = 0.000	0.001	0.00	-65.47	39.7
4031	4024	11-Mar-94	3:31:36	20-0 CAM, RPM= 1078 VOR = 0.15 ALFSU = 5.00 CT/SIGMA = 0.076	0.007	0.15	912.00	59.6
4031	4041	11-Mar-94	3:38:01	20-0 CAM, RPM= 1078 VOR = 0.15 ALFSU = 5.00 CT/SIGMA = 0.076	0.007	0.15	931.77	59.3
999	4042	11-Mar-94	3:41:52	20-10 CAM, RPM= 0000 VOR = 0.00 ALFSU = 0.00 CT/SIGMA = 0.000	####	0.00	-27.11	0.0
4045	4043	11-Mar-94	4:36:07	20-10 CAM, RPM= 1087 VOR = 0.00 ALFSU = 0.00 CT/SIGMA = 0.000	0.001	0.01	-27.68	38.9
4034	4044	11-Mar-94	4:41:32	20-10 CAM, RPM= 1077 VOR = 0.15 ALFSU = 3.00 CT/SIGMA = 0.076	0.007	0.15	910.82	62.6
4034	4061	11-Mar-94	4:47:44	20-10 CAM, RPM= 1077 VOR = 0.15 ALFSU = 3.00 CT/SIGMA = 0.076	0.007	0.15	936.92	62.5
4055	4062	11-Mar-94	4:51:05	20-10 CAM, RPM= 1077 VOR = 0.20 ALFSU = 7.50 CT/SIGMA = 0.087	0.008	0.20	1039.70	40.6
4055	4079	11-Mar-94	4:57:17	20-10 CAM, RPM= 1077 VOR = 0.20 ALFSU = 7.50 CT/SIGMA = 0.087	0.008	0.20	1055.00	39.8
4056	4080	11-Mar-94	4:59:34	20-10 CAM, RPM= 1080 VOR = 0.20 ALFSU = 8.50 CT/SIGMA = 0.087	0.008	0.20	1041.10	36.8
4056	4097	11-Mar-94	5:05:43	20-10 CAM, RPM= 1080 VOR = 0.20 ALFSU = 8.50 CT/SIGMA = 0.087	0.008	0.20	1060.50	35.9
4945	4098	11-Mar-94	5:07:57	20-10 CAM, RPM= 1082 VOR = 0.20 ALFSU = 2.00 CT/SIGMA = 0.076	0.007	0.20	915.18	55.6
4945	4115	11-Mar-94	5:14:10	20-10 CAM, RPM= 1082 VOR = 0.20 ALFSU = 2.00 CT/SIGMA = 0.076	0.007	0.20	932.77	55.0
4049	4116	11-Mar-94	5:16:25	20-10 CAM, RPM= 1082 VOR = 0.20 ALFSU = 6.00 CT/SIGMA = 0.076	0.007	0.20	903.11	41.1
999	4131	11-Mar-94	5:24:49	20-10 CAM, RPM= 0000 VOR = 0.00 ALFSU = 0.00 CT/SIGMA = 0.000	####	0.00	32.46	0.0
4845	4132	11-Mar-94	18:37:52	20-15 CAM, RPM= 1087 VOR = 0.00 ALFSU = 0.00 CT/SIGMA = 0.000	0.001	0.01	-26.53	38.7
4817	4133	11-Mar-94	18:55:28	20-15 CAM, RPM= 1079 VOR = 0.15 ALFSU = 5.00 CT/SIGMA = 0.076	0.007	0.15	921.66	58.2
4817	4150	11-Mar-94	19:01:34	20-15 CAM, RPM= 1079 VOR = 0.15 ALFSU = 5.00 CT/SIGMA = 0.076	0.007	0.15	942.86	58.0
4824	4151	11-Mar-94	19:03:45	20-15 CAM, RPM= 1083 VOR = 0.20 ALFSU = 5.00 CT/SIGMA = 0.076	0.007	0.20	925.61	46.0
4824	4168	11-Mar-94	19:09:46	20-15 CAM, RPM= 1083 VOR = 0.20 ALFSU = 5.00 CT/SIGMA = 0.076	0.007	0.20	932.55	45.6
4828	4189	11-Mar-94	19:11:38	20-15 CAM, RPM= 1085 VOR = 0.20 ALFSU = 4.50 CT/SIGMA = 0.087	0.008	0.20	1059.10	54.4
4828	4186	11-Mar-94	19:17:45	20-15 CAM, RPM= 1085 VOR = 0.20 ALFSU = 4.50 CT/SIGMA = 0.087	0.008	0.20	1059.40	54.0
4845	4187	11-Mar-94	19:20:13	20-15 CAM, RPM= 1087 VOR = 0.00 ALFSU = 0.00 CT/SIGMA = 0.000	0.002	0.01	0.41	39.1
999	4188	11-Mar-94	19:21:04	20-15 CAM, RPM= 0000 VOR = 0.00 ALFSU = 0.00 CT/SIGMA = 0.000	####	9.00	9.18	0.0
5845	4189	11-Mar-94	21:17:48	17.5-20 CAM, RPM= 1087 VOR = 0.00 ALFSU = 0.00 CT/SIGMA = 0.000	0.001	0.01	-23.58	36.3
5830	4190	11-Mar-94	21:24:27	17.5-20 CAM, RPM= 1077 VOR = 0.20 ALFSU = 7.50 CT/SIGMA = 0.087	0.008	0.20	1042.20	37.5
5830	4207	11-Mar-94	21:30:31	17.5-20 CAM, RPM= 1077 VOR = 0.20 ALFSU = 7.50 CT/SIGMA = 0.087	0.008	0.20	1057.40	36.8
8531	4208	11-Mar-94	21:33:04	17.5-20 CAM, RPM= 1082 VOR = 0.20 ALFSU = 8.50 CT/SIGMA = 0.087	0.008	0.20	1038.90	33.3
8531	4225	11-Mar-94	21:39:01	17.5-20 CAM, RPM= 1082 VOR = 0.20 ALFSU = 8.50 CT/SIGMA = 0.087	0.008	0.20	1050.40	32.4
5845	4226	11-Mar-94	21:42:30	17.5-20 CAM, RPM= 1087 VOR = 0.00 ALFSU = 0.00 CT/SIGMA = 0.000	0.002	0.00	19.51	36.0
999	4227	11-Mar-94	21:43:17	17.5-20 CAM, RPM= 0000 VOR = 0.00 ALFSU = 0.00 CT/SIGMA = 0.000	####	0.00	27.34	0.0
5045	4228	11-Mar-94	22:03:20	17.5+140 CAM, RPM= 1087 VOR = 0.00 ALFSU = 0.00 CT/SIGMA = 0.000	0.001	0.00	-26.76	36.0
5032	4229	11-Mar-94	22:09:06	17.5+140 CAM, RPM= 1078 VOR = 0.15 ALFSU = 5.00 CT/SIGMA = 0.076	0.007	0.15	925.17	52.5





TEST	POINT	DATE			CT	Mu	Lift (lbs)	HP
7506	4539	12-Mar-94	15:43:20	3P2A-15 CAM, RPM= 1087 VOR = 0.00 ALFSU = 0.00 CT/SIGMA = 0.000	0.001	0.01	13.71	26.3
7509	4540	12-Mar-94	15:44:03	3P2A-15 CAM, RPM= 1087 COLL = 1.0	0.001	0.01	80.56	28.2
7510	4541	12-Mar-94	15:44:41	3P2A-15 CAM, RPM= 1087 COLL = 2.0 DEG	0.002	0.01	166.80	32.4
7511	4542	12-Mar-94	15:45:11	3P2A-15 CAM, RPM= 1087 COLL = 3.0 DEG	0.002	0.02	261.39	38.4
7512	4543	12-Mar-94	15:45:40	3P2A-15 CAM, RPM= 1087 COLL = 4.0 DEG	0.003	0.03	357.96	45.6
7513	4544	12-Mar-94	15:46:12	3P2A-15 CAM, RPM= 1087 COLL = 5.0 DEG	0.004	0.02	484.05	56.7
7514	4545	12-Mar-94	15:46:42	3P2A-15 CAM, RPM= 1087 COLL = 6.0 DEG	0.004	0.04	584.80	66.9
7515	4546	12-Mar-94	15:47:26	3P2A-15 CAM, RPM= 1087 COLL = 7.0 DEG	0.006	0.03	732.56	82.6
7516	4547	12-Mar-94	15:48:03	3P2A-15 CAM, RPM= 1087 COLL = 8.0 DEG	0.006	0.04	851.65	98.1
999	4549	12-Mar-94	16:09:08	3P2A-15 CAM, RPM= 0000 COLL = 0.0 DEG	####	9.00	50.86	0.0
6506	4550	12-Mar-94	22:57:05	5P4A-9 CAM, RPM= 1087 COLL = 0.0 DEG	0.001	0.00	10.66	26.2
6505	4551	12-Mar-94	22:57:48	5P4A-9 CAM, RPM= 1033 COLL = 0.0 DEG	0.001	0.00	8.93	22.6
6504	4552	12-Mar-94	22:58:31	5P4A-9 CAM, RPM= 978 COLL = 0.0 DEG	0.001	0.01	10.92	19.6
6503	4553	12-Mar-94	22:59:07	5P4A-9 CAM, RPM= 870 COLL = 0.0 DEG	0.001	0.00	8.34	13.9
6502	4554	12-Mar-94	22:59:40	5P4A-9 CAM, RPM= 781 COLL = 0.0 DEG	0.001	0.00	8.71	9.6
6501	4555	12-Mar-94	23:00:25	5P4A-9 CAM, RPM= 652 COLL = 0.0 DEG	0.001	0.00	10.15	6.4
6506	4556	12-Mar-94	23:01:20	5P4A-9 CAM, RPM= 1087 COLL = 0.0 DEG	0.001	0.00	22.62	26.3
6509	4557	12-Mar-94	23:02:07	5P4A-9 CAM, RPM= 1087 COLL = 1.0 DEG	0.001	0.01	111.40	29.2
6510	4558	12-Mar-94	23:02:38	5P4A-9 CAM, RPM= 1087 COLL = 2.0 DEG	0.002	0.01	175.19	32.4
6511	4559	12-Mar-94	23:03:12	5P4A-9 CAM, RPM= 1087 COLL = 3.0 DEG	0.002	0.01	269.03	38.3
6512	4560	12-Mar-94	23:03:42	5P4A-9 CAM, RPM= 1087 COLL = 4.0 DEG	0.003	0.02	370.19	46.3
6513	4561	12-Mar-94	23:04:06	5P4A-9 CAM, RPM= 1087 COLL = 5.0 DEG	0.004	0.02	483.52	56.4
6514	4562	12-Mar-94	23:04:41	5P4A-9 CAM, RPM= 1087 COLL = 6.0 DEG	0.005	0.02	602.77	67.9
6515	4563	12-Mar-94	23:05:14	5P4A-9 CAM, RPM= 1087 COLL = 7.0 DEG	0.005	0.03	716.02	81.0
6516	4564	12-Mar-94	23:05:47	5P4A-9 CAM, RPM= 1087 COLL = 8.0 DEG	0.006	0.04	832.96	96.3
6517	4565	12-Mar-94	23:06:25	5P4A-9 CAM, RPM= 1087 COLL = 9.0 DEG	0.007	0.04	974.96	116.3
6507	4566	12-Mar-94	23:08:10	5P4A-9 CAM, RPM= 1120 COLL = 0.0 DEG	0.001	0.01	48.35	29.4
6506	4567	12-Mar-94	23:08:40	5P4A-9 CAM, RPM= 1087 COLL = 0.0 DEG	0.001	0.01	46.17	27.0
6510	4568	12-Mar-94	23:09:19	5P4A-9 CAM, RPM= 1087 COLL = 2.0 DEG	0.002	0.02	193.57	32.8
6519	4569	12-Mar-94	23:10:08	5P4A-9 CAM, RPM= 1087 COLL = 2.0 DEG, LAT = 2.0 DEG	0.002	0.02	206.94	35.3
6520	4570	12-Mar-94	23:10:56	5P4A-9 CAM, RPM= 1087 COLL = 2.0 DEG, LONG = 2.0 DEG	0.002	0.01	206.67	35.1
6506	4571	12-Mar-94	23:11:33	5P4A-9 CAM, RPM= 1087 COLL = 0.0 DEG	0.001	0.00	39.44	26.5
6521	4572	12-Mar-94	23:14:41	5P4A-9 CAM, RPM= 1072 VOR=0.10 ALFSU=-0.92	0.006	0.10	793.11	65.4
6523	4573	12-Mar-94	23:18:13	5P4A-9 CAM, RPM= 1075 VOR=0.15 ALFSU=-1.89	0.006	0.15	785.94	56.2
6526	4574	12-Mar-94	23:20:22	5P4A-9 CAM, RPM= 1077 VOR=0.20 ALFSU=-0.70	0.006	0.20	801.74	48.5
6528	4575	12-Mar-94	23:22:50	5P4A-9 CAM, RPM= 1077 VOR=0.20 ALFSU=-0.70 CT/SIGMA=0.087	0.008	0.20	1061.30	67.0
6528	4592	12-Mar-94	23:29:06	5P4A-9 CAM, RPM= 1077 VOR=0.20 ALFSU=-0.70 CT/SIGMA=0.087	0.008	0.20	1060.50	66.2
6590	4593	12-Mar-94	23:31:42	5P4A-9 CAM, RPM= 1081 VOR=0.20 ALFSU=3.50 CT/SIGMA=0.087	0.008	0.20	1055.30	46.6
6590	4610	12-Mar-94	23:37:48	5P4A-9 CAM, RPM= 1081 VOR=0.20 ALFSU=3.50 CT/SIGMA=0.087	0.008	0.20	1051.70	46.5
6530	4611	12-Mar-94	23:41:15	5P4A-9 CAM, RPM= 1084 VOR=0.25 ALFSU=-3.00 CT/SIGMA=0.065	0.006	0.25	799.95	58.0
6532	4612	12-Mar-94	23:42:34	5P4A-9 CAM, RPM= 1084 VOR=0.25 ALFSU=-2.50 CT/SIGMA=0.087	0.008	0.25	1072.00	76.6
6534	4613	12-Mar-94	23:46:09	5P4A-9 CAM, RPM= 1089 VOR=0.30 ALFSU=-5.00 CT/SIGMA=0.065	0.006	0.30	800.79	71.7
6536	4614	12-Mar-94	23:47:42	5P4A-9 CAM, RPM= 1090 VOR=0.30 ALFSU=-4.00 CT/SIGMA=0.087	0.008	0.30	1068.00	91.0
6506	4615	12-Mar-94	23:50:58	5P4A-9 CAM, RPM= 1087 VOR=0.00 ALFSU=0.00 CT/SIGMA=0.000	0.001	0.00	18.31	27.0
999	4616	12-Mar-94	23:51:46	5P4A-9 CAM, RPM= 0000 VOR=0.00 ALFSU=0.00 CT/SIGMA=0.000	####	0.00	7.86	0.0
6606	4617	13-Mar-94	0:12:02	5P4A+9 CAM, RPM= 1087 VOR=0.00 ALFSU=0.00 CT/SIGMA=0.000	0.001	0.00	7.77	27.0
6621	4618	13-Mar-94	0:15:33	5P4A+9 CAM, RPM= 1077 VOR=0.10 ALFSU=0.92 CT/SIGMA=0.065	0.006	0.10	797.77	68.5
6622	4619	13-Mar-94	0:17:05	5P4A+9 CAM, RPM= 1077 VOR=0.10 ALFSU=-0.81 CT/SIGMA=0.087	0.008	0.10	1080.10	100.8
6623	4620	13-Mar-94	0:20:07	5P4A+9 CAM, RPM= 1080 VOR=0.15 ALFSU=-1.89 CT/SIGMA=0.065	0.006	0.15	801.85	58.7
6624	4621	13-Mar-94	0:21:53	5P4A+9 CAM, RPM= 1080 VOR=0.15 ALFSU=-1.81 CT/SIGMA=0.087	0.008	0.15	1059.80	82.1
6625	4622	13-Mar-94	0:24:27	5P4A+9 CAM, RPM= 1081 VOR=0.20 ALFSU=-0.70 CT/SIGMA=0.065	0.006	0.20	797.89	48.7
6627	4623	13-Mar-94	0:25:57	5P4A+9 CAM, RPM= 1082 VOR=0.20 ALFSU=-0.70 CT/SIGMA=0.087	0.008	0.20	1058.40	67.4
6627	4640	13-Mar-94	0:32:02	5P4A+9 CAM, RPM= 1082 VOR=0.20 ALFSU=-0.70 CT/SIGMA=0.087	0.008	0.20	1071.70	66.9
6630	4641	13-Mar-94	0:35:04	5P4A+9 CAM, RPM= 1085 VOR=0.25 ALFSU=-3.00 CT/SIGMA=0.065	0.006	0.25	787.50	55.1
6632	4642	13-Mar-94	0:36:30	5P4A+9 CAM, RPM= 1086 VOR=0.25 ALFSU=-2.50 CT/SIGMA=0.087	0.008	0.25	1059.10	71.4
6634	4643	13-Mar-94	0:39:00	5P4A+9 CAM, RPM= 1090 VOR=0.30 ALFSU=-5.00 CT/SIGMA=0.065	0.006	0.30	796.39	67.8
6636	4644	13-Mar-94	0:40:04	5P4A+9 CAM, RPM= 1090 VOR=0.30 ALFSU=-4.00 CT/SIGMA=0.087	0.008	0.30	1053.50	84.6
6606	4645	13-Mar-94	0:42:52	5P4A+9 CAM, RPM= 1087 VOR=0.00 ALFSU=0.00 CT/SIGMA=0.000	0.001	0.00	66.96	27.7
999	4646	13-Mar-94	0:43:33	5P4A+9 CAM, RPM= 0000 VOR=0.00 ALFSU=0.00 CT/SIGMA=0.000	####	0.00	34.69	0.0
6706	4647	13-Mar-94	0:53:55	5P4A+45 CAM, RPM= 1087 VOR=0.00 ALFSU=0.00 CT/SIGMA=0.000	0.001	0.00	36.01	26.7
6721	4648	13-Mar-94	0:56:40	5P4A+45 CAM, RPM= 1080 VOR=0.10 ALFSU=0.92 CT/SIGMA=0.065	0.006	0.10	800.04	66.0
6722	4649	13-Mar-94	0:58:12	5P4A+45 CAM, RPM= 1080 VOR=0.10 ALFSU=-0.81 CT/SIGMA=0.087	0.008	0.10	1086.70	100.5
6723	4650	13-Mar-94	1:00:43	5P4A+45 CAM, RPM= 1080 VOR=0.15 ALFSU=-1.89 CT/SIGMA=0.065	0.006	0.15	806.09	57.2
6724	4651	13-Mar-94	1:01:58	5P4A+45 CAM, RPM= 1081 VOR=0.15 ALFSU=-1.61 CT/SIGMA=0.087	0.008	0.15	1057.50	79.5
6726	4652	13-Mar-94	1:04:02	5P4A+45 CAM, RPM= 1081 VOR=0.20 ALFSU=-0.70 CT/SIGMA=0.065	0.006	0.20	792.72	47.7
6728	4653	13-Mar-94	1:05:13	5P4A+45 CAM, RPM= 1082 VOR=0.20 ALFSU=-0.70 CT/SIGMA=0.087	0.008	0.20	1073.20	66.7
6730	4654	13-Mar-94	1:07:23	5P4A+45 CAM, RPM= 1085 VOR=0.25 ALFSU=-3.00 CT/SIGMA=0.065	0.006	0.25	784.95	54.0
6732	4655	13-Mar-94	1:08:49	5P4A+45 CAM, RPM= 1086 VOR=0.25 ALFSU=-2.50 CT/SIGMA=0.087	0.008	0.25	1057.50	70.7
6734	4656	13-Mar-94	1:11:19	5P4A+45 CAM, RPM= 1090 VOR=0.30 ALFSU=-5.00 CT/SIGMA=0.065	0.006	0.30	798.58	66.8
6736	4657	13-Mar-94	1:12:38	5P4A+45 CAM, RPM= 1093 VOR=0.30 ALFSU=-4.00 CT/SIGMA=0.087	0.008	0.30	1064.60	83.1
6706	4658	13-Mar-94	1:15:06	5P4A+45 CAM, RPM= 1087 VOR=0.00 ALFSU=0.00 CT/SIGMA=0.000	0.001	0.01	79.89	28.4
999	4659	13-Mar-94	1:18:00	5P4A+45 CAM, RPM= 0000 VOR=0.00 ALFSU=0.00 CT/SIGMA=0.000	####	0.00	39.71	0.0
6806	4660	14-Mar-94	18:02:20	5P4A+27.5 CAM, RPM= 1087 VOR=0.00 ALFSU=0.00 CT/SIGMA=0.000	0.001	0.01	42.75	25.9
6821	4661	14-Mar-94	18:05:32	5P4A+27.5 CAM, RPM= 1089 VOR=0.10 ALFSU=-0.92 CT/SIGMA=0.065	0.006	0.10	786.42	66.0
6822	4662	14-Mar-94	18:07:02	5P4A+27.5 CAM, RPM= 1089 VOR=0.10 ALFSU=-0.81 CT/SIGMA=0.087	0.008	0.10	1043.00	98.7
6823	4663	14-Mar-94	18:09:34	5P4A+27.5 CAM, RPM= 1091 VOR=0.15 ALFSU=-1.89 CT/SIGMA=0.065	0.006	0.15	780.95	55.9
6824	4664	14-Mar-94	18:11:02	5P4A+27.5 CAM, RPM= 1091 VOR=0.15 ALFSU=-1.81 CT/SIGMA=0.087	0.008	0.15	1041.50	79.0
6826	4665	14-Mar-94	18:14:46	5P4A+27.5 CAM, RPM= 1091 VOR=0.20 ALFSU=-0.70 CT/SIGMA=0.065	0.006	0.20	778.29	46.7
6828	4666	14-Mar-94	18:17:25	5P4A+27.5 CAM, RPM= 1093 VOR=0.20 ALFSU=-0.70 CT/SIGMA=0.087	0.008	0.20	1037.90	65.3
6828	4683	14-Mar-94	18:23:29	5P4A+27.5 CAM, RPM= 1093 VOR=0.20 ALFSU=-0.70 CT/SIGMA=0.087	0.008	0.20	1038.20	64.5
6830	4684	14-Mar-94	18:28:19	5P4A+27.5 CAM, RPM= 1088 VOR=0.25 ALFSU=-3.00 CT/SIGMA=0.065	0.006	0.25	784.22	54.4
6832	4685	14-Mar-94	18:28:45	5P4A+27.5 CAM, RPM= 1099 VOR=0.25 ALFSU=-2.50 CT/SIGMA=0.087	0.008	0.25	1040.20	70.1
6834	4686	14-Mar-94	18:31:54	5P4A+27.5 CAM, RPM= 1103 VOR=0.30 ALFSU=-5.00 CT/SIGMA=0.065	0.006	0.30	785.07	67.3
6836	4687	14-Mar-94	18:33:57	5P4A+27.5 CAM, RPM= 1102 VOR=0.30 ALFSU=-4.00 CT/SIGMA=0.087	0.008	0.30	1044.00	85.6
6806	4688	14-Mar-94	18:37:19	5P4A+27.5 CAM, RPM= 1087 VOR=0.00 ALFSU=0.00 CT/SIGMA=0.000	0.001	0.01	35.12	27.8

REPORT DOCUMENTATION PAGE			Form Approved OMB No. 0704-0188		
Public reporting burden for this collection of information is estimated to average 1 hour per response, including the time for reviewing instructions, searching existing data sources, gathering and maintaining the data needed, and completing and reviewing the collection of information. Send comments regarding this burden estimate or any other aspect of this collection of information, including suggestions for reducing this burden, to Washington Headquarters Services, Directorate for Information Operations and Reports, 1215 Jefferson Davis Highway, Suite 1204, Arlington, VA 22202-4302, and to the Office of Management and Budget, Paperwork Reduction Project (0704-0188), Washington, DC 20503.					
1. AGENCY USE ONLY (Leave blank)		2. REPORT DATE July 1995	3. REPORT TYPE AND DATES COVERED Contractor Report		
4. TITLE AND SUBTITLE Blade Mounted Flap Control For BVI Noise Reduction Proof-of-Concept Test			5. FUNDING NUMBERS C NAS1-19060 TA 8  WU 505-63-36-03		
6. AUTHOR(S) Seth Dawson, Ahmed Hassan, Friedrich Straub and Hormoz Tadghighi					
7. PERFORMING ORGANIZATION NAME(S) AND ADDRESS(ES) McDonnell Douglas Aerospace McDonnell Douglas Helicopter Systems 5000 E. McDowell Rd. Mesa, AZ 85215			8. PERFORMING ORGANIZATION REPORT NUMBER  L6BCK-FR-94001		
9. SPONSORING/MONITORING AGENCY NAME(S) AND ADDRESS(ES) National Aeronautics and Space Administration Langley Research Center Hampton, VA 23681-0001			10. SPONSORING/MONITORING AGENCY REPORT NUMBER  NASA CR-195078		
11. SUPPLEMENTARY NOTES  Langley Technical Monitor: Michael A. Marcolini Final Report - Task 8					
12a. DISTRIBUTION/AVAILABILITY STATEMENT  Unclassified - Unlimited  Subject Category 71			12b. DISTRIBUTION CODE		
13. ABSTRACT (Maximum 200 words)  This report describes a wind tunnel test of the McDonnell Douglas Helicopter Systems (MDHS) Active Flap Model Rotor at the NASA Langley 14- by 22-Foot Subsonic Tunnel. The test demonstrated that BVI noise reductions and vibration reductions were possible with the use of an active flap. Aerodynamic results supported the acoustic data trends, showing a reduction in the strength of the tip vortex with the deflection of the flap. Acoustic results showed that the flap deployment, depending on the peak deflection angle and azimuthal shift in its deployment schedule, can produce BVI noise reductions as much as 6 dB on the advancing and retreating sides. The noise reduction was accompanied by an increase in low frequency harmonic noise and high frequency broadband noise. A brief assessment of the effect of the flap on vibration showed that significant reductions were possible. The greatest vibration reductions (as much as 76%) were found in the four per rev pitching moment at the hub. Performance improvement can results were inconclusive, as the improvements were predicted to be smaller than the resolution of the rotor balance.					
14. SUBJECT TERMS  Active Flap Rotor, Blade-Vortex Interaction, Active Controls, Rotor Noise			15. NUMBER OF PAGES 193		
			16. PRICE CODE A09		
17. SECURITY CLASSIFICATION OF REPORT  Unclassified	18. SECURITY CLASSIFICATION OF THIS PAGE  Unclassified	19. SECURITY CLASSIFICATION OF ABSTRACT	20. LIMITATION OF ABSTRACT		

TEST	POINT	DATE			CT	Mu	Lift (lbs)	HP
999	4689	14-Mar-94	18:38:10	5P4A+27.5 CAM, RPM= 0000 VOR=0.00 ALFSU= 0.00 CT/SIGMA=0.000	####	0.00	-1.93	0.0
6906	4690	14-Mar-94	19:12:15	5P4A+0 CAM, RPM= 1087 VOR=0.00 ALFSU= 0.00 CT/SIGMA=0.000	0.001	0.01	-11.62	25.2
6921	4691	14-Mar-94	19:15:30	5P4A+0 CAM, RPM= 1087 VOR=0.10 ALFSU=-0.92 CT/SIGMA=0.065	0.006	0.10	798.32	69.7
6923	4692	14-Mar-94	19:17:16	5P4A+0 CAM, RPM= 1090 VOR=0.15 ALFSU=-1.89 CT/SIGMA=0.065	0.006	0.15	788.01	58.9
6926	4693	14-Mar-94	19:19:28	5P4A+0 CAM, RPM= 1093 VOR=0.20 ALFSU=-0.70 CT/SIGMA=0.065	0.006	0.20	783.85	48.6
6930	4694	14-Mar-94	19:21:31	5P4A+0 CAM, RPM= 1096 VOR=0.25 ALFSU=-3.00 CT/SIGMA=0.065	0.006	0.25	774.97	54.2
6934	4695	14-Mar-94	19:23:43	5P4A+0 CAM, RPM= 1100 VOR=0.30 ALFSU=-5.00 CT/SIGMA=0.065	0.006	0.30	781.64	67.1
6906	4696	14-Mar-94	19:26:25	5P4A+0 CAM, RPM= 1087 VOR=0.00 ALFSU= 0.00 CT/SIGMA=0.000	0.001	0.00	25.48	26.8
999	4697	14-Mar-94	19:27:09	5P4A+0 CAM, RPM= 0000 VOR=0.00 ALFSU= 0.00 CT/SIGMA=0.000	####	0.00	-0.37	0.0
6956	4698	14-Mar-94	19:43:48	5P4A+18 CAM, RPM= 1087 VOR=0.00 ALFSU= 0.00 CT/SIGMA=0.000	0.001	0.00	30.09	26.2
6971	4699	14-Mar-94	19:46:46	5P4A+18 CAM, RPM= 1090 VOR=0.10 ALFSU=-0.92 CT/SIGMA=0.065	0.006	0.10	783.97	67.0
6973	4700	14-Mar-94	19:48:27	5P4A+18 CAM, RPM= 1089 VOR=0.15 ALFSU=-1.89 CT/SIGMA=0.065	0.006	0.15	781.08	56.5
6976	4701	14-Mar-94	19:50:16	5P4A+18 CAM, RPM= 1091 VOR=0.20 ALFSU=-0.70 CT/SIGMA=0.065	0.006	0.20	778.21	46.8
6980	4702	14-Mar-94	19:52:24	5P4A+18 CAM, RPM= 1094 VOR=0.25 ALFSU=-3.00 CT/SIGMA=0.065	0.006	0.25	783.28	52.8
6984	4703	14-Mar-94	19:54:37	5P4A+18 CAM, RPM= 1100 VOR=0.30 ALFSU=-5.00 CT/SIGMA=0.065	0.006	0.30	785.13	65.4
6956	4704	14-Mar-94	19:57:24	5P4A+18 CAM, RPM= 1087 VOR=0.00 ALFSU= 0.00 CT/SIGMA=0.000	0.001	0.00	52.36	27.5
999	4705	14-Mar-94	19:58:10	5P4A+18 CAM, RPM= 0000 VOR=0.00 ALFSU= 0.00 CT/SIGMA=0.000	####	0.00	33.23	0.0
5000	4706	14-Mar-94	22:36:10	NO HORN, RPM= 1087 VOR=0.00 ALFSU= 0.00 CT/SIGMA=0.000	0.001	0.01	46.89	21.8
5509	4707	14-Mar-94	22:37:00	NO HORN, RPM= 1087 COLL=1.0 ALFSU= 0.00 CT/SIGMA=0.000	0.001	0.01	103.77	23.1
5510	4708	14-Mar-94	22:37:38	NO HORN, RPM= 1087 COLL=2.0 ALFSU= 0.00 CT/SIGMA=0.000	0.002	0.02	186.33	27.0
5511	4709	14-Mar-94	22:39:11	NO HORN, RPM= 1087 COLL=3.0 ALFSU= 0.00 CT/SIGMA=0.000	0.002	0.01	266.01	31.7
5512	4710	14-Mar-94	22:39:51	NO HORN, RPM= 1087 COLL=4.0 ALFSU= 0.00 CT/SIGMA=0.000	0.003	0.02	370.64	38.7
5513	4711	14-Mar-94	22:40:35	NO HORN, RPM= 1087 COLL=5.0 ALFSU= 0.00 CT/SIGMA=0.000	0.004	0.03	477.43	47.2
5514	4712	14-Mar-94	22:41:15	NO HORN, RPM= 1087 COLL=6.0 ALFSU= 0.00 CT/SIGMA=0.000	0.005	0.03	582.45	58.1
5515	4713	14-Mar-94	22:41:52	NO HORN, RPM= 1087 COLL=7.0 ALFSU= 0.00 CT/SIGMA=0.000	0.005	0.03	690.89	68.5
5516	4714	14-Mar-94	22:42:33	NO HORN, RPM= 1087 COLL=8.0 ALFSU= 0.00 CT/SIGMA=0.000	0.006	0.03	794.29	83.2
5517	4715	14-Mar-94	22:43:15	NO HORN, RPM= 1087 COLL=9.0 ALFSU= 0.00 CT/SIGMA=0.000	0.007	0.03	922.27	100.6
5518	4716	14-Mar-94	22:44:09	NO HORN, RPM= 1087 COLL=10.0 ALFSU= 0.00 CT/SIGMA=0.000	0.008	0.03	1066.30	121.1
5000	4717	14-Mar-94	22:45:53	NO HORN, RPM= 1087 VOR = 0.00 ALFSU= 0.00 CT/SIGMA=0.000	0.001	0.01	71.02	21.9
999	4718	14-Mar-94	22:53:52	NO HORN, RPM= 0000 VOR = 0.00 ALFSU= 0.00 CT/SIGMA=0.000	####	9.00	41.97	0.0
5000	4719	14-Mar-94	23:13:13	NO HORN, RPM= 1087 VOR = 0.00 ALFSU= 0.00 CT/SIGMA=0.000	0.001	0.01	32.67	21.6
5010	4720	14-Mar-94	23:22:04	NO HORN, RPM= 1087 VOR = 0.15 ALFSU= 7.00 CT/SIGMA=0.076	0.007	0.15	908.37	34.2
5010	4737	14-Mar-94	23:28:15	NO HORN, RPM= 1087 VOR = 0.15 ALFSU= 7.00 CT/SIGMA=0.076	0.007	0.15	924.81	33.8
5001	4738	14-Mar-94	23:32:14	NO HORN, RPM= 1082 VOR = 0.15 ALFSU= 5.00 CT/SIGMA=0.076	0.007	0.15	906.71	39.8
5001	4755	14-Mar-94	23:36:31	NO HORN, RPM= 1082 VOR = 0.15 ALFSU= 5.00 CT/SIGMA=0.076	0.007	0.15	914.48	39.4
5011	4756	14-Mar-94	23:40:50	NO HORN, RPM= 1082 VOR = 0.15 ALFSU= 3.00 CT/SIGMA=0.076	0.007	0.15	906.75	45.5
5011	4773	14-Mar-94	23:47:08	NO HORN, RPM= 1082 VOR = 0.15 ALFSU= 3.00 CT/SIGMA=0.076	0.007	0.15	907.19	44.2
5005	4774	14-Mar-94	23:52:21	NO HORN, RPM= 1085 VOR = 0.20 ALFSU= 4.00 CT/SIGMA=0.076	0.007	0.20	911.46	31.1
5005	4791	14-Mar-94	23:58:42	NO HORN, RPM= 1085 VOR = 0.20 ALFSU= 4.00 CT/SIGMA=0.076	0.007	0.20	922.80	30.6
5004	4792	15-Mar-94	0:01:33	NO HORN, RPM= 1088 VOR = 0.20 ALFSU= 2.00 CT/SIGMA=0.076	0.007	0.20	906.83	38.0
5004	4809	15-Mar-94	0:07:38	NO HORN, RPM= 1088 VOR = 0.20 ALFSU= 2.00 CT/SIGMA=0.076	0.007	0.20	913.76	37.5
5007	4810	15-Mar-94	0:10:28	NO HORN, RPM= 1088 VOR = 0.20 ALFSU= 2.50 CT/SIGMA=0.087	0.008	0.20	1037.80	43.6
5007	4827	15-Mar-94	0:16:45	NO HORN, RPM= 1088 VOR = 0.20 ALFSU= 2.50 CT/SIGMA=0.087	0.008	0.20	1045.00	42.9
5000	4828	15-Mar-94	0:21:07	NO HORN, RPM= 1087 VOR = 0.00 ALFSU= 0.00 CT/SIGMA=0.000	0.001	0.00	54.59	22.3
999	4829	15-Mar-94	0:21:52	NO HORN, RPM= 0000 VOR = 0.00 ALFSU= 0.00 CT/SIGMA=0.000	####	0.00	16.47	0.0
5000	4830	15-Mar-94	1:07:33	NO HORN, RPM= 1087 VOR = 0.00 ALFSU= 0.00 CT/SIGMA=0.000	0.001	0.00	45.66	21.6
5006	4831	15-Mar-94	1:12:28	NO HORN, RPM= 1085 VOR = 0.20 ALFSU= 4.50 CT/SIGMA=0.087	0.008	0.20	1034.30	34.0
5006	4848	15-Mar-94	1:18:49	NO HORN, RPM= 1085 VOR = 0.20 ALFSU= 4.50 CT/SIGMA=0.087	0.008	0.20	1055.30	34.0
5013	4849	15-Mar-94	1:21:20	NO HORN, RPM= 1088 VOR = 0.20 ALFSU= 6.00 CT/SIGMA=0.076	0.007	0.20	911.11	23.0
5013	4866	15-Mar-94	1:27:33	NO HORN, RPM= 1088 VOR = 0.20 ALFSU= 6.00 CT/SIGMA=0.076	0.007	0.20	921.56	22.6
5015	4867	15-Mar-94	1:29:45	NO HORN, RPM= 1088 VOR = 0.20 ALFSU= 6.50 CT/SIGMA=0.087	0.008	0.20	1033.10	25.5
5015	4884	15-Mar-94	1:35:56	NO HORN, RPM= 1088 VOR = 0.20 ALFSU= 6.50 CT/SIGMA=0.087	0.008	0.20	1049.00	24.1
5000	4885	15-Mar-94	1:39:18	NO HORN, RPM= 1087 VOR = 0.00 ALFSU= 0.00 CT/SIGMA=0.000	0.001	0.00	104.41	23.0
999	4886	15-Mar-94	1:40:03	NO HORN, RPM= 0, END OF TEST PROGRAM	####	0.00	53.86	0.0